2017

Design, Synthesis, Characterization and Evaluation of Near Infrared BODIPY Dyes for Various Applications

Qianli Meng
Louisiana State University and Agricultural and Mechanical College

DESIGN, SYNTHESIS, CHARACTERIZATION AND EVALUATION OF NEAR INFRARED BODIPY DYES FOR VARIOUS APPLICATIONS

A Dissertation

Submitted to the Graduate Faculty of the
Louisiana State University and
Agricultural and Mechanical College
in partial fulfillment of the
requirements for the degree of
Doctor of Philosophy

In

The Department of Chemistry

by
Qianli Meng
B.E., Anhui Normal University, 2011
May 2017

I would like to dedicate this dissertation to my parents, Ming Meng and Min Li for their love and encouragement. And of course, to my dearest wife, Jingyuan for her unconditional support and patience through my graduate career.

ACKNOWLEDGEMENTS

First of all, I would like to thank my doctoral advisor, Dr. M. Graça H. Vicente for giving me a chance to study in her research group, for her support and valuable suggestions throughout my graduate career. Dr. Vicente was always working hard as an excellent role model, and always in the office and laboratories to help me with my research and life.

I also appreciate all help and advice from Prof. Kevin M. Smith. His insightful ideas on research, especially on pyrrole and porphyrin chemistry, inspired me and taught me how to think about chemistry like a real chemist. He's also among the most professional professor, since he could always pick up any error or typo in my presentations, and helped me to learn how to prepare professional schemes.

I would also like to thank my doctoral committee members, Dr. Justin Ragains and Dr. Donghui Zhang for taking time out of their demanding schedule and to serve on my advisory Committee, and for all their help on my job applications. In addition, I offer my appreciation to Dr. Geoff Clayton to serve on my Committee as the Dean's representative. I am deeply grateful for the collaboration with Dr. Michael Mathis's and Dr. Karl Kadish's research group from Veterinary School of Louisiana State university and University of Houston, for sharing their electrochemical knowledge with me. To Dr. Frank R. Fronczek for the crystal structure determinations, Dr. Thomas Weldeghiorghis for his expertise in NMR facility, and Ms. Connie David for the support in mass spectrometry. I have to acknowledge my undergraduate research advisors, Prof. Erhong Hao and Prof. Lijuan Jiao, who trained me with all organic experimental skills and motivated me to step into the fluorescent BODIPY area.

My sincerest gratitude goes to the wonderful chemists in the Vicente and Smith groups. Thank you Dr. Timsy K. Uppal, Dr. Moses I. Ihachi, Dr. Haijun Wang, Dr. R. G. Waruna

Jinadasa, Dr. N. V. S. Dinesh Bhupathiraju, Dr. Jaime H. Gibbs, Dr. Alex L. Nguyen, Dr. Ning Zhao, Dr. Sunting Xuan, Tyrslai Williams, Eliazabeth Okoth, Daniel J. LaMaster, Maodie Wang, Nichole E. Kaufman, Guanyu Zhang and Zehua Zhou for friendship, and sharing their suggestions and knowledge. During my graduate career, I was so honored to work with three undergraduate students, Ha Nguyen, Evan Courville and Kaitlin Griffin, and their excellent performances helped me a lot.

At the end, I would like to express my greatest thanks to my wife Jingyuan for her patience and encouragement throughout my graduate years in LSU. To my beloved parents and parents-in-law and other family members, for their continuous love and care. This dissertation will not be completed without everyone's encouragement and guidance.

Table of Contents

ACKNOWLEDGEMENTS iii

GLOSSARY OF ABBREVIATIONS vii

ABSTRACT ix

CHAPTER I: INTRODUCTION 1

1.1 BODIPY® Structure 1
1.2 BODIPY Synthetic Methodologies 4
1.3 Derivatization of the BODIPY Platform 7
1.4 BODIPY's Applications 13
1.5 Research Outlook 17
1.6 References 18

CHAPTER II: SYNTHESIS OF IODINATED BODIPYS AND INVESTIGATIONS OF THEIR PD-CATALYZED CROSS COUPLING REACTIONS 25

2.1 Introduction 25
2.2 Results and Discussion 28
2.3 Conclusions 46
2.4 Experimental 47
2.5 References 59

Chapter III: AROMATIC SUBSTITUTION REACTIONS ON IODINATED-BODIPYS 63

3.1 Introduction 63
3.2 Results and Discussion 67
3.3 Conclusions 83
3.4 Experimental 83
3.5 References 97

CHAPTER IV: PREPARATION OF NEAR-IR BODIPYS VIA BENZO-FUSIONS 101

4.1 Introduction 101
4.2 Results and Discussion 108
4.3 Conclusions 119
4.4 Experimental 119
4.5 References 131

CHAPTER V: PREPARATION OF NITROPHENYL FUNCTIONALIZED BODIPYS FOR ELECTRO-CHEMICAL STUDIES 136

5.1 Introduction 136
5.2 Results and Discussion 139
5.3 Conclusions 147
5.4 Experimental 147
5.5 References 154

APPENDIX 155

APPENDIX A: NMR Characterization of Compounds Found in Chapter 2.....155
APPENDIX B: NMR Characterization of Compounds Found in Chapter 3.....180
APPENDIX C: NMR Characterization of Compounds Found in Chapter 4.....209
APPENDIX D: NMR Characterization of Compounds Found in Chapter 5.....245
Letters of Permission.....259
VITA.....263

GLOSSARY OF ABBREVIATIONS

δ	Chemical shift
λ_{max}	Maximum wavelength
aza-BODIPY	Aza-boron Dipyrromethene
^{11}B NMR	Boron 11 Nuclear Magnetic Resonance
BODIPY	Boron Dipyrromethene
^{13}C NMR	Carbon 13 Nuclear Magnetic Resonance
CuTc	Copper(I) thienyl-2-carboxylate
DCM	Dichloromethane
DDQ	2,3-Dichloro-5,6-dicyano-1,4-benzoquinone
DNA	Deoxyribonucleic acid
E	Extinction coefficient
Et	Ethyl
EtOAc	Ethyl acetate
^{19}F NMR	Fluoride 19 Nuclear Magnetic Resonance
FRET	Förster Resonance Energy Transfer
^{1}H NMR	Proton Nuclear Magnetic Resonance
HRMS-ESI	High Resolution Mass Spectrometry Electrospray Ionization
h	Hours
HOMO	Highest Occupied Molecular Orbital
HPLC	High-Performance Liquid Chromatography
Hz	Hertz
ICT	Intramolecular Charge Transfer
IDG	Indocyanine Green
J	Coupling constant (Hz)
LUMO	Lowest Unoccupied Molecular Orbital
M	Molarity
m/z	Mass to charge ratio
Me	Methyl
Mg	Milligram
MHz	Megahertz

Min	Minutes
mL	Milliliter
MP	Melting Point
NIR	Near-infrared
Nm	Nanometer
PDT	Photodynamic Therapy
PEG	Polyethylene Glycol
PET	Positron Emission Tomography
Ph	Phenyl
Ppm	Parts per million
rDA	Retro-Diels-Alder
RNA	Ribonucleic Acid
Rt	Room temperature
s	Singlet
S_NAr	Nucleophilic Aromatic Substitution
SPECT	Single-Photo Emission Computed Tomography
t	Triplet
THF	Tetrahydrofuran
TLC	Thin Layer Chromatography
UV-Vis	Ultra violet-visible

ABSTRACT

4,4-Difluoro-4-bora-3a,4a-diaza-5-indacene (BODIPY) have drawn a large number of research attention, for its numerous useful application in the fields of material and biology. Small modification of this well-known fluophore has been shown to optimize its photophysical and chemical properties. This work mainly focuses on functionalization of BODIPY cores with halogenated atoms, particularly iodine, and their subsequent post-functionalization reactions, mainly cross-coupling reaction and substitutions, for various further applications.

Chapter 1 of this dissertation gives a general overview of BODIPYs including their synthetic strategies, post-functionalization, and how BODIPYs are utilized in many biological applications.

Chapter 2 mainly focuses on the synthesis and characterization of 3,5-diiodo-BODIPYs' and 2,3,5,6-tetraiodo-BODIPY's cross coupling products, together with the best coupling reaction methodology developments.

Chapter 3 presents various aromatic substitution reactions of 3,5-diiodo-BODIPYs and 2,3,5,6-tetraiodo-BODIPY. The methods are developed with the best solvents, temperature and equivalents of nucleophiles. Due to the high reactivity of the 3,5-iodines, ^{123}I radio labeling reactions were also attempted to produce ^{123}I exchanged BODIPYs within one hour.

Chapter 4 investigates the aromatization reactions on β,β'-bicyclo-BODIPYs, and a full scan of all 3,5-substited groups shows that only electron withdrawing groups are stable during the aromatization reactions. Based on this conclusion, a bis(isothiocyanate)-BODIPY that emits in the near-IR region was prepared and conjugated to an EGFR-L1 peptide.

Chapter 5 reports the synthesis of nitrophenyl BODIPYs, and their electrochemical properties were studied, in collaboration with Dr. Karl Kadish group from University of Houston. In the

reductive area, reversible peaks are found, which are corresponded to the reductive reactions on the nitrophenyl units.

CHAPTER I: INTRODUCTION

1.1 BODIPY® Structure

Fluorescent dyes attract the attention of scientists from numerous fields, such as material science, molecular biology, drug discovery, tissue diagnostics, analytical chemistry and environmental chemistry.[1-3] An increasing number of applications are now requiring design and synthesis of fluorescent chromophores to emit in the red or near infrared (NIR) region. The development on fluorescent chromophores' physical and biological properties, including high stability and solubility and low toxicity, are being investigated by numerous research groups. Though a variety of fluorescent organic dyes, including fluorescein, rhodamines, cyanine and phthalocyanines, are commercially available, BODIPY, which is the abbreviation for boron dipyrromethene (4,4-difluoro-4-bora-3a,4a-diaza-s-indacene), has been discovered and studied over the past two decades as a highly popular fluorophore in many applications.

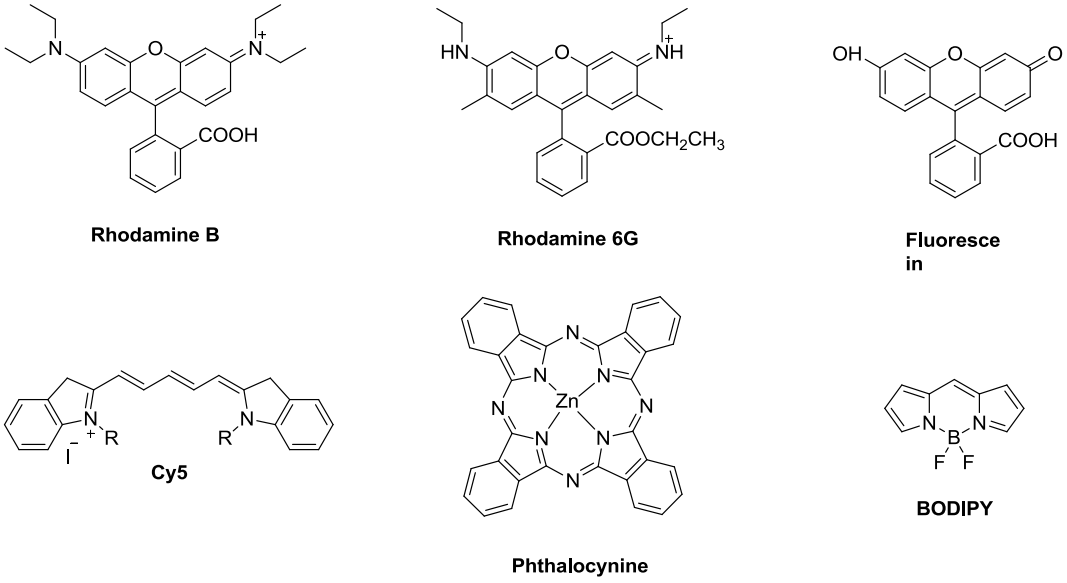

Figure 1.1: Structure of common fluorophores

BODIPY is usually prepared from the complexation of a dipyrromethene molecule with a disubstituted boron unit, and this is often completed by using boron trifluoride diethyl etherate. The dipyrromethene's structure if formed by linking the α-positions of two pyrroles via an sp^2 carbon. The complexation of the dipyrromethene with the BF_2 unit forms a rigid system and prevents the *cis/trans* isomerization of the dipyrromethene molecule. This stable rigidification allows the conjugation of π-electron system along the carbon-nitrogen backbone, and it leads to unusually intense fluorescence quantum yields.[4]

Several numbering systems have been reported for the BODIPY core. The first system utilizes the similarity between BODIPY and s-indacene, which is an all-carbon tricyclic analog (Figure 1.2). In this numbering system, the 3- and 5- carbons are referred to as alpha and the 1, 2, 6 and 7 are denoted as beta, which is similar to pyrroles. The C-8 position is referred to as the *meso*- position, following porphyrinic systems, and positions 4 and 4' are for the two fluoride atoms on the boron atom.[2]

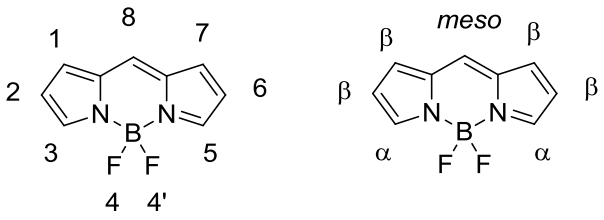

Figure 1.2: Numbering system of BODIPY structure

BODIPYs have a variety of applications because of their valuable characteristics, such as sharp bands in the absorption and emission spectra giving high sensitivity, large molar absorption coefficients (40000-110000 M^{-1} cm^{-1}), relatively high fluorescence quantum yields, long excited singlet- state lifetimes (1-10 ns), high chemical and photo- chemical stability in both solution and solid states, versatile charge- transfer properties, good solubility in most common solvents and resistance toward aggregation in solution.[2-3]

The absorption band of a typical BODIPY is a narrow and intense band due to the S_0- S_1 (π- π^*) transition, around 500- 525 nm, a shoulder at high energy around 480± 5 nm due to the 0-1 vibrational transition, and a weak and broad band around 375± 5 nm attributed to the S_0- S_2 (π- π^*) transition.[5-6] BODIPY has a narrow and Stokes- shifted emission band, of mirror image shape to the absorption band, with λ_{max} located between 530- 560 nm, which comes from the S_1 state. Low phosphorescence is observed from BODIPY dyes mainly due to negligible triple state formation and a fairly slow rate of intersystem crossing (except for heavy- atom effect of 2,6-diiodo-BODIPYs).[7]

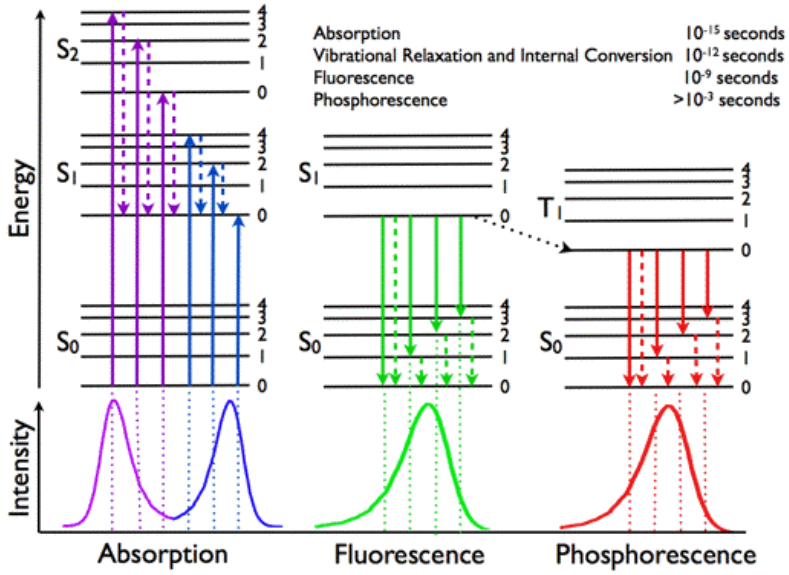

Figure 1.3: Jablonski diagram[8]

The replacement of C-8 in the BODIPY with a nitrogen atom gives a so-called aza-BODIPY structure. In addition to the advantages of normal BODIPY molecules, aza-BODIPYs have a *ca*. 90 nm red shift[9] of the absorption and emission bands. Besides being a promising agent for photodynamic therapy,[10] aza-BODIPYs can also be utilized as luminescent chemosensors.[11]

Near-infrared fluorophores (700- 900 nm) have optimal optical sensitivity for biological studies, including minimal interference from endogenous chromophores, optimal photon penetration through tissue, reduced light scattering, and lower damage to the cells and tissues under observation.[12-15] The absorption and emission bands of BODIPY dyes have been tuned to the red or NIR region by a number of chemical reactions aimed at extending their π-systems, and other photophysical characteristics of BODIPYs can also be optimized. Consequently, many research groups have studied many synthetic methodologies to these systems.

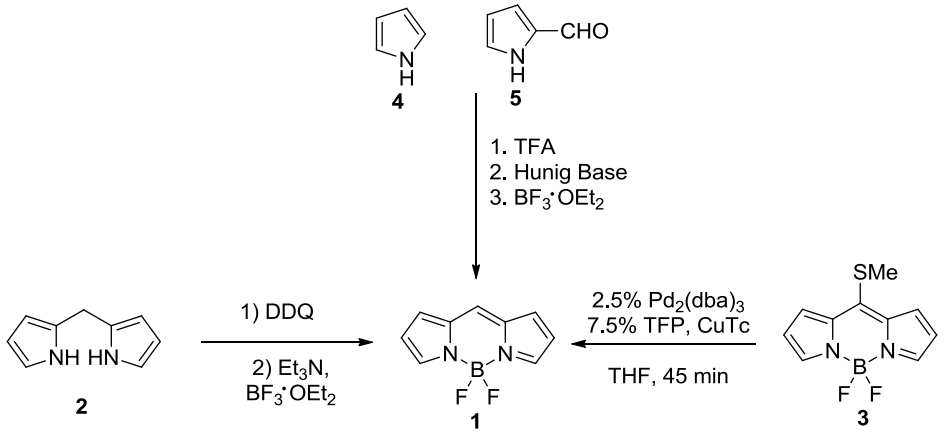

Scheme 1.1: Methods for syntheses of unsubstituted BODIPY.

1.2 BODIPY Synthetic Methodologies

1.2.1 Synthesis of unsubstituted BODIPYs

Though numerous reports of synthesis of BODIPY are seen in the literature, the fully unsubstituted BODIPY **1** remained to be a challenge due to the very low stability of this compound and its intermediates. There are so far three methods reported on syntheses of unsubstituted BODIPY **1**. The first method started from dipyrromethane **2**, which is oxidized to the corresponding dipyrromethene using DDQ. To avoid other reactions such as decomposition or polymerization, the oxidation step is carried out at low temperature (-78 °C). The complexation step with $BF_3 \cdot OEt_2$ is performed *in situ* in the presence of an organic base to give

the desired compound in relatively low yield.[16] Second, a reactive electrophilic pyrrole carbaldehyde **5** and nucleophilic α-free-pyrrole **4** afford the corresponding dipyrromethene, which is deprotonated using a secondary or tertiary amine, followed by complexation with boron trifluoride etherate ($BF_3 \cdot OEt_2$) to give the BODIPY. Interestingly, the unsubstituted BODIPY was synthesized in 98% yield from an efficient method, which was developed by Pena-Cabrera and coworkers.[17] A *meso*-thiomethyl BODIPY **3** was treated with trimethylsilane under mild conditions, using copper(I) thienyl-2-carboxylate (CuTc) and palladium(0) in refluxing THF. According to the literature, no reaction was observed in the absence of CuTc or palladium(0). This method afforded BODIPY **1** in high yield (93%), as shown in Scheme 1.1.[18]

1.2.2 Synthesis of substituted BODIPYs

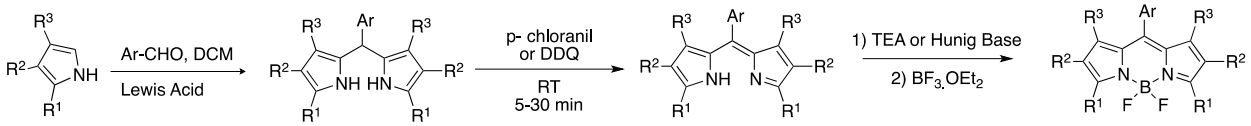

Scheme 1.2: Synthetic route to BODIPY using an arylaldehyde and an α-free pyrrole

The most common reported and used methodology for the preparation of 8-substituted BODIPYs is by a condensation reaction among two α-free pyrroles and an aldehyde under acidic conditions, as shown in Scheme 1.2. An oxidation step is also required for the formation of the dipyrromethene (common used oxidants are DDQ or p-chloranil), with a subsequent complexation step with $BF_3 \cdot OEt_2$.

Another synthesis of 8-substituted BODIPYs is via the condensation of acyl chlorides or anhydrides with α-free pyrroles, as shown in Scheme 1.3. This reaction directly produces a dipyrromethene without the need for an additional oxidation step. The only problem with this route is the high reactivity of acyl chlorides that often lead to side-products.

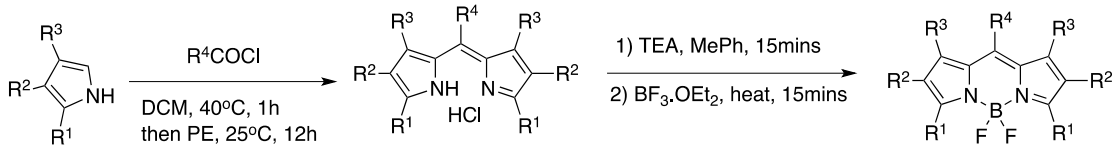

Scheme 1.3: Synthetic routes to BODIPY using an acyl chloride and an α-free pyrrole

Asymmetrically substituted BODIPYs can be obtained via preparation of ketopyrrole or formylpyrrole intermediates, with another α- free pyrrole, as shown in Scheme 1.4.

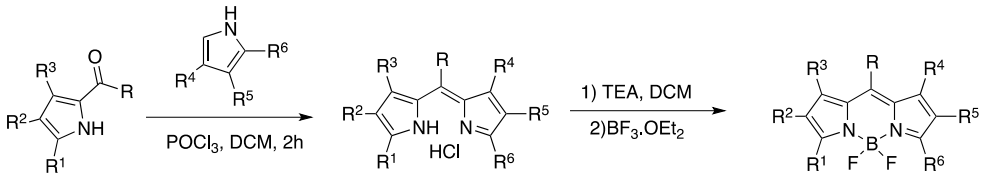

Scheme 1.4: Synthesis of asymmetric BODIPY from ketopyrroles

Anhydrides are also employed to react with an *α*-free pyrrole to give the corresponding dipyrromethene, followed by a complexation step to give BODIPYs with linkers and carboxylic acids at the chain ends, as shown in Scheme 1.5. This method allows the preparation of BODIPY-acids for subsequent conjugating reactions.

Although the introduction of aromatic groups to the BODIPY's *meso*-positions is not able to extend the π-conjugation significantly due to the nearly perpendicular geometry of the aryl groups, it increases the BODIPY stability, because the *meso*-positions are relatively reactive under many reaction conditions.[2-3, 19-20]

1.2.3 Synthesis of aza-BODIPYs

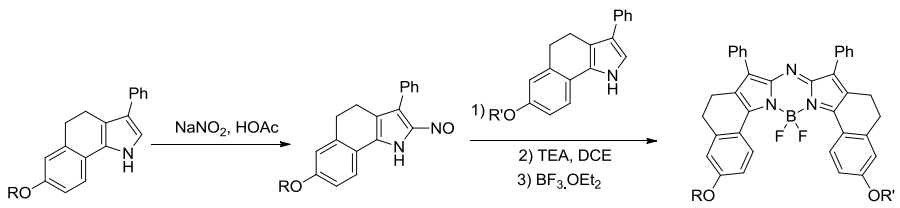

Scheme 1.5: Synthesis of aza-BODIPY through nitroso-pyrroles

The aza-BODIPY's precursor, the azadipyrromethene chromophore, was first described in the 1940s, but aza-BODIPY's research was only developed in last two decades, mainly by O'Shea's group. The classical way to synthesize aza-BODIPYs is via a nitrosation of a 2,4- diaryl pyrrole, followed by a reaction with an α-free pyrrole and generation of azadipyrromethenes, as shown in Scheme 1.6.[21] Phthalonitrile was treated with aryl Grignard reagents, and water distillation was able to give aza-dipyrromethenes after 24 hours. The aza-dipyrromethenes were then complexed to give dibenzo-fused aza-BODIPYs, as shown in Scheme 1.7.[9] In 2010, Li *et al* reacted 2-chloroindole with 1,3-diiminoisoindoline, and after complexation, an indole- based aza-BODIPY was prepared, as shown in Scheme 1.8.[22]

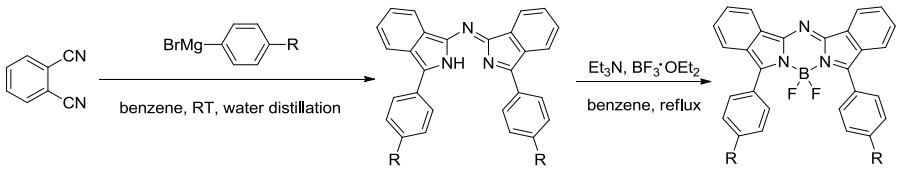

Scheme 1.6: Synthesis of benzo-fused aza-BODIPYs

1.3 Derivatization of the BODIPY Platform

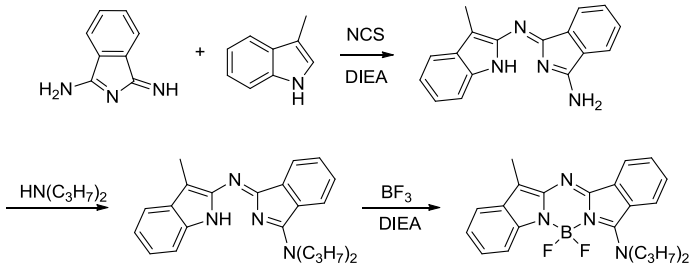

Scheme 1.7: An aza-BODIPY synthesis from 1,3-diiminoisoindoline

Several BODIPYs are commercially available, and most of them are synthesized in just a few steps, following earlier literature. Their prices are relatively inexpensive, particularly as fluorescent molecules with activated acids, as shown in Table 1.1. However, looking at their λ_{max} (abs) and λ_{max} (emi) wavelengths, most of these molecules' wavelengths are still within the 500-

600 nm region, and their Stokes' shifts are relatively small. In addition, due to the absence of *meso*-aryl groups in most of these structures, their stability is not compatible for some of their desirable applications.

Table 1.1: Commercially available BODIPYs ready for amino-conjugation (the numbers below the structures show their λ_{max} (abs.) and λ_{max} (emi.) wavelengths)

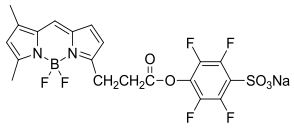 **500/510**	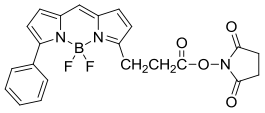 **527/546**	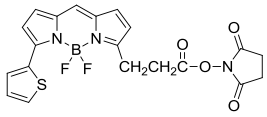 **558/568**	Price: 5mg/ ~$300
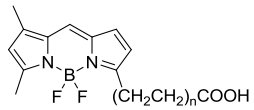 **500/510**	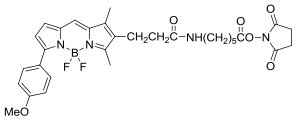 **541/569**	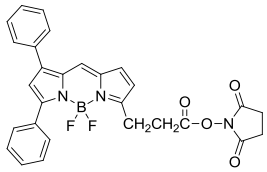 **530/550**	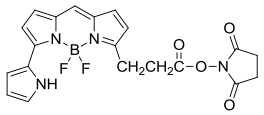 **576/589**
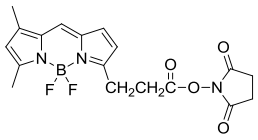 **500/510**	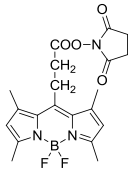 **493/503**	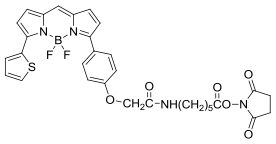 **590/620**	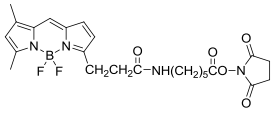 **500/510**
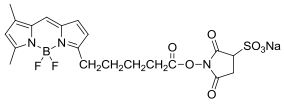 **500/510**	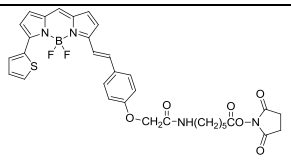 **630/650**	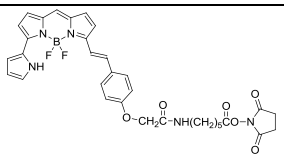 **650/665**	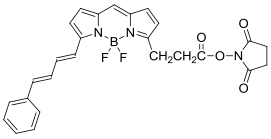 **581/591**

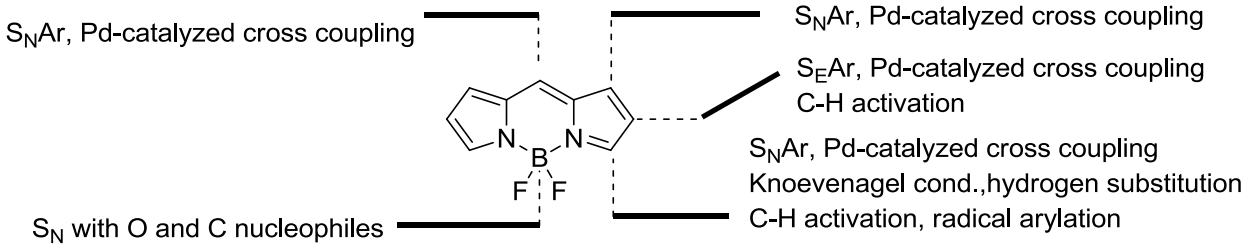

Figure 1.4: An overview of possible functionalizations on BODIPY molecules[23]

1.3.1: Functionalization at the *meso*-position

Functionalization at the *meso*-position is relatively easy, compared to the substitution at the other pyrrolic positions, since it can be achieved by condensation of pyrroles with suitable aryl aldehydes or acyl chlorides. This method is still the most common method used for direct introduction of various aryl units on the BODIPY core, such as ligands,[1, 3, 24] chiral auxiliaries, donor-acceptor groups[25-27] and water-solubilizing groups[15, 28] for various applications, as shown in Figure 1.5. The introduction of *ortho*-substituents on the *meso*-phenyl ring, the replacement of phenyl with bulkier groups and/or the introduction of 1,7-substituents on the BODIPY skeleton, are able to improve the fluorescence emission quantum yields significantly, due to restricted intramolecular rotation and steric hindrance between the substituents.

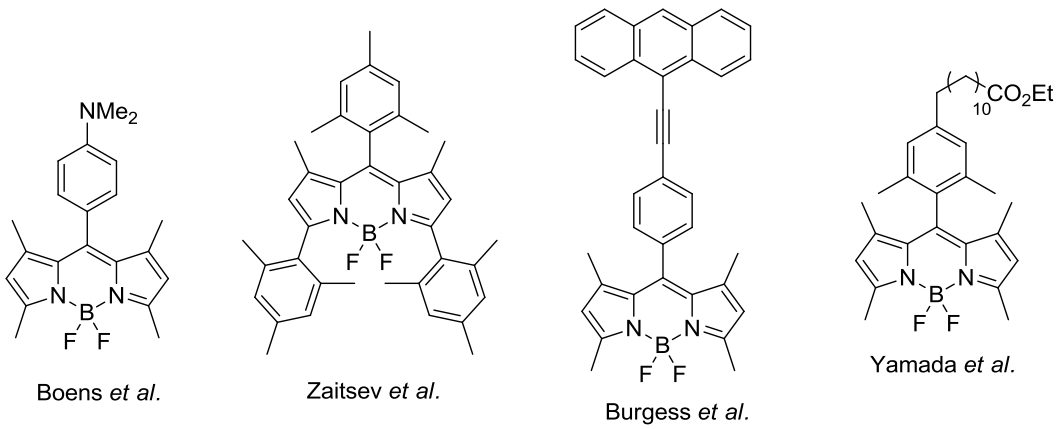

Figure 1.5: Several *meso*- functionalized BODIPYs[2-3, 29-31]

In 2012 and 2014, the synthesis of *meso*-chloro-BODIPYs was reported from dipyrroketone,[32-33] and the reactive BODIPYs opened a door to more *meso*-functionalizations.[34-39] A dipyrrylketone was chlorinated to give 5-chloro-dipyrromethene, which was then complexed to give *meso*-chloro-BODIPY, as shown in Scheme 1.9. Further reactions indicated this chlorine was a good leaving group for subsequent cross-coupling reactions and substitution reactions.

1.3.2: Functionalization at the 1,3,5,7-positions

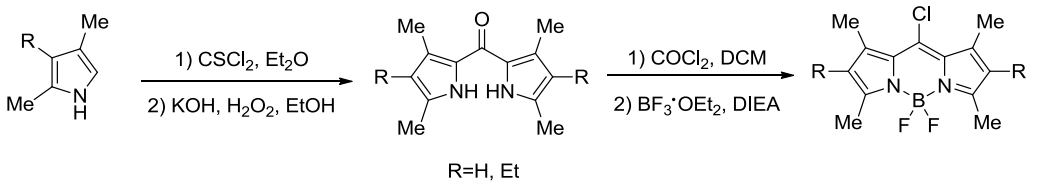

Scheme 1.8: Synthesis of *meso*-chloro-BODIPYs from dipyrrylketone

The photophysical properties of the BODIPY core can be easily tuned by switching the substituents on the carbon framework, particularly at the 1,3,5,7-positions. The 3,5-methyl groups are relatively acidic, due to being in close proximity to the pyrrolic nitrogen atom. In order to extend the π-conjugation system, the methyl groups can be deprotonated and further condensed with aromatic aldehydes through Knoevenagel reactions, generating *trans*-stryryl groups.[40-41] Although the Knoevenagel condensation reactions require large excess of aldehydes and prolonged refluxing time, extension of π-conjugation is still mainly accomplished through this method. Addition of conjugation at the 3,5-positions generally produces a greater bathochromic shift (*ca.* 50 - 100 nm) than adding conjugation through the 2,6-positions, producing the greatest shift when all four methyls are converted to styryl groups.[2] Addition of halogens, particularly iodine atoms, at the 3,5-positions allows BODIPY to become highly reactive toward nucleophilic aromatic substitutions (S_NAr) and palladium-catalyzed cross-coupling, which will be discussed in detail in the following chapters.

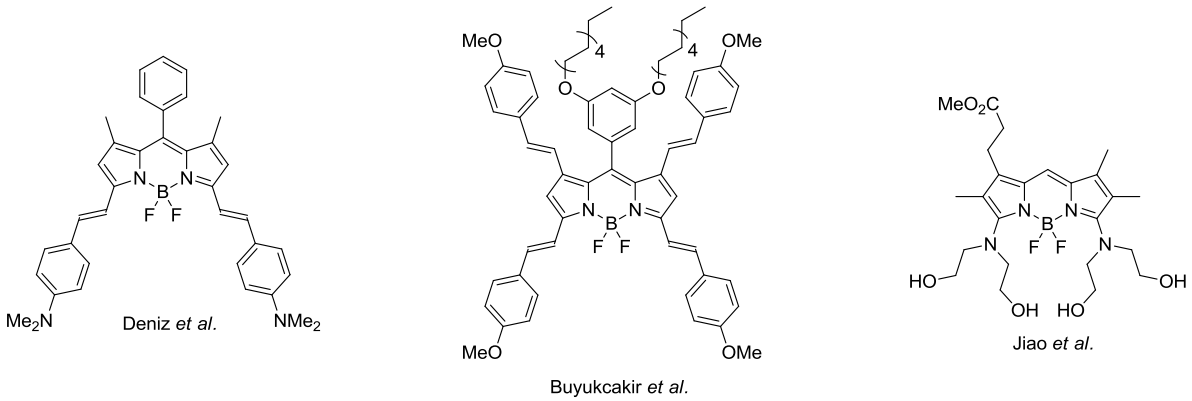

Figure 1.6: Several cases with functionalizations at 1,3,5,7-positions[42-44]

1.3.3 Functionalization at the 2,6-Positions

The reactivity of the BODIPY core can be predicted based on the resonance structure, as shown in Figure 1.7, where the 2- and 6-positions contain the least positive charge. For this reason, they are susceptible to undergo electrophilic aromatic substitution. Different functional groups have been introduced at the 2- and 6-positions via reactions including halogenation,[45-46] nitration,[47-48] sulfonation,[49-50] and formylation.[51] For example, the introduction of sulfonate groups is able to largely increase the BODIPY's water solubility for potential biological applications. Though sulfonate groups do not make significance changes in the absorption and emission spectra, BODIPYs containing sulfonates are still highly fluorescent in polar solvents, and more stable than their precursors. It was also reported that the addition of nitro groups at the 2,6-positions reduces the BODIPY fluorescence quantum yields.[52]

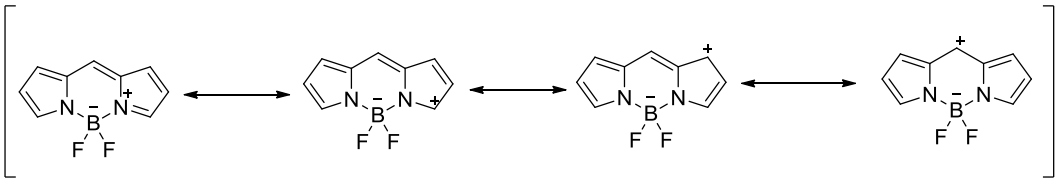

Figure 1.7: Resonance structures of BODIPY core

The addition of halogen groups (bromide or iodide) at the 2- and 6-positions is able to produce red shifts in the absorption and fluorescence emission maxima, but this transformation largely quenches the quantum yield, due to the heavy atom effect.[46, 53] Furthermore, post-modification on these 2,6-halogenated BODIPYs typically involves palladium-catalyzed cross-coupling reactions, such as Suzuki,[37, 54] Sonagashira,[55] and Heck reactions.[56]

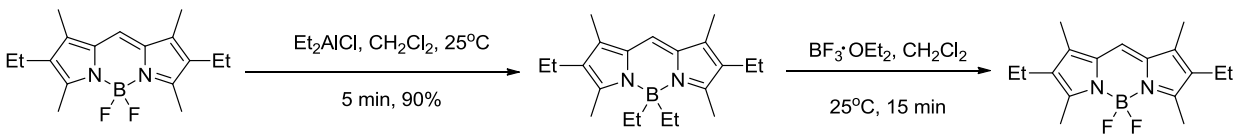

Scheme 1.9: Protection and deprotection strategy for the BF_2-BODIPY

1.3.4 Functionalization at the Boron-Positions

Boron-substituted BODIPYs have been investigated in the past ten years, mainly to increase the stability, and in the preparation of energy cassettes. Most reports employ oxygen and carbon nucleophiles (sp^3 and sp carbons) to replace the fluorines. The first 4,4-dialkyl-BODIPYs were synthesized via the reaction of dipyrromethenes with boron-alkyl chemicals. Alternatively, Ziessel *et al* investigated the synthesis of 4,4-dialkyl-, 4,4-diaryl-, and 4,4-diethynyl-BODIPYs by treating BODIPY with Grignard and organolithium reagents.[49, 57-64] These boron-aryl BODIPYs have relatively larger Stokes shifts compared to their corresponding BF_2 molecules. Cyano groups were also reported to replace the fluoride atoms, using trimethylsilyl cyanide, and the reactions were performed in high yields, in the presence of a Lewis acid.[49] Recently, Ankush *et al* reported a new method to introduce ethyl groups onto the boron center in high yields via treating BODIPY with Et_2AlCl, and the boron atom can be deprotected by boron trifluoride etherate, to give the BF_2 BODIPY, as shown in Scheme 1.9.[65]

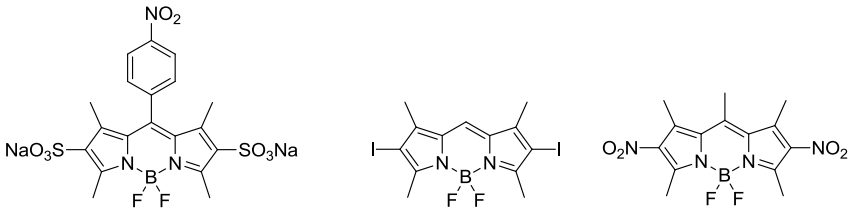

Li *et al.* Yogo *et al.* Pavlopoulos *et al.*

Figure 1.8: Several 2,6-functionalized BODIPY via electrophilic substitution reactions

Oxygen groups on the boron atom are expected to increase the solubility of BODIPY in aqueous solution. In 1999, the Burgess group reported the first oxygen substitution on the boron center by intramolecular cyclization.[66] Since then, a series of 4,4-dialkoxy- and diaryloxy-BODIPYs were synthesized and reported, either by treating with sodium alkoxide in refluxing alcohol, or with alcohols in the presence of a Lewis acid.[67] On the other hand, Courtis *et al* conducted a synthesis of mono-alkoxy BODIPYs for further bioimaging applications.[68]

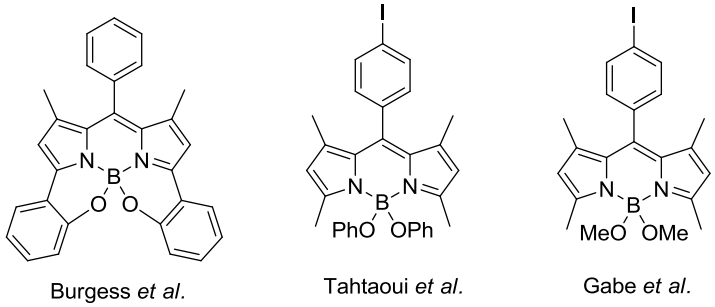

Figure 1.9: Several boron-functionalized BODIPYs

1.4 BODIPY's Applications

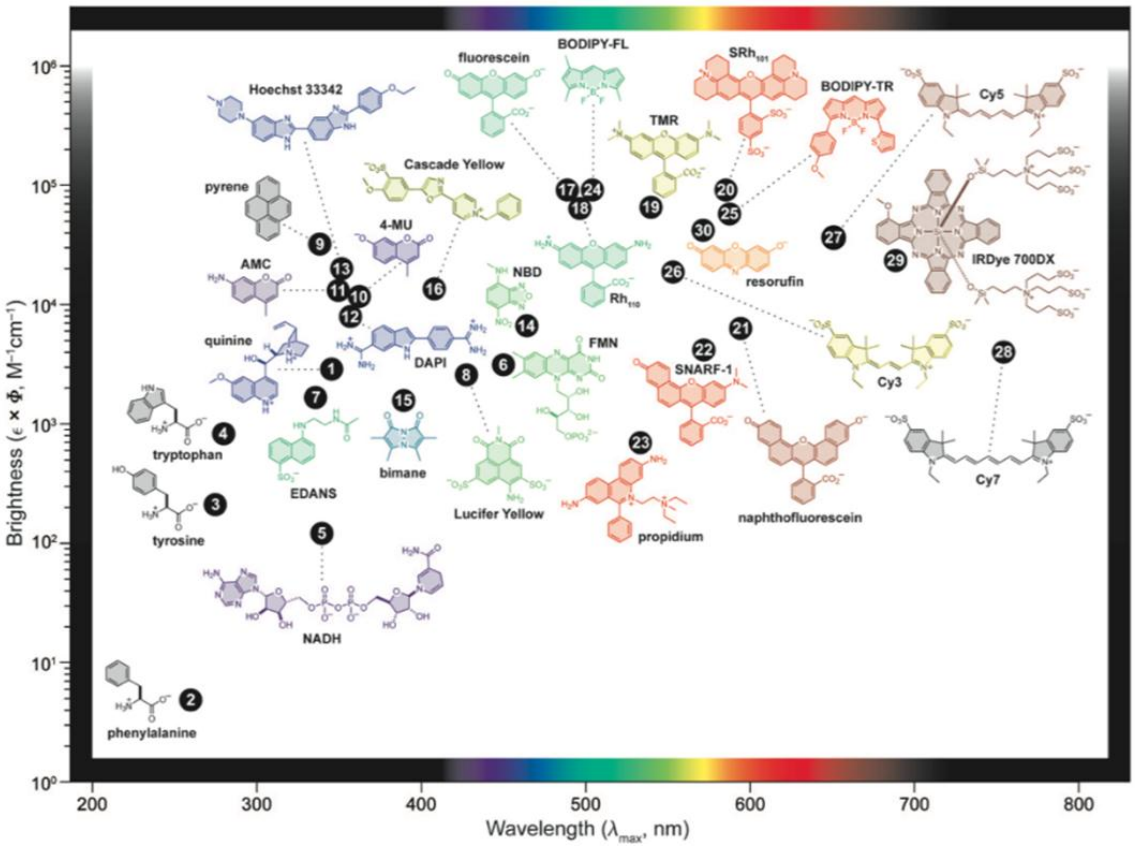

Figure 1.10: Common fluorescent dyes with different emissive wavelengths and brightness.[69]

Reprint with permission from Copyright (2008) American Chemical Society.

1.4.1 Biological Labels

BODIPYs linked to a biomolecule, can facilitate visualization of interactions between proteins, enzymes and other targets in living cells via fluorescence detection, especially for systems that lack detectable signals by other means.

BODIPYs usually have low dark toxicities, high fluorescent intensity and do not significantly influence the biological functions because of their small sizes. BODIPY-based probes can be functionalized with reactive ligands for bio-conjugations. BODIPYs with ligands have been studied for the detection and visualization of various proteins. Additionally, many BODIPY probes are being employed to label biomolecules.

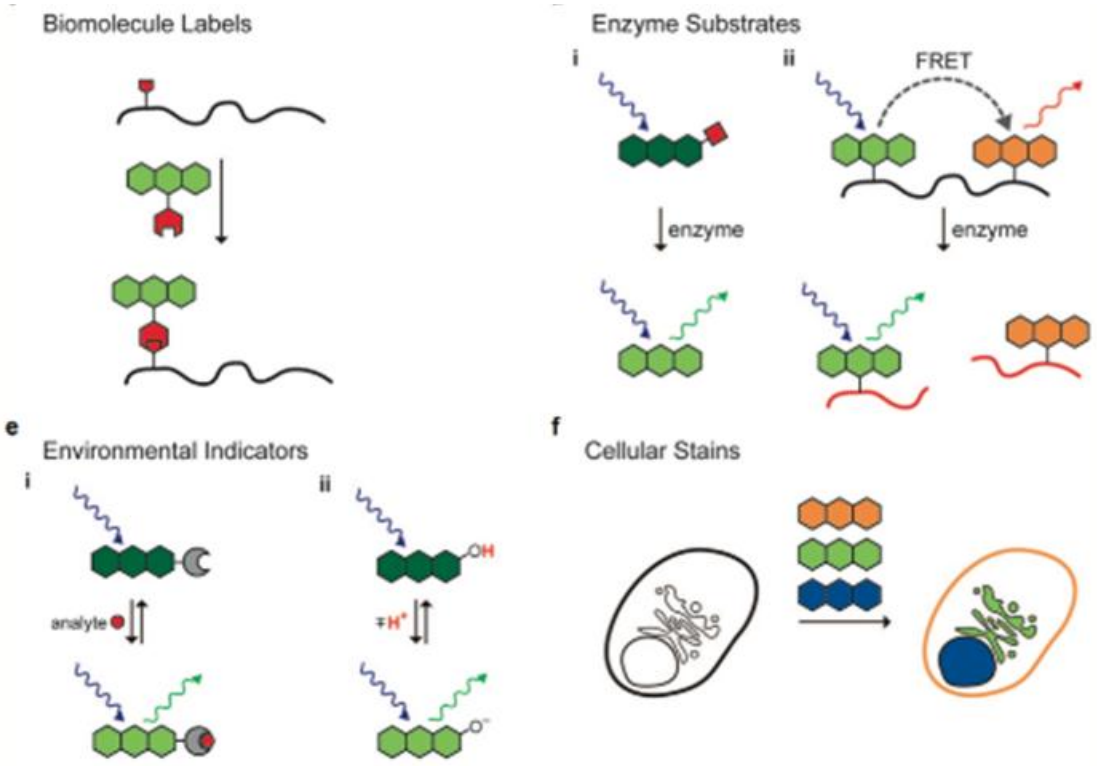

Figure 1.11: Biological applications of molecular fluorescent probes.[69] Reprint with permission from Copyright (2008) American Chemical Society

1.4.2 Environmental Indicators

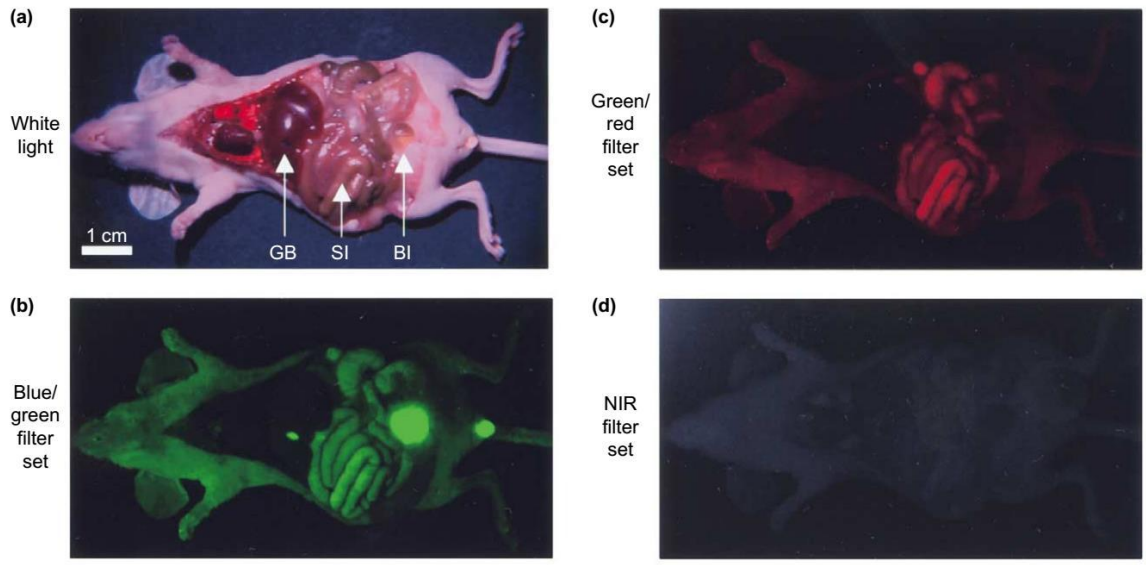

Figure 1.12: Mouse's vital organs and BODIPY fluids autofluorescence with different excitation/emission filters. a) no filter; b) blue/green (460-500nm/505-560nm) filter; c) green/red (525-555nm/590-650 nm) filter; d) NIR (725-775nm/790-830nm) filter. GB = gall bladder, SI = small intestine, BL = bladder. Reprinted with permission from Copyright (2002) Elsevier.[70]

BODIPY dyes can be selective and sensitive fluorescent chemosensors for intracellular pH and a variety of metal ions. Fluorescent sensors are either constructed as fluorophore- spacer-receptor or as intrinsic fluorescent probes.

Fluorophore-spacer-receptor systems operate on the basis of photoinduced electron transfer (PET) and internal charge transfer (ICT) processes. After binding the analyte to the sensor, alteration in either the fluorescence intensity or wavelength is detected. In PET sensors, binding of the analyte inhibits the PET while increasing the fluorescence intensity without much change in the spectral shift. In contrast, ICT sensors show a moderate increase in their emission intensity followed by significant shifts in their λ_{max}. A series of BODIPY based sensors have been reported for detection of H^+, K^+, Ni^{2+}, Cu^{2+}, Zn^{2+}, Hg^{2+}, etc metal ions in living cells, examples are shown in Figure 1.13.[44, 71-76]

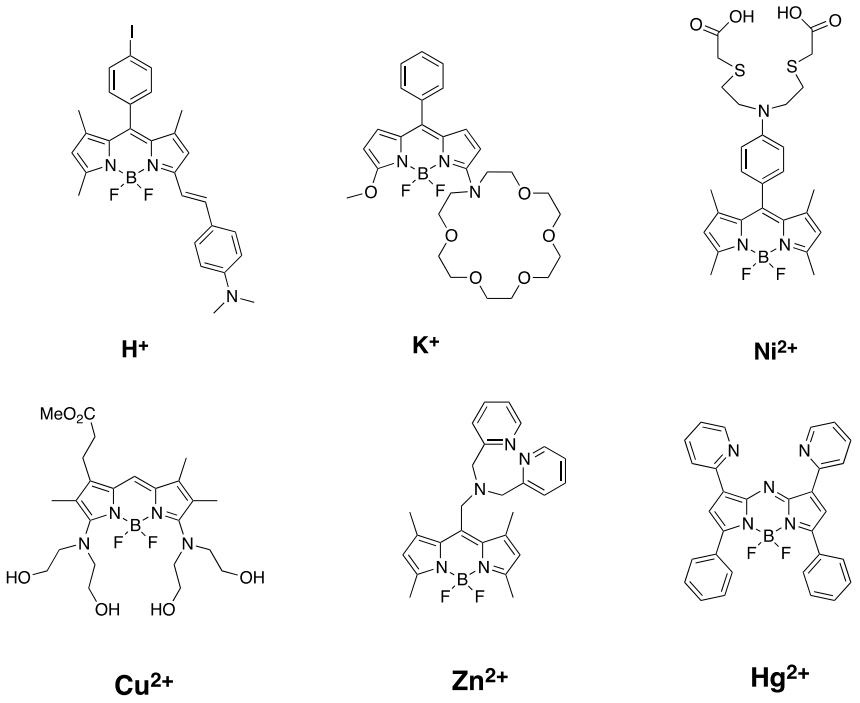

Figure 1.13: Some BODIPY chemosensors

1.4.3 Cellular Stains

Many biological samples and cells are transparent under the microscope. The internal parts of the cells, such as the organelles are transparent and therefore hard to be seen. As organelle stains, small BODIPY dyes can pass through viable cell membranes more efficiently than large molecules and remain inside the cell. For example, BODIPY ceramide is commercially available and used to specifically label ER/ Golgi, as shown in Figure 1.14.

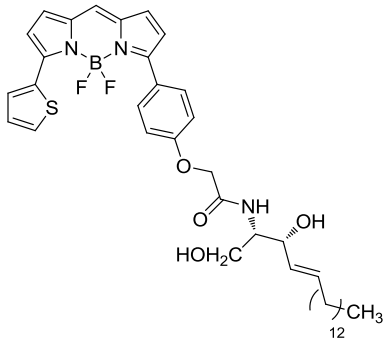

Figure 1.14: Chemical structure of BODIPY TR ceramide[77]

1.4.4 Photodynamic Therapy

Photodynamic therapy (PDT) is a new form of treatment that utilizes a photosensitizer (PS), a specific wavelength of light that can excite the PS and tissue oxygen to kill cancer cells in a selected region of the patient's body. When in the dark cell environment, both the PS and oxygen ($^3O_2$) present in the cell is not toxic. The conversion from triplet oxygen to singlet oxygen can only take place upon light activation of the PS.[78] Once the PS absorbs photon energy and is excited to higher energy levels, it can relax through non-radiative decay, fluorescence or phosphoresce. Molecules that go through ISC take a longer time in the excited triplet state and therefore have a higher probability of reacting. The energy lost is taken up by molecular oxygen to generate a highly reactive cytocidal $^1O_2$.[78-80]

A number of BODIPYs have been observed to show low dark toxicities but high photo toxicities. Most phototoxic BODIPYs have two halogen atoms (Br or I) on the 2,6- positions,[81] but not all BODIPYs with two halogen atoms on the 2,6-positions are phototoxic. Electron-donating 8-substituents are also necessary for phototoxicity.[46, 82] Computational studies show that 2,6- substituted BODIPYs favor ISC and singlet oxygen generation.[53]

1.5 Research Outlook

Though a number of reports are published with various methods to functionalize BODIPYs, we are still investigating efficient platforms and methodologies to prepare BODIPY with near-IR absorptions and emissions, high fluorescence quantum yields, high stability, solubility, and cell permeability. In this dissertation, the design, synthesis, characterization, and evaluation of near-IR BODIPYs for various applications is discussed in the next Chapters.

1.6 References

1. Boens, N.; Leen, V.; Dehaen, W., Fluorescent indicators based on BODIPY. *Chem. Soc. Rev.* **2012,** *41* (3), 1130-1172.

2. Loudet, A.; Burgess, K., BODIPY Dyes and Their Derivatives: Syntheses and Spectroscopic Properties. *Chem. Rev. (Washington, DC, U. S.)* **2007,** *107* (11), 4891-4932.

3. Ulrich, G.; Ziessel, R.; Harriman, A., The Chemistry of Fluorescent Bodipy Dyes: Versatility Unsurpassed. *Angew. Chem. Int. Ed.* **2008,** *47* (7), 1184-1201.

4. Descalzo, A. B.; Xu, H.-J.; Shen, Z.; Rurack, K., Red/Near-infrared Boron–Dipyrromethene Dyes as Strongly Emitting Fluorophores. *Ann. N. Y. Acad. Sci.* **2008,** *1130* (1), 164-171.

5. Qin, W.; Baruah, M.; De Borggraeve, W. M.; Boens, N., Photophysical properties of an on/off fluorescent pH indicator excitable with visible light based on a borondipyrromethene-linked phenol. *J. Photochem. Photobiol. A* **2006,** *183* (1–2), 190-197.

6. Meng, G.; Velayudham, S.; Smith, A.; Luck, R.; Liu, H., Color Tuning of Polyfluorene Emission with BODIPY Monomers. *Macromolecules* **2009,** *42* (6), 1995-2001.

7. Qin, W.; Leen, V.; Dehaen, W.; Cui, J.; Xu, C.; Tang, X.; Liu, W.; Rohand, T.; Beljonne, D.; Averbeke, B. V.; Clifford, J. N.; Driesen, K.; Binnemans, K.; Auweraer, M. V. d.; Boens, N., 3,5-Dianilino Substituted Difluoroboron Dipyrromethene: Synthesis, Spectroscopy, Photophysics, Crystal Structure, Electrochemistry, and Quantum-Chemical Calculations†. *The Journal of Physical Chemistry C* **2009,** *113* (27), 11731-11740.

8. http://www.photobiology.info/Visser-Rolinski.html.

9. Donyagina, V. F.; Shimizu, S.; Kobayashi, N.; Lukyanets, E. A., Synthesis of N,N-difluoroboryl complexes of 3,3′-diarylazadiisoindolylmethenes. *Tetrahedron Lett.* **2008,** *49* (42), 6152-6154.

10. Gorman, A.; Killoran, J.; O'Shea, C.; Kenna, T.; Gallagher, W. M.; O'Shea, D. F., In Vitro Demonstration of the Heavy-Atom Effect for Photodynamic Therapy. *J. Am. Chem. Soc.* **2004,** *126* (34), 10619-10631.

11. McDonnell, S. O.; O'Shea, D. F., Near-Infrared Sensing Properties of Dimethlyamino-Substituted BF2−Azadipyrromethenes. *Org. Lett.* **2006,** *8* (16), 3493-3496.

12. Escobedo, J. O.; Rusin, O.; Lim, S.; Strongin, R. M., NIR dyes for bioimaging applications. *Curr. Opin. Chem. Biol.* **2010,** *14* (1), 64-70.

13. Byron, B.; Lauren, A. E.; Alan, S. W., Fluorescence Imaging of Tumors In Vivo. *Curr. Med. Chem.* **2005,** *12* (7), 795-805.

14. Amiot, C.; Xu, S.; Liang, S.; Pan, L.; Zhao, J., Near-Infrared Fluorescent Materials for Sensing of Biological Targets. *Sensors* **2008,** *8* (5), 3082.

15. Niu, S.-l.; Massif, C.; Ulrich, G.; Renard, P.-Y.; Romieu, A.; Ziessel, R., Water-Soluble Red-Emitting Distyryl-Borondipyrromethene (BODIPY) Dyes for Biolabeling. *Chem. Eur. J.* **2012,** *18* (23), 7229-7242.

16. Tram, K.; Yan, H.; Jenkins, H. A.; Vassiliev, S.; Bruce, D., The synthesis and crystal structure of unsubstituted 4,4-difluoro-4-bora-3a,4a-diaza-s-indacene (BODIPY). *Dyes Pigm.* **2009,** *82* (3), 392-395.

17. Schmitt, A.; Hinkeldey, B.; Wild, M.; Jung, G., Synthesis of the Core Compound of the BODIPY Dye Class: 4,4′-Difluoro-4-bora-(3a,4a)-diaza-s-indacene. *J. Fluoresc.* **2009,** *19* (4), 755-758.

18. Arroyo, I. J.; Hu, R.; Merino, G.; Tang, B. Z.; Peña-Cabrera, E., The Smallest and One of the Brightest. Efficient Preparation and Optical Description of the Parent Borondipyrromethene System. *J. Org. Chem.* **2009,** *74* (15), 5719-5722.

19. Zheng, Q.; Xu, G.; Prasad, P. N., Conformationally Restricted Dipyrromethene Boron Difluoride (BODIPY) Dyes: Highly Fluorescent, Multicolored Probes for Cellular Imaging. *Chem. Eur. J.* **2008,** *14* (19), 5812-5819.

20. Nepomnyashchii, A. B.; Cho, S.; Rossky, P. J.; Bard, A. J., Dependence of Electrochemical and Electrogenerated Chemiluminescence Properties on the Structure of BODIPY Dyes. Unusually Large Separation between Sequential Electron Transfers. *J. Am. Chem. Soc.* **2010,** *132* (49), 17550-17559.

21. Hall, M. J.; McDonnell, S. O.; Killoran, J.; O'Shea, D. F., A Modular Synthesis of Unsymmetrical Tetraarylazadipyrromethenes. *J. Org. Chem.* **2005,** *70* (14), 5571-5578.

22. Li, Y.; Dolphin, D.; Patrick, B. O., Synthesis of a BF_2 complex of indol-2-yl-isoindol-1-ylidene-amine: a fully conjugated azadipyrromethene. *Tetrahedron Lett.* **2010,** *51* (5), 811-814.

23. Boens, N.; Verbelen, B.; Dehaen, W., Postfunctionalization of the BODIPY Core: Synthesis and Spectroscopy. *Eur. J. Org. Chem.* **2015,** *2015* (30), 6577-6595.

24. Ulrich, G.; Ziessel, R., Convenient and Efficient Synthesis of Functionalized Oligopyridine Ligands Bearing Accessory Pyrromethene-BF_2 Fluorophores. *J. Org. Chem.* **2004,** *69* (6), 2070-2083.

25. Zrig, S.; Rémy, P.; Andrioletti, B.; Rose, E.; Asselberghs, I.; Clays, K., Engineering Tuneable Light-Harvesting Systems with Oligothiophene Donors and Mono- or Bis-Bodipy Acceptors. *J. Org. Chem.* **2008,** *73* (4), 1563-1566.

26. Wu, L.; Loudet, A.; Barhoumi, R.; Burghardt, R. C.; Burgess, K., Fluorescent Cassettes for Monitoring Three-Component Interactions in Vitro and in Living Cells. *J. Am. Chem. Soc.* **2009,** *131* (26), 9156-9157.

27. Ziessel, R.; Bonardi, L.; Ulrich, G., Boron dipyrromethene dyes: a rational avenue for sensing and light emitting devices. *Dalton Trans.* **2006,** (23), 2913-2918.

28. Thivierge, C.; Bandichhor, R.; Burgess, K., Spectral Dispersion and Water Solubilization of BODIPY Dyes via Palladium-Catalyzed C−H Functionalization. *Org. Lett.* **2007,** *9* (11), 2135-2138.

29. Baruah, M.; Qin, W.; Flors, C.; Hofkens, J.; Vallée, R. A. L.; Beljonne, D.; Van der Auweraer, M.; De Borggraeve, W. M.; Boens, N., Solvent and pH Dependent Fluorescent Properties of a Dimethylaminostyryl Borondipyrromethene Dye in Solution. *J. Phys. Chem. A* **2006,** *110* (18), 5998-6009.

30. Wan, C.-W.; Burghart, A.; Chen, J.; Bergström, F.; Johansson, L. B. Å.; Wolford, M. F.; Kim, T. G.; Topp, M. R.; Hochstrasser, R. M.; Burgess, K., Anthracene–BODIPY Cassettes: Syntheses and Energy Transfer. *Chem. Eur. J.* **2003,** *9* (18), 4430-4441.

31. Yamada, K.; Toyota, T.; Takakura, K.; Ishimaru, M.; Sugawara, T., Preparation of BODIPY probes for multicolor fluorescence imaging studies of membrane dynamics. *New J. Chem.* **2001,** *25* (5), 667-669.

32. Leen, V.; Yuan, P.; Wang, L.; Boens, N.; Dehaen, W., Synthesis of Meso-Halogenated BODIPYs and Access to Meso-Substituted Analogues. *Org. Lett.* **2012,** *14* (24), 6150-6153.

33. Wang, H.; Vicente, M. G. H.; Fronczek, F. R.; Smith, K. M., Synthesis and Transformations of 5-Chloro-2,2′-Dipyrrins and Their Boron Complexes, 8-Chloro-BODIPYs. *Chem. Eur. J.* **2014,** *20* (17), 5064-5074.

34. Wang, H.; Fronczek, F. R.; Vicente, M. G. H.; Smith, K. M., Functionalization of 3,5,8-Trichlorinated BODIPY Dyes. *J. Org. Chem.* **2014,** *79* (21), 10342-10352.

35. Gibbs, J. H.; Wang, H.; Bhupathiraju, N. V. S. D. K.; Fronczek, F. R.; Smith, K. M.; Vicente, M. G. H., Synthesis and properties of a series of carboranyl-BODIPYs. *J. Organomet. Chem.* **2015,** *798, Part 1*, 209-213.

36. Zhao, N.; Vicente, M. G. H.; Fronczek, F. R.; Smith, K. M., Synthesis of 3,8-Dichloro-6-ethyl-1,2,5,7-tetramethyl–BODIPY from an Asymmetric Dipyrroketone and Reactivity Studies at the 3,5,8-Positions. *Chem. Eur. J.* **2015,** *21* (16), 6181-6192.

37. Zhao, N.; Xuan, S.; Fronczek, F. R.; Smith, K. M.; Vicente, M. G. H., Stepwise Polychlorination of 8-Chloro-BODIPY and Regioselective Functionalization of 2,3,5,6,8-Pentachloro-BODIPY. *J. Org. Chem.* **2015,** *80* (16), 8377-8383.

38. Zhao, N.; Xuan, S.; Byrd, B.; Fronczek, F. R.; Smith, K. M.; Vicente, M. G. H., Synthesis and regioselective functionalization of perhalogenated BODIPYs. *Org. Biomol. Chem.* **2016,** *14* (26), 6184-6188.

39. Xuan, S.; Zhao, N.; Ke, X.; Zhou, Z.; Fronczek, F. R.; Kadish, K. M.; Smith, K. M.; Vicente, M. G. H., Synthesis and Spectroscopic Investigation of a Series of Push–Pull Boron Dipyrromethenes (BODIPYs). *J. Org. Chem.* **2017,** *82* (5), 2545-2557.

40. Deniz, E.; Isbasar, G. C.; Bozdemir, Ö. A.; Yildirim, L. T.; Siemiarczuk, A.; Akkaya, E. U., Bidirectional Switching of Near IR Emitting Boradiazaindacene Fluorophores. *Org. Lett.* **2008,** *10* (16), 3401-3403.

41. Buyukcakir, O.; Bozdemir, O. A.; Kolemen, S.; Erbas, S.; Akkaya, E. U., Tetrastyryl-Bodipy Dyes: Convenient Synthesis and Characterization of Elusive Near IR Fluorophores. *Org. Lett.* **2009,** *11* (20), 4644-4647.

42. Rohand, T.; Qin, W.; Boens, N.; Dehaen, W., Palladium-Catalyzed Coupling Reactions for the Functionalization of BODIPY Dyes with Fluorescence Spanning the Visible Spectrum. *Eur. J. Org. Chem.* **2006,** *2006* (20), 4658-4663.

43. Rohand, T.; Baruah, M.; Qin, W.; Boens, N.; Dehaen, W., Functionalisation of fluorescent BODIPY dyes by nucleophilic substitution. *Chem. Commun.* **2006,** (3), 266-268.

44. Jiao, L.; Li, J.; Zhang, S.; Wei, C.; Hao, E.; Vicente, M. G. H., A selective fluorescent sensor for imaging Cu2+ in living cells. *New J. Chem.* **2009,** *33* (9), 1888-1893.

45. Yogo, T.; Urano, Y.; Ishitsuka, Y.; Maniwa, F.; Nagano, T., Highly Efficient and Photostable Photosensitizer Based on BODIPY Chromophore. *J. Am. Chem. Soc.* **2005,** *127* (35), 12162-12163.

46. Gibbs, J. H.; Robins, L. T.; Zhou, Z.; Bobadova-Parvanova, P.; Cottam, M.; McCandless, G. T.; Fronczek, F. R.; Vicente, M. G. H., Spectroscopic, computational modeling and cytotoxicity of a series of meso-phenyl and meso-thienyl-BODIPYs. *Bioorg. Med. Chem.* **2013,** *21* (18), 5770-5781.

47. Shah, M.; Thangaraj, K.; Soong, M.-L.; Wolford, L. T.; Boyer, J. H.; Politzer, I. R.; Pavlopoulos, T. G., Pyrromethene–BF2 complexes as laser dyes:1. *Heteroat. Chem.* **1990,** *1* (5), 389-399.

48. Pavlopoulos, T. G.; Boyer, J. H.; Sathyamoorthi, G., Laser action from a 2,6,8-position trisubstituted 1,3,5,7-tetramethylpyrromethene-BF2 complex: part 3. *Appl. Opt.* **1998,** *37* (33), 7797-7800.

49. Li, L.; Nguyen, B.; Burgess, K., Functionalization of the 4,4-difluoro-4-bora-3a,4a-diaza-s-indacene (BODIPY) core. *Bioorg. Med. Chem. Lett.* **2008,** *18* (10), 3112-3116.

50. Li, L.; Han, J.; Nguyen, B.; Burgess, K., Syntheses and Spectral Properties of Functionalized, Water-Soluble BODIPY Derivatives. *J. Org. Chem.* **2008,** *73* (5), 1963-1970.
51. Jiao, L.; Yu, C.; Li, J.; Wang, Z.; Wu, M.; Hao, E., β-Formyl-BODIPYs from the Vilsmeier−Haack Reaction. *J. Org. Chem.* **2009,** *74* (19), 7525-7528.

52. Pavlopoulos, T. G.; Boyer, J. H.; Shah, M.; Thangaraj, K.; Soong, M.-L., Laser action from 2,6,8-position trisubstituted 1,3,5,7-tetramethylpyrromethene-BF_2 complexes: part 1. *Appl. Opt.* **1990,** *29* (27), 3885-3886.

53. Ortiz, M. J.; Agarrabeitia, A. R.; Duran-Sampedro, G.; Bañuelos Prieto, J.; Lopez, T. A.; Massad, W. A.; Montejano, H. A.; García, N. A.; Lopez Arbeloa, I., Synthesis and functionalization of new polyhalogenated BODIPY dyes. Study of their photophysical properties and singlet oxygen generation. *Tetrahedron* **2012,** *68* (4), 1153-1162.

54. Zhai, J.; Pan, T.; Zhu, J.; Xu, Y.; Chen, J.; Xie, Y.; Qin, Y., Boronic Acid Functionalized Boron Dipyrromethene Fluorescent Probes: Preparation, Characterization, and Saccharides Sensing Applications. *Anal. Chem.* **2012,** *84* (23), 10214-10220.

55. Goeb, S.; Ziessel, R., Synthesis of novel tetrachromophoric cascade-type Bodipy dyes. *Tetrahedron Lett.* **2008,** *49* (16), 2569-2574.

56. Chen, J.; Mizumura, M.; Shinokubo, H.; Osuka, A., Functionalization of Boron Dipyrrin (BODIPY) Dyes through Iridium and Rhodium Catalysis: A Complementary Approach to α- and β-Substituted BODIPYs. *Chem. Eur. J.* **2009,** *15* (24), 5942-5949.

57. Ulrich, G.; Goze, C.; Guardigli, M.; Roda, A.; Ziessel, R., Pyrromethene Dialkynyl Borane Complexes for "Cascatelle" Energy Transfer and Protein Labeling. *Angew. Chem. Int. Ed.* **2005,** *44* (24), 3694-3698.

58. Niu, S. L.; Ulrich, G.; Ziessel, R.; Kiss, A.; Renard, P.-Y.; Romieu, A., Water-Soluble BODIPY Derivatives. *Org. Lett.* **2009,** *11* (10), 2049-2052.

59. Goze, C.; Ulrich, G.; Mallon, L. J.; Allen, B. D.; Harriman, A.; Ziessel, R., Synthesis and Photophysical Properties of Borondipyrromethene Dyes Bearing Aryl Substituents at the Boron Center. *J. Am. Chem. Soc.* **2006,** *128* (31), 10231-10239.

60. Goze, C.; Ulrich, G.; Ziessel, R., Unusual Fluorescent Monomeric and Dimeric Dialkynyl Dipyrromethene−Borane Complexes. *Org. Lett.* **2006,** *8* (20), 4445-4448.

61. Goze, C.; Ulrich, G.; Ziessel, R., Tetrahedral Boron Chemistry for the Preparation of Highly Efficient "Cascatelle" Devices. *J. Org. Chem.* **2007,** *72* (2), 313-322.

62. Goeb, S.; Ziessel, R., Convenient Synthesis of Green Diisoindolodithienylpyrromethene-Dialkynyl Borane Dyes. *Org. Lett.* **2007,** *9* (5), 737-740.

63. Bonardi, L.; Ulrich, G.; Ziessel, R., Tailoring the Properties of Boron−Dipyrromethene Dyes with Acetylenic Functions at the 2,6,8 and 4-B Substitution Positions. *Org. Lett.* **2008,** *10* (11), 2183-2186.

64. Ulrich, G.; Goeb, S.; De Nicola, A.; Retailleau, P.; Ziessel, R., Chemistry at Boron: Synthesis and Properties of Red to Near-IR Fluorescent Dyes Based on Boron-Substituted Diisoindolomethene Frameworks. *J. Org. Chem.* **2011,** *76* (11), 4489-4505.

65. More, A. B.; Mula, S.; Thakare, S.; Sekar, N.; Ray, A. K.; Chattopadhyay, S., Masking and Demasking Strategies for the BF2–BODIPYs as a Tool for BODIPY Fluorophores. *J. Org. Chem.* **2014,** *79* (22), 10981-10987.

66. Kim, H.; Burghart, A.; B. Welch, M.; Reibenspies, J.; Burgess, K., Synthesis and spectroscopic properties of a new 4-bora-3a,4a-diaza-s-indacene (BODIPY®) dye. *Chem. Commun.* **1999,** (18), 1889-1890.

67. Nguyen, A. L.; Bobadova-Parvanova, P.; Hopfinger, M.; Fronczek, F. R.; Smith, K. M.; Vicente, M. G. H., Synthesis and Reactivity of 4,4-Dialkoxy-BODIPYs: An Experimental and Computational Study. *Inorg. Chem.* **2015,** *54* (7), 3228-3236.

68. Courtis, A. M.; Santos, S. A.; Guan, Y.; Hendricks, J. A.; Ghosh, B.; Szantai-Kis, D. M.; Reis, S. A.; Shah, J. V.; Mazitschek, R., Monoalkoxy BODIPYs—A Fluorophore Class for Bioimaging. *Bioconjugate Chem.* **2014,** *25* (6), 1043-1051.

69. Lavis, L. D.; Raines, R. T., Bright Ideas for Chemical Biology. *ACS Chem. Biol.* **2008,** *3* (3), 142-155.

70. Frangioni, J. V., In vivo near-infrared fluorescence imaging. *Curr. Opin. Chem. Biol.* **2003,** *7* (5), 626-634.

71. Ziessel, R.; Ulrich, G.; Harriman, A.; Alamiry, M. A. H.; Stewart, B.; Retailleau, P., Solid-State Gas Sensors Developed from Functional Difluoroboradiazaindacene Dyes. *Chem. Eur. J.* **2009,** *15* (6), 1359-1369.

72. Baruah, M.; Qin, W.; Vallée, R. A. L.; Beljonne, D.; Rohand, T.; Dehaen, W.; Boens, N., A Highly Potassium-Selective Ratiometric Fluorescent Indicator Based on BODIPY Azacrown Ether Excitable with Visible Light. *Org. Lett.* **2005,** *7* (20), 4377-4380.

73. Dodani, S. C.; He, Q.; Chang, C. J., A Turn-On Fluorescent Sensor for Detecting Nickel in Living Cells. *J. Am. Chem. Soc.* **2009,** *131* (50), 18020-18021.

74. Peng, X.; Du, J.; Fan, J.; Wang, J.; Wu, Y.; Zhao, J.; Sun, S.; Xu, T., A Selective Fluorescent Sensor for Imaging Cd2+ in Living Cells. *J. Am. Chem. Soc.* **2007,** *129* (6), 1500-1501.

75. Wu, Y.; Peng, X.; Guo, B.; Fan, J.; Zhang, Z.; Wang, J.; Cui, A.; Gao, Y., Boron dipyrromethene fluorophore based fluorescence sensor for the selective imaging of Zn(ii) in living cells. *Org. Biomol. Chem.* **2005,** *3* (8), 1387-1392.

76. Coskun, A.; Yilmaz, M. D.; Akkaya, E. U., Bis(2-pyridyl)-Substituted Boratriazaindacene as an NIR-Emitting Chemosensor for Hg(II). *Org. Lett.* **2007,** *9* (4), 607-609.

77. https://www.thermofisher.com/order/catalog/product/D7540.

78. Chen, J.; Keltner, L.; Christophersen, J.; Zheng, F.; Krouse, M.; Singhal, A.; Wang, S., New technology for deep light distribution in tissue for phototherapy. *Cancer Journal* **2002,** *8* (2), 154-163.

79. Mellish, K. J.; Cox, R. D.; Vernon, D. I.; Griffiths, J.; Brown, S. B., In Vitro Photodynamic Activity of a Series of Methylene Blue Analogues. *Photochem. Photobiol.* **2002,** *75* (4), 392-397.

80. Rio, Y.; Salome Rodriguez-Morgade, M.; Torres, T., Modulating the electronic properties of porphyrinoids: a voyage from the violet to the infrared regions of the electromagnetic spectrum. *Org. Biomol. Chem.* **2008,** *6* (11), 1877-1894.

81. Carpenter, B.; Situ, X.; Scholle, F.; Bartelmess, J.; Weare, W.; Ghiladi, R., Antiviral, Antifungal and Antibacterial Activities of a BODIPY-Based Photosensitizer. *Molecules* **2015,** *20* (6), 10604.

82. Gibbs, J. H.; Zhou, Z.; Kessel, D.; Fronczek, F. R.; Pakhomova, S.; Vicente, M. G. H., Synthesis, spectroscopic, and in vitro investigations of 2,6-diiodo-BODIPYs with PDT and bioimaging applications. *J. Photochem. Photobiol. B* **2015,** *145*, 35-47.

CHAPTER II: SYNTHESIS OF IODINATED BODIPYS AND INVESTIGATIONS OF THEIR PD-CATALYZED CROSS COUPLING REACTIONS

2.1 Introduction

2.1.1 Cross-Coupling Reactions

Organometallic catalyst cross-coupling reactions were largely developed in last two decades, mainly providing a method to generate carbon-carbon and aromatic carbon-nitrogen bonds, which brought opportunities of building more organic synthesis than those of traditional chemistry, as shown in Scheme 2.1.[1-4] During a general catalytic cycle for the cross-coupling reactions, three major processes are involved: oxidative addition, transmetalation and reductive elimination. The oxidative addition is considered as the rate-determining step, and the relative reactivity increases in the order of Cl<<Br<OTf<I.[5]

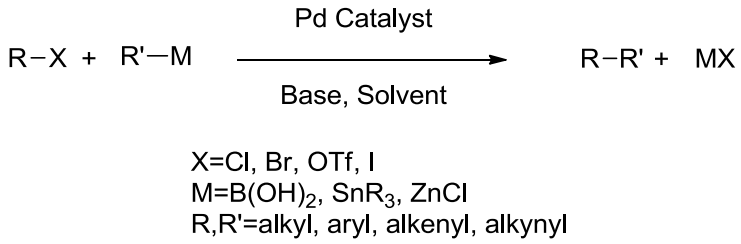

Scheme 2.1: Cross coupling reactions

There are various methods reported to functionalize the 3,5-positions of BODIPYs, including cross-coupling reactions, aromatic substitutions, Knoevenagel condensations, radical arylations and C-H arylations.[6] For the functionalizations of the 2,6-positions, cross-coupling reactions with 2,6-dihalogenated BODIPYs were also reported. [7]Among these, the Pd(0)-catalyzed cross-coupling, including mainly Suzuki, Stille, Sonogashira and Heck coupling reactions, are particularly convenient due to the variety of commercially available boronic acids, tin reagents, alkene and alkynes.

2.1.2 Halogenated BODIPYs

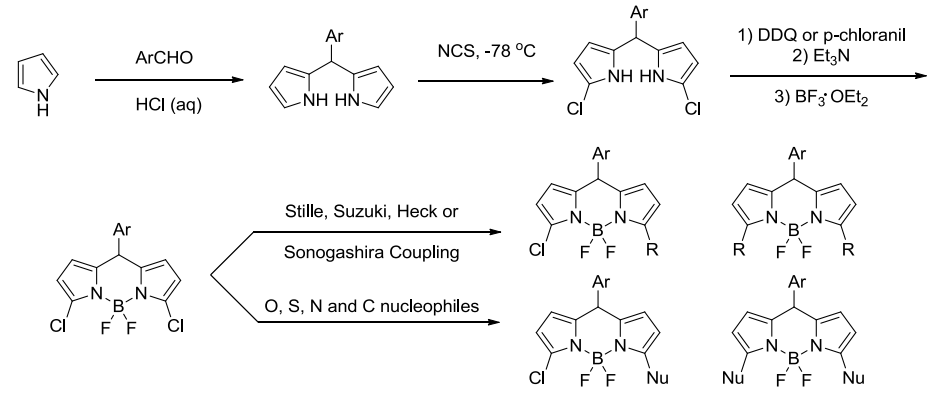

Scheme 2.2: Syntheses of 3,5-dichloro-BODIPYs and their post-functionalizations[8-9]

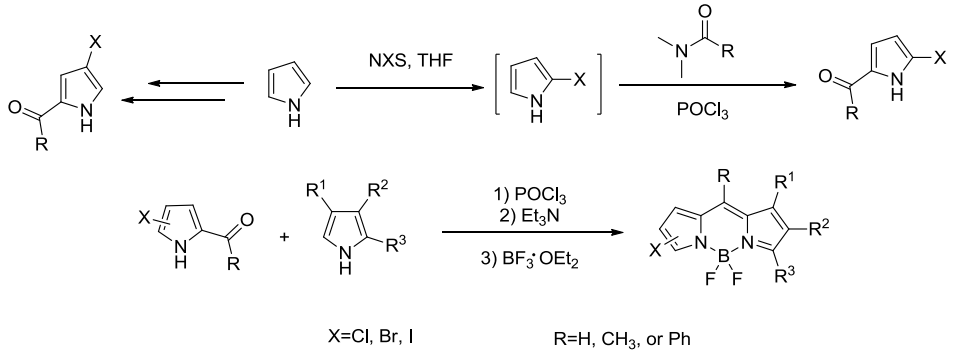

Scheme 2.3: Syntheses of halogenated pyrroles and unsymmetric BODIPYs[10]

The preparation of a variety of halogenated BODIPYs has been reported in the last ten years. Dehaen *et al* contributed several methods to produce chlorinated BODIPYs. They first reported the synthesis of 3,5-dichloro-BODIPYs, by NCS chlorination at -78°C on unsubstituted dipyrromethanes, followed by DDQ or p-chloranil oxidation and typical complexation conditions with a tertiary amine (mainly triethylamine) and boron trifluoride etherate, as shown in Scheme 2.2.[8-9, 11-12] Another main contribution to the synthesis of halogenated BODIPYs by Dehean *et al* was to start the routes from halogenated pyrroles with 2-acyl groups. The acylated pyrroles were then condensed with another α-free pyrrole in the presence of $POCl_3$ and finally complexed to give unsymmetrical halogenated BODIPYs, as shown in Scheme 2.3.[10, 13]

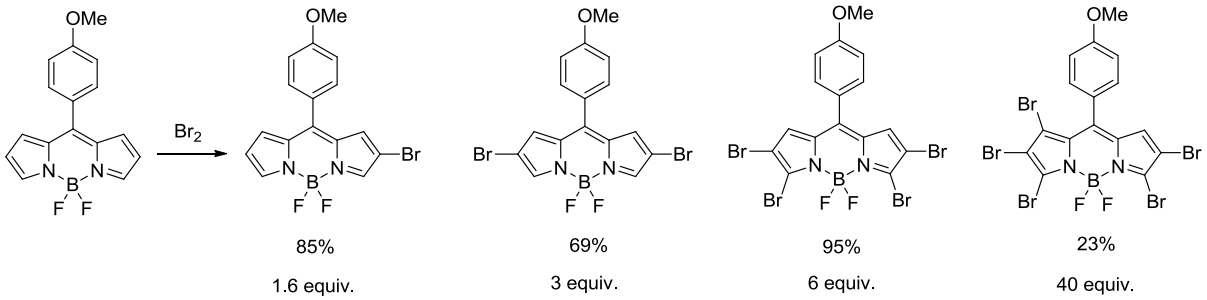

Scheme 2.4: A stepwise bromination on an unsubstituted BODIPY[14]

In 2010, Hao & Jiao and co-workers published an elegant stepwise bromination study, with results showing that mono-, di-, tetra- and pentabromo-BODIPYs can be prepared by reacting a *meso*-aryl-BODIPY with 1.6, 3.0, 6.0 and 40 equivalents of bromine.[14] As shown in Scheme 2.4, the bromination was regioselective, first at the 2,6-positions, followed by the 3,5-positions and finally the 1,7-positions, which was also demonstrated by X-ray analysis results.

Ortiz group investigated BODIPY's halogenation with two different conditions, including ICl and HIO_3/I_2. Especially with different equivalents of iodic acid and iodine, the degree of iodination on the BODIPY core was controlled, which enabled the synthesis of mono-, di- and polyiodinated BODIPYs.[15]

Our group also contributed to this topic with several publications on globally halogenation and 3,5-diiodinations of BODIPYs. Starting from an unsubstituted *meso*-chloro-BODIPY,[16] our group found that the chlorination was controlled to stepwisely occur at the 2-, 6-, 3- and 5-positions with 1.3, 2.3, 5.0 and 10 equivalents of trichloroisocyanuric acid in acetic acid,[17] and Br_2 was able to further substitute the 1,7-positions in DCM, to give perhalogenated BODIPYs, as shown in Scheme 2.5.[18] We also reported the synthesis and further reactions of 3,5-diiodo-BODIPYs. The route began with a dipyrromethane bearing two α-carboxybenzyl which were hydrolyzed, iodinated, followed by oxidation to dippyromethene and boron compelcation to give a 3,5-diiodo-BODIPY, as shown in Scheme 2.6.[19-20]

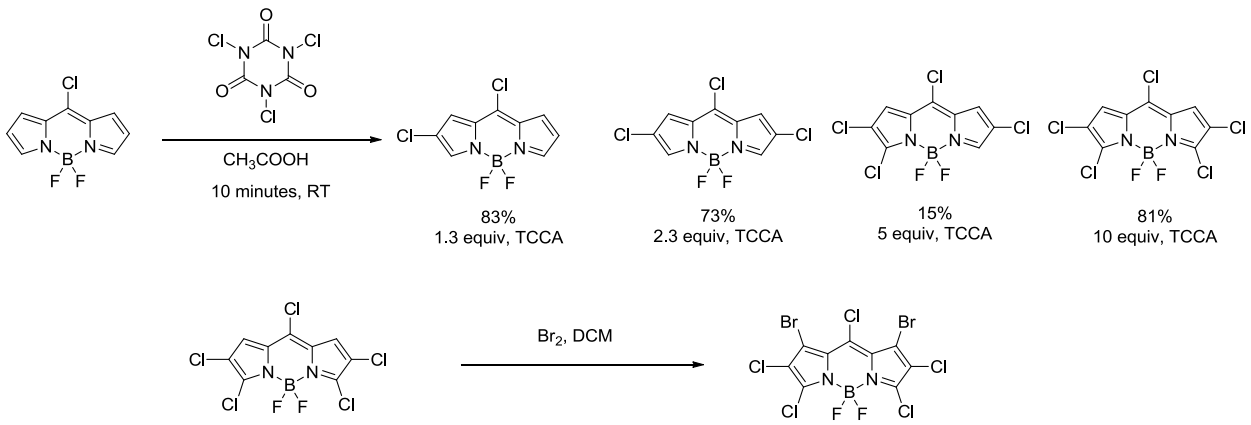

Scheme 2.5: Syntheses of pentachloro-BODIPY and its further bromination reactions

My research involved the synthesis of two kinds of iodinated BODIPYs, based on their stability, further functionalizing diversity, and the commercial availability of starting materials. All BODIPYs were designed to contain meso-aryl groups to enhance their stabilities. In the 3,5-diiodo-BODIPY cases, the β, β'-bicyclic structure not only provides further aromatization reaction possibilities, but also facilitate the starting pyrrole's preparation.

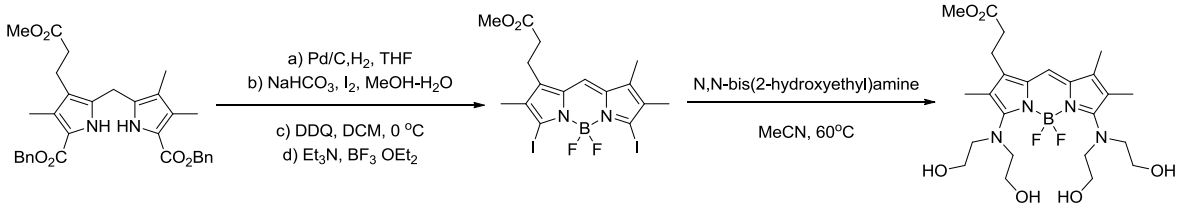

Scheme 2.6: Syntheses of 3,5-diiodo-BODIPY and its further functionalizations

2.2 Results and Discussion

2.2.1 Syntheses

2.2.1.1 Syntheses of 3,5-DiiodoBODIPYs and 2,3,5,6-TetraiodoBODIPYs

3,5-Diiodo-BODIPY **6a** and **6b**, with two bicyclo-rings that could potentially be aromatized, was prepared as shown in Scheme 2.7.[21] Tetrahydroisoindole **2** was prepared as previous literature described[22] from 1-nitro-1-cyclohexene and ethyl isocyanoacetate, and it was treated with arylaldehyde under acidic condition in the presence of nBu_4NI, to give

dipyrromethanes **3a** and **3b** in 85% yield. The ethyl esters were hydrolyzed under classical basic conditions, followed by acidic work-up, and the acid **4** precipitated out. This acid was then iodinated and oxidized in one step by I_2/MeOH/H_2O conditions to afford 3, 5-diiodo-dipyrromethene **5a** and **5b**. The oxidation from dipyrromethane to dipyrromethene was not performed by I_2 in previous BODIPY iodination conditions, thus the *meso*-phenyl group is key role to help fulfill this step. Dipyrromethenes **5a** and **5b** were complexed with $BF_3 \cdot Et_2O$ *in situ* under basic conditions to afford BODIPY **6a** and **6b**, in 40% overall yields for 4 steps. BODIPY **6b** bearing methoxy groups on the *meso*-phenyl could potentially show enhanced water solubility. The structure of BODIPY **6a** was confirmed by its X-ray structure, as shown in Figure 2.1.

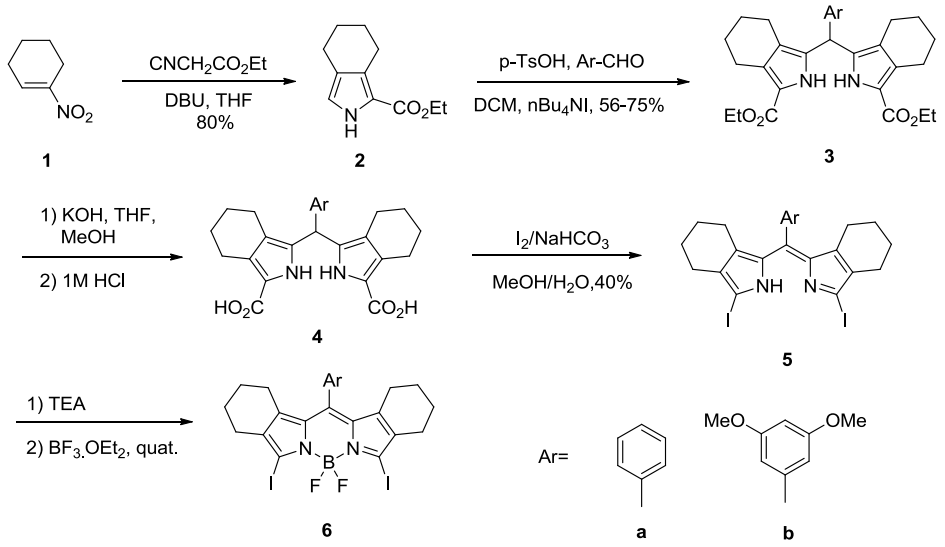

Scheme 2.7: Preparation of 3,5-diiodo-BODIPYs **6a**,**b** from 1-nitro-1-cyclohexene

The average length of C-I bonds is 2.06 Å, indicating these long bonds favor palladium (0) insertion. The plane of the *meso*-phenyl ring is nearly perpendicular to the central plane, forming a dihedral angle of 86.9°.

2,3,5,6-Tetraiodo-BODIPY was prepared from a multi-iodination reaction of *meso*-aryl BODIPYs, as shown in Scheme 2.8. Three equivalents of pyrrole were treated with one

equivalent of arylaldehyde in HCl solution, and the dipyrromethane was precipitated. The dipyrromethane was oxidized with p-chloranil and further complexed with boron trifluoride etherate, producing BODIPYs **8a**,**b** in 31-36% overall yields from pyrrole. The 3,5-dimethoxyphenyl group was installed at the *meso*-position due to its reported enhancement of the phototoxicity and solubility.[23] However, the attempts to iodinate unsubstituted BODIPY **8b** failed due to the reactivity of the *meso*-phenyl group under those conditions, which produced a mixture of iodinated BODIPYs that were difficult to isolate in good yields. *Meso*-tolyl BODIPY **8a** was iodinated at the 2,3,5,6-positions by reacting **8a** with 4.5 equivalents of iodic acid and 4 equivalents of iodine, in refluxing anhydrous ethanol, [15] and the tetraiodo-BODIPY **9a** was obtained in 76% yield.

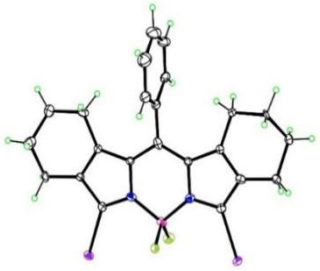

Figure 2.1: X-ray crystal structure of β,β'-bicyclo-3,5-diiodo-BODIPY **6a**

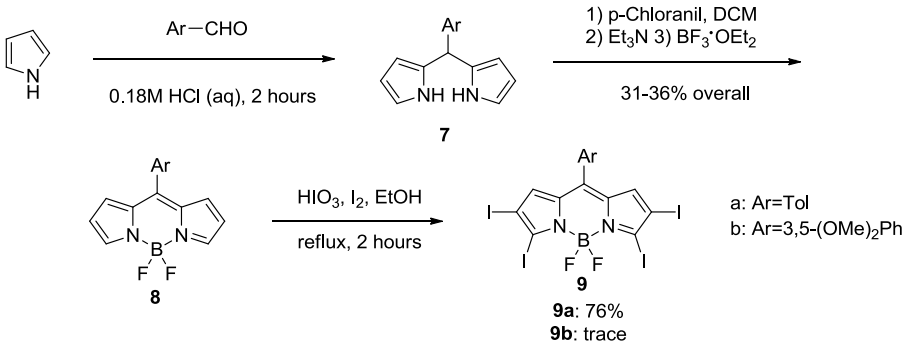

Scheme 2.8: Preparation of *meso*-aryl BODIPYs **8a**,**b** and their tetra-iodination

2.2.1.2 Pd-Catalyzed Stille Coupling on Iodinated BODIPYs 6a,b and 9a

Pd-Catalyzed Stille cross coupling reactions were investigated first, due to previous reports on *meso*-chloro-BODIPY's showing that this reaction might proceed without a base,[16, 24-25] although Dehean *et al* used base in their investigations of 3,5-dichloro-BODIPYs.[9] We assumed that the *meso*-chloro-BODIPY's C-Cl bonds are less steric hindered, and PdL_n units are easier to insert into the longer C-I bonds. As C-I bonds are longer than the C-Cl bonds, no base was present in the attempts of the Stille coupling reactions on 3,5-diiodo-BODIPYs. BODIPY **6a** was treated with ten equivalents of 2-(tributylstannyl)-thiophene, and the reaction was heated in toluene at 110°C in the presence of a catalytic amount (5 mol%) of tetrakis(triphenylphosphine)-palladium(0). The reaction was monitored by TLC, which indicated that the reaction was complete after 2 hours, producing 3,5-dithienyl-BODIPY **10a** in 88% yield, as shown in Scheme 2.9. We then decreased the temperature to 100°C, 90°C and 80°C, and at 100°C and 90°C BODIPY **10a** was obtained in similar yields of 88% and 89%, but at 80 °C no product was even obtained after 24 hours, as monitored by TLC and UV-Vis spectroscopy.

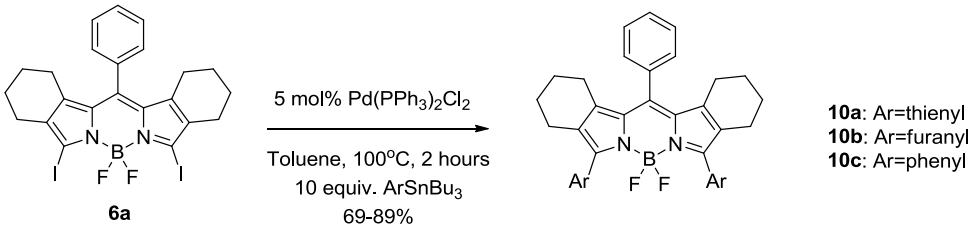

Scheme 2.9: Symmetric Stille cross-coupling reactions

Bis(triphenylphosphine) palladium(II) dichloride, which generates Pd(0) in situ, is cheaper than tetrakis(triphenylphosphine)palladium(0), and can be stored longer on bench-top at room temperature, rather than a 0 °C for $Pd(PPh_3)_4$. The Stille coupling reaction of **6a** was then performed with 5 mol% of $Pd(PPh_3)_2Cl_2$, and the yield obtained for **10a** is the same. The optimized conditions (5 mol% $Pd(PPh_3)_2Cl_2$, toluene, 90 °C for 2 hours) was applied to two other

commercially available tin reagents, 2-(tributylstannyl)-furan and tributylphenylstannane, and BODIPYs **10b** and **10c** were obtained 80% and 69% yield, as shown in Scheme 2.9.

Unsymmetrical Stille coupling reactions were studied using the same catalyst, and initially mono-coupling product was attempted to be prepared by controlling the equivalents of tin reagents. A one-pot reaction condition was attempted by reacting one equivalent of 3,5-diiodo-BODIPY **6a** with one equivalent of 2-(tributylstannyl)-thiophene, and when the mono-coupling product was observed on TLC, another two equivalents of 2-(tributylstannyl)-furan were added without any work-up or purification of the first step, and BODIPY **11** was obtained in only trace amount, as shown in Scheme 2.10. This low yield is not only due to the difficulty of purification, but also mainly because the reaction between BODIPY **11** and only one equivalent of the tin reagent was slow, while prolonged heat would lead to decomposition and side reactions, such as reduction generating 3,5-unsubstituted BODIPYs.

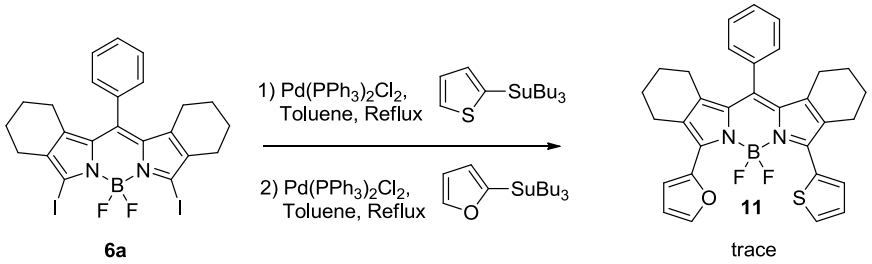

Scheme 2.10: "One-pot" Stille coupling reaction without isolation of the mono-iodo intermediate

Since the "one-pot" conditions did not give the unsymmetric BODIPY in good yield, the route was designed as a stepwise way. BODIPY **6a** was treated with 2,3,4 and 5 equivalents of 2-(tributylstannyl)-furan in 100^{o}C toluene, and the reactions were monitored by TLC. This comparative study showed that three equivalents of tin reagent gave the mono-coupling product as a major product, after 25 minutes reaction time. Another Suzuki cross-coupling reaction was then performed at the other iodinated position, by treating BODIPY **12** with 2 equivalents of 5-

methyl-2-thienylboronic acid in refluxing toluene, and BODIPY **13** was obtained in 38% overall yield, with a catalytic amount of $Pd(PPh_3)_2Cl_2$, as shown in Scheme 2.11.

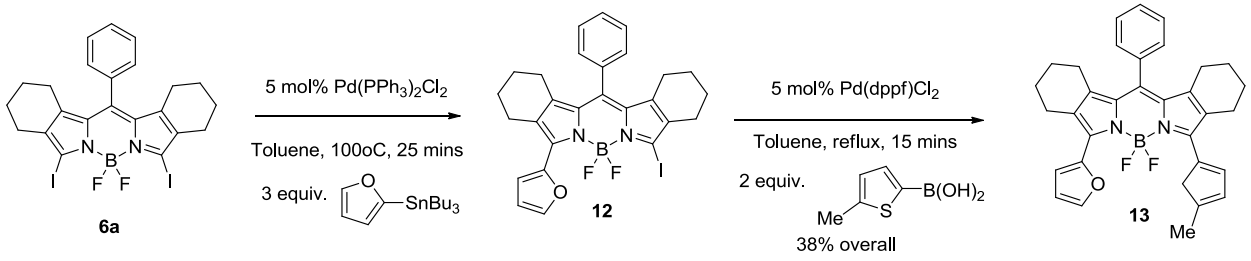

Scheme 2.11: Mono- Stille coupling followed with a Suzuki cross-coupling on BODIPY **6a**

The Stille cross-coupling conditions were also utilized in tetraiodo-BODIPY's functionalization. Using toluene as the solvent, BODIPY **9a** reacted with ten equivalents of phenylstannane, in the presence of 10 mol% $Pd(PPh_3)_2Cl_2$, and BODIPY **14** was isolated in 53% yield, as shown in Scheme 2.12.

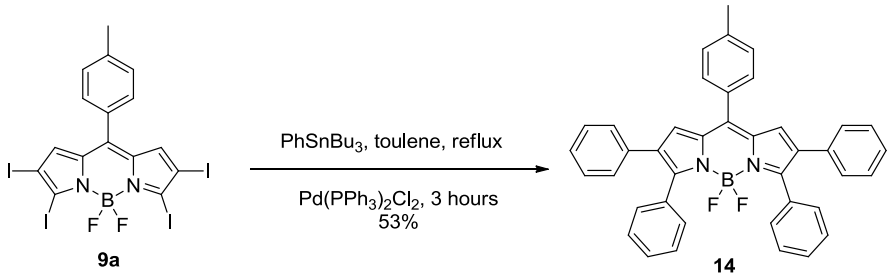

Scheme 2.12: Stille cross-coupling reactions on tetraiodo-BODIPY **9a**

2.2.1.3 Pd-Catalyzed Suzuki Coupling on Iodinated BODIPYs

Halogenated BODIPY's Suzuki cross-coupling have been studied often, due to a variety of commercially available boronic acids, relatively low toxicity and the ease of removal after the reaction. Three palladium catalysts, $Pd(PPh_3)_4$, $Pd(OAc)_2/PPh_3$ and $Pd(PPh_3)_2Cl_2$ were employed in the attempted coupling reaction between BODIPY **6a** and the phenyl boronic acid, using toluene as the solvent and K_2CO_3 as the base. After refluxing in toluene for 8 hours, the 3,5-diphenyl-BODIPY **10c** was obtained in 45%, 35% and 52% yields, respectively. These moderate

yields and prolonged reaction time led us to investigate a bidentate ligand complexed catalyst, [1,1′-bis(diphenylphosphino)ferrocene] dichloropalladium(II) ($Pd(dppf)Cl_2$), since this complex is reported to be relatively more reactive in the oxidative addition step, with a fairly cheap price. BODIPY **10c** was produced from **6a** in 73% yield, using $Pd(dppf)Cl_2$ as the catalyst. The reaction took 2 hours only, in refluxing toluene and in the presence of K_2CO_3. The reaction conditions were further optimized by employing a co-solvent system, toluene and THF in 1:1 ratio,[26] and after the optimization BODIPY **10c** was obtained in 85% yield. The developed conditions were then used for the coupling reactions of all other boronic acids, such as 2-thienylboronic acid, 2-furanylboronic acid, 4-nitrophenylboronic acid and the products from these reactions, BODIPYs **10a**, **10b** and **15** were isolated in high yields, as shown in Scheme 2.13.

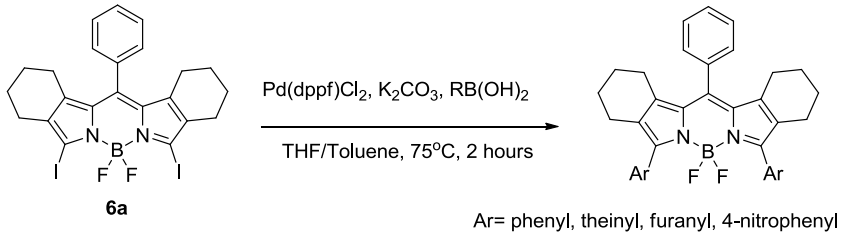

Scheme 2.13: Symmetric Suzuki cross-coupling reactions on 3,5-diiodo-BODIPY **6a**

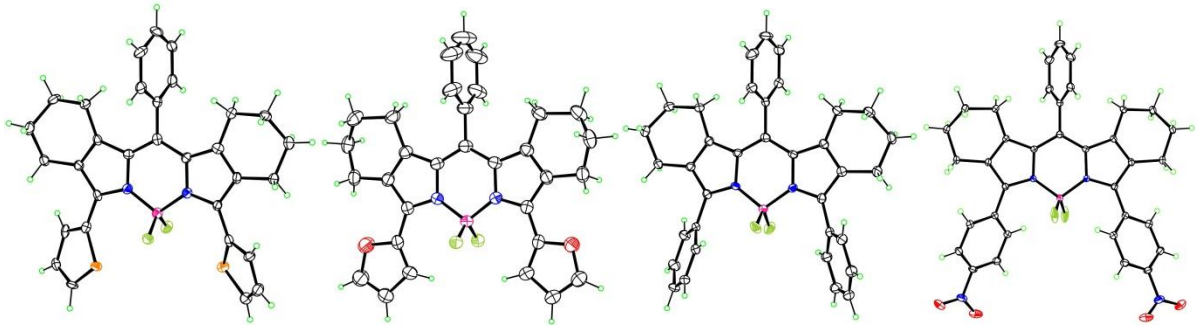

10a **10b** **10c** **15**

Figure 2.2: Suitable crystal structure of BODIPY **10a**, **10b**, **10c** and **15**.

Suitable crystals for X-ray analysis were obtained for BODIPYs **10a**, **10b**, **10c** and **15**, and they are shown in Figure 2.2. BODIPY **10a**'s central ring and the *meso*-phenyl gave a 77.3^{o} dihedral angle, and a 40.3^{o} dihedral angel between the thienyl group and the central ring. The dihedral angle between BODIPY **10b**'s furanyl ring and central C_3N_2B is surprisingly low as 1.2^{o}, and the *meso*-phenyl is almost perpendicular to the central ring, with an 86.1^{o} dihedral angle. In BODIPY **10c**, the central C_3N_2B ring is nearly planar, with mean deviation 0.014 Å. Its *meso*-phenyl ring forms a dihedral angle of 79.8° with the central ring, and its 3,5-phenyl rings form a dihedral angle of 56.2° with the central ring. BODIPY **15**'s central ring is slightly twisted, with the carbon atoms lying 0.076 Å off the plane, and the N atoms 0.072 Å. The *meso*-phenyl group forms a dihedral angle of 60.4° with the central C_3N_2B plane, and the 3,5-diphenyl groups 47.2°.

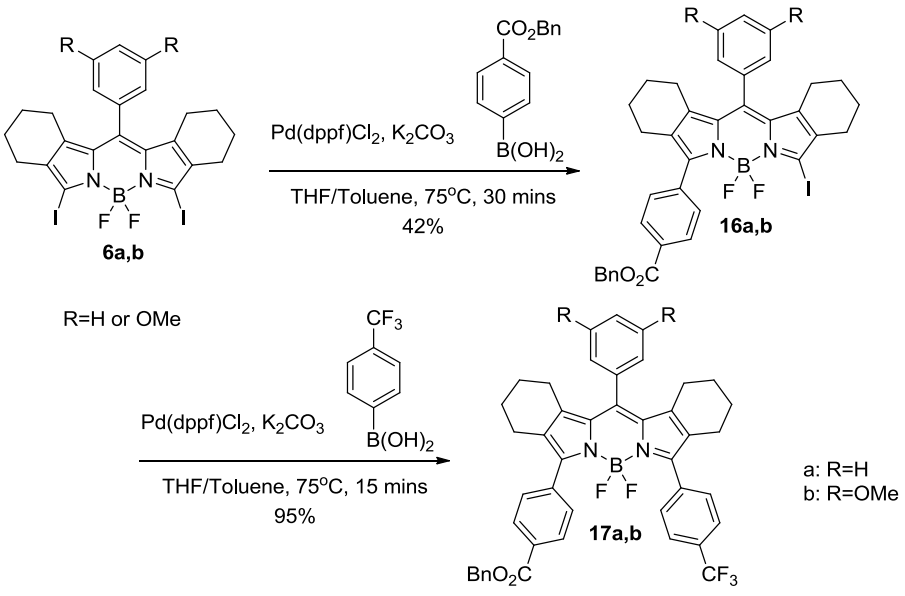

Scheme 2.14: Unsymmetric Suzuki cross-coupling reactions on BODIPYs **6a** and **6b**

BODIPY **6a** was also subjected to unsymmetric functionalization reactions, using two different boronic acids, as shown in Scheme 2.14. Following the experience from Stille unsymmetric coupling, BODIPY **6a** was treated with 2,3,4 and 5 equivalents of (4-

(benzyloxycarbonyl)phenyl) boronic acid, and 3 equivalents of boronic acid produced mono-coupling BODIPY **16a** after 30 minutes reaction time. After a quick work up and purification with a flash column, BODIPY **16a** was immediately subjected to a second Suzuki cross-coupling reaction in the presence of five equivalents of 4-(trifluoromethyl)phenylboronic acid for 15 minutes, affording BODIPY **17a** in 95% yield.

Due to the availability of a variety of boronic acids, BODIPY **9a** was also functionalized with phenyl boronic acid, 3,5-dimethoxyphenyl boronic acid and 3,4,5-trimethoxyphenyl boronic acid, in the presence of 10 mol% $Pd(dppf)Cl_2$, and 2,3,5,6-tetraaryl-BODIPYs **14**, **18** and **19** were produced in 45%, 48% and 48% yields, as shown in Scheme 2.15.

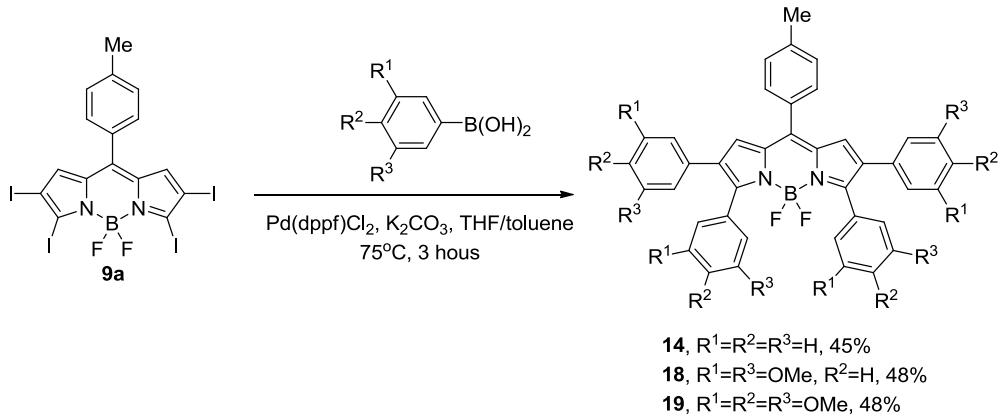

Scheme 2.15: Suzuki cross-coupling reactions on tetraiodo-BODIPY **9a**

2.2.1.4 Pd-Catalyzed Heck Coupling reactions on Iodinated BODIPYs

Reported typical Heck cross-coupling reactions require relatively high temperature and long reaction time, and some BODIPYs decompose or polymerize under such conditions, thus Heck cross-coupling reactions on BODIPYs are not investigated as often as Stille and Suzuki cross-coupling reactions. However, the extension of π-systems of BODIPYs is important, due to arylstyryl substitution at 3,5-positions red-shift BODIPY's absorption and emission spectra by up to 250 nm,[27-28] and they can also increase fluorescence quantum yields when they are at the

2,6-positions.[29] Knoevenagel condensation reactions are widely reported to functionalize the 3,5[27-28] and *meso*[30] positions with arylstyryl units due to the ease of preparation of methylated BODIPYs and the readily availability of aryl aldehydes. One example is shown in Scheme 2.16. However the low yields and prolonged reaction times limit the synthesis of BODIPYs with arylstryl groups. Another drawback of the condensation reaction is that Knoevenagel reactions are not accessible for 2,6-methyl groups, probably due to their relatively low acidity. The Heck reaction is considered a candidate to replace classical condensation reactions, and we are expecting to develop Heck cross-coupling conditions that require lower temperature, shorter reaction time and fewer reagents to avoid further reactions on styrylated BODIPYs.

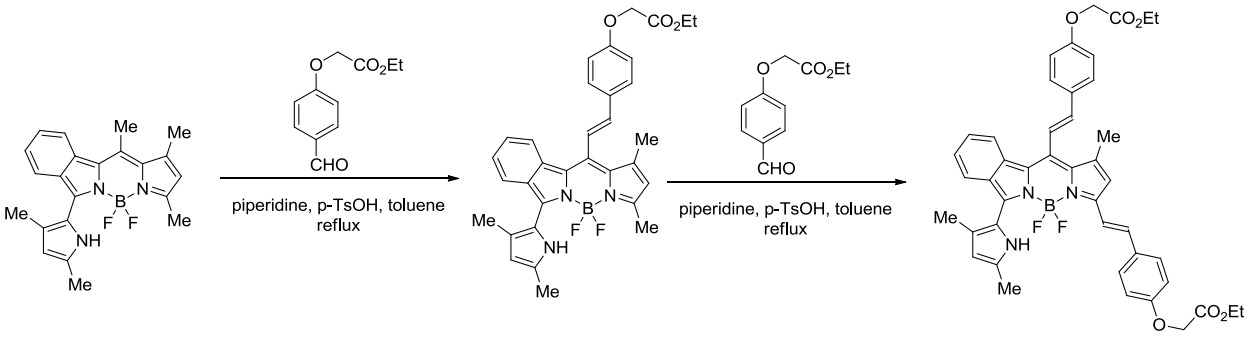

Scheme 2.16: A typical Knoevenagel reaction condition[30]

Other than halide compounds and olefins, a typical Heck reaction condition also requires reagents including a base, a Pd catalyst and high boiling point solvents. We chose anhydrous DMF as the first solvent to try since it was mostly reported in previous literature[9] (boiling point: 153 ^{o}C), and triethylamine was employed as the base due to its high solubility. Pd(dppf)Cl_2 was attempted as the first catalyst due to its efficient catalytic performance in Suzuki and Stille cross-coupling reactions. BODIPY **6a** was treated with 10 equivalents of 4-vinyl-anisole, and 3 hours later TLC indicated a consumption of the starting material and a new green fluorescent was seen. However, after a quick work up and column chromatography, no desired product was obatined.

This failure was mainly because the target BODIPY's solubility is very low in most organic solvents. BODIPY **6** was then employed, since the methoxyl groups on the *meso*-phenyl unit enhance solubility largely, and BODIPY **20** was obtained in 55% yield, using the same conditions. We then perform the same reaction condition in refluxing toluene (110^{o}C) for three hours to lower down the reaction temperature, and BODIPY **20** was isolated in a higher yield, 64%, as shown in Scheme 2.17. Other attempted optimizations, such as lowering the temperature to 90^{o}C or replace triethylamine with potassium carbonate, did not produce BODIPY **20** at all. BODIPY **6** was also treated with 10 equivalents of 4-vinyl-anisole, and BODIPY **21** was obtained after 3 hours, in 60% yield. The Heck reaction's yields from **6b** clearly indicated the *meso*-(3,5-dimethoxy)-phenyl groups increased solubility of the 3,5-styrylated BODIPYs.

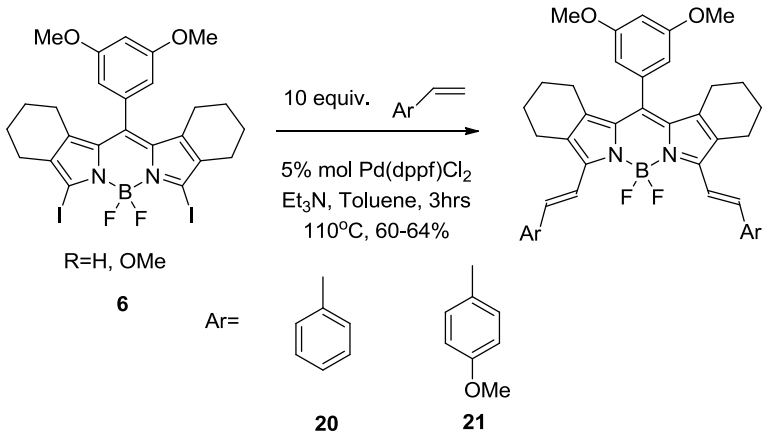

Scheme 2.17: Symmetric Heck cross-coupling reactions on BODIPY **6b**

The relatively longer Heck reaction time shows it might be easier to perform mono-Heck cross-coupling reactions with lower equivalents of olefins. BODIPY **6** was subjected to unsymmetric functionalization, first a Heck cross-coupling reaction, followed by a Suzuki coupling reaction, as shown in Scheme 2.18. Following the experience from Stille unsymmetric coupling, BODIPY **6** was treated with 4, 5 and 6 equivalents of 4-vinyl-anisole, and 6 equivalents of the olefin produced mono-coupling BODIPY **22** after 2 hour reaction time. After

quick work up and purification with a flash column, BODIPY **22** was subjected to a Suzuki cross-coupling reaction in the presence of five equivalents of 2-furanyl boronic acid for 15 minutes, affording BODIPY **23** in 24% overall yield from **6a**.

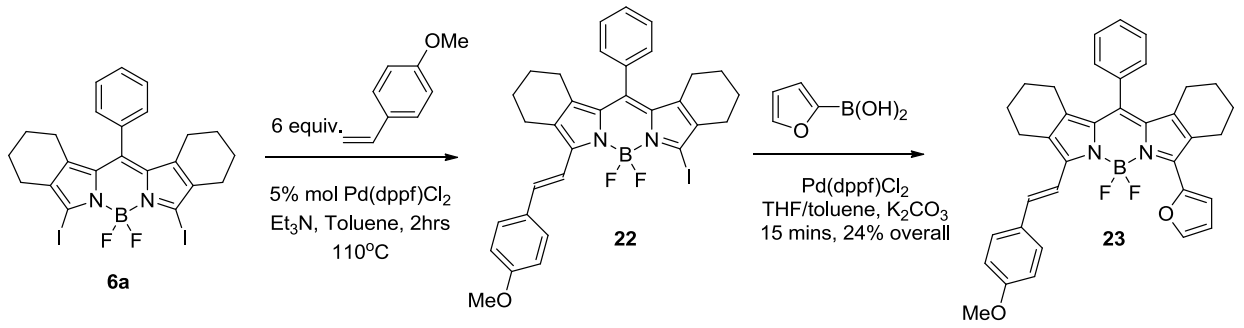

Scheme 2.18: Mono- Heck coupling on BODIPY **6a** followed by a Suzuki coupling reaction

2.2.2 Structural Characterization

All BODIPYs were characterized by ^{1}H-, ^{13}C- and ^{11}B-NMR, HRMS, UV-Vis and fluorescence. All ^{11}B-NMR show triplets for the BF_2 units, demonstrating no cross-coupling reactions affected the BF_2 units.

In proton NMR of 3,5-diiodo-BODIPYs **6a** and **6b** and their derivatives, in addition to signals from aromatic protons and methoxy groups, the bicyclic units show CH_2 peaks between 2.8 to 1.3 ppm. Symmetric BODIPYs generally show four signals of four protons each due to the symmetry of the BODIPY, while unsymmetric BODIPYs produced two triplet signals in the 2.8 ppm to 2.4 ppm region, indicating those two CH_2 units are in different environment, as shown in Figure 2.3 and 2.4. The carbon NMRs also agree with this observation, because the sp^3-C region shows four signals when the BODIPY is symmetric and eight signals when the BODIPY is unsymmetric with two different units at the 3,5-positions, as shown in Figures 2.5 and 2.6.

The NMR spectra of tetraiodo-BODIPY **9a** and its derivatives show relatively high symmetry. Through iodination reactions, the 1,7-protons remained around 7.0 ppm, and the protons at the 2,3,5,6-positions disappeared. After the installation of four aryl groups, a number

of aromatic signals overlap with each other, and the signals from the methoxy groups were clearly isolated, as shown in Figure 2.7 shows.

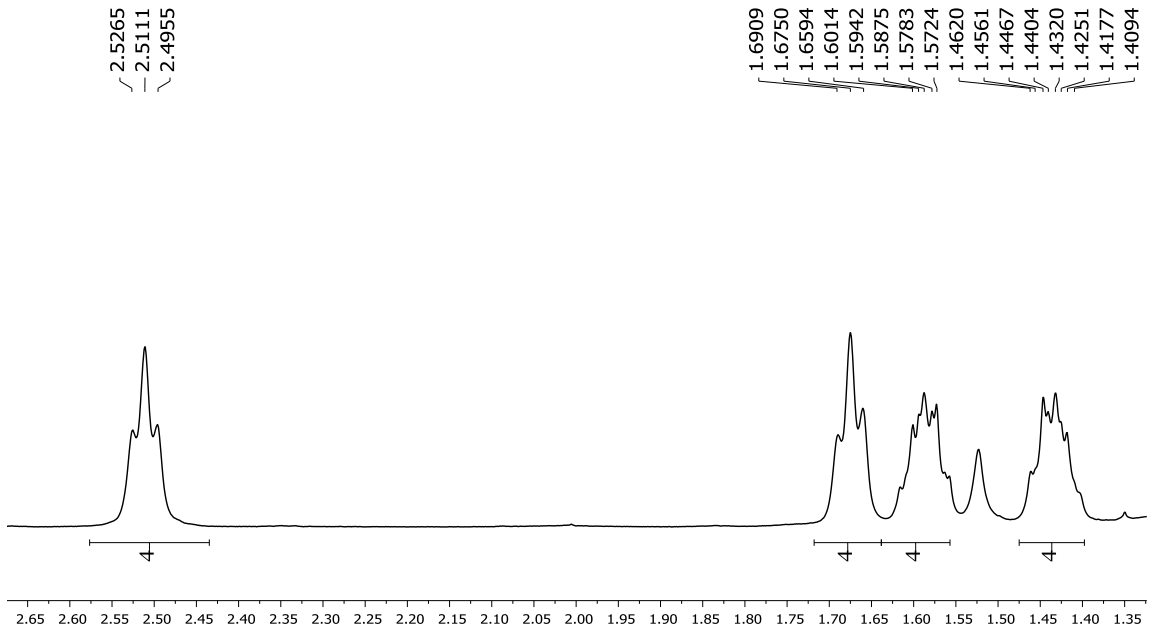

Figure 2.3: The 2.7-1.3 ppm region from the ^{1}H-NMR of BODIPY **10a**

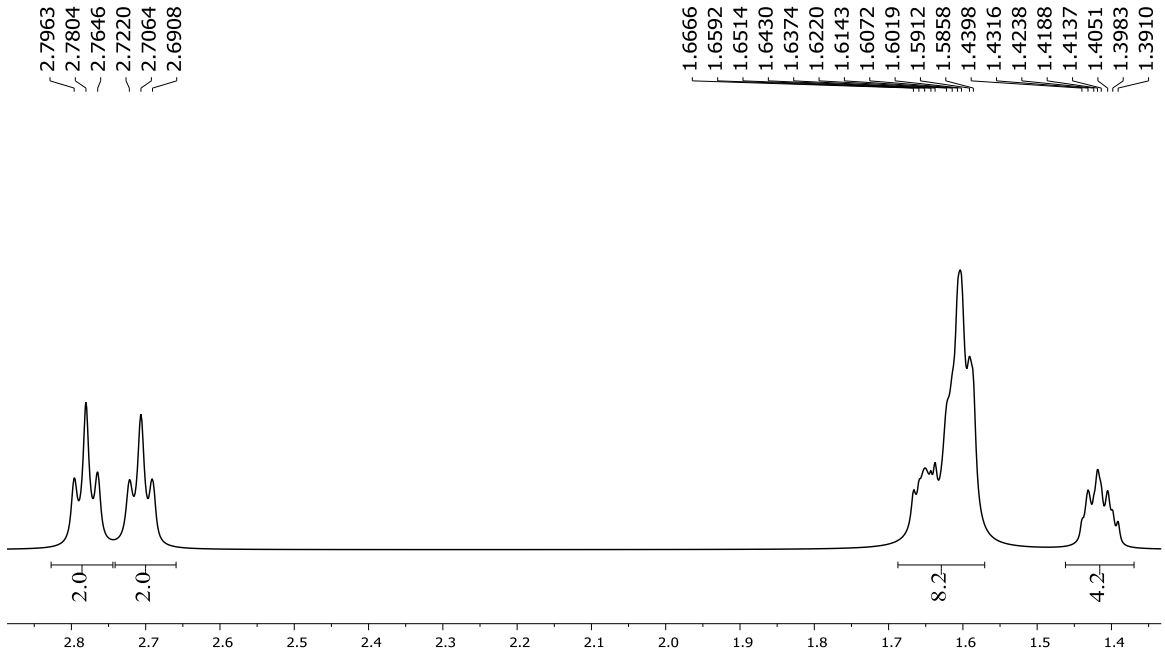

Figure 2.4: The 2.9-1.3 ppm region from the ^{1}H-NMR of BODIPY **23**

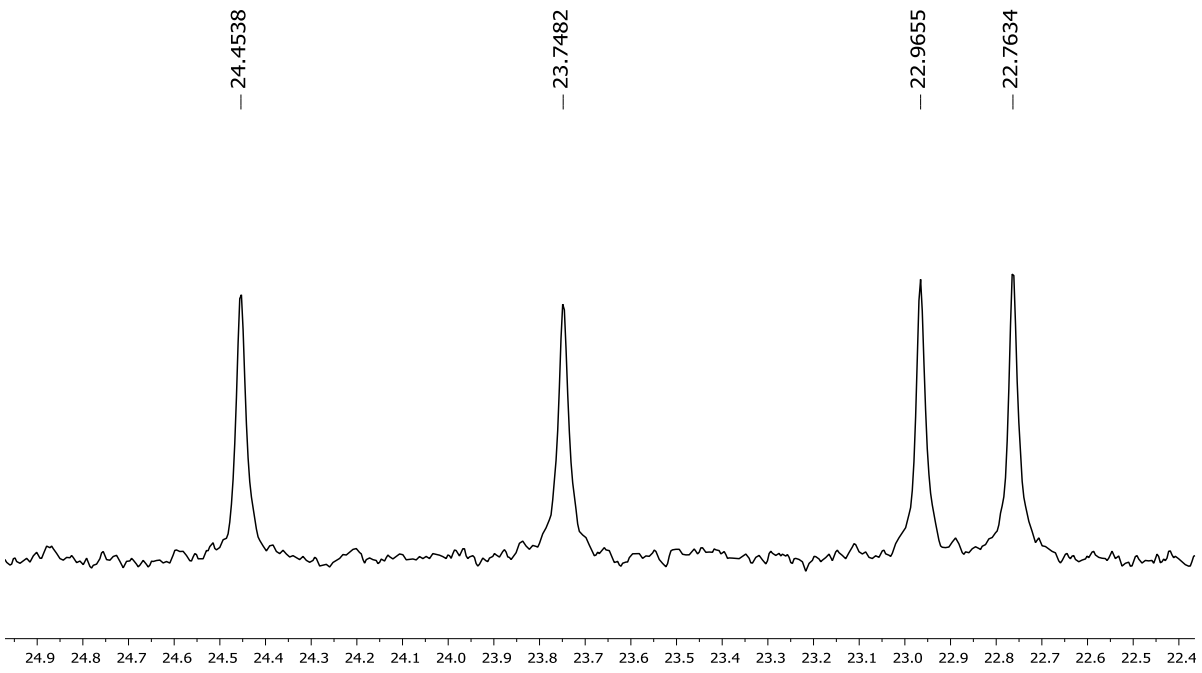

Figure 2.5: The 25-22 ppm region from the ^{13}C-NMR of BODIPY **10a**

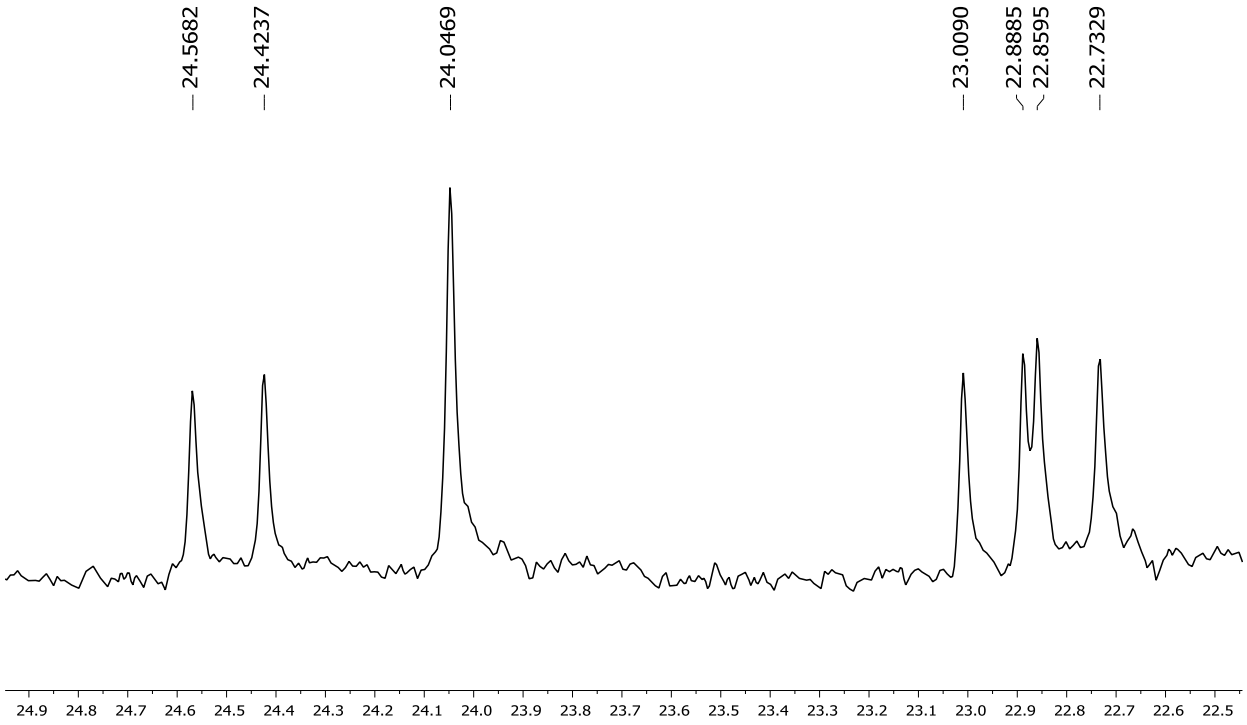

Figure 2.6: The 25-22 ppm region from the ^{13}C-NMR of BODIPY **13**

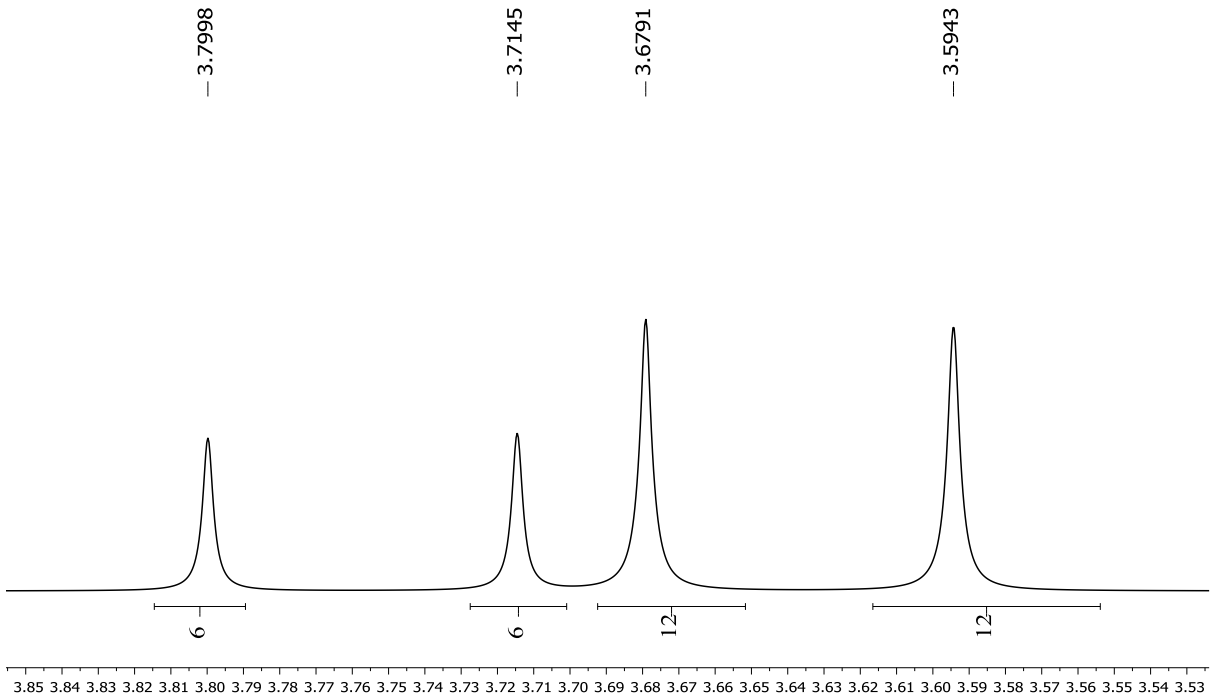

Figure 2.7: The 3.9-3.5 ppm region from the ^{1}H-NMR of BODIPY **19** with OCH_3 signals

2.2.3 Spectroscopic Study

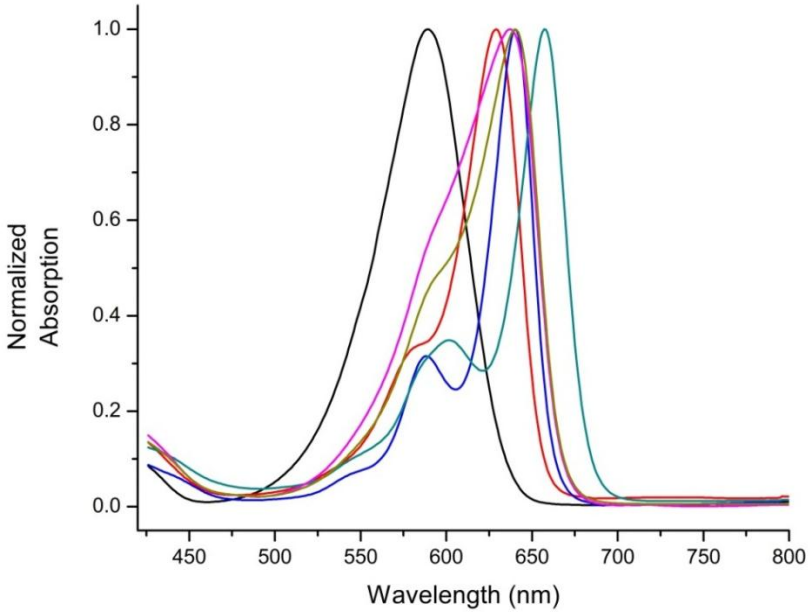

Figure 2.8: Normalized absorption spectra of BODIPYs **10a** (black)**, 10b** (red), **20** (blue), **21** (cyan), **13** (magenta) and **23** (yellow) in THF at RT.

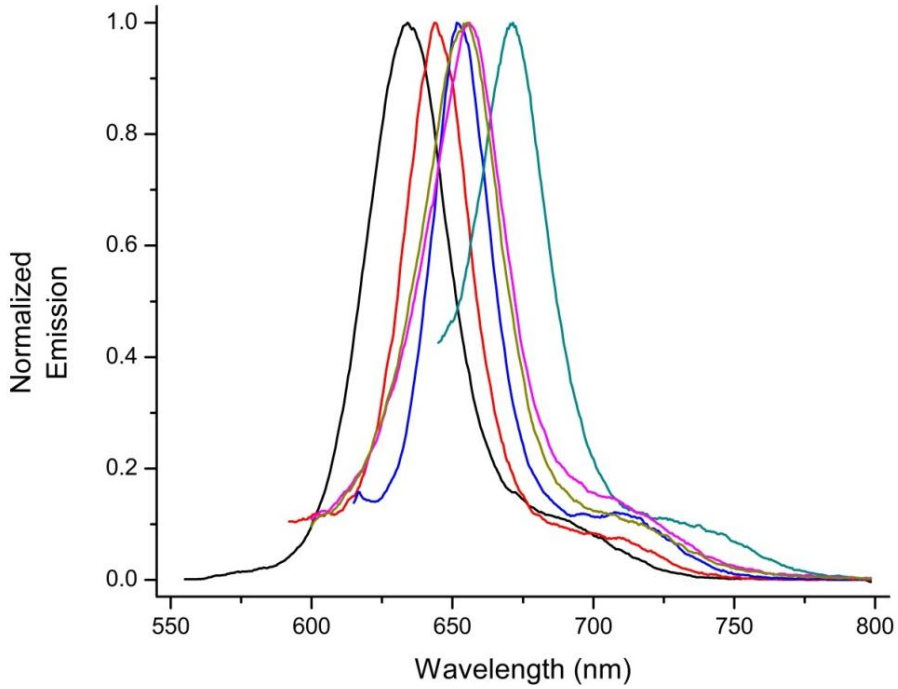

Figure 2.9: Normalized emission spectra of BODIPYs **10a** (black)**, 10b** (red), **20** (blue), **21** (cyan), **13** (magenta) and **23** (yellow) in THF at RT

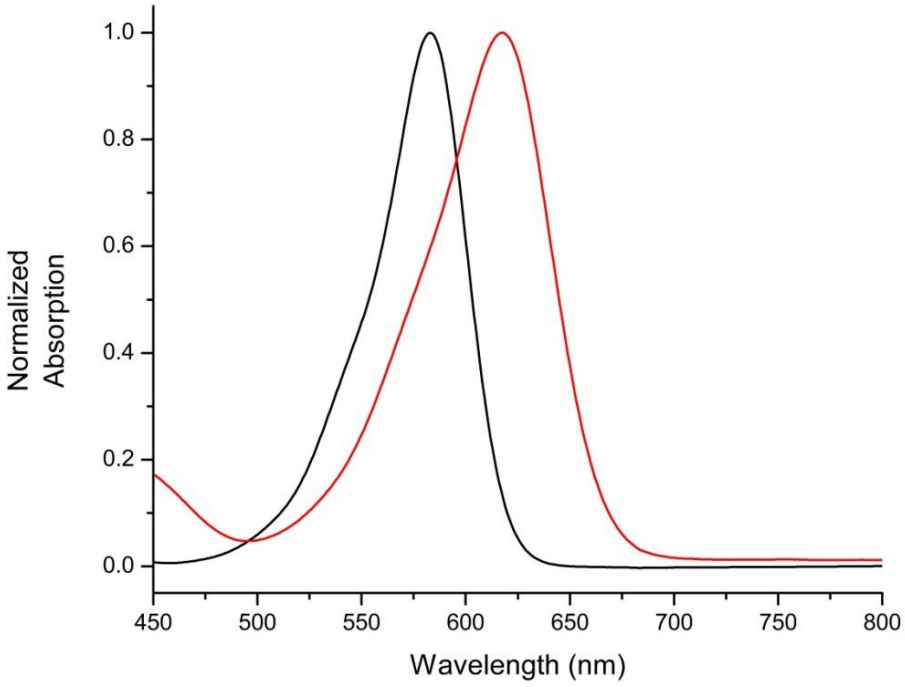

Figure 2.10: Normalized absorption spectra of BODIPYs **14** (black) and **19** (red) in THF at RT

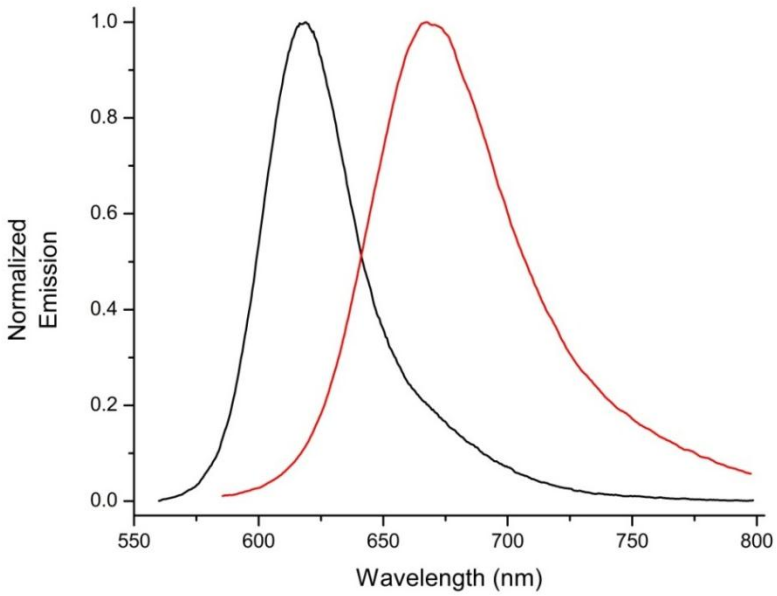

Figure 2.11: Normalized emission spectra of BODIPYs **14** (black) and **19** (red) in THF at RT

The spectroscopic properties of BODIPYs were investigated in THF. BODIPY **6a**, **6b** and their derivatives showed absorption bands between 550 and 657 nm and emission bands between 559 and 671 nm in THF with strong absorption bands (log ε= 4.7-5.0), as Table 2.1 shows. The thienyl group was able to red-shift 39 nm for the absorption, and its Stokes shift is also the highest, showing that the free rotation of thienyl groups is relatively fast. The furanyl group largely shifts BODIPY's absorption by 69 nm, but its Stokes' shift is reduced to 15 nm. BODIPY **6a** and **6b**'s low quantum yields are probably due to the heavy-atom effect caused by the iodine atoms. The introduction of styryl groups induced greatly red-shifts of 79–90 nm and 92–112 nm for the absorption and emission, respectively, due to further extension of the π-conjugation. In addition, the methoxy- group on styryl groups red-shifts BODIPY's absorption and emission spectra with a further 17 nm and 20 nm, respectively, and this can be explained by a push-pull effect.[31] Both 3,5-distyrylated BODIPYs show a shoulder at lower wavelength that is attributed to the vibrational transitions. The broader and weaker absorption bands seen in the absorption spectra of the styryl-BODIPYs centered at 560 nm are likely due to the S_0–S_2

transition.[32] Most BODIPYs produced by cross-coupling reactions show higher fluorescence quantum yields than the 3,5-diiodo-BODIPYs **6a** and **6b**, and their quantum yields are in agreement with similar BODIPY's reports.[31]

Table 2.1: Spectroscopic properties of BODIPYs **6a**, **6b**, **10a**, **10b**, **10c**, **13**, **20**, **21** and **23** in THF at RT

BODIPYs	Abs. λ_{max} (nm)	log ε ($M^{-1}cm^{-1}$)	Emission λ_{max} (nm)	Φf	Stokes shift (nm)
6a	550	5.00	560	0.14	10
6b	550	5.00	559	0.14	9
10a	589	4.69	634	0.74	45
10b	629	4.76	644	0.63	15
10c	548	4.74	574	0.42	26
20	640	4.78	651	0.53	11
21	657	4.81	671	0.28	14
13	637	4.74	656	0.65	19
23	640	4.79	655	0.49	15

BODIPY **14**, **18** and **19** showed absorption bands between 577 and 617 nm and emission bands between 597 and 668 nm in THF with high extinction coefficients (log ε= 4.9-5.0), as Table 2.2 shows. Comparing with BODIPY **6a**, BODIPY **9a**'s red-shifts from absorption and emission spectra are mainly due to the 2,6-iodine groups. BODIPY **14** and **18** show similar λ_{max} in the absorption and emission spectra, but BODIPY **14**'s quantum yield is higher, because of the relatively fast rotation of the aryl groups on BODIPY **18**'s 2,3,5,6-positions. BODIPY **19**'s large

red-shifts of the absorption and emission spectra are due to a push-pull effect, and the fastest free rotation rate induces the lowest quantum yield.

Table 2.2: Spectroscopic properties of BODIPYs **9a, 14, 18** and **19** in THF at RT

BODIPYs	Abs. λ_{max} (nm)	log ε ($M^{-1}cm^{-1}$)	Emission λ_{max} (nm)	Φf	Stokes shift (nm)
9a	577	5.02	597	0.09	20
14	583	4.87	619	0.36	36
18	585	4.99	623	0.10	38
19	617	5.06	668	<0.01	51

2.3 Conclusions

In summary, two types of iodinated BODIPYs were successfully prepared and their reactivity under Pd-catalyzed cross-coupling reactions were investigated. We were able to synthesize a series of symmetric and unsymmetric BODIPYs with aryl and/or styryl groups. Stille cross-coupling reactions are accessible with most Pd(0) catalysts, but Suzuki and Heck coupling reactions favor $Pd(dppf)Cl_2$ as the most efficient catalyst. Methodology development provided methods to functionalize BODIPY's 2,3,5,6-positions with aryl and styryl groups in higher yields and shorter time, compared with the yields from chlorinated and brominated BODIPYs. The Heck cross-coupling reaction on iodinated BODIPYs also provided a better method to replace the Knoevenagel reaction. Most cross-coupling products show red-shifted absorption and emission spectra, thus iodinated BODIPYs could potentially be functionalized with cross-coupling reactions to produce near-IR platforms for bio-imaging and other applications.

2.4 Experimental

2.4.1 General Information

All the reagents and solvents were purchased from Sigma-Aldrich and were used without further purification. All reactions were carried out with oven-dried glassware under a dry argon atmosphere. All the reactions were monitored using Sorbent Technologies 0.2 mm silica gel TLC plates with UV-254 nm indicator. Flash column chromatography was performed using Sorbent Technologies 60 Å silica gel (230-400 mesh). Prep-TLC 60 Å silica gel 20 x 20 cm (210-270 μm) was used. All ^{1}H-, ^{13}C-, and ^{11}B-NMR spectra were collected on a Bruker AV-400 and AV-500 spectrometer in deuterated chloroform or dichloromethane. The $CDCl_3$ chemical shifts (δ) are reported in ppm using as reference 7.26 for proton and 77.00 for carbon and BF_3•OEt_2 was used as reference (0.00 δ) for boron NMR. The CD_2Cl_2 chemical shifts (δ) are reported in ppm using as reference 5.32 for proton and 53.50 for carbon.

Coupling constants are reported in Hertz (Hz). All the mass spectra were collected using an Agilent 6210 ESI-TOF mass spectrometer. All melting points were recorded using a MEL-TEMP electrothermal instrument.

2.4.2 Synthesis

Synthesis of 3,5-diiodo-8-aryl-BODIPYs 6a,b. To a solution of tetrahydroisoindole **2** (772 mg, 4.00 mmol) *p*-TsOH monohydrate (40.0mg, 0.210 mmol) and nBu_4NI (20.0 mg, 0.0541 mmol) in dicloromethane (50 mL) was added 0.6 equiv. of arylaldehyde. The reaction was stirred for 12 h at room temperature under inert atmosphere. The mixture was washed with sat. $NaHCO_3$ (1 x 50 mL) and with sat. NaCl (1 x 50 mL) before being dried over anhydrous Na_2SO_4. The solvent was removed under vacuum and the residue was purified by silica gel column chromatography (elution: hexanes/ethyl acetate 5:1). Dipyrromethanes **3a** (from benzaldehyde) and **3b** (from 3,5-dimethoxybenzaldehyde) were obtained in 95% and 86% yield, respectively, and **3a**'s NMR and

MS are in agreement with those reported.[33] For **3b**: Orange solid, mp(°C) 89; ^{1}H NMR ($CDCl_3$, 400 MHz) δ 9.39 (s, 2H), 6.33 (t, *J* = 2.3 Hz, 1H), 6.24 (d, *J* = 2.3 Hz, 2H), 5.40 (s, 1H), 4.19 – 4.09 (m, 4H), 3.67 (s, 6H), 2.76 (d, *J* = 6.3 Hz, 4H), 2.27 (d, *J* = 5.5 Hz, 4H), 1.73 – 1.64 (m, 8H), 1.24 (t, *J* = 7.1 Hz, 6H); ^{13}C NMR ($CDCl_3$, 100 MHz) δ 161.9, 161.0, 141.7, 130.8, 129.0, 119.7, 116.7, 106.5, 98.3, 59.7, 55.1, 40.3, 23.3, 23.2, 23.1, 21.3, 14.3; HRMS (ESI-TOF) m/z 535.2811 $[M+H]^+$ calcd for $C_{31}H_{39}N_2O_6$ 535.2803. Dipyrromethane **3a** or **3b** (1.00 mmol) was dissolved in THF/methanol 1:1 (12 mL) and a solution of KOH (504 mg, 8.98 mmol) in water (10 mL) was added. The final mixture was refluxing for 4 h before being cooled to room temperature, poured into 2 M HCl (50 mL) and stirred at room temperature for 15 min. The precipitate was collected under vacuum filtration and dissolved in 45 mL methanol. A solution of $NaHCO_3$ (0.54 g) and I_2 (0.50 g) in water (15 mL) was added, the mixture was sonicated for 5 min and then stirred for 24 h under Ar. The mixture was filtered and the precipitate washed with cold hexanes to remove excess iodine. The precipitate was dissolved in dichloromethane (50 mL) and cooled with an ice bath. Triethylamine (2.0 mL) and $BF_3{\cdot}OEt_2$ (3.0 mL) were added. After 5 min the ice bath was removed and the solution was stirred at room temperature for 2 h. The solvents were removed under vacuum and the resulting residue was dissolved in ethyl acetate (100 mL) and washed with 1M HCl (1 x 100 mL), sat. $NaHCO_3$ (1 x 50 mL) and sat. NaCl (1 x 50 mL). Ethyl acetate was removed and the oily residue was purified by silica gel column chromatography (elution: hexanes/dichloromethane 1:2). 3,5-Diiodo-BODIPYs **6a** and **6b** were obtained in 40% and 42% yields, respectively, as brown solids.

3,5-Diiodo-8-phenyl-BODIPY 1a. mp(°C) 220; ^{1}H NMR ($CDCl_3$, 400 MHz) δ 7.49 (dd, *J* = 5.1, 1.9 Hz, 3H), 7.26 – 7.20 (m, 2H), 2.30 (tt, *J* = 6.3, 1.3 Hz, 4H), 1.62 – 1.56 (m, 4H), 1.53 (t, *J* = 6.3 Hz, 4H), 1.42 – 1.36 (m, 4H); ^{13}C NMR ($CDCl_3$, 125 MHz) δ 142.2, 139.1, 136.3,

134.6, 134.3, 129.5, 129.4, 127.7, 106.2, 24.4, 24.2, 23.1, 22.4; ^{11}B NMR ($CDCl_3$,128 MHz) δ 0.47 (t, *J* = 30.7 Hz); HRMS (ESI-TOF) m/z 649.9796 $[M+Na]^+$ calcd for $C_{23}H_{21}BF_2I_2N_2Na$ 649.9784.

3,5-Diiodo-8-(3,5-dimethoxyphenyl)-BODIPY 1b. mp(°C) 226; ^{1}H NMR ($CDCl_3$, 400 MHz) δ 6.55 (t, *J* = 2.3 Hz, 1H), 6.39 (d, *J* = 2.3 Hz, 2H), 3.80 (s, 6H), 2.31 (t, *J* = 6.3 Hz, 4H), 1.74 (t, *J* = 6.2 Hz, 4H), 1.65 – 1.59 (m, 4H), 1.48 – 1.40 (m, 4H); ^{13}C NMR ($CDCl_3$, 125 MHz) δ 161.7, 142.1, 138.6, 136.09, 136.06, 135.7, 134.2, 106.1, 105.4, 101.1, 55.6, 24.2, 23.8, 23.1, 22.3; ^{11}B NMR ($CDCl_3$, 128 MHz) δ 0.44 (t, *J* = 30.6 Hz); HRMS (ESI-TOF) m/z 668.0104 $[M-F]^+$ calcd for $C_{25}H_{24}BFI_2N_2O_2$ 668.0113.

Synthesis of unsubstituted *meso*-aryl BODIPYs 8a and 8b. 3.10 mL (45.0 mmol) pyrrole and 15.0 mmol arylaldehyde were mixed and stirred in 100 ml of 0.18 M hydrochloric acid solution for 3 hours. The resulting dipyrromethane precipitates and was filtered. The solid was then dissolved in 100 mL and washed with 2 x 50 mL saturated sodium bicarbonate solution before being dried over anhydrous Na_2SO_4. The solution was concentrated down under vacuum to 20 mL and then 1.1 equiv. (16.5 mmol) of p-chloranil was added slowly. The reaction was stirred under inert atmosphere for 2 hours and then 9.0 mL of triethylamine (75.0 mmol) was added. After 10 minutes, $BF_3{\cdot}OEt_2$ (9.8 mL, 105 mmol) were added via a syringe dropwisely at 0^{o}C. The ice bath was removed after the addition of BF_3 etherate and the solution was allowed to stir in room temperature for 4 hours. The solvents were removed under vacuum and the resulting residue was dissolved in ethyl acetate (100 mL) and washed with 1M HCl (1 x 100 mL), sat. $NaHCO_3$ (1 x 50 mL) and sat. NaCl (1 x 50 mL). Ethyl acetate was removed and the oily residue was purified by silica gel column chromatography. BODIPYs **8a** and **8b** were obtained in 36% and 31% yields, respectively, as brown and yellow solids.

BODIPY **8a**: ^{1}H NMR (500 MHz, $CDCl_3$) δ 7.93 (s, 2H), 7.47 (d, *J* = 8.1 Hz, 2H), 7.34 (d, *J* = 7.8 Hz, 2H), 6.96 (d, *J* = 4.2 Hz, 2H), 6.60 – 6.50 (m, 2H), 2.48 (s, 3H); HRMS (ESI-TOF) m/z 283.1210 $[M+H]^+$ calcd for $C_{16}H_{14}BF_2N_2$ 283.1218.

BODIPY **8b**: ^{1}H NMR (400 MHz, CD_2Cl_2) δ 7.91 (s, 2H), 7.06 (d, *J* = 4.2 Hz, 2H), 6.71 (dd, *J* = 18.2, 2.3 Hz, 3H), 6.63 – 6.50 (m, 2H), 3.83 (s, 6H); HRMS (ESI-TOF) m/z 329.1262 $[M+H]^+$ calcd for $C_{17}H_{15}BF_2N_2O_2$ 329.1273.

Tetra-iodination reaction conditions. 70.0 mg of BODIPY **8a** (0.25 mmol) and 283.4 mg of iodine (1.12 mmol) were mixed and dissolved in 20 mL ethanol. 174.6 mg of iodic acid (1.0 mmol) was dissolved in minimum amount of water and was added dropwisely into the solution. The brown solution was refluxing for 3 hours until TLC indicated all starting material was gone, and the solution's color turned to dark pink. Ethanol was removed under vacuum, and the residue green solids were dissolved in 100 mL DCM, and washed with 2 x 50 mL of saturated sodium thiosulfate solution before being dried over anhydrous Na_2SO_4. DCM was removed under vacuum and the residue was purified by silica gel column chromatography. BODIPY **9a** was obtained in 76% yield as a dark green solid. mp(°C) 283; ^{1}H NMR (400 MHz, CD_2Cl_2) δ 7.41 (d, *J* = 8.2 Hz, 2H), 7.37 – 7.33 (m, 2H), 7.08 – 7.01 (m, 2H), 2.46 (s, 3H); ^{13}C NMR (125 MHz, CD_2Cl2) δ 142.4, 141.0, 139.3, 137.8, 130.6, 129.5, 129.0, 115.3, 90.6, 21.3; ^{11}B NMR (128 MHz, CD_2Cl_2) δ 0.00 (t, *J* = 29.2 Hz); HRMS (ESI-TOF) m/z 766.7034 $[M-F]^+$ calcd for $C_{16}H_9BFI_4N_2$ 766.7022.

General Stille cross-coupling conditions on 3,5-diiodo-BODIPYs. For symmetric BODIPYs, 62.8 mg (0.100 mmol) **6a**, and 5.00 mg $Pd(PPh_3)_2Cl_2$ and 5 equiv (0.500 mmol) of tin reagent were mixed under inert atmosphere. Toluene (2 mL) were added via syringe and the solution was heated at 90 ^{o}C in an oil bath for 3 min. Tin reagent was added via syringe and the reaction was

monitored by TLC until complete consumption of 3,5-diiodo-BODIPY. The cooled solution was filtered through celite to remove excess palladium, and the solvent was concentrated under vacuum. The residue was purified by silica gel column chromatography to afford the corresponding 3,5-diaryl-BODIPYs as red solids, which were recrystallized using 1:1 dichloromethane/hexane. For the unsymmetric BODIPYs, 62.8 mg (0.100 mmol) BODIPY **6a** and 5.00 mg $Pd(PPh_3)_2Cl_2$ were mixed under inert atmosphere. Toluene (2 mL) was added via syringe and the solution was heated at 90 ^oC for 3 minutes. Three equivalents of the tin reagent were added via syringe and the reaction was heated at 70 ^oC for 25 min. The cooled solution was filtered through celite and the solvent removed under vacuum. The residue was purified by silica gel column chromatography. The second band corresponding to the 3-aryl-5-iodo-BODIPY was collected, and immediately reacted with 5.00 mg $Pd(dppf)Cl_2$ and 5 equiv of 5-methyl-2-thienylboronic acid under inert atmosphere. Toluene (2 mL) and THF (2 mL) were added via syringe and the solution was heated at 70 ^oC for 3 minutes. K_2CO_3 (1 M, 0.5 mL) solution was added via syringe and the reaction was heated at 70 ^oC for 30 min. The cooled solution was filtered through celite and the solvent removed under vacuum. The residue was purified by silica gel column chromatography and recrystallized using 1:1 dichloromethane/hexane.

BODIPY 10a: Yield 78%. mp(°C)> 300; ^1H NMR (400 MHz, CD_2Cl_2) δ 7.69 – 7.61 (m, 2H), 7.58 – 7.45 (m, 5H), 7.41 – 7.30 (m, 2H), 7.20 – 7.10 (m, 2H), 2.51 (t, *J* = 6.2 Hz, 4H), 1.68 (t, *J* = 6.3 Hz, 4H), 1.64 – 1.56 (m, 4H), 1.47 – 1.40 (m, 4H); ^{13}C NMR (100 MHz, CD_2Cl2) δ 146.9, 142.1, 135.5, 132.6, 132.1, 131.4, 131.3, 130.7, 129.24, 129.15, 128.5, 128.3, 127.3, 24.5, 23.8, 23.0, 22.8; ^{11}B NMR (128 MHz, $CDCl_3$) δ 1.10 (t, *J* = 32.8 Hz); HRMS (ESI-TOF) m/z 540.1788 $[M+H]^+$ calcd for $C_{31}H_{28}BF_2N_2S_2$ 540.1786.

BODIPY 10b: Yield 80%. mp(°C)> 300; ^{1}H NMR (400 MHz, CD_2Cl_2) δ 7.64 (d, *J* = 1.7 Hz, 1H), 7.59 (d, *J* = 3.6 Hz, 1H), 7.54 – 7.46 (m, 2H), 7.41 – 7.28 (m, 1H), 6.63 (dd, *J* = 3.6, 1.7 Hz, 1H), 2.92 – 2.64 (m, 2H), 1.71 – 1.56 (m, 4H), 1.46 – 1.37 (m, 2H); ^{13}C NMR (101 MHz, $CDCl_3$) δ 147.6, 143.9, 142.0, 141.4, 138.5, 135.8, 132.4, 130.6, 129.0, 128.9, 128.5, 116.1, 116.0, 115.9, 112.7, 24.4, 24.1, 22.8, 22.7; ^{11}B NMR (128 MHz, CD_2Cl_2) δ 1.28 (t, *J* = 33.5 Hz); HRMS (ESI-TOF) m/z 530.2045 $[M+Na]^+$ calcd for $C_{31}H_{27}BF_2N_2O_2Na$ 530.2062.

BODIPY 10c: Yield 85%. mp(°C)> 300; ^{1}H NMR (CD_2Cl_2, 400 MHz) δ 7.55 (dd, *J* = 5.0, 1.9 Hz, 3H), 7.50 (dd, *J* = 7.4, 2.3 Hz, 4H), 7.43 – 7.36 (m, 8H), 2.28 (s, 4H), 1.72 (t, *J* = 6.1 Hz, 4H), 1.54 (qd, *J* = 5.2, 2.9 Hz, 4H), 1.45 (ddp, *J* = 9.5, 6.4, 2.8 Hz, 4H); ^{13}C NMR ($CDCl_3$, 125 MHz) δ 154.5, 141.6, 141.6, 135.7, 132.2, 131.3, 129.7, 129.62, 129.59, 129.57, 129.1, 129.0, 128.5, 128.1, 127.7, 24.3, 23.1, 22.7, 22.6; ^{11}B NMR ($CDCl_3$, 128 MHz) δ 0.87 (t, *J* = 32.0 Hz); HRMS (ESI-TOF) m/z 508.2638 $[M-F]^+$ calcd for $C_{35}H_{31}BFN_2$ 508.2595.

BODIPY 13: Yield 38%. mp(°C)> 300; ^{1}H NMR (400 MHz, CD_2Cl_2) δ 7.62 (d, *J* = 1.7 Hz, 1H), 7.54 (d, *J* = 3.7 Hz, 1H), 7.53 – 7.46 (m, 4H), 7.40 – 7.30 (m, 2H), 6.87 (dd, *J* = 3.7, 1.2 Hz, 1H), 6.59 (dd, *J* = 3.7, 1.7 Hz, 1H), 2.76 (t, *J* = 6.2 Hz, 2H), 2.57 (s, 3H), 2.52 (t, *J* = 6.2 Hz, 2H), 1.80 – 1.51 (m, 8H), 1.49 – 1.38 (m, 4H); ^{13}C NMR (101 MHz, CD_2Cl2) δ 147.6, 144.2, 143.9, 141.6, 139.4, 135.7, 132.4, 131.7, 130.5, 129.2, 129.0, 128.7, 128.5, 126.4, 126.0, 116.0, 112.5, 24.6, 24.4, 24.1, 23.0, 22.89, 22.86, 22.7, 15.2; ^{11}B NMR (128 MHz, $CDCl_3$) δ 1.22 (t, *J* = 33.3 Hz); HRMS (ESI-TOF) m/z 560.2007 $[M+Na]^+$ calcd for $C_{32}H_{29}BF_2N_2NaOS$ 560.1990.

General Stille cross-coupling conditions on 2,3,5,6-tetraiodo-BODIPYs. 78.6 mg (0.100 mmol) **9a**, and 10.00 mg $Pd(PPh_3)_2Cl_2$ and 10 equiv (1.000 mmol) of tin reagent were mixed under inert atmosphere. Toluene (3 mL) were added via syringe and the solution was heated at 90 ^{o}C in an oil bath for 3 min. Tin reagent was added via syringe and the reaction was monitored

by TLC until complete consumption of BODIPY **9a**. The cooled solution was filtered through celite to remove excess palladium, and the solvent was concentrated under vacuum. The residue was purified by silica gel column chromatography to afford the corresponding 2,3,5,6-tetraphenyl-BODIPY. Yield 53%. mp(°C)> 300; ^{1}H NMR (400 MHz, CD_2Cl_2) δ 7.65 (d, *J* = 8.1 Hz, 2H), 7.47 – 7.33 (m, 12H), 7.20 – 7.14 (m, 6H), 7.12 (d, *J* = 1.4 Hz, 2H), 7.08 – 7.00 (m, 4H), 2.52 (s, 3H); ^{13}C NMR (100 MHz, CD_2Cl2) δ 156.1, 145.0, 141.3, 134.7, 134.6, 134.51, 134.48, 133.9, 132.2, 131.5, 131.0, 130.42, 130.39, 130.37, 129.3, 129.1, 128.8, 128.3, 128.2, 127.8, 127.0, 21.3; ^{11}B NMR (128 MHz, CD_2Cl_2) δ 0.78 (t, *J* = 30.7 Hz); HRMS (ESI-TOF) m/z 566.2435 $[M-F]^+$ calcd for $C_{40}H_{29}BFN_2$ 566.2439.

General Suzuki cross-coupling conditions. For symmetric BODIPYs, 62.8 mg (0.100 mmol) **6a** or 68.8 mg (0.100 mmol) **6b**, 5.00 mg Pd(dppf)Cl_2 and 5 equiv (0.500 mmol) of aryl boronic acid were mixed under inert atmosphere. Toluene (2 mL) and THF (2 mL) were added via syringe and the solution was heated at 70 ^{o}C in an oil bath for 3 min. K_2CO_3 (1 M, 0.5 mL) solution was added via syringe and the reaction was monitored by TLC until complete consumption of 3,5-diiodo-BODIPY. The cooled solution was filtered through celite to remove excess palladium and boronic acid, and the solvent was concentrated under vacuum. The residue was purified by silica gel column chromatography to afford the corresponding 3,5-diaryl-BODIPYs as red solids, which were recrystallized using 1:1 dichloromethane/hexane. For the unsymmetric BODIPYs, 62.8 mg (0.100 mmol) BODIPY **6a** or 68.8 mg (0.100 mmol) BODIPY **6b**, 5.00 mg Pd(dppf)Cl_2 and 3 equiv (0.300 mmol) of 4-(benzyloxy)carbonyl)phenyl)boronic acid were mixed under inert atmosphere. Toluene (2 mL) and THF (2 mL) were added via syringe and the solution was heated at 70 ^{o}C for 3 minutes. K_2CO_3 (1 M, 0.5 mL) solution was added via syringe and the reaction was heated at 70 ^{o}C for 30 min. The cooled solution was

filtered through celite and the solvent removed under vacuum. The residue was purified by silica gel column chromatography. The second band corresponding to the 3-aryl-5-iodo-BODIPY was collected, and immediately reacted with 5.00 mg $Pd(dppf)Cl_2$ and 5 equiv of 4-(trifluoromethyl)phenylboronic acid under inert atmosphere. Toluene (2 mL) and THF (2 mL) were added via syringe and the solution was heated at 70 ^oC for 3 minutes. K_2CO_3 (1 M, 0.5 mL) solution was added via syringe and the reaction was heated at 70 ^oC for 30 min. The cooled solution was filtered through celite and the solvent removed under vacuum. The residue was purified by silica gel column chromatography and recrystallized using 1:1 dichloromethane/hexane.

BODIPY 15: Yield 83%. mp(°C)> 300; ^1H NMR (CD_2Cl_2, 400 MHz) δ 8.25 – 8.18 (m, 4H), 7.75 – 7.65 (m, 4H), 7.61 – 7.54 (m, 3H), 7.44 – 7.35 (m, 2H), 2.27 (t, *J* = 6.1 Hz, 4H), 1.74 (t, *J* = 6.1 Hz, 4H), 1.56 (ddt, *J* = 8.1, 6.2, 2.4 Hz, 4H), 1.50 – 1.42 (m, 4H);^{13}C NMR (CD_2Cl_2, 100 MHz) δ 152.0, 147.8, 144.0, 143.4, 138.7, 134.8, 132.3, 130.79, 130.75, 130.7, 130.4, 129.52, 129.46, 127.9, 122.9, 24.4, 23.0, 22.5, 22.4; ^{11}B NMR (CD_2Cl_2, 128 MHz) δ 0.67 (t, *J* = 32.5 Hz); HRMS (ESI-TOF) m/z 617.2260 $[M]^+$ calcd for $C_{35}H_{29}BF_2N_2O_4$ 617.2281.

BODIPY 17a: Yield 36%. mp(°C)> 300; ^1H NMR ($CDCl_3$, 400 MHz) δ 8.17 – 8.11 (m, 2H), 7.75 – 7.64 (m, 6H), 7.58 (dd, *J* = 5.0Hz, 1.9 Hz, 3H), 7.51 – 7.46 (m, 2H), 7.45 – 7.36 (m, 5H), 5.40 (s, 2H), 2.31 (dt, *J* = 6.5, 3.2 Hz, 4H), 1.75 (t, *J* = 6.0 Hz, 4H), 1.63 – 1.54 (m, 4H), 1.50 (dp, *J* = 9.0, 3.4, 2.6 Hz, 4H); ^{13}C NMR ($CDCl_3$, 100 MHz) δ 166.0, 153.5, 152.7, 142.7, 142.4, 142.2, 136.6, 135.9, 135.6, 135.1, 131.8, 131.6, 130.4, 130.0, 129.9, 129.6, 129.2, 129.1, 128.5, 128.2, 128.1, 127.8, 124.7, 124.7, 66.7, 24.3, 22.9, 22.5, 22.4; ^{11}B NMR ($CDCl_3$, 128 MHz) δ 0.82 (t, *J* = 32.1 Hz); HRMS (ESI-TOF) m/z 729.2839 $[M]^+$ calcd for $C_{44}H_{36}BF_5N_2O_2$ 729.2821.

BODIPY 17b: Yield 40%. mp(°C)> 300; ^{1}H NMR (CD_2Cl_2, 400 MHz) δ 8.12 – 8.05 (m, 2H), 7.65 (s, 4H), 7.63 – 7.57 (m, 2H), 7.48 – 7.43 (m, 2H), 7.42 – 7.33 (m, 3H), 6.62 (t, *J* = 2.3 Hz, 1H), 6.55 (d, *J* = 2.3 Hz, 2H), 5.36 (s, 2H), 3.84 (s, 6H), 2.27 (t, *J* = 6.0 Hz, 4H), 1.95 (t, *J* = 6.1 Hz, 4H), 1.61 – 1.49 (m, 8H); ^{13}C NMR (CD_2Cl_2, 100 MHz) δ 165.9, 161.9, 153.6, 152.6, 143.0, 142.9, 142.7, 136.9, 136.7, 136.3, 136.1, 131.6, 131.4, 130.4, 130.33, 130.25, 130.14, 130.07, 129.8, 129.0, 128.62, 128.58, 128.2, 128.1, 127.3, 125.6, 124.69, 124.66, 122.9, 105.8, 101.2, 66.8, 55.7, 24.2, 23.1, 22.6, 22.5, 22.4; ^{11}B NMR (CD_2Cl_2, 128 MHz) δ 0.70 (t, *J* = 32.3 Hz); HRMS (ESI-TOF) m/z 812.2922 $[M+Na]^+$ calcd for $C_{46}H_{40}BF_5N_2O_4Na$ 812.2930.

General Suzuki cross-coupling conditions on BODIPY 9a. 78.6 mg (0.100 mmol) **9a**, 10.00 mg Pd(dppf)Cl_2 and 10 equiv (1.000 mmol) of aryl boronic acid were mixed under inert atmosphere. Toluene (2 mL) and THF (2 mL) were added via syringe and the solution was heated at 70 ^{o}C in an oil bath for 3 min. K_2CO_3 (1 M, 0.5 mL) solution was added via syringe and the reaction was monitored by TLC until complete consumption of BODIPY **9a**. The cooled solution was filtered through celite to remove excess palladium and boronic acid, and the solvent was concentrated under vacuum. The residue was purified by silica gel column chromatography to afford the corresponding 2,3,5,6-tetraaryl-BODIPYs as purple solids.

BODIPY 18: Yield 48%. mp(°C)> 300. ^{1}H NMR (500 MHz, $CDCl_3$) δ 7.56 (d, *J* = 7.8 Hz, 2H), 7.38 (d, *J* = 7.8 Hz, 2H), 7.02 (s, 2H), 6.70 (d, *J* = 2.2 Hz, 4H), 6.46 (t, *J* = 2.3 Hz, 2H), 6.26 (dd, *J* = 21.4, 2.2 Hz, 6H), 3.68 (s, 12H), 3.58 (s, 12H), 2.51 (s, 3H); ^{13}C NMR (125 MHz, $CDCl_3$) δ 160.4, 160.0, 155.9, 144.6, 140.9, 135.6, 134.4, 134.04, 134.02, 133.5, 131.4, 130.7, 129.2, 128.4, 124.2, 108.48, 108.46, 108.4, 106.2, 102.1, 99.5, 55.4, 55.2; ^{11}B NMR (128 MHz, CD_2Cl_2) δ 0.72 (t, *J* = 30.4 Hz); HRMS (ESI-TOF) m/z 807.3257 $[M+H]^+$ calcd for $C_{48}H_{46}BF_2N_2O_8$ 826.3346.

BODIPY 19: Yield 48%. mp(°C)> 300; ^{1}H NMR (400 MHz, CD_2Cl_2) δ 7.69 – 7.57 (m, 2H), 7.43 (d, *J* = 7.8 Hz, 2H), 7.06 (d, *J* = 1.4 Hz, 2H), 6.77 (s, 4H), 6.30 (s, 4H), 3.80 (s, 6H), 3.71 (s, 6H), 3.68 (s, 12H), 3.59 (s, 12H), 2.52 (s, 3H); ^{13}C NMR (100 MHz, CD_2Cl2) δ 155.8, 153.1, 152.9, 141.3, 139.2, 137.6, 134.5, 134.4, 131.5, 131.0, 129.4, 129.3, 127.9, 127.2, 108.5, 105.9, 60.63, 60.56, 56.5, 56.2, 56.0, 21.3; ^{11}B NMR (128 MHz, CD_2Cl_2) δ 0.89 (t, *J* = 30.9 Hz); HRMS (ESI-TOF) m/z 946.3745 $[M+H]^+$ calcd for $C_{52}H_{54}BF_2N_2O_{12}$ 946.3769.

General Heck cross-coupling conditions. For symmetric BODIPYs, 68.8 mg (0.100 mmol) **6b** and 5.00 mg Pd(dppf)Cl_2 and were mixed under inert atmosphere. Toluene (4 mL) was added via syringe and the solution was heated at 100 ^{o}C in an oil bath for 3 min. 10 equiv (0.500 mmol) of styrene and one drop of triethylamine were added via syringe and the reaction was monitored by TLC until complete consumption of 3,5-diiodo-BODIPY **6b**. The cooled solution was filtered through celite to remove excess palladium, and the solvent was concentrated under vacuum. The residue was purified by silica gel column chromatography to afford the corresponding 3,5-distyryl-BODIPYs. For the unsymmetric BODIPYs, 68.8 mg (0.100 mmol) BODIPY **6b**, 68.8 mg (0.100 mmol) **6b** and 5.00 mg Pd(dppf)Cl_2 and were mixed under inert atmosphere. Toluene (4 mL) was added via syringe and the solution was heated at 100 ^{o}C in an oil bath for 3 min. 6 equiv (0.500 mmol) of styrene and one drop of triethylamine were added via syringe and the reaction was monitored by TLC until the purple mono-coupling product was the major spot. The cooled solution was filtered through celite to remove excess palladium, and the solvent was concentrated under vacuum. The residue was purified by silica gel column chromatography. The second band corresponding to the 3-styryl-5-iodo-BODIPY was collected, and immediately reacted with 5.00 mg Pd(dppf)Cl_2 and 5 equiv. of 2-furanylboronic acid under inert atmosphere. Toluene (2 mL) and THF (2 mL) were added via syringe and the solution was heated at 70 ^{o}C for

3 minutes. K_2CO_3 (1 M, 0.5 mL) solution was added via syringe and the reaction was heated at 70 ^oC for 30 min. The cooled solution was filtered through celite and the solvent removed under vacuum. The residue was purified by silica gel column chromatography.

BODIPY 20: Yield 60%. mp (°C) 186 (decomposed); ^1H NMR (400 MHz, $CDCl_3$) δ 7.90 (s, 1H), 7.85 (s, 1H), 7.63 (d, *J* = 7.2 Hz, 4H), 7.40 (t, *J* = 7.5 Hz, 4H), 7.31 (t, *J* = 7.5 Hz, 2H), 7.25 (s, 1H), 7.21 (s, 1H), 6.56 (s, 1H), 6.46 (d, *J* = 2.3 Hz, 2H), 3.82 (s, 6H), 2.74 (t, *J* = 6.3 Hz, 4H), 1.84 (t, *J* = 6.3 Hz, 4H), 1.69 (dq, *J* = 7.8, 5.4, 4.2 Hz, 4H), 1.52 – 1.45 (m, 4H); ^{13}C NMR (100 MHz, $CDCl_3$) δ 161.4, 149.7, 141.1, 137.32, 137.29, 136.5, 132.0, 129.6, 128.7, 128.6, 127.3, 120.5, 106.4, 100.9, 55.6, 25.0, 23.9, 22.8; ^{11}B NMR (128 MHz, $CDCl_3$) δ 1.17 (t, *J* = 34.6 Hz); HRMS (ESI-TOF) m/z 620.3136 $[M-F]^+$ calcd for $C_{41}H_{39}BFN_2O_2$ 620.3119.

BODIPY 21: Yield 64%. mp (°C) 170 (decomposed); ^1H NMR (400 MHz, $CDCl_3$) δ 7.78 (s, 1H), 7.74 (s, 1H), 7.58 (d, *J* = 8.8 Hz, 4H), 7.21 (s, 1H), 7.17 (s, 1H), 6.93 (d, *J* = 8.8 Hz, 4H), 6.55 (t, *J* = 2.4 Hz, 1H), 6.47 (d, *J* = 2.4 Hz, 2H), 3.86 (s, 6H), 3.82 (s, 6H), 2.73 (t, *J* = 6.2 Hz, 4H), 1.83 (t, *J* = 6.2 Hz, 4H), 1.73 – 1.63 (m, 4H), 1.53 – 1.45 (m, 4H); ^{13}C NMR (101 MHz, $CDCl_3$) δ 161.4, 160.2, 149.7, 140.7, 137.5, 136.4, 136.0, 131.8, 130.3, 129.3, 128.7, 118.6, 114.2, 106.5, 100.8, 55.6, 55.4, 25.1, 23.9, 22.8; ^{11}B NMR (128 MHz, $CDCl_3$) δ 1.22 (t, *J* = 34.8 Hz); HRMS (ESI-TOF) m/z 701.3334 $[M+H]^+$ calcd for $C_{43}H_{44}BF_2N_2O_4$ 701.3362.

BODIPY 23: Yield 24%. mp (°C) 178 (decomposed); ^1H NMR (400 MHz, $CDCl_3$) δ 7.76 (d, *J* = 16.8 Hz, 1H), 7.69 (d, *J* = 3.6 Hz, 1H), 7.64 – 7.52 (m, 2H), 7.51 – 7.39 (m, 2H), 7.33 – 7.27 (m, 2H), 7.19 (d, *J* = 16.7 Hz, 1H), 6.92 (d, *J* = 8.8 Hz, 1H), 6.62 (dd, *J* = 3.6, 1.7 Hz, 1H), 3.85 (s, 3H), 2.78 (t, *J* = 6.3 Hz, 2H), 2.71 (t, *J* = 6.2 Hz, 2H), 1.72 – 1.57 (m, 8H), 1.47 – 1.36 (m, 2H); ^{13}C NMR (100 MHz, $CDCl_3$) δ 160.3, 150.8, 147.8, 143.7, 141.4, 140.6, 137.6, 136.5, 135.8, 130.2, 130.0, 129.0, 128.8, 128.5, 118.5, 115.3, 114.2, 112.6, 55.4, 25.1, 24.4, 24.2,

24.0, 22.9, 22.72, 22.69; ^{11}B NMR (128 MHz, $CDCl_3$) δ 1.28 (t, *J* = 33.9 Hz); HRMS (ESI-TOF) m/z 554.2654 $[M-F]^+$ calcd for $C_{36}H_{33}BFN_2O_2$ 554.2650.

2.4.3 X-ray Determined Molecular Structures

X-ray data were collected at low temperature with MoKα radiation on Bruker Kappa Apex-II DUO or Nonius KappaCCD diffactometers. data reduction: Bruker *SAINT*; program(s) used to solve structure: *SHELXS97* (Sheldrick, 2008); program(s) used to refine structure: *SHELXL97* (Sheldrick, 2008); molecular graphics: *ORTEP-3 for Windows* (Farrugia, 2012); software used to prepare material for publication: *SHELXL97* (Sheldrick, 2008).

Crystal Data: **6a**, $C_{23}H_{21}BF_2I_2N_2$, CH_2Cl_2, M=712.95, orthorhombic, a=8.2966(4), b=23.4782(12), c=25.1750(11) Å, T=100 K, space group $P2_12_12_1$, Z=8, 64679 reflections measured, 10489 unique (R_{int}=0.046), θ_{max}=26.8°, final R=0.053, CCDC 1435988;

Crystal Data: **10a**: $C_{31}H_{27}BF_2N_2S_2$, M=540.48, orthorhombic, a=25.3519(11), b=7.8512(3), c=25.1917(10) Å, T=100K, space group $Pna2_1$, Z=8, 19680 reflections measured, 5672 unique (R_{int}=0.034), θ_{max}=59.0°, final R=0.034;

Crystal Data: **10b**: $C_{31}H_{27}BF_2N_2O_2$, M=508.36, orthorhombic, a=13,8100(13), b=21.839(2), c=7.9190(10) Å, T=100K, space group Pbcn, Z=4, 21079 reflections measured, 2045 unique (R_{int}=0.035), θ_{max}=69.8°, final R=0.035;

Crystal Data: **10c**, $C_{35}H_{31}BF_2N_2$, M=528.43, orthorhombic, a=11.0477(15), b=14.069(2), c=17.029(3) Å, T=100 K, space group $P2_12_12_1$, Z=4, 79037 reflections measured, 5446 unique (R_{int}=0.055), θ_{max}=25.4°, final R=0.033, CCDC 1435989;

Crystal Data: **15**, $C_{35}H_{29}BF_2N_2O_4$, M=618.43, monoclinic, a=15.7880(6), b=12.5007(6), c=15.9397(7) Å, β=116.931(4)°, T=90 K, space group C2/c, Z=4, 31542 reflections measured, 5374 unique (R_{int}=0.042), θ_{max}=33.2°, final R=0.047, CCDC 1435990.

2.4.4 Steady-state Absorption and Fluorescence Spectroscopy

The photophysical properties of compounds **6a, 6b, 9a, 10a, 10b, 13, 14, 18, 19, 20, 21** and **23** were determined by preparing a stock solution with a concentration of 1×10^{-4} M and diluting it to appropriate concentrations for absorbance and emission spectra measurements. All the absorption spectra were obtained using a Perkin Elmer Lambda 35 UV-visible spectrophotometer. The optical density, ε, were taken by preparing solution concentrations at $1x10^{-5}$ M in order to get λ_{max} between 0.5 and 1.0. Emission spectra were measured on a LS-55 Perkin-Elmer spectro-fluorometer with the slit width set at 5 nm for BODIPYs **9a** and **19**, and 2.5 nm for all other BODIPYs. All absorbance and emission spectra were acquired within 6 h of fresh solution preparation, at room temperature. Rhodamine 6G (Φ = 0.86 in MeOH)[34] was used as the reference for compounds **6a** and **6b** in THF. Cresyl violet (Φ = 0.55 in MeOH)[34] was used as the reference for compounds **9a, 10a, 14** and **18** in THF. Methylene blue (Φ = 0.03 in MeOH)[34] was used as the reference for compounds **10b, 13, 19, 20, 21** and **23** in THF. Quartz spectrophotometric cells with path lengths of 10 mm were used. For the determination of quantum yields, dilute solutions with different absorbance between 0.02-0.08 at the particular excitation wavelength were used. Molar absorption coefficients (ε) was determined from the plots of integrated absorbance vs concentrations. The following equation was used for the calculations of the relative fluorescence quantum yields (Φ_f)[35]: $\Phi_s = \Phi_{st} \times (Grad_x/Grand_{st}) \times (n_x^2 / n_{st}^2)$ where Φ and n are the fluorescence quantum yields and refractive indexes, respectively; Grad represents gradient of integrated fluorescence intensity vs absorbance at the particular wavelength, subscripts s and x refer to the standards and the tested samples.

2.5 References

1. Miyaura, N.; Suzuki, A., Palladium-Catalyzed Cross-Coupling Reactions of Organoboron Compounds. *Chem. Rev.* **1995,** *95* (7), 2457-2483.

2. Negishi, E.-i.; Anastasia, L., Palladium-Catalyzed Alkynylation. *Chem. Rev.* **2003,** *103* (5), 1979-2018.

3. Yin, L.; Liebscher, J., Carbon−Carbon Coupling Reactions Catalyzed by Heterogeneous Palladium Catalysts. *Chem. Rev.* **2006,** *107* (1), 133-173.

4. Beletskaya, I. P.; Cheprakov, A. V., The Heck Reaction as a Sharpening Stone of Palladium Catalysis. *Chem. Rev.* **2000,** *100* (8), 3009-3066.

5. Corbet, J.-P.; Mignani, G., Selected Patented Cross-Coupling Reaction Technologies. *Chem. Rev.* **2006,** *106* (7), 2651-2710.

6. Boens, N.; Verbelen, B.; Dehaen, W., Postfunctionalization of the BODIPY Core: Synthesis and Spectroscopy. *Eur. J. Org. Chem.* **2015,** *2015* (30), 6577-6595.

7. Loudet, A.; Burgess, K., BODIPY Dyes and Their Derivatives: Syntheses and Spectroscopic Properties. *Chem. Rev.* **2007,** *107* (11), 4891-4932.

8. Rohand, T.; Baruah, M.; Qin, W.; Boens, N.; Dehaen, W., Functionalisation of fluorescent BODIPY dyes by nucleophilic substitution. *Chem. Commun.* **2006,** (3), 266-268.

9. Rohand, T.; Qin, W.; Boens, N.; Dehaen, W., Palladium-Catalyzed Coupling Reactions for the Functionalization of BODIPY Dyes with Fluorescence Spanning the Visible Spectrum. *Eur. J. Org. Chem.* **2006,** *2006* (20), 4658-4663.

10. Leen, V.; Braeken, E.; Luckermans, K.; Jackers, C.; Van der Auweraer, M.; Boens, N.; Dehaen, W., A versatile, modular synthesis of monofunctionalized BODIPY dyes. *Chem. Commun.* **2009,** (30), 4515-4517.

11. Basaric, N.; Baruah, M.; Qin, W.; Metten, B.; Smet, M.; Dehaen, W.; Boens, N., Synthesis and spectroscopic characterisation of BODIPY® based fluorescent off-on indicators with low affinity for calcium. *Org. Biomol. Chem.* **2005,** *3* (15), 2755-2761.

12. Baruah, M.; Qin, W.; Vallée, R. A. L.; Beljonne, D.; Rohand, T.; Dehaen, W.; Boens, N., A Highly Potassium-Selective Ratiometric Fluorescent Indicator Based on BODIPY Azacrown Ether Excitable with Visible Light. *Org. Lett.* **2005,** *7* (20), 4377-4380.

13. Sonnet, P. E., Preparation and properties of ternary iminium salts of pyrrole aldehydes and ketones. Synthesis of 4-substituted pyrrole-2-carboxaldehydes. *J. Org. Chem.* **1972,** *37* (7), 925-929.

14. Jiao, L.; Pang, W.; Zhou, J.; Wei, Y.; Mu, X.; Bai, G.; Hao, E., Regioselective Stepwise Bromination of Boron Dipyrromethene (BODIPY) Dyes. *J. Org. Chem.* **2011,** *76* (24), 9988-9996.

15. Ortiz, M. J.; Agarrabeitia, A. R.; Duran-Sampedro, G.; Bañuelos Prieto, J.; Lopez, T. A.; Massad, W. A.; Montejano, H. A.; García, N. A.; Lopez Arbeloa, I., Synthesis and functionalization of new polyhalogenated BODIPY dyes. Study of their photophysical properties and singlet oxygen generation. *Tetrahedron* **2012,** *68* (4), 1153-1162.

16. Wang, H.; Vicente, M. G. H.; Fronczek, F. R.; Smith, K. M., Synthesis and Transformations of 5-Chloro-2,2′-Dipyrrins and Their Boron Complexes, 8-Chloro-BODIPYs. *Chem. Eur. J.* **2014,** *20* (17), 5064-5074.

17. Zhao, J.; Xu, K.; Yang, W.; Wang, Z.; Zhong, F., The triplet excited state of Bodipy: formation, modulation and application. *Chem. Soc. Rev.* **2015 ,** *44,* 8904-8939.

18. Zhao, N.; Xuan, S.; Byrd, B.; Fronczek, F. R.; Smith, K. M.; Vicente, M. G. H., Synthesis and regioselective functionalization of perhalogenated BODIPYs. *Org. Biomol. Chem.* **2016,** *14* (26), 6184-6188.

19. Jiao, L.; Yu, C.; Uppal, T.; Liu, M.; Li, Y.; Zhou, Y.; Hao, E.; Hu, X.; Vicente, M. G. H., Long wavelength red fluorescent dyes from 3,5-diiodo-BODIPYs. *Org. Biomol. Chem.* **2010,** *8* (11), 2517-2519.

20. Jiao, L.; Li, J.; Zhang, S.; Wei, C.; Hao, E.; Vicente, M. G. H., A selective fluorescent sensor for imaging Cu2+ in living cells. *New J. Chem.* **2009,** *33* (9), 1888-1893.

21. Meng, Q.; Fronczek, F. R.; Vicente, M. G. H., Synthesis and Spectroscopic Properties of β,β'-Dibenzo-3,5,8-triaryl-BODIPYs. *New J. Chem.* **2016**, 5740-5751.

22. H.R. Barton, D.; Kervagoret, J.; Zard, S. Z., A useful synthesis of pyrroles from nitroolefins. *Tetrahedron* **1990,** *46* (21), 7587-7598.

23. Gibbs, J. H.; Robins, L. T.; Zhou, Z.; Bobadova-Parvanova, P.; Cottam, M.; McCandless, G. T.; Fronczek, F. R.; Vicente, M. G. H., Spectroscopic, computational modeling and cytotoxicity of a series of meso-phenyl and meso-thienyl-BODIPYs. *Biorg. Med. Chem.* **2013,** *21* (18), 5770-5781.

24. Wang, H.; Fronczek, F. R.; Vicente, M. G. H.; Smith, K. M., Functionalization of 3,5,8-Trichlorinated BODIPY Dyes. *J. Org. Chem.* **2014,** *79* (21), 10342-10352.

25. Zhao, N.; Vicente, M. G. H.; Fronczek, F. R.; Smith, K. M., Synthesis of 3,8-Dichloro-6-ethyl-1,2,5,7-tetramethyl–BODIPY from an Asymmetric Dipyrroketone and Reactivity Studies at the 3,5,8-Positions. *Chem. Eur. J.* **2015,** *21* (16), 6181-6192.

26. Lakhe, D.; Jairaj, K. K.; Pradhan, M.; Ladiwala, U.; Agarwal, N., Synthesis and photophysical studies of heteroaryl substituted-BODIPy derivatives for biological applications. *Tetrahedron Lett.* **2014,** *55* (51), 7124-7129.

27. Gibbs, J. H.; Zhou, Z.; Kessel, D.; Fronczek, F. R.; Pakhomova, S.; Vicente, M. G. H., Synthesis, spectroscopic, and in vitro investigations of 2,6-diiodo-BODIPYs with PDT and bioimaging applications. *J. Photochem. Photobiol., B* **2015,** *145*, 35-47.

28. Uppal, T.; Bhupathiraju, N. V. S. D. K.; Vicente, M. G. H., Synthesis and cellular properties of Near-IR BODIPY–PEG and carbohydrate conjugates. *Tetrahedron* **2013,** *69* (23), 4687-4693.

29. Gai, L.; Mack, J.; Lu, H.; Yamada, H.; Kuzuhara, D.; Lai, G.; Li, Z.; Shen, Z., New 2,6-Distyryl-Substituted BODIPY Isomers: Synthesis, Photophysical Properties, and Theoretical Calculations. *Chem. Eur. J.* **2014,** *20* (4), 1091-1102.

30. Yu, C.; Xu, Y.; Jiao, L.; Zhou, J.; Wang, Z.; Hao, E., Isoindole-BODIPY Dyes as Red to Near-Infrared Fluorophores. *Chem. Eur. J.* **2012,** *18* (21), 6437-6442.

31. Jiao, L.; Wu, Y.; Wang, S.; Hu, X.; Zhang, P.; Yu, C.; Cong, K.; Meng, Q.; Hao, E.; Vicente, M. G. H., Accessing Near-Infrared-Absorbing BF2-Azadipyrromethenes via a Push–Pull Effect. *J. Org. Chem.* **2014,** *79* (4), 1830-1835.

32. Baruah, M.; Qin, W.; Flors, C.; Hofkens, J.; Vallée, R. A. L.; Beljonne, D.; Van der Auweraer, M.; De Borggraeve, W. M.; Boens, N., Solvent and pH Dependent Fluorescent Properties of a Dimethylaminostyryl Borondipyrromethene Dye in Solution. *The Journal of Physical Chemistry A* **2006,** *110* (18), 5998-6009.

33. Uppal, T.; Hu, X.; Fronczek, F. R.; Maschek, S.; Bobadova-Parvanova, P.; Vicente, M. G. H., Synthesis, Computational Modeling, and Properties of Benzo-Appended BODIPYs. *Chem. Eur. J.* **2012,** *18* (13), 3893-3905.

34. Olmsted, J., Calorimetric determinations of absolute fluorescence quantum yields. *The Journal of Physical Chemistry* **1979,** *83* (20), 2581-2584.

35. Gorka, A. P.; Nani, R. R.; Zhu, J.; Mackem, S.; Schnermann, M. J., A Near-IR Uncaging Strategy Based on Cyanine Photochemistry. *J. Am. Chem. Soc.* **2014,** *136* (40), 14153-14159.

Chapter III: AROMATIC SUBSTITUTION REACTIONS ON IODINATED-BODIPYS

3.1 Introduction

Functionalization on BODIPY molecules opens a door to numerous BODIPY applications, particularly as chemeosensors. Numerous novel BODIPYs with a variety of physical, chemical and biological properties have been prepared via aromatic substitution reactions, thus this type of reaction has drawn tremendous attention in the last ten years. [1-2]

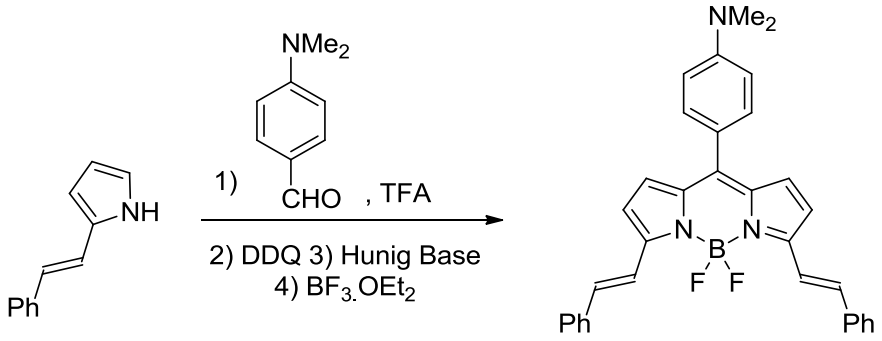

Scheme 3.1: Syntheses of a BODIPY with styryl groups from styrylated pyrrole[3]

Arylated and styrylated BODIPYs can be prepared via post-functionalization reactions on halogenated BODIPYs, for example via Stille, Suzuki, Sonogashira and Heck cross-coupling reactions[4-14], or they can be produced from condensations of arylated or styrylated pyrroles or isoindoles, as shown in Scheme 3.1. The introduction of heteroatoms at the 3,5-positions significantly changes a number of physical and chemical properties of BODIPY chromophores, such as water solubility, absorption and emission spectra and electron density. However the corresponding pyrroles are rarely reported and prepared, due to their relatively difficult preparation and low stability. Therefore, the investigation of functionalizing BODIPY at the 3, 5-positions was attempted, by using 3, 5-dichloro- and 3, 5-dibromo-BODIPYs with various nucleophiles.

3.1.1 Advantages of aromatic substitution reactions on 3,5-dihalogenated BODIPYs

In 2005, Boens and co-workers reported the synthesis of a novel fluorescent sensor. They prepared a 3-methoxy-5-chloro-BODIPY via an aromatic substitution reaction on a 3,5-dichloro-BODIPY, and the second chlorine was replaced by aza-18-crown-6 to give the sensor molecule in the presence of an amine, as shown in Scheme 3.2.[15]

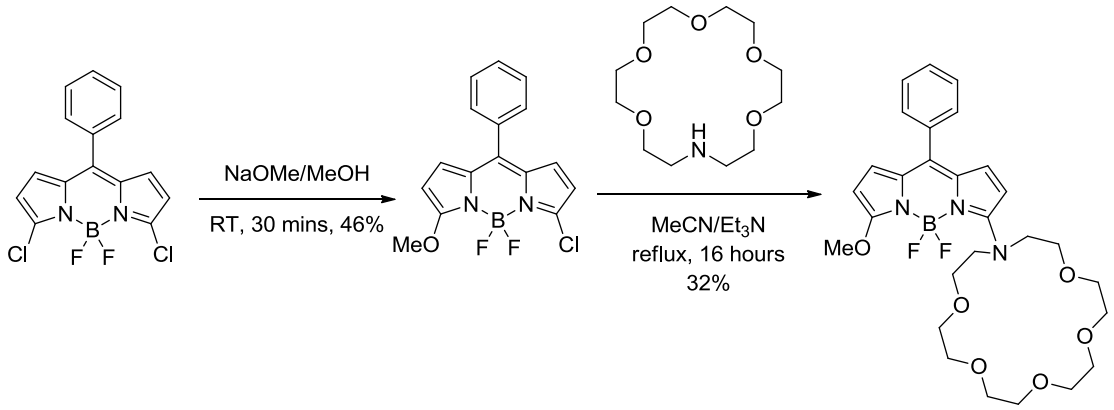

Scheme 3.2: Synthesis of a K^+ sensor via S_NAr reactions on a3,5-Cl_2-BODIPY[15]

When the sensor is treated with potassium ion, significant changes in absorption and emission were observed, due to the coordination of the cation to the donor nitrogen atom of the aza-crown. This inhibits the intramolecular charge transfer (ICT) process to the acceptor BODIPY, thus after a fast ICT process, a large cation-induced fluorescence enhancement was observed.

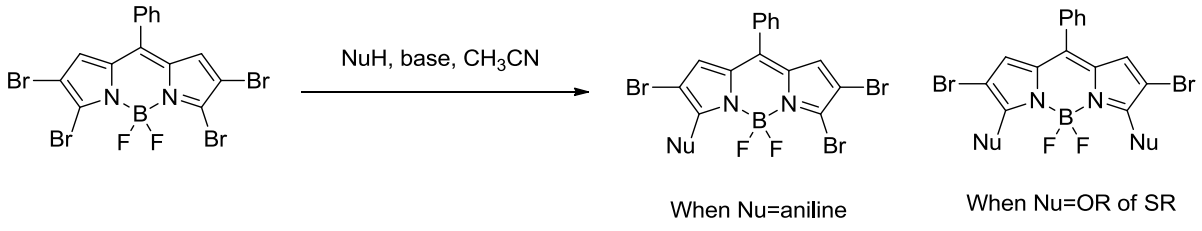

Scheme 3.3: Aromatic substitution reactions on a tetrabromo-BODIPY

The Hao and Jiao research group reported the synthesis of polybrominated BODIPYs and their further substitution reactions. Several aromatic substitution reactions were performed on

tetra- and hepta-brominated BODIPYs, giving substituted BODIPYs in high yields and short reaction times, as shown in Scheme 3.3.[16] They also discovered that pyrroles are reactive nucleophiles in the substitution chloro- and bromo- groups on BODIPYs to give the formation of new C-C bonds, in the presence or absence of Lewis acids.[17-19] The highly regioselective substitution reactions did not require Pd catalysts, and they produced highly red-shifted BODIPYs, which were synthetic precursors of oligopyrroles for medicinal, material and supramolecular chemistry applications. In 2009, the syntheses of a water-soluble BODIPY was also reported by treating a 3,5-diiodo-BODIPY with N,N-bis(2-hydroxyethyl)amine. The resulting BODIPY detects Cu^{2+} in aqueous solution, showing a quenched emission with 0.1 equiv. of Cu^{2+},[20] as shown in Scheme 3.4.

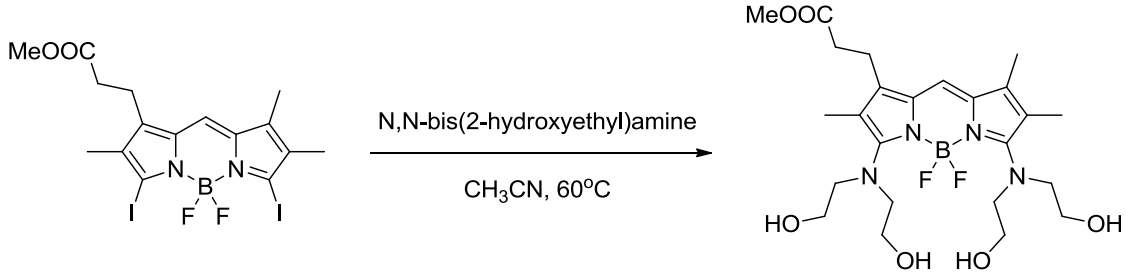

Scheme 3.4: Aromatic substitution on a 3,5-diiodoBODIPY to give a sensor for Cu^{2+}

3.1.2 SPECT and PET

Positron emission tomography/computed tomography (PET/CT) is a nuclear medicinal technique that is been used to observe various metabolic processes in clinical studies, which was commercially introduced in 2001. PET detects radiolabeled compounds containing a positron-emitting radionuclide (tracer), such as ^{18}F and ^{64}Cu, which is usually introduced into the body on a bio-molecule. The combined CT method improves quantitation of more accurate functional images. [21]

Single-photon emission computed tomography (SPECT) is another nuclear medicine imaging technique that detects gamma rays, as in PET. However, the tracers used in SPECT are often prepared in situ, by using commercially available reagents and kits, followed by detection. As a result, SPECT scans are significantly cheaper than PET scans, mainly because SPECT uses longer-lived and easier obtained radio-isotopes, such as ^{123}I and ^{111}In. [22]

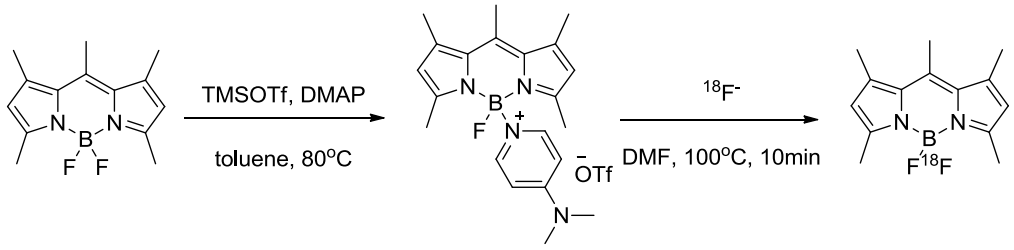

Scheme 3.5: BF_2 unit's activation with DMAP and TMSOTf[21]

In 2012, Weissleder & Mazitschek employed TMSOTf and DMAP to functionalize BODIPY's BF_2 units, by replacing one fluoride atom with a DMAP molecule. The highly reactive intermediate was quickly replaced by $^{18}F^-$ in DMF to give $^{18}F^-$ radiolabeled BODIPYs, as shown in Scheme 3.5. With a stable N-hydroxysuccinimide ester (unreactive in the presence of TMSOTf) at the *meso*- position, the radioactive BODIPY was conjugated with Trastuzumab at room temperature in a PBS-solution.[21] In 2012, Denat *et al* reported similar research with $^{18}F^-$ labeled BODIPY. However, instead of using a NHS group at the *meso*- position, they employed isothiocyanate or azide group at the *meso*- position. Gabbai *et al* not only developed BODIPYs with an NHS group at the 3-position, but also employed ionized p-dimethylaminophenyl groups at the *meso*- position to enhance the water solubilitity.[23]

Denat *et al* reported the synthesis of BODIPY-DOTA (1,4,5,10-tetraazacyclododecane-1,4,7,10-tetraacetic acid) derivatives, and a DOTA unit was installed at the *meso*- phenyl groups. The ^{111}In-DOTA-BODIPY-LPS was visualized over 24 hours in a whole animal by SPECT-CT, and a major amount was localized in the liver.[22]

3.1.4 Research goals

Since 3,5-diiodo-BODIPYs and 2,3,5,6-tetraiodo-BODIPYs are important precursors, we performed various aromatic substitution reactions to prepare a variety of functionalized BODIPYs. The substitution reactions, particularly between the iodinated BODIPY and the ^{123}I anion, is also a potential method for radiolabeling BODIPY with ^{123}I for future SPECT studies.

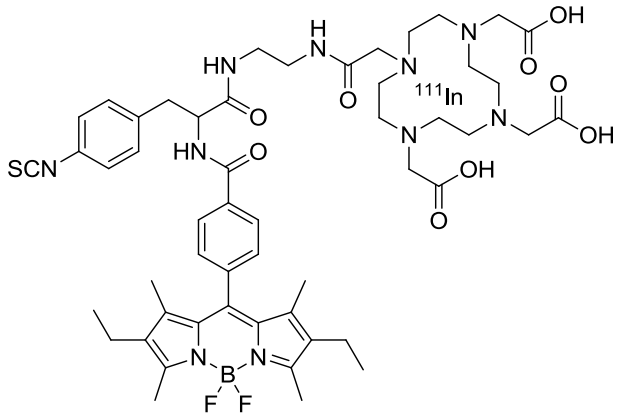

Figure 3.1: BODIPY-DOTA derivatives for SPECT-CT studies

In 2013 and 2015, our research group reported the synthesis and biological evaluation of a series of BODIPYs containing iodine at the 2,6-positions, and *in vitro* studies indicated that *meso*-methoxyphenyl groups enhanced phototoxicity significantly, while unsymmetric BODIPYs tended to show higher photoxicity. In this Chapter, we will also study aromatic substitution reactions to produce potential BODIPY photosensitizers with heteroatoms at the 3- and/or 5-positions.

3.2 Results and Discussion

3,5-Diiodo-BODIPY **1a** and **1b**'s synthesis was described in Chapter II. Herein we employed them as major platforms to perform aromatic substitution reactions. 2,3,5,6-Tetraiodo-*meso*-tolyl-BODIPY **2**, also prepared in Chapter II, was expected to be more reactive toward

aromatic substitution conditions, due to the electro-withdrawing effect from the iodine groups at the 2,6-positions.

3.2.1 S_NAr substitution on 3,5-diiodo-BODIPYs

3.2.1.1 S_NAr substitution of 3,5-diiodo-BODIPY with S nucleophiles

Based on the developed methods of S_NAr reactions performed on chlorinated and brominated BODIPYs, BODIPY **1a** was treated with excess benzenethiol in anhydrous dichloromethane. When no base was present, no desired substitution product was obtained. Triethylamine and potassium carbonate were both attempted as the organic and inorganic base with similar pK_a values, and the reactions were performed at room temperature and monitored by TLC. When one drop (~0.05 mL) of triethylamine was used, the desired BODIPY **3a** was obtained within 10 minutes in 88% yield. Ten equivalents of potassium carbonate were also able to produce BODIPY **3a** after 12 hours, in 81% yield, which indicated that the inorganic base is less efficient in catalyzing the thiol substitution reaction, mainly due to its low solubility. A crystal of BODIPY **3a** was obtained, and X-ray crystallography analysis gave the structure shown in Figure 3.2. The two thiol groups sit on the same side of the BODIPY molecule, and the average C-S bond length of C-S bonds is 1.750 Å. The aryl groups from thiol form an average dihedral angle of 80.9º with the BODIPY core, and the *meso*-aryl group is almost perpendicular with the C_3N_2B plane.

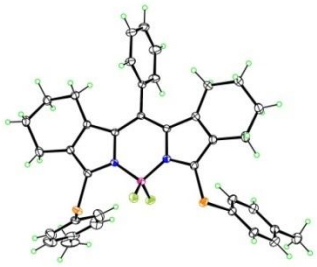

Figure 3.2: Molecular structure of BODIPY **3a** from X-ray crystal structure.

4-Methylbenzenethiol was also employed as another aryl thiol, and in presence of one drop of triethylamine, BODIPY **3b** was obtained in a similar yield of 86% in 10 minutes. Benzene mercaptan was further investigated as an alkyl thiol to substitute at the 3,5-positions, and BODIPY **3c** was obtained in a 75% yield after 2 hours. One or less equivalent of aryl and alkyl thiols were used with BODIPY **1a** to prepare unsymmetrical BODIPYs with only one iodine atom replaced, but all attempts failed, and the products were a mixture of starting material **1a** and disubstituted BODIPYs. This was probably due to the fast reaction rate of the di-substitution reaction, and all nucleophiles were consumed before the reaction stopped at the mono-substituted intermediate stage.

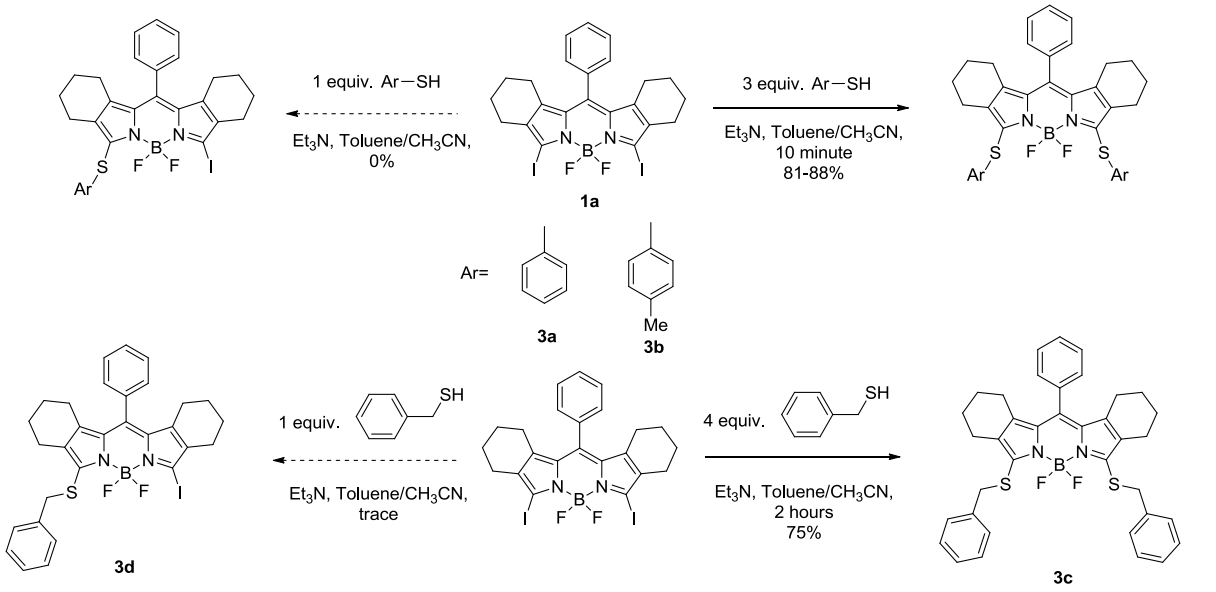

Scheme 3.5: S_NAr reactions on 3,5-diiodo-BODIPY **1a** with thiol nucleophiles

3.2.1.2 S_NAr substitution of 3,5-diiodo-BODIPY with O nucleophiles

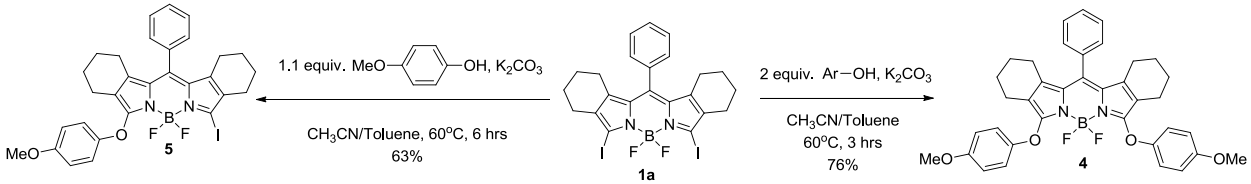

Scheme 3.6: Mono- and di-S_NAr reactions between 3,5-diiodo-BODIPY **1a** and 4-OMe-phenol

4-Methoxyphenol was employed as an oxygen nucleophile, but no desired substitution product was obtained, following identical conditions from the thiol S_NAr reactions, probably because the phenolic nucleophiles are less reactive. Acetonitrile is a common solvent for most S_NAr reactions on brominated and chlorinated BODIPYs due to its relatively high polarity,[16, 24] but since it only dissolved BODIPY **1a** slightly, toluene was added as a co-solvent to enhance the solubility. Three equivalents of 4-methoxyphenol were able to replace two iodine atoms on BODIPY **1a**, in the presence of 10 equivalents of potassium carbonate, to give BODIPY **4** in 76% yield, after heating at 60 ^oC for 3 hours. Additional equivalents of 4-methoxyphenol were even more efficient to push the equilibrium to the products, but the removal of the excess nucleophile was difficulty. When BODIPY **1a** was treated with one equivalent of 4-methoxyphenol, unsymmetrical BODIPY **5** was prepared and isolated after 12 hours in 63% yield, as shown in Scheme 3.6.

The reactivity of BODIPY **5**'s iodic-position was then investigated. BODIPY **5** was mixed with one equivalent of 4-methylbenzenethiol, in the presence of one drop of triethylamine, and the completion of reaction was achieved within one minute, which was confirmed by TLC. However, ^{1}H-NMR, and UV-Vis spectroscopy demonstrated the product was

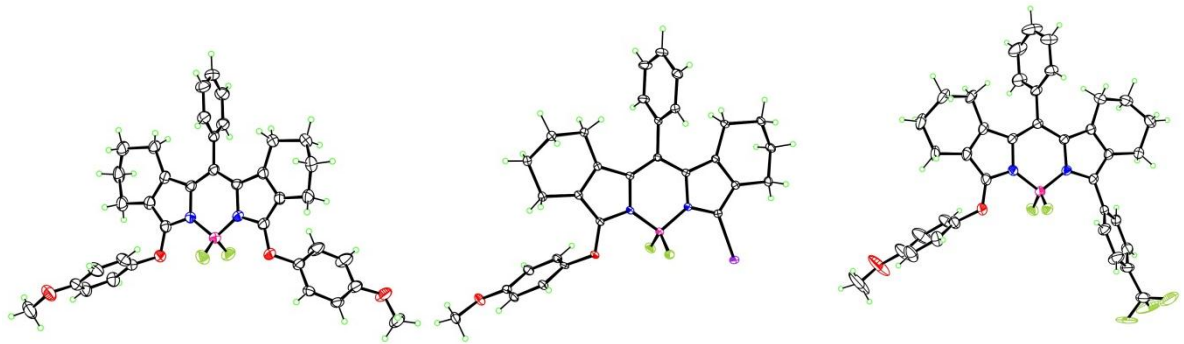

4 **5** **7**

Figure 3.3: Molecular structures of BODIPYs **4**, **5** and **7** from X-ray crystallography.

BODIPY **3b** in an 82% yield. This result indicated that the phenoxide ion is a better leaving group, and sulfur-substituted BODIPYs are more stable. Palladium-catalyzed cross coupling reactions were also attempted, including Stille and Suzuki coupling reactions, developed in Chapter II. A typical Stille reaction conditions, including 5 equivalents of 2-(tributylstannyl)thiophene and catalytic amount of $Pd(dppf)Cl_2$, were applied on BODIPY **5** in refluxing toluene, but the corresponding BODIPY **6** was isolated in only a trace amount. This result might be due to decomposition of BODIPY **5** under the high temperature during the Stille reaction. A Suzuki reaction between BODIPY **5** and five equivalents of 4-trifluoromethylphenyl boronic acid was performed, in the presence of a catalytic amount of $Pd(dppf)Cl_2$ and ten equivalents of potassium carbonate, and BODIPY **7** was isolated in 88% yield, as shown in Scheme 3.7.

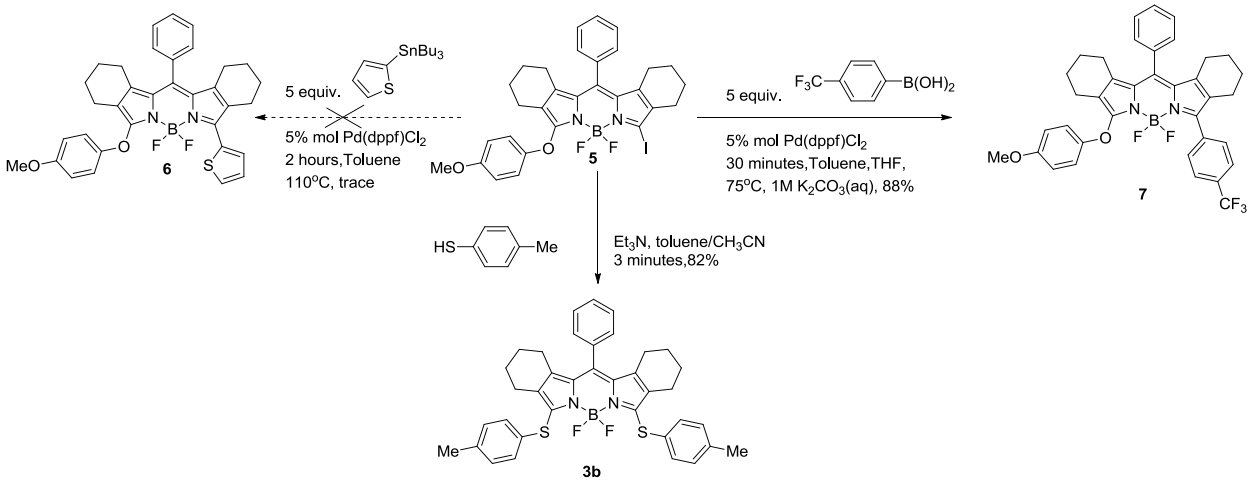

Scheme 3.7: Stille, Suzuki cross-coupling reactions and a thiol S_NAr reaction on BODIPY **5**

BODIPYs **4**, **5** and **7** were characterized by X-ray crystallography, and their structures are shown in Figure 3.3. The lengths of the C-O bonds are in the range 1.345-1.360 Å, which are relatively shorter than the C-S bond. BODIPY **5**'s C-I bond is fairly long with 2.066 Å, and this also explains the high efficiency of the Suzuki cross coupling reaction, but not the Stille reaction.

The *meso*-phenyl rings form dihedral angles in the range 72.4-79.1º with the C_3N_2B planes, and the phenyl groups from the phenols form dihedral angles in the range 76.6-88.4º with the central cores. The phenyl group with trifluoromethyl unit forms a 72.4º angle with the BODIPY core, which is similar to the previous report. [6]

3.2.1.3 S_NAr substitution of 3,5-diiodo-BODIPY with C nucleophiles

Since the aromatic substitution reaction between 3,5-diiodo-BODIPY and amine nucleophiles were studied and reported in 2007,[20] carbon nucleophiles were then employed to functionalize BODIPY **1a**, and sodium hydride was employed as the base to deprotonate the α-proton from the malonate molecule. The reaction was performed in refluxing acetonitrile and toluene (1:1) mixture by treating BODIPY **1a** with 3 equivalents of diethyl malonate. The mono-substituted BODIPY was collected in 5% yield after 2 hours, and this low yield is probably due to the relatively low solubility. BODIPY **1b** was employed to react with three equivalents of diethyl malonate under the same conditions, and mono-substituted BODIPY **8a** was produced in 65% yield after overnight reflux. Ten equivalents of ethyl malonate after 24 hours were able to give di-substituted BODIPY **8b** in 33% yield, and more than twenty equivalents of diethyl malonate were able to facilitate the di-substitution reaction much faster, but the removal of the unreacted malonate was difficult. The conditions and yields are shown in Scheme 3.8.

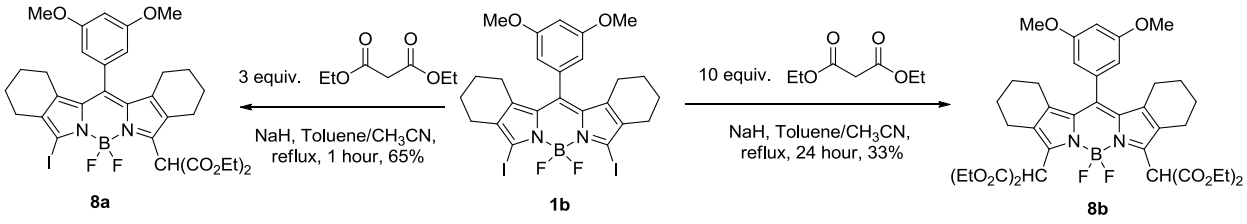

Scheme 3.8: Mono- and di-S_NAr reactions between 3,5-diiodo-BODIPY and ethyl malonate

3.2.1.4 S_NAr substitution of 3,5-iodinated BODIPY with phenyl and OMe on the boron

To further investigate the reactivity of the 3,5-diiodo-BODIPYs, we also substituted BODIPY's BF_2 unit with a phenyl and a methoxy group. Diiodo-dipyrromethene **9** was activated with triethylamine in anhydrous DCM, and then phenyl boron dichloride was added to give a reactive intermediate with the chlorine atom as a good leaving group. The boron was then substituted with methoxy group by reacting with sodium methoxide, and BODIPY **10** was obtained in 58% yield.

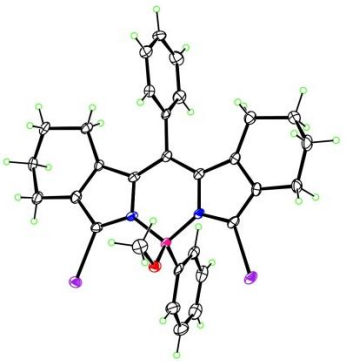

Figure 3.4**:** Molecular structure of BODIPY **10** from X-ray crystallography

A suitable crystal structure for X-ray crystallography was obtained, as shown in Figure 3.4, demonstrating that the iodine atoms at the 3,5-positions of the BODIPY were not replaced by methoxide ions. The *meso*-phenyl ring forms a dihedral angle of 72.4º, while the phenyl and methoxy units on the boron atom are almost perpendicular with the main core. The relatively long C-I bonds (average: 2.064 Å) promote the reactivity of the 3,5-positions of the BODIPY molecule.

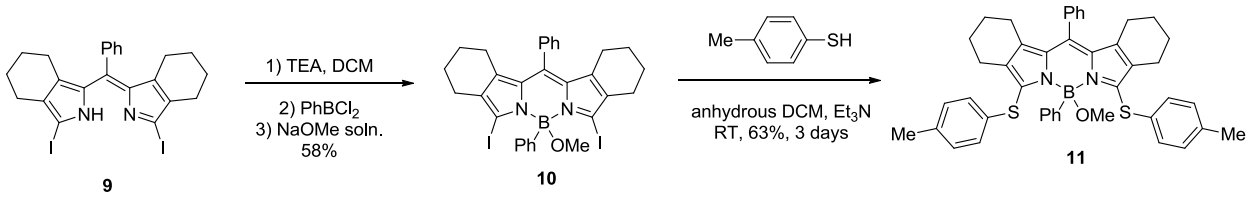

Scheme 3.9: Preparation of boron substituted BODIPY **10** and its S_NAr reaction

BODIPY **10**'s reactivity under aromatic substitution conditions was studied via thiol substitution, by treating BODIPY **10** with excess 4-methyl-benzenethiol, in the presence of an organic base. The substitution reaction was much slower than the one of BODIPY **1a**, but the targeting product was still produced and isolated after a 3-day reaction at room temperature in 63% yield, as shown in Scheme 3.9.

3.2.1.5 Radiolabeling of 3,5-Diiodo-BODIPYs 1a,b with ^{123}I

Since 3,5-diiodo-BODIPY **1a** and **1b** show relatively high reactivity under most aromatic substitutions, we also apply this result to obtain $^{123}I^-$ labeled BODIPYs for potential SPECT studies, by treating **1a,b** with ^{123}I sources as shown in Scheme 3.10. The only commercial source of ^{123}I is 1.0 mCi $Na^{123}I$ (< 10^{-6} M) in 0.1 N NaOH, which is a challenge due to potential side reactions at the boron atom.

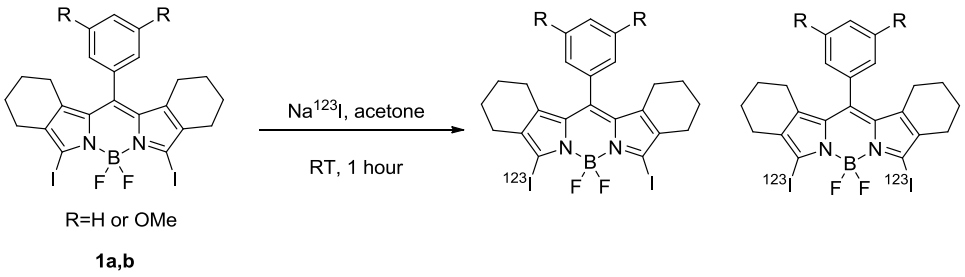

Scheme 3.10: Proposed radio-labeling reaction of 3,5-diiodo-BODIPYs **1a,b**

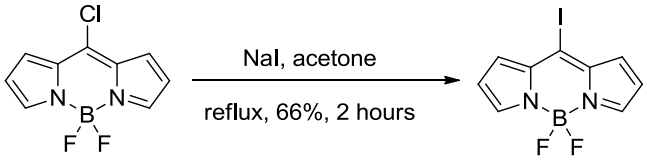

Scheme 3.11: Preparation of a *meso*-iodo-BODIPY from a *meso*-chloro-BODIPY

In 2012, Dehaen *et al* reported that *meso*-chloro-BODIPY was able to be substituted by iodide ions in acetone, giving *meso*-iodo-BODIPY in 66% yield, as shown in Scheme 3.11. BODIPY **1b** reacted with NaCl or NaBr in acetone, respectively, and 1 hour later mass spectroscopy results indicated the formation of mono- and di-substituted BODIPYs. This result

demonstrated partial substitution reaction occurred between 3,5-diiodo-BODIPY and halide anions, as shown in Scheme 3.12.

Although the iodine atoms at the 3,5-position are relatively stable in the presence of oxygen nucleophiles (NaOMe and 4-methoxy-phenol) at room temperature, the stability of the BODIPY under basic conditions needed to be confirmed. The BF_2 units of BODIPYs could potentially be substituted with hydroxyl groups to give $B(OH)_2$ units, and the $B(OH)_2$ units would chelate with another hydroxyl group to leave as a boronic acid and give low fluorescent dipyrromethene, as shown in Scheme 3.13. BODIPY **1b** reacted with 1 equivalent of sodium hydroxide in acetone, and after one hour, both ^{11}B NMR and fluorescence emission measurements demonstrated almost no decomposition occurred.

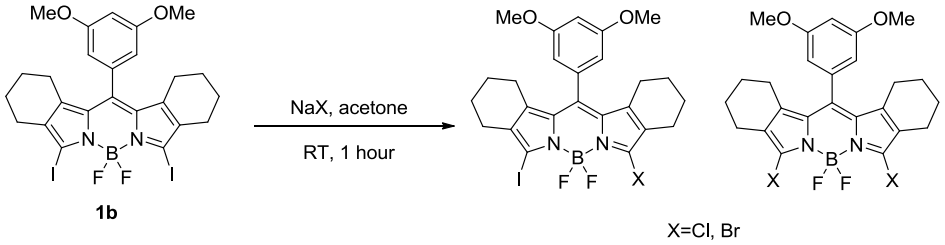

Scheme 3.12: Reactivity studies on 3,5-diiodo-BODIPY **1b**

BODIPY **1b** was then dissolved in acetone, and different concentrations at BODIPY **1b** solutions were reacted with $Na^{123}I$ in the presence of NaOH. Time-dependent TLC and film visualization results indicated that ^{123}I was successfully loaded onto the BODIPY platform, as shown in Figure 3.5. The iodinated BODIPY showed an approximately R_f value≈0.5 in EtOAc:Hex=1:4, and the radiolabeled molecules were visualized on the film after overnight exposure. As the spots were getting darker, higher amounts of iodinated BODIPYs were successfully replaced with ^{123}I anion, from 5 minutes to 1 hour.

3.2.2 S_NAr Substitution on 2,3,5,6-Tetraiodo-BODIPYs

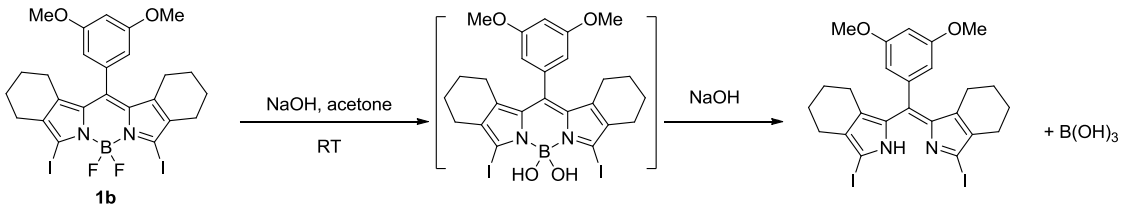

Scheme 3.13: Potential decomposition reactions caused by NaOH

Among the reported 2,3,5,6-tetrabromo-BODIPY and 2,3,5,6,8-pentachloro-BODIPY, the halogen atoms at the 2,6-positions are unreactive under S_NAr conditions, because of the partially negative charge at the 2,6-positions.[14, 16] Some 2,6-dibromo- and 2,6-diiodo-BODIPYs are reported as photosensitizers and singlet oxygen generators, but most of their 3,5-positions are blocked or substituted by alkyl, aryl or styryl units.

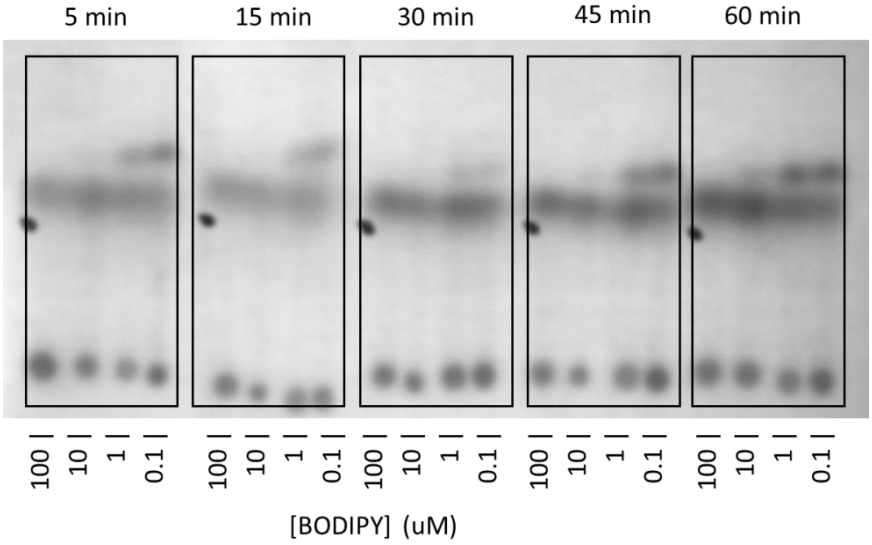

Figure 3.5: Film-visualization demonstration of ^{123}I radio-labeling

3.2.2.1 S_NAr substitution of 2,3,5,6-tetraiodo-BODIPY with S nucleophiles

4-Methyl-benzenethiol was first employed as the nucleophile, and similar conditions to those used for 3,5-diiodo-BODIPY **1a,b** were applied. BODIPY **2** reacted with two equivalents of thiol in acetonitrile, in the presence of triethylamine. The reaction was rapidly completed upon addition of triethylamine and the resulting 3,5-disubstituted BODIPY **12** was isolated in 94%

yield, as shown in Scheme 3.14. Mono-substitution was also attempted too, by treating one equivalent of thiol with BODIPY **2**, but TLC indicated the resulting solution was a mixture of starting material and di-substituted product **12**. This is probably due to the very high reactivity of the 3,5-positions towards thiol substitution reactions.

3.2.2.2 S_NAr substitution of 2,3,5,6-tetraiodo-BODIPY with O nucleophiles

Oxygen nucleophiles were then studied, following similar conditions to those described earlier for BODIPY **1a**, **b's** substitution. Excess amount of 4-methoxyphenol were added into a solution of BODIPY **2** in CH_3CN in the presence of potassium carbonate, and TLC indicated the consumption of BODIPY **2** within 5 minutes, affording BODIPY **13** in 89% yield. To investigate the mono-substitution reaction, BODIPY **2** was treated with one equivalent of 4-methoxyphenol, followed by addition of two equivalents of potassium carbonate. The completion of this reaction was detected after five minutes, and BODIPY **14** was obtained in 89% yield, as shown in Scheme 3.15. Instead of requirements of prolonged reaction time, heat, and large excess of base, tetraiodo-BODIPY **2** showed much higher reactivity in S_NAr reactions, and both mono- and di-substitution reactions were accomplished at room temperature and shorter time.

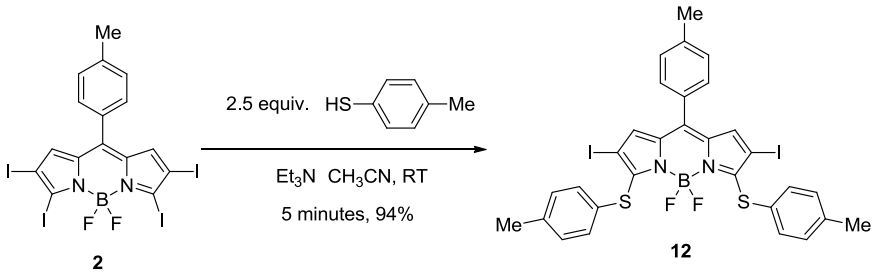

Scheme 3.14: S_NAr reactions between tetraiodo-BODIPY **2** and 4-methyl-benzenethiol

3.2.2.3 S_NAr substitution of 2,3,5,6-tetraiodo-BODIPY with N nucleophiles

Aniline was employed as the nitrogen nucleophile to investigate the reactivity of tetraiodo-BODIPY 2. One equivalent of aniline was mixed with BODIPY **2**, and it afforded

mono-substituted BODIPY **15** in 78% yield after 30 minutes, without the presence of an additional base, as shown in Scheme 3.16. However, the aromatic substitution reaction stopped at the mono-substitution product, even when a large excess of aniline or additional organic base, and heating conditions were employed. This observation is in agreement with previous published results by Ortiz *et al*.[25]

3.2.2.4 S_NAr substitution of 2,3,5,6-tetraiodo-BODIPY with C nucleophiles

Tetraiodo-BODIPY's reactivity was also studied with carbon nucleophile, and ethyl malonate was employed as the nucleophile. The mono-substitution reaction was performed in refluxing acetonitrile, in the presence of one equivalent of ethyl malonate and sodium hydride, and BODIPY **16** was produced after 10 minutes in 72% yield. Changing the ethyl malonate's equivalents to 2.5 equivalents afforded BODIPY **17** in 69% yield after 5 hour reaction time.

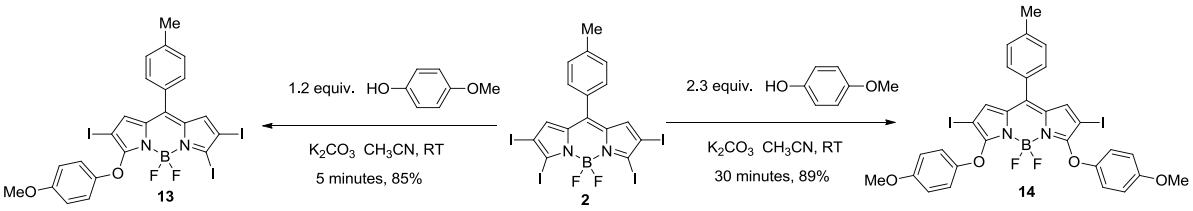

Scheme 3.15: Mono- and di-S_NAr reactions between tetraiodo-BODIPY **2** and 4-OMe-phenol

For BODIPY **16**, although one iodine atom was replaced by the malonate, the other iodo-position was expected to be relatively reactive, due to the electron withdrawing effect of the iodines at the 2,6-positions. BODIPY **16** reacted with one equivalent of 4-methyl-benzenethiol, 4-methoxy-phenol and aniline, respectively, and all three reactions were performed in acetonitrile in room temperature. Unsymmetric BODIPYs **18**, **19** and **20** were produced in 68%, 66% and 58% yields, respectively, as shown in Scheme 3.18. The second S_NAr reactions all required longer time, probably due to the less reactivity and steric hindering effect from the first substituent malonate group.

3.2.3 Structural Characterization

All BODIPYs were characterized by ^{1}H-, ^{13}C- and ^{11}B-NMR, HRMS, UV-Vis and fluorescence spectroscopy. All ^{11}B-NMR except those for BODIPYs **10** and **11**, show triplets for the BF_2 units, demonstrating that among our developed conditions, no nucleophiles replaced the fluoride atoms on the boron. Boron functionalized BODIPYs **10** and **11** show a broad singlet in their ^{11}B-NMR spectra because there is no more fluoride atom that split the boron signal.

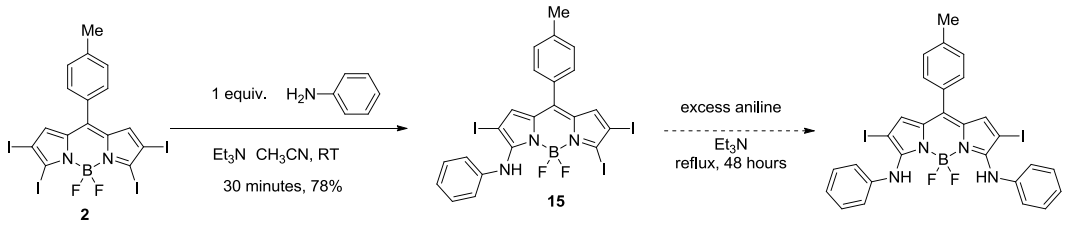

Scheme 3.16: Mono S_NAr reaction between BODIPY **2** and aniline

In proton NMR of 3,5-diiodo-BODIPYs **1a** and **1b**'s derivatives, the bicyclic units gave CH_2 peaks between 2.8 to 1.3 ppm. In the 2.8 ppm to 2.4 ppm region, symmetric BODIPYs showed a triplet of four protons, while unsymmetric BODIPYs produced two triplets signals, indicating those two CH_2 units are in different environment. The carbon NMR also agreed with this observation, because the sp^3-C region showed four signals for the symmetric BODIPYs and eight signals for the unsymmetric BODIPYs, with two different groups at the 3,5-positions.

3.2.4 Spectroscopic Studies

The spectroscopic properties of BODIPYs were investigated in THF. BODIPY **1a** and **1b**'s derivatives showed absorption bands between 528 and 580 nm and emission bands between 542 and 600 nm in THF with strong absorption bands (log ε= 4.6-5.0), as Table 3.1 summarizes. We noticed that thiol substitution was the only reaction to red-shift BODIPY's absorption and emission spectra, and phenol and malonate di-substitution gave blue-shifts. Thiol and malonate

substitution produced higher fluorescent quantum yields. 4-Trifluoromethylphenyl group not only increased the quantum yield of BODIPY **5**, but also increased the Stokes shift slightly.

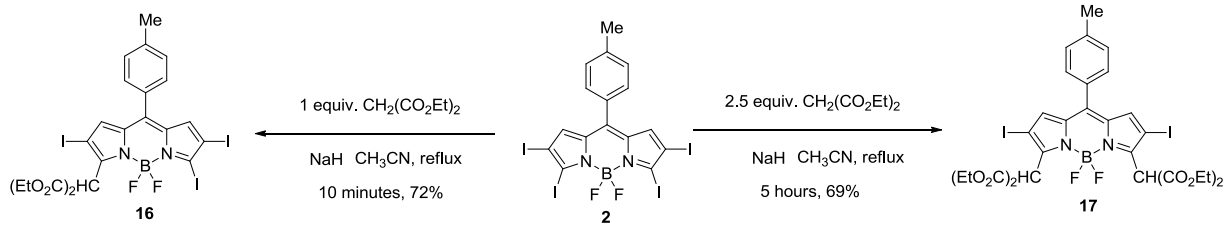

Scheme 3.17: Mono- and di-S_NAr reactions between tetraiodo-BODIPY **2** and ethyl malonate

BODIPY **2** and its derivatives showed absorption bands between 543 nm and 605 nm and emission bands between 575 nm and 637 nm (log ε= 4.7-5.2), as Table 3.2 shows. All compounds show relatively low fluorescent quantum yields, and this is because of the heavy atom effect that facilitates the S_1 to T_1 intersystem crossing process. Thiol substitution also produced the largest bathochromic shifts in the absorption and emission spectra. Aniline substitution products **15** and **20**'s absorption and emission spectra were broader than the ones of other BODIPYs and their Stokes' shifts are surprisingly higher than others. This observation is in agreement with previous papers,[26] and probably can be explained by the hydrogen bonding between the N-H and fluoride atoms from the BF_2 units.

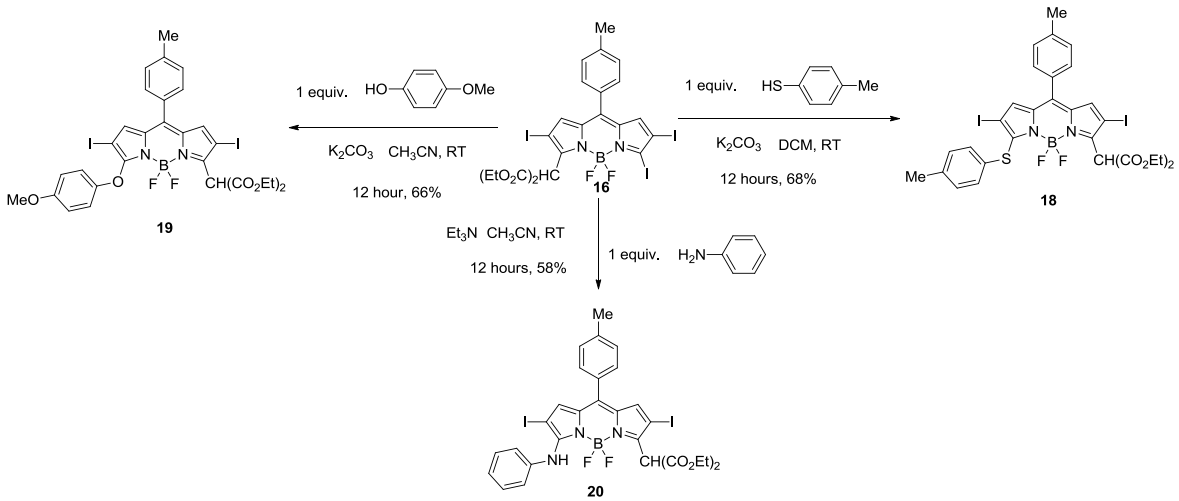

Scheme 3.18: Further S_NAr reactions on BODIPY **16** with S, O and N nucleophiles

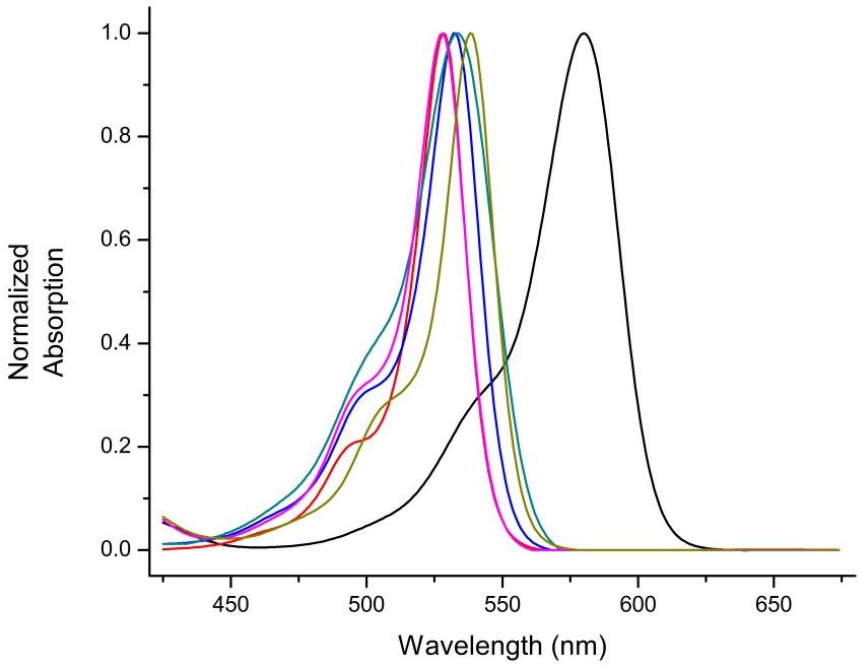

Figure 3.6: Normalized absorption spectra of BODIPYs **3b** (black), **4** (red), **5** (blue), **7** (cyan), **8a** (magenta) and **8b** (dark yellow) in THF at RT

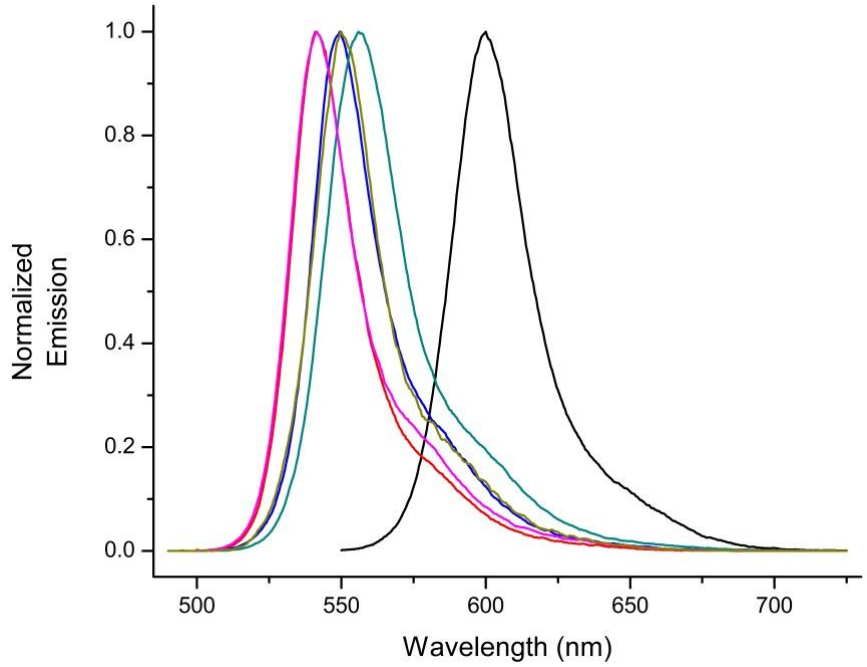

Figure 3.7: Normalized emission spectra of **3b** (black), **4** (red), **5** (blue), **7** (cyan), **8a** (magenta) and **8b** (dark yellow) in THF at RT

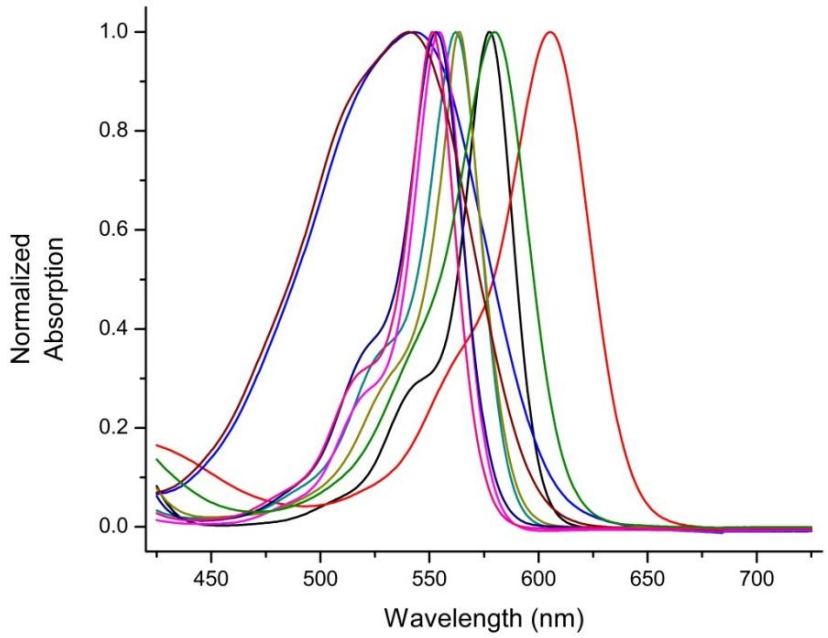

Figure 3.8: Normalized absorption spectra of BODIPYs **2** (black), **12** (red), **13** (cyan), **14** (magenta), **15** (blue), **16** (yellow), **17** (navy), **18**(olive), **19** (pink) and **20** (wine) in THF at RT

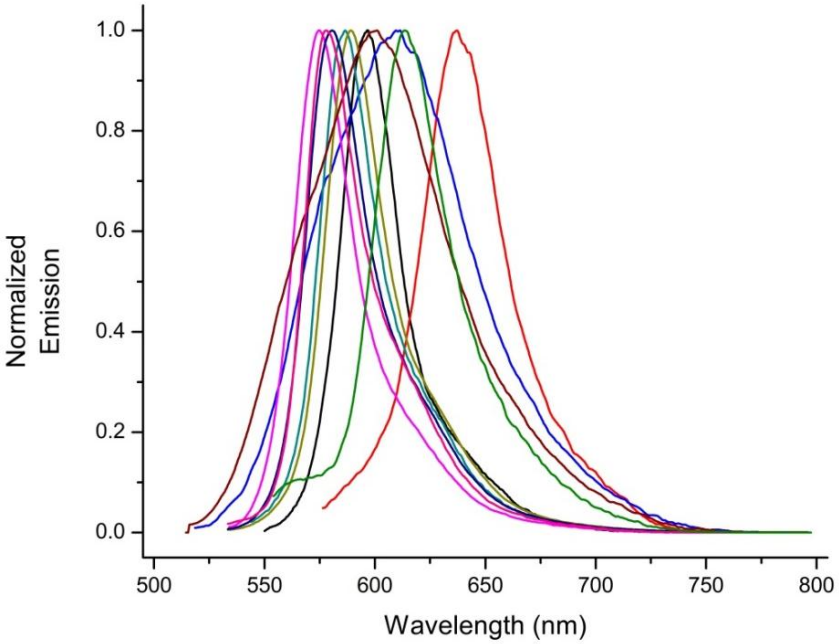

Figure 3.9: Normalized emission spectra of BODIPYs **2** (black), **12** (red), **13** (cyan), **14** (magenta), **15** (blue), **16** (yellow), **17** (navy), **18**(olive), **19** (pink) and **20** (wine) in THF at RT

Table 3.1: Absorption and emission spectral properties of BODIPYs **1a** and **1b**'s derivatives in THF at RT

BODIPY	**Abs. λ_{max} (nm) THF**	**log ε ($M^{-1}cm^{-1}$)**	**Emission λ_{max} (nm) THF**	**Φf**	**Stokes shift (nm)**
3b	580	4.58	600	0.74	20
4	528	4.68	542	0.34	14
5	532	4.87	550	0.18	18
7	533	4.75	556	0.43	23
8a	528	4.82	542	0.23	14
8b	538	4.86	550	0.41	12

3.3 Conclusions

In summary, two 3,5-diiodo-BODIPYs and one 2,3,5,6-tetraiodo-BODIPY were studied on their reactivity towards unsymmetric and symmetric aromatic substitution reactions with S, O, N and C nucleophiles. Sulfur nucleophiles show the highest reactivity, affording the most red-shifted substituted BODIPYs. The BODIPY's boron unit was stable during the substitution conditions, indicating the iodide groups at the 3,5-positions were fairly reactive among most functionalization reactions. The high reactivity of iodinated BODIPYs was further applied for ^{123}I-radiolabeling with significant transformation observed. The very low fluorescence quantum yields of BODIPY **2**'s derivatives suggested that they might be promising photodynamic therapy agents.

3.4 Experimental

3.4.1 General Information

Table 3.2: Absorption and emission spectral properties of BODIPYs **2**'s derivatives in THF at room temperature

BODIPYs	**Abs. λ_{max} (nm) THF**	**log ε ($M^{-1}cm^{-1}$)**	**Emission λ_{max} (nm) THF**	**Φf**	**Stokes shift (nm)**
12	605	5.12	637	0.02	32
13	562	5.23	587	0.09	25
14	554	5.21	575	0.11	21
15	543	4.97	612	0.05	69
16	564	4.79	589	0.12	25
17	553	4.74	581	0.15	28
18	580	4.97	614	0.07	34
19	552	4.93	578	0.04	26
20	541	4.82	601	0.01	60

All the reagents and solvents were purchased from Sigma-Aldrich and VWR and were used without further purification. All reactions were carried out with oven-dried glassware under a dry argon atmosphere. All the reactions were monitored using Sorbent Technologies 0.2 mm silica gel TLC plates with UV-254 nm indicator. Flash column chromatography was performed using Sorbent Technologies 60 Å silica gel (230-400 mesh). Prep-TLC 60 Å silica gel 20 x 20 cm (210-270 μm) was used. All ^{1}H-, ^{13}C-, and ^{11}B-NMR spectra were collected on a Bruker AV-400 and AV-500 spectrometer in deuterated chloroform or dichloromethane. The $CDCl_3$ chemical shifts (δ) are reported in ppm using as reference 7.26 for proton and 77.00 for carbon

and BF_3•OEt_2 was used as reference (0.00 δ) for boron NMR. The CD_2Cl_2 chemical shifts (δ) are reported in ppm using as reference 5.32 for proton and 53.50 for carbon.

Coupling constants are reported in Hertz (Hz). All the mass spectra were collected using an Agilent 6210 ESI-TOF mass spectrometer. All melting points were recorded using a MEL-TEMP electrothermal instrument.

2.4.2 Synthesis

S_NAr reactions between BODIPY 1a and thiols:

Organic base method: To a mixture of 31.4 mg (0.05 mmol) BODIPY **1a** and 0.11 mmol thiol, 10 mL dichloromethane was added. 1 drop of triethylamine was added via syringe and the reaction was allowed to stir in room temperature under inert atmosphere for 10 minutes. After thin layer chromatography confirmed the consumption of BODIPY **1a**, the reaction was poured to 100 mL dichloromethane, and was washed with 2 x 50 mL saturated sodium bicarbonate solution. Dichloromethane was removed under vacuum. The dark purple residue was purified by silica gel column chromatography (elution: hexane/dichloromethane=1:2) and recrystallized using 1:1 dichloromethane/hexane.

Inorganic base method: To a mixture of 31.4 mg (0.05 mmol) BODIPY **1a**, 0.11 g (1.0 mmol) potassium carbonate and 0.11 mmol thiol, 10 mL dichloromethane was added. The reaction was allowed to stir in room temperature under inert atmosphere for 12 hours. The work-up and purifying procedure are the same with the organic base method.

BODIPY 3a: Yield 86%. mp (°C) 235; ^{1}H NMR (500 MHz, $CDCl_3$) δ 7.43 – 7.38 (m, 3H), 7.35 (dd, *J* = 7.5, 1.8 Hz, 4H), 7.26 – 7.10 (m, 8H), 1.80 (t, *J* = 6.1 Hz, 4H), 1.49 (t, *J* = 6.1 Hz, 4H), 1.34 – 1.27 (m, 4H), 1.23 – 1.19 (m, 4H); ^{13}C NMR (126 MHz, $CDCl_3$) δ 147.9, 141.5, 139.0, 134.9, 133.7, 133.42, 133.39, 133.38, 132.1, 131.99, 130.96, 129.1, 129.98, 128.95, 127.9,

127.6, 127.1, 24.1, 22.6, 22.2, 22.1; ^{11}B NMR (128 MHz, $CDCl_3$) δ 0.72 (t, *J* = 31.0 Hz); HRMS (ESI-TOF) m/z 592.1998 $[M]^+$ calcd for $C_{35}H_{31}BF_2N_2S_2$ 592.1990.

BODIPY 3b: Yield 88%. mp (°C) 278; ^{1}H NMR (400 MHz, CD_2Cl_2) δ 7.49 (q, *J* = 3.7 Hz, 3H), 7.36 – 7.26 (m, 6H), 7.13 (d, *J* = 7.9 Hz, 4H), 2.33 (s, 6H), 1.89 (t, *J* = 6.2 Hz, 4H), 1.59 (t, *J* = 6.8 Hz, 4H), 1.44 – 1.36 (m, 4H), 1.31 – 1.26 (m, 4H); ^{13}C NMR (100 MHz, CD_2Cl2) δ 148.0, 141.8, 139.1, 137.8, 134.9, 133.5, 133.4, 132.1, 131.3, 129.93, 129.85, 129.2, 129.1, 128.1, 24.3, 22.8, 22.5, 22.3, 20.9; ^{11}B NMR (128 MHz, $CDCl_3$) δ 0.73 (t, *J* = 31.1 Hz); HRMS (ESI-TOF) m/z 601.2300 $[M-F]^+$ calcd for $C_{37}H_{35}BFN_2S_2$ 601.2319.

BODIPY 3c: Yield 75%. mp (°C) 150 (decomposed); ^{1}H NMR (500 MHz, CD_2Cl_2) δ 7.50 (q, *J* = 2.7 Hz, 3H), 7.39 – 7.19 (m, 12H), 4.29 (s, 4H), 2.23 – 2.13 (m, 4H), 1.65 – 1.53 (m, 4H), 1.49 – 1.41 (m, 4H), 1.36 – 1.27 (m, 4H); ^{13}C NMR (125 MHz, CD_2Cl2) δ 148.5, 141.4, 139.7, 137.7, 135.04, 135.01, 134.9, 132.8, 129.20, 129.17, 129.1, 128.5, 128.0, 127.3, 40.3, 24.2, 22.9, 22.5, 22.4; ^{11}B NMR (128 MHz, $CDCl_3$) δ 0.80 (t, *J* = 31.0 Hz); HRMS (ESI-TOF) m/z 601.2327 $[M-FH]^+$ calcd for $C_{37}H_{35}BFN_2S_2$ 601.2319.

S_NAr reactions between BODIPY 1a and 4-OMe-phenol

For the di-substitution, to a mixture of 31.4 mg (0.05 mmol) BODIPY **1a**, 18.6 mg (0.15 mmol) 4-methoxyphenol and 0.11 g (1.0 mmol) potassium carbonate, 5 mL toluene and 5 mL acetonitrile were added. The reaction was heated under 60 ^oC under inert atmosphere until thin layer chromatography confirmed the consumption of BODIPY **1a**, and the solvents were removed under vacuum. The residue was dissolved in 100 mL dichloromethane and washed with 2 x 50 mL water. Dichloromethane was removed under vacuum. The residue was purified by silica gel column chromatography (elution: 100% dichloromethane) and recrystallized using dichloromethane/hexane=1:1. BODIPY **4** was obtained in 76% yield. For the mono-substitution,

to a mixture of 31.4 mg (0.05 mmol) BODIPY **1a**, 9.3 mg (0.08 mmol) 4-methoxyphenol and 0.11 g (1.0 mmol) potassium carbonate, 5 mL toluene and 5 mL acetonitrile were added. The reaction was heated under 60 ^{o}C under inert atmosphere for 6 hours. After thin layer chromatography confirmed the consumption of BODIPY **1a**, the rest work-up procedure was all similar to the one of di-substitution reactions.

BODIPY 4: Yield 76%. mp (°C) 264; ^{1}H NMR (400 MHz, $CDCl_3$) δ 7.50 – 7.42 (m, 3H), 7.36 – 7.29 (m, 2H), 7.12 – 7.04 (m, 4H), 6.85 – 6.76 (m, 4H), 3.77 (s, 6H), 1.79 (t, *J* = 6.1 Hz, 4H), 1.39 – 1.28 (m, 8H); ^{13}C NMR (126 MHz, $CDCl_3$) δ 158.2, 156.1, 149.5, 142.3, 138.1, 135.5, 128.9, 128.8, 128.4, 123.9, 119.6, 116.0, 114.4, 55.6, 24.2, 22.7, 22.1, 21.3; ^{11}B NMR (128 MHz, $CDCl_3$) δ 0.28 (t, *J* = 29.0 Hz); HRMS (ESI-TOF) m/z 601.2675 $[M+H]^+$ calcd for $C_{37}H_{35}BFN_2O_4$ 601.2674.

BODIPY 5: Yield 63%. mp (°C) 150 (decomposed); ^{1}H NMR (400 MHz, $CDCl_3$) δ 7.50 – 7.42 (m, 3H), 7.30 – 7.24 (m, 2H), 7.16 – 7.10 (m, 2H), 6.88 – 6.82 (m, 2H), 3.80 (s, 3H), 2.30 (t, *J* = 6.2 Hz, 2H), 1.68 (t, *J* = 6.2 Hz, 2H), 1.56 (q, *J* = 6.2 Hz, 6H), 1.40 – 1.28 (m, 6H); ^{13}C NMR (100 MHz, $CDCl_3$) δ 162.7, 156.9, 148.4, 146.6, 137.9, 137.6, 134.8, 133.6, 133.5, 132.6, 129.04, 129.02, 128.1, 126.4, 120.6, 119.2, 114.5, 95.7, 55.6, 24.4, 24.3, 23.8, 23.4, 22.5, 22.2, 21.8, 21.6; ^{11}B NMR (128 MHz, $CDCl_3$) δ 0.33 (t, *J* = 29.9 Hz); HRMS (ESI-TOF) m/z 605.1289 $[M-F]^+$ calcd for $C_{30}H_{28}BFIN_2O_2$ 605.1273.

Suzuki cross-coupling reaction on BODIPY 5

To a mixture of 62.4 mg (0.1 mmol) BODIPY **5**, 5 mg $Pd(dppf)Cl_2$ and 95.0 mg (0.5 mmol) 4-CF_3-phenylboronic acid, 2 mL toluene and 2 mL tetrahydrofuran were added under inert atmosphere. The reaction was heated under 75^{o}C for 2 minutes and 0.1 mL 1M potassium carbonate solution was added via syringe. The reaction was monitored by thin layer

chromatography until complete consumption of BODIPY **5**. The cooled solution was filtered through celite cake to remove excess palladium catalyst and boronic acid, and the solvent was then evaporated under vacuum. The residue was purified by silica gel column chromatography (elution: hexane/dichloromethane=1:2) to afford BODIPY **7** in 88% yield, and was recrystallized using dichloromethane/hexane=1:1.**BODIPY 7**: mp (°C) >300; ^{1}H NMR (400 MHz, CD_2Cl_2) δ 7.75 (d, *J* = 8.2 Hz, 2H), 7.68 (d, *J* = 8.2 Hz, 2H), 7.56 – 7.49 (m, 3H), 7.41 – 7.34 (m, 2H), 7.09 – 7.03 (m, 2H), 6.89 – 6.83 (m, 2H), 3.78 (s, 3H), 2.33 (t, *J* = 6.1 Hz, 2H), 1.74 – 1.62 (m, 6H), 1.60 – 1.51 (m, 2H), 1.50 – 1.41 (m, 2H), 1.41 – 1.28 (m, 4H); ^{13}C NMR (126 MHz, CD_2Cl_2) δ 162.0, 157.0, 148.4, 147.2, 146.7, 139.8, 138.6, 136.9, 135.2, 130.4, 130.34, 130.31, 129.72, 129.67, 129.5, 129.2, 129.1, 128.4, 127.63, 127.61, 126.3, 125.5, 124.63, 124.60, 124.57, 124.5, 123.3, 120.2, 119.3, 114.7, 55.6, 24.6, 24.1, 23.3, 22.9, 22.5, 22.4, 21.9, 21.6; ^{11}B NMR (128 MHz, CD_2Cl_2) δ 0.50 (t, *J* = 30.9 Hz); HRMS (ESI-TOF) m/z 623.2501 $[M+H]^+$ calcd for $C_{37}H_{32}BF_4N_2O_2$ 623.2493.

S_NAr reactions between BODIPY 1b and ethyl malonate

For the di-substitution, to a mixture of 34.4 mg (0.05 mmol) BODIPY **1b**, 113.9 μL (0.75 mmol) ethyl malonate and 18.0 mg (0.75 mmol) sodium hydride, 5 mL toluene and 5 mL acetonitrile were added. The reaction was refluxed at 82 ^{o}C under inert atmosphere until thin layer chromatography confirmed the consumption of BODIPY **1b**, and the solvents were removed under vacuum. The residue was dissolved in 100 mL dichloromethane and washed with 2 x 50 mL water. Dichloromethane was removed under vacuum. The residue was purified by silica gel column chromatography. BODIPY **8a** was obtained in 33% yield. For the mono-substitution, to a mixture of 34.4 mg (0.05 mmol) BODIPY **1b**, 22.7 μL (0.15 mmol) 4-methoxyphenol and 3.6 mg (0.15 mmol) sodium hydride, 5 mL toluene and 5 mL acetonitrile

were added. The following reaction condition, work up and purification procedure were all similar to the ones of di-substitution reactions.

BODIPY 8a: mp (°C) 260; ^{1}H NMR (400 MHz, $CDCl_3$) δ 6.54 (t, *J* = 2.3 Hz, 1H), 6.45 (d, *J* = 2.3 Hz, 2H), 5.52 (s, 2H), 4.26 (q, *J* = 7.1 Hz, 8H), 3.81 (s, 6H), 2.35 (t, *J* = 6.2 Hz, 4H), 1.81 (t, *J* = 6.2 Hz, 4H), 1.55 (s, 4H), 1.43 (s, 4H), 1.29 (t, *J* = 7.1 Hz, 12H); ^{13}C NMR (126 MHz, $CDCl_3$) δ 166.5, 161.6, 146.3, 142.9, 142.5, 136.5, 130.3, 130.0, 105.3, 101.2, 62.1, 55.6, 51.5, 23.9, 22.8, 22.2, 21.7, 14.0; ^{11}B NMR (128 MHz, $CDCl_3$) δ 0.54 (t, *J* = 35.3 Hz); HRMS (ESI-TOF) m/z 774.3216 $[M+Na]^+$ calc. $C_{39}H_{47}BF_2N_2NaO_{10}$ 774.3220.

BODIPY 8b: mp (°C) 186; ^{1}H NMR (400 MHz, $CDCl_3$) δ 6.55 (s, 1H), 6.42 (d, *J* = 2.2 Hz, 2H), 5.60 (s, 1H), 4.41 – 4.11 (m, 4H), 3.80 (s, 6H), 2.37 (t, *J* = 6.2 Hz, 2H), 2.30 (t, *J* = 6.2 Hz, 2H), 1.95 – 1.71 (m, 4H), 1.65 – 1.52 (m, 4H), 1.52 – 1.40 (m, 4H), 1.30 (t, *J* = 7.1 Hz, 6H); ^{13}C NMR (101 MHz, $CDCl_3$) δ 166.4, 161.6, 147.8, 143.4, 141.6, 140.6, 136.1, 135.5, 134.0, 130.7, 105.4, 103.9, 101.2, 62.1, 55.6, 51.5, 24.2, 24.0, 23.7, 23.1, 22.7, 22.3, 22.2, 21.7, 14.1; ^{11}B NMR (128 MHz, $CDCl_3$) δ 0.47 (t, *J* = 32.9 Hz); HRMS (ESI-TOF) m/z 701.1698 $[M-F]^+$ calc. $C_{32}H_{36}BFIN_2O_6$ 701.1695.

Synthesis of BODIPY with phenyl and methoxy units on the boron

57.9 mg (0.1 mmol) dipyrromethene **9** was dissolved in 10 mL anhydrous DCM, and 69.6 μL (0.5 mmol) triethylamine was added. The solution was stirred under inert atmosphere for 5 minutes, and then 68.2 μL (0.5 mmol) $PhBCl_2$ was added via a syringe dropwisely, and 2.1 mL of 0.5 M NaOMe in methanol solution was added one hour later. The reaction was quenched after 10 minutes by removing all solvents under vacuum, and the crude product was directly purified by silica gel column chromatography to afford BODIPY **10** in 58% yield, and was recrystallized using EtOAc/hexane=1:1. **BODIPY 10**: mp (°C) 100 (decomposed); ^{1}H NMR

(400 MHz, $CDCl_3$) δ 7.75 – 7.45 (m, 5H), 7.46 – 7.35 (m, 2H), 7.24 – 7.07 (m, 3H), 3.25 (s, 3H), 2.50 – 2.08 (m, 4H), 1.75 – 1.50 (m, 8H), 1.47 – 1.32 (m, 4H); ^{13}C NMR (101 MHz, $CDCl_3$) δ 140.1, 139.1, 135.5, 134.9, 134.4, 133.8, 129.2, 129.1, 129.0, 127.91, 127.86, 126.1, 125.9, 107.0, 49.2, 24.5, 24.1, 23.2, 22.3; ^{11}B NMR (128 MHz, $CDCl_3$) δ 4.01 (s); HRMS (ESI-TOF) m/z 736.0132 $[M+K]^+$ calc. $C_{30}H_{29}BI_2KN_2O_{10}$ 736.0130.

S_NAr reactions between BODIPY 10 and thiols:

To a mixture of 34.9 mg (0.05 mmol) BODIPY **10** and 18.6 mg (0.15 mmol) 4-methyl-benzenethiol, 10 mL dichloromethane was added. One drop of triethylamine was added via syringe and the reaction was allowed to stir in room temperature under inert atmosphere for 3 days. After thin layer chromatography confirmed the consumption of BODIPY **10**, the reaction was quenched by removing all solvent under vacuum. The dark purple residue was purified by silica gel column chromatography to give BODIPY **11** in a 63% yield. **BODIPY 11**: mp (°C) 80 (decomposed); ^1H NMR (400 MHz, CD_2Cl_2) δ 7.85 – 7.27 (m, 8H), 7.25 – 7.03 (m, 4H), 6.92 (d, *J* = 7.8 Hz, 3H), 6.74 (dd, *J* = 15.8, 7.8 Hz, 3H), 3.45 – 2.99 (m, 3H), 2.24 (s, 6H), 1.88 – 1.48 (m, 8H), 1.48 – 1.30 (m, 8H); ^{13}C NMR (100 MHz, CD_2Cl_2) δ 152.0, 141.2, 140.6, 138.9, 138.6, 137.7, 137.3, 135.7, 135.5, 134.4, 134.1, 133.9, 133.6, 133.2, 133.1, 132.6, 132.5, 132.0, 131.5, 131.1, 130.7, 130.6, 129.8, 129.6, 129.62, 129.59, 129.5, 129.3, 129.20, 129.15, 129.13, 129.10, 129.1, 129.99, 128.97, 128.9, 128.83, 128.79, 128.4, 128.3, 128.0, 126.7, 126.6, 126.3, 126.2, 126.2, 126.0, 125.9, 125.7, 125.5, 106.5, 102.4, 49.4, 49.1, 48.9, 24.72, 24.66, 24.5, 24.4, 24.3, 24.2, 23.6, 23.4, 23.00, 22.97, 22.9, 22.8, 22.6, 22.44, 22.42, 22.39, 22.3, 20.88, 20.85; ^{11}B NMR (128 MHz, CD2Cl2) δ 3.38 (s) ; HRMS (ESI-TOF) m/z 712.2795 $[M+Na]^+$ calc. $C_{44}H_{43}BN_2NaOS_2$ 712.2838.

S_NAr reactions between BODIPY 2 and thiols:

To a mixture of 38.8 mg (0.05 mmol) BODIPY **2** and 13.6 mg (0.11 mmol) 4-methyl-benzenethiol, 10 mL dichloromethane was added. 1 drop of triethylamine was added via syringe and the reaction was allowed to stir in room temperature under inert atmosphere for one minute. After thin layer chromatography confirmed the consumption of BODIPY **2**, the reaction was poured to 100 mL dichloromethane, and was washed with 2 x 50 mL saturated sodium bicarbonate solution. Dichloromethane was removed under vacuum. The dark purple residue was purified by silica gel column chromatography in a 94% yield. **BODIPY 12**: mp (°C) >300; ^{1}H NMR (400 MHz, CD_2Cl_2) δ 7.44 (d, *J* = 8.1 Hz, 2H), 7.40 – 7.27 (m, 6H), 7.15 (d, *J* = 8.6 Hz, 6H), 2.47 (s, 3H), 2.33 (s, 6H); ^{13}C NMR (101 MHz, CD_2Cl2) δ 153.0, 142.1, 142.0, 138.8, 138.1, 137.2, 131.3, 130.7, 130.2, 130.1, 129.9, 129.5, 21.3, 21.0; ^{11}B NMR (128 MHz, CD_2Cl_2) δ 0.34 (t, *J* = 28.6 Hz); HRMS (ESI-TOF) m/z 776.9502 $[M]^-$ calc. $C_{30}H_{23}BF_2I_2S_2$ 776.9495.

S_NAr reactions between BODIPY 2 and 4-OMe-phenol

For the di-substitution, to a mixture of 38.8 mg (0.05 mmol) BODIPY **2**, 13.6 mg (0.11 mmol) 4-methoxyphenol and 0.11 g (1.0 mmol) potassium carbonate, and 5 mL acetonitrile were added. The reaction was stirred in room temperature for 30 minutes under inert atmosphere until thin layer chromatography confirmed the consumption of BODIPY **2**, and the solvents were removed under vacuum. The residue was dissolved in 100 mL dichloromethane and washed with 2 x 50 mL water. Dichloromethane was removed under vacuum. The residue was purified by silica gel column chromatography and BODIPY **14** was obtained in 89% yield. For the mono-substitution, to a mixture of 38.8 mg (0.05 mmol) BODIPY **2**, 7.4 mg (0.06 mmol) 4-methoxyphenol and 0.11 g (1.0 mmol) potassium carbonate, and 5 mL acetonitrile were added. The reaction was stirred in room temperature for 5 minutes. After thin layer chromatography

confirmed the consumption of BODIPY **2**, the rest work-up procedure was all similar to the one of di-substitution reactions, and BODIPY **13** was isolated in an 85% yield.

BODIPY 13: mp (°C) 120 (decomposed); ^{1}H NMR (400 MHz, CD_2Cl_2) δ 7.45 – 7.39 (m, 2H), 7.35 (d, *J* = 7.7 Hz, 2H), 7.23 (s, 1H), 7.11 – 7.07 (m, 2H), 6.95 – 6.90 (m, 3H), 3.81 (s, 3H), 2.46 (s, 3H); ^{13}C NMR (126 MHz, CD_2Cl2) δ 163.1, 157.29, 157.27, 148.60, 148.59, 142.1, 141.82, 141.81, 140.5, 138.3, 134.6, 131.2, 130.6, 130.52, 130.50, 129.5, 129.4, 129.28, 129.26, 120.10, 120.08, 114.79, 114.78, 107.4, 87.4, 64.0, 55.7, 21.3; ^{11}B NMR (128 MHz, CD_2Cl_2) δ -0.14 (t, *J* = 28.0 Hz); HRMS (ESI-TOF) m/z 777.9808 $[M]^-$ calc. $C_{30}H_{23}BF_2I_2N_2O_4$ 776.9850.

BODIPY 14: mp (°C)>300; ^{1}H NMR (400 MHz, CD_2Cl_2) δ 7.48 – 7.42 (m, 2H), 7.39 – 7.34 (m, 2H), 7.10 (s, 2H), 7.05 – 6.99 (m, 4H), 6.92 – 6.84 (m, 4H), 3.78 (s, 6H), 2.47 (s, 3H); ^{13}C NMR (126 MHz, CD_2Cl2) δ 160.3, 156.6, 149.6, 141.6, 141.5, 138.4, 130.6, 129.8, 129.42, 129.40, 119.1, 114.6, 55.7; ^{11}B NMR (128 MHz, CD_2Cl_2) δ -0.24 (t, *J* = 27.2 Hz); HRMS (ESI-TOF) m/z 780.8441 $[M]^-$ calc. $C_{23}H_{16}BF_2I_3N_2O_2$ 780.8433.

S_NAr reactions between BODIPY 2 and aniline

38.8 mg (0.05 mmol) BODIPY **2** and 45.1 μL (0.75 mmol) aniline were mixed in 5 mL acetonitrile and stirred at room temperature for 30 minutes under inert atmosphere until thin layer chromatography confirmed the consumption of BODIPY **2**, and the solvents were removed under vacuum. The residue was dissolved in 30 mL dichloromethane and washed with 2 x 15 mL water. Dichloromethane was removed under vacuum. The residue was purified by silica gel column chromatography to give BODIPY **15** in a 78% yield.

BODIPY 15: mp (°C) 110 (decomposed); ^{1}H NMR (400 MHz, CD_2Cl_2) δ 8.19 (s, 1H), 7.45 (dd, *J* = 8.3, 6.8 Hz, 2H), 7.40 – 7.34 (m, 3H), 7.33 – 7.22 (m, 5H), 6.64 (s, 1H), 2.44 (s, 3H); ^{13}C NMR (126 MHz, CD_2Cl2) δ 157.1, 145.3, 140.5, 137.8, 135.6, 134.5, 131.8, 130.3,

130.0, 129.4, 129.3, 128.9, 127.8, 127.1, 53.9, 53.7, 53.5, 53.3, 53.1, 21.2; ^{11}B NMR (128 MHz, CD_2Cl_2) δ 0.33 (t, *J* = 33.3 Hz); HRMS (ESI-TOF) m/z 789.8115 $[M+K]^+$ calc. $C_{22}H_{15}BF_2I_3N_3K$ 789.8104.

S_NAr reactions between BODIPY 2 and ethyl malonate

For the di-substitution, to a mixture of 38.8 mg (0.05 mmol) BODIPY **2**, 22.8 μL (0.15 mmol) ethyl malonate and 3.6 mg (0.15 mmol) sodium hydride, and 5 mL acetonitrile were added. The reaction was refluxed at 82 ^oC under inert atmosphere until thin layer chromatography confirmed the consumption of BODIPY **2**, and the solvents were removed under vacuum. The residue was dissolved in 50 mL dichloromethane and washed with 2 x 25 mL water. Dichloromethane was removed under vacuum. The residue was purified by silica gel column chromatography. BODIPY **17** was obtained in 69% yield. For the mono-substitution, to a mixture of 38.8 mg (0.05 mmol) BODIPY **1b**, 9.1 μL (0.06 mmol) ethyl malonate and 2.4 mg (0.06 mmol) sodium hydride, and 5 mL acetonitrile were added. The following reaction condition, work up and purification procedure were all similar to the ones of di-substitution reactions, and BODIPY **16** was produced in a 72% yield.

BODIPY 16: mp (°C) 150 (decomposed); ^{1}H NMR (400 MHz, CD_2Cl_2) δ 7.44 (d, *J* = 8.0 Hz, 2H), 7.37 (d, *J* = 7.9 Hz, 2H), 7.22 – 7.12 (m, 1H), 7.04 (d, *J* = 1.3 Hz, 1H), 5.51 (s, 1H), 4.29 (q, *J* = 7.1 Hz, 4H), 2.47 (s, 3H), 1.31 (t, *J* = 7.1 Hz, 6H); ^{13}C NMR (126 MHz, CD_2Cl2) δ 164.9, 143.4, 142.5, 139.9, 139.2, 137.7, 135.4, 130.7, 129.5, 129.5, 62.7, 21.3, 13.9; ^{11}B NMR (128 MHz, CD_2Cl_2) δ 0.09 (t, *J* = 31.3 Hz); HRMS (ESI-TOF) m/z 817.8622 $[M]^-$ calc. $C_{23}H_{20}BF_2I_3N_2O_4$ 817.8618.

BODIPY 17: mp (°C) >300; ^{1}H NMR (400 MHz, $CDCl_3$) δ 7.44 (d, *J* = 8.1 Hz, 2H), 7.35 (d, *J* = 7.9 Hz, 2H), 7.12 (d, *J* = 1.5 Hz, 2H), 5.55 (s, 2H), 4.30 (q, *J* = 7.1, 2.3 Hz, 8H), 2.48

(s, 3H), 1.31 (t, *J* = 7.2 Hz, 12H); ^{13}C NMR (101 MHz, $CDCl_3$) δ 165.0, 151.2, 145.3, 142.1, 139.4, 135.1, 130.6, 129.9, 129.5, 62.6, 52.1, 29.7, 21.5, 14.0; ^{11}B NMR (128 MHz, $CDCl_3$) δ 0.21 (t, *J* = 33.8 Hz); HRMS (ESI-TOF) m/z 850.0210 $[M]^-$ calc. $C_{30}H_{31}BF_2I_2N_2O_8$ 774.3220.

S_NAr reactions between BODIPY 16 and thiols:

To a mixture of 41.4 mg (0.05 mmol) BODIPY **16** and 12.4 mg (0.10 mmol) 4-methyl-benzenethiol, 10 mL dichloromethane was added. 1 drop of triethylamine was added via syringe and the reaction was allowed to stir in room temperature under inert atmosphere for 12 hours. After thin layer chromatography confirmed the consumption of BODIPY **16**, the reaction was poured to 100 mL dichloromethane, and was washed with 2 x 50 mL saturated sodium bicarbonate solution. Dichloromethane was removed under vacuum. The dark purple residue was purified by silica gel column chromatography to give BODIPY **18** in a 68% yield. **BODIPY 18**: mp (°C) 170 (decomposed); ^{1}H NMR (400 MHz, CD_2Cl_2) δ 7.49 – 7.41 (m, 2H), 7.37 (d, *J* = 7.9 Hz, 2H), 7.34 – 7.25 (m, 2H), 7.21 – 7.08 (m, 4H), 5.55 (s, 1H), 4.29 (q, *J* = 7.2 Hz, 4H), 2.47 (s, 3H), 2.33 (s, 3H), 1.33 – 1.28 (m, 6H); ^{13}C NMR (101 MHz, CD_2Cl2) δ 165.2, 152.8, 151.5, 144.1, 142.3, 139.4, 139.3, 138.2, 137.0, 135.5, 131.2, 130.8, 130.1, 129.9, 129.8, 129.6, 129.5, 62.7, 21.3, 21.0, 13.9; ^{11}B NMR (128 MHz, CD_2Cl_2) δ 0.25 (t, *J* = 31.2 Hz); HRMS (ESI-TOF) m/z 835.9770 $[M+Na]^+$ calc. $C_{30}H_{27}BF_2I_2N_2NaO_4$ 774.3220.

S_NAr reactions between BODIPY 16 and 4-OMe-phenol

To a mixture of 41.4 mg (0.05 mmol) BODIPY **16**, 12.4 mg (0.10 mmol) 4-methoxyphenol and 0.11 g (1.0 mmol) potassium carbonate, and 5 mL acetonitrile were added. The reaction was stirred in room temperature for 12 hours under inert atmosphere until thin layer chromatography confirmed the consumption of BODIPY **16**, and the solvents were removed under vacuum. The residue was dissolved in 100 mL dichloromethane and washed with 2 x 50

mL water. Dichloromethane was removed under vacuum. The residue was purified by silica gel column chromatography and BODIPY **19** was obtained in 89% yield. **BODIPY 19**: mp (°C) 213; ^{1}H NMR (400 MHz, CD_2Cl_2) δ 7.44 (d, *J* = 8.1 Hz, 2H), 7.36 (d, *J* = 7.9 Hz, 2H), 7.23 (s, 1H), 7.13 – 7.01 (m, 3H), 6.96 – 6.85 (m, 2H), 5.44 (s, 1H), 4.26 (q, *J* = 7.1 Hz, 4H), 3.81 (s, 3H), 2.47 (s, 3H), 1.29 (t, *J* = 7.1 Hz, 6H); ^{13}C NMR (100 MHz, CD_2Cl2) δ 165.5, 162.5, 157.2, 148.6, 146.9, 142.7, 141.9, 141.7, 136.4, 134.1, 130.8, 130.5, 129.6, 129.3, 119.9, 114.8, 62.4, 55.6, 21.2, 13.8; ^{11}B NMR (128 MHz, CD_2Cl_2) δ 0.01 (t, *J* = 30.8 Hz); HRMS (ESI-TOF) m/z 794.0012 $[M-F]^+$ calc. $C_{30}H_{27}BFI_2N_2O_6$ 794.0066.

S_NAr reactions between BODIPY 16 and aniline

41.4 mg (0.05 mmol) BODIPY **16** and 10.0 μL (0.15 mmol) aniline were mixed in 5 mL acetonitrile and stirred at room temperature for 12 hours under inert atmosphere until thin layer chromatography confirmed the consumption of BODIPY **2**, and the solvents were removed under vacuum. The residue was dissolved in 30 mL dichloromethane and washed with 2 x 15 mL water. Dichloromethane was removed under vacuum. The residue was purified by silica gel column chromatography to give BODIPY **20** in a 78% yield. **BODIPY 20**: mp (°C) 142; ^{1}H NMR (400 MHz, CD_2Cl_2) δ 8.07 (s, 1H), 7.59 – 7.06 (m, 10H), 6.73 (s, 1H), 5.36 (s, 1H), 4.27 (q, *J* = 7.1 Hz, 4H), 2.45 (s, 3H), 1.30 (t, *J* = 7.1 Hz, 6H); ^{13}C NMR (101 MHz, CD_2Cl2) δ 166.3, 156.9, 145.3, 140.6, 139.6, 135.8, 134.1, 133.8, 133.5, 130.4, 130.3, 129.4, 129.3, 127.8, 127.1, 62.3, 21.2, 14.0; ^{11}B NMR (128 MHz, CD_2Cl_2) δ 0.60 (t, *J* = 35.9 Hz); HRMS (ESI-TOF) m/z 784.0141 $[M+H]^+$ calc. $C_{29}H_{27}BF_2I_2N_3O_4$ 784.0152.

3.4.3 X-ray Determined Molecular Structures

X-ray data were collected at low temperature with MoKα radiation on Bruker Kappa Apex-II DUO or Nonius KappaCCD diffactometers. Data reduction: Bruker *SAINT*; program(s)

used to solve structure: *SHELXS97* (Sheldrick, 2008); program(s) used to refine structure: *SHELXL97* (Sheldrick, 2008); molecular graphics: *ORTEP-3 for Windows* (Farrugia, 2012); software used to prepare material for publication: *SHELXL97* (Sheldrick, 2008).

Crystal Data: **3b**, $C_{37}H_{35}BF_2N_2S_2$, M=620.60, monoclinic, a=17.1401(9), b=10.6673(5), c=18.0721(9) Å, T=100 K, space group $P2_1/n$, Z=4, 167674 reflections measured, 12394 unique (R_{int}=0.039), θ_{max}=36.4°, final R=0.037;

Crystal Data: **4**, $C_{37}H_{35}BF_2N_2O_4$, M=620.48, monoclinic, a=11.0091(9), b=24.4103(18), c=12.6266(11) Å, T=150 K, space group $P2_1/n$, Z=4, 37510 reflections measured, 4712 unique (R_{int}=0.063), θ_{max}=28.3°, final R=0.050;

Crystal Data: **5**, $C_{30}H_{28}BF_2IN_2O_2$, M=624.25, Triclinic, a=9.8023(4), b=11.1021(4), c=13.2217(5) Å, T=90 K, space group P1, Z=2, 22581 reflections measured, 8829 unique (R_{int}=0.031), θ_{max}=33.2°, final R=0.030;

Crystal Data: **6**, $C_{37}H_{32}BF_5N_2O_2$, M=642.45, monoclinic, a=13.2597(9), b=8.4023(5), c=14.1888(7) Å, T=90 K, space group $P2_1$, Z=2, 12821 reflections measured, 5228 unique (R_{int}=0.020), θ_{max}=25.7°, final R=0.039;

Crystal Data: **10**, $C_{30}H_{29}BI_2N_2O$, M=698.16, Triclinic, a=11.5055(6), b=16.1724(10), c=16.5198(8) Å, T=90 K, space group P1, Z=4, 59600 reflections measured, 9238 unique (R_{int}=0.042), θ_{max}=27.2°, final R=0.034.

3.4.4 Steady-state Absorption and Fluorescence Spectroscopy

The photophysical properties of compounds **3b, 4, 5, 7, 8a, 8b,** and **12-23** were determined by preparing a stock solution with a concentration of 1×10^{-4} M and diluting it to appropriate concentrations for absorbance and emission spectra measurements. All the absorption spectra were obtained using a Perkin Elmer Lambda 35 UV-visible

spectrophotometer. The optical density, ε, were taken by preparing solution concentrations at $1x10^{-5}$ M in order to get λ_{max} between 0.5 and 1.0. Emission spectra were measured on a LS-55 Perkin-Elmer spectro-fluorometer with the slit width set at 2.5 nm for all other BODIPYs. All absorbance and emission spectra were acquired within 6 h of fresh solution preparation, at room temperature. Cresyl violet (Φ = 0.55 in MeOH)[27] was used as the reference for compounds **3b, 12, 13** and **18** in THF. Rhodamine 6G (Φ = 0.86 in MeOH)[27] was used as the reference for all rest compounds in THF. Quartz spectrophotometric cells with path lengths of 10 mm were used. For the determination of quantum yields, dilute solutions with different absorbance between 0.02-0.08 at the particular excitation wavelength were used. Molar absorption coefficients (ε) were determined from the plots of integrated absorbance vs concentrations. The following equation was used for the calculations of the relative fluorescence quantum yields (Φ_f)[28]: $\Phi_s = \Phi_{st}x(Grad_x/Grand_{st})x(n_x^2/n_{st}^2)$ where Φ and n are the fluorescence quantum yields and refractive indexes, respectively; Grad represents gradient of integrated fluorescence intensity vs absorbance at the particular wavelength, subscripts s and x refer to the standards and the tested samples.

3.5 References

1. Loudet, A.; Burgess, K., BODIPY Dyes and Their Derivatives: Syntheses and Spectroscopic Properties. *Chem. Rev. (Washington, DC, U. S.)* **2007,** *107* (11), 4891-4932.

2. Ulrich, G.; Ziessel, R.; Harriman, A., The Chemistry of Fluorescent Bodipy Dyes: Versatility Unsurpassed. *Angew. Chem. Int. Ed.* **2008,** *47* (7), 1184-1201.

3. Rurack, K.; Kollmannsberger, M.; Daub, J., A highly efficient sensor molecule emitting in the near infrared (NIR): 3,5-distyryl-8-(p-dimethylaminophenyl)difluoroboradiaza-s-indacene. *New J. Chem.* **2001,** *25* (2), 289-292.

4. Rohand, T.; Qin, W.; Boens, N.; Dehaen, W., Palladium-Catalyzed Coupling Reactions for the Functionalization of BODIPY Dyes with Fluorescence Spanning the Visible Spectrum. *Eur. J. Org. Chem.* **2006,** *2006* (20), 4658-4663.

5. Leen, V.; Braeken, E.; Luckermans, K.; Jackers, C.; Van der Auweraer, M.; Boens, N.; Dehaen, W., A versatile, modular synthesis of monofunctionalized BODIPY dyes. *Chem. Commun.* **2009,** (30), 4515-4517.

6. Meng, Q.; Fronczek, F. R.; Vicente, M. G. H., Synthesis and Spectroscopic Properties of β,β'-Dibenzo-3,5,8-triaryl-BODIPYs. *New J. Chem.* **2016**, 5740-5751.

7. Leen, V.; Leemans, T.; Boens, N.; Dehaen, W., 2- and 3-Monohalogenated BODIPY Dyes and Their Functionalized Analogues: Synthesis and Spectroscopy. *Eur. J. Org. Chem.* **2011,** *2011* (23), 4386-4396.

8. Leen, V.; Miscoria, D.; Yin, S.; Filarowski, A.; Molisho Ngongo, J.; Van der Auweraer, M.; Boens, N.; Dehaen, W., 1,7-Disubstituted Boron Dipyrromethene (BODIPY) Dyes: Synthesis and Spectroscopic Properties. *J. Org. Chem.* **2011,** *76* (20), 8168-8176.

9. Leen, V.; Yuan, P.; Wang, L.; Boens, N.; Dehaen, W., Synthesis of Meso-Halogenated BODIPYs and Access to Meso-Substituted Analogues. *Org. Lett.* **2012,** *14* (24), 6150-6153.

10. Jiao, L.; Yu, C.; Uppal, T.; Liu, M.; Li, Y.; Zhou, Y.; Hao, E.; Hu, X.; Vicente, M. G. H., Long wavelength red fluorescent dyes from 3,5-diiodo-BODIPYs. *Org. Biomol. Chem.* **2010,** *8* (11), 2517-2519.

11. Wang, H.; Vicente, M. G. H.; Fronczek, F. R.; Smith, K. M., Synthesis and Transformations of 5-Chloro-2,2′-Dipyrrins and Their Boron Complexes, 8-Chloro-BODIPYs. *Chem. Eur. J.* **2014,** *20* (17), 5064-5074.

12. Wang, H.; Fronczek, F. R.; Vicente, M. G. H.; Smith, K. M., Functionalization of 3,5,8-Trichlorinated BODIPY Dyes. *J. Org. Chem.* **2014,** *79* (21), 10342-10352.

13. Zhao, N.; Vicente, M. G. H.; Fronczek, F. R.; Smith, K. M., Synthesis of 3,8-Dichloro-6-ethyl-1,2,5,7-tetramethyl–BODIPY from an Asymmetric Dipyrroketone and Reactivity Studies at the 3,5,8-Positions. *Chem. Eur. J.* **2015,** *21* (16), 6181-6192.

14. Zhao, N.; Xuan, S.; Fronczek, F. R.; Smith, K. M.; Vicente, M. G. H., Stepwise Polychlorination of 8-Chloro-BODIPY and Regioselective Functionalization of 2,3,5,6,8-Pentachloro-BODIPY. *J. Org. Chem.* **2015,** *80* (16), 8377-8383.

15. Baruah, M.; Qin, W.; Vallée, R. A. L.; Beljonne, D.; Rohand, T.; Dehaen, W.; Boens, N., A Highly Potassium-Selective Ratiometric Fluorescent Indicator Based on BODIPY Azacrown Ether Excitable with Visible Light. *Org. Lett.* **2005,** *7* (20), 4377-4380.

16. Jiao, L.; Pang, W.; Zhou, J.; Wei, Y.; Mu, X.; Bai, G.; Hao, E., Regioselective Stepwise Bromination of Boron Dipyrromethene (BODIPY) Dyes. *J. Org. Chem.* **2011,** *76* (24), 9988-9996.

17. Yu, C.; Xu, Y.; Jiao, L.; Zhou, J.; Wang, Z.; Hao, E., Isoindole-BODIPY Dyes as Red to Near-Infrared Fluorophores. *Chem. Eur. J.* **2012,** *18* (21), 6437-6442.

18. Yu, C.; Jiao, L.; Tan, X.; Wang, J.; Xu, Y.; Wu, Y.; Yang, G.; Wang, Z.; Hao, E., Straightforward Acid-Catalyzed Synthesis of Pyrrolyldipyrromethenes. *Angew. Chem. Int. Ed.* **2012,** *51* (31), 7688-7691.

19. Jiang, T.; Zhang, P.; Yu, C.; Yin, J.; Jiao, L.; Dai, E.; Wang, J.; Wei, Y.; Mu, X.; Hao, E., Straightforward Synthesis of Oligopyrroles through a Regioselective SNAr Reaction of Pyrroles and Halogenated Boron Dipyrrins. *Org. Lett.* **2014,** *16* (7), 1952-1955.

20. Jiao, L.; Li, J.; Zhang, S.; Wei, C.; Hao, E.; Vicente, M. G. H., A selective fluorescent sensor for imaging Cu^{2+} in living cells. *New J. Chem.* **2009,** *33* (9), 1888-1893.

21. Hendricks, J. A.; Keliher, E. J.; Wan, D.; Hilderbrand, S. A.; Weissleder, R.; Mazitschek, R., Synthesis of [^{18}F]BODIPY: Bifunctional Reporter for Hybrid Optical/Positron Emission Tomography Imaging. *Angew. Chem. Int. Ed.* **2012,** *51* (19), 4603-4606.

22. Duheron, V.; Moreau, M.; Collin, B.; Sali, W.; Bernhard, C.; Goze, C.; Gautier, T.; Pais de Barros, J.-P.; Deckert, V.; Brunotte, F.; Lagrost, L.; Denat, F., Dual Labeling of Lipopolysaccharides for SPECT-CT Imaging and Fluorescence Microscopy. *ACS Chem. Biol.* **2014,** *9* (3), 656-662.

23. Liu, S.; Lin, T.-P.; Li, D.; Leamer, L.; Shan, H.; Li, Z.; Gabbai, F. P.; Conti, P. S., Lewis Acid-Assisted Isotopic 18F-19F Exchange in BODIPY Dyes: Facile Generation of Positron Emission Tomography/Fluorescence Dual Modality Agents for Tumor Imaging. *Theranostics* **2013,** *3* (3), 181-189.

24. Rohand, T.; Baruah, M.; Qin, W.; Boens, N.; Dehaen, W., Functionalisation of fluorescent BODIPY dyes by nucleophilic substitution. *Chem. Commun.* **2006,** (3), 266-268.

25. Ortiz, M. J.; Agarrabeitia, A. R.; Duran-Sampedro, G.; Bañuelos Prieto, J.; Lopez, T. A.; Massad, W. A.; Montejano, H. A.; García, N. A.; Lopez Arbeloa, I., Synthesis and functionalization of new polyhalogenated BODIPY dyes. Study of their photophysical properties and singlet oxygen generation. *Tetrahedron* **2012,** *68* (4), 1153-1162.

26. Qin, W.; Leen, V.; Dehaen, W.; Cui, J.; Xu, C.; Tang, X.; Liu, W.; Rohand, T.; Beljonne, D.; Averbeke, B. V.; Clifford, J. N.; Driesen, K.; Binnemans, K.; Auweraer, M. V. d.; Boens, N., 3,5-Dianilino Substituted Difluoroboron Dipyrromethene: Synthesis, Spectroscopy, Photophysics, Crystal Structure, Electrochemistry, and Quantum-Chemical Calculations†. *The Journal of Physical Chemistry C* **2009,** *113* (27), 11731-11740.

27. Olmsted, J., Calorimetric determinations of absolute fluorescence quantum yields. *The Journal of Physical Chemistry* **1979,** *83* (20), 2581-2584.

28. Gorka, A. P.; Nani, R. R.; Zhu, J.; Mackem, S.; Schnermann, M. J., A Near-IR Uncaging Strategy Based on Cyanine Photochemistry. *J. Am. Chem. Soc.* **2014,** *136* (40), 14153-14159.

CHAPTER IV: PREPARATION OF NEAR-IR BODIPYS VIA BENZO-FUSIONS

4.1 Introduction

4.1.1 Overview

In the last decade, research in the synthesis of organic chromophores with absorption and fluorescence spectra in the near infrared (NIR) region became popular, because such chromophores have many applications such as in imaging,[1-5], electrophoresis,[6-7] labels[8] and sensors.[9-11] The biological window is in the 650–1000 nm region, where auto-fluorescence, and absorption by water and tissues are minimized, so laser light could penetrate deeper. The development of low-cost instruments for NIR excitation sources and detectors, have inspired the design of new fluorophores with high molar absorption coefficients and fluorescence quantum yield.

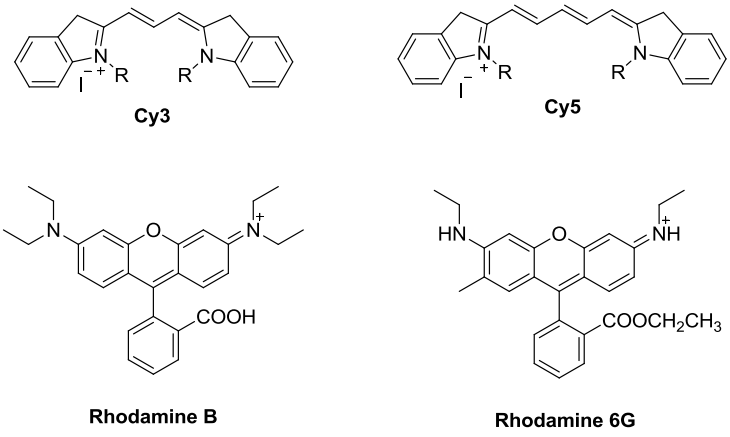

Figure 4.1**:** Cyanine dyes and rhodamine dyes

So far cyanine dyes, such as Cy3 or Cy5, have been the most common choice in many applications, but their low photostability and low quantum yields are the major drawbacks. Though some rigid or bridged cyanines have been developed, the flexible bonds can still cause non-emissive deactivation.[12-13] Rhodamine dyes are occasionally employed as alternatives due to

their relatively higher structural rigidity and high quantum yields in aqueous solvents, as shown in Figure 4.1. However, their absorption and emission peaks are below 600 nm. In addition, since rhodamine dyes are with positively charged ions, the solubility of rhodamines is restricted to polar solvents.[14]

4.1.2 BODIPY's Wavelength Tuning Strategies

Classical BODIPY's spectral properties are typically within the 470–530 nm region. Around 50 nm red-shifts of the absorption and emission maxima have been achieved through functionalization at the BODIPY periphery. Our research goal is to synthesize near infrared BODIPY dyes with high stability, solubility and fluorescence quantum yields. A great number of papers are published on the synthesis, properties and applications of near infrared BODIPY dyes, and their major red-shifting methods are listed below.

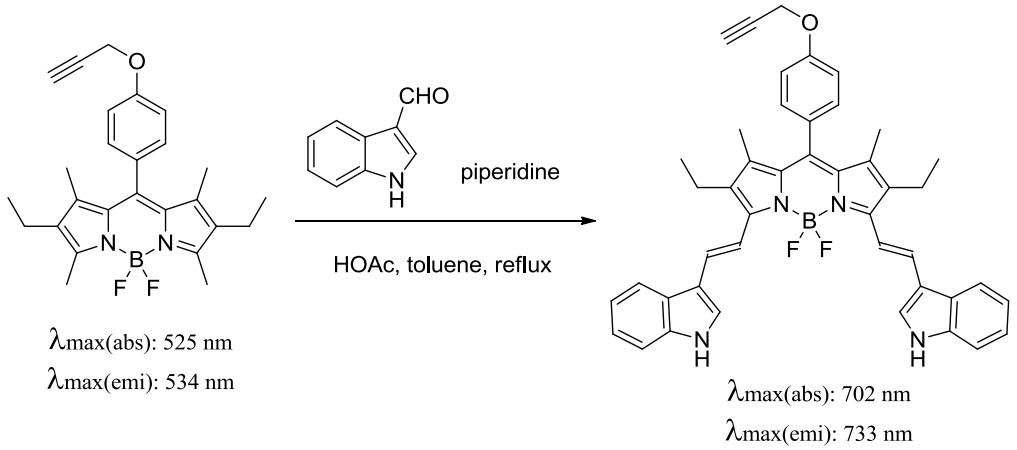

Scheme 4.1: A 3,5-Knovenagel condensation reaction that red-shifts the BODIPY[15]

4.1.2.1 Functionalizations with aryl, styryl and arylethynyl units

The introduction of aryl substituents is a common method in BODIPY's synthetic chemistry, and the aryl units can be installed either on the pyrrole precursors or at the postfunctionalization stage of BODIPYs. This method to produces significant red-shifts due to a

destabilization of the HOMO orbitals while phenyl groups are incorporated at the 3,5-positions, where large MO coefficients are anticipated.[16-17]

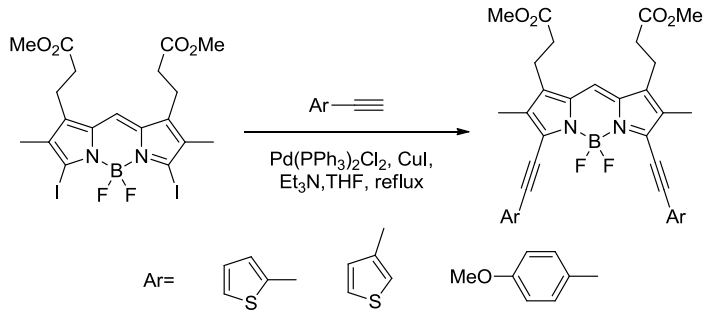

Scheme 4.2: Sonogashira cross-coupling reactions to give arylethynyl BODIPYs[18]

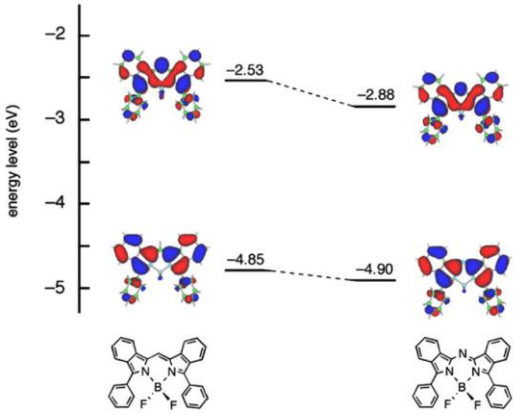

Figure 4.2: Calculated MO diagrams of BODIPY and aza-BODIPY[19] Reprint with permission from Elsevier (2008).

Styryl groups are commonly introduced to BODIPYs by Knoevenagel condensations, or are able to be installed with Heck cross-coupling reactions, as Chapter II describes. When indole-3-carbaldehyde was employed in Knoevenagel reactions, the 3,5-distyryl groups induced red-shifts in the order of 178 nm in the absorption and 198 nm in the emission spectra, as shown in Scheme 4.1.[15] Arylethynyl functionalization, particularly with thiophene, gives BODIPYs that absorb up to 649 nm and emit up to 681 nm, as shown in Scheme 4.2 shows.[18]

4.1.2.2 Replacing the *meso*-carbon atom with a nitrogen atom to form aza-BODIPYs

Computational studies show that the red-shifted absorption band mainly comes from a transition from HOMO to LUMO.[19] The energies of the HOMO and LUMO are both stabilized, but the stabilization of the HOMO of the aza-BODIPY is less than that of LUMO, since the LUMO is delocalized over the *meso*-position by the stronger electron-withdrawing effect of the nitrogen atom. The HOMO–LUMO gap for the aza-BODIPY is smaller than that for the *meso*-carbon BODIPY, resulting in obvious red-shifts, as shown in Figure 4.2.

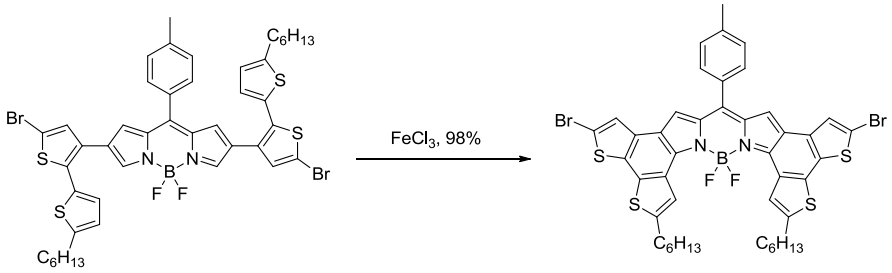

Scheme 4.3: Rigidification of the 2,6-aryl groups to produce red-shifts[20]

4.1.2.3 Rigidification of free-rotatable moieties

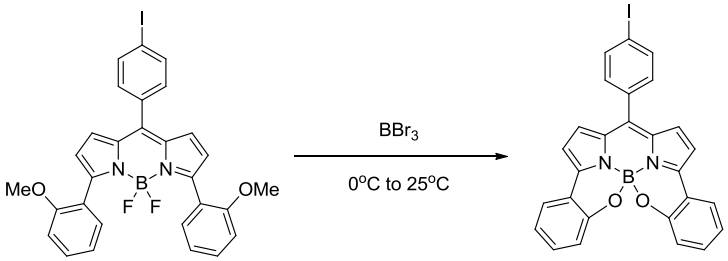

Scheme 4.4: Rigidification of 3,5-diaryl groups to produce red-shifts[21]

Various rotatable moieties were attempted to be prevented on BODIPY molecules, mainly including the ones from *meso*-, 3,5- and 2,6-positions. Wu *et al* used $FeCl_3$/$MeNO_2$/DCM conditions to rigidify the anthracene unit on BODIPY's 1,7-positions and the new dye shows four major bands above 600 nm: 606, 650, 760, and 826 nm.[22] The Burgess group first installed two 2-methoxy-phenyl on the 3,5-positions of BODIPY, and then employed BBr_3 to hydrolyze the OMe to hydroxyl group following by chelation with boron atom, as shown in Scheme 4.4.

The BODIPY showed red-shifted 80 nm in the absorption spectra and 47 nm in the emission spectra.[21] Ziessel *et al* prepared a BODIPY with dithienyl units and through $FeCl_3$/DCM condition, the β-position of the thiophene was coupled with the BODIPY's 3,5-positions to give a near-IR BODIPY that absorbs at 665 nm, as shown in Scheme 4.3.[23]

4.1.2.4 Push-pull Effects

Aza-BODIPYs with 4-methoxy-phenyl groups at the 3,5-positions and 4-cyano-phenyl groups at the 1,7-positions show 28 nm red-shifts in the absorption and 32 nm red-shifts in the emission spectra, as shown in Figure 4.3.[24] This phenomenon is probably due to the reducing of the band gap by increasing the HOMO, and decreasing the LUMO energy. BODIPYs bearing electron donating groups at the 2,3,5-positions, and electron withdrawing groups at the 6,8-positions show the λ_{max} absorption at 635-653 nm, and emission at 706-707 nm and the largest Stokes shift (54−71 nm) in different solvents, as shown in Figure 4.4 show.[25]

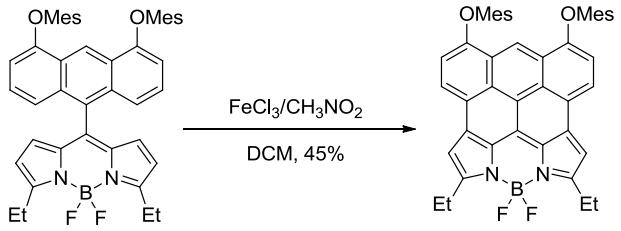

Scheme 4.5: Rigidification of the *meso*-aryl group to produce red-shifting[22]

4.1.2.5 Benzo-fusions

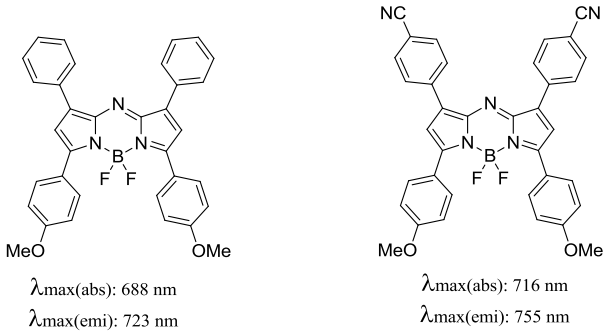

Figure 4.3: Push-pull effect to produce bathochromic shifts of aza-BODIPYs[24]

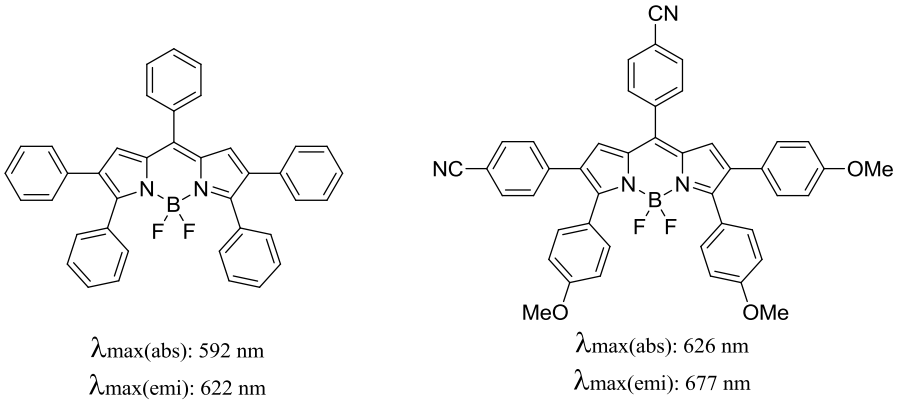

Figure 4.4: Push-pull effect to produce bathochromic shifts on BODIPYs[25]

Π-extented BODIPYs, with aromatic ring fusion at the β, β'-pyrrolic positions, are highly constrained, planar and hydrophobic. The rigid aromatic rings largely red-shift BODIPY's absorption and emission spectra (ca. 50 nm per annulated benzene ring), and the quantum yields are also enhanced.[26] Several π-extented BODIPYs have been synthesized via different methods and high cell permeability was shown, particularly the *meso*-aryl-substituted benzo-BODIPYs. The Ono method starts from an α-free bicyclo-octadiene-fused pyrrole with methyl, ester or aryl groups on the other α-position, as Route A shows in Figure 4.5, and a series of BODIPY's benzo-fusions were generated from retro-Diels-Alder reactions under harsh conditions.[27-28] On the other hand the isoindole precursors required by Route B are relatively unstable, so only the Hao&Jiao method reported a total synthesis of monobenzo-fused BODIPYs from 2-chloro-5-formyl-isoindole[29-30] and Ziessel method reported a total synthesis of *meso*-free dibenzo-BODIPYs via a bis-isoindolylmethane retro-aldol formaldehyde elimination.[31] Furthermore, as di- and/or tetra-hydroisoindole pyrroles have been used as precursors for the synthesis of tetrabenzoporphyrins,[32] they were reported in preparation of π-extended dipyrrins and BODIPYs. In 2010, π-extended dipyrrins were prepared from dihydroisoindole's aromatization with DDQ in THF and room temperature, as Route C shows.[33] In 2012, our group reported the synthesis of a

series of π-extended BODIPYs from a more readily prepared tetrahydroisoindole, with ethoxycarbonyl substituent on the 3,5-positions, as shown by route E, which decreases the quantum yields due to its high flexibility and limits further chemical and biological functionalization.[26] Route D and Route F both form isoindole intermediates that produce dibenzo-dipyrromethene in "one-pot" synthesis, thus they are efficient methods to prepare symmetric dibenzo-BODIPYs as well.[31, 34]

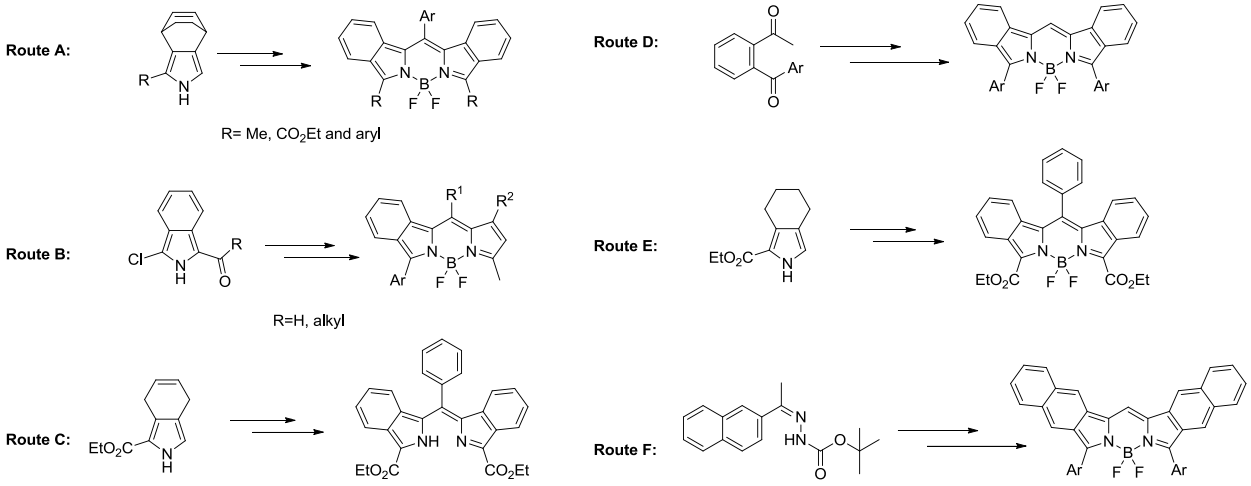

Figure 4.5: Synthetic strategies to prepare β,β'-benzo-fused BODIPYs and precursors

4.1.3 Epidermal Growth Factor Receptor

Epidermal growth factor receptor (EGFR) is employed in tumor targeted diagnosis and therapy, since its overexpression was reported to be found in breast, colon, and ovarian cancers. Colorectal cancer (CRC) is causing the second leading cancer-related deaths in the US. Colon cancer develops over several years from adenomatous polyps to carcinoma, and colon screening, detection, and removal of polyp adenomas or early stage cancer reduces the incidence of CRC. Current detecting methods for CRC include flexible sigmoidoscopy, radiography, standard colonoscopy, and computer tomography (CT) colonoscopy. EGFR has strong association with colorectal cancer, so it has been targeted by various ligands such as peptides, antibodies and

conjugates.[35] Our group prepared a series of phthalocyanine-peptide and porphyrin-peptide conjugates, and via *in vitro* and *in vivo* studies we found that those conjugates targeted EGFR selectively.[37-38]

4.1.4 Research Prospective

Based on the results from Chapter II and III, we have synthesized and characterized a number of BODIPY dyes that can be further transformed to near-IR BODIPY derivatives, and we are investigating their further bio-conjugation reactions to produce novel near-IR imaging reagents.

4.2 Results and Discussion

4.2.1 Syntheses

All sample prepared in Chapters II and III with bicyclo-moieties at the 1,2,6,7-positions, were investigated in oxidation reaction to produce dibenzo moieties to induce red-shifts. Bicyclo-BODIPYs and DDQ were dissolved in toluene, and the solutions were refluxed and monitored by TLC and by UV-Vis, as shown in Scheme 4.6. Only BODIPYs with phenyl and 4-nitro-phenyl groups were successfully oxidized to their dibenzo-derivatives. The solutions of BODIPYs with 3,5-electron-rich aryl groups red-shifted by approximately 70-90 nm, but TLC indicated the new formed compounds were insoluble and very polar, requiring 100% acetone as the eluent. Previous experience indicated that most BODIPY molecules were relatively non-polar and very soluble in DCM. Thus we think the aromatized BODIPYs formed, but they were quickly polymerized to polymers immediately, due to the high electron density on the 3,5-groups. The other BODIPYs with hetero-substituents, styryl and arylethynyl groups decomposed within 30 minutes, as observed by lack of the UV-Vis absorption bands, and the solutions completely lost the fluorescence. Other milder aromatizing conditions were also attempted on all bicyclo

BODIPYs, including $FeCl_3$, H_2O_2 and I_2/DMSO,[39] but the results still turned out to be either polymerization or decomposition.

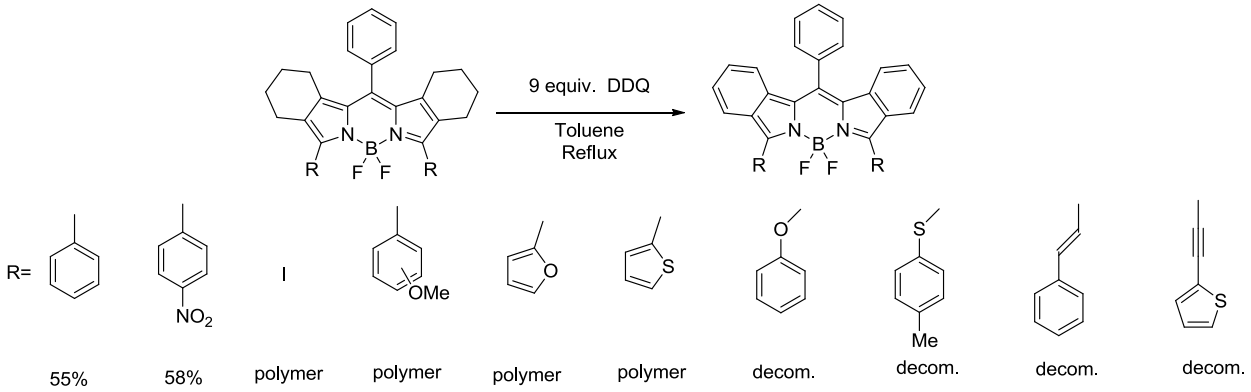

Scheme 4.6: Attempts to aromatize bicyclo-BODIPYs bearing substituents at the 3,5-positions

Since bicyclo-BODIPYs bearing phenyl, 4-nitrophenyl and ethyl ester groups[26] were successfully aromatized under DDQ conditions, we then plan to prepare a series of symmetric and unsymmetric bicyclo-BODIPYs bearing aryl groups containing electro-withdrawing units. The targeted molecules are expected to have three "handles" at the *meso*-, 3- and 5-positions for three different purposes, as Figure 4.6 shows, and these molecules are expected to retain high stability due to the strong sp^2C-sp^2C bonding.

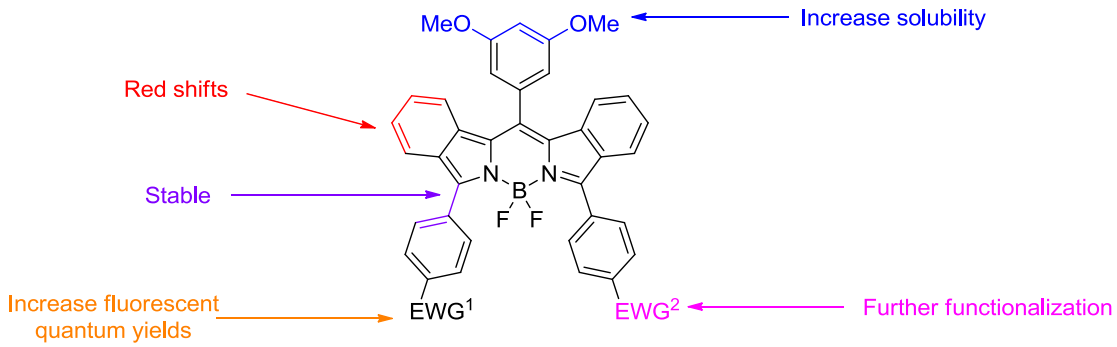

Figure 4.6: A designed near-IR BODIPY structure with three "handles"

4.2.1.1 Synthesis of bicyclo-BODIPYs with 3,5-diaryl groups

The optimized conditions from Chapter II were then used for the coupling of boronic acids (4-cyanophenyl-, 4-(trifluoromethyl)phenyl- and 4-(benzyloxycarbonyl)phenyl boronic acids) and the products from these reactions, BODIPYs **2a–i** were isolated consistently in high yields, and the highest yield (92%) was obtained for **2i** due to the enhanced solubility in organic solvents. The yields of all prepared bicyclo-BODIPYs, including **2a** and **2b** which were investigated in Chapter II, are ummarized in Table 4.1.

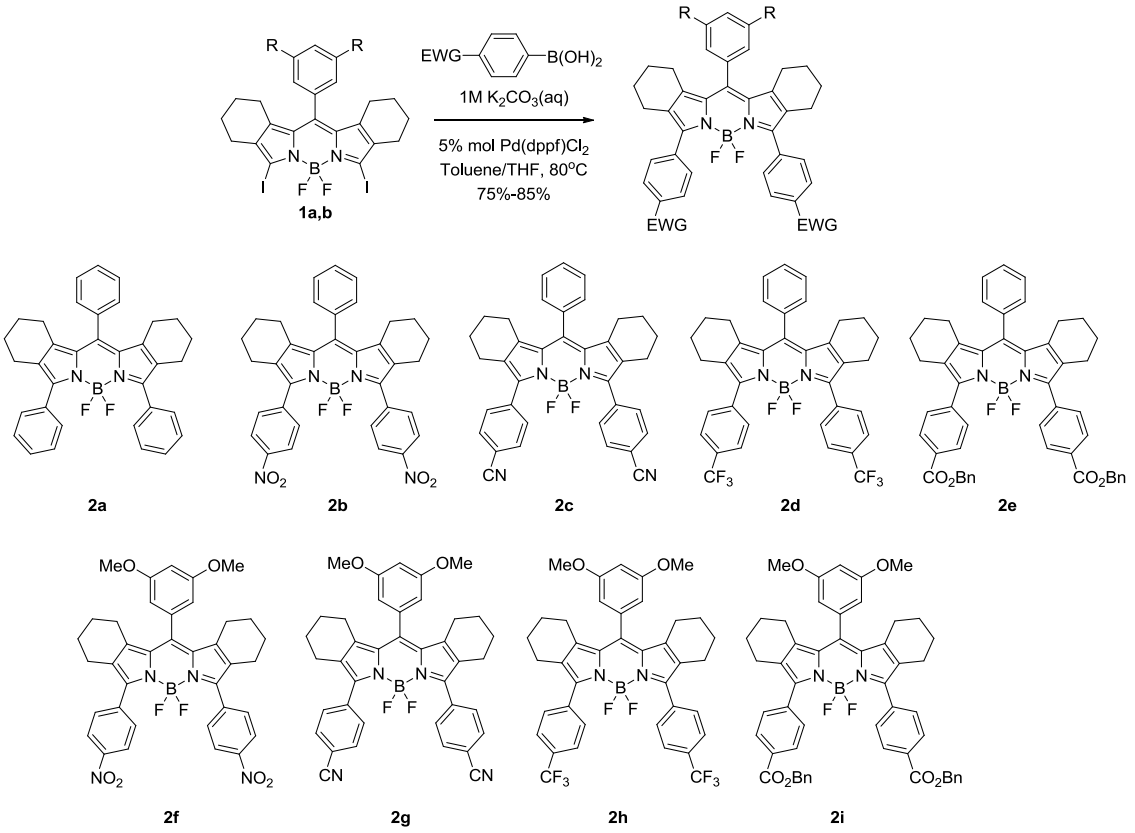

Scheme 4.7: Symmetric Suzuki cross-coupling reactions on 3,5-diiodo-BODIPY **1a** and **1b**

Crystals suitable for X-ray analysis were obtained for BODIPYs **2b**, **2c**, **2d**, **2e**, **2f**, **2h** and **2i**, as shown in Figure 4.7. In BODIPY **2a**, the C_3N_2B ring is almost planar. Its *meso*-phenyl ring forms a dihedral angle of 79.8° with the central ring, and its 3,5-diphenyl rings form a dihedral angle of 56.2° with the central C_3N_2B ring. BODIPY **2b**'s central ring is slightly twisted, with carbon atoms lying 0.076 Å out of the plane, and the nitrogen atoms 0.072 Å. Its *meso*-

phenyl group forms a dihedral angle of 60.4° with the central plane, and the 3,5-daryl groups 47.2°. In BODIPY **2c**, the central C_3N_2B ring is non-planar, as the boron atom lies out of the C_3N_2 best plane. The *meso*-phenyl group forms a dihedral angle of 72.8° with the central plane, and the 3,5-diaryl groups form an average of 61.0° with the central plane. In BODIPY **2d**, the central C_3N_2B ring is highly planar. Its *meso*-phenyl ring forms a dihedral angle of 74.4° with the central plane, and the 3,5-diaryl groups an average of 52.9°. In BODIPY **2e**, the central C_3N_2B ring is also highly planar. Its *meso*-phenyl group forms a dihedral angle of 82.4° with the central plane, and the 3,5-diphenyl rings an average of 59.8° with it.

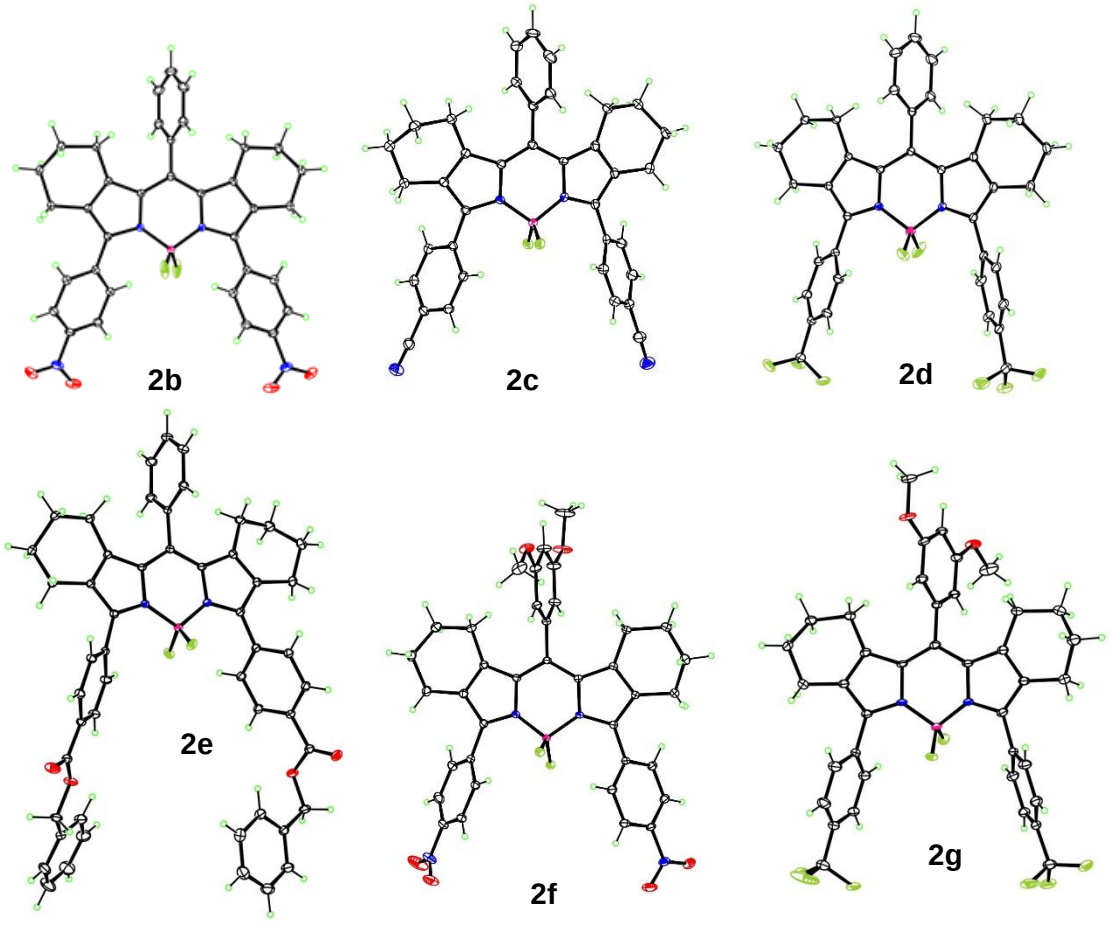

Figure 4.7: Crystal structure of BODIPYs **2b, 2c, 2d, 2e, 2f,** and **2h**[41]

4.2.1.2 DDQ aromatization

To obtaining the best aromatizing conditions, bicyclo-BODIPY **2b** reacted with 9 equivalents of DDQ in refluxing toluene. In the first attempt, BODIPY **2b** was dissolved in approximately 20 mL toluene, and DDQ was added. The reaction took 3 hours to be completed and the yield was only 15%. Polar byproducts were observed in this reaction, probably as a result of a radical polymerization process. Such polar compounds were the major products obtained from the DDQ aromatization of BODIPYs bearing electron-donating groups at the 3,5-positions. To avoid the intermolecular polymerization, we then diluted the reaction solution to 50 mL, but the yield was even lower (4%), after longer time (5 hours). Considering the aromatization reaction rate is highly related with the concentration, BODIPY **2b** was dissolved in only 5 mL of toluene, and the reaction was successfully completed within 30 minutes, with a highest yield of 32%. The same conditions were applied for all other BODIPYs **2a**, **2c-i**, as well as two unsymmetric BODIPYs from Chapter II, **3a** and **3b**, and all aromatization reactions were successful, producing BODIPYs **4a-k** in 32-56%. The lowest yield was obtained for BODIPY **4b**, due to the strongest electron-withdrawing character of the nitro units, and its lowest solubility compared with the other BODIPYs.

Table 2.1: Products and yields obtained in the Suzuki cross-couplings (**2a-f**) and DDQ aromatization (**4a-f**) of BODIPYs **1a** and **1b**.

BODIPY	Ar group	R group	Yield of 5 (%)	Yield of 6 (%)
2a/4a	Ph	H	85	50
2b/4b	Ph	NO_2	83	32
2c/4c	Ph	CN	85	52
2d/4d	Ph	CF_3	82	48
2e/4e	Ph	CO_2Bn	86	54
2f/2f	3,5-$(OMe)_2$Ph	CO_2Bn	92	52

BODIPYs **4a**, **4b** and **4c** were characterized by X-ray crystallography, as shown in Figure 4.8. BODIPY **4a** has a similar twisted conformation from **2b**, although the BODIPY only has the C2 symmetry. The *meso*-phenyl group forms a dihedral angle of 68.3° with the central plane, and the 3,5-phenyl groups 60.6°. The central ring of BODIPY **4b** is as non-planar as **2c**, with the boron atom lying out of the plane. The *meso*-phenyl ring forms a dihedral angle of 76.8° with the central plane, and the 3,5-diphenyl groups 57.2°. The central ring of both independent BODIPY **4c** has the boron atom lying out of the central plane. The *meso*-phenyl group forms a dihedral angle of 82.2° with the central plane, and the 3,5-diaryl groups 50.2°.

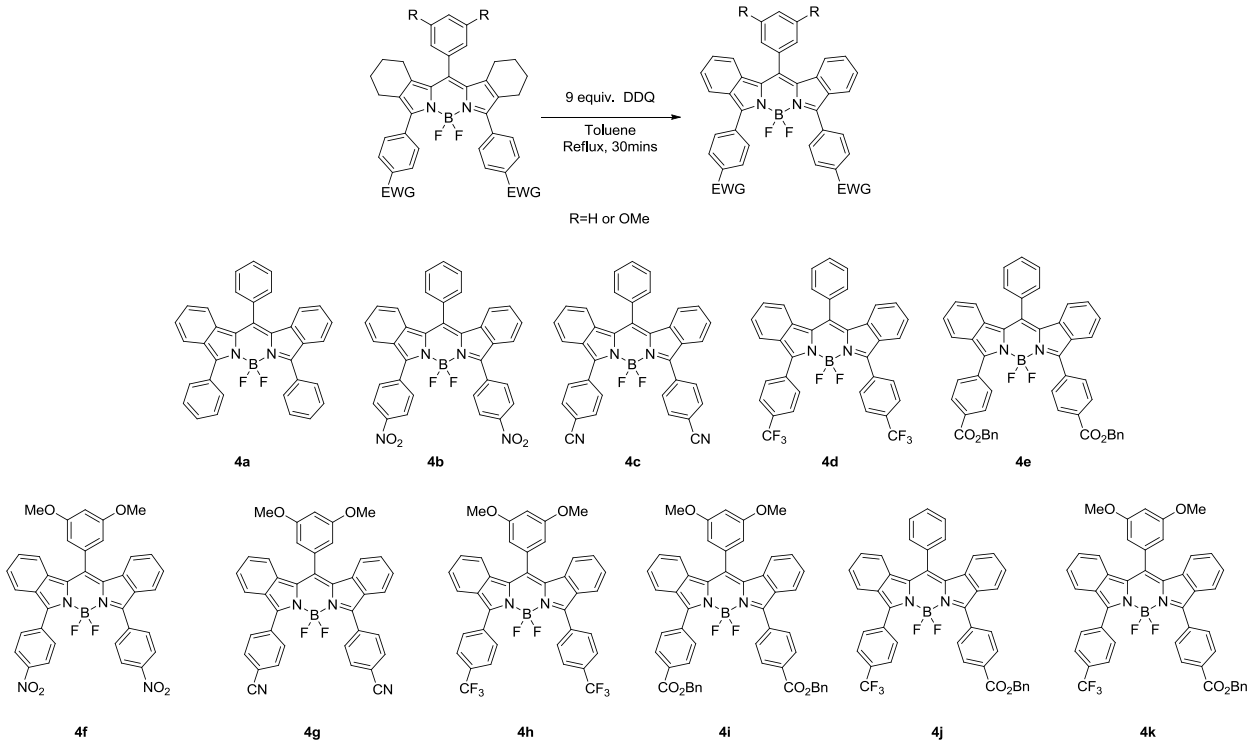

Scheme 4.8: Aromatization reactions to produce dibenzo-BODIPYs

4.2.1.3 Conversion of nitrophenyl-BODIPYs to isothiocyanate-BODIPYs

Nitrophenyl BODIPYs **4b** and **4f** were further functionalized since nitro groups are relatively easy to be reduced to amino groups via a variety of reducing conditions, and amino-BODIPYs are promising candidates for further bio-conjugations. Since nitrophenyl units on the

meso-position were reported to be reduced by hydrazine and Pd/C in refluxed ethanol,[42] BODIPYs **4b** and **4f** were treated with excess hydrazine hydrate in the presence of 10 % Pd/C, and the solution was refluxed in a co-solvent of THF and ethanol, since ethanol wasn't able to dissolve **4b** and **4f**. The reduction reactions were completed after two to three hours, producing diaminophenyl-BODIPY **5a** and **5b** in 21 and 87 % yield, respectively, as shown in Scheme 4.9. The lower yield of **5a** was mainly due to its low solubility. However, the stability of **5a** and **5b** were both relatively low, and even during purification and characterization time they were partially decomposed to dark insoluble solids.

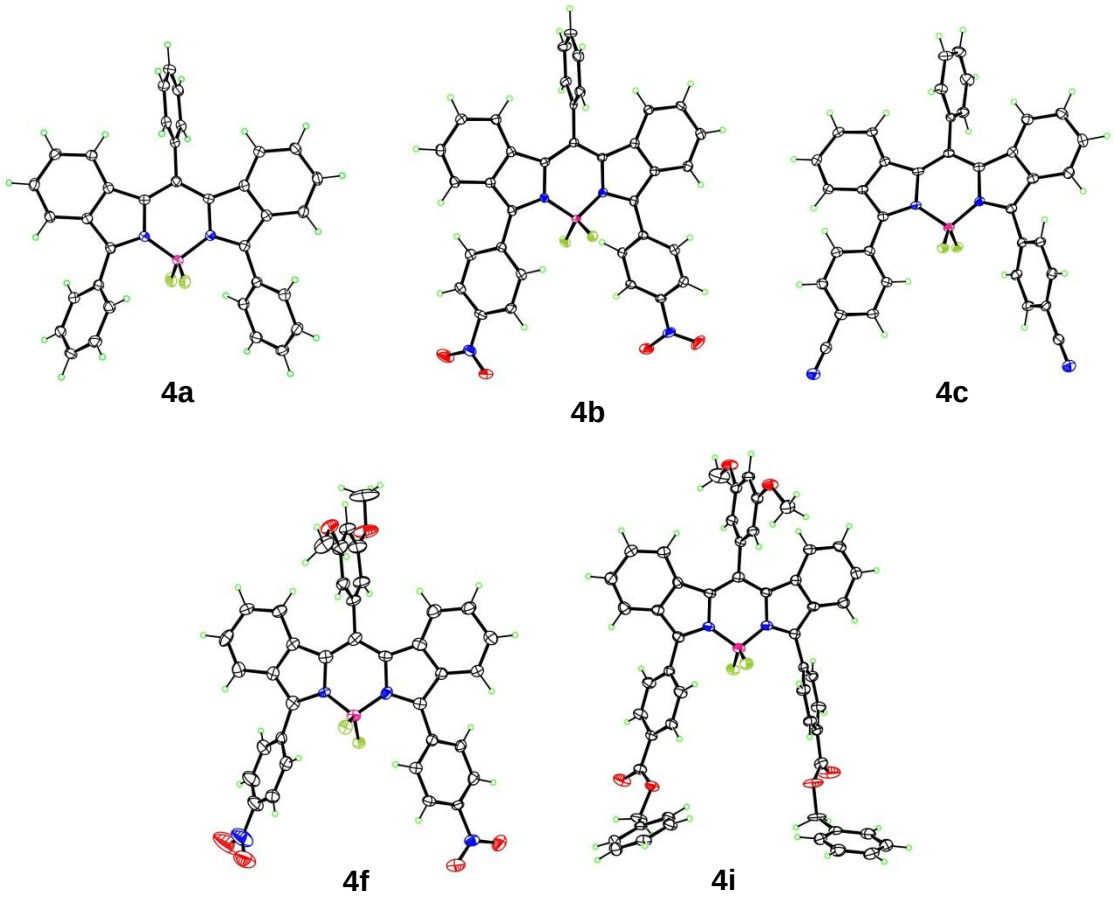

Figure 4.8: Crystal structure of BODIPYs **4a, 4b, 4c,**[40] **4f,** and **4i**

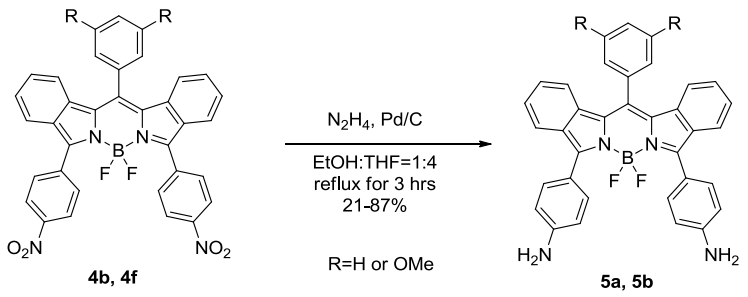

Scheme 4.9: Reduction of nitrophenyl BODIPYs to aminophenyl-BODIPYs

Due to the low stability of diaminophenyl-BODIPYs, we decided to convert them to more stable peptide conjugating precursor isothiocyanate BODIPYs, which also requires mild conjugation conditions, and readily prepared peptides with free amino groups. Diaminophenyl BODIPYs **5a** and **5b** were then converted to isothiocyanate BODIPYs **6a** and **6b**, by reacting with excess amounts of 1,1′-thiocarbonyldi-2(1*H*)-pyridone for 24 hours.[43] Diisothiocyanate BODIPYs **7a** and **7b** were produced in 21 and 87% yields, as shown in Scheme 4.10. The lower yield of **7a** was also due to its low solubility. We then chose BODIPY **7b** as the candidate for further bio-conjugation, because its overall yield from the dinitrophenyl BODIPY is much higher.

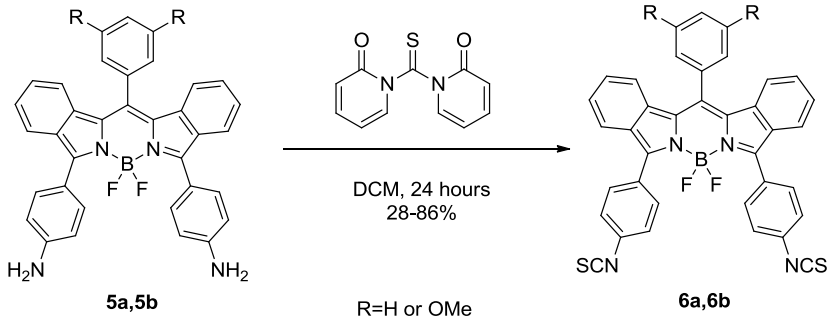

Scheme 4.10: Conversion of diaminophenyl-BODIPYs to diisothiocyanate BODIPYs

4.2.1.4 Conjugation between PEGylated EGFR-L1 and isothiocyanate-BODIPY

BODIPY **7b** was then employed for conjugation reaction, and we chose PEGylated EGFR-L1(LARLLT) due to its better cellular properties[36-37] and its PEGylated linker to reduce the steric hindering effect. By treating BODIPY **7b** with 2 equivalents of $(PEG)_3$-EGFR-L1 in

anhydrous DMF in the presence of triethylamine, mono-conjugated BODIPY **8** was obtained in 86% after 30 minutes, as shown in Scheme 4.11, and after HPLC purification using 100% acetonitrile as the eluent, as shown in Figure 4.9. To obtain a bis(EGFR-L1)-BODIPY, larger equivalents of EGFG-L1 were treated with BODIPY **7b**, or BODIPY **8** was reacted with another 2 equivalents of EGFR-L1, but MALDI-MS spectrometry result didn't present any corresponding product.

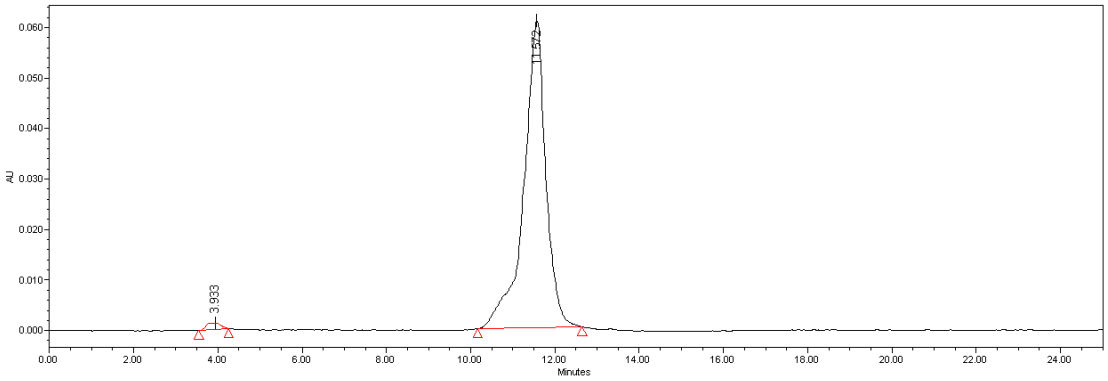

Figure 4.9: An HPLC purification spectra of BODIPY **8**

4.2.2 Structural Characterization

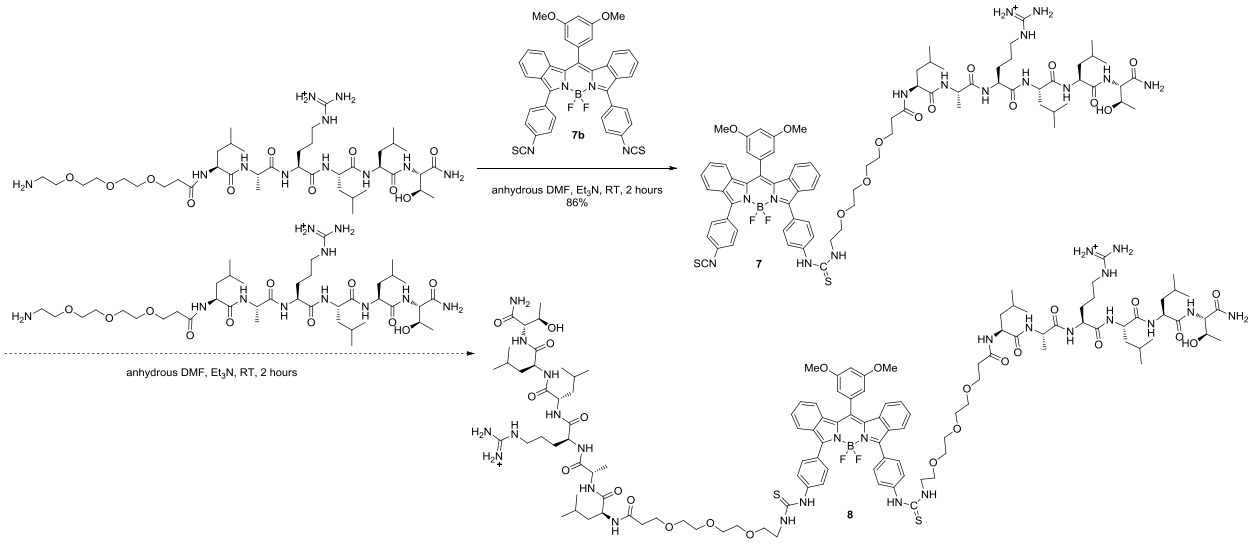

Scheme 4.11: Conjugation reactions between BODIPY **7b** and $(PEG)_3$-EGFR-L1

All BODIPYs were characterized by ^{1}H-, ^{13}C- ^{11}B- and ^{19}F-NMR, HRMS, UV-Vis and fluorescence. The products from the Suzuki cross-coupling reactions, the β,β'-bicyclo-3,5,8-triaryl-BODIPYs **2a-i** and **3a,b** showed ^{1}H and ^{13}C chemical shifts for the 3,5-aryl groups characteristically. After aromatization to the β,β'-dibenzo-BODIPYs, the chemical shifts for the 3,5-aryl groups almost did not shift. However, the ^{1}H and ^{13}C chemical shifts for the fused benzene rings characteristically moved to the aromatic regions.

Table 4.2: ^{11}B- and ^{19}F-NMR chemical shifts of BF_2 group. In ^{11}B-NMR the signal is a triplet and in ^{19}F-NMR the signals are a quartet and septet (J_{11BF} =32 Hz, J_{10BF} = 10 Hz)

BODIPY	**^{11}B NMR (ppm)**	**^{19}F NMR (ppm)**
2a	0.87	-131.45, -131.53
2b	0.67	-131.81, -130.89
2c	0.70	-131.06, -131.13
2d	0.78	-131.48, -131.55
2e	0.77	-131.40, -131.47
2i	0.73	-131.25, -131.32
4a	1.81	-129.13, -129.20
4b	1.67	-128.20, -128.28
4c	1.68	-128.19, -128.26
4d	1.74	-128.56, -128.64
4e	1.76	-128.56, -129.63
4i	1.70	-129.34, -129.41
3a	1.72	-131.28, -131.35
3b	1.68	-131.25, -131.32
4j	0.82	-128.52, -128.60
4k	0.70	-128.59, -128.67

Differences were also seen in the ^{11}B and ^{19}F NMR spectra of the BODIPYs, as shown in Table 4.2. All BODIPYs showed a triplet signal in ^{11}B-NMR with ca. J_{BF} = 32 Hz. In ^{19}F-NMR

the isotopes ^{11}B (I = 3/2, 80%) and ^{10}B (I = 3, 20%) split the BF_2 signals into a mixture of a quartet (J_{11BF} = 32 Hz) and a septet (J_{10BF} = 10 Hz). The signals in ^{11}B-NMR shifted downfield from ca. 0.5 ppm for the β,β'-bicyclo-3,5-diiodo-BODIPYs to ca. 0.8 ppm for the β,β'-bicyclo-3,5,8-triaryl-BODIPYs, and finally about 1.7 ppm for the β,β'-dibenzo-3,5,8-triaryl-BODIPYs. In ^{19}F-NMR the signals shifted downfield too, following the same trend. These changes are due to interactions of the aryl groups with the BF_2 unit, and to the extension of π-conjugation systems.

4.2.3 Spectroscopic study

The spectroscopic properties of BODIPYs **2a-2e**, **2i**, **4a-e**, **4i**, **3a,b** and **4a,j** in THF, including their maximum absorption and emission wavelengths, molar coefficients, Stokes shifts, and fluorescence quantum yields, were investigated and are shown in Table 4.3. Figures 4.11 and 4.12 show the normalized absorption and emission spectra of some selected BODIPYs, respectively. The BODIPYs show characteristic absorption and emission spectra, with high molar absorption coefficients (log ε = 4.63-5.00) and Stokes-shifted narrow fluorescent emission bands. BODIPY **2b** bearing two nitro groups showed the most red-shifted absorption and emission bands, and the largest Stokes shift. However, BODIPY **2b** with two nitro groups shows the lowest fluorescence quantum yield and BODIPY **2d** bearing two trifluoromethyl groups shows the highest fluorescence quatum yield. *p*-Nitrophenyl groups have been reported to quench the fluorescence of BODIPYs via PET process, due to the strong electron-withdrawing effect of the nitro. The presence of a trifluoromethyl at the *meso*-position of BODIPYs was previously reported to induce high fluorescence quantum yields.[44]

The β,β'-dibenzo-BODIPYs showed 77-89 nm red-shifts in the absorption and emission bands, compared with the corresponding β,β'-bicyclo-BODIPYs as expected. In general, the fluorescence quantum yields were higher for the β,β'-dibenzo-BODIPYs compared with the

corresponding β,β'-bicyclo-BODIPYs, except in the case of the 3,5-dinitrophenyl-BODIPY **2b**. Diisothiocyanate BODIPY **7b**'s emission spectra show the highest peak in 683nm, indicating it's an excellent near-IR conjugation precursor.

4.3 Conclusions

The functionalization of 3,5-diiodo-BODIPYs via Suzuki cross-coupling reactions gave the β,β'-bicyclo-3,5,8-triaryl-BODIPYs in 82-92% yields. DDQ aromatization of these β,β'-bicyclo-3,5,8-triaryl-BODIPYs produced the corresponding β,β'-dibenzo-3,5,8-triaryl-BODIPYs in 32-54% yields. Downfield shifts were observed in their ^{11}B and ^{19}F-NMR spectra. The β,β'-dibenzo-3,5,8-triaryl-BODIPYs showed 77-89 nm red-shifted absorptions and fluorescence emissions, decreased Stokes shifts, and in general higher quantum yields, compared with their corresponding β,β'-bicyclo-BODIPYs. The 3,5-(*p*-nitrophenyl) groups caused the largest red-shifts and Stokes shifts, although they slightly quenched the fluorescence quantum yield of the BODIPYs. On the other hand, BODIPYs bearing 3,5-(*p*-trifluoromethylphenyl) groups showed the highest fluorescence quantum yields among this series. Nitrophenyl BODIPYs were successfully converted to diisothiocyanate BODIPYs and the following bio-conjugating reactions were performed to give BODIPY-peptide conjugates for further imaging studies.

4.4 Experimental

4.4.1 General Information

All the reagents and solvents were purchased from Sigma-Aldrich and were used without further purification. All reactions were carried out with oven-dried glassware under a dry argon atmosphere. All the reactions were monitored using Sorbent Technologies 0.2 mm silica gel TLC plates with UV-254 nm indicator. Flash column chromatography was performed using Sorbent Technologies 60 Å silica gel (230-400 mesh). Prep-TLC 60 Å silica gel 20 x 20 cm (210-270 μm)

was used. All ^{1}H-, ^{13}C-, ^{11}B- and ^{19}F-NMR spectra were collected on a Bruker AV-400 and AV-500 spectrometer in deuterated chloroform or dichloromethane. The $CDCl_3$ chemical shifts (δ) are reported in ppm using as reference 7.26 for proton and 77.00 for carbon and BF_3•OEt_2 was used as reference (0.00 δ) for boron NMR. The CD_2Cl_2 chemical shifts (δ) are reported in ppm using as reference 5.32 for proton and 53.50 for carbon. Coupling constants are reported in Hertz (Hz). All the mass spectra were collected using an Agilent 6210 ESI-TOF mass spectrometer. All melting points were recorded using a MEL-TEMP electrothermal instrument.

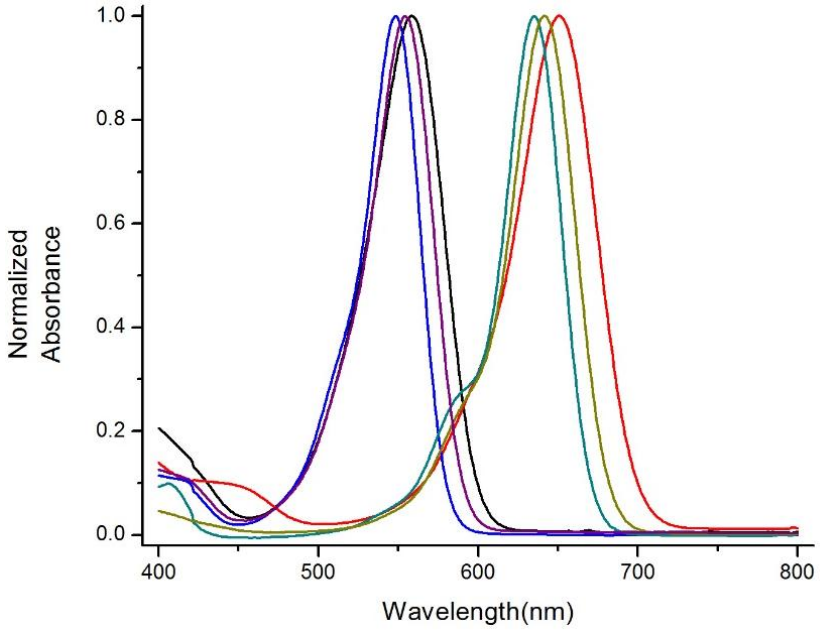

Figure 4.11: Normalized UV-Vis spectra of selected BODIPYs **2b** (black), **2c** (blue), **2d** (purple), **2b** (red), **2c** (cyan) and **2d** (dark yellow) in THF at room temperature.

4.4.2 Synthesis

General Suzuki cross-coupling conditions. For symmetric BODIPYs, 62.8 mg (0.100 mmol) **1a** or 68.8 mg (0.100 mmol) **1b**, 5.00 mg Pd(dppf)Cl_2 and 5 equiv (0.500 mmol) of aryl boronic acid were mixed under inert atmosphere. Toluene (2 mL) and THF (2 mL) were added via syringe and the solution was heated at 70 ^{o}C in an oil bath for 3 min. K_2CO_3 (1 M, 0.5 mL)

solution was added via syringe and the reaction was monitored by TLC until complete consumption of 3,5-diiodo-BODIPY. The cooled solution was filtered through celite to remove excess palladium and boronic acid, and the solvent was concentrated under vacuum. The residue was purified by silica gel column chromatography to afford the corresponding 3,5-diaryl-BODIPYs as red solids, which were recrystallized using 1:1 dichloromethane/hexane.

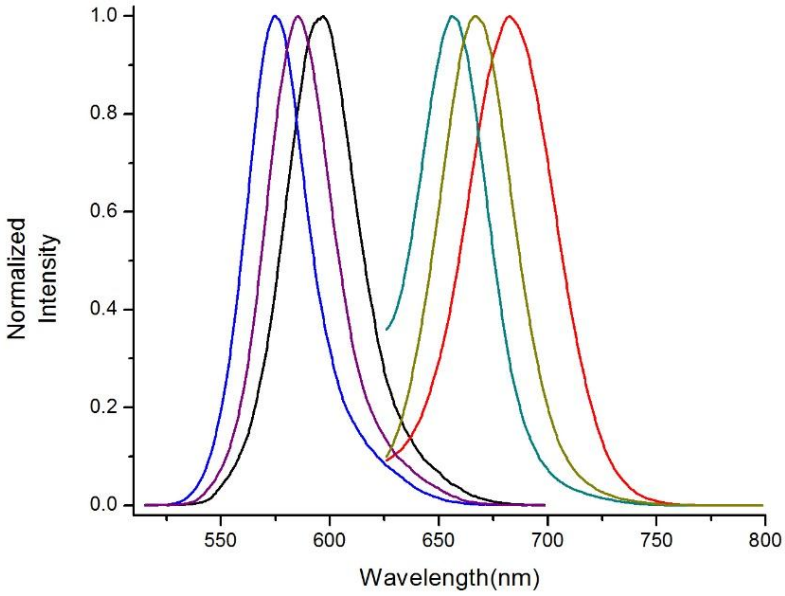

Figure 4.11 Normalized fluorescent emission spectra of selected BODIPYs **2b** (black), **2c** (blue), **2d** (purple), **2b** (red), **2c** (cyan) and **2d** (dark yellow) in THF at room temperature.

BODIPY 2c: Yield 85%. mp(°C)> 300; ^{1}H NMR (CD_2Cl_2, 400 MHz) δ 7.72 – 7.60 (m, 8H), 7.60 – 7.53 (m, 3H), 7.42 – 7.35 (m, 2H), 2.25 (t, *J* = 5.9 Hz, 4H), 1.72 (t, *J* = 6.1 Hz, 4H), 1.57 – 1.52 (m, 4H), 1.46 (d, *J* = 5.6 Hz, 4H); ^{13}C NMR (CD_2Cl_2, 100 MHz) δ 152.3, 143.8, 143.2, 136.7, 134.9, 132.1, 131.6, 130.4, 130.40, 130.37, 130.3, 129.5, 129.4, 127.9, 118.6, 112.4, 24.4, 23.0, 22.5, 22.4; ^{11}B NMR ($CDCl_3$, 128 MHz) δ 0.70 (t, *J* = 32.3 Hz); ^{19}F NMR ($CDCl_3$,

376 MHz) δ -131.00-131.26 (m); HRMS (ESI-TOF) m/z 600.2407 $[M+Na]^+$ calcd for $C_{37}H_{29}BF_2N_4Na$ 600.2382.

Table 4.3: Spectroscopic properties of BODIPYs in THF.

BODIPY	Abs λ_{max} (nm)	log ε ($M^{-1}cm^{-1}$)	Emi λ_{max} (nm)	Φ_f	Stokes shift (cm^{-1})
5a	548	4.74	574	0.42	827
5b	558	4.66	597	0.35	1171
5c	554	4.63	585	0.43	957
5d	548	4.75	575	0.52	857
5e	554	4.74	586	0.42	986
5i	555	4.76	585	0.40	924
6a	631	4.78	651	0.64	487
6b	651	4.72	683	0.23	720
6c	643	4.77	670	0.48	627
6d	635	4.79	656	0.67	504
6e	641	4.94	667	0.48	608
6i	642	4.99	667	0.46	584
3a	638	4.94	664	0.55	614
3b	638	4.89	663	0.55	591
4j	551	4.79	579	0.45	878
4k	551	4.75	580	0.46	907

BODIPY 2d: Yield 82%. mp(°C)> 300; ^{1}H NMR ($CDCl_3$, 400 MHz) δ 7.65 (q, *J* = 8.4 Hz, 8H), 7.55 (dd, *J* = 4.9, 1.9 Hz, 3H), 7.42 – 7.33 (m, 2H), 2.26 (t, *J* = 6.0 Hz, 4H), 1.70 (t, *J* = 6.1 Hz, 4H), 1.57 – 1.52 (m, 4H), 1.49 – 1.42 (m, 4H); ^{13}C NMR ($CDCl_3$, 125 MHz) δ 154.6, 141.72, 135.8, 132.3, 131.4, 129.9, 129.8, 129.2, 129.1, 128.7, 128.3, 127.9, 24.4, 23.3, 22.84, 22.77; ^{11}B NMR ($CDCl_3$, 128 MHz) δ 0.78 (t, *J* = 32.1 Hz); ^{19}F NMR ($CDCl_3$, 376 MHz) δ -

62.70(s), δ -131.42-131.68 (m); HRMS (ESI-TOF) m/z 644.2352 $[M-F]^+$ calcd for $C_{37}H_{29}BF_7N_2$ 644.2343.

BODIPY 2e: Yield 86%. mp(°C)> 300; ^{1}H NMR (CD_2Cl_2, 400 MHz) δ 8.22 (s, 2H), 8.11 (dt, *J* = 8.0, 1.5 Hz, 2H), 7.81 (dt, *J* = 7.9, 1.4 Hz, 2H), 7.58 (dd, *J* = 5.2, 1.9 Hz, 3H), 7.53 – 7.45 (m, 6H), 7.45 – 7.34 (m, 8H), 5.37 (s, 4H), 2.29 (t, *J* = 6.0 Hz, 4H), 1.76 (t, *J* = 6.1 Hz, 4H), 1.61 – 1.53 (m, 4H), 1.48 (dp, *J* = 9.4, 3.6, 2.7 Hz, 4H); ^{13}C NMR (CD_2Cl_2, 100 MHz) δ 165.9, 153.3, 143.1, 142.7, 137.0, 136.4, 135.2, 131.9, 130.3, 130.2, 129.80, 129.77, 129.3, 129.0, 128.6, 128.2, 128.09, 128.06, 66.7, 24.5, 23.1, 22.6, 22.5; ^{11}B NMR (CD_2Cl_2, 128 MHz) δ 0.77 (t, *J* = 32.3 Hz); ^{19}F NMR ($CDCl_3$, 376 MHz) δ -131.34-131.60 (m); HRMS (ESI-TOF) m/z 818.3172 $[M+Na]^+$ calcd for $C_{51}H_{43}BF_2N_2O_4Na$ 818.3212.

BODIPY 2f: Yield 91%. mp(°C)> 300; ^{1}H NMR ($CDCl_3$, 400 MHz) δ 8.22 (d, *J* = 8.4 Hz, 4H), 7.71 (d, *J* = 8.4 Hz, 4H), 6.62 (s, 1H), 6.52 (d, *J* = 2.2 Hz, 2H), 3.86 (s, 6H), 2.27 (d, *J* = 6.1 Hz, 4H), 1.92 (d, *J* = 6.1 Hz, 4H), 1.73 – 1.44 (m, 8H); ^{13}C NMR ($CDCl_3$, 100 MHz) δ 161.8, 152.1, 147.7, 143.3, 143.1, 138.4, 136.4, 131.8, 130.64, 130.60, 130.57, 130.1, 123.0, 105.6, 101.2, 55.6, 24.0, 22.9, 22.42, 22.36; ^{11}B NMR ($CDCl_3$, 128 MHz) δ 0.69 (t, *J* = 32.4 Hz); HRMS (ESI-TOF) m/z 659.2489 $[M-F]^+$ calcd for $C_{37}H_{33}BFN_4O_6$ 659.2477.

BODIPY 2g: Yield 88%. mp(°C)> 300; ^{1}H NMR (400 MHz, CD_2Cl_2) δ 7.77 – 7.46 (m, 8H), 6.64 (t, *J* = 2.3 Hz, 1H), 6.54 (d, *J* = 2.3 Hz, 2H), 3.85 (s, 6H), 2.27 (t, *J* = 6.0 Hz, 4H), 1.95 (d, *J* = 6.0 Hz, 4H), 1.63 – 1.47 (m, 8H); ^{13}C NMR (100 MHz, CD_2Cl_2) δ 162.0, 152.3, 143.4, 143.2, 136.7, 136.4, 131.8, 131.5, 130.41, 130.38, 130.35, 130.23, 130.20, 118.6, 112.4, 105.7, 101.2, 55.7, 24.1, 23.0, 22.5, 22.4; ^{11}B NMR (128 MHz, CD_2Cl_2) δ 0.67 (t, *J* = 32.5 Hz); HRMS (ESI-TOF) m/z 619.2666 $[M-F]^+$ calcd for $C_{39}H_{33}BFN_4O_2$ 619.2681.

BODIPY 2h: Yield 86%. mp(°C)> 300; ^{1}H NMR (400 MHz, CDCl3) δ 7.65 (q, *J* = 8.4 Hz, 8H), 6.60 (t, *J* = 2.3 Hz, 1H), 6.53 (d, *J* = 2.3 Hz, 2H), 3.85 (s, 6H), 2.27 (t, *J* = 6.0 Hz, 4H), 1.91 (t, *J* = 6.0 Hz, 4H), 1.55 (m, 6H); ^{13}C NMR (100 MHz, CD_2Cl_2) δ 162.0, 152.9, 143.1, 142.9, 136.7, 136.1, 131.5, 130.5, 130.19, 130.16, 130.1, 125.6, 124.80, 124.76, 124.72, 124.68, 122.9, 105.8, 101.3, 55.7, 24.2, 23.1, 22.6, 22.5; ^{11}B NMR (128 MHz, CD_2Cl_2) δ 0.70 (t, *J* = 32.3 Hz); HRMS (ESI-TOF) m/z 705.2551 $[M-F]^+$ calcd for $C_{39}H_{33}BF_7N_2O_2$ 705.2523.

BODIPY 2i: Yield 92%. mp(°C)> 300; ^{1}H NMR ($CDCl_3$, 400 MHz) δ 8.06 (d, *J* = 8.0 Hz, 4H), 7.59 (d, *J* = 8.1 Hz, 4H), 7.45 (d, *J* = 7.2 Hz, 4H), 7.42 – 7.31 (m, 6H), 6.61 (t, *J* = 2.2 Hz, 1H), 6.54 (d, *J* = 2.2 Hz, 2H), 5.35 (s, 4H), 3.84 (s, 6H), 2.27 (t, *J* = 5.9 Hz, 4H), 1.93 (t, *J* = 6.0 Hz, 4H), 1.67 – 1.37 (m, 8H); ^{13}C NMR (CD_2Cl_2, 125 MHz) δ 165.9, 161.9, 153.3, 142.7, 136.9, 136.7, 136.3, 131.5, 130.3, 130.1, 129.77, 129.75, 129.7, 128.9, 128.6, 128.2, 128.1, 124.9, 105.8, 101.2, 66.7, 55.7, 24.1, 23.1, 22.6, 22.5; ^{11}B NMR ($CDCl_3$, 128 MHz) δ 0.73 (t, *J* = 32.0 Hz); ^{19}F NMR (CD_2Cl_2, 376 MHz) δ -131.19-131.45 (m); HRMS (ESI-TOF) m/z 836.3535 $[M-F]^+$ calcd for $C_{53}H_{47}BFN_2O_6$ 836.3542.

General procedure for DDQ aromatization. 0.100 mmol bicyclo-3,5-diaryl-BODIPYs and 204 mg (0.900 mmol) of DDQ were dissolved in 5 mL toluene. The solution was then refluxed under inert atmosphere for 30 min. The reaction was monitored by TLC and UV-Vis spectroscopy. The solvent was removed under vacuum and the residue was dissolved in 100 mL dichloromethane and washed with sat. $NaHCO_3$ (1 x 100 mL). The aqueous solution was extracted with dichloromethane (2 x 50 mL) and the organic solvent was removed under vacuum. The residue was purified by silica gel column chromatography and the product was recrystallized in 1:1 dichloromethane/hexane.

BODIPY 4a: Yield 50%. mp(°C)> 300; ^{1}H NMR (CD_2Cl_2, 400 MHz) δ 7.80 (d, J = 7.0 Hz, 4H), 7.72 (d, J = 6.8 Hz, 3H), 7.64 (d, J = 6.9 Hz, 2H), 7.51 (dd, J = 14.3, 7.7 Hz, 8H), 7.07 (dt, J = 23.6, 7.3 Hz, 4H), 6.24 (d, J = 8.3 Hz, 2H); ^{13}C NMR (CD_2Cl_2, 100 MHz) δ 151.7, 135.3, 134.3, 131.2, 131.0, 130.3, 129.6, 129.5, 129.4, 129.1, 128.8, 128.2, 126.4, 124.7, 123.6, 121.4; ^{11}B NMR ($CDCl_3$, 128 MHz) δ 1.81 (t, J = 31.2 Hz); ^{19}F NMR ($CDCl_3$, 376 MHz) δ -129.0-129.33 (m); HRMS (ESI-TOF) m/z 519.1960 [M]+ calcd for $C_{35}H_{23}BF_2N_2$ 519.1953.

BODIPY 4b: Yield 32%. mp(°C)> 300; ^{1}H NMR (CD_2Cl_2, 400 MHz) δ 8.39 – 8.28 (m, 4H), 7.99 – 7.91 (m, 4H), 7.80 – 7.74 (m, 3H), 7.66 (dq, *J* = 6.5, 2.2 Hz, 2H), 7.52 (dt, *J* = 8.2, 1.1 Hz, 2H), 7.20 (ddd, *J* = 8.1, 6.9, 1.1 Hz, 2H), 7.13 (ddd, *J* = 8.1, 6.9, 1.1 Hz, 2H), 6.32 (dd, *J* = 8.3, 1.1 Hz, 2H); ^{13}C NMR (CD_2Cl_2, 125MHz) δ 149.2, 148.3, 138.1, 137.4, 134.62, 134.55, 131.5, 131.42, 131.39, 131.0, 130.9, 130.0, 129.9, 129.6, 128.9, 128.8, 127.7, 125.8, 124.9, 123.4, 122.8, 121.9; ^{11}B NMR ($CDCl_3$, 128MHz) δ 1.67 (t, *J* = 31.8 Hz); ^{19}F NMR (CD_2Cl_2, 376MHz) δ -128.1-128.40 (m); HRMS (ESI-TOF) m/z 610.1739 $[M+H]^+$ calcd for $C_{35}H_{22}BF_2N_2O_4$ 611.1739.

BODIPY 4c: Yield 52%. mp(°C)> 300; ^{1}H NMR (CD_2Cl_2, 400 MHz) δ 7.89 (d, *J* = 8.0 Hz, 4H), 7.84 – 7.74 (m, 7H), 7.64 (d, *J* = 6.4 Hz, 2H), 7.49 (d, *J* = 8.1 Hz, 2H), 7.18 (t, *J* = 7.5 Hz, 2H), 7.11 (t, *J* = 7.6 Hz, 2H), 6.31 (d, *J* = 8.3 Hz, 2H); ^{13}C NMR (CD_2Cl_2, 100 MHz) δ 149.4, 135.5, 134.6, 132.0, 131.04, 131.01, 130.97, 129.92, 129.86, 129.5, 128.9, 125.7, 122.8, 121.8, 118.5, 113.2; ^{11}B NMR ($CDCl_3$, 128 MHz) δ 1.68 (t, *J* = 31.7 Hz); ^{19}F NMR ($CDCl_3$, 376 MHz) δ -128.13-128.39 (m); HRMS (ESI-TOF) m/z 550.1918 $[M-F]^+$ calcd for $C_{37}H_{20}BFN_4$ 550.1874.

BODIPY 4d: Yield 48%. mp(°C)> 300; ^{1}H NMR (CD_2Cl_2, 400 MHz) δ 7.91 (d, *J* = 8.1 Hz, 4H), 7.82 – 7.74 (m, 7H), 7.67 – 7.62 (m, 2H), 7.51 – 7.46 (m, 2H), 7.17 (m, 2H), 7.10 (ddd, *J* = 8.1, 6.8, 1.2 Hz, 2H), 6.34 – 6.27 (m, 2H); ^{13}C NMR (CD_2Cl_2, 100 MHz) δ 150.0, 134.8,

134.5, 131.1, 130.8, 129.8, 129.4, 128.9, 127.1, 125.4, 125.2, 125.1, 123.0, 121.7; ^{11}B NMR ($CDCl_3$, 128 MHz) δ 1.74 (t, *J* = 31.6 Hz); ^{19}F NMR (CD_2Cl_2, 376 MHz) δ -63.02, δ -128.51-128.76 (m); HRMS (ESI-TOF) m/z 636.1695 $[M-F]^+$ calcd for $C_{37}H_{21}BF_7N_2$ 636.1717.

BODIPY 4e: Yield 54%. mp(°C)> 300; ^{1}H NMR (CD_2Cl_2, 400 MHz) δ 8.22 (d, *J* = 8.0 Hz, 4H), 7.87 (d, *J* = 8.1 Hz, 4H), 7.80 – 7.72 (m, 3H), 7.64 (d, *J* = 6.7 Hz, 2H), 7.52 (dd, *J* = 8.0, 3.2 Hz, 6H), 7.42 (dt, *J* = 12.7, 6.7 Hz, 6H), 7.12 (dt, *J* = 25.4, 7.2 Hz, 4H), 6.32 (d, *J* = 8.3 Hz, 2H), 5.43 (s, 4H); ^{13}C NMR (CD_2Cl_2, 100 MHz) δ 165.8, 136.3, 135.6, 134.9, 134.5, 131.0, 130.4, 129.80, 129.78, 129.3, 129.2, 129.0, 128.6, 128.3, 128.2, 125.3, 123.1, 121.7, 66.9; ^{11}B NMR (CD_2Cl_2, 128 MHz) δ 1.76 (t, *J* = 31.5 Hz); ^{19}F NMR (CD_2Cl_2, 376 MHz) δ -128.51-128.76 (m); HRMS (ESI-TOF) m/z 787.2701 $[M]^+$ calcd for $C_{51}H_{35}BF_2N_2O_4$ 787.2689.

BODIPY 4f: Yield 34%. mp(°C)> 300; ^{1}H NMR (400 MHz, CD_2Cl_2) δ 8.41 – 8.26 (m, 4H), 8.05 – 7.79 (m, 4H), 7.58 – 7.47 (m, 2H), 7.27 – 7.15 (m, 4H), 6.85 (t, *J* = 2.3 Hz, 1H), 6.80 (d, *J* = 2.3 Hz, 2H), 6.66 – 6.49 (m, 2H), 3.88 (s, 6H); ^{13}C NMR (126 MHz, CD_2Cl2) δ 162.2, 149.1, 148.3, 137.7, 137.3, 136.1, 134.4, 134.4, 131.42, 131.39, 131.37, 131.0, 130.94, 130.92, 130.90, 129.8, 127.4, 125.9, 123.3, 122.7, 122.2, 106.6, 101.8, 55.8; ^{11}B NMR (128 MHz, CD_2Cl_2) δ 1.66 (t, *J* = 31.9 Hz); HRMS (ESI-TOF) m/z 693.1731 $[M+Na]^+$ calcd for $C_{37}H_{25}BF_2N_4O_6Na$ 693.1733.

BODIPY 4g: Yield 54%. mp(°C)> 300; ^{1}H NMR (400 MHz, $CDCl_3$) δ 7.89 (d, *J* = 8.2 Hz, 4H), 7.79 (d, *J* = 8.3 Hz, 4H), 7.53 – 7.45 (m, 2H), 7.25 – 7.16 (m, 4H), 6.83 (d, *J* = 2.3 Hz, 1H), 6.79 (d, *J* = 2.3 Hz, 2H), 6.61 – 6.50 (m, 2H), 3.88 (s, 6H); ^{13}C NMR (100 MHz, $CDCl_3$) δ 162.0, 149.4, 137.4, 136.1, 135.3, 134.29, 134.26, 132.0, 130.93, 130.89, 130.86, 130.81, 130.77, 129.7, 127.0, 125.7, 122.7, 122.1, 118.5, 113.2, 106.5, 102.1, 55.7; ^{11}B NMR (128 MHz, $CDCl_3$)

δ 1.64 (t, *J* = 31.8 Hz); HRMS (ESI-TOF) m/z 630.2033 $[M]^+$ calcd for $C_{39}H_{25}BF_2N_4O_2$ 630.2039.

BODIPY 4h: Yield 49%. mp(°C)> 300; ^{1}H NMR (400 MHz, CD_2Cl_2) δ 7.90 (d, *J* = 8.1 Hz, 4H), 7.79 (d, *J* = 8.1 Hz, 4H), 7.53 – 7.46 (m, 2H), 7.23 – 7.15 (m, 4H), 6.82 (dd, *J* = 13.9, 2.3 Hz, 3H), 6.61 – 6.53 (m, 2H), 3.87 (s, 6H); ^{13}C NMR (101 MHz, CD_2Cl_2) δ 162.2, 150.0, 137.4, 136.4, 134.8, 134.3, 131.2, 131.1, 130.9, 130.82, 130.79, 129.6, 127.8, 126.8, 125.6, 125.5, 125.23, 125.19, 125.16, 125.1, 122.93, 122.85, 122.0, 106.7, 101.9, 55.8; ^{11}B NMR (128 MHz, CD_2Cl_2) δ 1.67 (t, *J* = 31.6 Hz); HRMS (ESI-TOF) m/z 697.1882 $[M-F]^+$ calcd for $C_{39}H_{25}BF_7N_2O_2$ 697.1897.

BODIPY 4i: Yield 52%. mp(°C)> 300; ^{1}H NMR (CD_2Cl_2, 400 MHz) δ 8.19 (d, *J* = 8.1 Hz, 4H), 7.84 (d, *J* = 8.0 Hz, 4H), 7.50 – 7.46 (m, 4H), 7.44 – 7.33 (m, 6H), 7.20 – 7.14 (m, 3H), 6.83 (t, *J* = 2.3 Hz, 1H), 6.79 (d, *J* = 2.3 Hz, 2H), 5.40 (s, 4H), 3.86 (s, 6H); ^{13}C NMR (CD_2Cl_2, 125 MHz) δ 165.8, 162.1, 136.3, 131.0, 130.4, 129.4, 129.3, 128.6, 128.24, 128.15, 125.4, 123.0, 122.0, 106.6, 101.8, 66.9, 55.8; ^{11}B NMR ($CDCl_3$, 128 MHz) δ 1.70 (t, *J* = 31.5 Hz); ^{19}F NMR ($CDCl_3$, 376 MHz) δ -129.28-129.54 (m); HRMS (ESI-TOF) m/z 848.2931 $[M+H]^+$ calcd for $C_{53}H_{40}BF_2N_2O_6$ 848.2978.

BODIPY 4j: Yield 54%. mp(°C)> 300; ^{1}H NMR (CD_2Cl_2, 400 MHz) δ 8.25 – 8.17 (m, 2H), 7.94 – 7.83 (m, 4H), 7.81 – 7.71 (m, 5H), 7.67 – 7.60 (m, 2H), 7.55 – 7.46 (m, 4H), 7.45 – 7.33 (m, 3H), 7.19 – 7.06 (m, 4H), 6.30 (d, *J* = 8.3 Hz, 2H), 5.41 (s, 2H); ^{13}C NMR (CD_2Cl_2, 125 MHz) δ 166.3, 151.3, 150.2, 138.0, 136.8, 136.0, 135.3, 135.1, 134.9, 131.6, 131.5, 131.34, 131.31, 131.0, 130.3, 129.9, 129.7, 129.4, 129.1, 128.8, 128.7, 125.91, 125.85, 125.64, 125.61, 123.6, 123.4, 122.17; ^{11}B NMR ($CDCl_3$, 128 MHz) δ 1.72 (t, *J* = 31.5 Hz); ^{19}F NMR (CD_2Cl_2,

376 MHz) δ -62.98(s), -128.47-128.72 (m); HRMS (ESI-TOF) m/z 702.2183 $[M-F]^+$ calcd for $C_{44}H_{28}BF_4N_2O_2$ 702.2211.

BODIPY 4k: Yield 51%. mp(°C)> 300; ^{1}H NMR (CD_2Cl_2, 400 MHz) δ 8.25 – 8.16 (m, 2H), 7.92 – 7.82 (m, 4H), 7.82 – 7.75 (m, 2H), 7.55 – 7.46 (m, 4H), 7.45 – 7.34 (m, 3H), 7.21 – 7.15 (m, 4H), 6.84 (t, J = 2.3 Hz, 1H), 6.61 – 6.52 (m, 2H), 5.40 (s, 2H), 3.87 (s, 6H); ^{13}C NMR (CD_2Cl_2, 100 MHz) δ 165.8, 162.2, 136.4, 136.3, 135.5, 131.1, 131.0, 130.8, 130.4, 129.5, 129.42, 129.35, 128.6, 128.3, 128.2, 125.5, 125.4, 125.2, 125.14, 125.10, 125.06, 123.1, 122.9, 122.0, 106.7, 101.8, 66.9, 55.8; ^{11}B NMR (CD_2Cl_2, 128 MHz) δ 1.68 (t, J = 31.5 Hz); ^{19}F NMR (CD_2Cl_2, 376 MHz) δ -63.0 (s), δ -128.54-128.79 (m); HRMS (ESI-TOF) m/z 820.2039 $[M+K]^+$ calcd for $C_{46}H_{32}BF_5N_2O_4K$ 820.2043.

Preparation of isothiocyanate BODIPYs: To a mixture of 3,5-dinitrophenyl BODIPY **4a** or **4f** (0.09 mmol) and 0.45 mL (0.9 mmol) hydrazine hydrate, 5 mL ethanol and 5 mL THF were added. After all solids were dissolved, 0.24 g (0.23 mmol) of 10% Pd/C was added. The solution was refluxed until TLC indicated the consumption of the starting material. All solvents were removed under vacuum and the residue was dissolved in DCM to pass through a celite cake to remove all Pd/C. After DCM was removed under vacuum, a flash column using EtOAc:DCM=1:1 was able to isolate the diaminophenyl BODIPYs **5a** and **5b**, in 21 and 86% yield, respectively. BODIPY **5a**'s solubility was too low to be characterized. BODIPY **5b**: mp(°C)> 100 (decom.); ^{1}H NMR (400 MHz, CD_2Cl_2) δ 7.61 (d, *J* = 7.6 Hz, 6H), 7.12 (t, *J* = 5.5 Hz, 4H), 6.80 (d, *J* = 8.4 Hz, 7H), 6.51 (d, *J* = 7.6 Hz, 2H), 4.05 (d, *J* = 13.4 Hz, 4H), 3.85 (s, 6H); HRMS (ESI-TOF) m/z 590.2399 $[M-F]^+$ calcd for $C_{37}H_{29}BFN_4O_2$ 590.2398. 47.2 mg (0.077 mmol) BODIPY **5b** and 71.8 mg (0.31 mmol) 1,1′-thiocarbonyldi-2(1*H*)-pyridone were dissolved in 10 mL anhydrous DCM, and the solution was stirred for 24 hours. Then DCM was

removed under vacuum and the residue was purified by silica gel column chromatography. BODIPY 6b: Yield 86%. mp(°C)> 90(decom.); ^{1}H NMR (400 MHz, CD_2Cl_2) δ 7.78 (d, *J* = 8.1 Hz, 4H), 7.55 – 7.48 (m, 2H), 7.39 (d, *J* = 8.1 Hz, 4H), 7.18 (dq, *J* = 6.0, 3.9, 2.2 Hz, 4H), 6.83 (t, *J* = 2.3 Hz, 1H), 6.78 (d, *J* = 2.3 Hz, 2H), 6.58 – 6.51 (m, 2H), 3.86 (s, 6H); ^{13}C NMR (101 MHz, CD_2Cl_2) δ 162.2, 150.1, 136.7, 136.5, 134.3, 132.4, 131.7, 131.0, 130.1, 129.4, 126.7, 125.6, 125.4, 123.0, 122.0, 106.7, 101.8, 55.8;^{11}B NMR (128 MHz, $CDCl_3$) δ 0.68 (t, *J* = 32.4 Hz).; HRMS (ESI-TOF) m/z 674.1540 $[M-F]^+$ calcd for $C_{39}H_{25}BFN_4O_2S_2$ 674.1527.

4.4.3 X-ray Determined Molecular Structures

X-ray data were collected at low temperature with MoKα radiation on Bruker Kappa Apex-II DUO or Nonius KappaCCD diffactometers. data reduction: Bruker *SAINT*; program(s) used to solve structure: *SHELXS97* (Sheldrick, 2008); program(s) used to refine structure: *SHELXL97* (Sheldrick, 2008); molecular graphics: *ORTEP-3 for Windows* (Farrugia, 2012); software used to prepare material for publication: *SHELXL97* (Sheldrick, 2008).

2c: $C_{37}H_{29}BF_2N_4$. CH_2Cl_2, M=663.38, triclinic, a=9.7694(8), b=13.1321(10), c=13.2027(8) Å, α=93.757(5), β=104.793(4), γ=102.323(4)°, T=90 K, space group P-1, Z=2, 24995 reflections measured, 8128 unique (R_{int}=0.062), θ_{max}=28.8°, final R=0.058, CCDC 1435991;

2d: $C_{37}H_{29}BF_8N_2$, M=664.43, triclinic, a=8.1559(9), b=13.0389(14), c=15.7981(18) Å, α=114.011(4), β=91.649(5), γ=102.179(5)°, T=90 K, space group P-1, Z=2, 35888 reflections measured, 11819 unique (R_{int}=0.028), θ_{max}=33.7°, final R=0.041, CCDC 1435992;

2e: $C_{51}H_{43}BF_2N_2O_4$, . CH_2Cl_2, M=881.61, monoclinic, a=9.5919(2), b=34.4320(6), c=13.4607(2) Å, β=107.8990(10)°, T=90 K, space group $P2_1/n$, Z=4, 50441 reflections measured, 20106 unique (R_{int}=0.037), θ_{max}=36.4°, final R=0.054, CCDC 1435993;

2f: $C_{37}H_{33}BF_2N_4O_6$•1.5(CH_2Cl_2), M=805.87, monoclinic, a=14.4025(11), b=8.5485(6), c=30.007(2) Å, β=98.229(2)°, T=90 K, space group $P2_1/n$, Z=4, 61391 reflections measured, 10885 unique (R_{int}=0.043), θ_{max}=33.2°, final R=0.060;

2h: $C_{40}H_{35}BCl_2F_8N_2O_2$, M=809.41, triclinic, a=11.1804(19), b=12.928(2), c=13.910(4) Å, β=76.767(15)°, T=90 K, space group P1, Z=2, 25162 reflections measured, 6505 unique (R_{int}=0.056), θ_{max}=30.5°, final R=0.059;

4a: $C_{35}H_{23}BF_2N_2$, M=520.36, triclinic, a=8.9607(14), b=10.4013(15), c=14.964(3) Å, α=98.262(9), β=106.170(6), γ=107.413(9)°, T=90 K, space group P-1, Z=2, 22864 reflections measured, 5881 unique (R_{int}=0.034), θ_{max}=27.9°, final R=0.044, CCDC 1435994;

4b: $C_{35}H_{21}BF_2N_2O_4$, M=610.37, monoclinic, a=12.2985(6), b=12.9578(6), c=18.4622(9) Å, β=108.407(2)°, T=90 K, space group $P2_1/c$, Z=4, 27177 reflections measured, 26528 unique (R_{int}=0.048), θ_{max}=27.3°, final R=0.053, CCDC 1435995;

4c: $C_{37}H_{20.95}BCl_{0.05}F_2N_2O_4$, M=572.02, monoclinic, a=13.2913(16), b=16.431(2), c=13.4762(16) Å, β=107.238(2)°, T=90 K, space group $P2_1$, Z=4, 21435 reflections measured, 12492 unique (R_{int}=0.023), θ_{max}=29.2°, final R=0.040, CCDC 1435996;

4f: $C_{37}H_{25}BF_2N_4O_6$, M=797.81, monoclinic, a=14.508(4), b=8.281(2), c=30.115(8) Å, β=99.189(10)°, T=90 K, space group $P2_1/n$, Z=4, 26932 reflections measured, 2931 unique (R_{int}=0.088), θ_{max}=25.1°, final R=0.073;

4i: $C_{53}H_{39}BF_2N_2O_6$, M=848.67, trichlinic, a=13.058(3), b=17.920(3), c=18.845(3) Å, β=107.450(12)°, T=90 K, space group P1, Z=4, 38985 reflections measured, 9107 unique (R_{int}=0.080), θ_{max}=26.6°, final R=0.060.

4.4.4 Steady-state Absorption and Fluorescence Spectroscopy

The photophysical properties of compounds were determined by preparing a stock solution with a concentration of 1×10^{-4} M and diluting it to appropriate concentrations for absorbance and emission spectra measurements. All the absorption spectra were obtained using a Perkin Elmer Lambda 35 UV-visible spectrophotometer. The optical density, ε, were taken by preparing solution concentrations at $1x10^{-5}$ M in order to get λ_{max} between 0.5 and 1.0. Emission spectra were measured on a LS-55 Perkin-Elmer spectro-fluorometer with the slit width set at 2.5 nm for all BODIPYs. All absorbance and emission spectra were acquired within 6 h of fresh solution preparation, at room temperature. Rhodamine 6G (Φ = 0.86 in MeOH)[44] was used as the reference for β,β'-bicyclo-BODIPYs in THF. Methylene blue (Φ = 0.03 in MeOH)[44] was used as the reference for β,β'-dibenzo-BODIPY in THF. Quartz spectrophotometric cells with path lengths of 10 mm were used. For the determination of quantum yields, dilute solutions with different absorbance between 0.02-0.08 at the particular excitation wavelength were used. Molar absorption coefficients (ε) was determined from the plots of integrated absorbance vs concentrations. The following equation was used for the calculations of the relative fluorescence quantum yields (Φ_f): $\Phi_s = \Phi_{st} \times (Grad_x/Grand_{st}) \times (n_x^2 / n_{st}^2)$ where Φ and n are the fluorescence quantum yields and refractive indexes, respectively; Grad represents gradient of integrated fluorescence intensity vs absorbance at the particular wavelength, subscripts s and x refer to the standards and the tested samples.

4.5 References

1. Brizet, B.; Goncalves, V.; Bernhard, C.; Harvey, P. D.; Denat, F.; Goze, C., DMAP-BODIPY Alkynes: A Convenient Tool for Labeling Biomolecules for Bimodal PET–Optical Imaging. *Chem. Eur. J.* **2014,** *20* (40), 12933-12944.

2. Duheron, V.; Moreau, M.; Collin, B.; Sali, W.; Bernhard, C.; Goze, C.; Gautier, T.; Pais de Barros, J.-P.; Deckert, V.; Brunotte, F.; Lagrost, L.; Denat, F., Dual Labeling of Lipopolysaccharides for SPECT-CT Imaging and Fluorescence Microscopy. *ACS Chemical Biology* **2014,** *9* (3), 656-662.

3. Lhenry, D.; Larrouy, M.; Bernhard, C.; Goncalves, V.; Raguin, O.; Provent, P.; Moreau, M.; Collin, B.; Oudot, A.; Vrigneaud, J.-M.; Brunotte, F.; Goze, C.; Denat, F., BODIPY: A Highly Versatile Platform for the Design of Bimodal Imaging Probes. *Chem. Eur. J.* **2015,** *21* (37), 13091-13099.

4. Ono, M.; Ishikawa, M.; Kimura, H.; Hayashi, S.; Matsumura, K.; Watanabe, H.; Shimizu, Y.; Cheng, Y.; Cui, M.; Kawashima, H.; Saji, H., Development of dual functional SPECT/fluorescent probes for imaging cerebral β-amyloid plaques. *Bioorg. Med. Chem. Lett.* **2010,** *20* (13), 3885-3888.

5. Ono, M.; Watanabe, H.; Kimura, H.; Saji, H., BODIPY-Based Molecular Probe for Imaging of Cerebral β-Amyloid Plaques. *ACS Chemical Neuroscience* **2012,** *3* (4), 319-324.

6. Hong, T.; Wang, T.; Guo, P.; Xing, X.; Ding, F.; Chen, Y.; Wu, J.; Ma, J.; Wu, F.; Zhou, X., Fluorescent Strategy Based on Cationic Conjugated Polymer Fluorescence Resonance Energy Transfer for the Quantification of 5-(Hydroxymethyl)cytosine in Genomic DNA. *Anal. Chem.* **2013,** *85* (22), 10797-10802.

7. Zhao, T.-T.; Chen, Q.-Y.; Wang, P.-D.; Chen, Z.-P., A DNA-Ag cluster as a sensor for BODIPY isomers and HepG-2 cells. *RSC Advances* **2014,** *4* (20), 10390-10394.

8. Sun, T.; Guan, X.; Zheng, M.; Jing, X.; Xie, Z., Mitochondria-Localized Fluorescent BODIPY-Platinum Conjugate. *ACS Medicinal Chemistry Letters* **2015,** *6* (4), 430-433.

9. Salim, M. M.; Owens, E. A.; Gao, T.; Lee, J. H.; Hyun, H.; Choi, H. S.; Henary, M., Hydroxylated near-infrared BODIPY fluorophores as intracellular pH sensors. *Analyst* **2014,** *139* (19), 4862-4873.

10. Strobl, M.; Rappitsch, T.; Borisov, S. M.; Mayr, T.; Klimant, I., NIR-emitting aza-BODIPY dyes - new building blocks for broad-range optical pH sensors. *Analyst* **2015,** *140* (21), 7150-7153.

11. Schutting, S.; Jokic, T.; Strobl, M.; Borisov, S. M.; Beer, D. d.; Klimant, I., NIR optical carbon dioxide sensors based on highly photostable dihydroxy-aza-BODIPY dyes. *Journal of Materials Chemistry C* **2015,** *3* (21), 5474-5483.

12. Benson, R. C.; Kues, H. A., Absorption and fluorescence properties of cyanine dyes. *Journal of Chemical & Engineering Data* **1977,** *22* (4), 379-383.

13. Sczepan, M.; Rettig, W.; L. Bricks, Y.; Slominski, Y. L.; Tolmachev, A. I., Unsymmetric cyanines: chemical rigidization and photophysical properties. *Journal of Photochemistry and Photobiology A: Chemistry* **1999,** *124* (1–2), 75-84.

14. Lavis, L. D.; Raines, R. T., Bright Ideas for Chemical Biology. *ACS Chemical Biology* **2008,** *3* (3), 142-155.

15. Uppal, T.; Bhupathiraju, N. V. S. D. K.; Vicente, M. G. H., Synthesis and cellular properties of Near-IR BODIPY–PEG and carbohydrate conjugates. *Tetrahedron* **2013,** *69* (23), 4687-4693.

16. Loudet, A.; Burgess, K., BODIPY Dyes and Their Derivatives: Syntheses and Spectroscopic Properties. *Chem. Rev.* **2007,** *107* (11), 4891-4932.

17. Lu, H.; Mack, J.; Yang, Y.; Shen, Z., Structural modification strategies for the rational design of red/NIR region BODIPYs. *Chem. Soc. Rev.* **2014,** *43* (13), 4778-4823.

18. Jiao, L.; Yu, C.; Uppal, T.; Liu, M.; Li, Y.; Zhou, Y.; Hao, E.; Hu, X.; Vicente, M. G. H., Long wavelength red fluorescent dyes from 3,5-diiodo-BODIPYs. *Org. Biomol. Chem.* **2010,** *8* (11), 2517-2519.

19. Donyagina, V. F.; Shimizu, S.; Kobayashi, N.; Lukyanets, E. A., Synthesis of N,N-difluoroboryl complexes of 3,3′-diarylazadiisoindolylmethenes. *Tetrahedron Lett.* **2008,** *49* (42), 6152-6154.

20. Poirel, A.; De Nicola, A.; Ziessel, R., Oligothienyl-BODIPYs: Red and Near-Infrared Emitters. *Org. Lett.* **2012,** *14* (22), 5696-5699.

21. Kim, H.; Burghart, A.; B. Welch, M.; Reibenspies, J.; Burgess, K., Synthesis and spectroscopic properties of a new 4-bora-3a,4a-diaza-s-indacene (BODIPY®) dye. *Chem. Commun.* **1999,** (18), 1889-1890.

22. Zeng, L.; Jiao, C.; Huang, X.; Huang, K.-W.; Chin, W.-S.; Wu, J., Anthracene-Fused BODIPYs as Near-Infrared Dyes with High Photostability. *Org. Lett.* **2011,** *13* (22), 6026-6029.

23. Heyer, E.; Retailleau, P.; Ziessel, R., α-Fused Dithienyl BODIPYs Synthesized by Oxidative Ring Closure. *Org. Lett.* **2014,** *16* (9), 2330-2333.

24. Jiao, L.; Wu, Y.; Wang, S.; Hu, X.; Zhang, P.; Yu, C.; Cong, K.; Meng, Q.; Hao, E.; Vicente, M. G. H., Accessing Near-Infrared-Absorbing BF2-Azadipyrromethenes via a Push–Pull Effect. *J. Org. Chem.* **2014,** *79* (4), 1830-1835.

25. Xuan, S.; Zhao, N.; Ke, X.; Zhou, Z.; Fronczek, F. R.; Kadish, K. M.; Smith, K. M.; Vicente, M. G. H., Synthesis and Spectroscopic Investigation of a Series of Push–Pull Boron Dipyrromethenes (BODIPYs). *J. Org. Chem.* **2017,** *82* (5), 2545-2557.

26. Uppal, T.; Hu, X.; Fronczek, F. R.; Maschek, S.; Bobadova-Parvanova, P.; Vicente, M. G. H., Synthesis, Computational Modeling, and Properties of Benzo-Appended BODIPYs. *Chem. Eur. J.* **2012,** *18* (13), 3893-3905.

27. Shen, Z.; Röhr, H.; Rurack, K.; Uno, H.; Spieles, M.; Schulz, B.; Reck, G.; Ono, N., Boron–Diindomethene (BDI) Dyes and Their Tetrahydrobicyclo Precursors—en Route to a New Class of Highly Emissive Fluorophores for the Red Spectral Range. *Chem. Eur. J.* **2004,** *10* (19), 4853-4871.

28. Tomimori, Y.; Okujima, T.; Yano, T.; Mori, S.; Ono, N.; Yamada, H.; Uno, H., Synthesis of π-expanded O-chelated boron–dipyrromethene as an NIR dye. *Tetrahedron* **2011,** *67* (18), 3187-3193.

29. Yu, C.; Xu, Y.; Jiao, L.; Zhou, J.; Wang, Z.; Hao, E., Isoindole-BODIPY Dyes as Red to Near-Infrared Fluorophores. *Chem. Eur. J.* **2012,** *18* (21), 6437-6442.

30. Yu, C.; Jiao, L.; Tan, X.; Wang, J.; Xu, Y.; Wu, Y.; Yang, G.; Wang, Z.; Hao, E., Straightforward Acid-Catalyzed Synthesis of Pyrrolyldipyrromethenes. *Angew. Chem. Int. Ed.* **2012,** *51* (31), 7688-7691.

31. Ulrich, G.; Goeb, S.; De Nicola, A.; Retailleau, P.; Ziessel, R., Chemistry at Boron: Synthesis and Properties of Red to Near-IR Fluorescent Dyes Based on Boron-Substituted Diisoindolomethene Frameworks. *J. Org. Chem.* **2011,** *76* (11), 4489-4505.

32. Filatov, M. A.; Cheprakov, A. V.; Beletskaya, I. P., A Facile and Reliable Method for the Synthesis of Tetrabenzoporphyrin from 4,7-Dihydroisoindole. *Eur. J. Org. Chem.* **2007,** *2007* (21), 3468-3475.

33. Filatov, M. A.; Lebedev, A. Y.; Mukhin, S. N.; Vinogradov, S. A.; Cheprakov, A. V., π-Extended Dipyrrins Capable of Highly Fluorogenic Complexation with Metal Ions. *J. Am. Chem. Soc.* **2010,** *132* (28), 9552-9554.

34. Yamazawa, S.; Nakashima, M.; Suda, Y.; Nishiyabu, R.; Kubo, Y., 2,3-Naphtho-Fused BODIPYs as Near-Infrared Absorbing Dyes. *J. Org. Chem.* **2016,** *81* (3), 1310-1315.

35. K. Vegesna, G.; Sripathi, S. R.; Zhang, J.; Zhu, S.; He, W.; Luo, F.-T.; Jahng, W. J.; Frost, M.; Liu, H., Highly Water-Soluble BODIPY-Based Fluorescent Probe for Sensitive and Selective Detection of Nitric Oxide in Living Cells. *ACS Appl. Mater. Interfaces* **2013,** *5* (10), 4107-4112.

36. www.cancer.org/cancer/colonandrectumcancer/detailedguide/colorectal-cancer-keystatistics.

37. Ongarora, B. G.; Fontenot, K. R.; Hu, X.; Sehgal, I.; Satyanarayana-Jois, S. D.; Vicente, M. G. H., Phthalocyanine–Peptide Conjugates for Epidermal Growth Factor Receptor Targeting. *J. Med. Chem.* **2012,** *55* (8), 3725-3738.

38. Fontenot, K. R.; Ongarora, B. G.; LeBlanc, L. E.; Zhou, Z.; Jois, S. D.; Vicente, M. G. H., Targeting of the epidermal growth factor receptor with mesoporphyrin IX-peptide conjugates. *J. Porphyrins Phthalocyanines* **2016,** *20* (01n04), 352-366.

39. Humne, V.; Dangat, Y.; Vanka, K.; Lokhande, P., Iodine-catalyzed aromatization of tetrahydrocarbazoles and its utility in the synthesis of glycozoline and murrayafoline A: a combined experimental and computational investigation. *Org. Biomol. Chem.* **2014,** *12* (27), 4832-4836.

40. Meng, Q.; Fronczek, F. R.; Vicente, M. G. H., Synthesis and Spectroscopic Properties of β,β'-Dibenzo-3,5,8-triaryl-BODIPYs. *New J. Chem.* **2016**, 5740-5751.

41. Chen, J.-B.; Zhang, H.-X.; Guo, X.-F.; Wang, H.; Zhang, H.-S., "Off–on" red-emitting fluorescent probes with large Stokes shifts for nitric oxide imaging in living cells. *Analytical and Bioanalytical Chemistry* **2013,** *405* (23), 7447-7456.

42. Sibrian-Vazquez, M.; Jensen, T. J.; Fronczek, F. R.; Hammer, R. P.; Vicente, M. G. H., Synthesis and Characterization of Positively Charged Porphyrin−Peptide Conjugates. *Bioconjugate Chem.* **2005,** *16* (4), 852-863.

43. Li, L.; Nguyen, B.; Burgess, K., Functionalization of the 4,4-difluoro-4-bora-3a,4a-diaza-s-indacene (BODIPY) core. *Bioorg. Med. Chem. Lett.* **2008,** *18* (10), 3112-3116.

44. Olmsted, J., Calorimetric determinations of absolute fluorescence quantum yields. *The Journal of Physical Chemistry* **1979,** *83* (20), 2581-2584.

CHAPTER V: PREPARATION OF NITROPHENYL FUNCTIONALIZED BODIPYS FOR ELECTRO-CHEMICAL STUDIES

5.1 Introduction

Various modern analytical chemistry methods and techniques are being utilized to investigate fluorophore's physical and chemical properties. Cyclic voltammetry (CV) has been employed as an excellent method to investigate electron transfer reactions of metalloporphyrins, for a better understanding of the energy transfer process in cytochromes and other respiratory enzymes.[1-2] In the last two decades, CV is widely used to characterize porphyrin, corroles and their derivatives.

The relationship between BODIPY structure and its electrochemical properties was studied in the last ten years mainly by Bard *et al*. By investigating the electrochemistry of a number of BODIPY dyes, they reported the presence of radical ions from unblocked BODIPYs, and large splitting (>1V) was seen between the first and second oxidation and reduction waves, compared to the observations from other aromatic molecules.[3] An interesting study was performed through electrogenerated chemiluminescent research, and they were able to detect the presence of dimers, trimers and polymers during electrochemical reactions.[4-5] By installing bipyridine units at the BODIPY's *meso*-positions, electrogenerated chemiluminescence was observed.[6]

5.1.1 Effects of nitrophenyl substitution on corrole's electrochemical properties

In 2014, Kadish *et al* investigated a series of nitrophenyl functionalized cobalt corroles, and their electrochemical properties were significantly modified, compared to normal cobalt corroles.[7] In both *meso*-nitrophenyl and β-nitrophenyl corroles, additional reduction processes

were observed, indicating that the nitrophenyl units on corroles are highly electroactive, as shown in Figure 5.1.

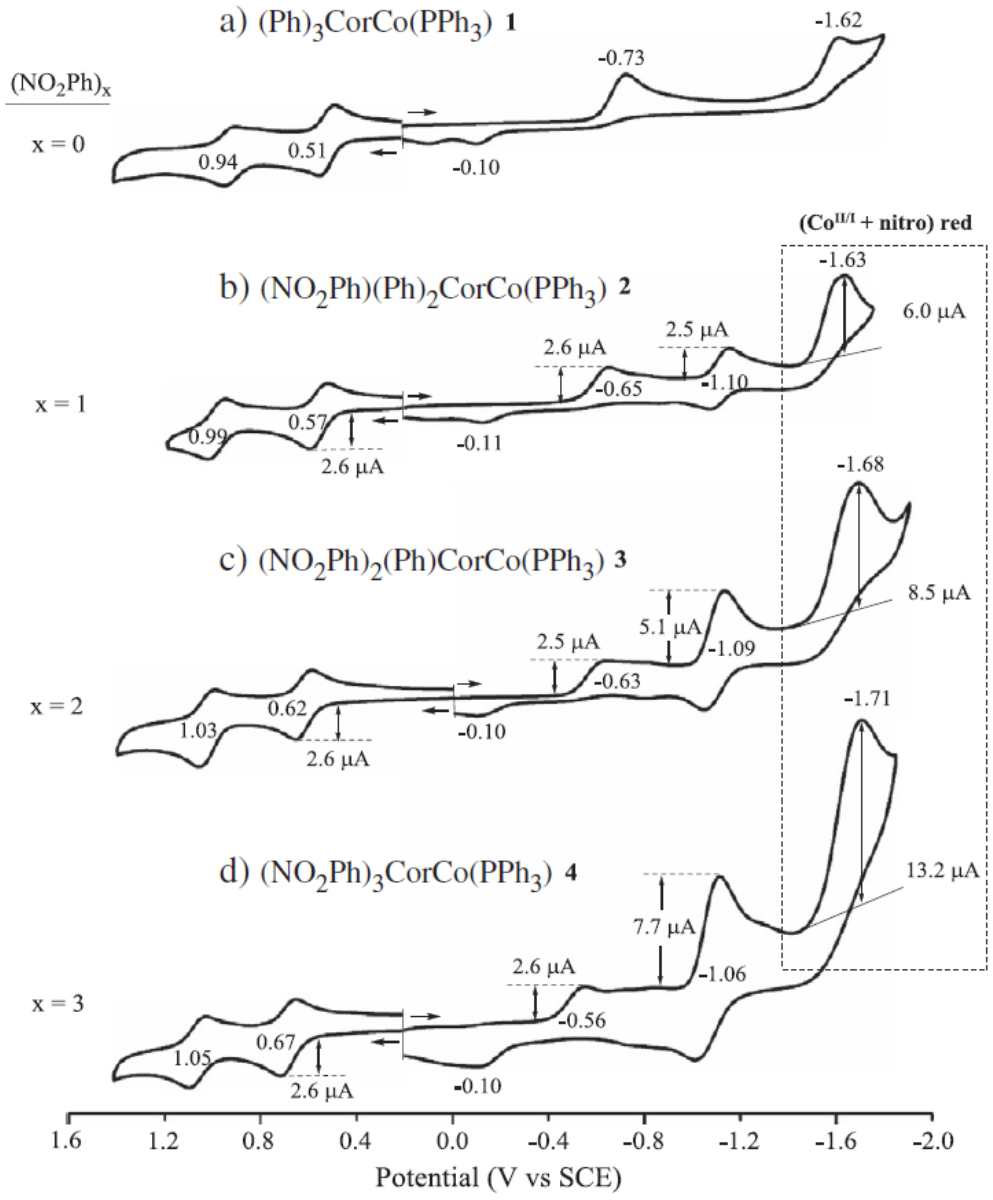

Figure 5.1: Cyclic voltammograms of nitrophenyl corroles in DCM containing 0.1 M TBAP at a scan rate of 0.1V/s.[7] Reprinted with permission from Copyright (2014) Elsevier.

5.1.2 Electro-Chemistry Study of Nitrophenyl Functionalized BODIPY Fluorophore:

3,5-DiPhNO_2-BODIPYs have been examined by CV in THF and CH_2Cl_2, and the cyclic voltammograms are given in Figure 5.2. As seen in the Figure, both 3,5-di-PhNO_2-BODIPYs

undergo three reversible one-electron reductions. The first reductions located at -0.74 and -0.64 V, are assigned to the BODIPY anion radical. The following two reactions located at -1.04, -1.31 and -0.95 and -1.29 V are assigned to the reduction of the nitrophenyl groups. Nitrophenyl groups on porphyrin and corrole macrocycles can gain multi-electron reductions as previous studies show, but this is the first time for BODIPY molecules bearing nitrophenyl to be studied by CV. The two reductions of 3,5-nitrophenyl were separately emerging, which may be interpreted that the two groups in these positions have intramolecular interactions. The dibenzo-BODIPY was easier to be reduced than the bicyclo- BODIPY because the benzo units expand the π-conjugation system of the molecule.

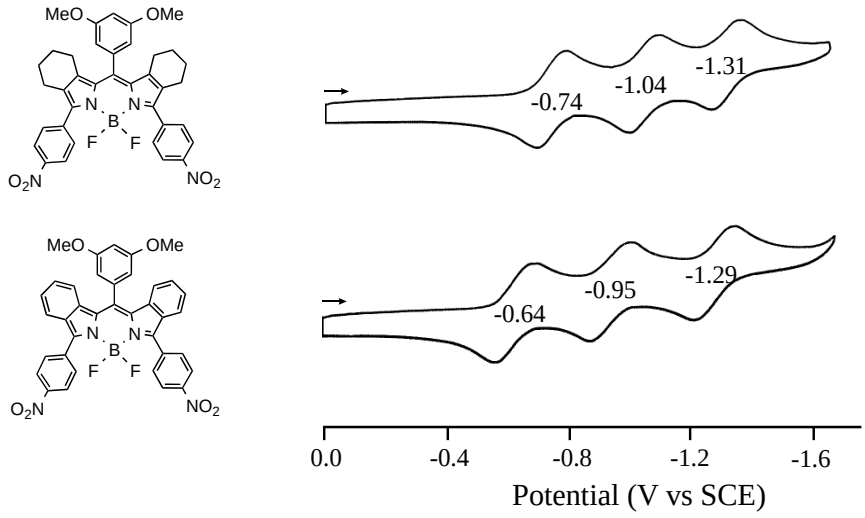

Figure 5.2: Cyclic voltammograms of investigated di-PhNO_2-BODIPYs in THF with 0.1 M TBAP, scan rate at 0.1V/s.

Due to the knowledge from nitrophenyl porphyrins and our preliminary discovery from 3,5-dinitrophenyl-BODIPYs, we wanted to investigate whether BODIPYs containing "N" nitrophenyl units would give "N+1" reversible peaks on the reductive parts of the cyclic voltammetry spectra. To further demonstrate our hypothesis, we prepared a series of nitrophenyl-functionalized BODIPYs for electrochemical studies.

Scheme 5.1: Synthesis of 1,3,5,7-tetramethyl-2,6-diethyl-8-nitrophenyl BODIPY

5.2 Results and Discussion

5.2.1 Design and Synthesis of Nitrophenyl BODIPYs

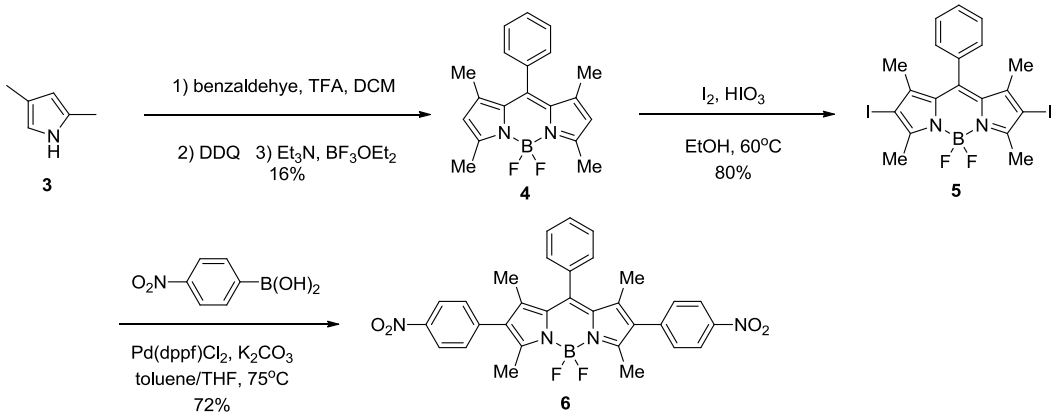

Scheme 5.2: Synthesis of 2,6-dinitrophenyl BODIPY

Nitrophenyl functionalized BODIPYs were designed to be prepared via a number of reactions, mainly by cross-coupling reactions between halogenated BODIPYs and 4-nitrophenyl boronic acids, since the Pd-catalyzed Suzuki cross-coupling reaction conditions are developed in previous Chapters with suitable Pd catalysts and solvents. For the installation of the *meso*-nitrophenyl groups, 4-nitro-benzaldehyde was condensed with pyrroles during the step of producing dipyrromethanes.

To demonstrate our hypothesis, we prepared a series of BODIPYs with mono-, di-, tri-, and tetranitrophenyl functionalized BODIPYs with nitrophenyl units at the *meso*-, 2, 3, 5, 6-positions. Mononitrophenyl BODIPYs were designed as the *meso*-PhNO_2-BODIPYs, and it was

prepared by reacting 2,4-dimethyl-3-ethyl-pyrrole and 4-nitro-benzaldehyde under acidic conditions, and the resulting dipyrromethane was then treated with DDQ and complexed to give *meso*-$PhNO_2$-BODIPY **2** in 12 % overall yield, as shown in Scheme 5.1.

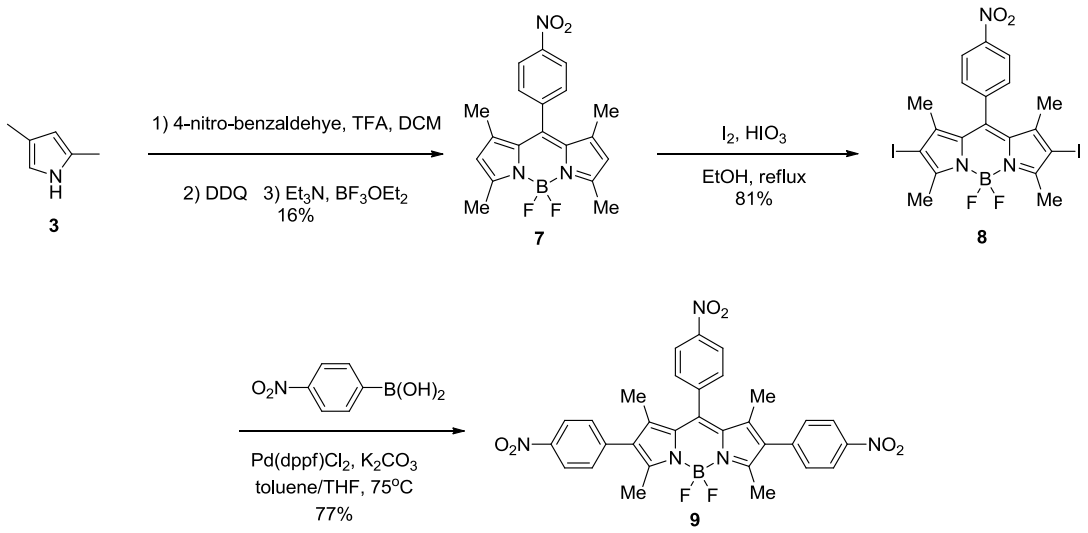

Scheme 5.3: Synthesis of 2,6,8-trinitrophenyl BODIPY **9**

Since 3,5-$(PhNO_2)_2$-BODIPYs were prepared and analyzed, we then designed 2,6-$(PhNO_2)_2$-BODIPY. BODIPY **4** was iodinated at the 2,6-positions with excess iodic acid and iodine to give 2,6-diiodo-BODIPY **5** in 80% yield, followed by a Suzuki cross-coupling reaction to give 2,6-$(PhNO_2)_2$-BODIPY **6** in 72% yield, as shown in Scheme 5.2.

There were two different trinitrophenyl-BODIPYs designed and synthesized in our research. A direct bromination or iodination on unsubstituted BODIPYs would functionalize at the 2,6-positions, and via this method we were able to produce 2,6,8-$(PhNO_2)_3$-BODIPY. The 3,5,8-$(PhNO_2)_3$-BODIPY's precursor, the 3,5-dihalogenated BODIPY, is prepared from α-halogenated dipyrromethanes. *Meso*-nitrophenyl-1,3,5,7-tetramethyl-BODIPY **7** was prepared from a classical "one-pot" route in 16% yield, and it was then iodinated at the 2,6-positions with excess iodic acid and iodine, in refluxing ethanol. The reactive 8-nitrophenyl-2,6-diiodo-BODIPY was subjected to a Suzuki cross-coupling reaction to produce 2,6,8-tri(nitrophenyl)-

BODIPY **9** in 77% yield, as shown in Scheme 5.3. 3,5-Dibromo-8-nitrophenyl-BODIPY **13** was prepared by treating dipyrromethane **11** with 2 equivalents of N-bromosuccinimide at -78^{o}C, and the resulting dipyrromethane **12** was then oxidized and complexed to give BODIPY **13** in 7% overall yield from dipyrromethane. Then BODIPY **13** was postfunctionalized with a Suzuki cross-coupling reaction, using $Pd(PPh_3)_2Cl_2$ as the catalyst, and 3,5,8-$(PhNO_2)_3$-BODIPY **14** was isolated in 60% yield, as shown in Scheme 5.4. The low yielding of the preparation of **13** and **14** is probably due to their low solubility, and partial amounts were lost during work up and purification.

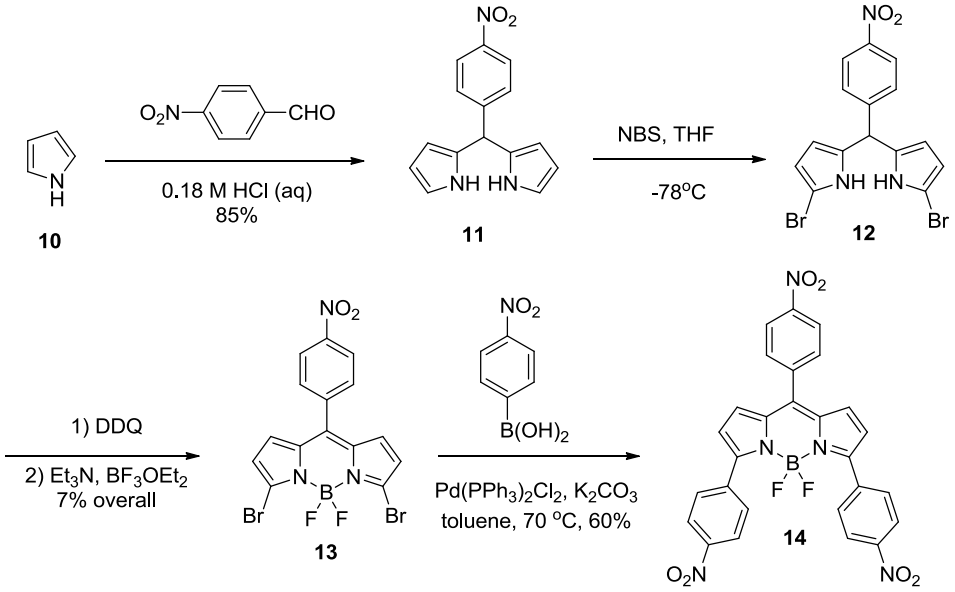

Scheme 5.4: Synthesis of 3,5,8-trinitrophenyl BODIPY **14**

Synthesis of tetranitrophenyl-BODIPY was attempted by reacting 2,3,5,6-tetraiodo-BODIPY **15** with 15 equivalents of 4-nitrophenyl boronic acid, in a typical Suzuki cross-coupling reaction condition, as shown in Scheme 5.5. However, no desired product was observed, and intermediates mono-, di- and tri-nitrophenyl BODIPYs precipitated, due to their relatively low solubility.

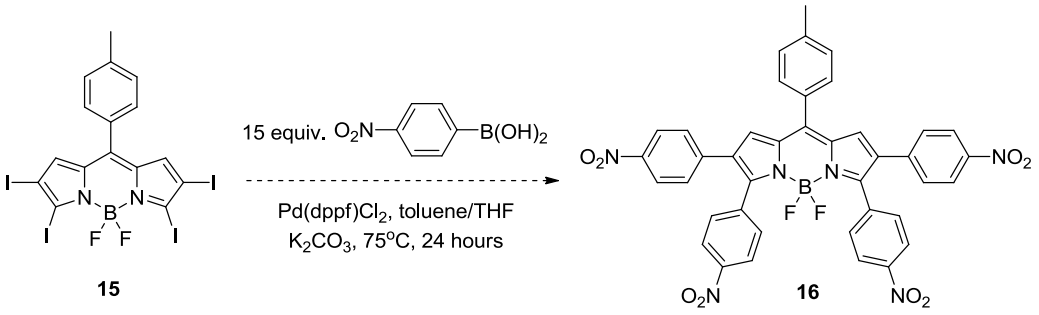

Scheme 5.5: Attempted synthesis of 2,3,5,6-tetranitrophenyl BODIPY **16**

To further confirm that only nitrophenyl units would give reversible peaks, we also prepared BODIPY with anisole units at 2,6- and 3,5-positions, respectively. 2,6-Dianisole-8-nitrophenyl-BODIPY **17** was prepared via a Suzuki cross-coupling reaction from BODIPY **8** in 82% yield, and 3,5-dianisole-8-nitrophenyl-BODIPY **18** was synthesized by post-functionalizing 3,5-dibromo-BODIPY **12** in 89% yield, as shown in Scheme 5.6.

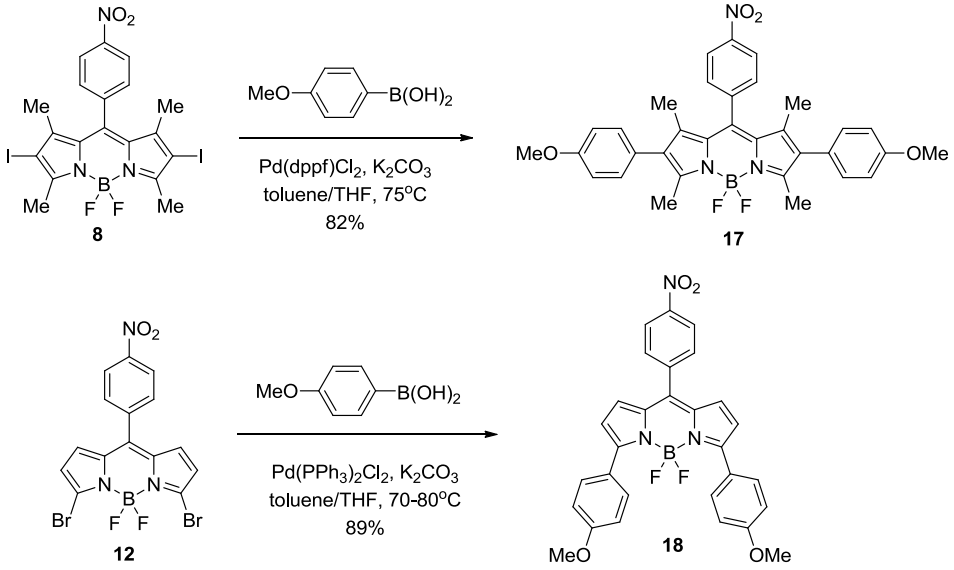

Scheme 5.6: Synthesis of 8-nitrophenyl BODIPYs with anisole units

5.2.2 Electrochemical Studies

The electrochemistry study of synthesized BODIPYs was carried out in CH_2Cl_2 and THF with 0.1M tetrabutylammonium perchlorate (TBAP) and a summary of potential values are

shown in Table 5.1. The representative cyclic voltammograms for selected BODIPY are shown in Figure 5.3 for BODIPYs **6, 12, 14, 18** which all have multiple reductions.

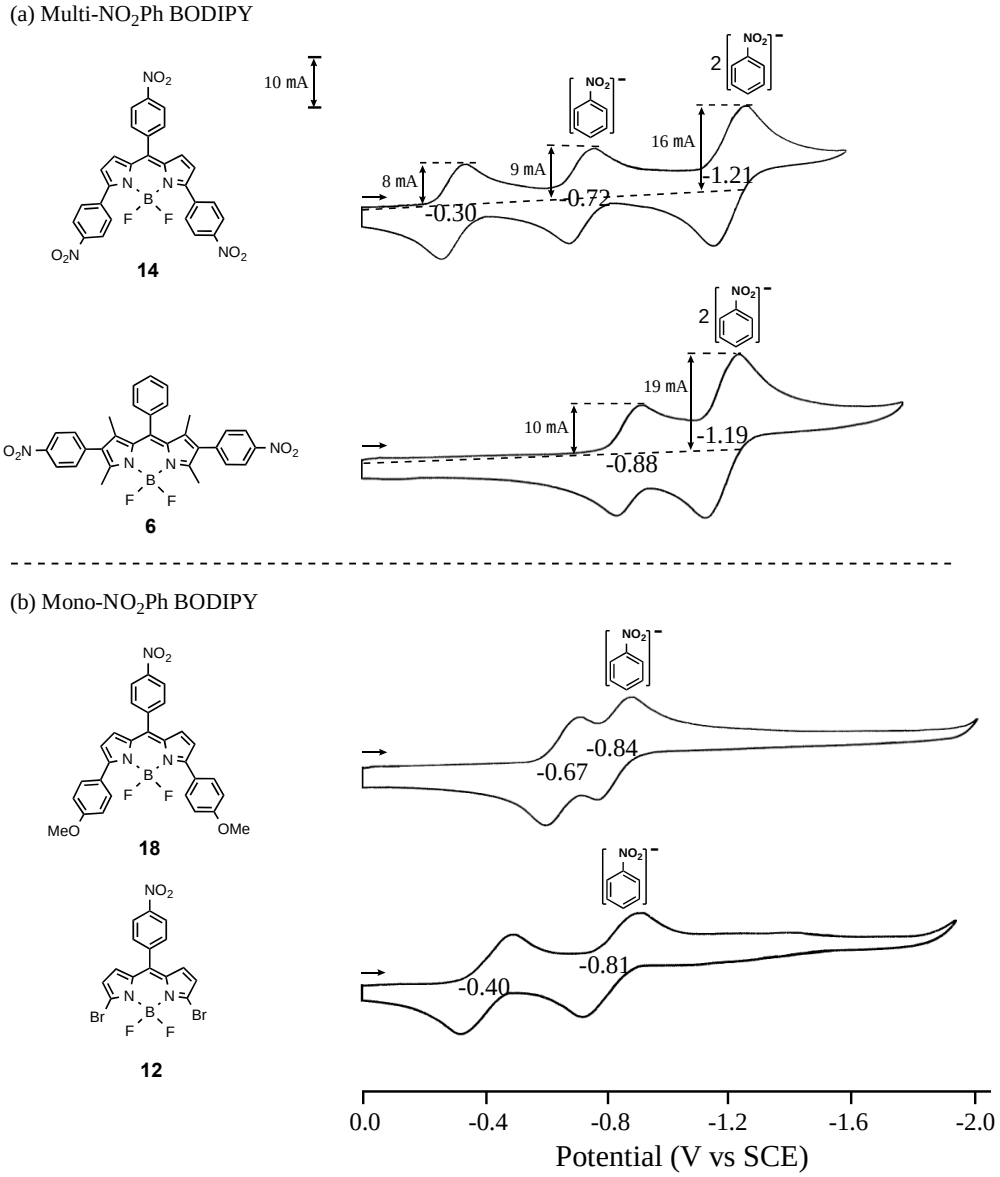

Figure 5.3: Cyclic voltammograms of (a) Multi-NO_2Ph BODIPY **14, 6** and (b) Mono-NO_2Ph BODIPY **18, 12** in THF containing 0.1M TBAP.

As shown in Figure 5.3 (a), compound **14** has three nitrophenyl substituted groups located at the 3,5,8-positions of BODIPY, thus this compound has three reversible reductions.

Table 5.1: Half-wave potentials (V vs SCE) for investigated BODIPYs in THF and CH2Cl2, 0.1M TBAP. Scan rate = 0.1 V/s.

		Oxidation		Reduction		
Solvent	Cpd #	2nd	1st	1st	2nd	3rd
CH_2Cl_2	**2**	1.86[a]	1.15	-1.02[a, b]		
	6		1.34	-0.98	-1.13	-1.21
	7	1.64[a]	1.30	-1.00[a, b]		
	8	1.86[a]	1.42	-0.84[a, b]		
	9		1.37	-0.89[a]	-1.21	
	13		1.76[a]	-0.49	-0.77	
	14		1.60	-0.32	-0.73	-1.18[b]
	17	1.57[a]	1.17	-1.00[a, b]		
	18	1.54	1.14	-0.72	-0.79	
THF	**6**			-0.88	-1.19[b]	
	12			-0.40	-0.81	
	14			-0.30	-0.72	-1.21[b]
	18			-0.67	-0.84	

[a]Peak potential, [b]overlapped peak (two electron transfer).

According to the current height of these three peaks showing in the Figure, the first two reductions were one-electron transfer processes, and the third one was a two-electron transfer reaction. The conjectural nitrophenyl reductions are also labeled in the Figure: the first reduction is assigned to generate the BODIPY anion radical, while the 2nd and the 3rd reductions described the reduction of the nitrophenyl groups. The 2nd reduction was due to the process of nitrophenyl located at the *meso*- position, and the 3rd reduction was due to the processes of nitrophenyls

located at 3,5- positions. The reason is probably that the nitrophenyl group is a fairly strong electron-withdrawing group, and it leads to all reactions shift.

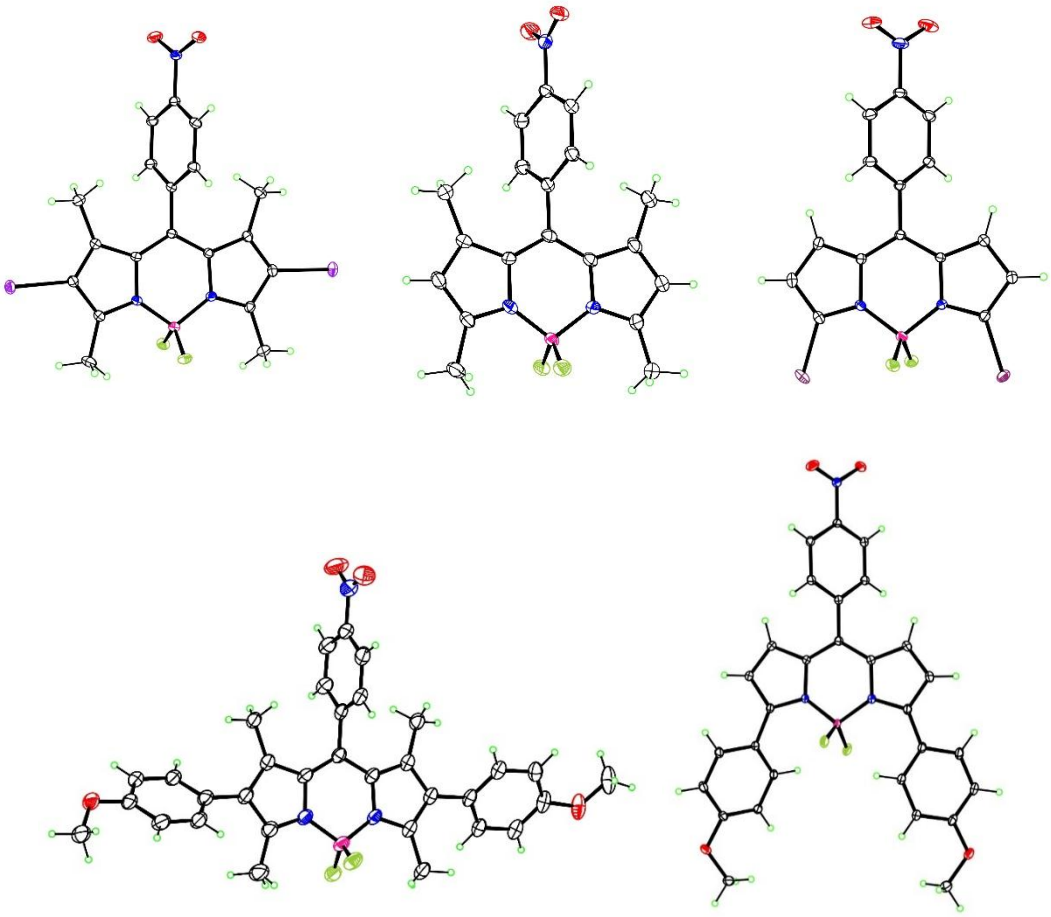

Figure 5.4: Crystal structures of mono-nitrophenyl BODIPYs **7, 8 ,13, 17** and **18**

BODIPY **6** showed two reversible processes, and the first one corresponds to the BODIPY anion and the second reduction belongs to the reductions of two nitrophenyl groups at the 2,6-positions. In Figure 5.3 (b), the two compounds studied were mononitrophenyl-BODIPYs, which are less electron withdrawing than the multi-substituted nitrophenyl BODIPYs. The first reductions (-0.67, -0.40 V) of BODIPY **18** and **12** belong to the BODIPY core, and the reductions of the nitrophenyl groups were at -0.81 and -0.84 V, which were 200 mV easier than

nitrobenzene.[7] This result gives the quantitatively potential difference of the positive shift values when the nitrophenyl groups are connected to the BODIPY core.

5.2.3 Structural Characterization

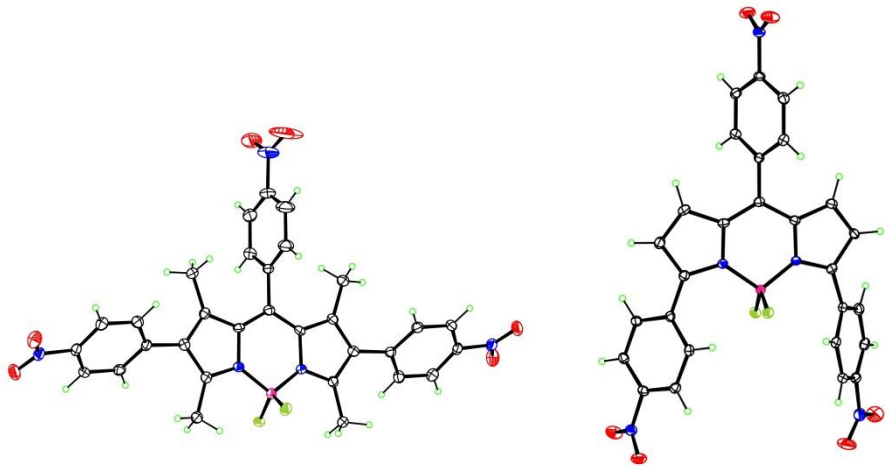

Figure 5.5: Crystal structures of tri-nitrophenyl BODIPYs **9** and **14**

All BODIPYs were characterized by ^{1}H-, ^{13}C-, and ^{11}B-NMR, HRMS, and in the case of **7, 8, 9, 13, 14, 17** and **18** also by X-ray crystallography. All BODIPYs contain triplets for the BF_2 in the ^{11}B-NMR, indicating that the BF_2 units were unreactive under the cross-coupling reactions. Other than BODIPY **14** and **18** that give downfield boron shifts (1.1 to 1.4 ppm), all rest BODIPYs' boron shifts are around 0.4-0.8 ppm. The nitrophenyl groups show two symmetric signals in ^{1}H-NMR around the 7.0-7.5 ppm region, and electron-withdrawing groups at the 3,5-positions downfield them to 7.5-8.5 ppm region.

Full structural confirmation of all compounds was obtained from the X-ray crystal structures. Crystals suitable for X-ray analysis were grown from slow evaporation of hexane diffused in dichloromethane. As expected, the *meso*-aryl groups are oriented perpendicular to the dipyrromethene core to avoid steric congestion caused by the 1,7-methyl groups in the structure of **7**, **8**, **9** and **17**. 3,5-Nitrophenyl units form dihedral 47-55° angles with the main BODIPY planes.

5.3 Conclusions

In summary, we have synthesized a series of nitrophenyl-functionalized BODIPYs containing nitrophenyl units at the *meso*, 2,3,5,6-positions in relatively high yields and efficient routes. Nitrophenyl installation at the *meso*-positions were achieved by using 4-nitro-benzaldehyde during preparation of starting BODIPYs, and the installation at the 2,3,5,6-positions were accomplished by regio-selective halogenation on BODIPYs or dipyrromethanes with bromine or iodine atoms, and then performing Suzuki cross-coupling reactions, using $Pd(PPh_3)_2Cl_2$ or $Pd(dppf)Cl_2$ as catalysts. A detailed electrochemistry study was carried out for selected nitrophenyl BODIPYs. In addition to get the anion radical for the BODIPY molecule, all the substituted nitrophenyl groups on the BODIPY periphery showed well-defined reversible reaction. The reductions overlapped or successively obtained based on the different structures for the multi-nitrophenyl BODIPYs.

5.4 Experimental

5.4.1 General Information

All the reagents and solvents were purchased from Sigma-Aldrich and were used without further purification. All reactions were carried out with oven-dried glassware under a dry argon atmosphere. All the reactions were monitored using Sorbent Technologies 0.2 mm silica gel TLC plates with UV-254 nm indicator. Flash column chromatography was performed using Sorbent Technologies 60 Å silica gel (230-400 mesh). Prep-TLC 60 Å silica gel 20 x 20 cm (210-270 μm) was used. Dichloromethane for electrochemistry (CH_2Cl_2, anhydrous, ≥99.8%, EMD Chemicals Inc.) were used as received. Tetrahydrofuran (THF, for HPLC, ≥99.9%) for electrochemistry was purchased from Sigma-Aldrich and freshly distilled using a Solvent System PS-MD-5-13-495 from Innovative Technology. Tetra-n-butylammonium perchlorate (TBAP) was purchased from

Sigma-Aldrich and stored in a drying oven at 40 °C. All ^{1}H-, ^{13}C-, and ^{11}B-NMR spectra were collected on Bruker AV-400 and AV-500 spectrometer in deuterated chloroform or deuterated dichloromethane. The $CDCl_3$ chemical shifts (δ) are reported in ppm using as reference 7.26 for proton and 77.0 for carbon and BF_3•OEt_2 was used as reference (0.00 δ) for boron NMR. The CD_2Cl_2 chemical shifts (δ) are reported in ppm using as reference 5.32 for proton and 53.50 for carbon. Coupling constants are reported in Hertz (Hz). BODIPY **2**, **6**, **8**, and **14**'s ^{13}C-NMR spectra is missing due to the low solubility. All the mass spectra were collected using an Agilent 6210 ESI-TOF mass spectrometer. All melting points were recorded using a MEL-TEMP electrothermal instrument.

5.4.2 Syntheses

"One-pot" synthesis of BODIPYs from alkylated pyrroles:

8.40 mmol pyrrole and 4.20 mmol arylaldyde were dissolved in 50 mL anhydrous DCM, and one drop of TFA was added. The reaction was stirred overnight until TLC indicated a consumption of the starting pyrroles. 0.95 g (4.20 mmol) DDQ was dissolved in a minimum amount of DCM and added slowly into the solution. The reaction was stirred for another 2 hours and 2.93 mL (21.0 mmol) triethylamine was added. Then BF_3 etherate was added dropwisely under iced water bath. The complexation reaction was allowed to stir for 4 hours, and the solvent was removed vacuum. The black residue was dissolved in 100 mL ethyl acetate, and then washed by 100 mL 1N HCl (aq), 100 mL saturated $NaHCO_3$ (aq) and 100 mL saturated NaCl (aq). Ethyl acetate was removed under vacuum after the solution was dried over anhydrous Na_2SO_4. The oily residue was purified by silica gel column chromatography and recrystallized in 1:1 DCM/Hexane.

BODIPY 2: Yield 12%. mp(°C) 248; ^{1}H NMR (400 MHz, CD_2Cl_2) δ 8.40 – 8.33 (m, 2H), 7.60 – 7.52 (m, 2H), 2.50 (s, 6H), 2.32 (q, *J* = 7.5 Hz, 4H), 1.28 (s, 6H), 0.98 (t, *J* = 7.6 Hz, 6H); ^{11}B NMR (128 MHz, CD_2Cl_2) δ 0.56 (t, *J* = 33.1 Hz); HRMS (ESI-TOF) m/z 406.2106 $[M-F]^+$ calcd for $C_{23}H_{26}BFN_3O_2$ 406.2107.

BODIPY 4: Yield 16%. mp(°C) 287; ^{1}H NMR (400 MHz, $CDCl_3$) δ 7.48 (dd, *J* = 5.2, 2.0 Hz, 3H), 7.31 – 7.26 (m, 2H), 5.97 (s, 2H), 2.55 (d, *J* = 1.2 Hz, 6H), 1.37 (s, 6H); HRMS (ESI-TOF) m/z 305.1633 $[M-F]^+$ calcd for $C_{19}H_{19}BFN_2$ 305.1625.

BODIPY 7: Yield 13%. mp(°C)>200 (decom.); ^{1}H NMR (400 MHz, CD_2Cl_2) δ 8.41 – 8.34 (m, 2H), 7.57 (d, *J* = 8.6 Hz, 2H), 6.05 (s, 2H), 2.52 (s, 6H), 1.38 (s, 6H); ^{13}C NMR (101 MHz, CD_2Cl_2) δ 156.5, 148.5, 143.0, 141.8, 138.8, 130.7, 129.8, 124.5, 121.8, 14.5; ^{11}B NMR (128 MHz, CD_2Cl_2) δ 0.54 (t, *J* = 32.7 Hz); HRMS (ESI-TOF) m/z 349.1504 $[M-F]^+$ calcd for $C_{19}H_{18}BFN_3O_2$ 349.1507.

Synthesis of 2,6-diiodo-BODIPYs

0.27 mmol 2,6-unsubstituted BODIPY was dissolved in 10 mL ethanol. 0.17 g (0.68 mmol) iodine was added, followed by addition of 95.0 mg (0.54 mmol) iodic acid in minimum amount of water. The solution was refluxed for 2 to 3 hours until TLC indicated a consumption of the starting BODIPY. Solvents were removed under vacuum, and the residue was dissolved in 100 mL DCM, and washed by 2 x 50 mL sat. sodium thiosulfate solution. DCM was removed under vacuum after being dried through anhydrous sodium sulfate. The residue was purified by silica gel column chromatography and recrystallized in 1:1 DCM/Hexane.

BODIPY 5: Yield 75%. mp(°C) 187; ^{1}H NMR (400 MHz, CD_2Cl_2) δ 7.60 – 7.48 (m, 3H), 7.35 – 7.23 (m, 2H), 2.62 (s, 6H), 1.40 (s, 6H); ^{13}C NMR (101 MHz, CD_2Cl_2) δ 156.7, 145.6, 141.8, 134.7, 131.4, 129.58, 129.56, 127.9, 85.5, 16.9, 15.9; ^{11}B NMR (128 MHz, CD_2Cl_2)

δ 0.43 (t, *J* = 32.2 Hz); HRMS (ESI-TOF) m/z 573.9512 $[M-H]^-$ calcd for $C_{19}H_{16}BF_2I_2N_2$ 573.9506.

BODIPY 8: Yield 88%. mp(°C) 223; ^{1}H NMR (400 MHz, $CDCl_3$) δ 8.46 – 8.36 (m, 2H), 7.57 – 7.48 (m, 2H), 2.66 (s, 6H), 1.38 (s, 6H); ^{13}C NMR (101 MHz, $CDCl_3$) δ 158.0, 148.6, 144.7, 141.5, 137.8, 130.5, 129.5, 124.6, 86.4, 17.3, 16.1;^{11}B NMR (128 MHz, $CDCl_3$) δ 0.38 (t, *J* = 31.8 Hz); HRMS (ESI-TOF) m/z 619.9381 $[M-H]^-$ calcd for $C_{19}H_{16}BF_2I_2N_3O_2$ 619.9435.

Synthesis of 3,5-dibromo-BODIPY 13:

1.0 mL (15.0 mmol) pyrrole was suspended in 33 mL (6.0 mmol) 0.18 M HCl (aq), and 0.75g (5.0 mmol) 4-nitrobenzaldeyde was added. The mixture was stirred for 2 hours to give dipyrromethane **11** as a precipitate. The filtered precipitate was dried under vacuum and then dissolved in anhydrous THF. 1.9g (10 mmol) recrystallized NBS was dissolved in THF and added into the dipyrromethane solution slowly under -78^{o}C. The reaction was allowed to stir for another 10 minutes, and 1.10 g (5 mmol) DDQ was dissolved in THF and added into the solution dropwisely. The solution then warmed to room temperature upon the addition of DDQ. THF was removed under vacuum and the residue was passed a flash column using 100% DCM as the eluent to remove insoluble byproducts. Dipyrromethane **11** was dissolved in DCM, followed by addition of 3.5 mL (25.0 mmol) Et_3N and 4.3 mL (35.0 mmol) BF_3 etherate. The complexation reaction was allowed to stir for 2 hours, and the solvent was removed vacuum. The black residue was dissolved in 100 mL ethyl acetate, and then washed by 100 mL 1N HCl (aq), 100 mL saturated $NaHCO_3$ (aq) and 100 mL saturated NaCl (aq). Ethyl acetate was removed under vacuum after the solution was dried over anhydrous Na_2SO_4. The oily residue was purified by silica gel column chromatography and recrystallized in 1:1 DCM/Hexane, and BODIPY **12** was obtained in a 7% overall yield. **BODIPY 8**: Yield 88%. mp(°C)> 300; ^{1}H NMR (400 MHz,

CD_2Cl_2) δ 8.41 – 8.34 (m, 2H), 7.75 – 7.68 (m, 2H), 6.76 (d, *J* = 4.4 Hz, 2H), 6.61 (d, *J* = 4.4 Hz, 2H); ^{11}B NMR (128 MHz, CD_2Cl_2) δ 0.56 (t, *J* = 33.1 Hz); HRMS (ESI-TOF) m/z 467.9096 $[M]^-$ calcd for $C_{15}H_8BBr_2F_2N_3O_2$ 467.9086.

Cross coupling conditions:

0.100 mmol halogenated BODIPY, 5 mol% Pd catalyst ($Pd(dppf)Cl_2$ was used for **6**, **9** and **17**, $Pd(PPh_3)_2Cl_2$ was used for **14** and **18**) and 10 equiv. of aryl boronic acid were mixed under inert atmosphere. Toluene (2 mL) and THF (2 mL) were added via syringe and the solution was heated at 70 ^oC in an oil bath for 3 min. K_2CO_3 (1 M, 0.5 mL) solution was added via syringe and the reaction was monitored by TLC until complete consumption of starting halogenated BODIPY. The cooled solution was filtered through celite to remove excess palladium and boronic acid, and the solvent was concentrated under vacuum. The residue was purified by silica gel column chromatography to afford the corresponding arylated BODIPY, which were recrystallized using 1:1 dichloromethane/hexane.

BODIPY 6: Yield 72%. mp(°C)> 300; ^{1}H NMR (400 MHz, $CDCl_3$) δ 8.31 – 8.23 (m, 4H), 7.54 (d, *J* = 6.3 Hz, 3H), 7.39 – 7.31 (m, 6H), 2.57 (s, 6H), 1.34 (s, 6H); ^{11}B NMR (128 MHz, $CDCl_3$) δ 0.79 (t, *J* = 32.5 Hz).; HRMS (ESI-TOF) m/z 546.1981 $[M-F]^{-+}$ calcd for $C_{31}H_{25}BFN_4O_4$ 546.1984.

BODIPY 9: Yield 77%. mp(°C)> 300; ^{1}H NMR (500 MHz, CD_2Cl_2) δ 8.46 – 8.39 (m, 2H), 8.26 (dd, *J* = 8.7, 2.8 Hz, 4H), 7.66 (dq, *J* = 5.9, 2.6 Hz, 2H), 7.36 (dq, *J* = 5.8, 2.6 Hz, 4H), 2.54 (s, 6H), 1.33 (s, 6H); ^{13}C NMR (126 MHz, CD_2Cl2) δ 155.3, 148.6, 147.1, 141.5, 140.2, 139.6, 132.4, 131.0, 130.9, 129.7, 124.7, 123.7, 13.3, 13.0; ^{11}B NMR (128 MHz, CD_2Cl_2) δ 0.73 (t, *J* = 32.1 Hz); HRMS (ESI-TOF) m/z 591.1802 $[M-F]^+$ calcd for $C_{31}H_{23}BFN_5O_6$ 591.1835.

BODIPY 17: Yield 82%. mp(°C)> 300; ^{1}H NMR (400 MHz, $CDCl_3$) δ 8.45 – 8.36 (m, 2H), 7.65 – 7.57 (m, 2H), 7.11 – 7.03 (m, 4H), 6.97 – 6.90 (m, 4H), 3.83 (s, 6H), 2.53 (s, 6H), 1.28 (s, 6H); ^{13}C NMR (101 MHz, $CDCl_3$) δ 158.9, 155.6, 148.4, 142.5, 138.3, 134.1, 131.2, 131.1, 130.9, 130.4, 129.8, 129.7, 125.3, 124.5, 124.4, 123.7, 114.0, 113.9, 55.2, 13.5, 13.1; ^{11}B NMR (128 MHz, $CDCl_3$) δ 0.78 (t, *J* = 32.7 Hz); HRMS (ESI-TOF) m/z 561.2348 $[M-F]^+$ calcd for $C_{33}H_{30}BFN_3O_4$ 561.2344.

BODIPY 14: Yield 60%. mp(°C) 288; ^{1}H NMR (400 MHz, CD_2Cl_2) δ 8.48 – 8.40 (m, 2H), 8.33 – 8.24 (m, 4H), 8.09 – 8.00 (m, 4H), 7.87 – 7.79 (m, 2H), 6.96 (dd, *J* = 4.4, 1.2 Hz, 2H), 6.81 (dd, *J* = 4.4, 1.3 Hz, 2H); ^{11}B NMR (128 MHz, CD_2Cl_2) δ 1.14 (t, *J* = 31.8 Hz).; HRMS (ESI-TOF) m/z 535.1218 $[M-F]^+$ calcd for $C_{27}H_{16}BFN_5O_6$ 535.1209.

BODIPY 18: Yield 89%. mp(°C)> 300; ^{1}H NMR (400 MHz, CD_2Cl_2) δ 8.38 (d, *J* = 8.2 Hz, 2H), 7.87 (d, *J* = 8.4 Hz, 4H), 7.78 (d, *J* = 8.2 Hz, 2H), 6.99 (d, *J* = 8.4 Hz, 4H), 6.80 (d, *J* = 4.3 Hz, 2H), 6.69 (d, *J* = 4.3 Hz, 2H), 3.87 (s, 6H); ^{13}C NMR (101 MHz, CD_2Cl_2) δ 161.3, 159.3, 149.0, 140.9, 139.2, 136.0, 131.7, 131.4, 131.33, 131.29, 130.0, 124.9, 123.5, 121.33, 121.29, 113.9, 107.7, 106.6, 55.5; ^{11}B NMR (128 MHz, $CDCl_3$) δ 1.39 (t, *J* = 32.2 Hz).; HRMS (ESI-TOF) m/z 505.1706 $[M-F]^+$ calcd for $C_{29}H_{22}BFN_3O_4$ 505.1718.

5.4.3 X-ray Determined Molecular Structures

Crystal structures were determined using low-temperature data from a Bruker Kappa APEX-II DUO diffractometer with either MoKα or CuKα radiation. For all structures, H atoms were located from difference maps but constrained in calculated positions during refinement.

4: $C_{19}H_{18}BF_2N_3O_2$, M=369.17, monoclinic, a=30.2933(12), b=11.7928(6), c=19.4126(4) Å, β=96.341(3)°, T=100 K, space group C2/c, *Z*=16, 17283 reflections measured, 4508 unique (R_{int}=0.050), θ_{max}=27.6°, final R=0.052;

8: $C_{19}H_{16}BF_2I_2N_3O_2$, M=620.96, triclinic, a=8.1914(11), b=9.5397(13), c=13.7575(19) Å, β=88.751(7)°, T=90 K, space group P_1, Z=2, 45131 reflections measured, 10220 unique (R_{int}=0.036), θ_{max}=40.4°, final R=0.029;

9: $C_{31}H_{24}BF_2N_5O_6$, M=654,45, monoclinic, a=8.1590(9), b=9.8314(11), c=19.581(2) Å, β=92.642(7)°, T=90 K, space group $P2_1$, Z=2, 8133 reflections measured, 5675 unique (R_{int}=0.014), θ_{max}=29.1°, final R=0.041;

13: $C_{15}H_8BBr_2F_2N_3O_2$, M=470.87, monoclinic, a=8.3873(2), b=13.1438(4), c=14,5793(4) Å, β=100.4009(15)°, T=90 K, space group $P2_1/n$, Z=4, 58239 reflections measured, 7792 unique (R_{int}=0.033), θ_{max}=40.3°, final R=0.031;

14: $C_{27}H_{16}BF_2N_5O_6$, M=555.26, orthorhombic, a=9.6987(18), b=11.886(2), c=20.278(3) Å, β=88.751(7)°, T=90 K, space group $P2_12_12_1$, Z=4, 21780 reflections measured, 6383 unique (R_{int}=0.035), θ_{max}=31.1°, final R=0.042;

17: $C_{29}H_{22}BF_2N_3O_4$, M=525.30, triclinic, a=7.0860(3), b=12.9107(7), c=13.2005(8) Å, β=79.572(3)°, T=90 K, space group P_1, Z=2, 21733 reflections measured, 7013 unique (R_{int}=0.023), θ_{max}=1.6°, final R=0.043;

18: $C_{33}H_{30}BCl_2F_2N_3O_4$, M=666.33, triclinic, a=9.9705(6), b=13.6149(9), c=13.9672(9) Å, β=71.667(7)°, T=90 K, space group P_1, Z=2, 19252 reflections measured, 4478 unique (R_{int}=0.043), θ_{max}=69.0°, final R=0.051;

5.4.4 Electrochemical Studies

Cyclic voltammetry was carried out using an EG&G Princeton Applied Research (PAR) 173 potentiostat coupled to an EG&GPAR Model 175 Universal Programmer. Current-voltage curves were recorded on an EG&G PAR R-0151 X-Y recorder. A homemade three-electrode cell was used for cyclic voltammetric measurements and consisted of a glassy carbon working

electrode, a platinum counter electrode and a homemade saturated calomel reference electrode (SCE). The SCE was separated from the bulk of the solution by a fritted bridge of low porosity, which contained the solvent/supporting electrolyte mixture.

5.5 References

1. Urry, D. W.; Eyring, H., AN IMIDAZOLE PUMP MODEL OF ELECTRON TRANSPORT. *Proceedings of the National Academy of Sciences of the United States of America* **1963,** *49* (2), 253-258.

2. Wilson, G. S.; Neri, B. P., CYCLIC VOLTAMMETRY OF PORPHYRINS AND METALLOPORPHYRINS*. *Ann. N. Y. Acad. Sci.* **1973,** *206* (1), 568-578.

3. Nepomnyashchii, A. B.; Cho, S.; Rossky, P. J.; Bard, A. J., Dependence of Electrochemical and Electrogenerated Chemiluminescence Properties on the Structure of BODIPY Dyes. Unusually Large Separation between Sequential Electron Transfers. *J. Am. Chem. Soc.* **2010,** *132* (49), 17550-17559.

4. Nepomnyashchii, A. B.; Bröring, M.; Ahrens, J.; Bard, A. J., Synthesis, Photophysical, Electrochemical, and Electrogenerated Chemiluminescence Studies. Multiple Sequential Electron Transfers in BODIPY Monomers, Dimers, Trimers, and Polymer. *J. Am. Chem. Soc.* **2011,** *133* (22), 8633-8645.

5. Nepomnyashchii, A. B.; Bröring, M.; Ahrens, J.; Bard, A. J., Chemical and Electrochemical Dimerization of BODIPY Compounds: Electrogenerated Chemiluminescent Detection of Dimer Formation. *J. Am. Chem. Soc.* **2011,** *133* (48), 19498-19504.

6. Qi, H.; Teesdale, J. J.; Pupillo, R. C.; Rosenthal, J.; Bard, A. J., Synthesis, Electrochemistry, and Electrogenerated Chemiluminescence of Two BODIPY-Appended Bipyridine Homologues. *J. Am. Chem. Soc.* **2013,** *135* (36), 13558-13566.

7. Li, B.; Ou, Z.; Meng, D.; Tang, J.; Fang, Y.; Liu, R.; Kadish, K. M., Cobalt triarylcorroles containing one, two or three nitro groups. Effect of NO_2 substitution on electrochemical properties and catalytic activity for reduction of molecular oxygen in acid media. *J. Inorg. Biochem.* **2014,** *136*, 130-139.

APPENDIX

APPENDIX A: NMR Characterization of Compounds Found in Chapter 2

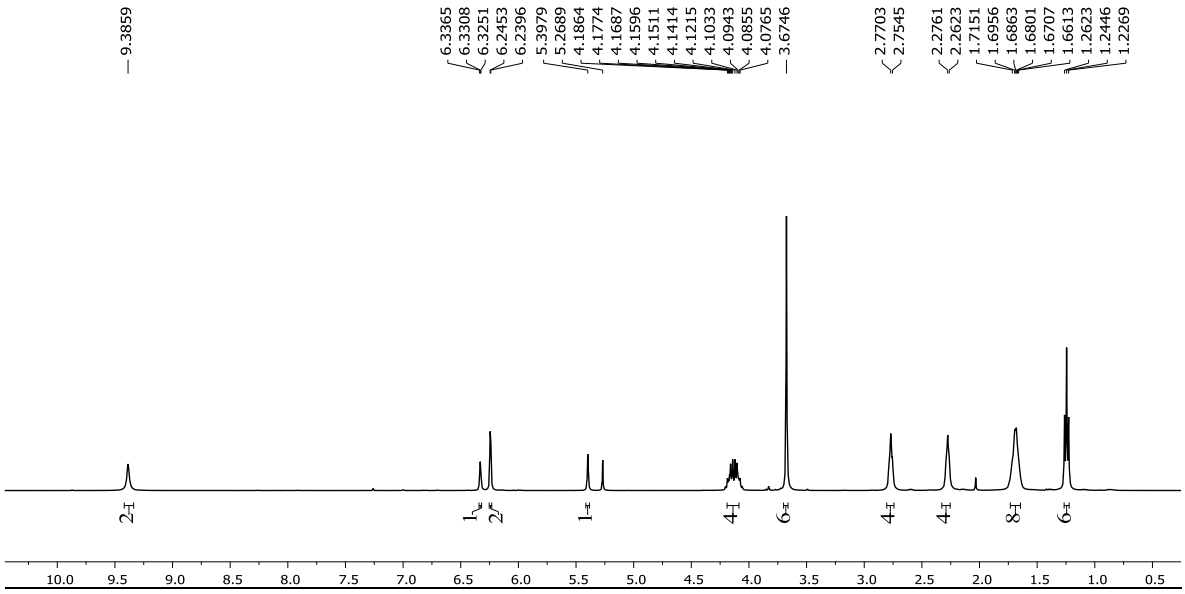

Figure A.1: ^{1}H NMR spectrum of **3b** in $CDCl_3$

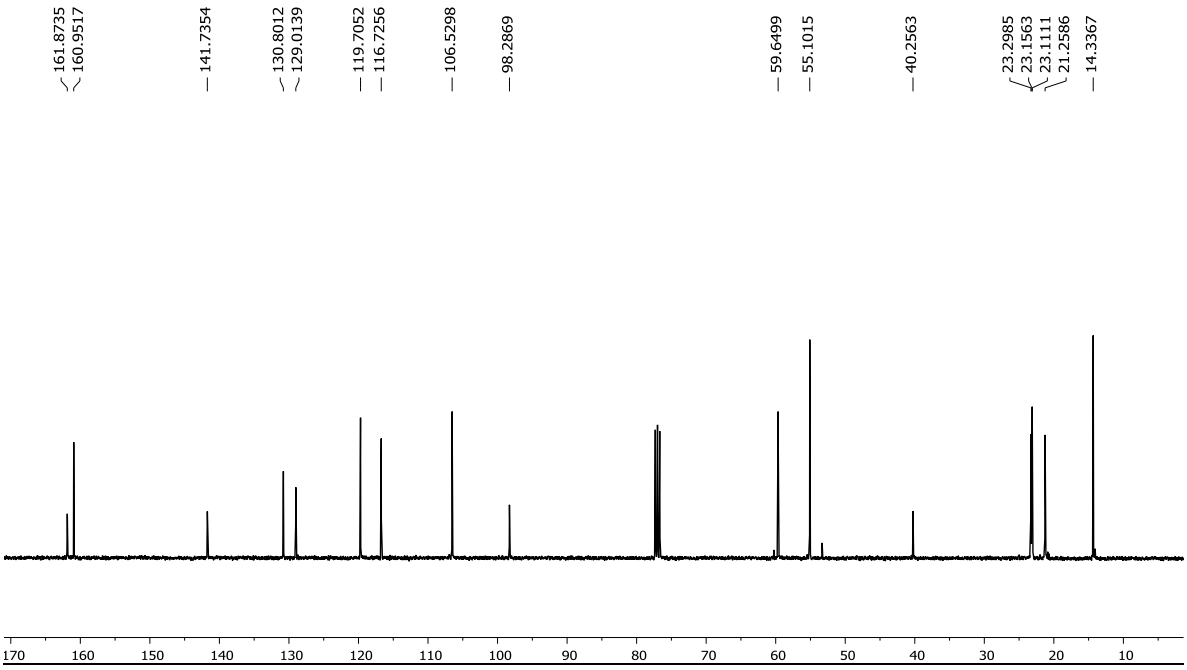

Figure A.2: ^{13}C NMR spectrum of **3b** in $CDCl_3$

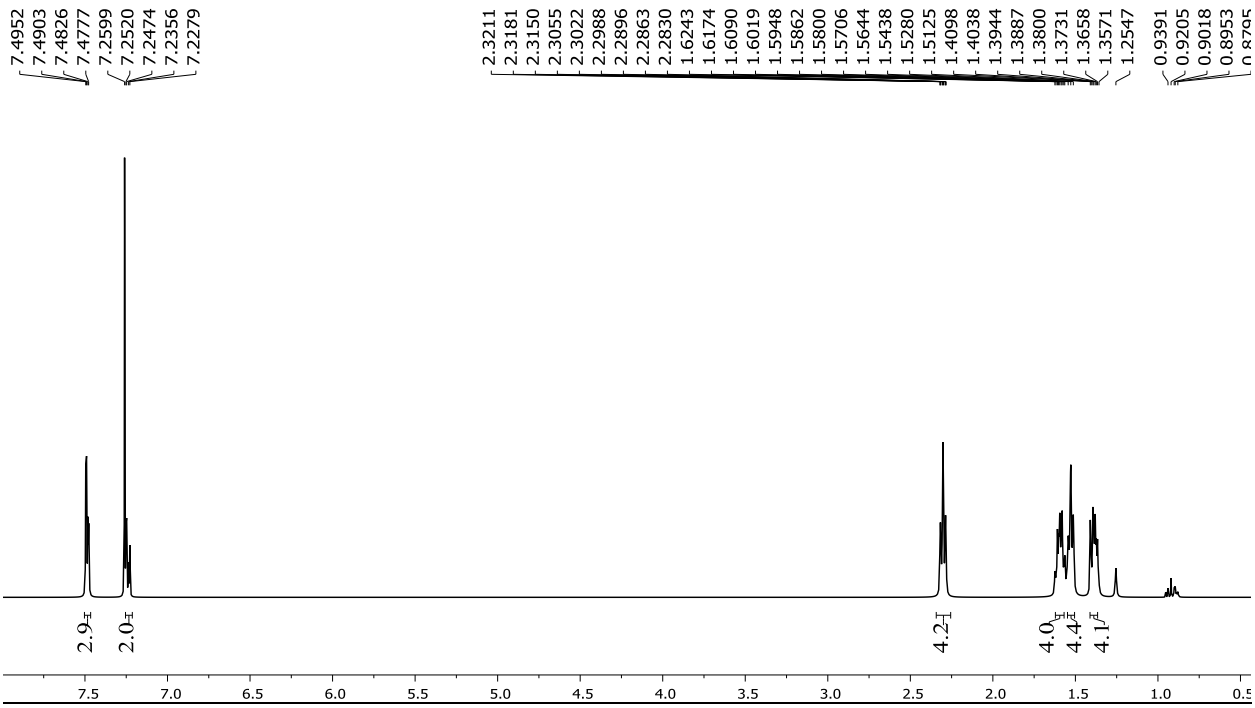

Figure A.3: ^{1}HNMR spectrum of **6a** in $CDCl_3$

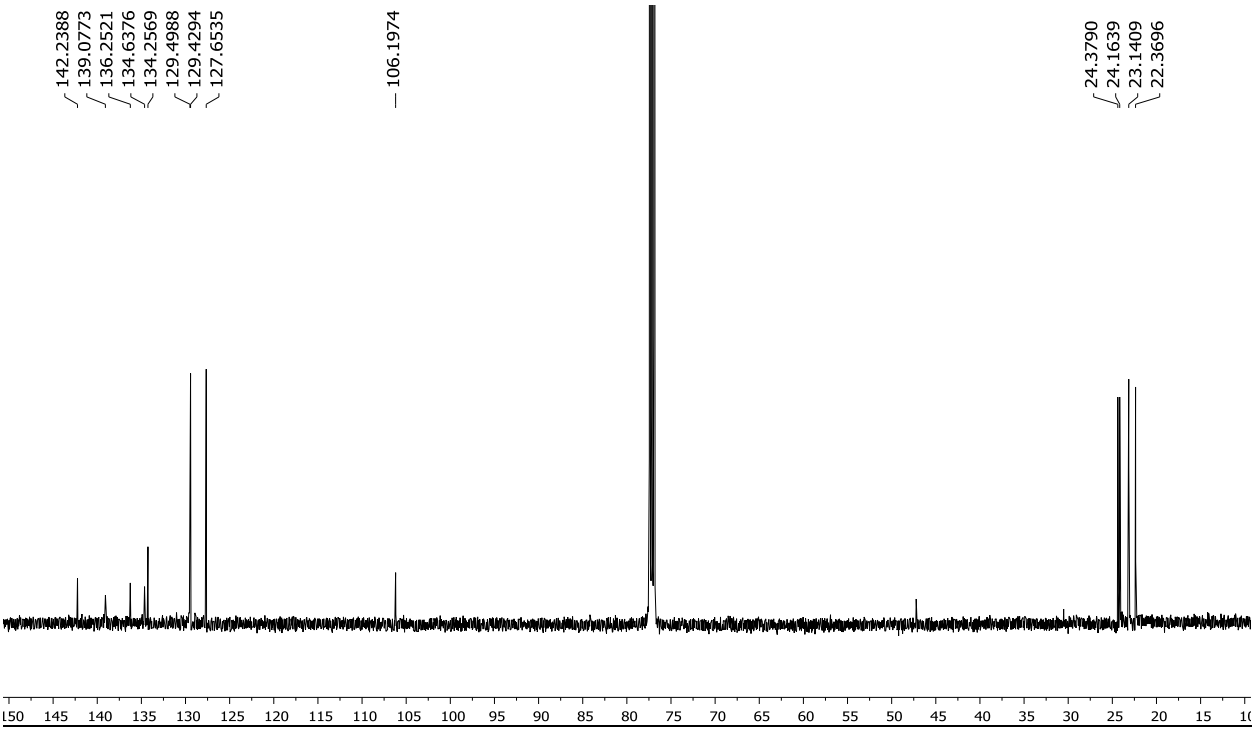

Figure A.4: ^{13}C NMR spectrum of **6a** in $CDCl_3$

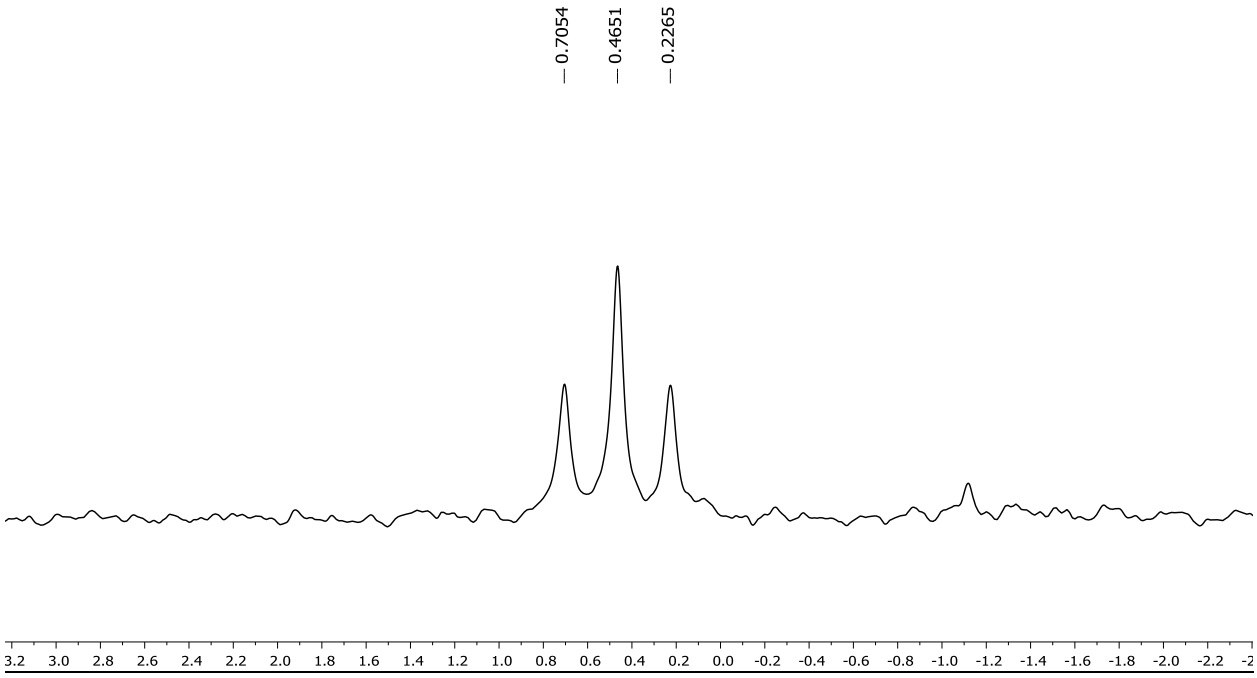

Figure A.5: ^{11}B NMR spectrum of **6a** in $CDCl_3$

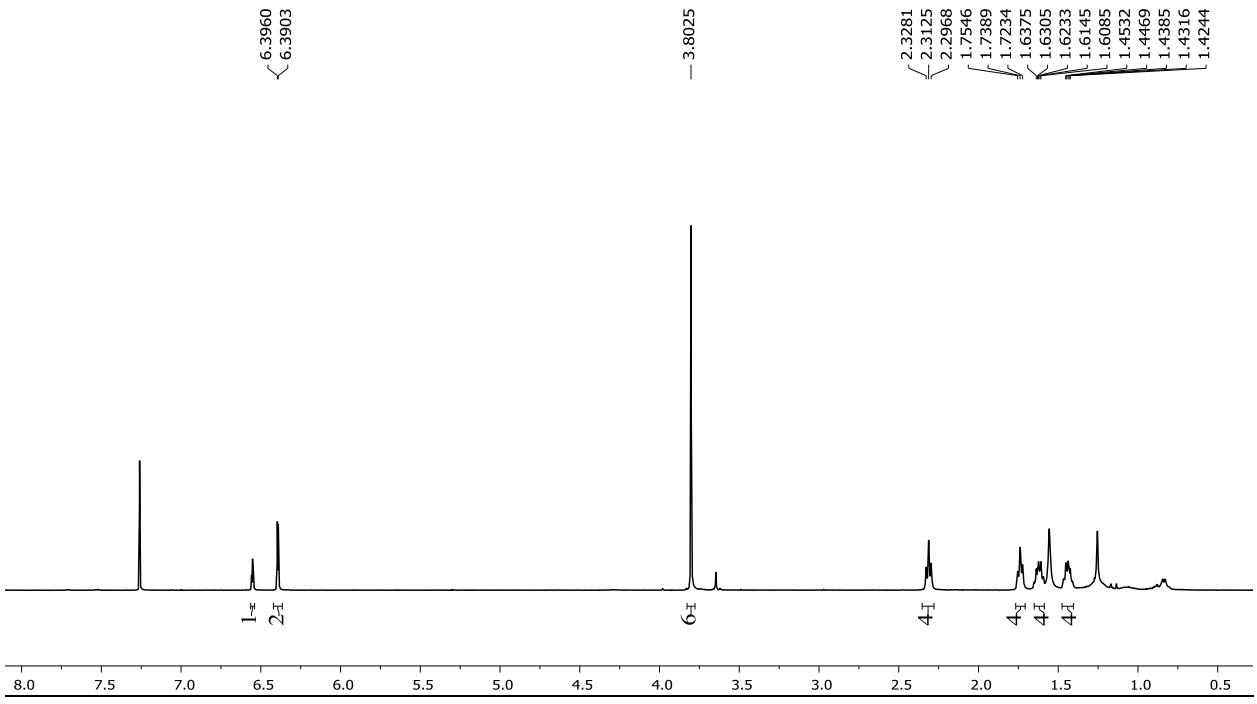

Figure A.6: ^{1}H NMR spectrum of **6b** in $CDCl_3$

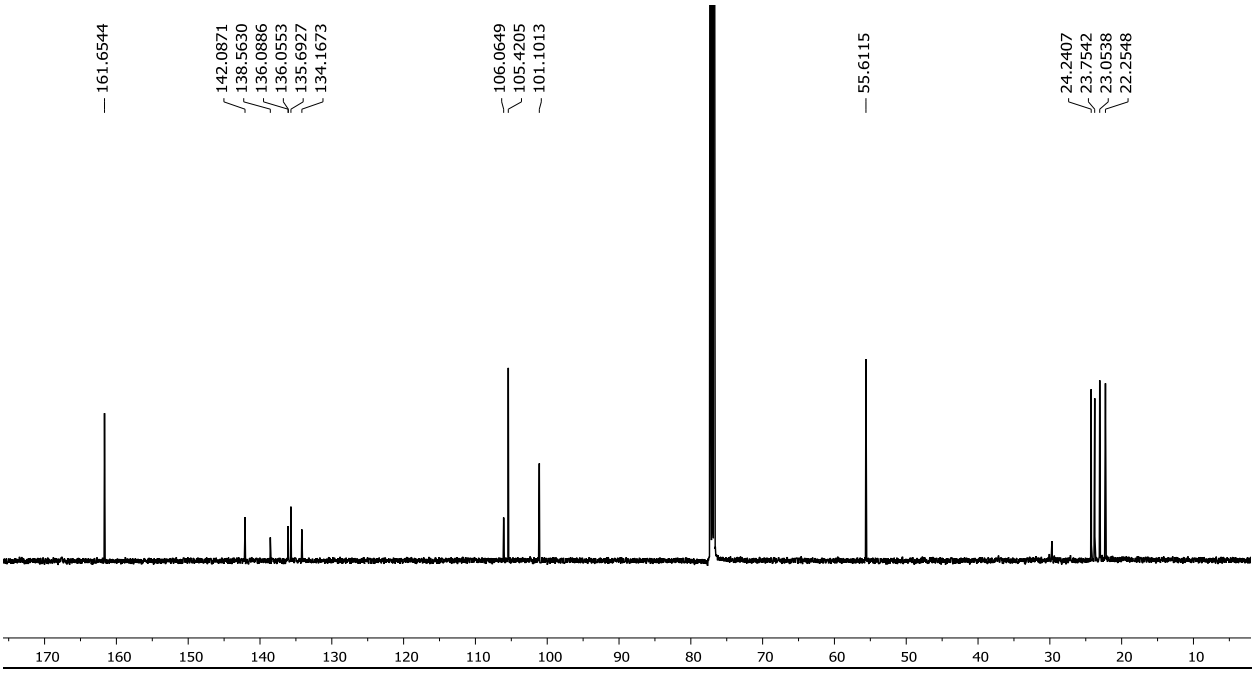

Figure A.7: ^{13}C NMR spectrum of **6b** in $CDCl_3$

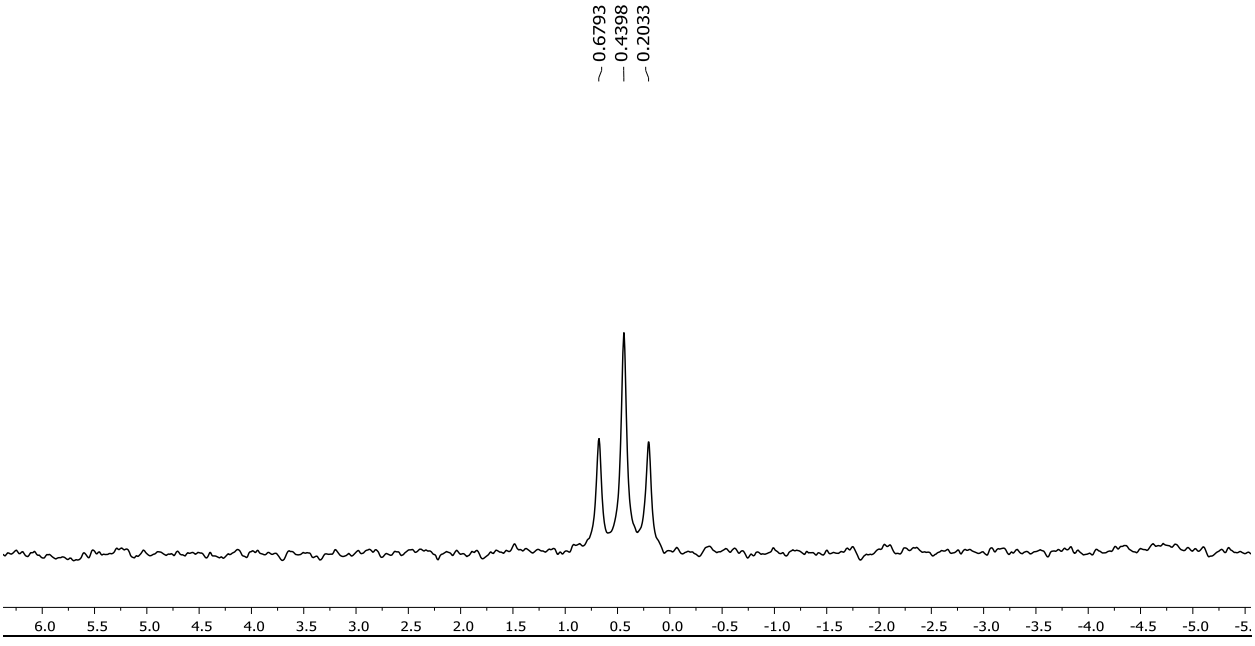

Figure A.8: ^{11}B NMR spectrum of **6b** in $CDCl_3$

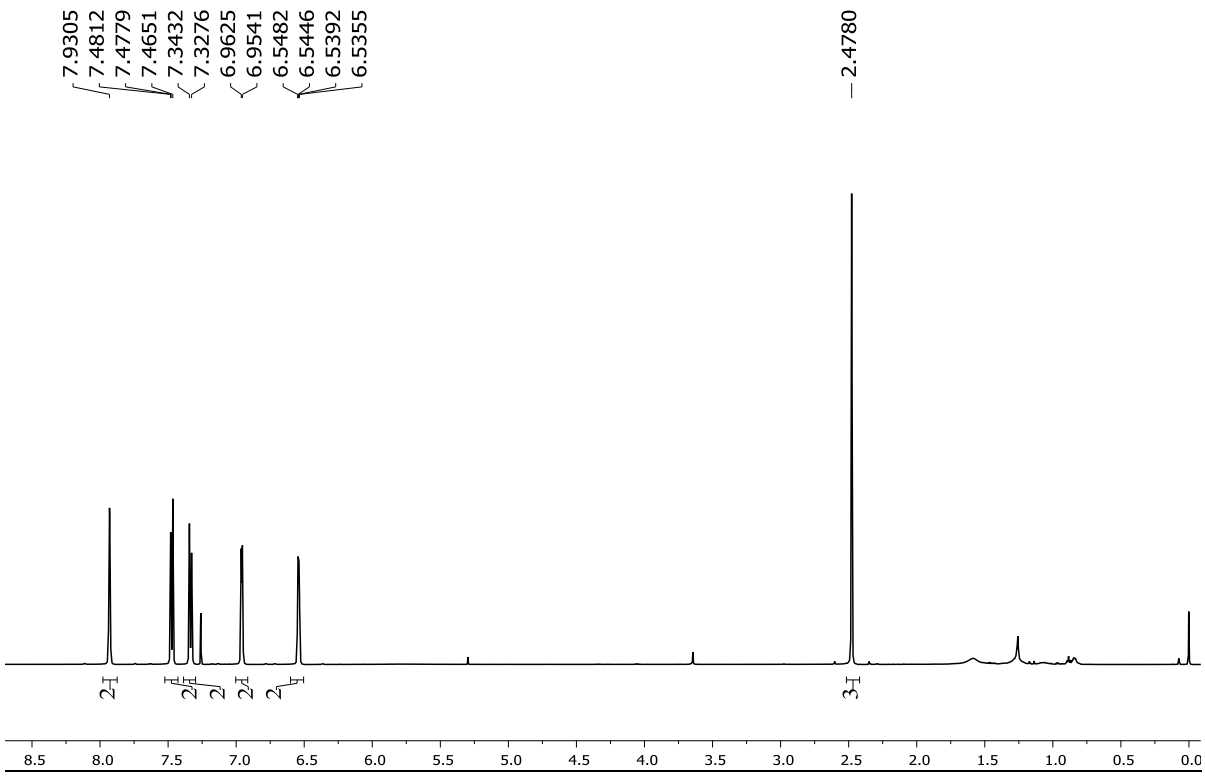

Figure A.9: ^{1}H NMR spectrum of **8a** in $CDCl_3$

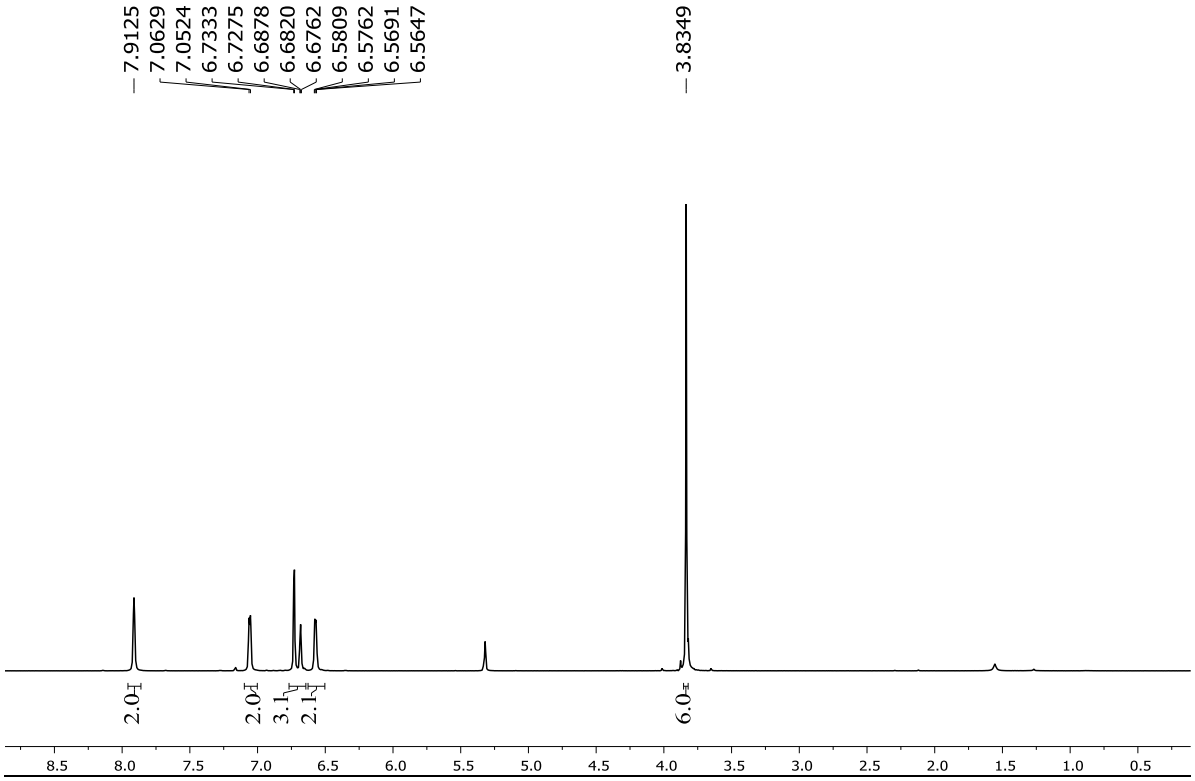

Figure A.10: ^{1}H spectrum of **8b** in CD_2Cl_2

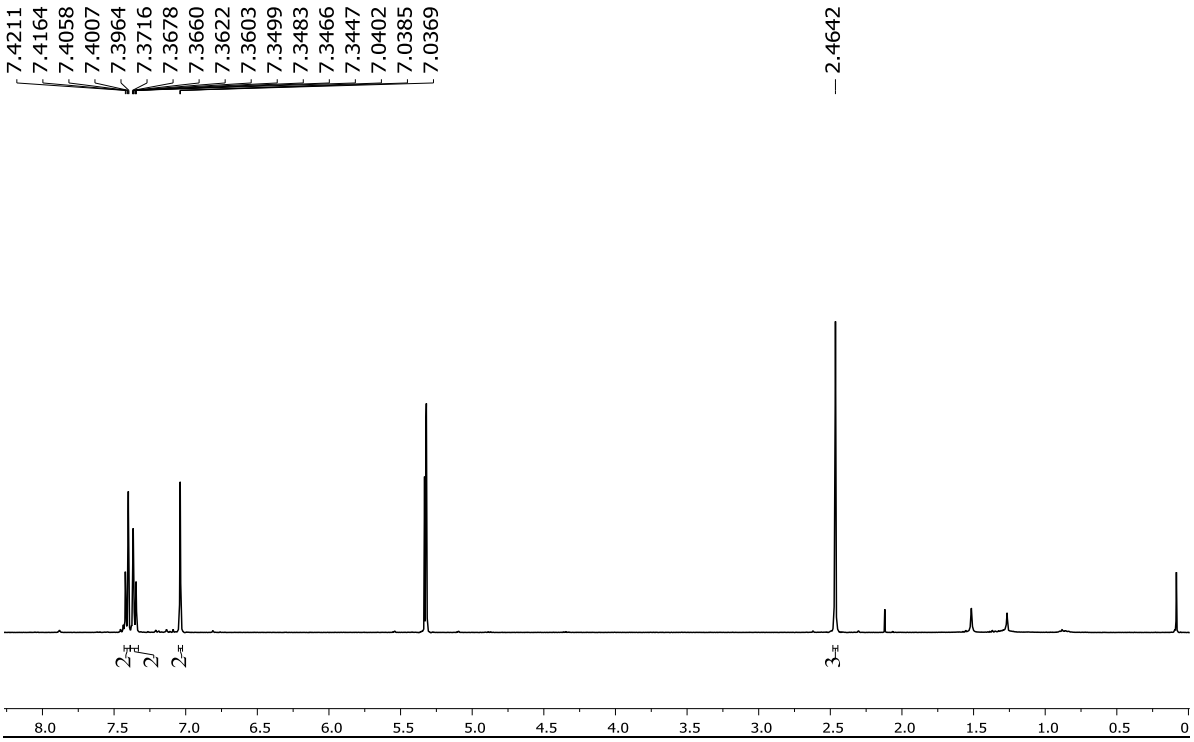

Figure A.11: ^{1}H NMR spectrum of **9a** in CD_2Cl_2

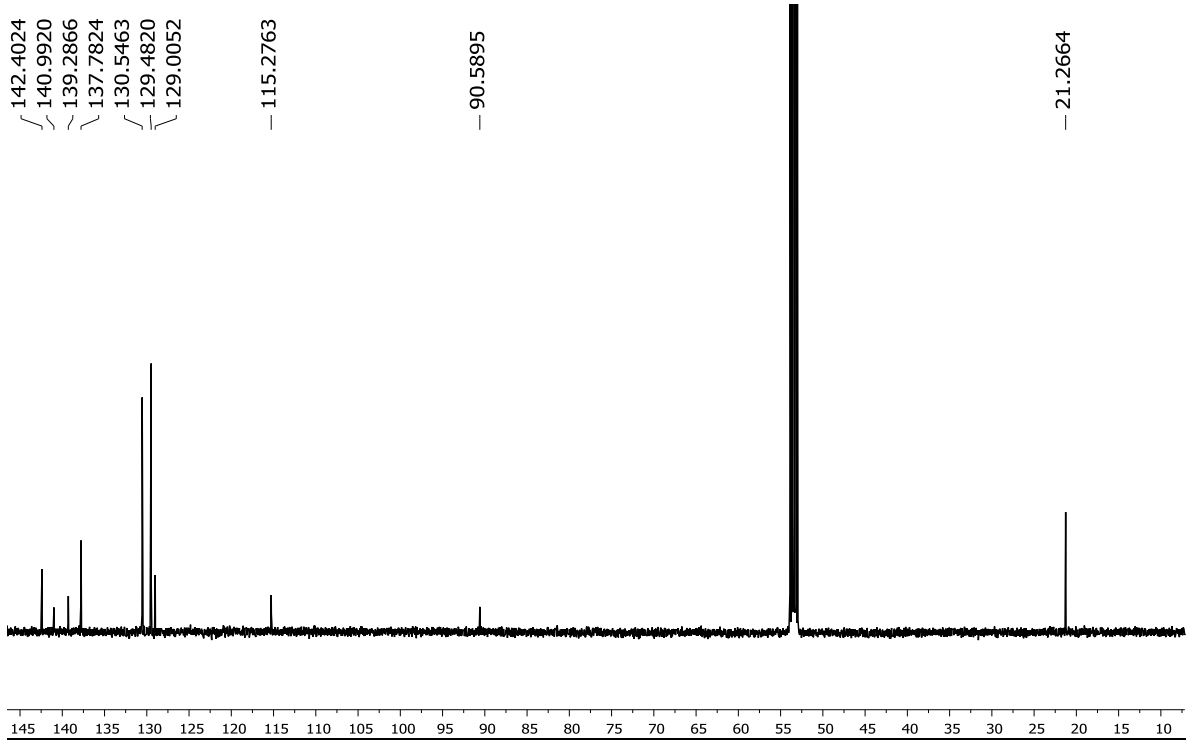

Figure A.12: ^{13}C NMR spectrum of **10a** in CD_2Cl_2

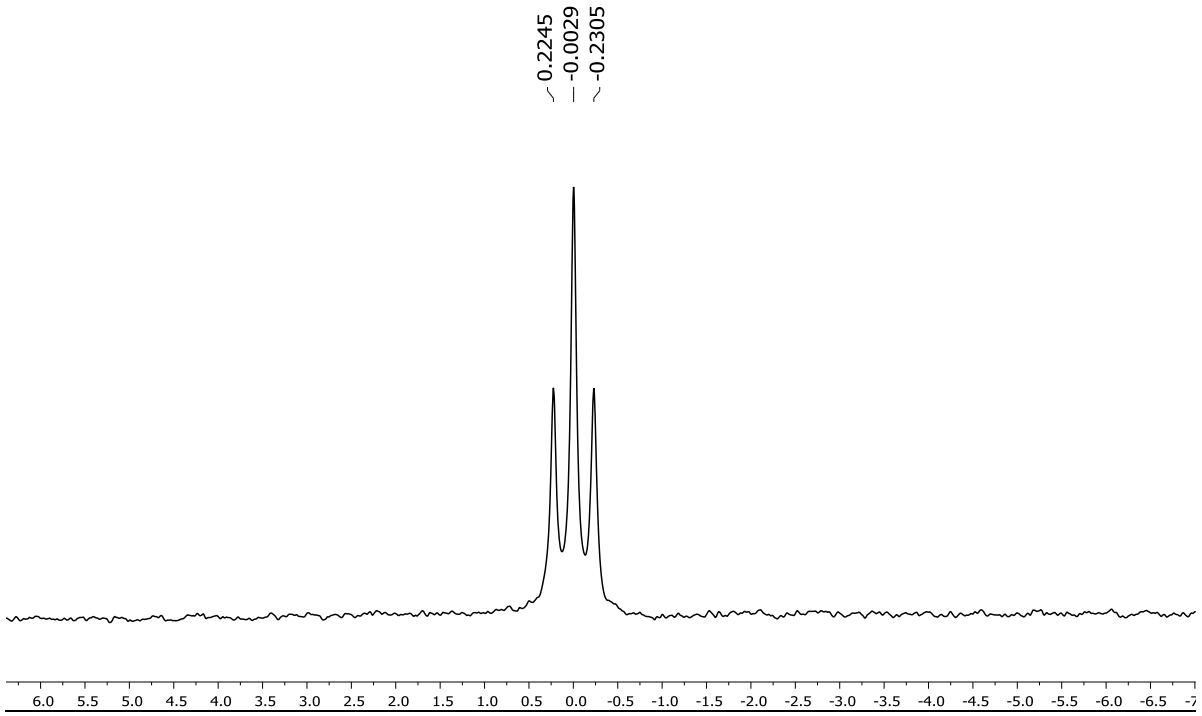

Figure A.13: ^{11}B NMR spectrum of **9a** in CD_2Cl_2

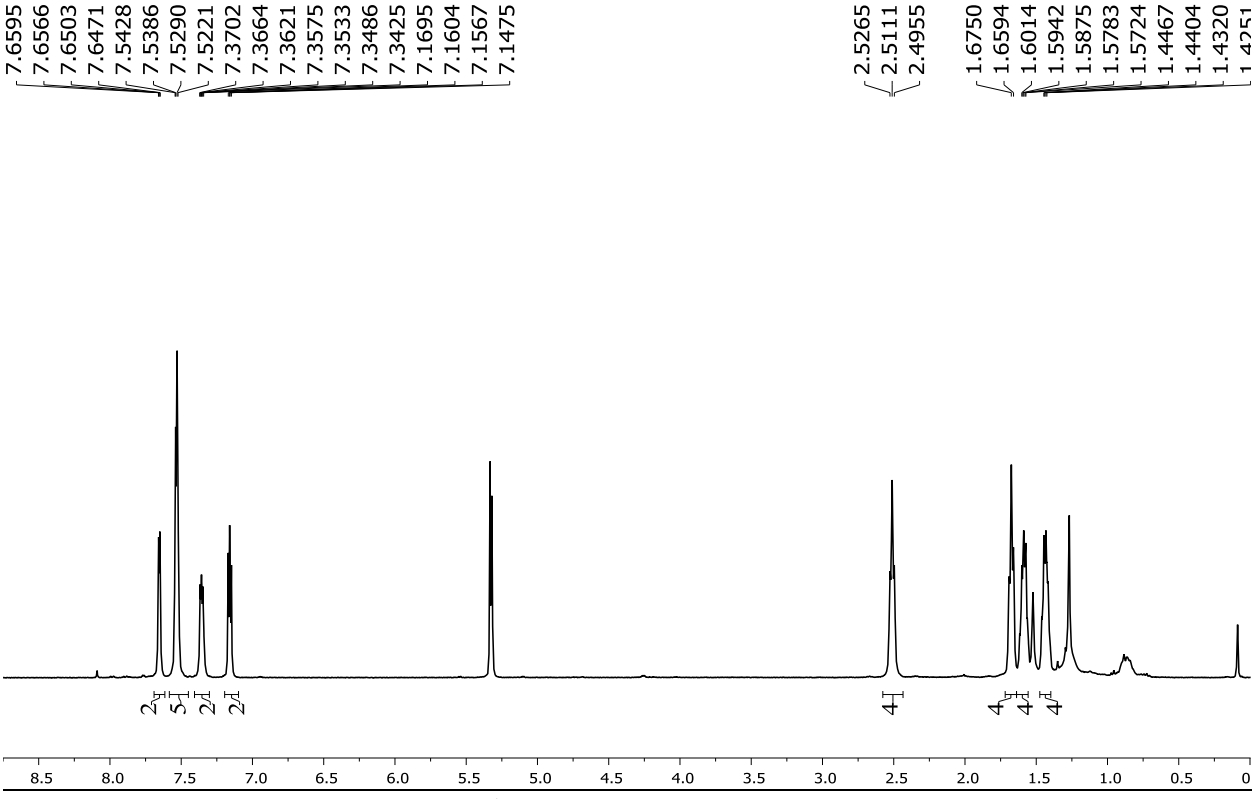

Figure A.14: ^{1}H NMR spectrum of **10a** in CD_2Cl_2

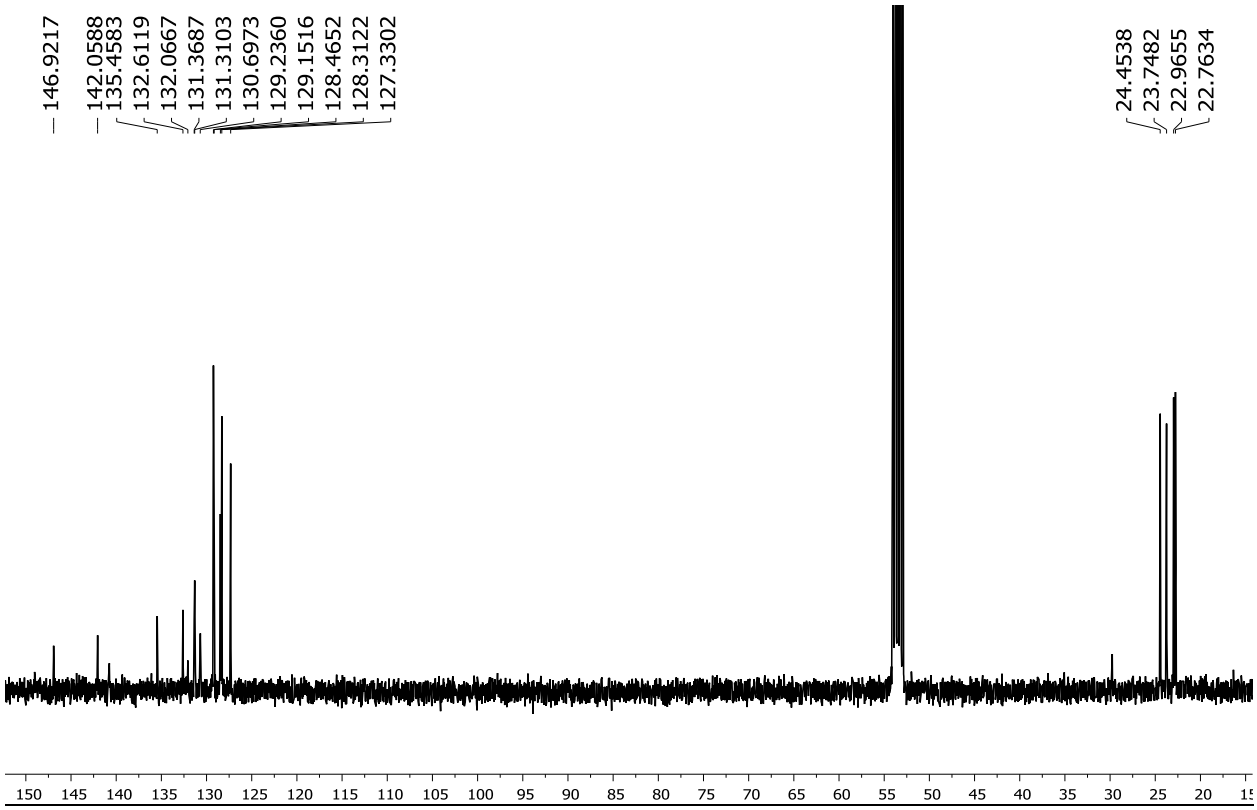

Figure A.15: ^{13}C NMR spectrum of **10a** in CD_2Cl_2

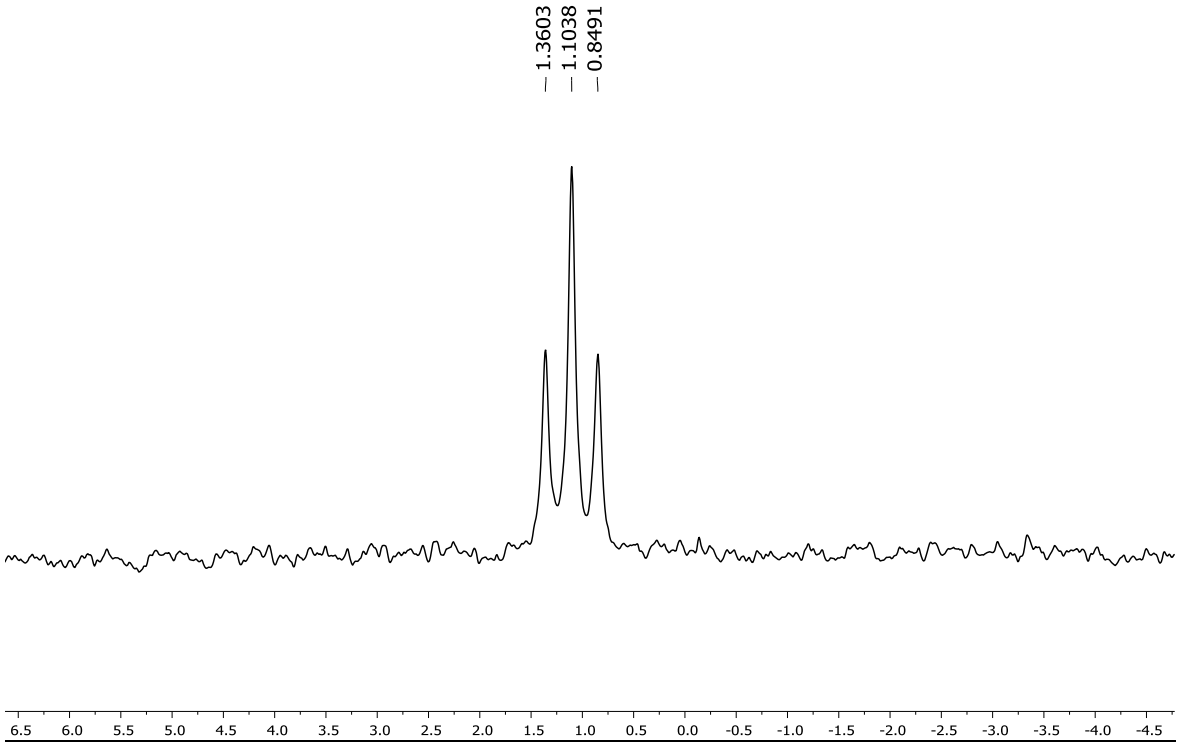

Figure A.16: ^{11}B NMR spectrum of **10a** in CD_2Cl_2

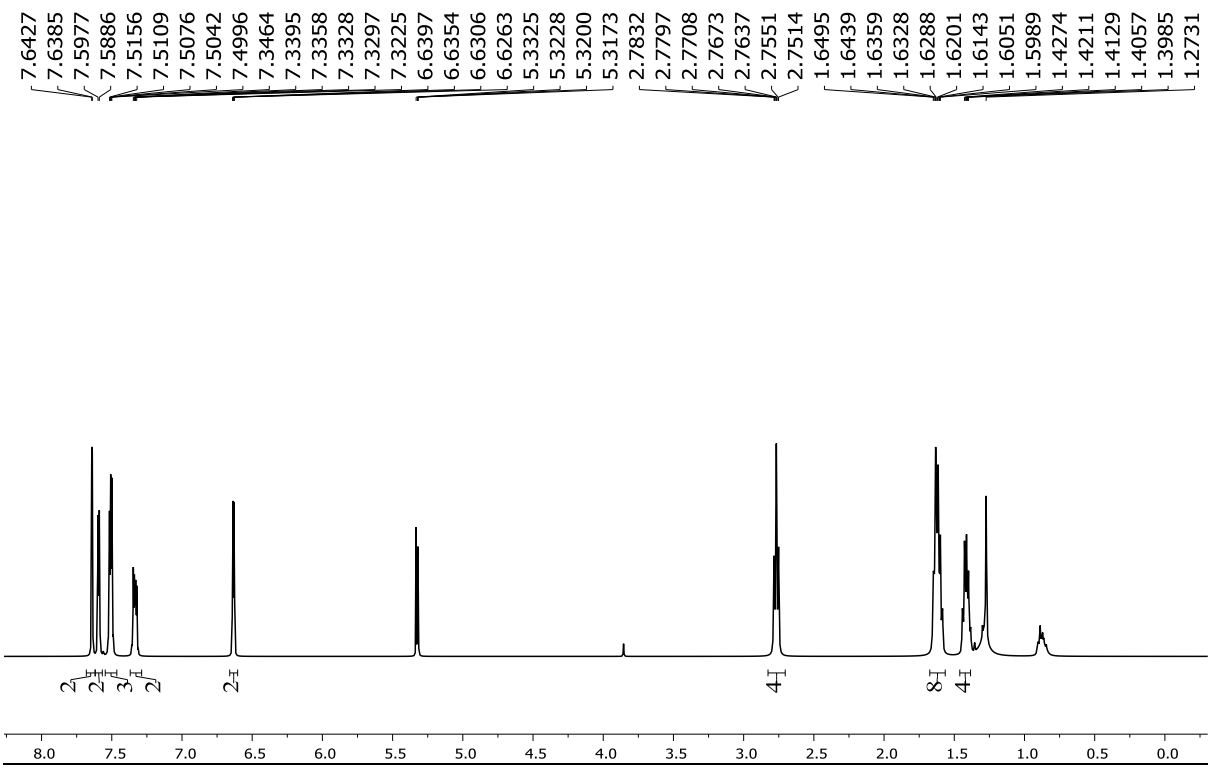

Figure A.17: ^{1}H NMR spectrum of **10b** in CD_2Cl_2

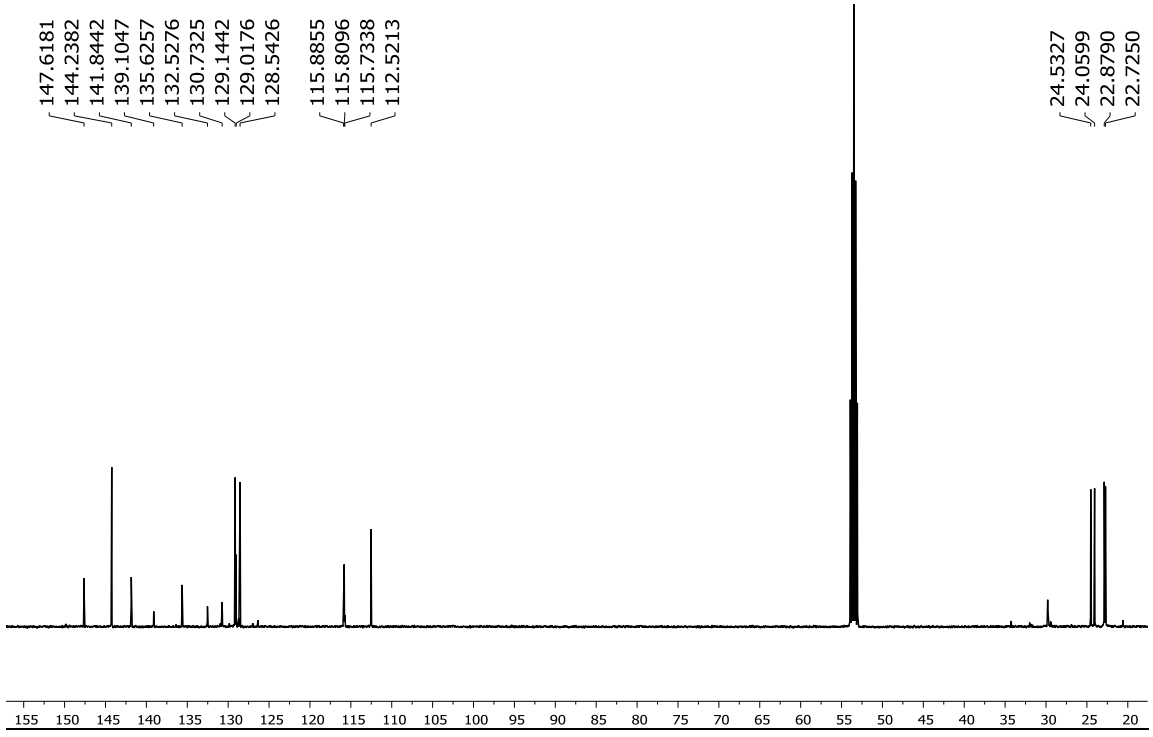

Figure A.18: ^{13}C NMR spectrum of **10b** in CD_2Cl_2

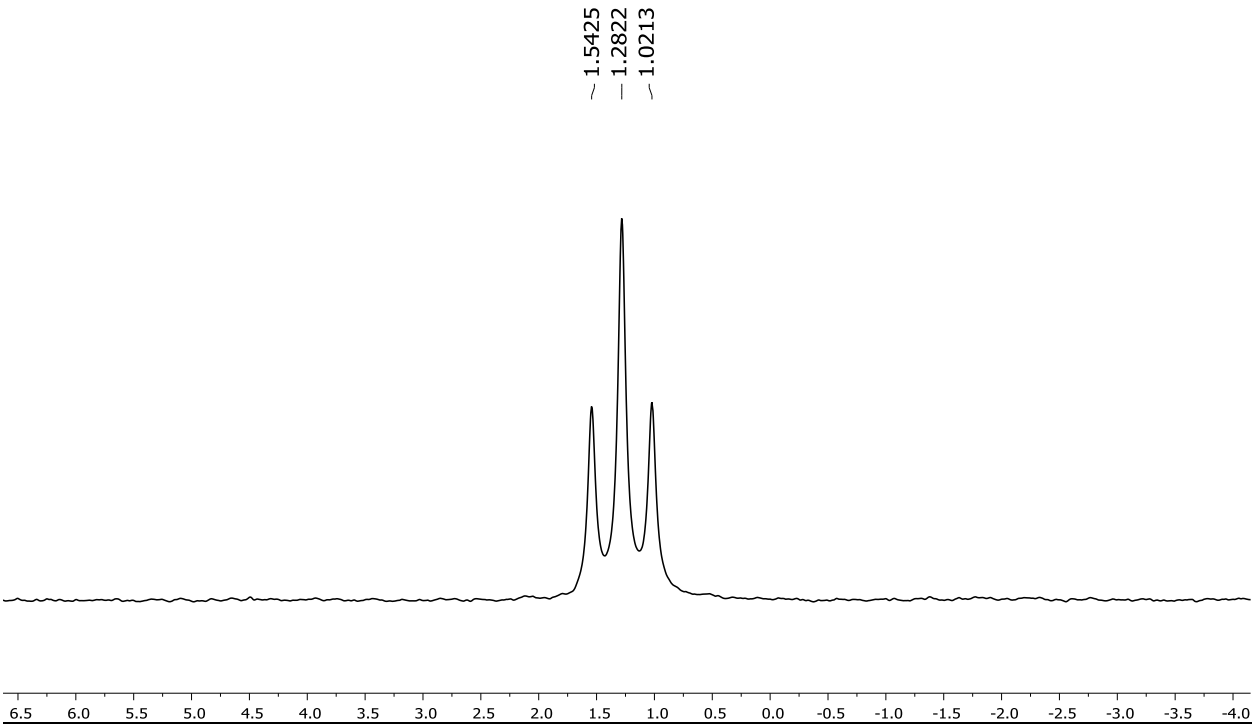

Figure A.19: ^{11}B NMR spectrum of **10b** in CD_2Cl_2

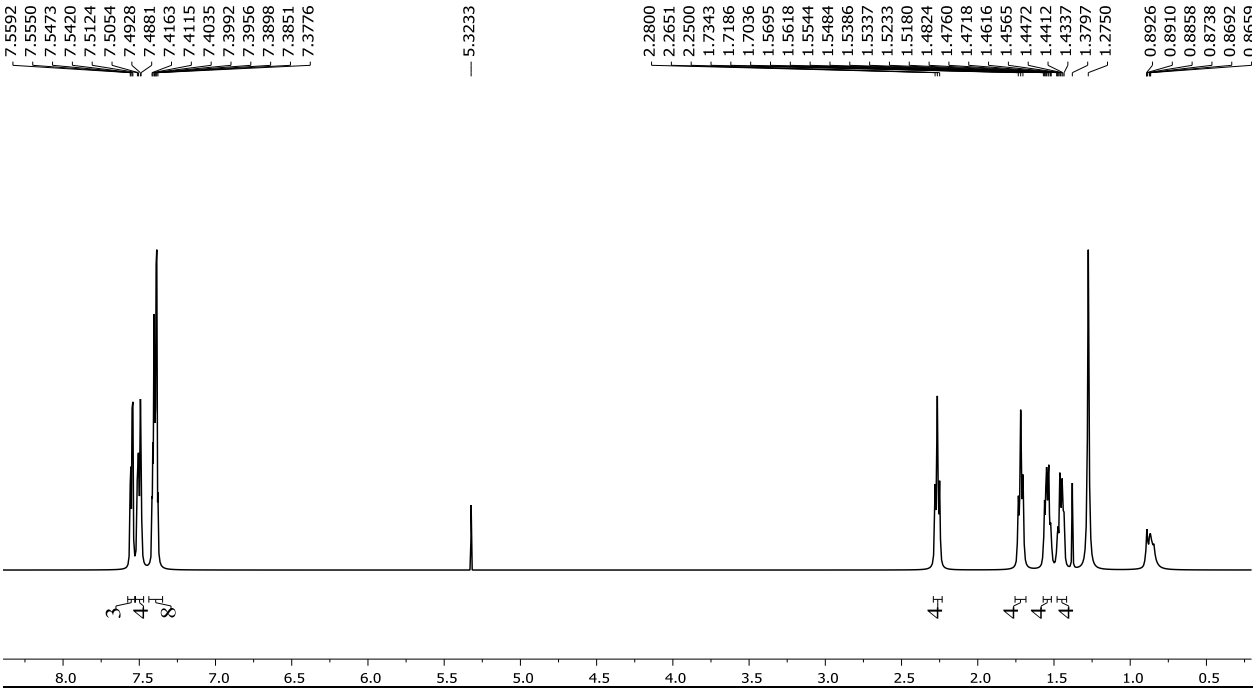

Figure A.20: ^{1}H NMR spectrum of **10c** in CD_2Cl_2

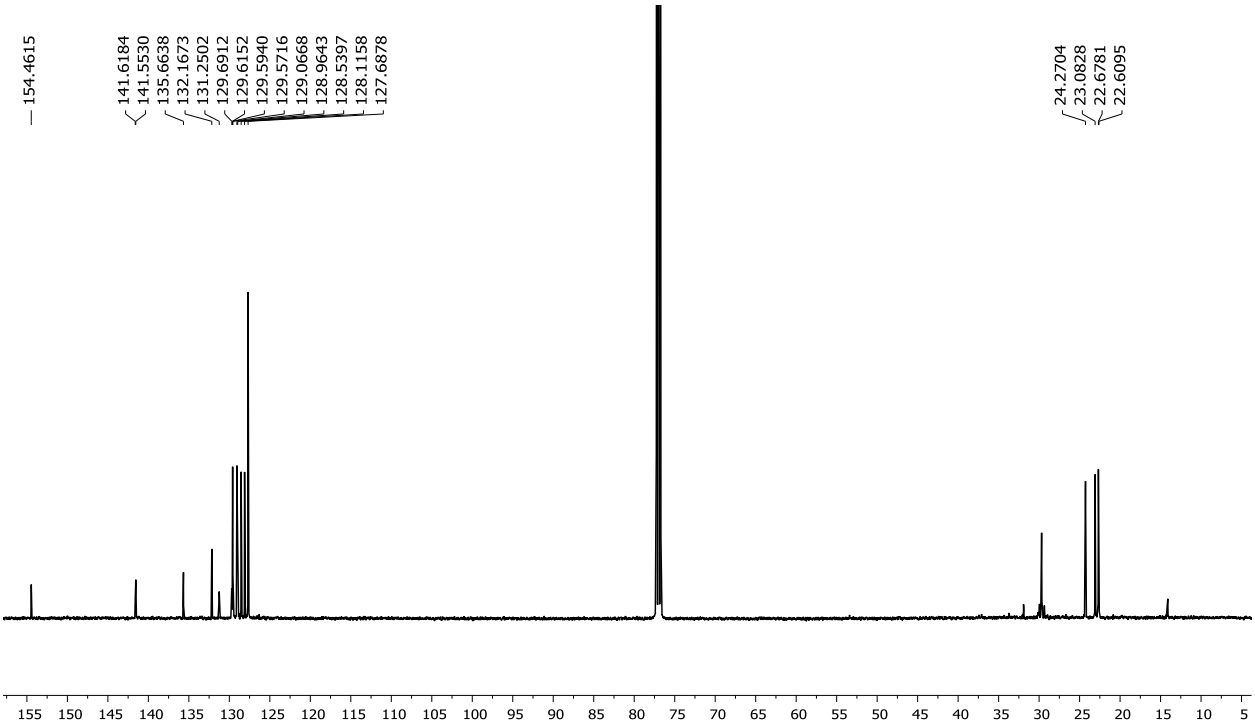

Figure A.21: ^{13}C NMR spectrum of **13** in $CDCl_3$

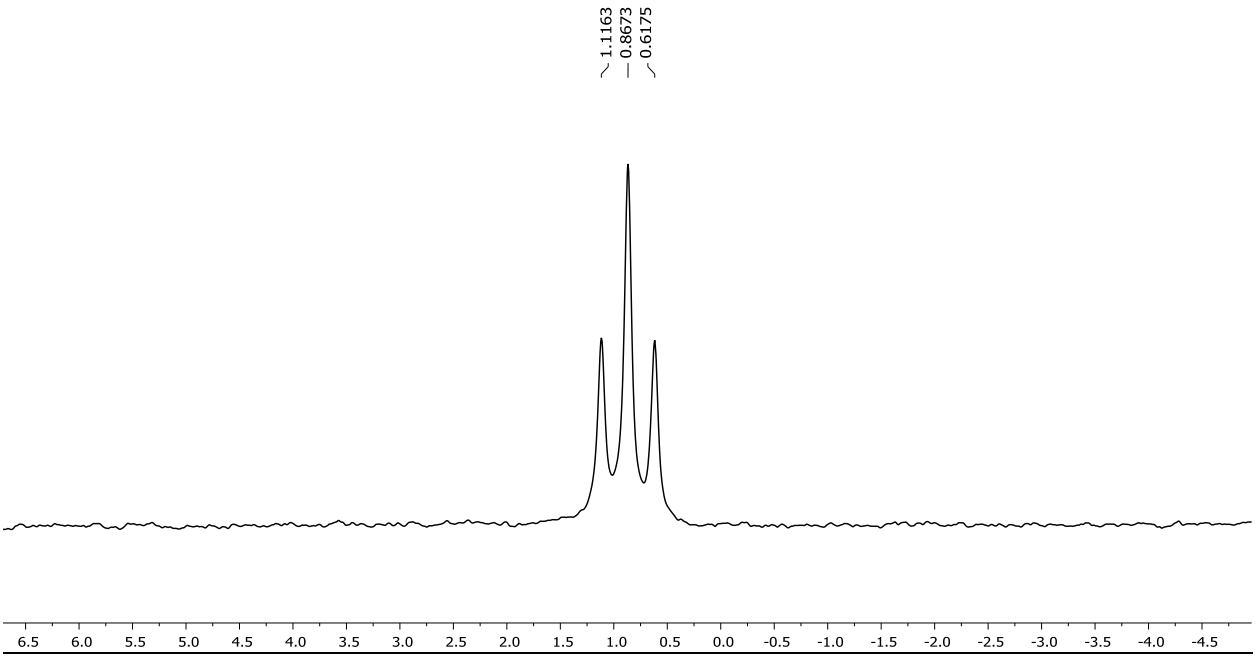

Figure A.22: ^{11}B NMR spectrum of **13** in CD_2Cl_2

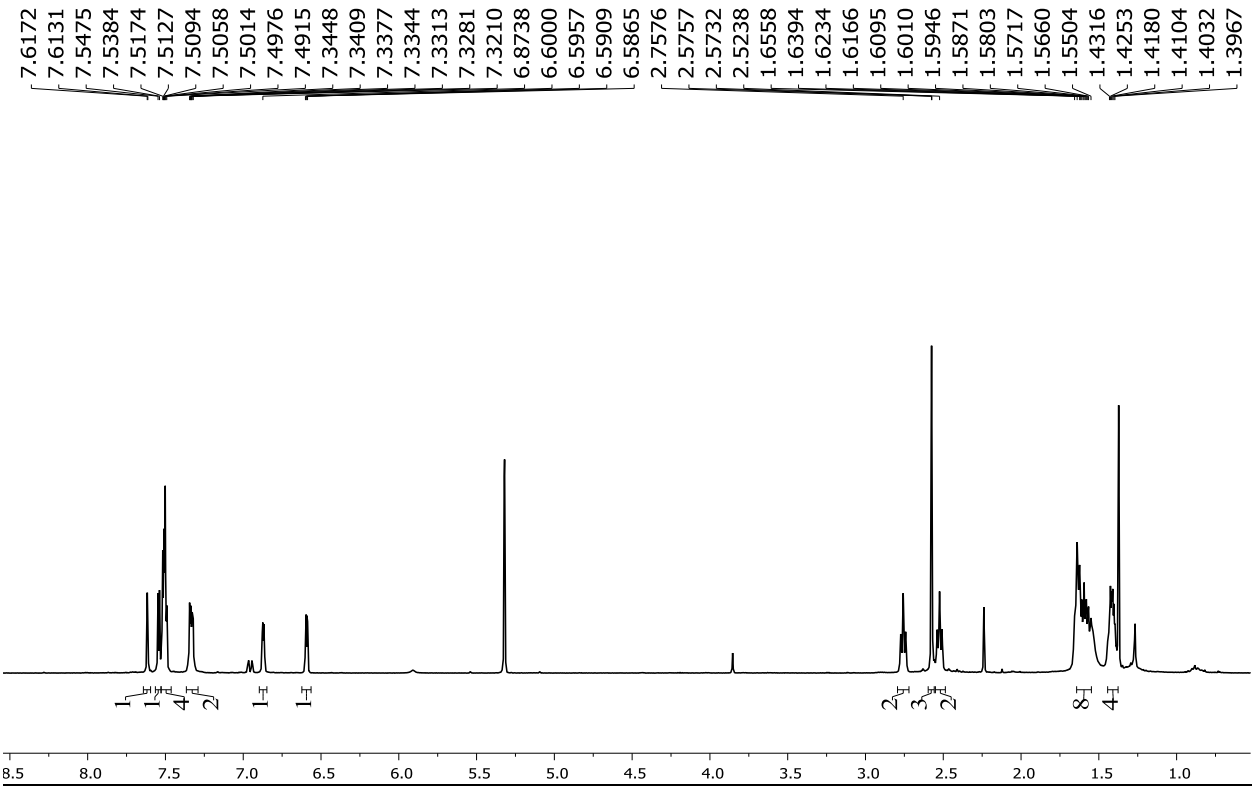

Figure A.23: ^{1}H NMR spectrum of **13** in CD_2Cl_2

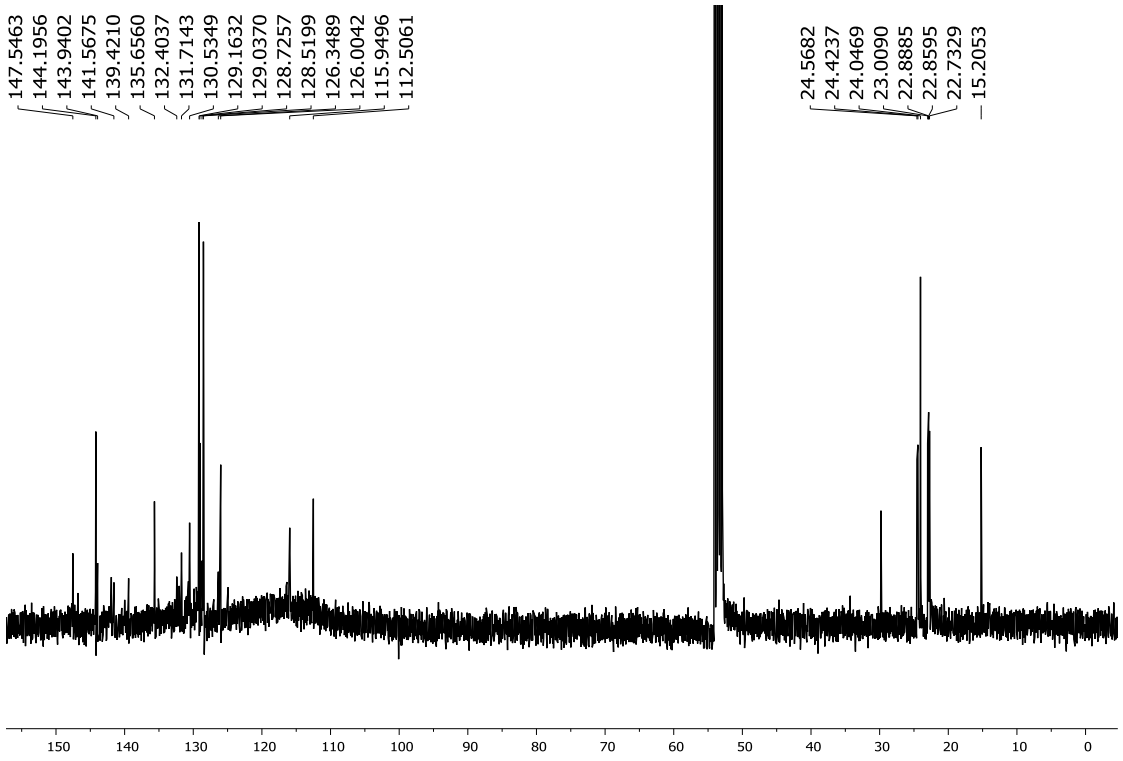

Figure A.24: ^{13}C NMR spectrum of **13** in CD_2Cl_2

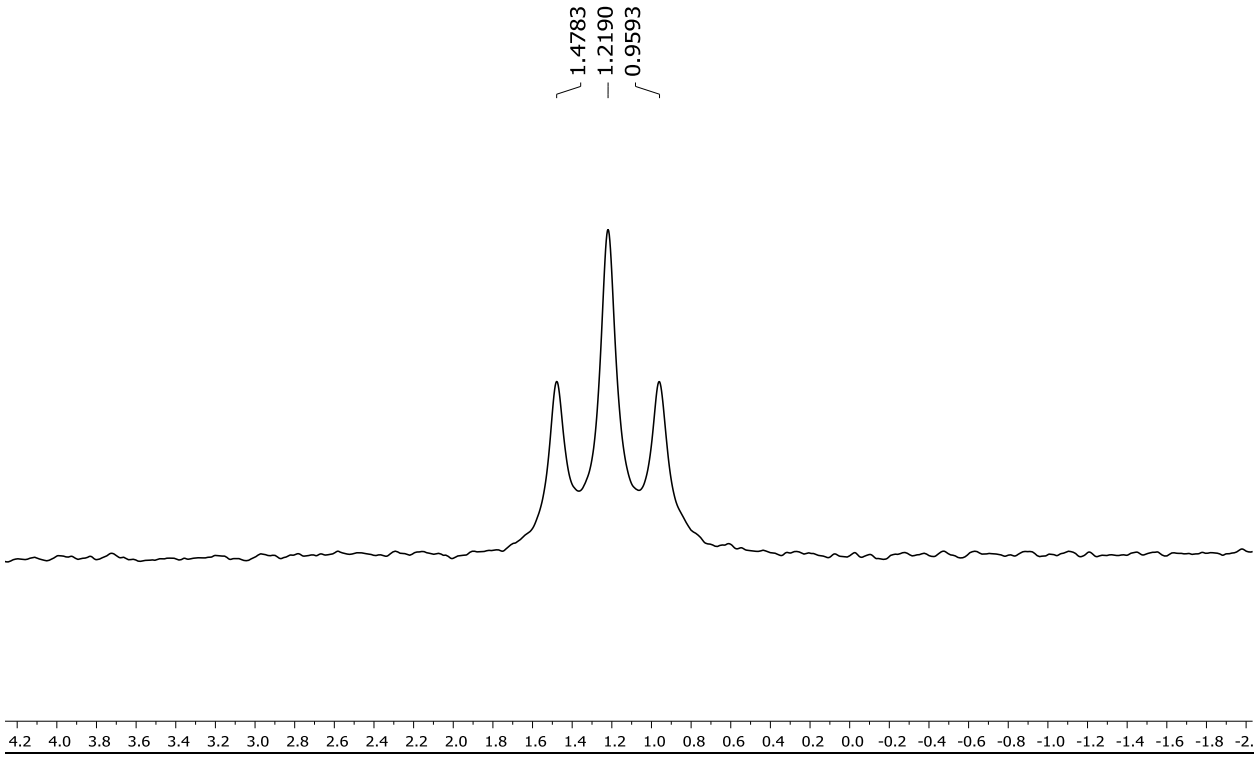

Figure A.25: ^{11}B NMR spectrum of **13** in CD_2Cl_2

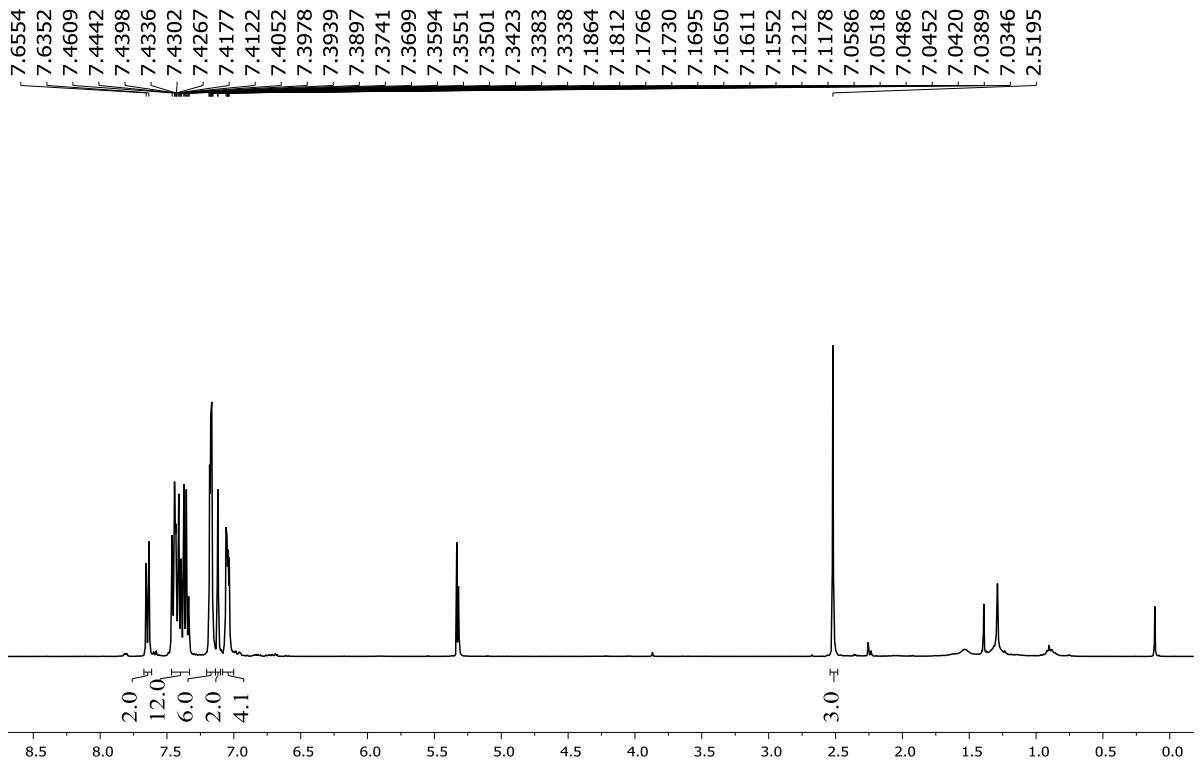

Figure A.26: ^{1}H NMR spectrum of **14** in CD_2Cl_2

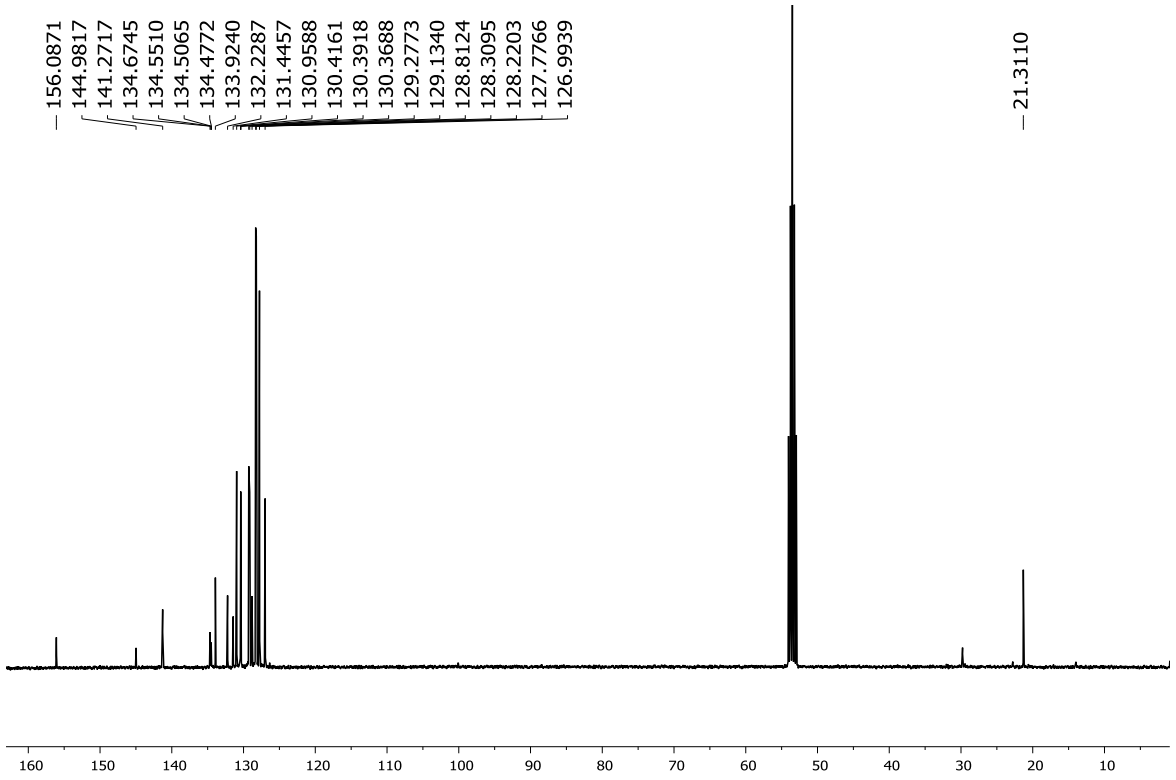

Figure A.27: ^{13}C NMR spectrum of **14** in CD_2Cl_2

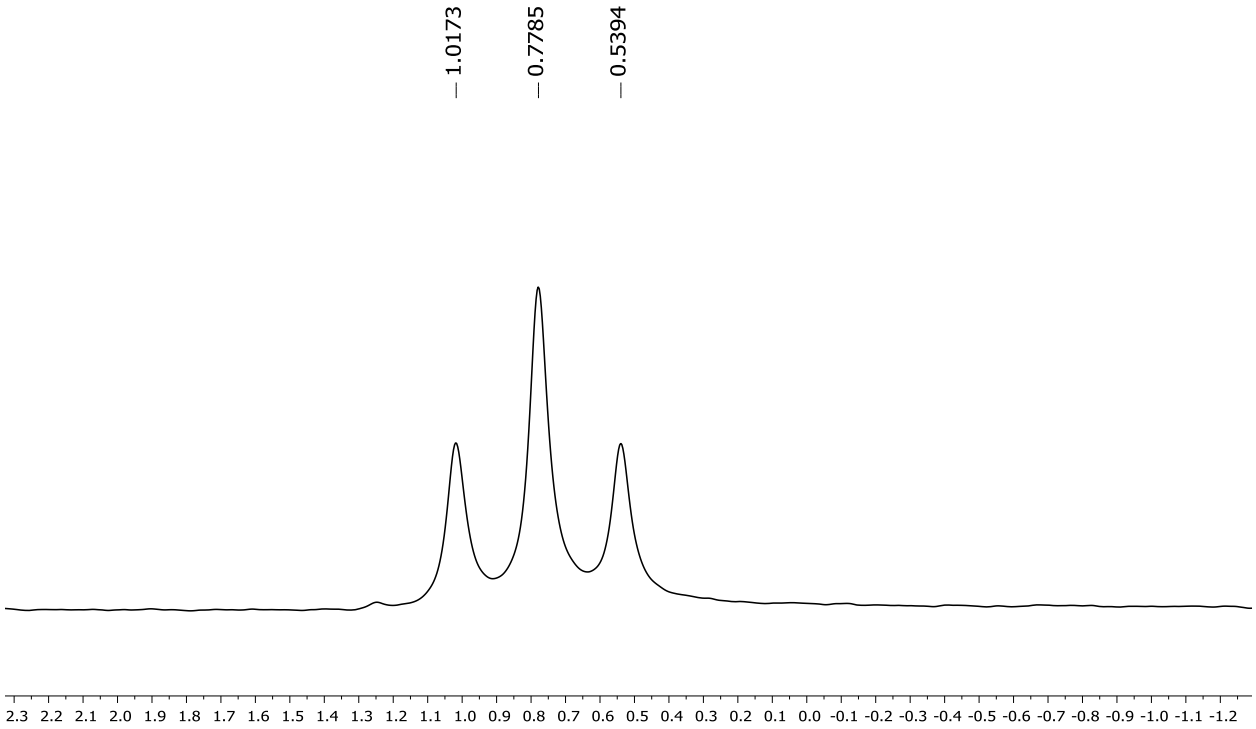

Figure A.28: ^{11}B NMR spectrum of **14** in CD_2Cl_2

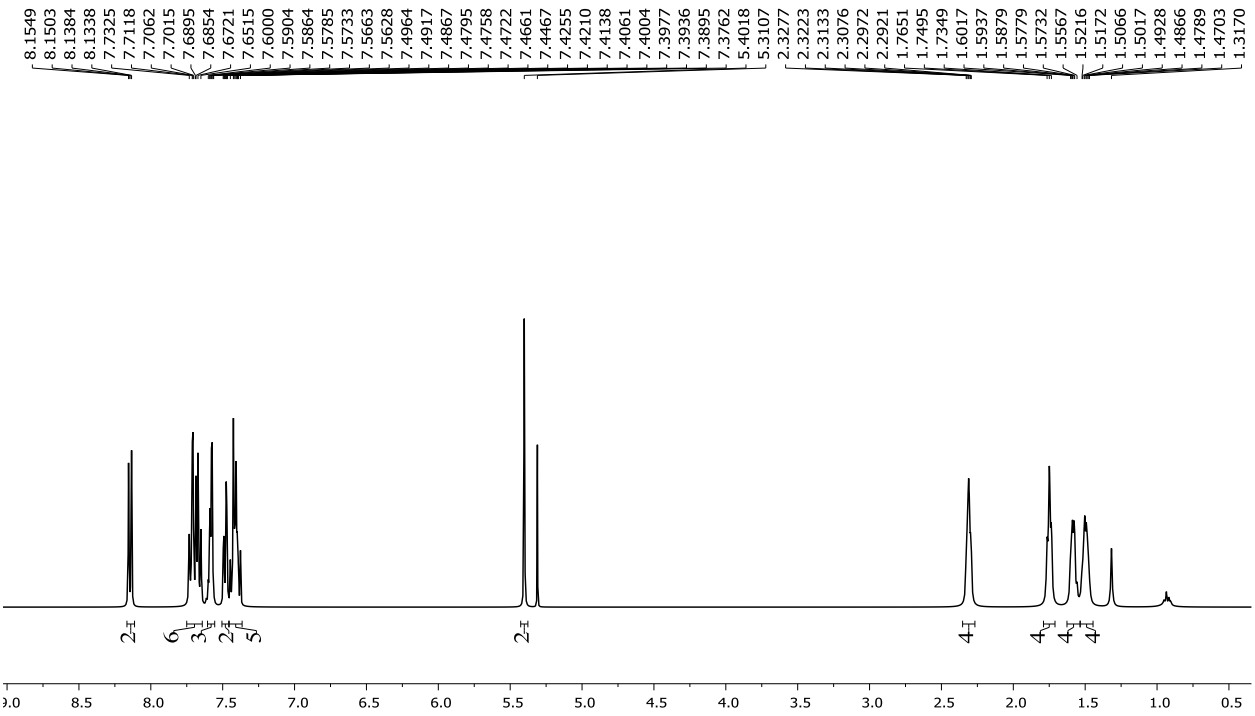

Figure A.29: ^{1}H NMR spectrum of **17a** in $CDCl_3$

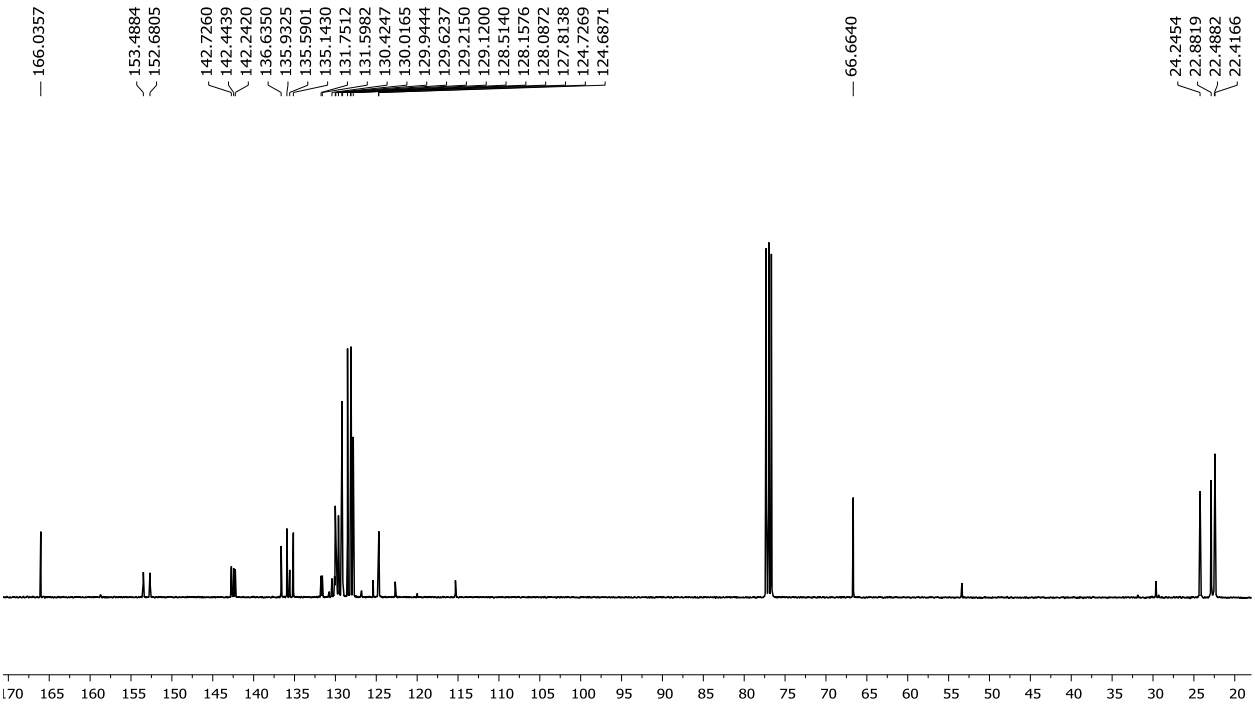

Figure A.30: ^{13}C NMR spectrum of **17a** in $CDCl_3$

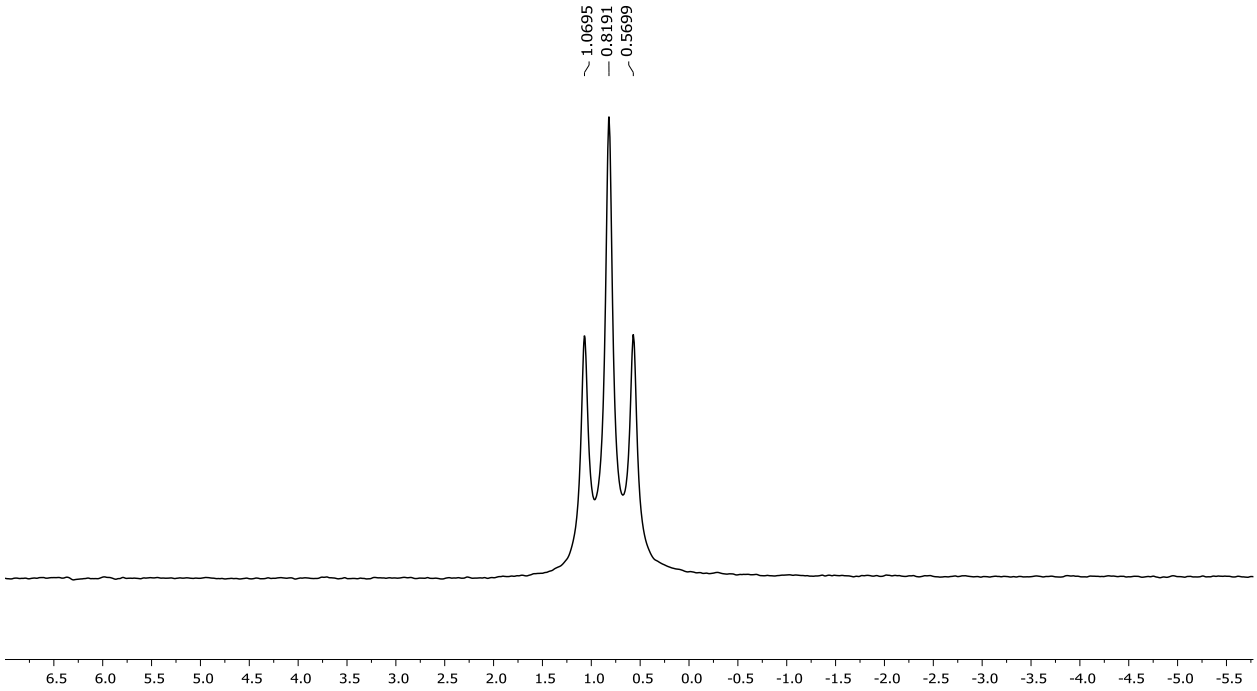

Figure A.31: ^{11}B NMR spectrum of **17a** in $CDCl_3$

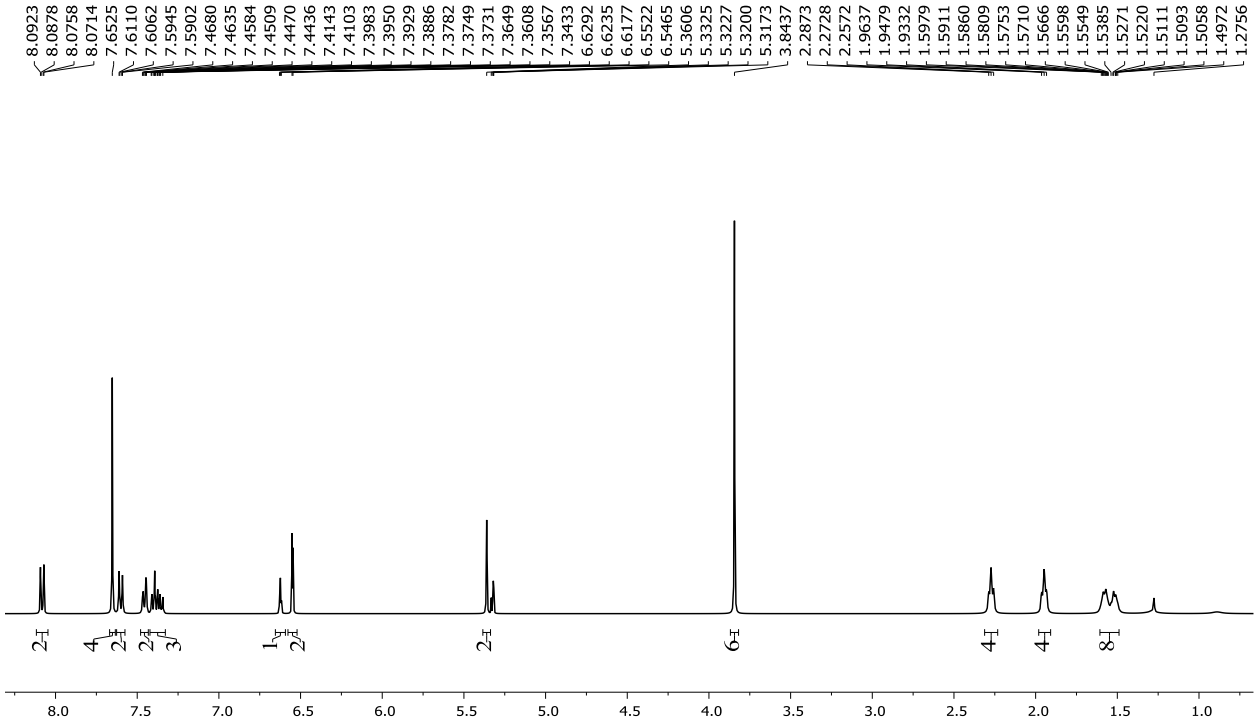

Figure A.32: ^{1}H NMR spectrum of **17b** in CD_2Cl_2

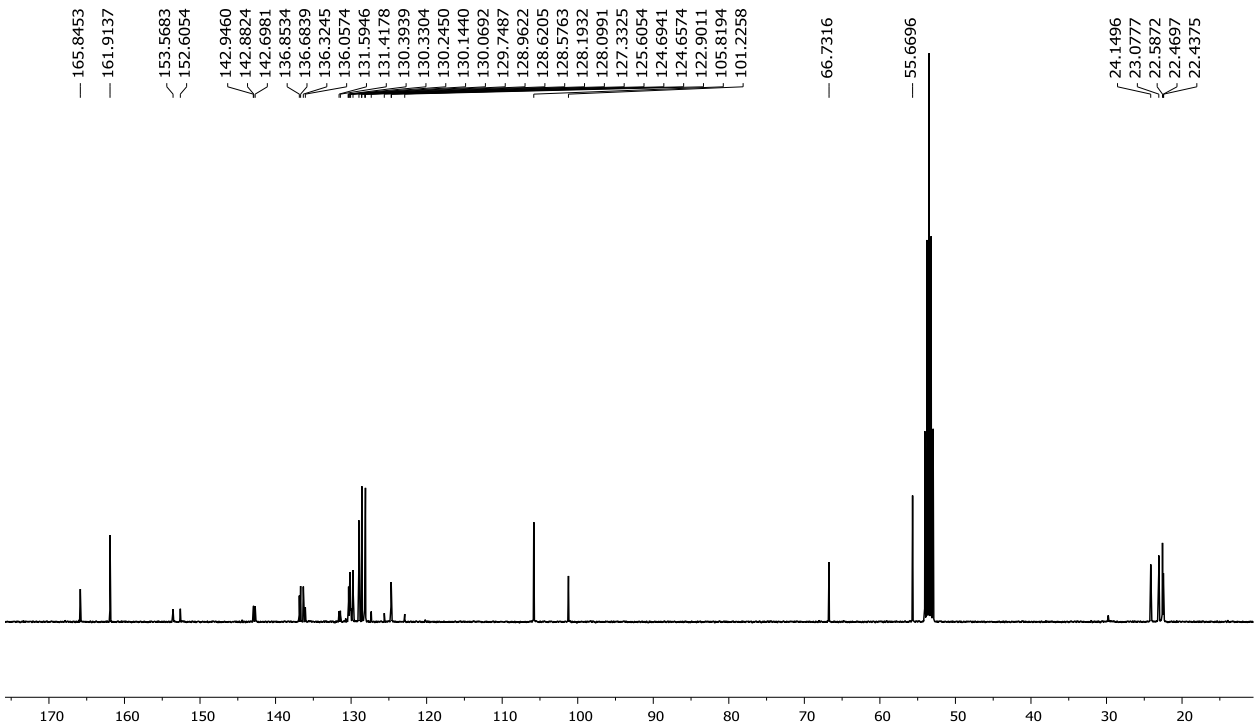

Figure A.33: ^{13}C NMR spectrum of **17b** in CD_2Cl_2

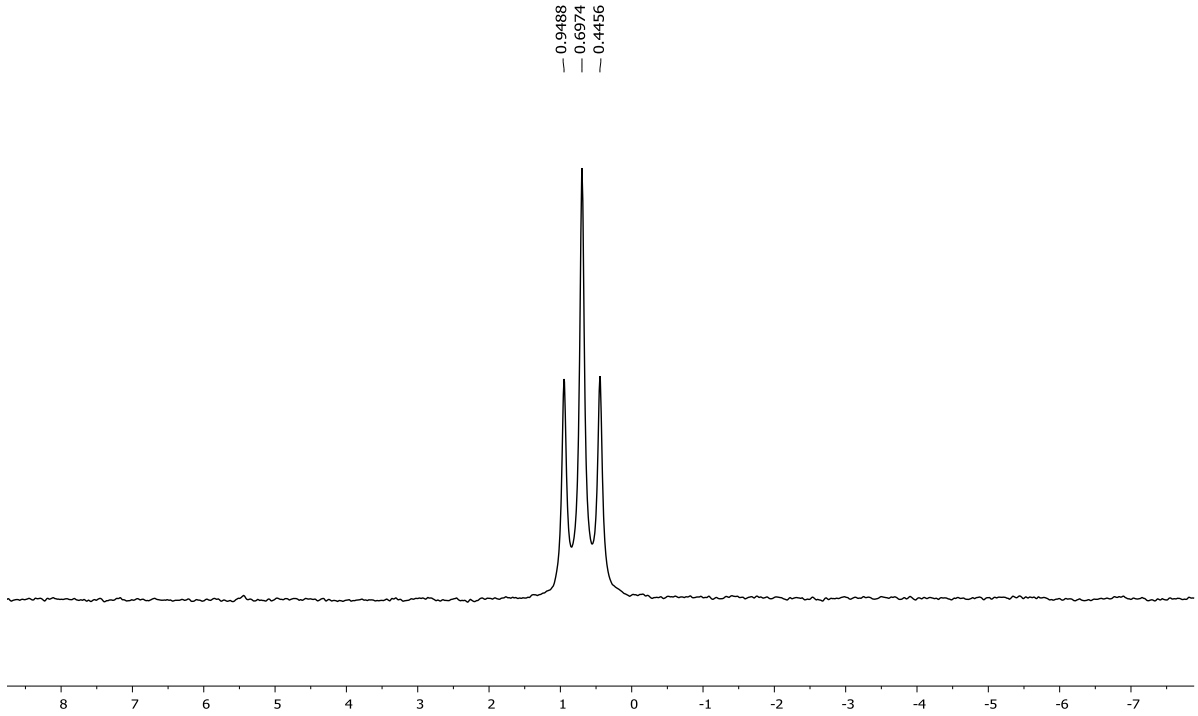

Figure A.34: ^{11}B NMR spectrum of **17b** in CD_2Cl_2

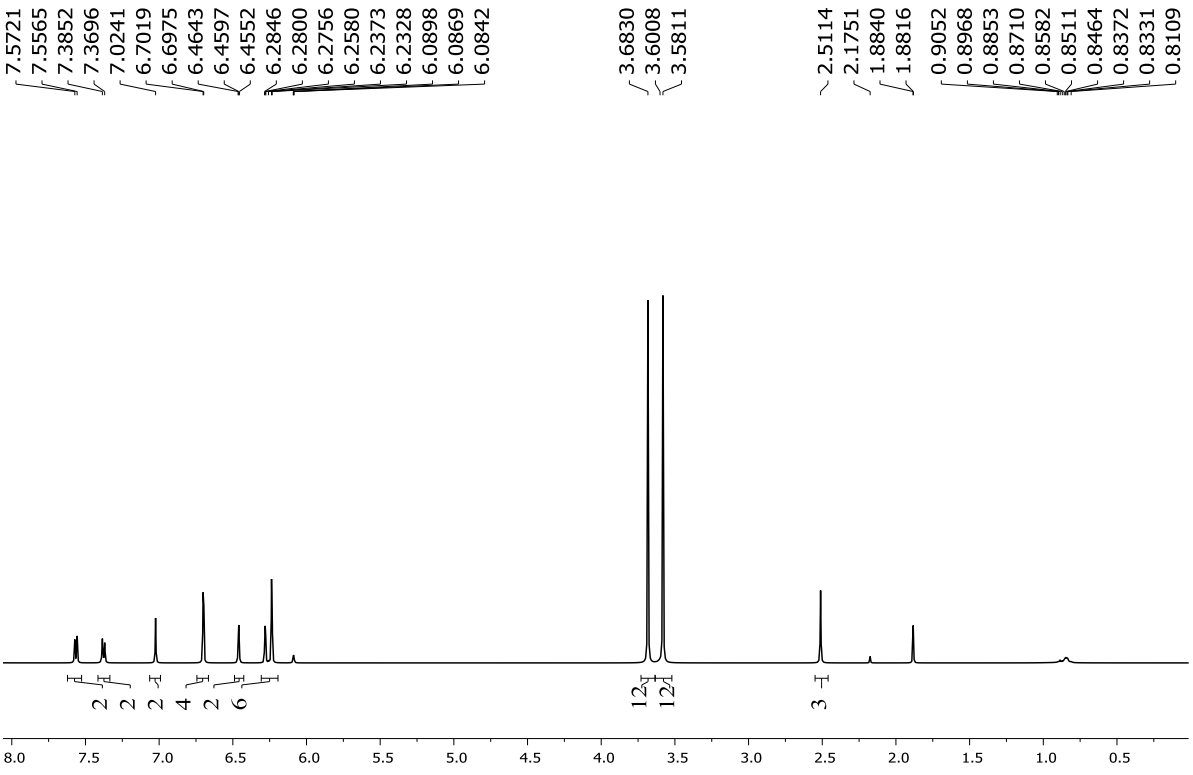

Figure A.35: ^{1}H NMR spectrum of **18** in CD_2Cl_2

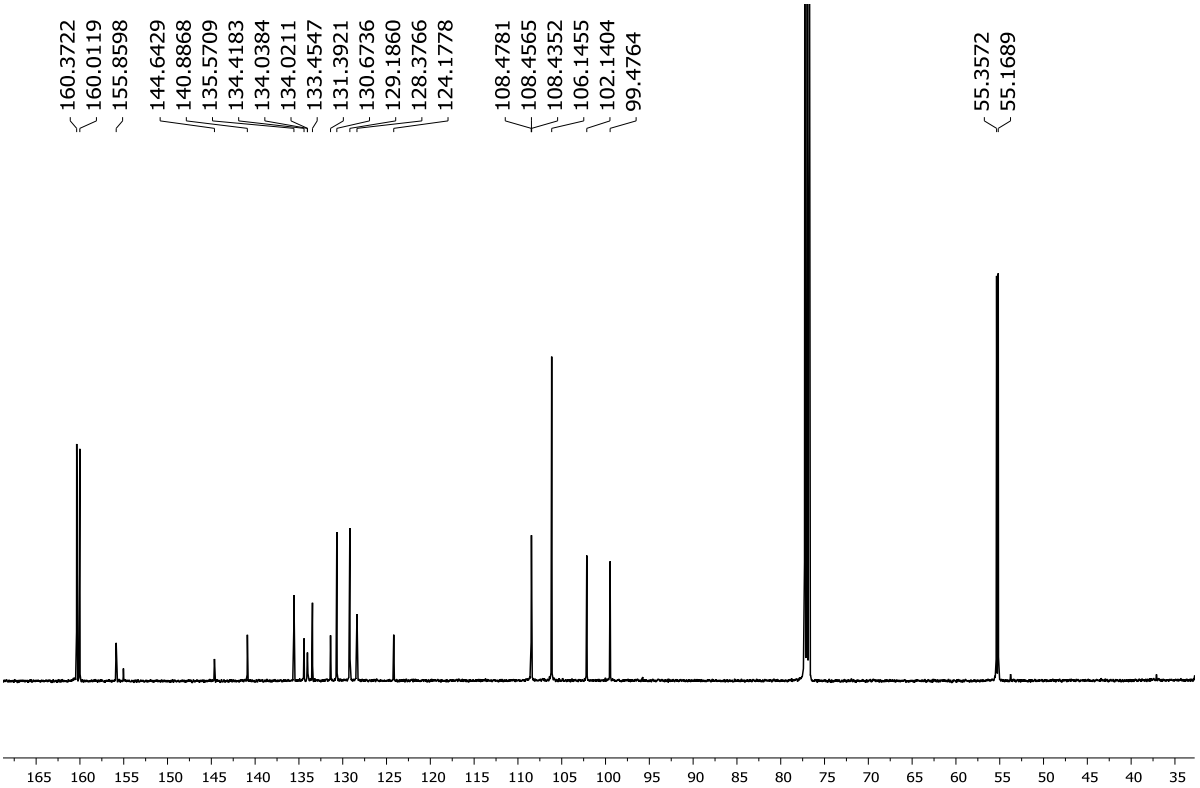

Figure A. 36: ^{13}C NMR spectrum of **18** in CD_2Cl_2

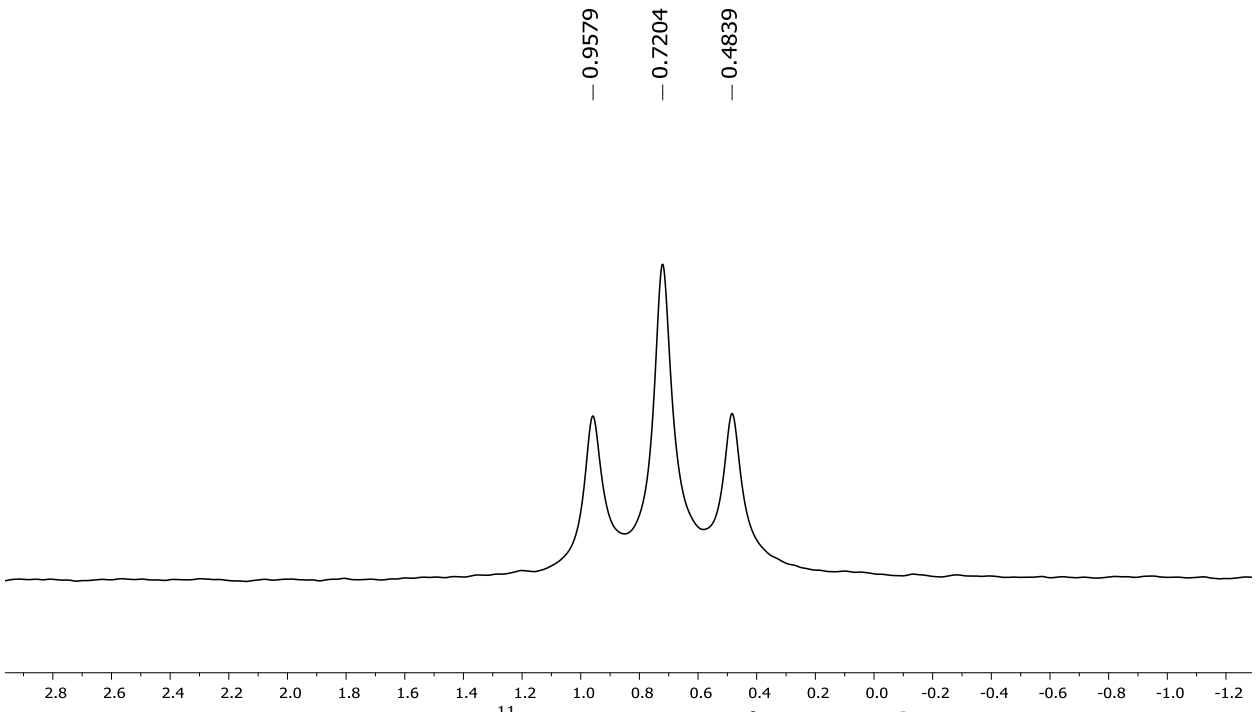

Figure A.37: ^{11}B NMR spectrum of **18** in CD_2Cl_2

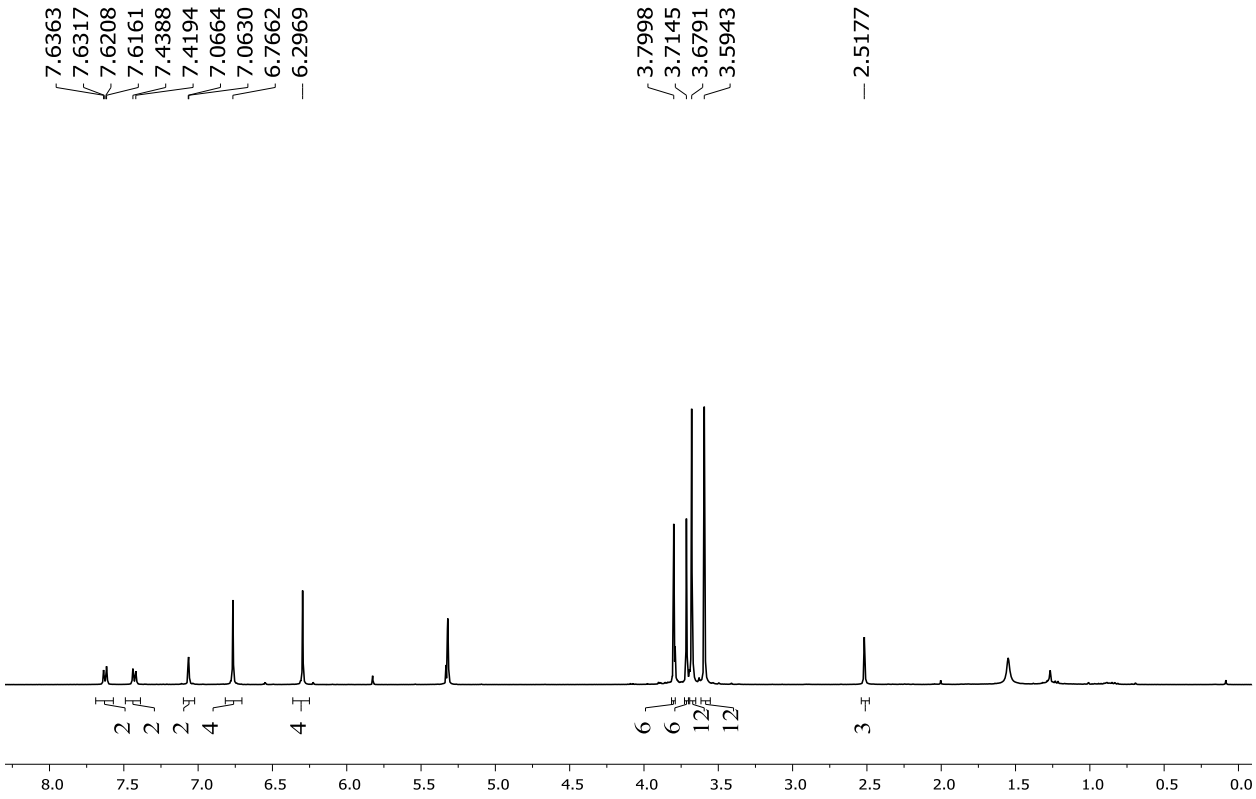

Figure A.38: ^{1}H NMR spectrum of **19** in CD_2Cl_2

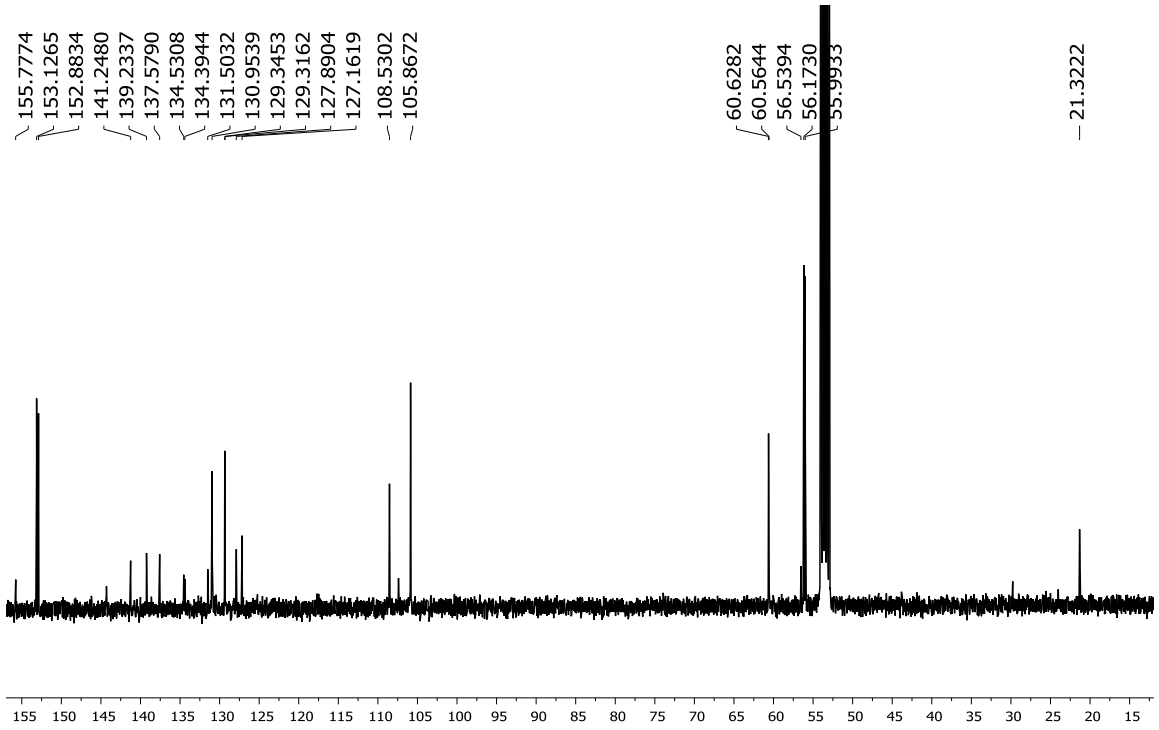

Figure A.39: ^{13}C NMR spectrum of **19** in CD_2Cl_2

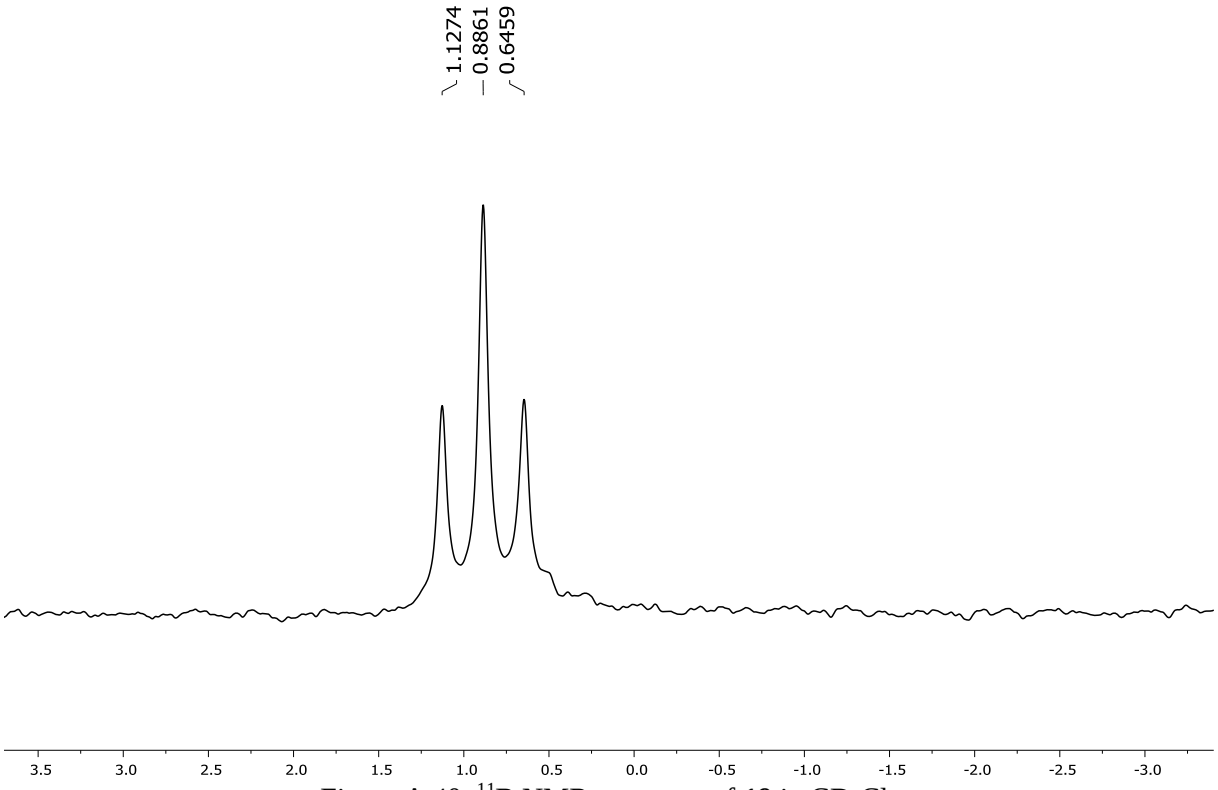

Figure A.40: ^{11}B NMR spectrum of **19** in CD_2Cl_2

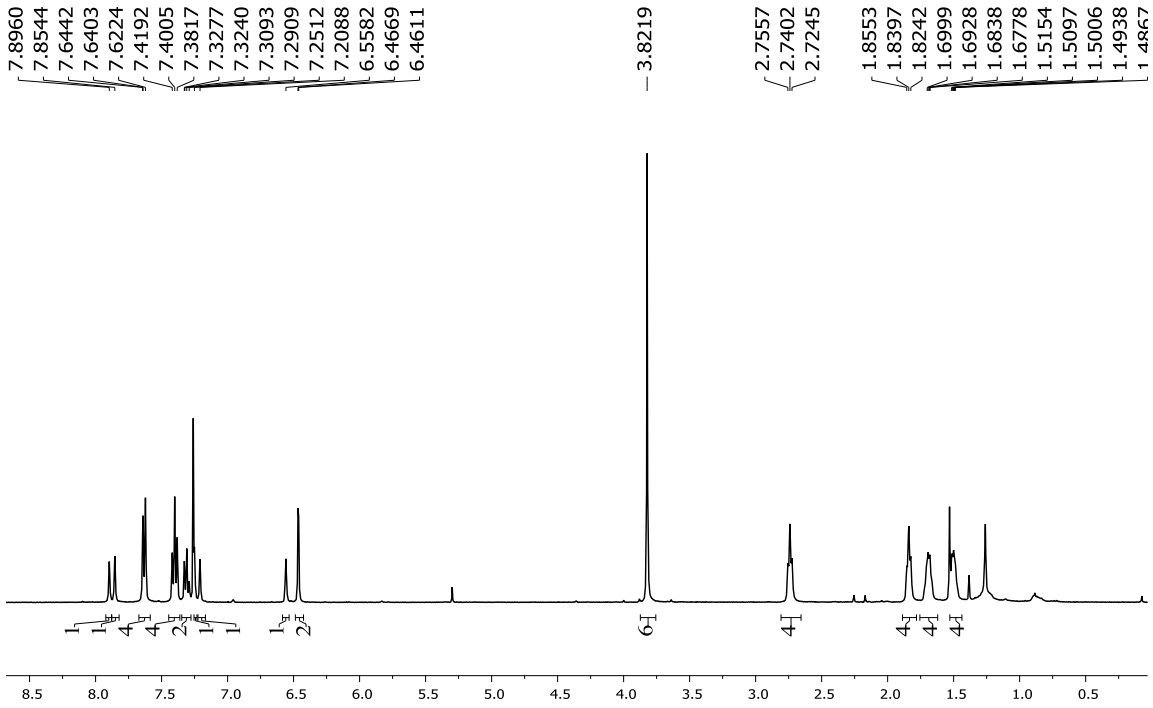

Figure A.41: ^{1}H NMR spectrum of **20** in $CDCl_3$

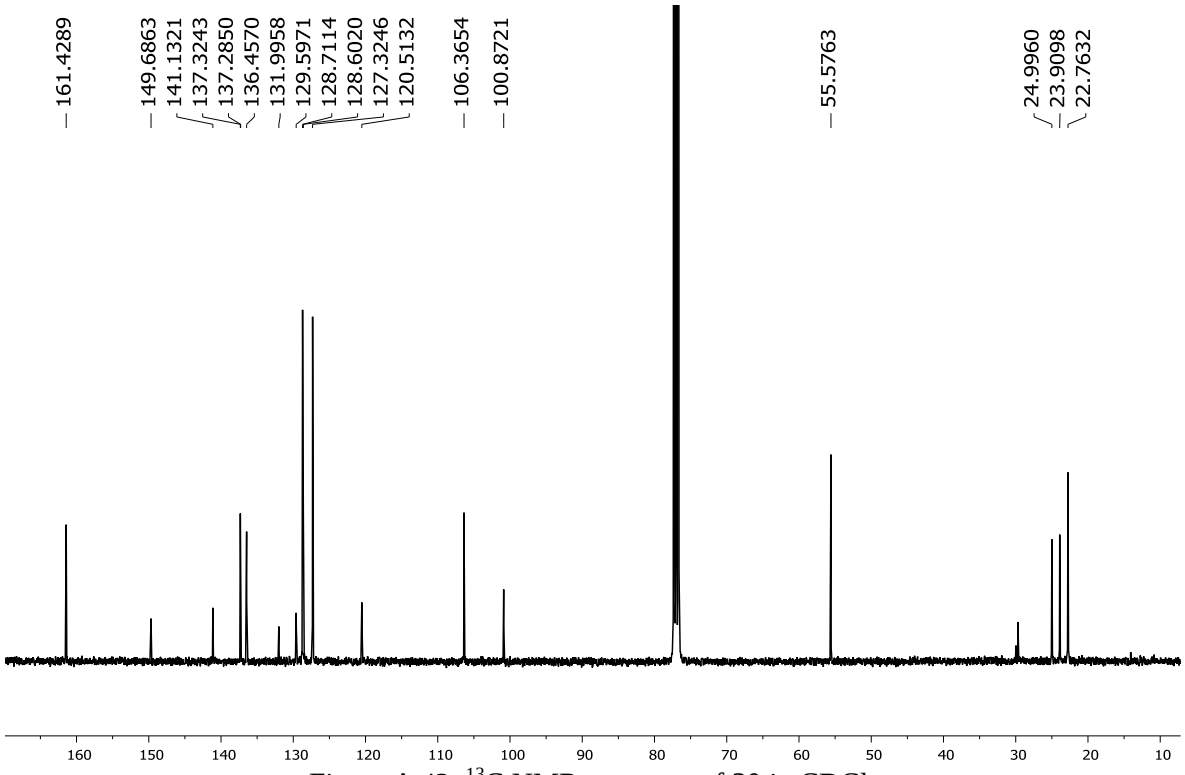

Figure A.42: ^{13}C NMR spectrum of **20** in $CDCl_3$

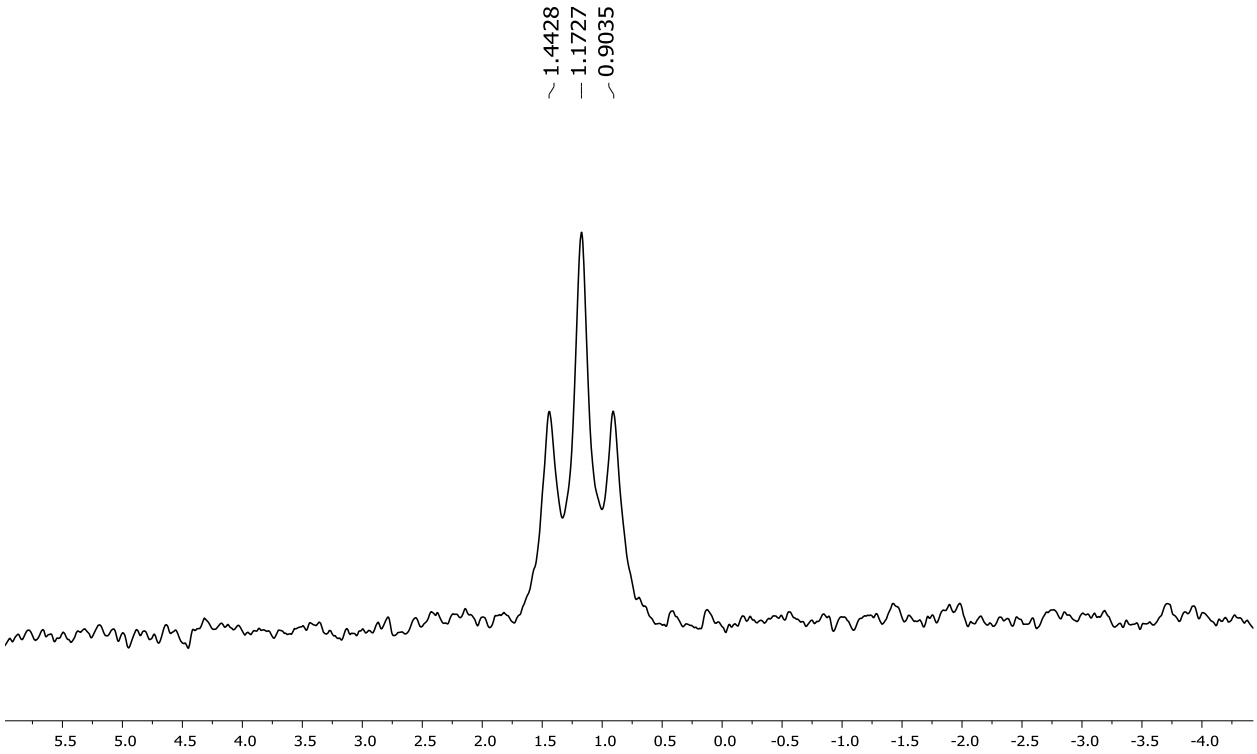

Figure A.43: ^{11}B NMR spectrum of **20** in $CDCl_3$

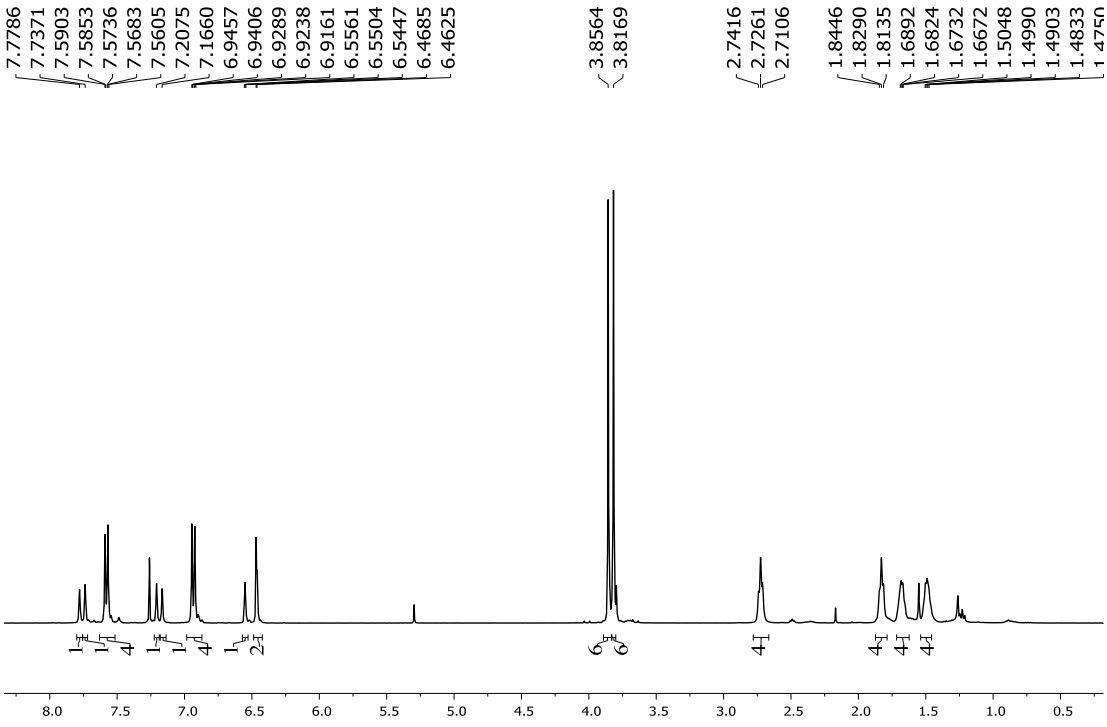

Figure A.44: ^{1}H NMR spectrum of **21** in $CDCl_3$

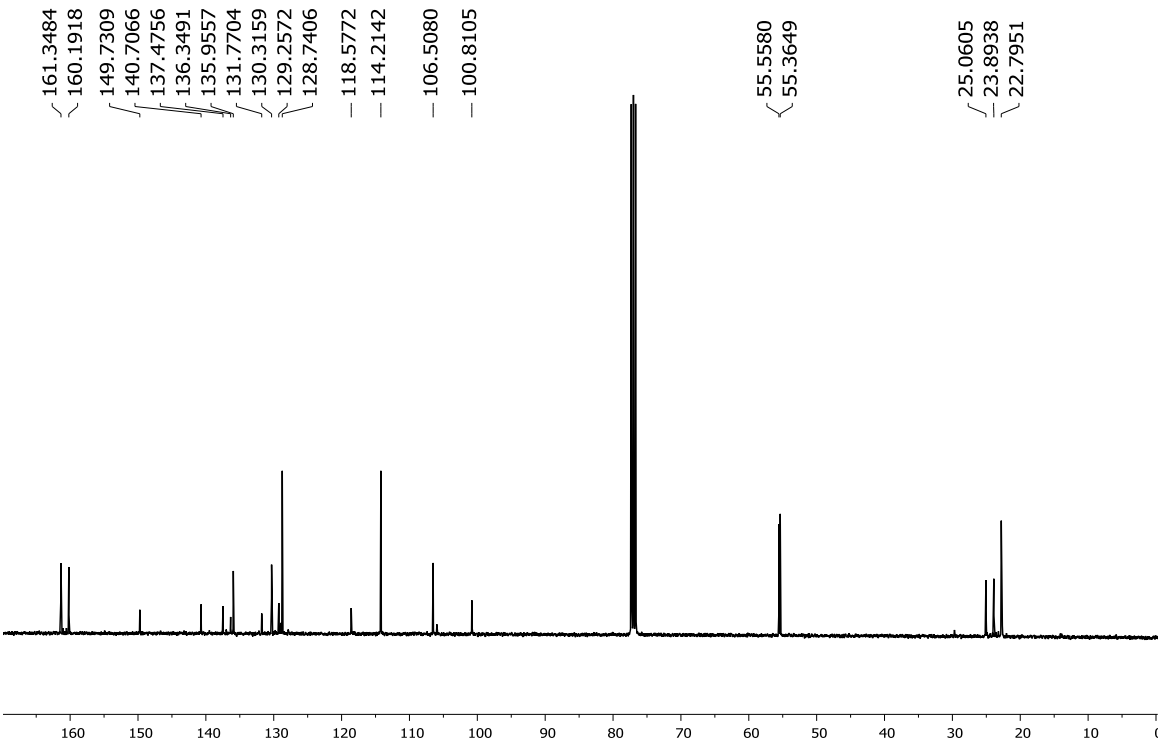

Figure A.45: ^{13}C NMR spectrum of **21** in $CDCl_3$

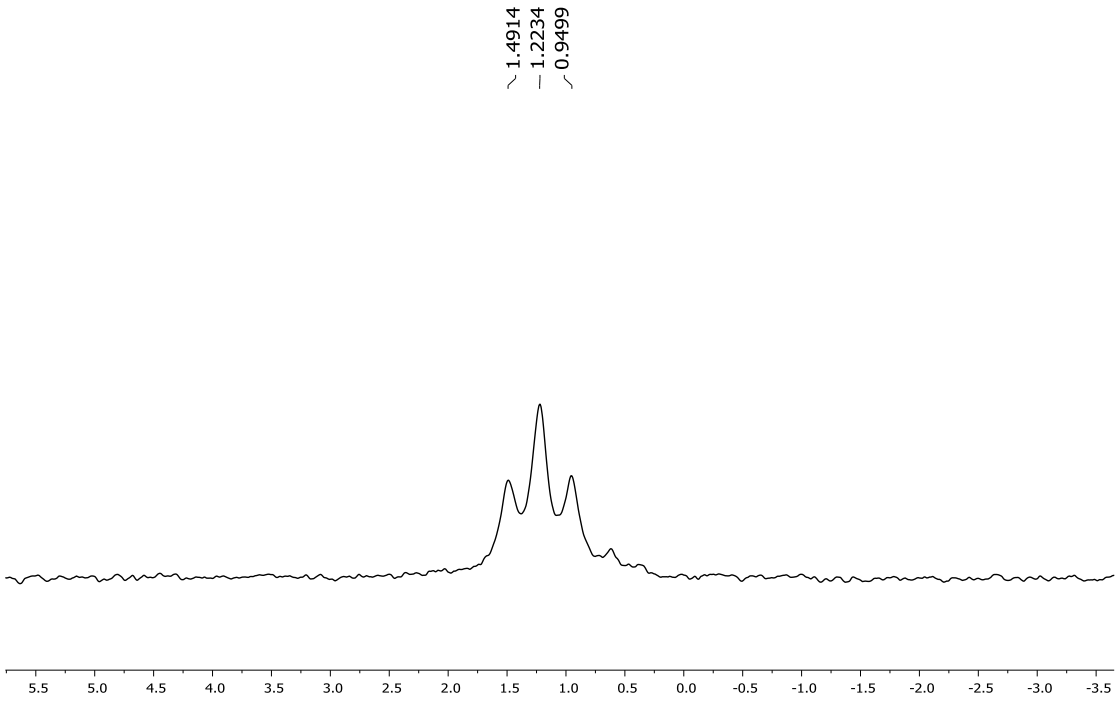

Figure A.46: ^{11}B NMR spectrum of **21** in $CDCl_3$

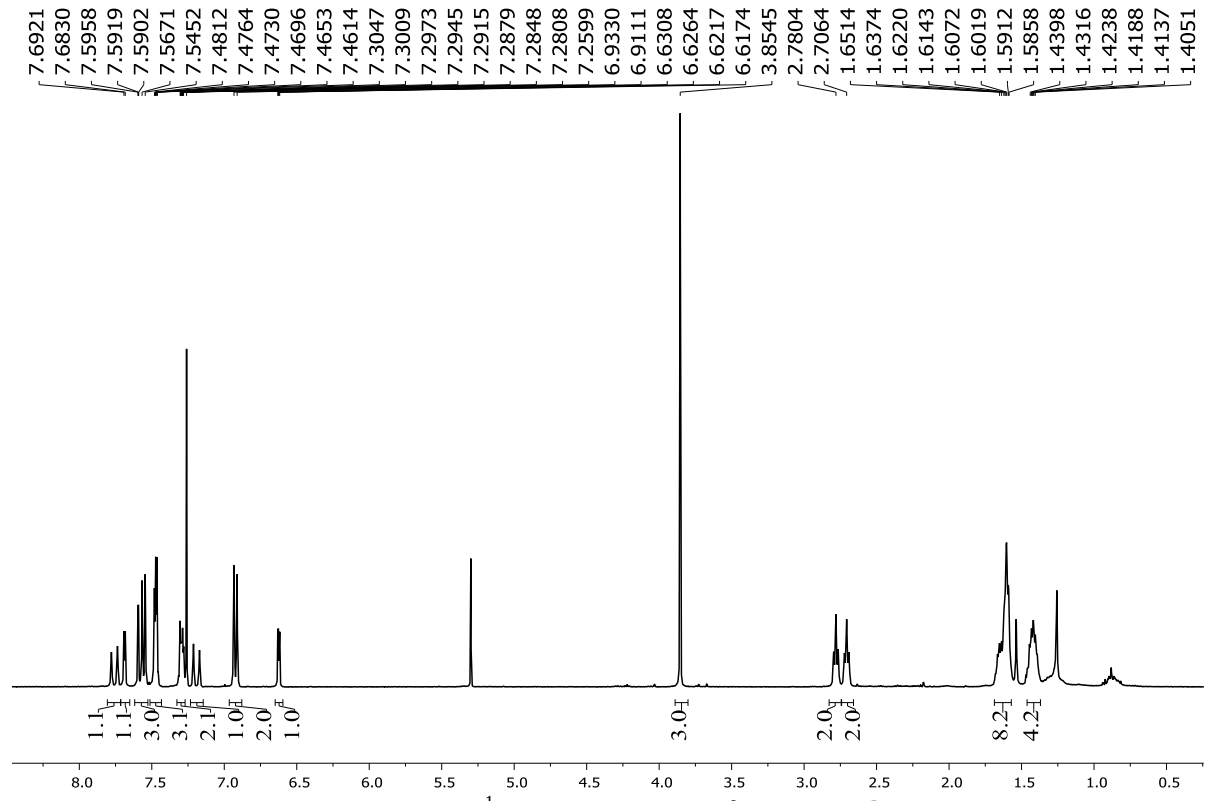

Figure A.47: ^{1}H NMR spectrum of **23** in $CDCl_3$

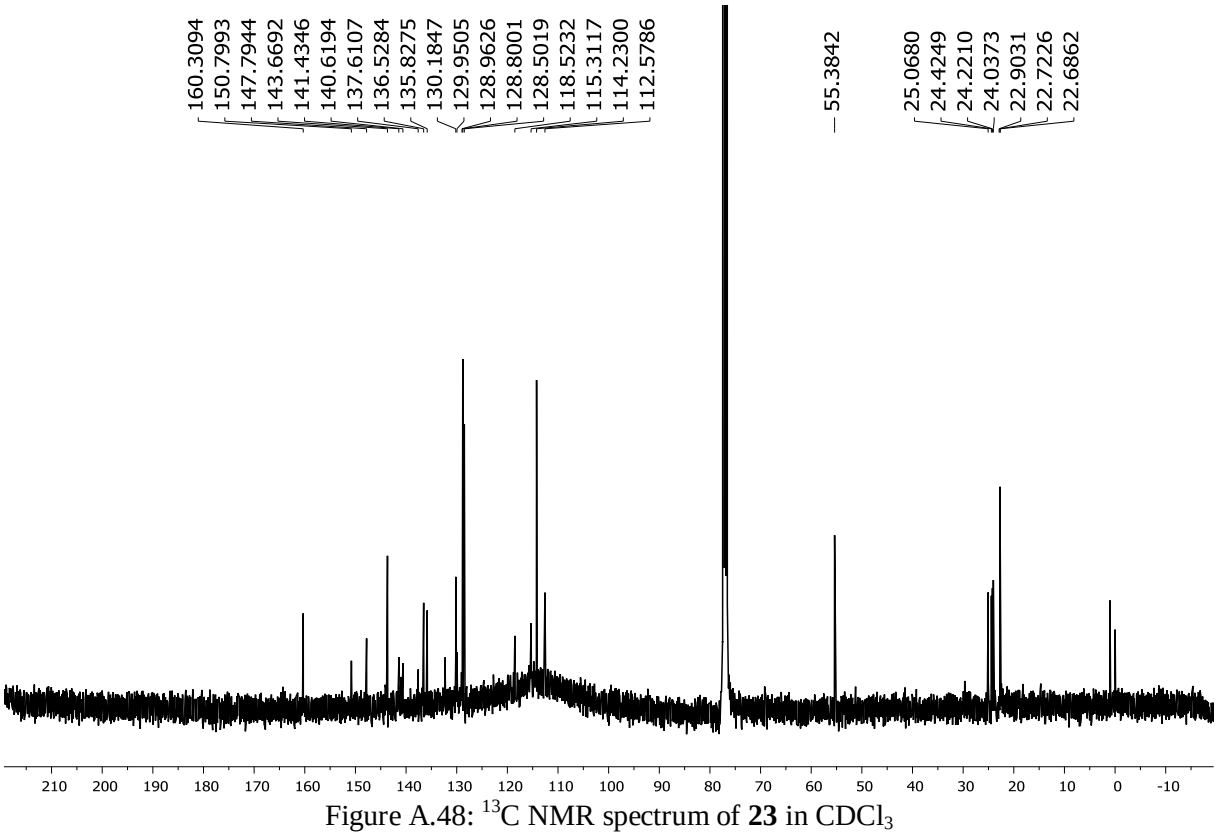

Figure A.48: ^{13}C NMR spectrum of **23** in $CDCl_3$

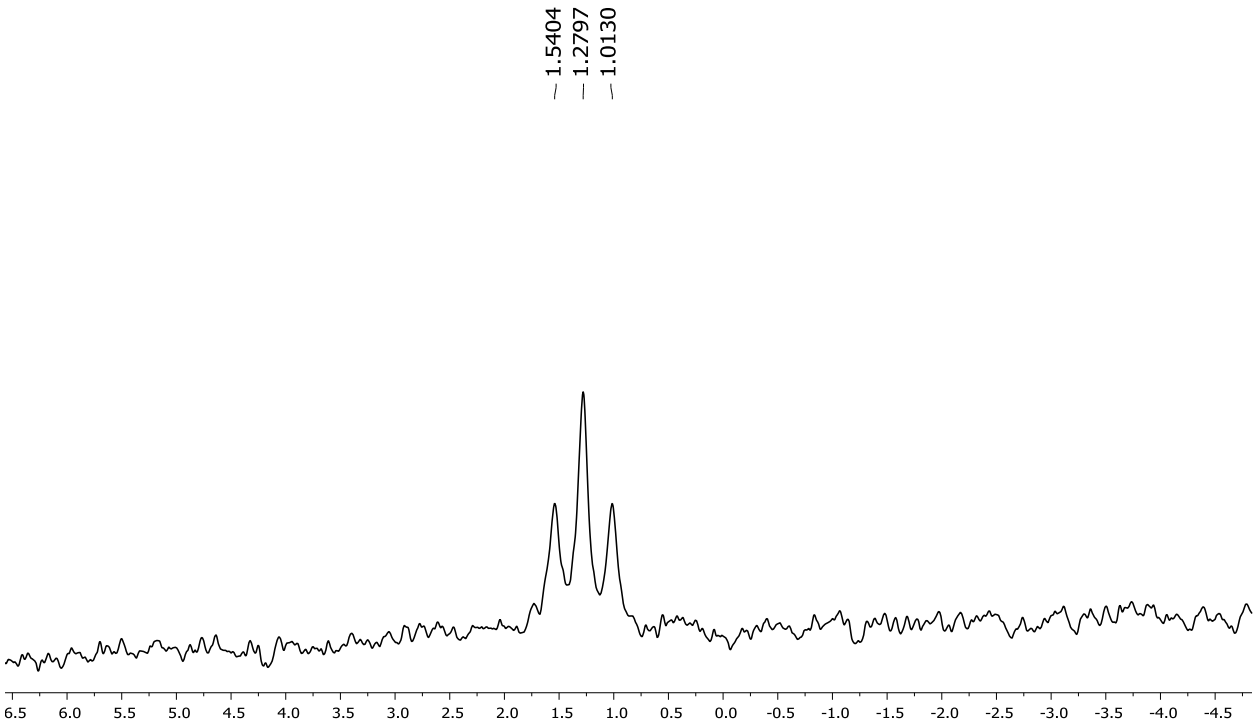

Figure A.49: ^{11}B NMR spectrum of **23** in $CDCl_3$

APPENDIX B: NMR Characterization of Compounds Found in Chapter 3

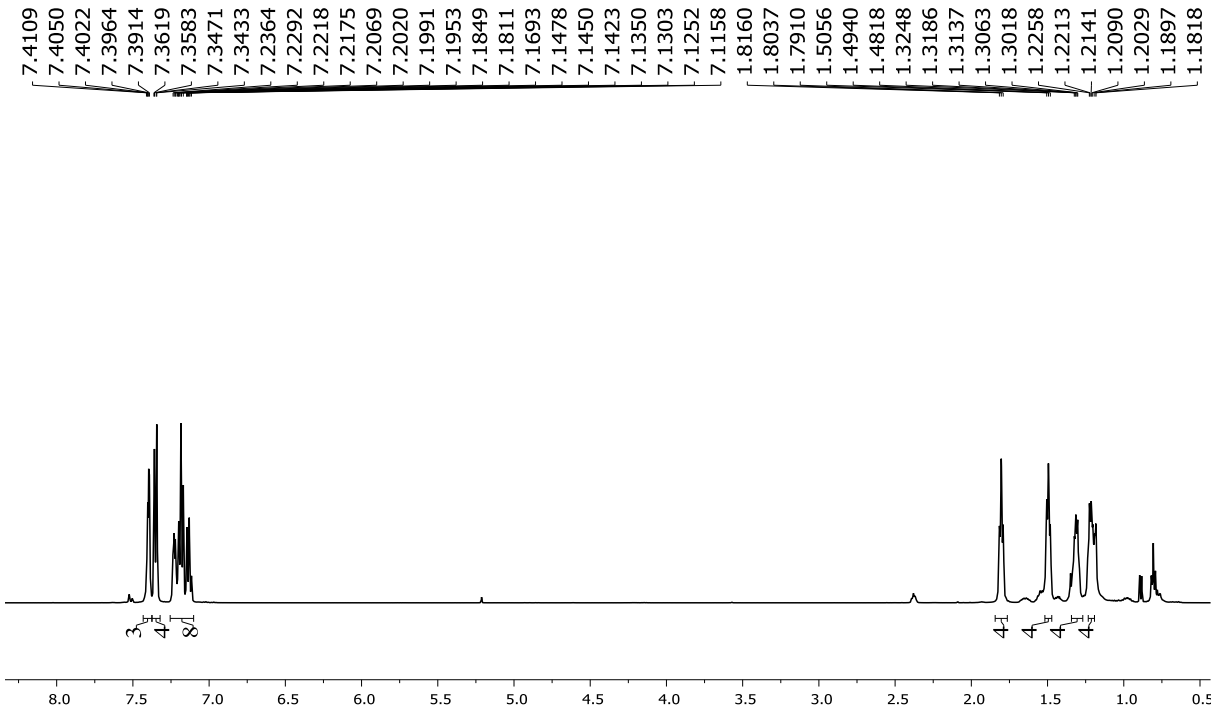

Figure B.1: ^{1}H NMR spectrum of **3a** in $CDCl_3$

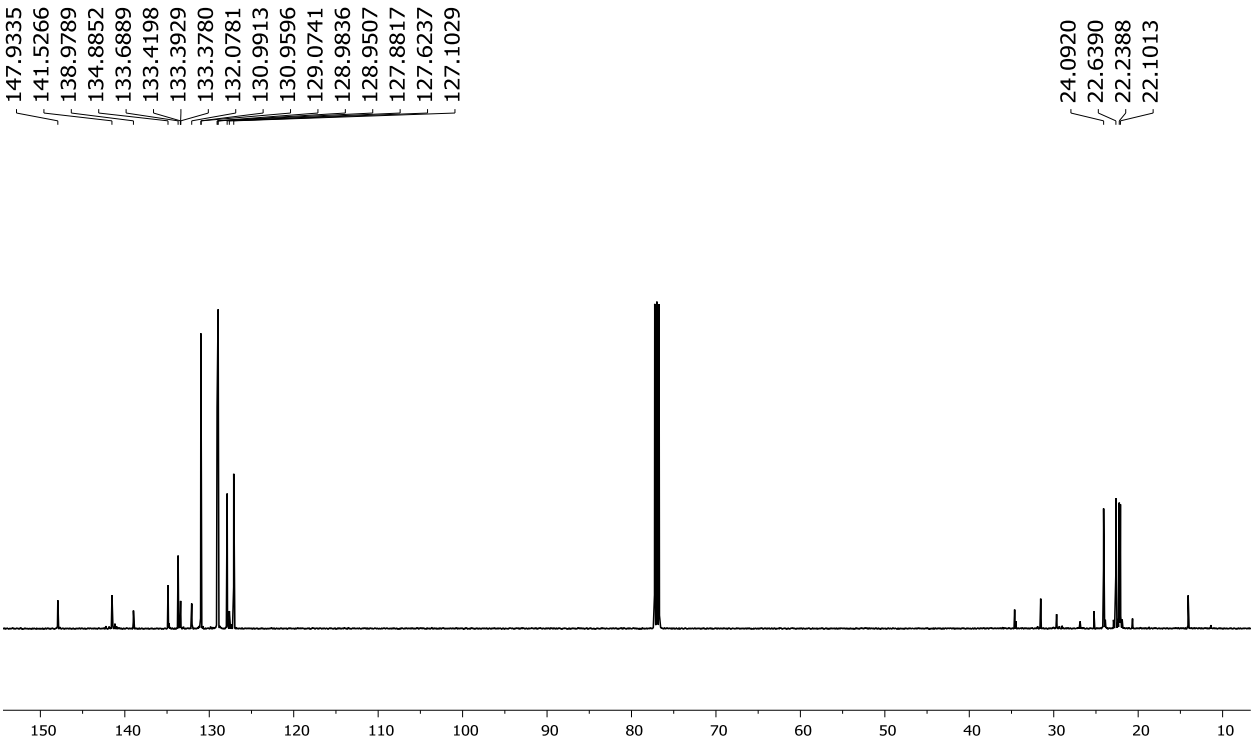

Figure B.2:^{13}C NMR spectrum of **3a** in $CDCl_3$

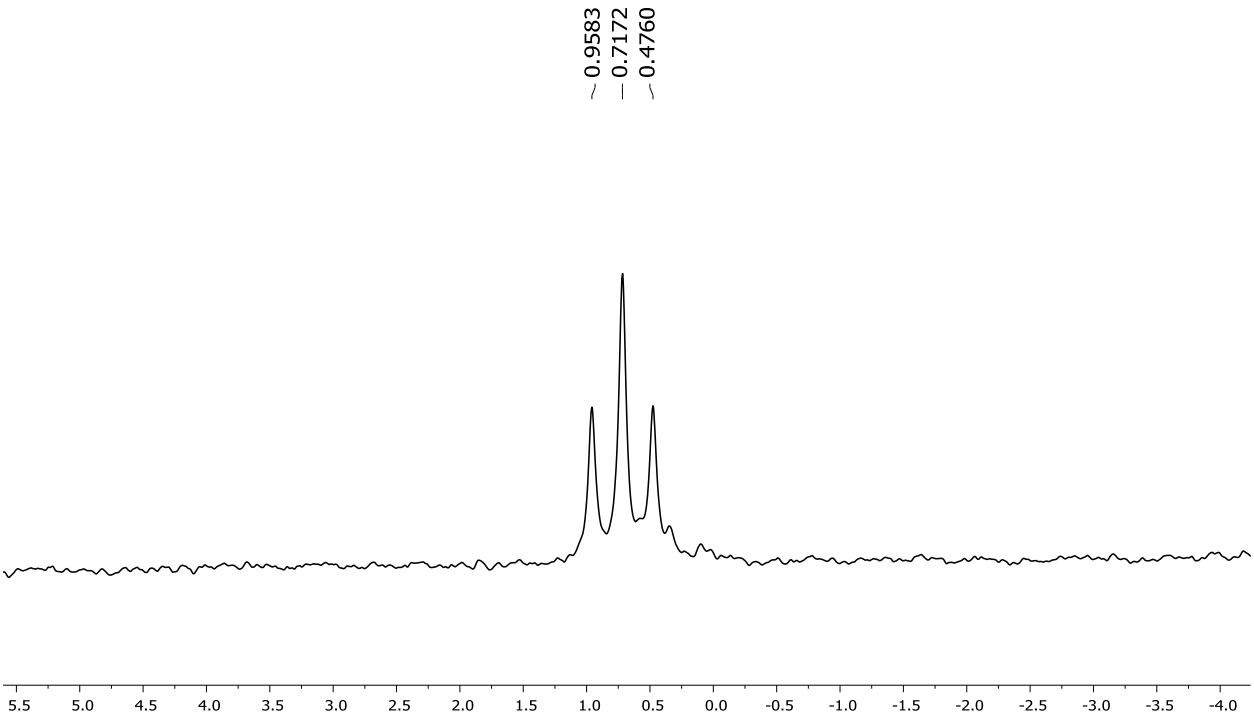

Figure B.3: ^{11}B NMR spectrum of **3a** in $CDCl_3$

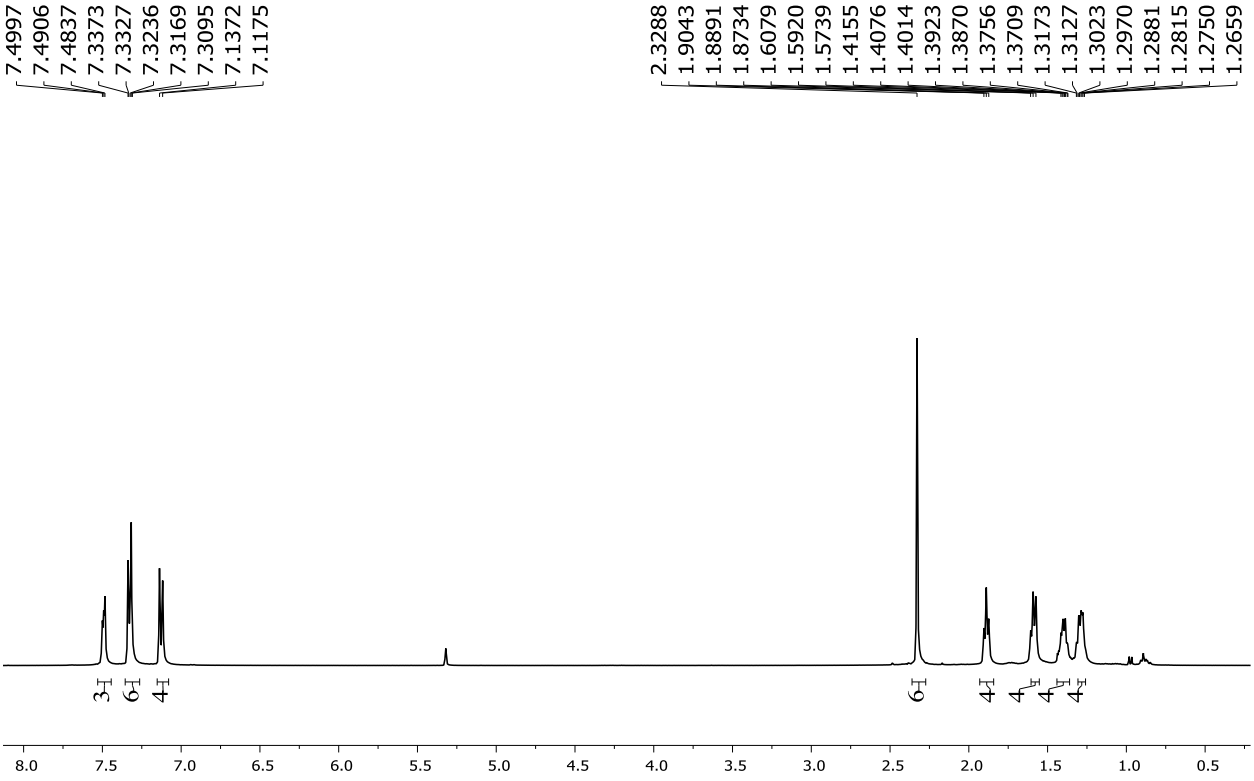

Figure B.4: ^{1}H NMR spectrum of **3b** in CD_2Cl_2

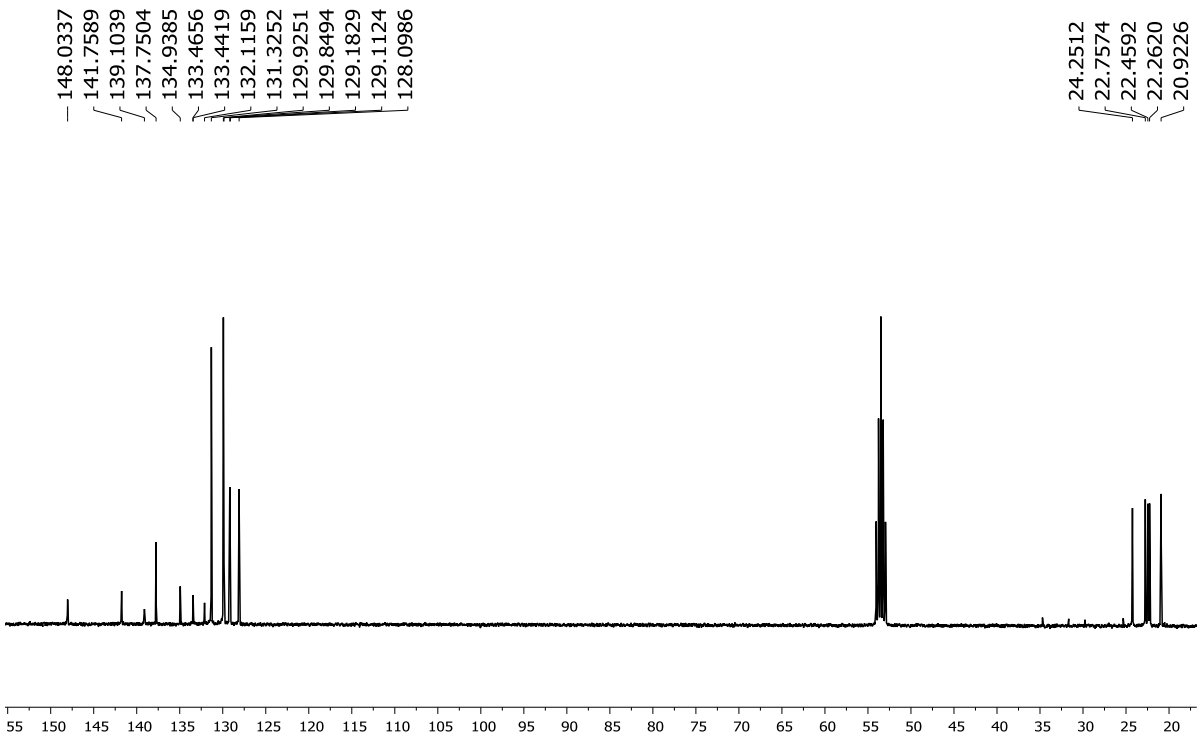

Figure B.5: ^{13}C NMR spectrum of **3b** in CD_2Cl_2

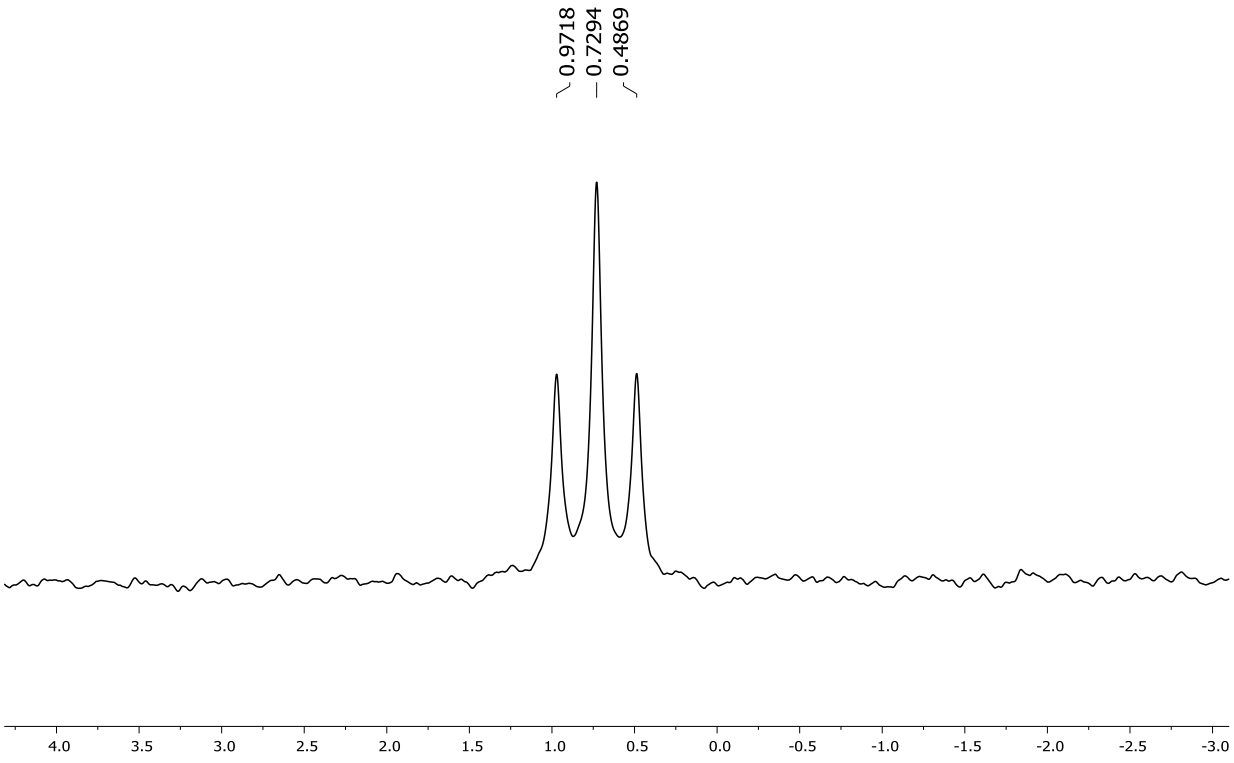

Figure B.6: ^{11}B NMR spectrum of **3b** in CD_2Cl_2

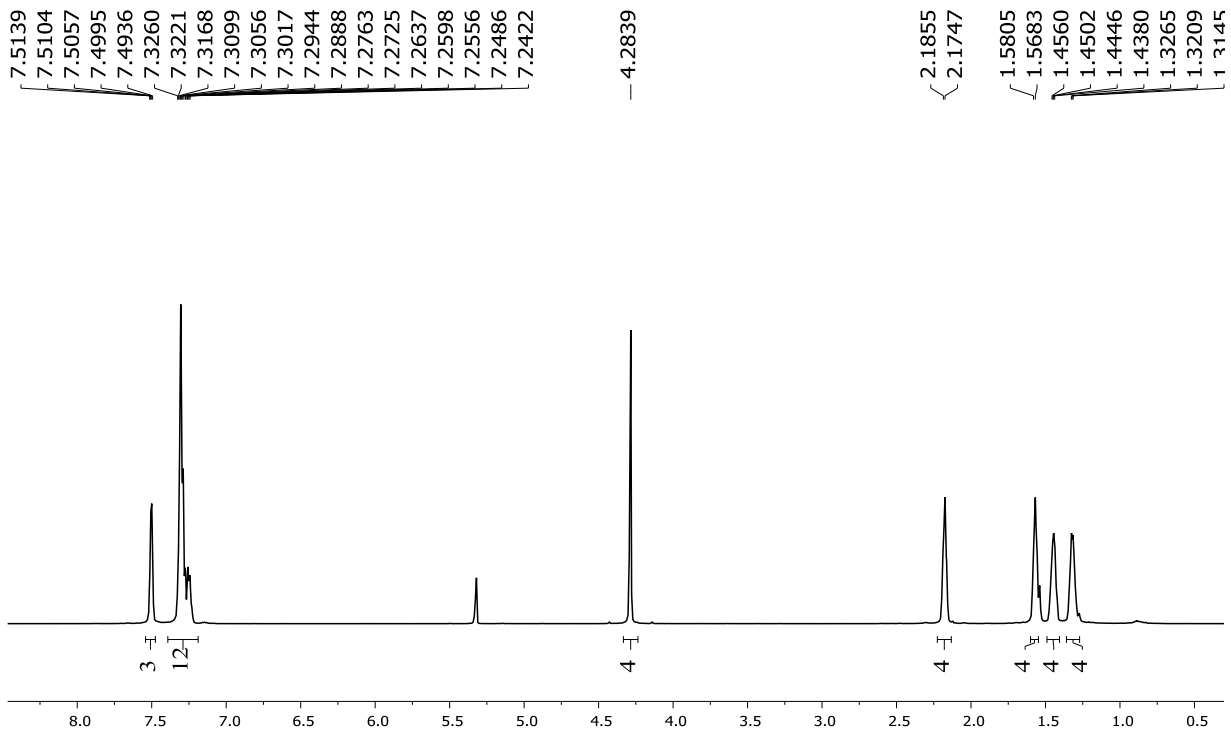

Figure B.7: ^{1}H NMR spectrum of **3c** in CD_2Cl_2

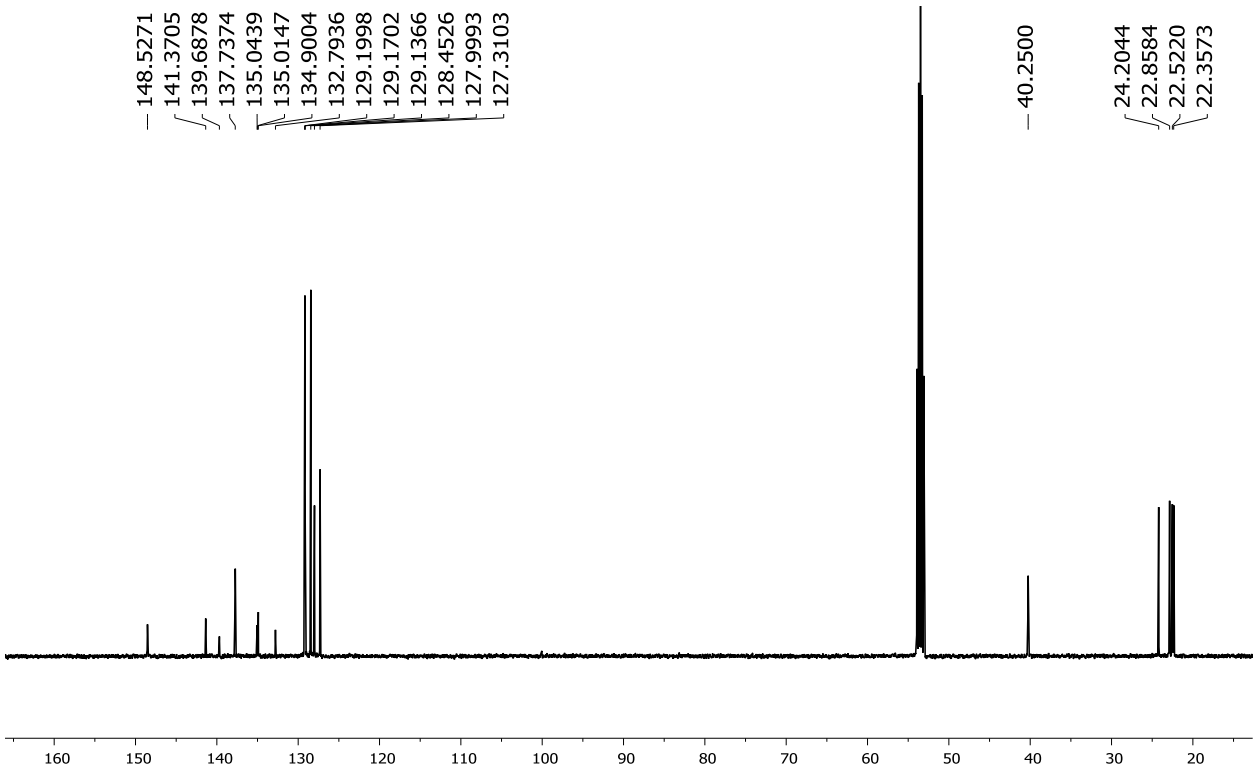

Figure B.8: ^{13}C NMR spectrum of **3c** in CD_2Cl_2

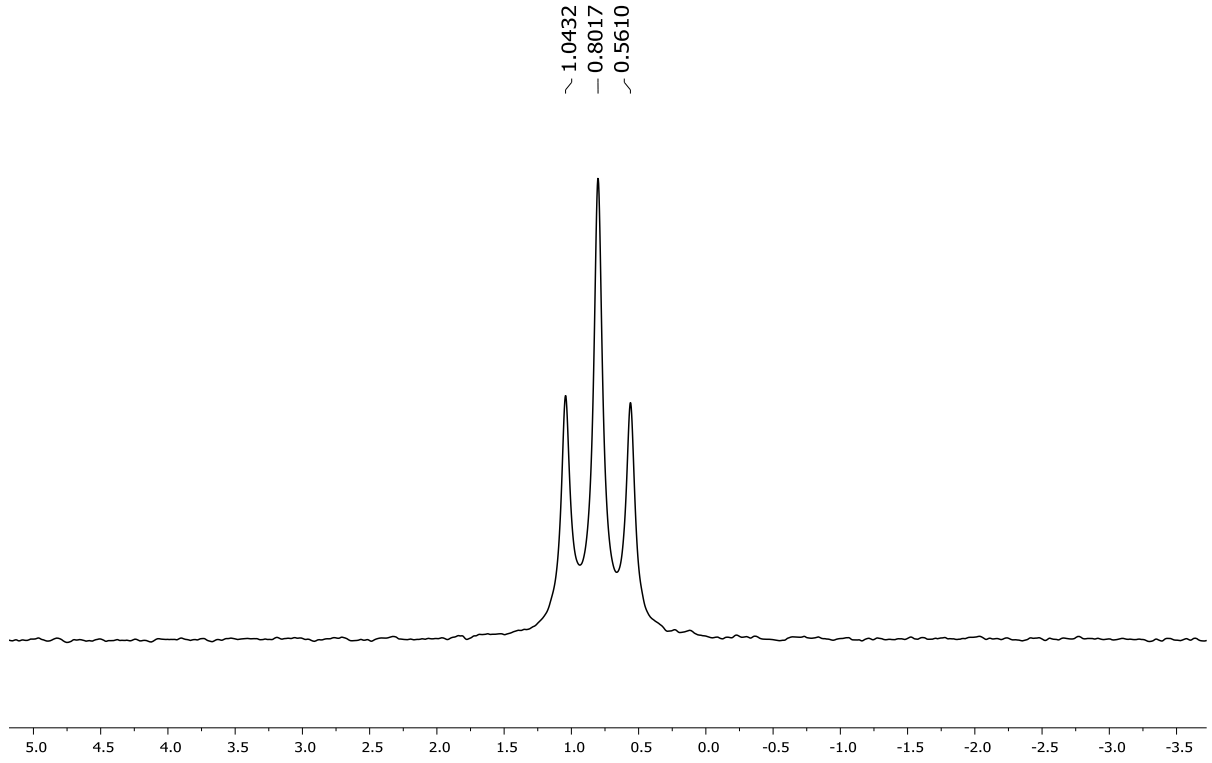

Figure B.9: ^{11}B NMR spectrum of **3c** in CD_2Cl_2

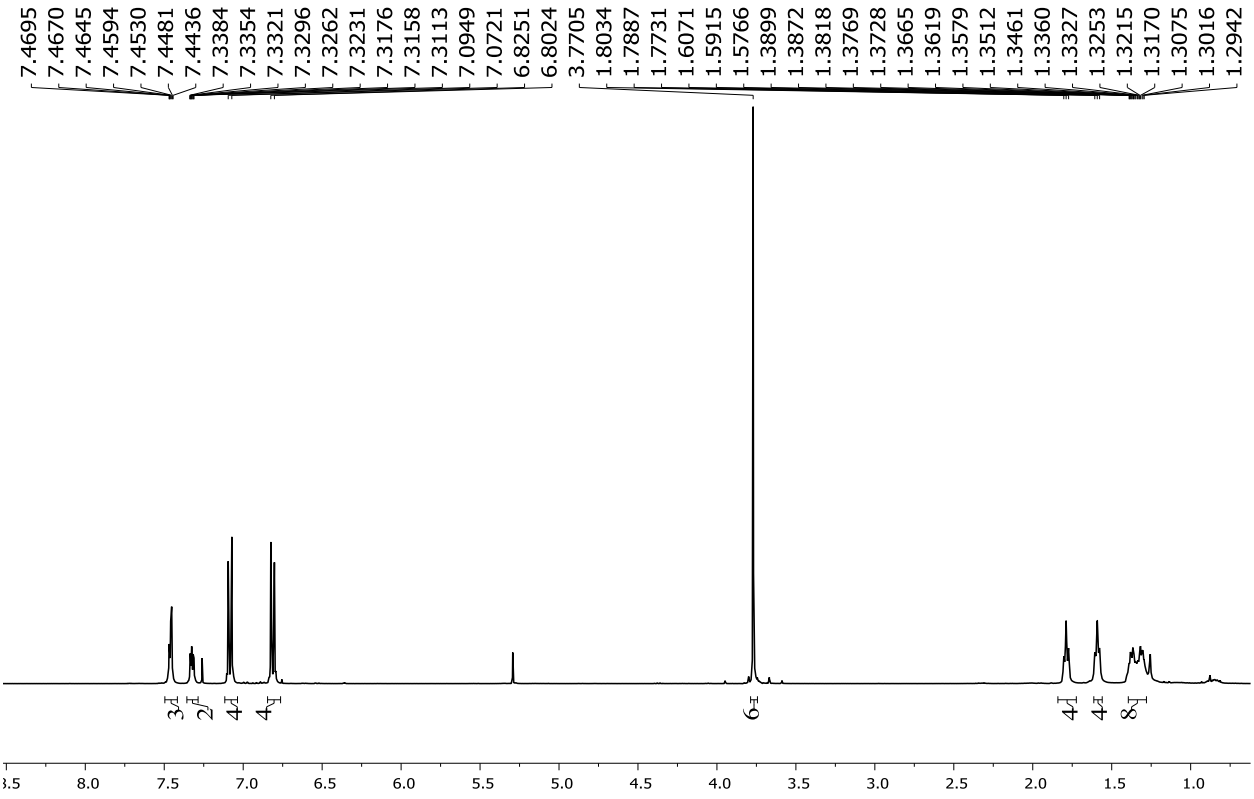

Figure B.10: ^{1}H NMR spectrum of **4** in $CDCl_3$

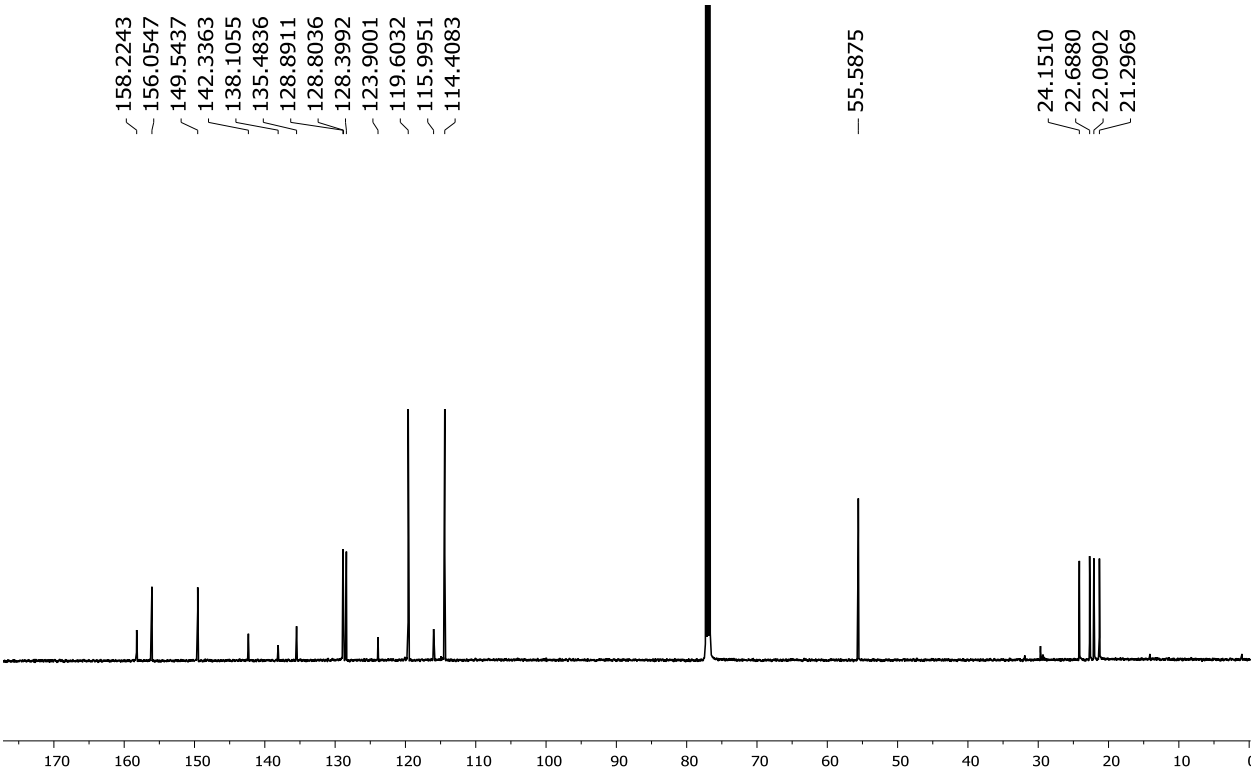

Figure B.11: ^{13}C NMR spectrum of **4** in $CDCl_3$

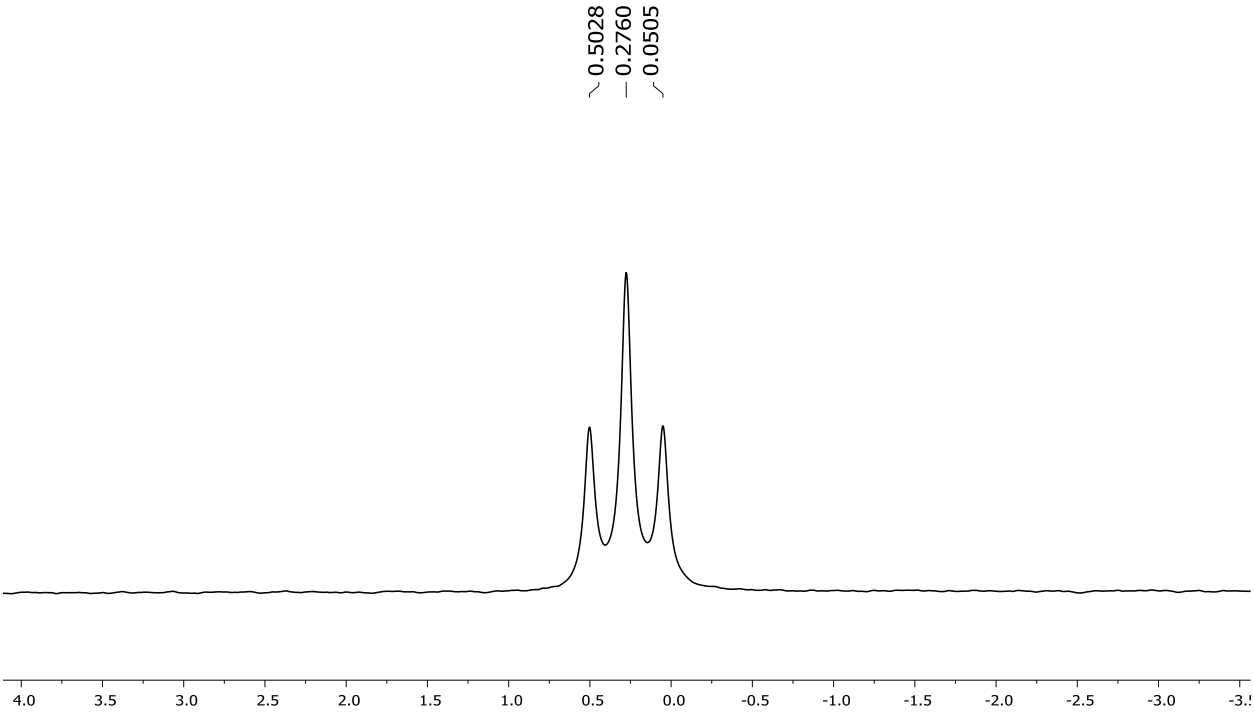

Figure B.12: ^{11}B NMR spectrum of **4** in $CDCl_3$

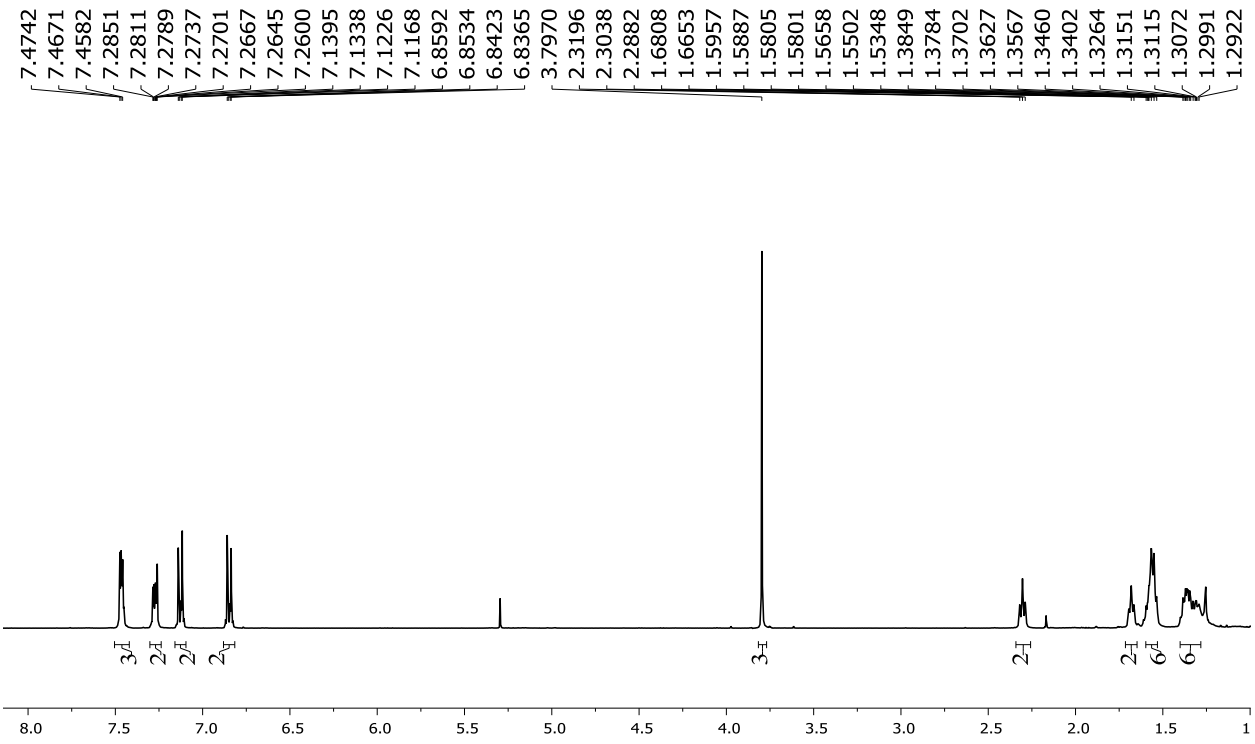

Figure B.13: ^{1}H NMR spectrum of **6** in $CDCl_3$

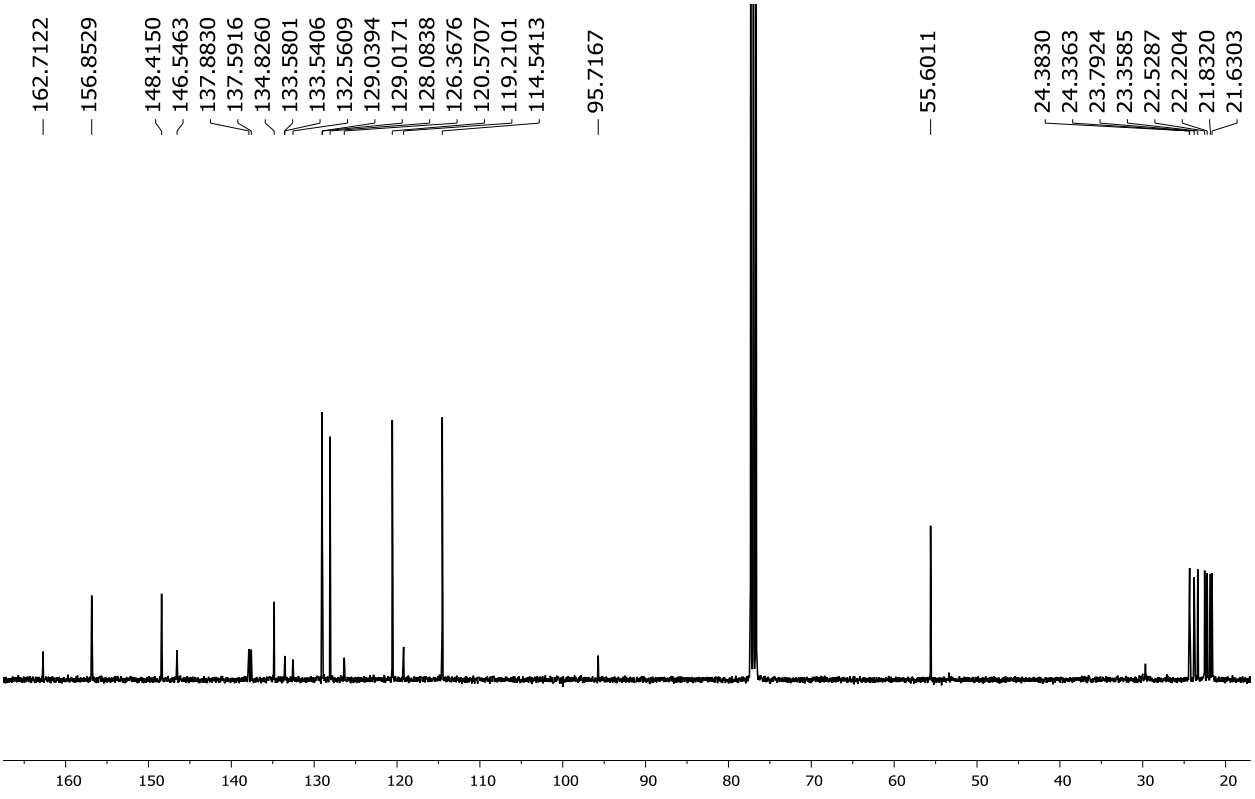

Figure B.14: ^{13}C NMR spectrum of **6** in $CDCl_3$

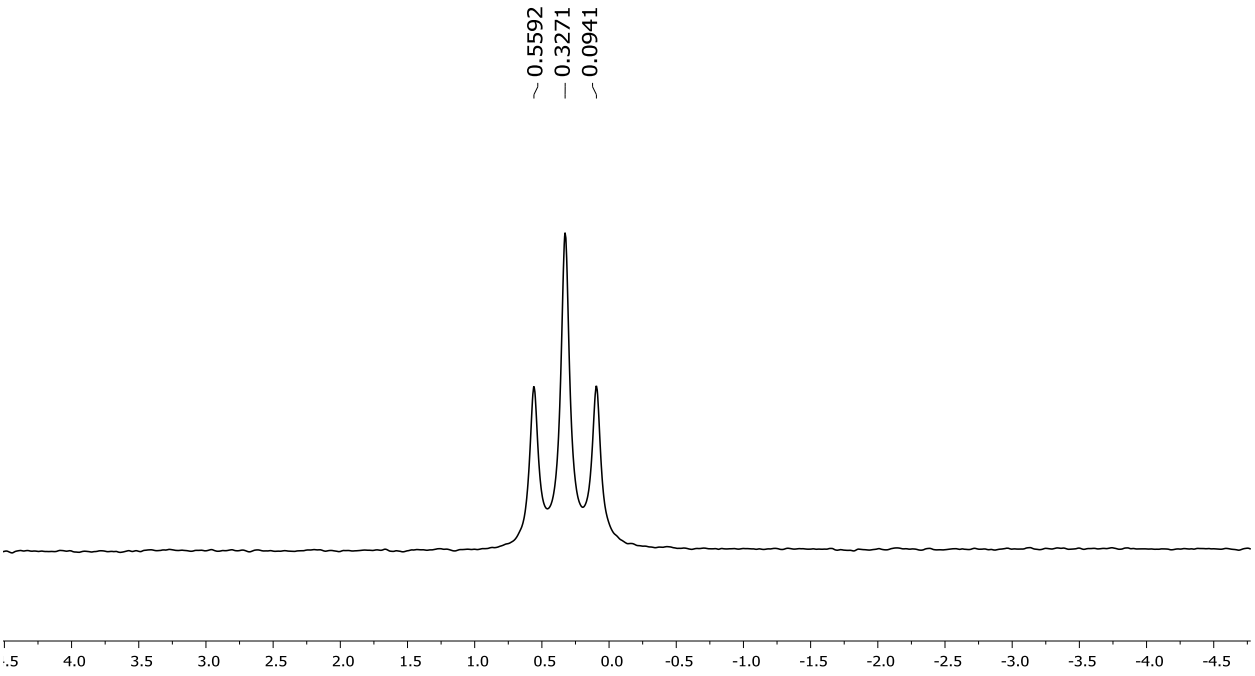

Figure B.15: ^{11}B NMR spectrum of **6** in $CDCl_3$

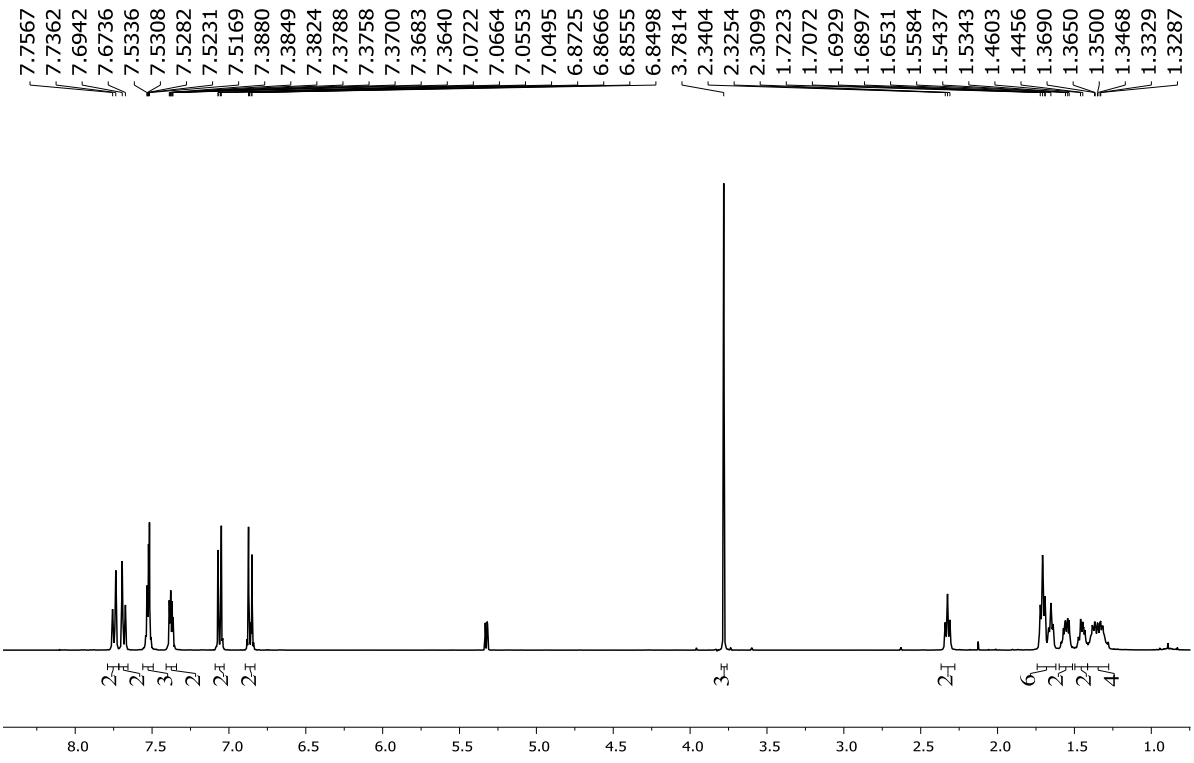

Figure B.16: ^{1}H NMR spectrum of **7** in CD_2Cl_2

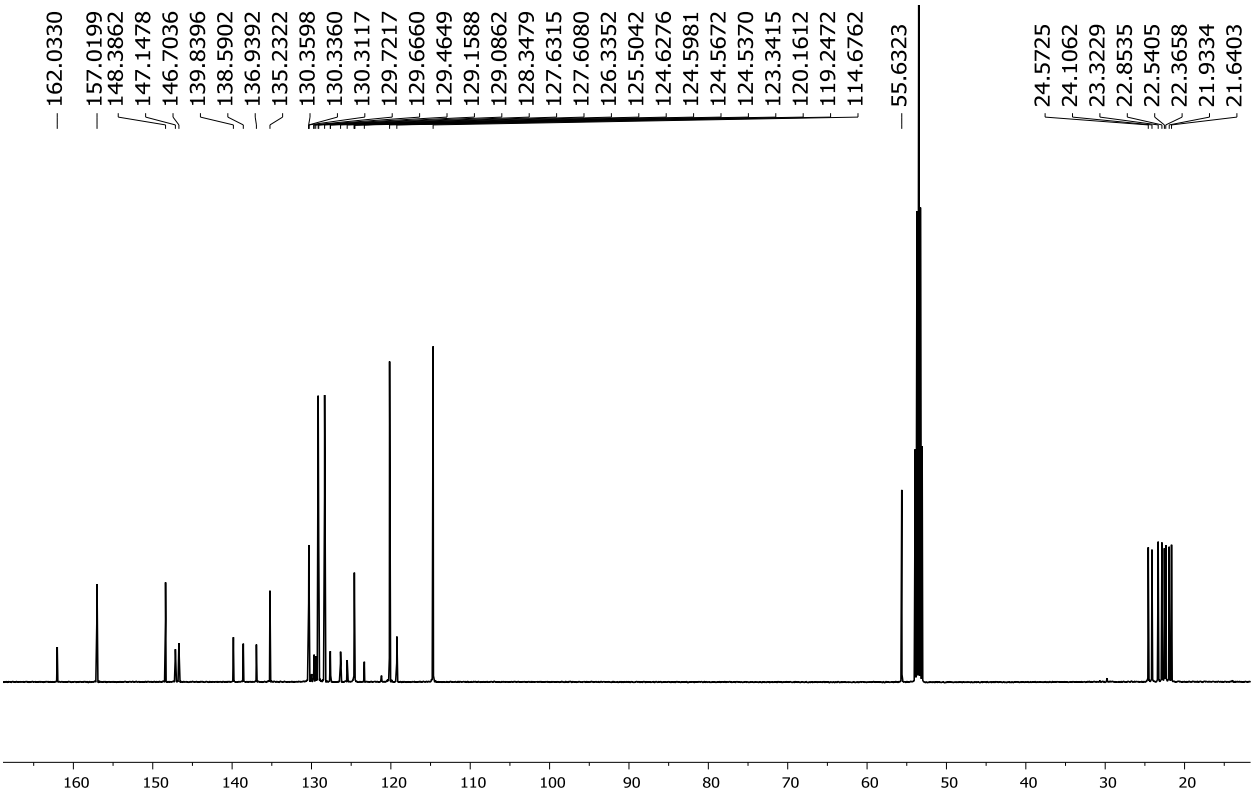

Figure B.17: ^{13}C NMR spectrum of **7** in CD_2Cl_2

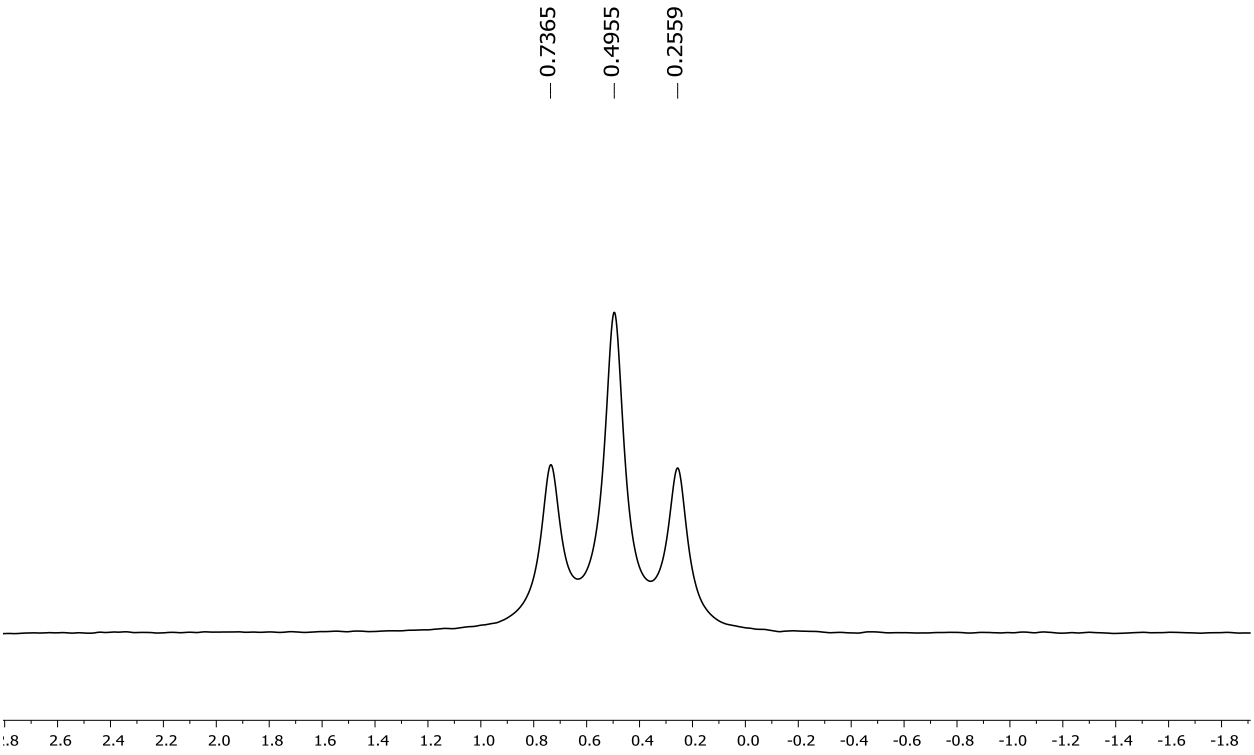

Figure B.18: ^{11}B NMR spectrum of **7** in CD_2Cl_2

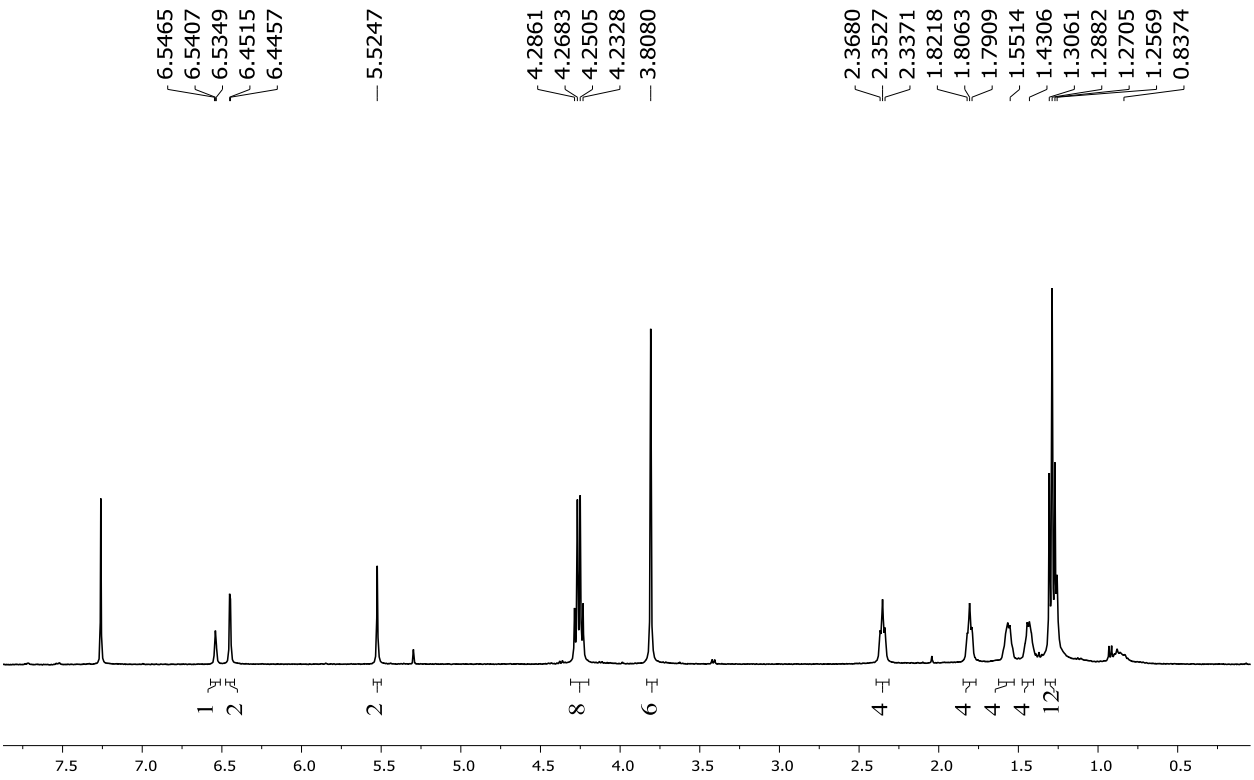

Figure B.19: ^{1}H NMR spectrum of **8a** in $CDCl_3$

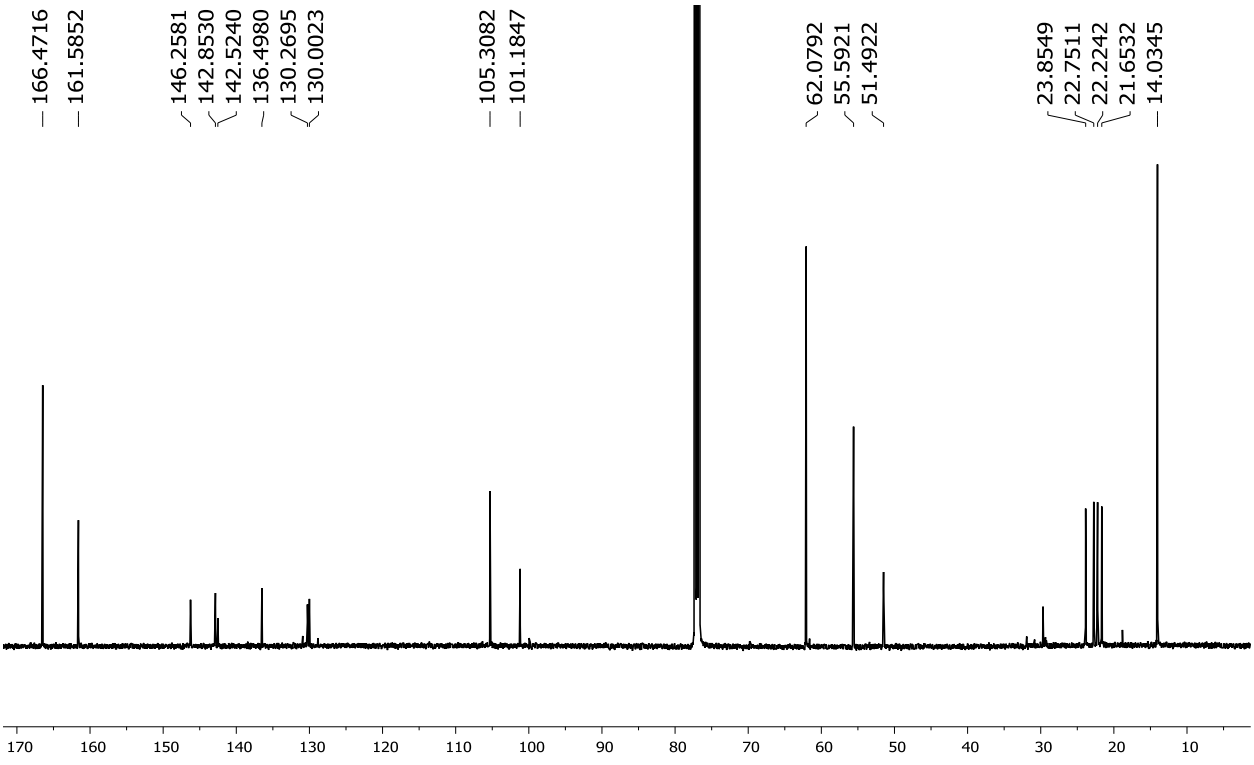

Figure B.20: ^{13}C NMR spectrum of **8a** in $CDCl_3$

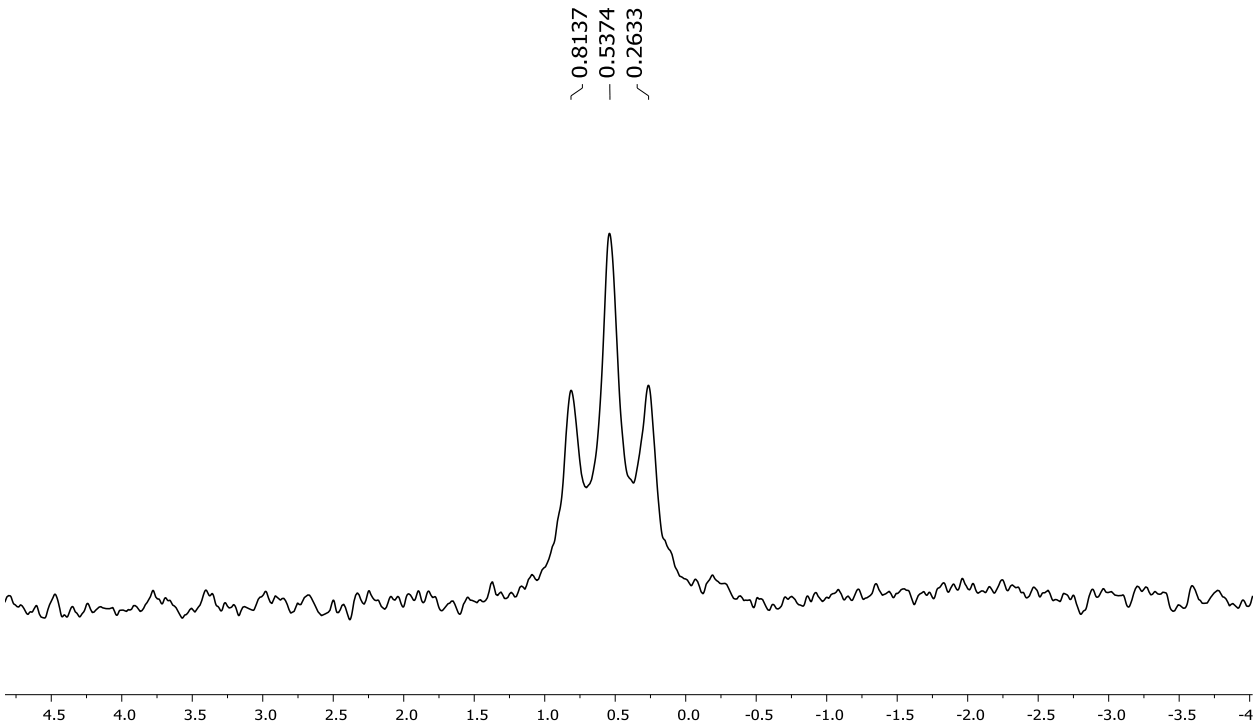

Figure B.21: ^{11}B NMR spectrum of **8a** in $CDCl_3$

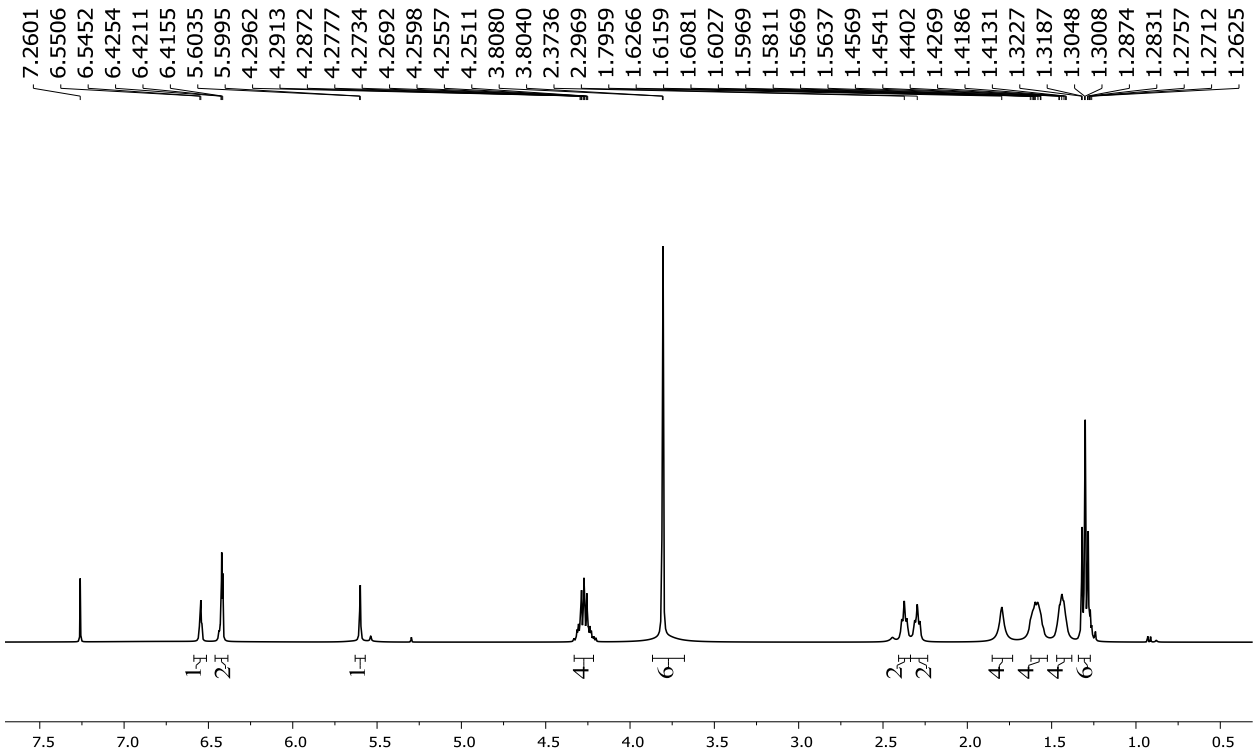

Figure B.22: ^{1}H NMR spectrum of **8b** in $CDCl_3$

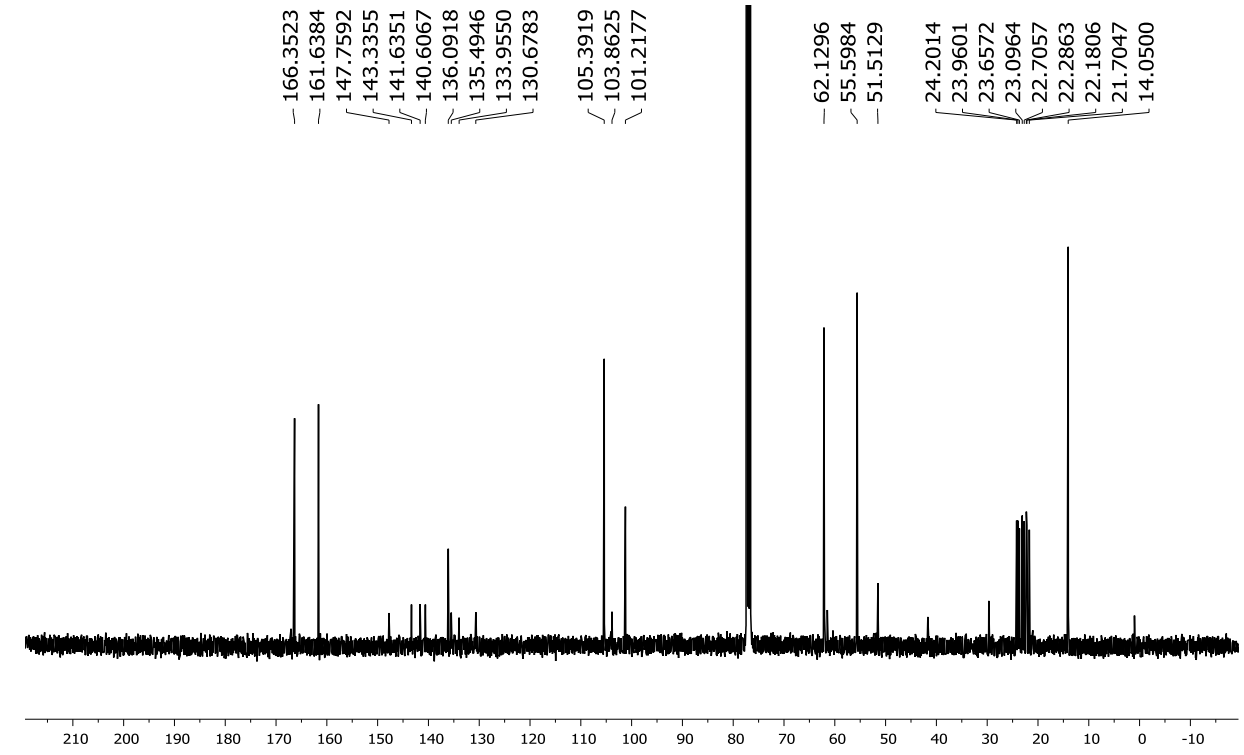

Figure B.23: ^{13}C NMR spectrum of **8b** in $CDCl_3$

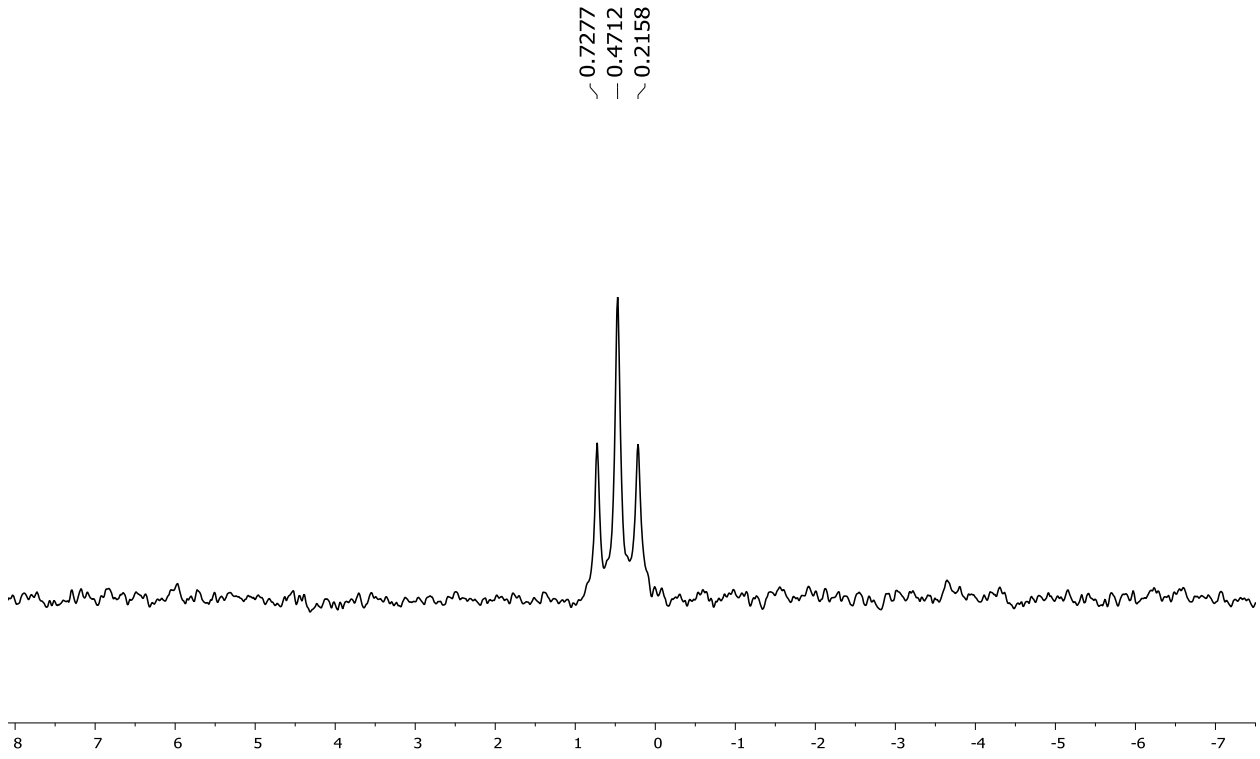

Figure B.24: ^{11}B NMR spectrum of **8b** in $CDCl_3$

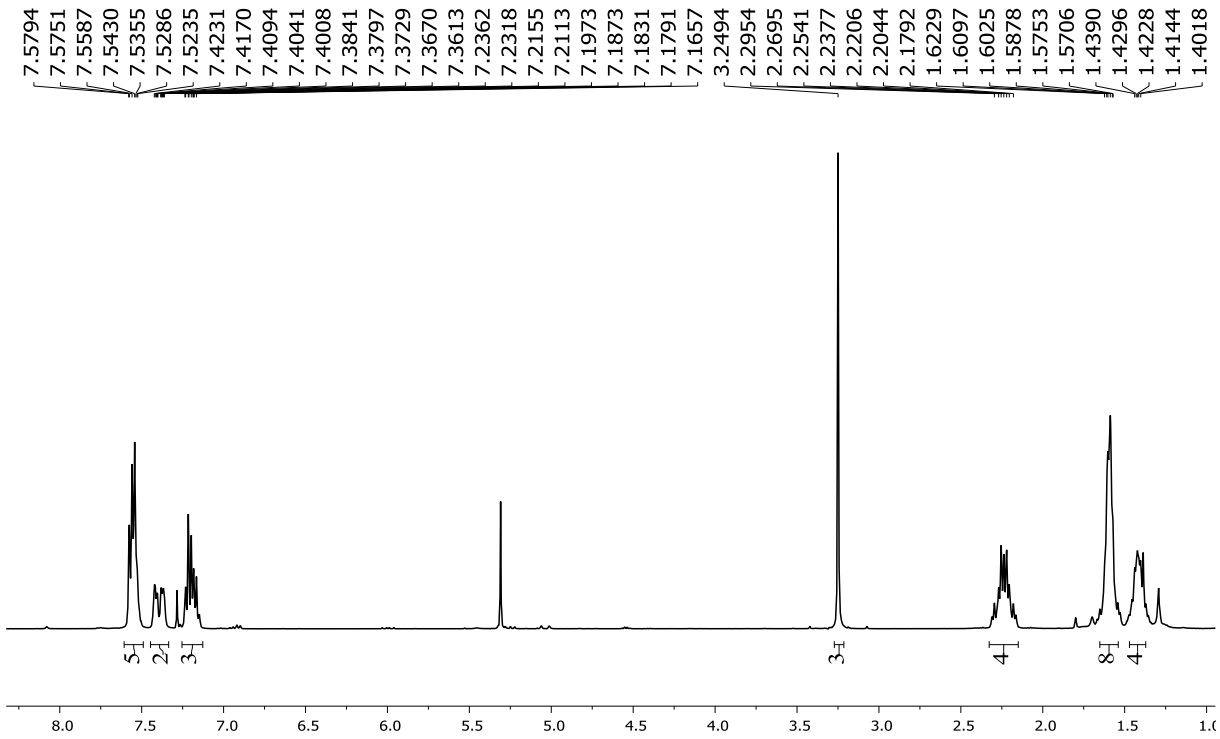

Figure B.25: ^{1}H NMR spectrum of **10** in $CDCl_3$

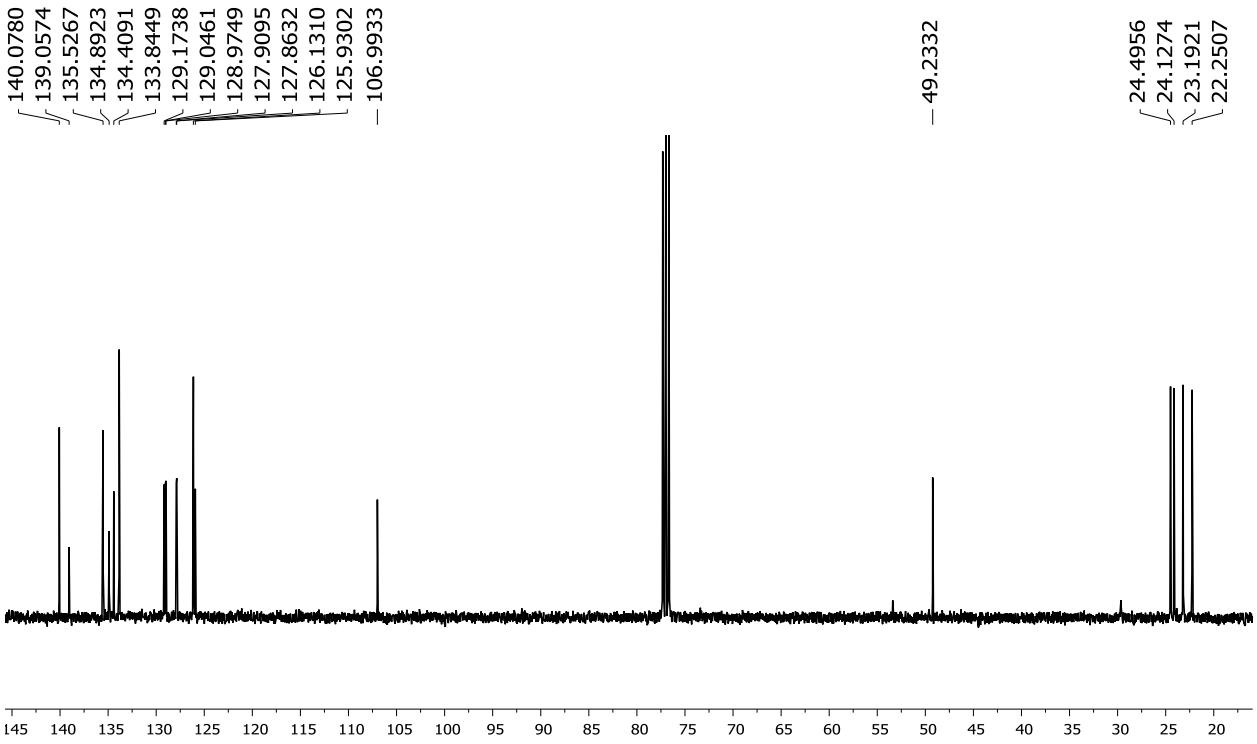

Figure B.26: ^{13}C NMR spectrum of **10** in $CDCl_3$

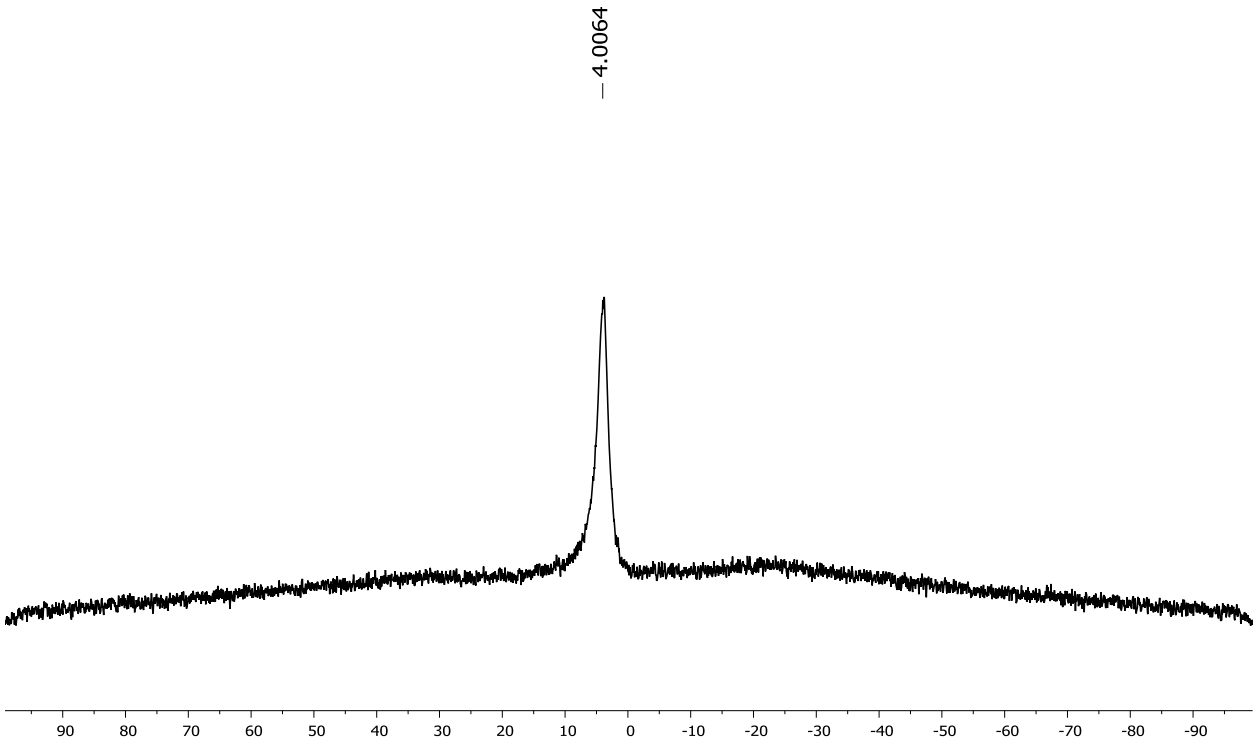

Figure B.27: ^{11}B NMR spectrum of **10** in $CDCl_3$

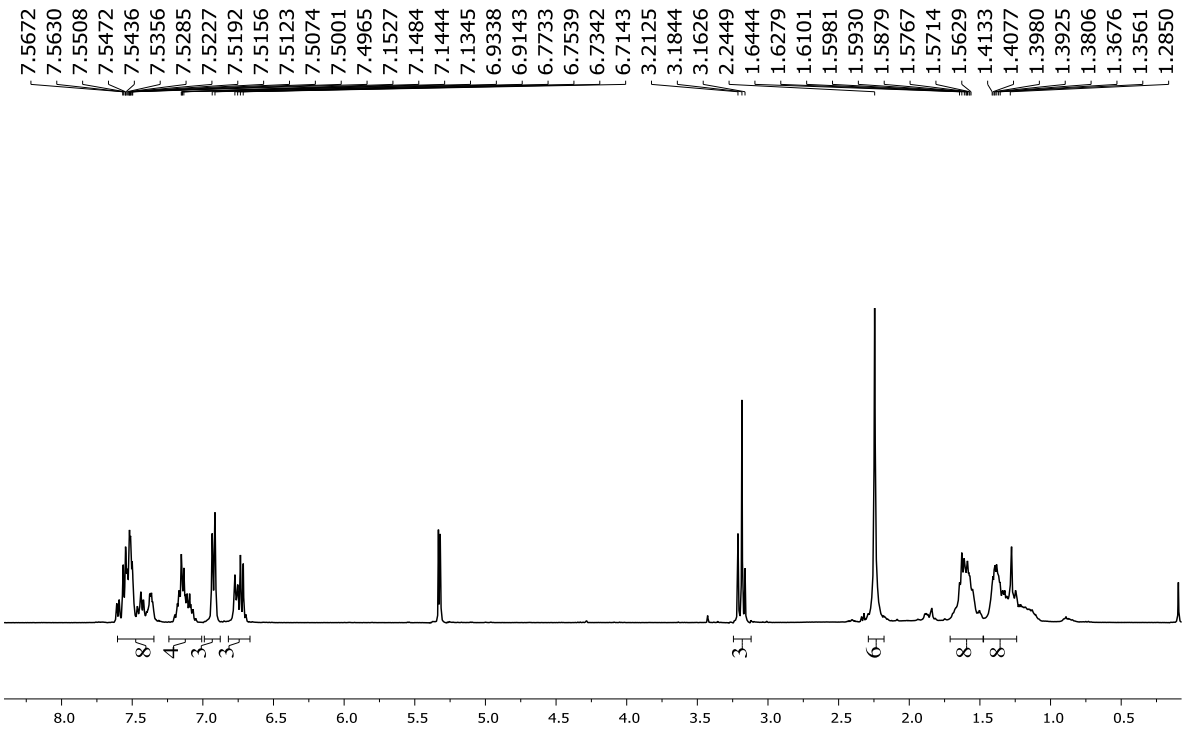

Figure B.28: ^{1}H NMR spectrum of **11** in CD_2Cl_2

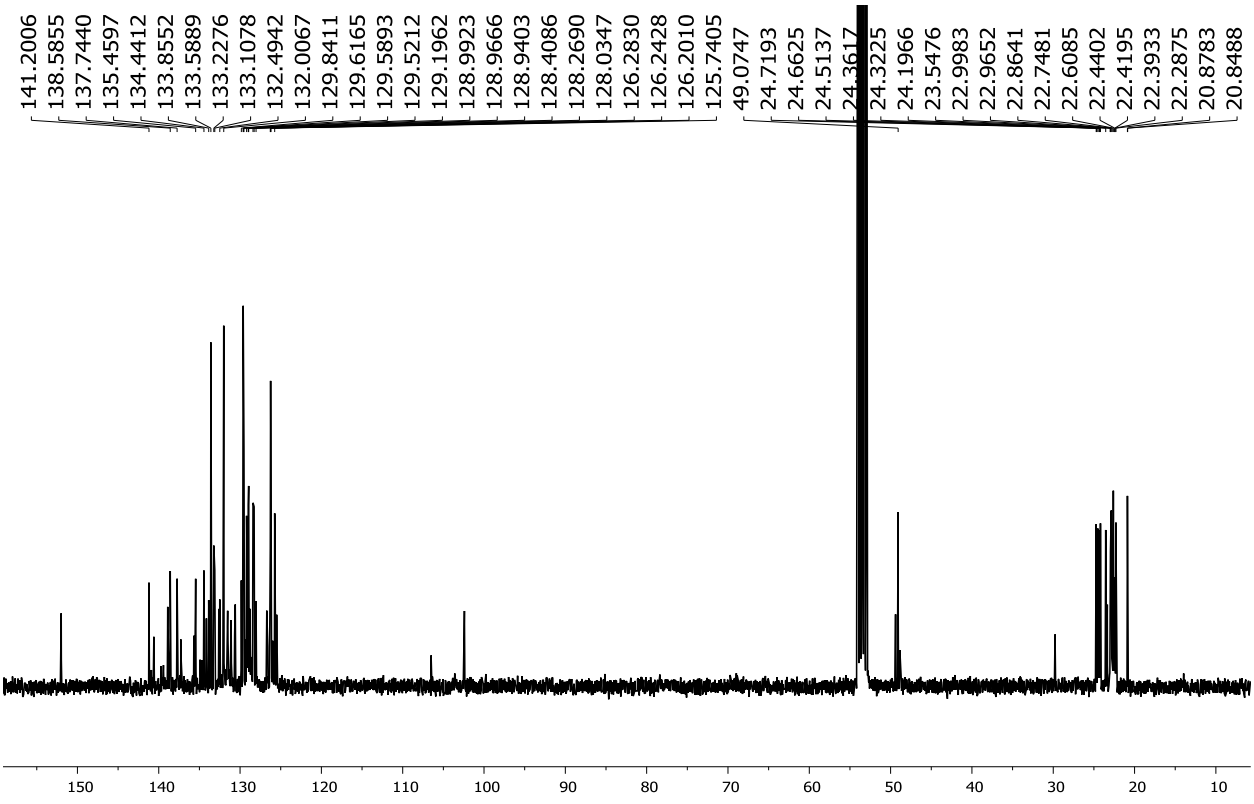

Figure B.29: ^{13}C NMR spectrum of **11** in CD_2Cl_2

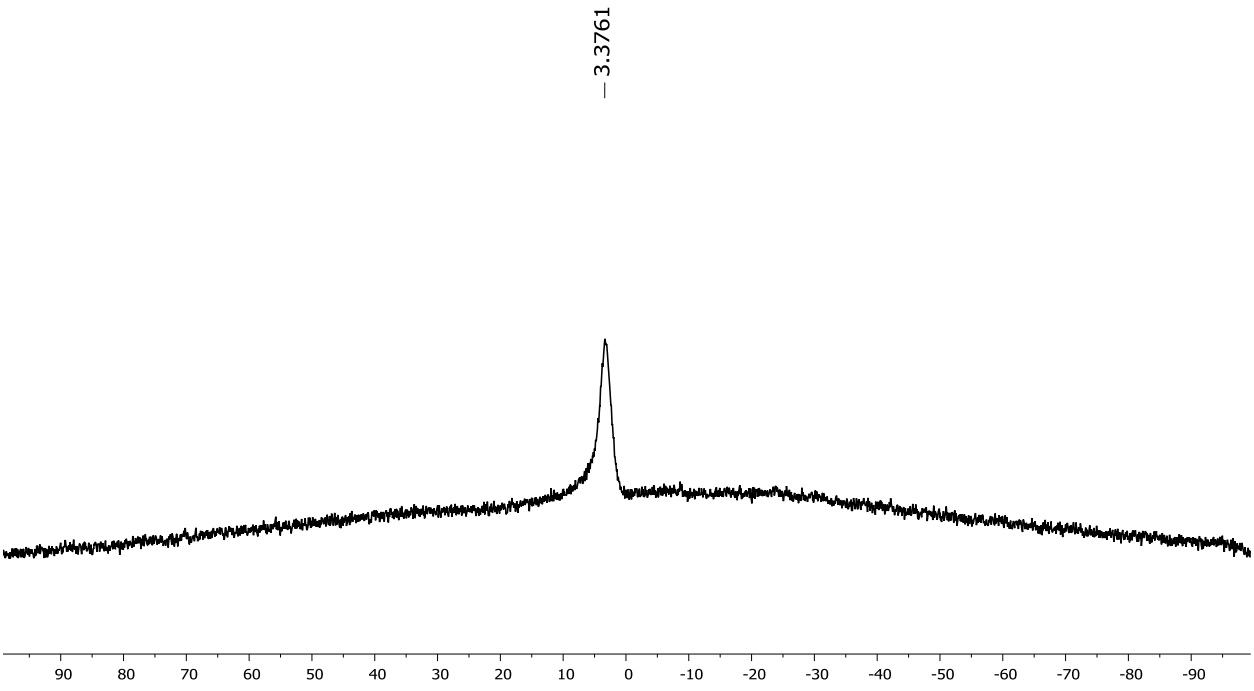

Figure B.30: ^{11}B NMR spectrum of **11** in CD_2Cl_2

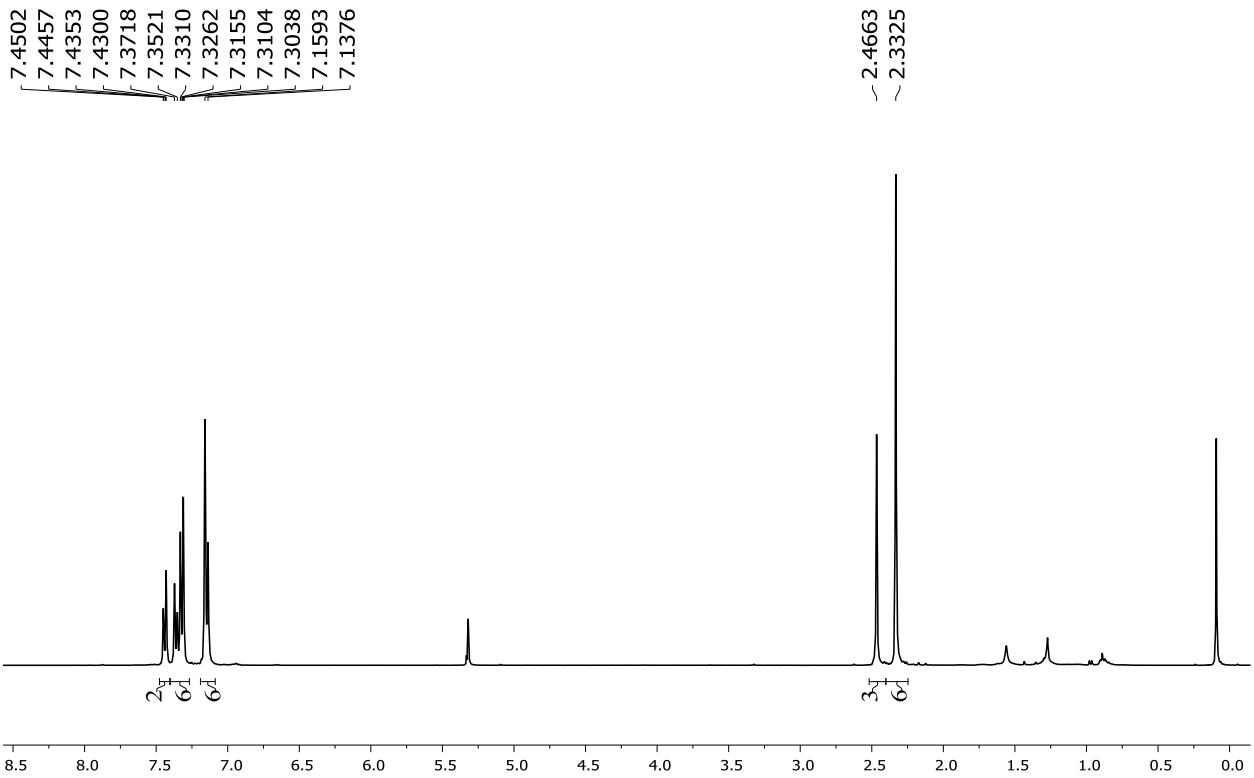

Figure B.31: ^{1}H NMR spectrum of **12** in CD_2Cl_2

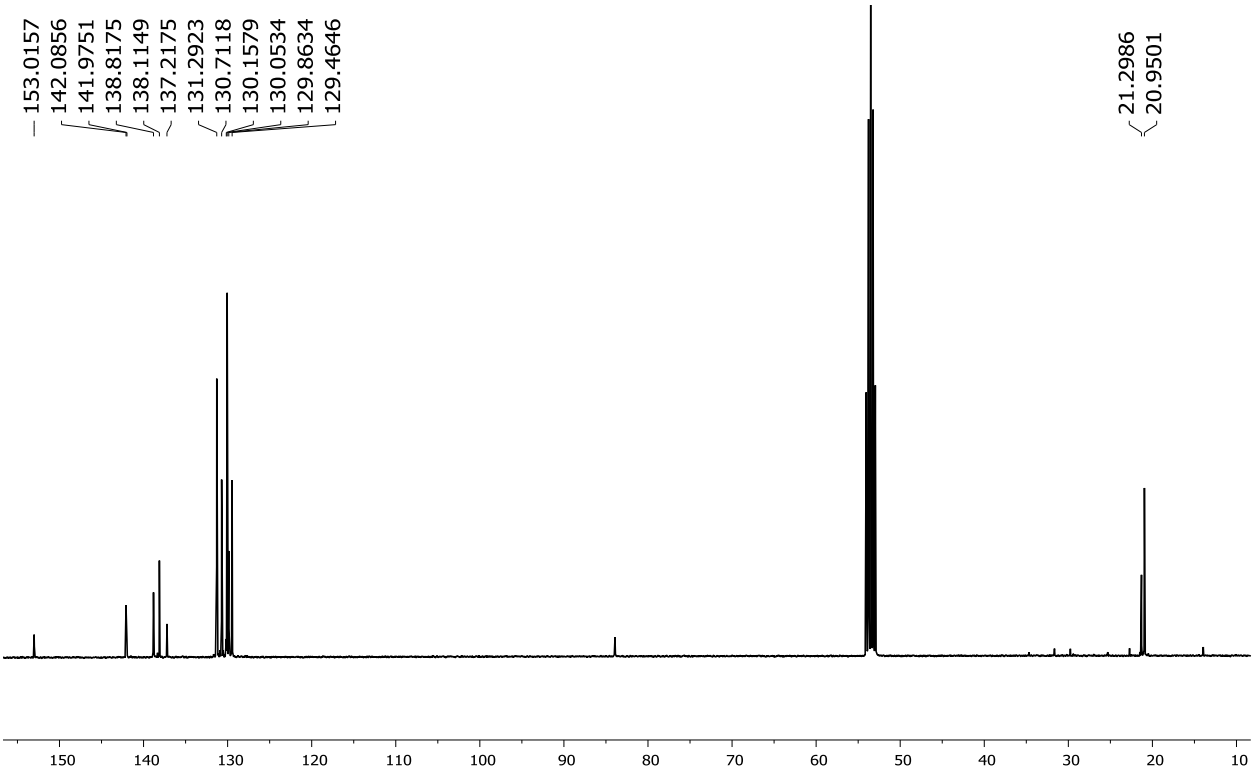

Figure B.32: ^{13}C NMR spectrum of **12** in CD_2Cl_2

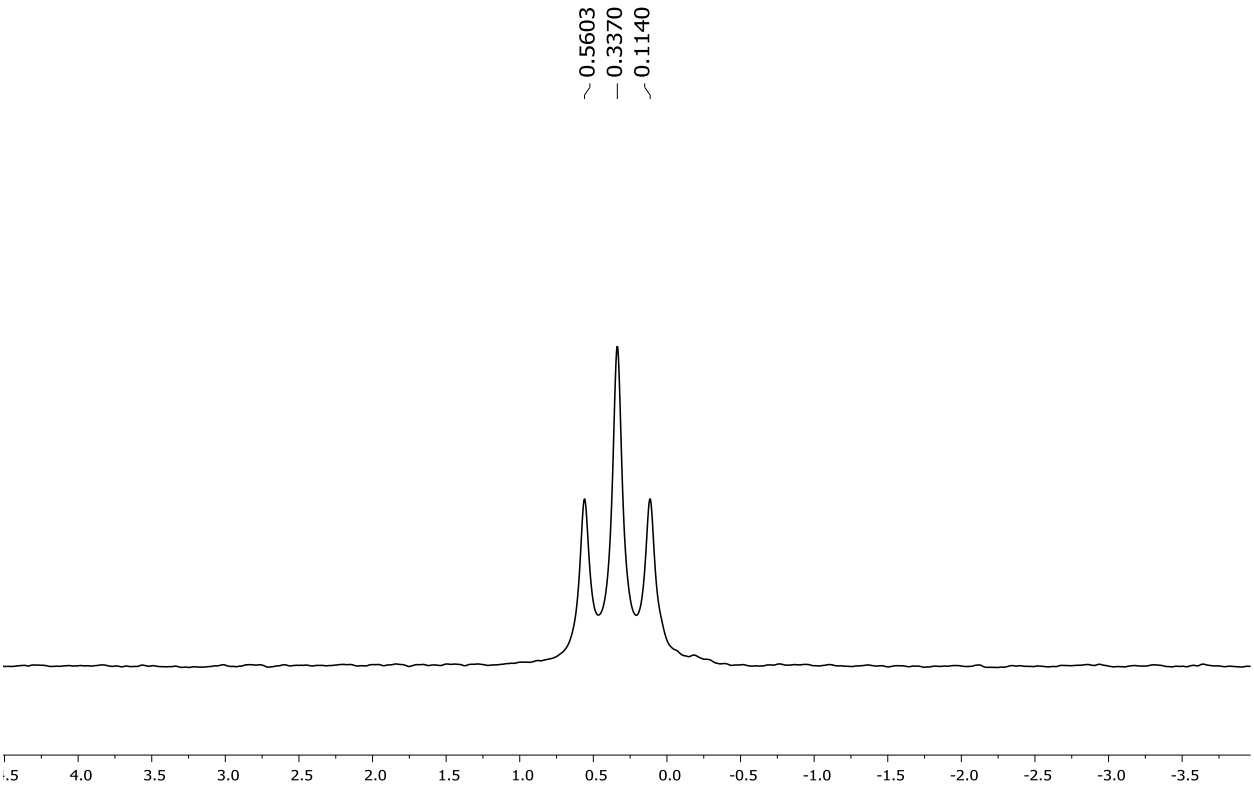

Figure B.33: ^{11}B NMR spectrum of **12** in CD_2Cl_2

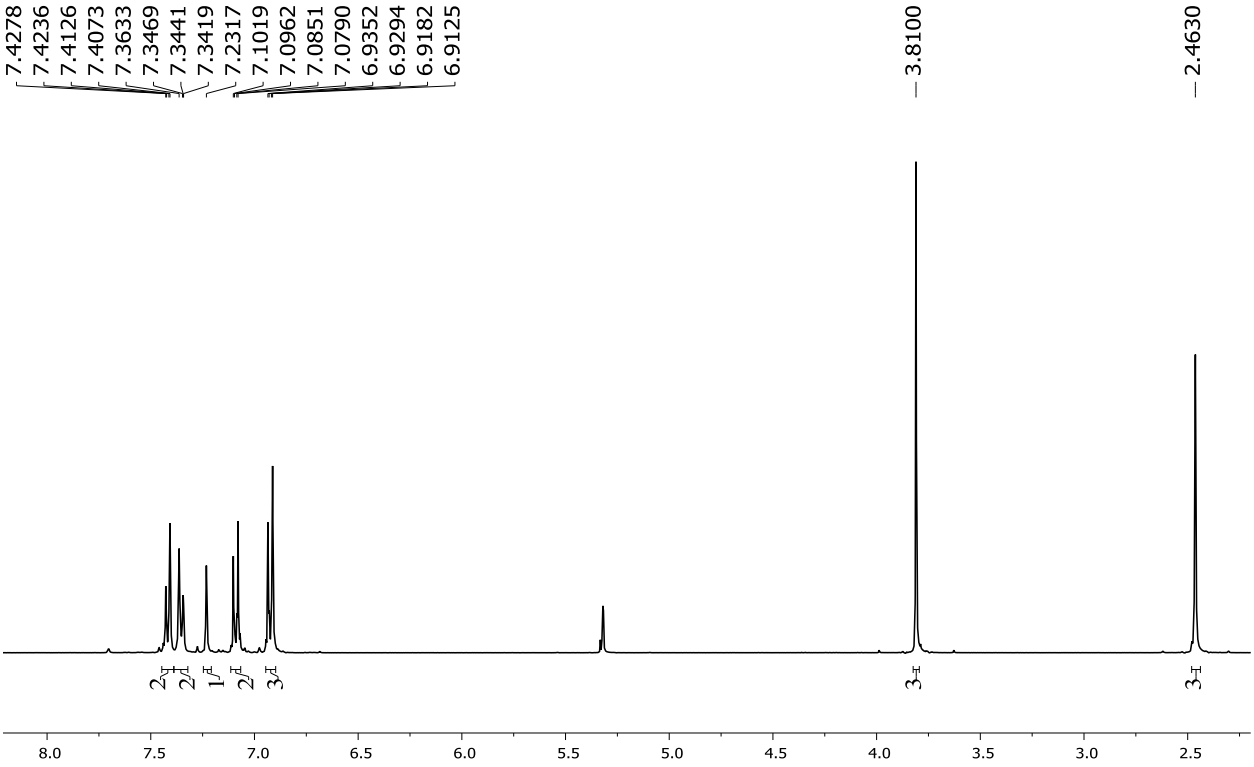

Figure B.34: ^{1}H NMR spectrum of **13** in CD_2Cl_2

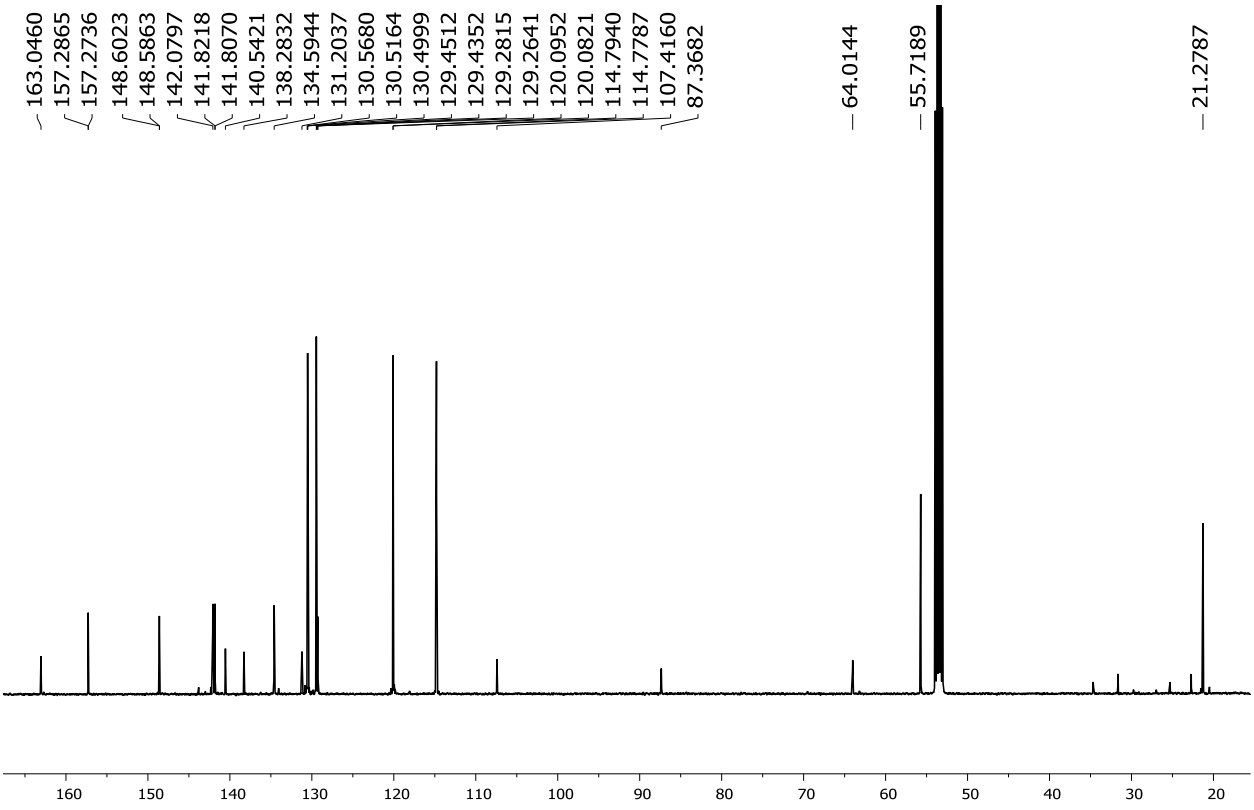

Figure B.35: ^{13}C NMR spectrum of **13** in CD_2Cl_2

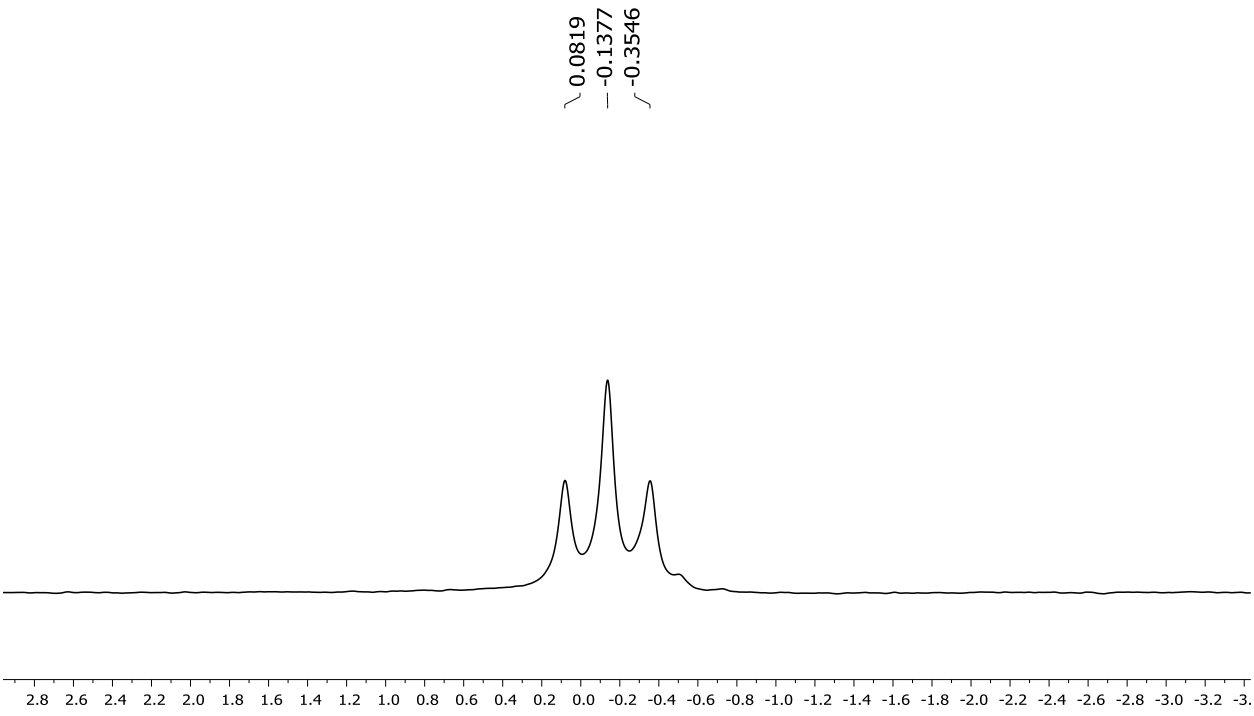

Figure B.36: ^{11}B NMR spectrum of **13** in CD_2Cl_2

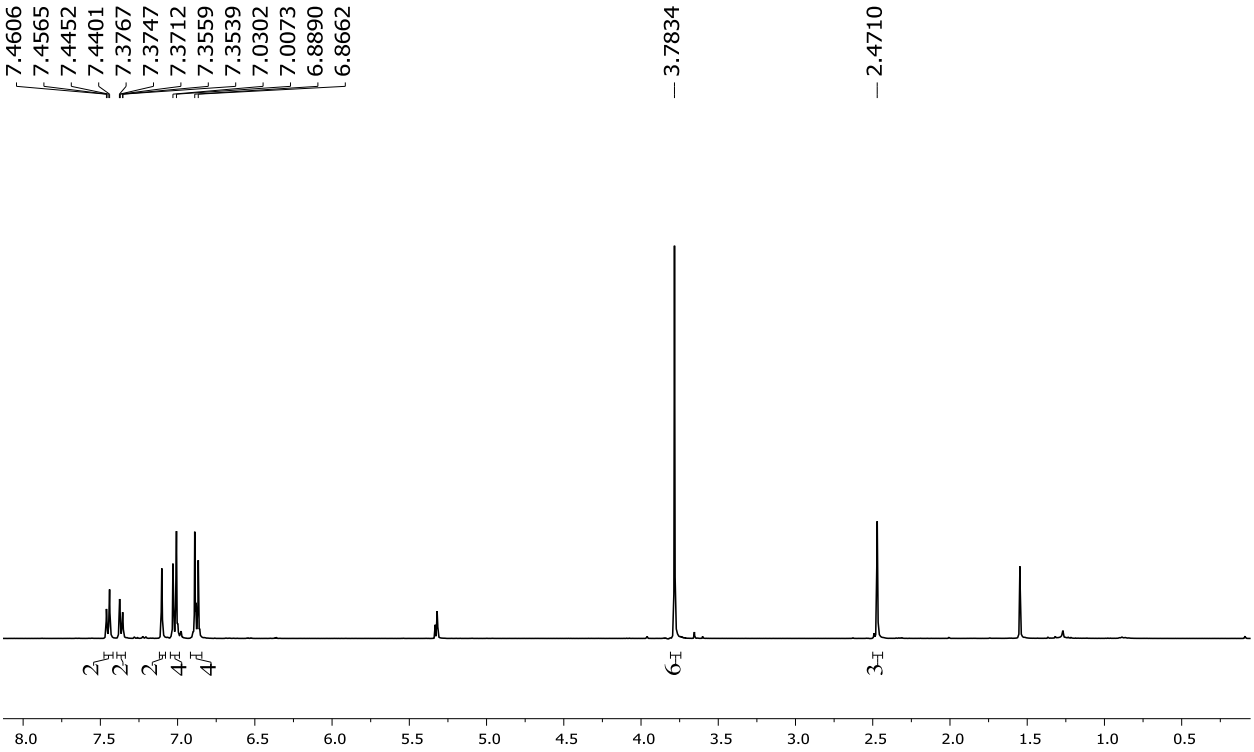

Figure B.37: ^{1}H NMR spectrum of **14** in CD_2Cl_2

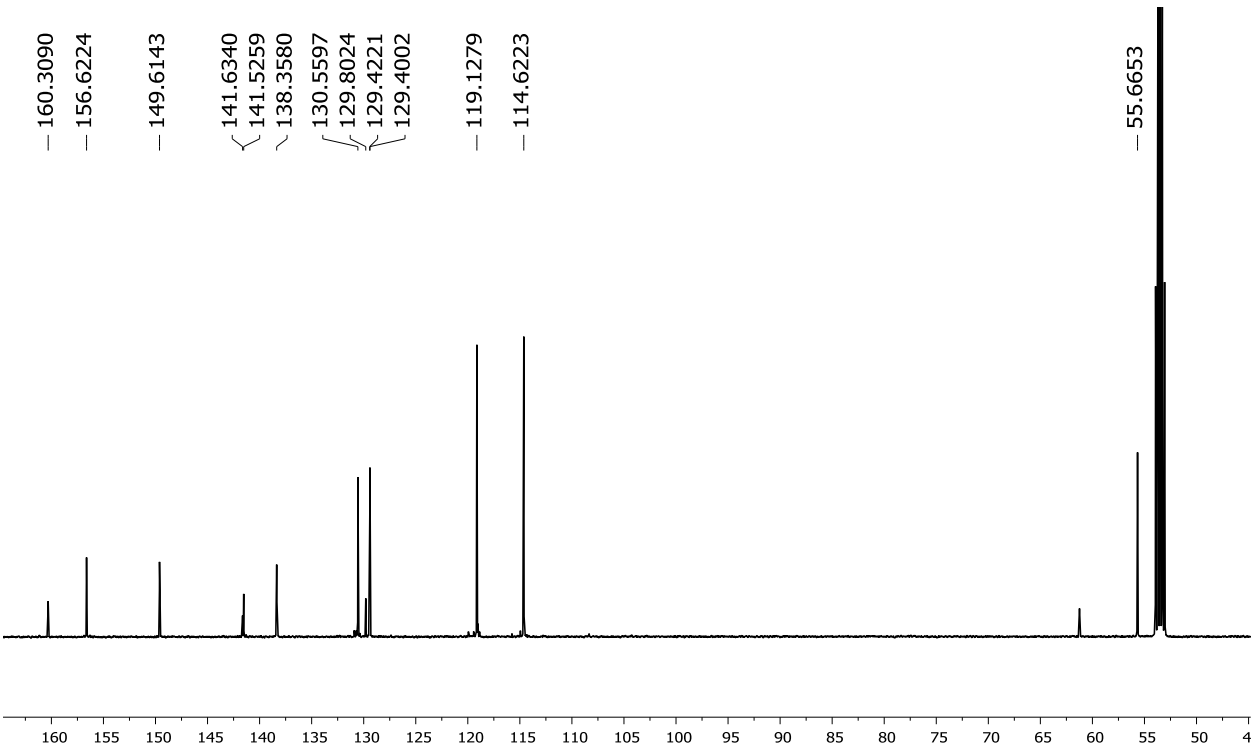

Figure B.38: ^{13}C NMR spectrum of **14** in CD_2Cl_2

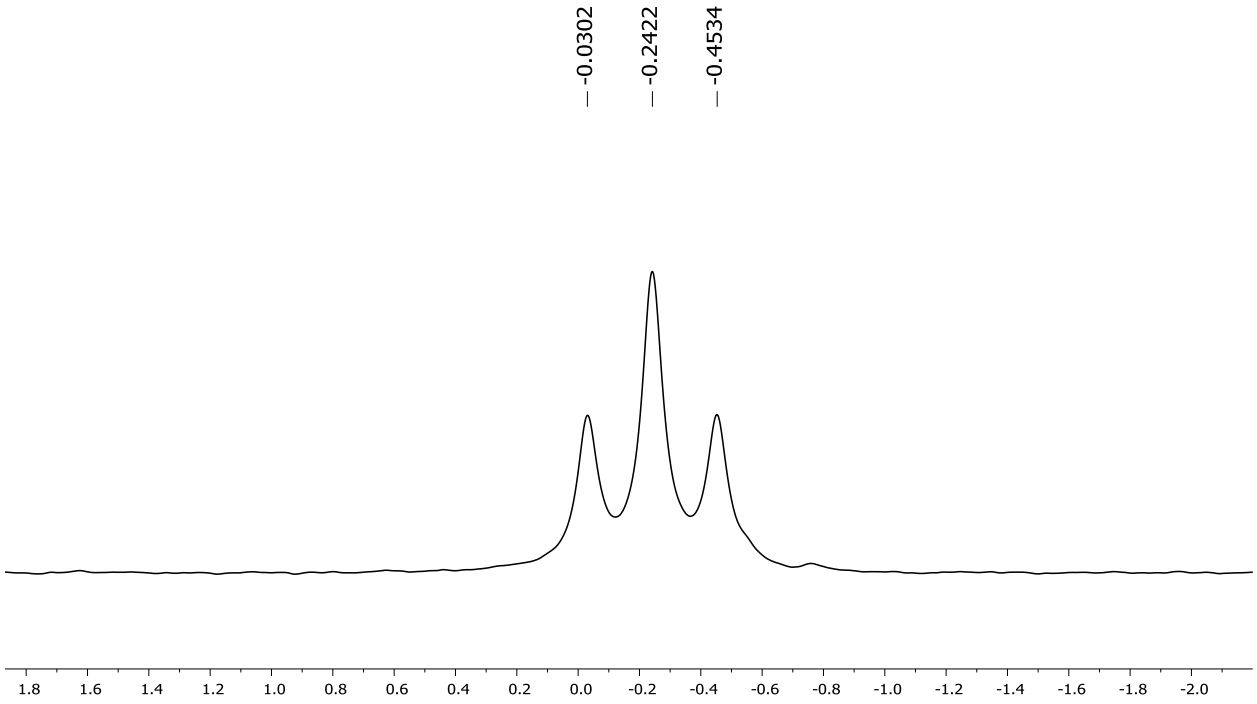

Figure B.39: ^{11}B NMR spectrum of **14** in CD_2Cl_2

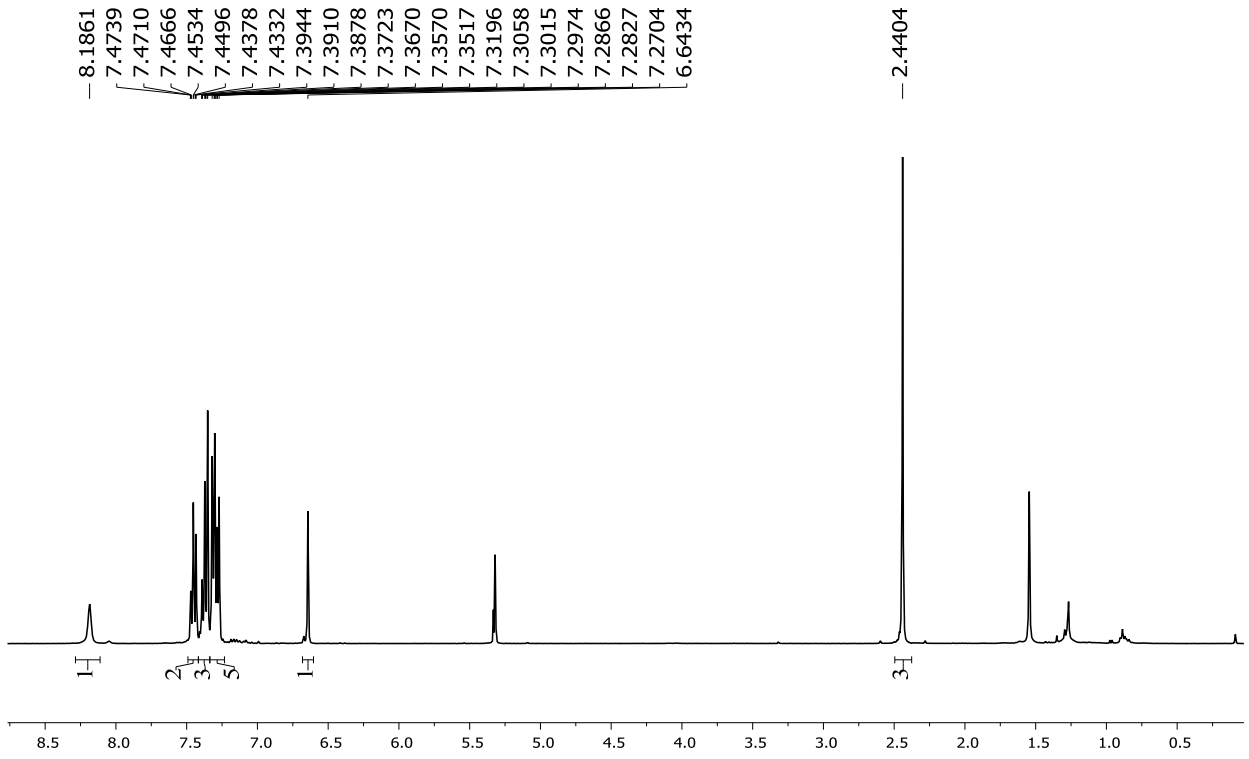

Figure B.40: ^{1}H NMR spectrum of **15** in CD_2Cl_2

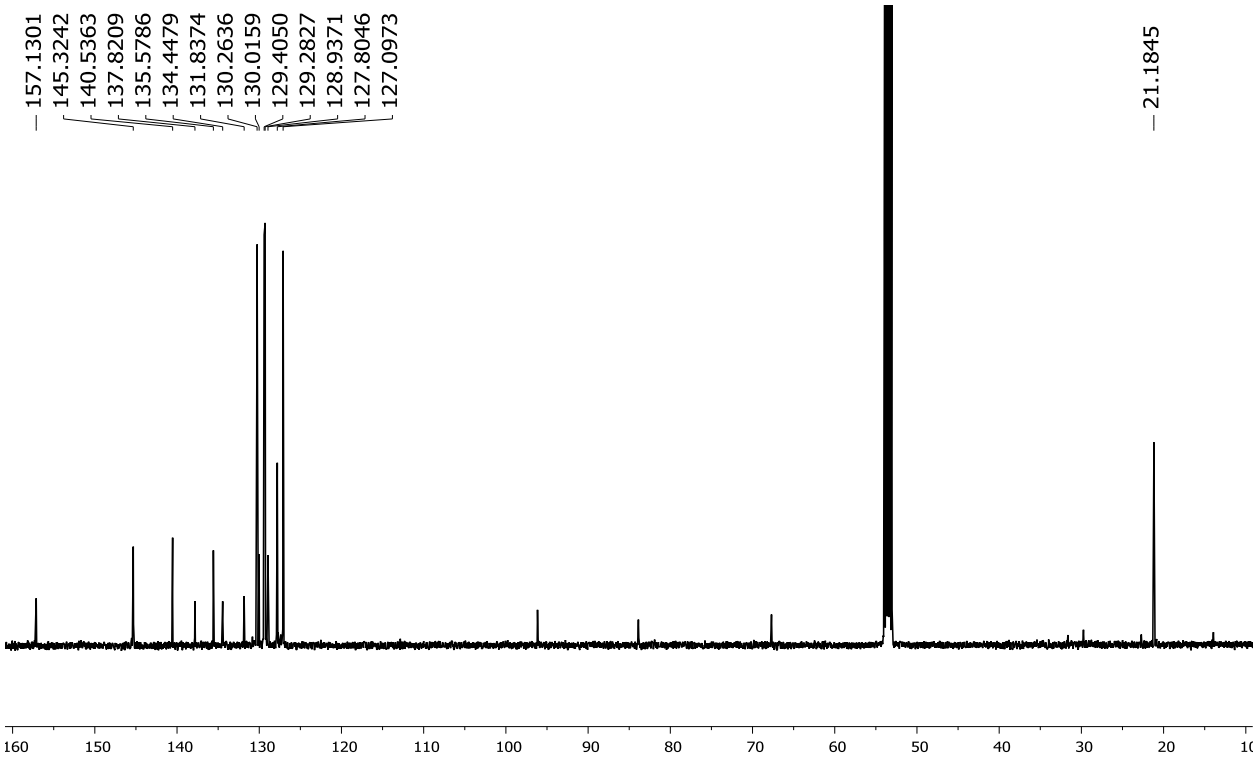

Figure B.41: ^{13}C NMR spectrum of **15** in CD_2Cl_2

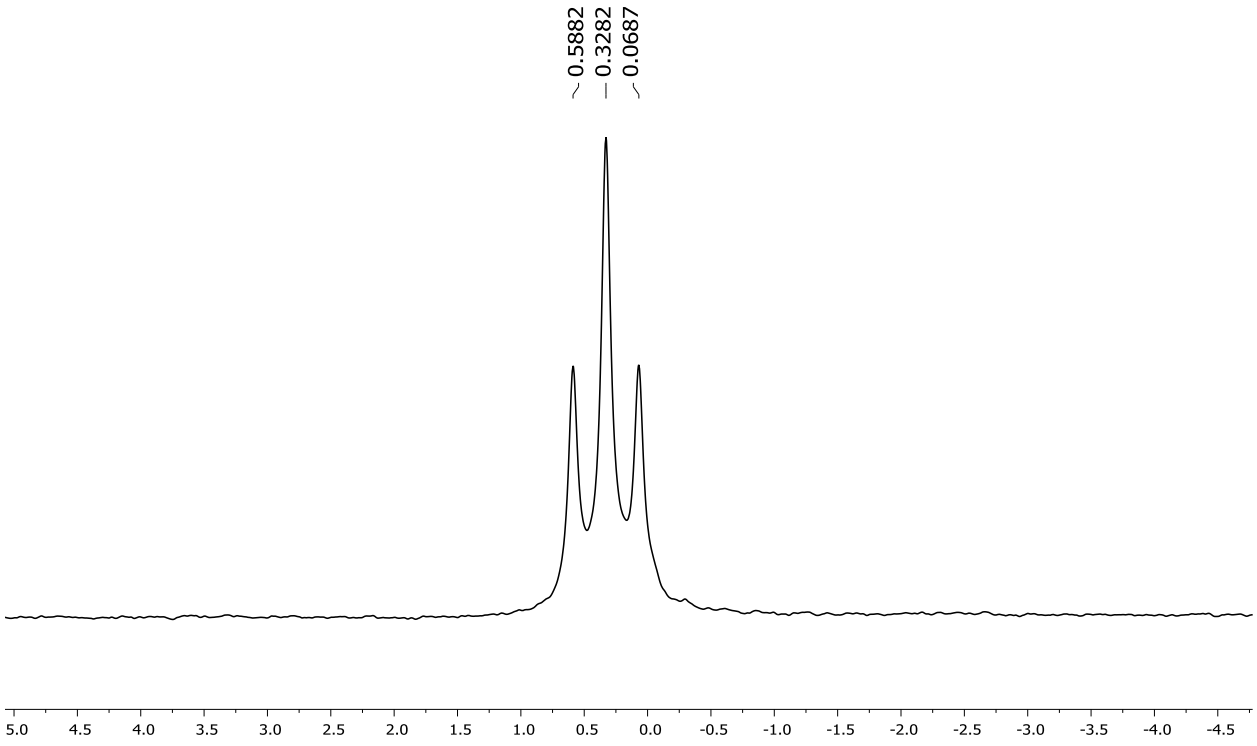

Figure B.42: ^{11}B NMR spectrum of **15** in CD_2Cl_2

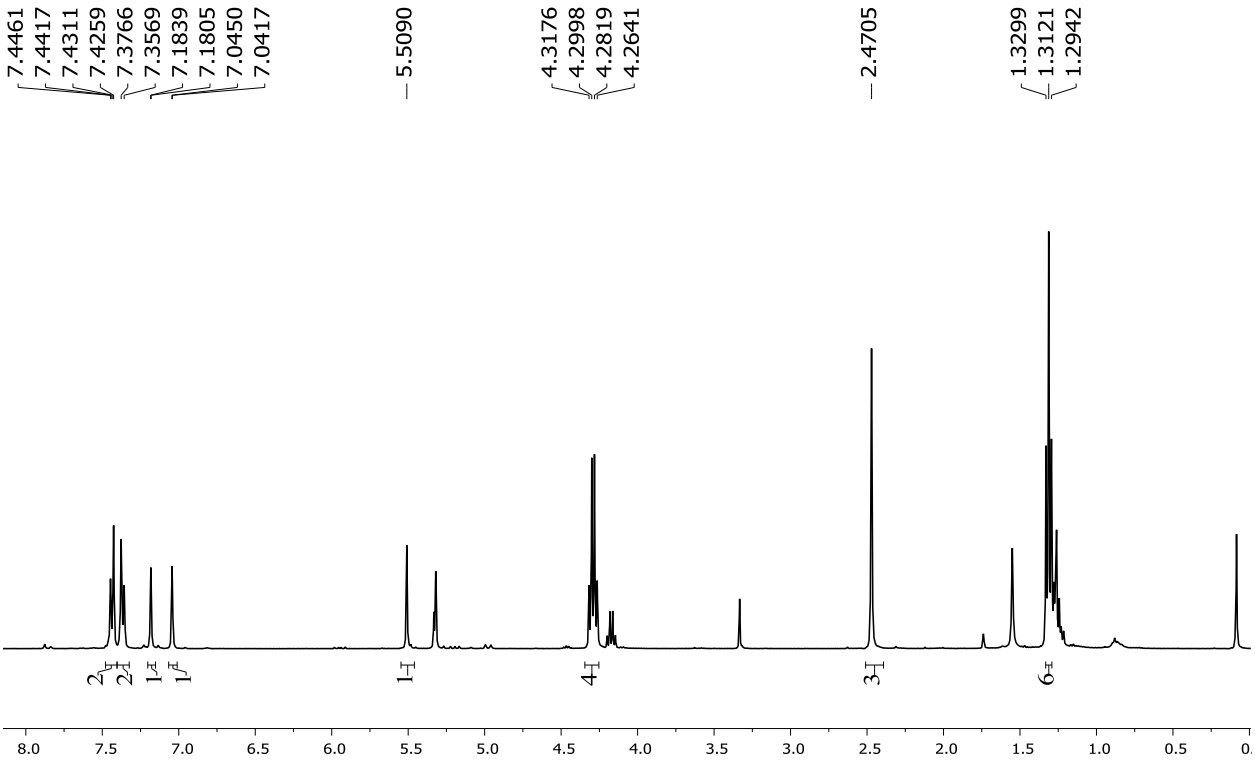

Figure B.43: ^{1}H NMR spectrum of **16** in CD_2Cl_2

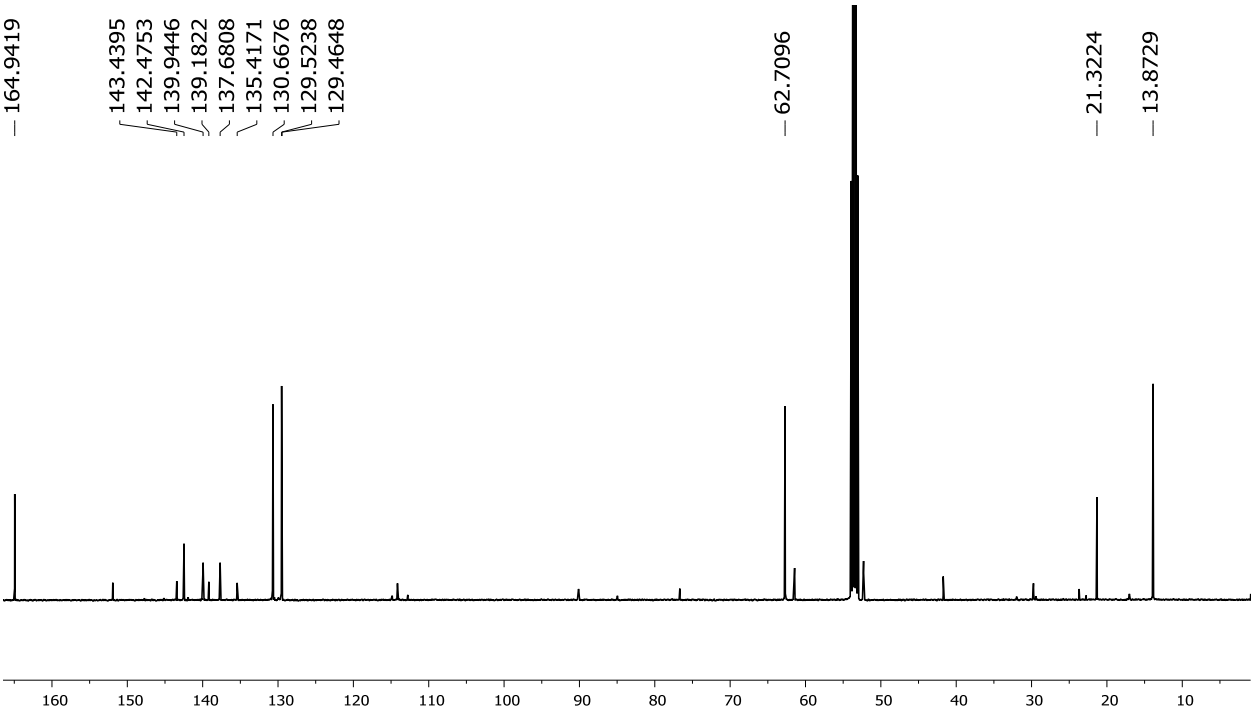

Figure B.44: ^{13}C NMR spectrum of **16** in CD_2Cl_2

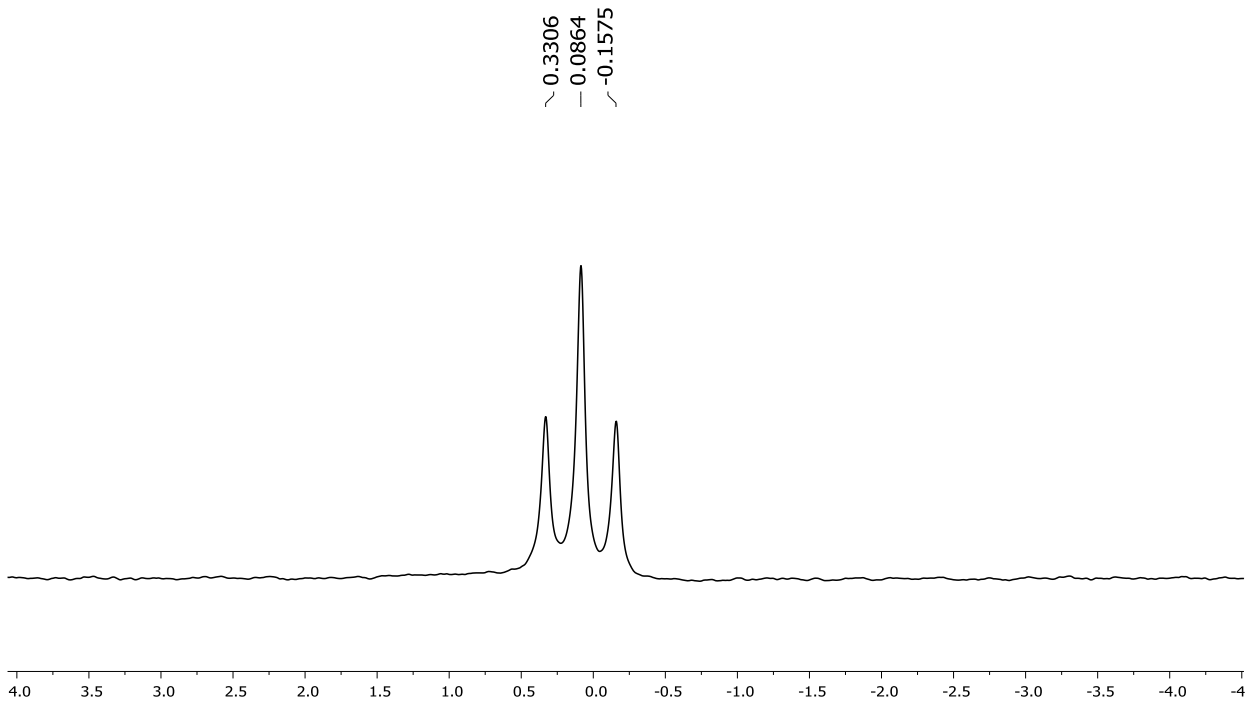

Figure B.45: ^{11}B NMR spectrum of **16** in CD_2Cl_2

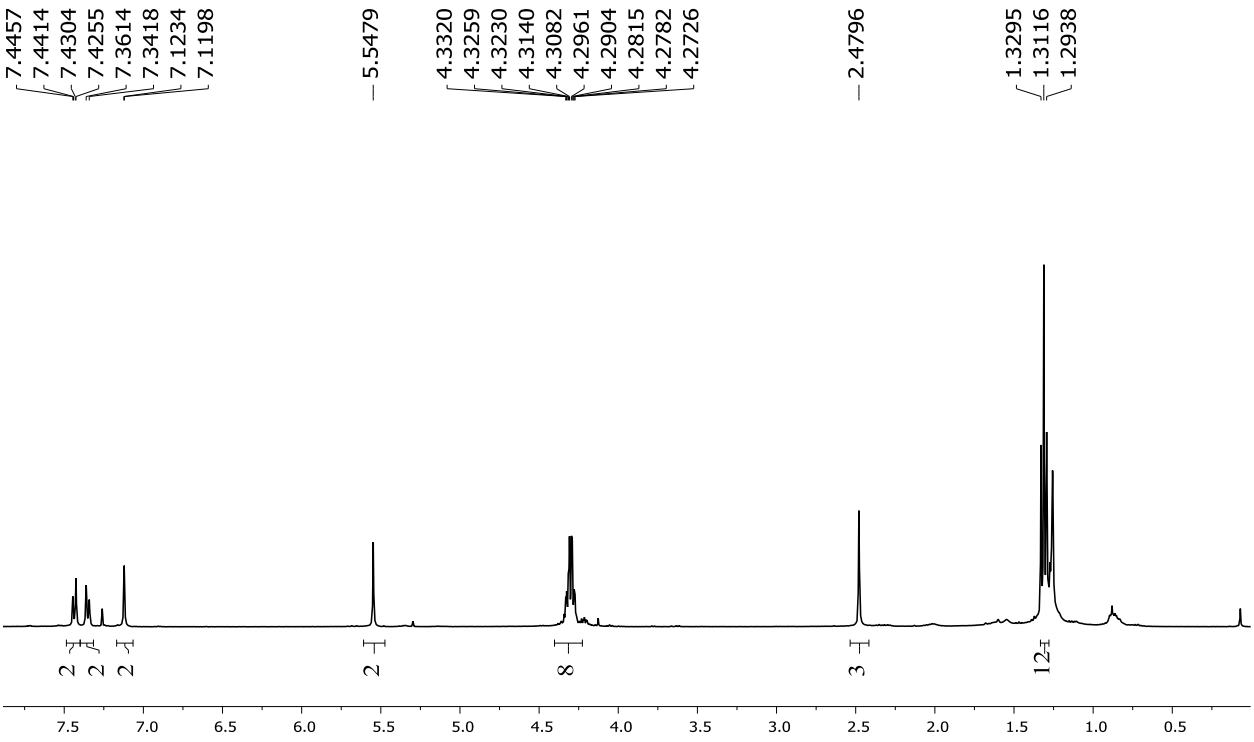

Figure B.46: ^{1}H NMR spectrum of **17** in $CDCl_3$

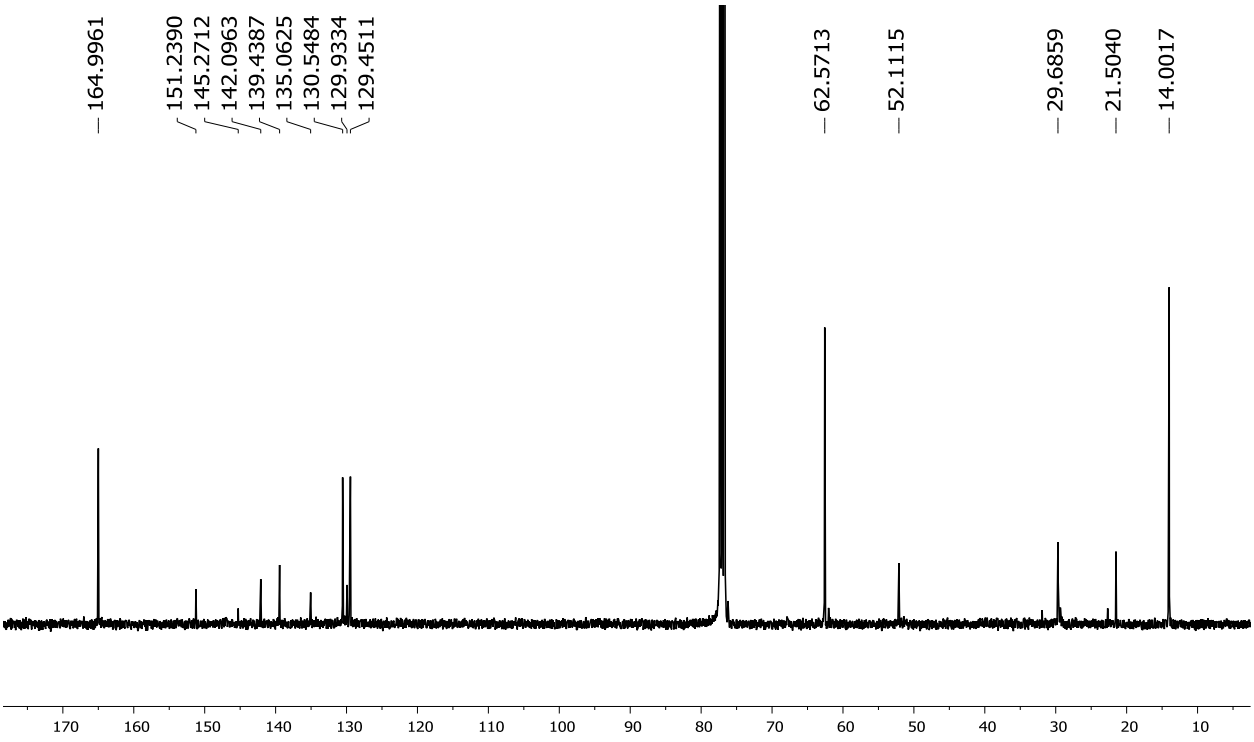

Figure B.47: ^{13}C NMR spectrum of **17** in $CDCl_3$

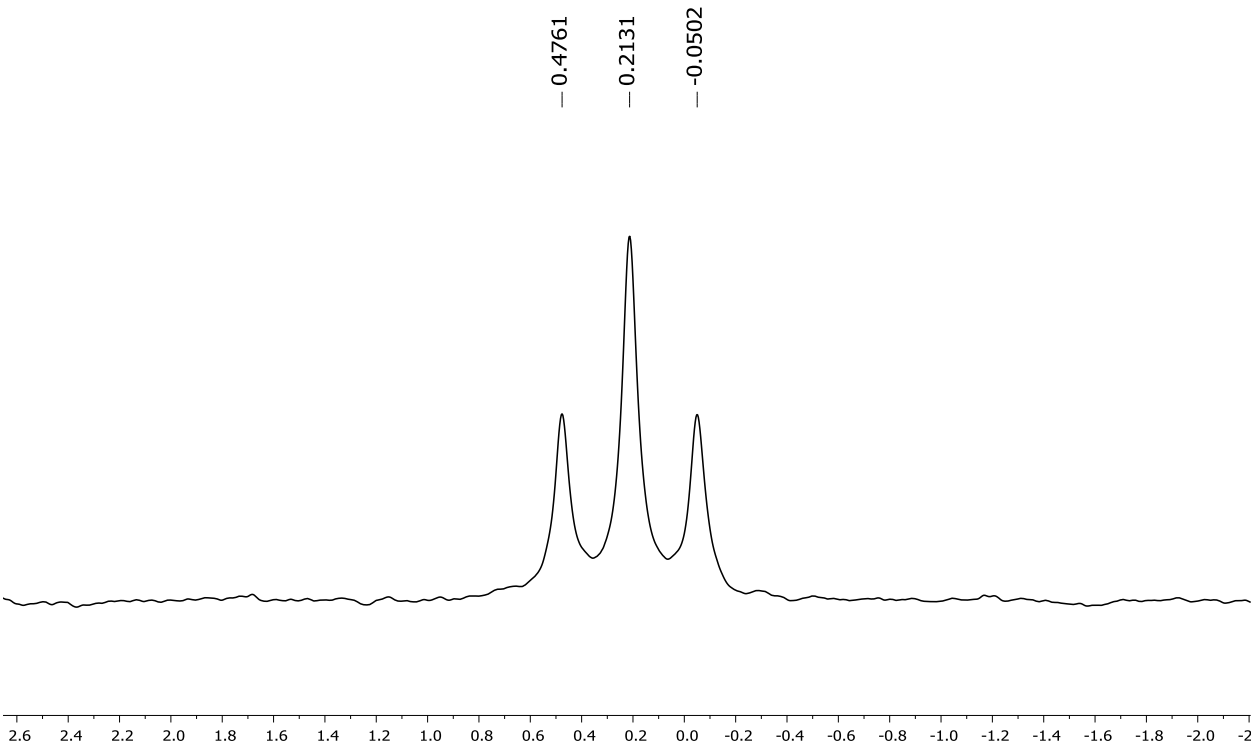

Figure B.48: ^{11}B NMR spectrum of **17** in $CDCl_3$

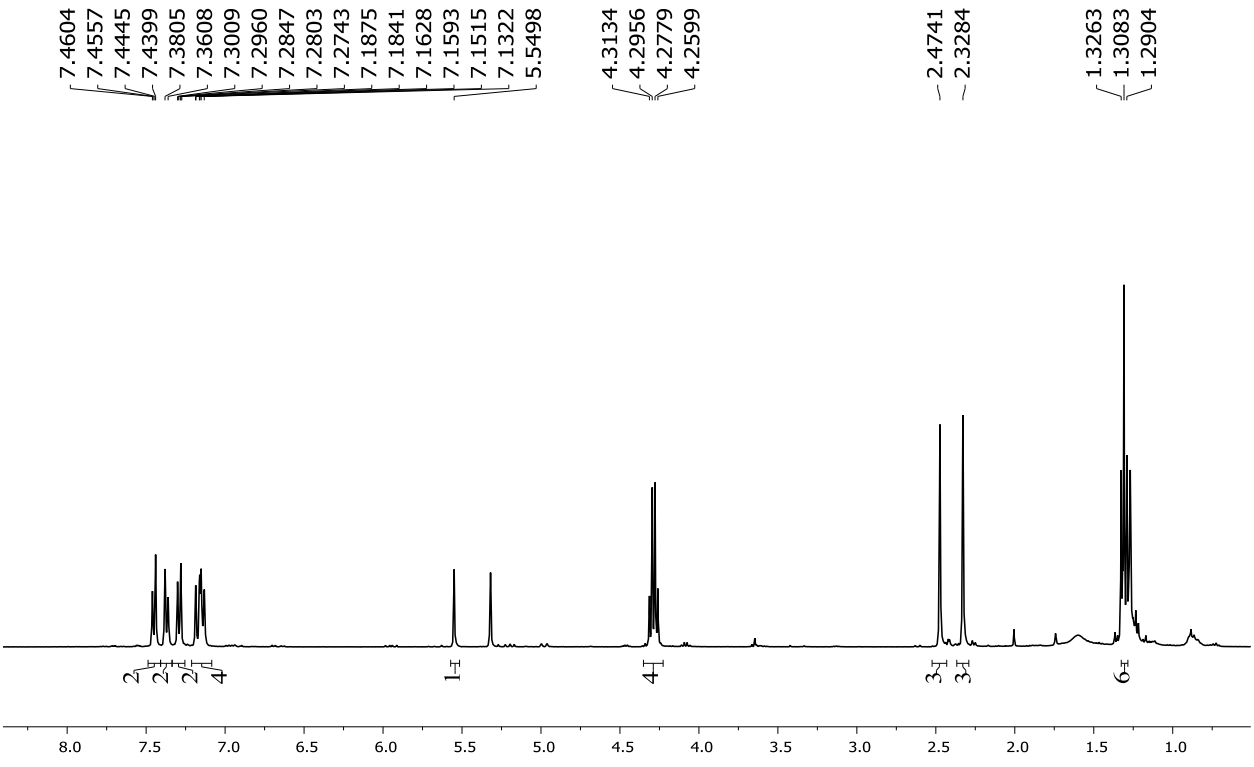

Figure B.49: ^{1}H NMR spectrum of **18** in CD_2Cl_2

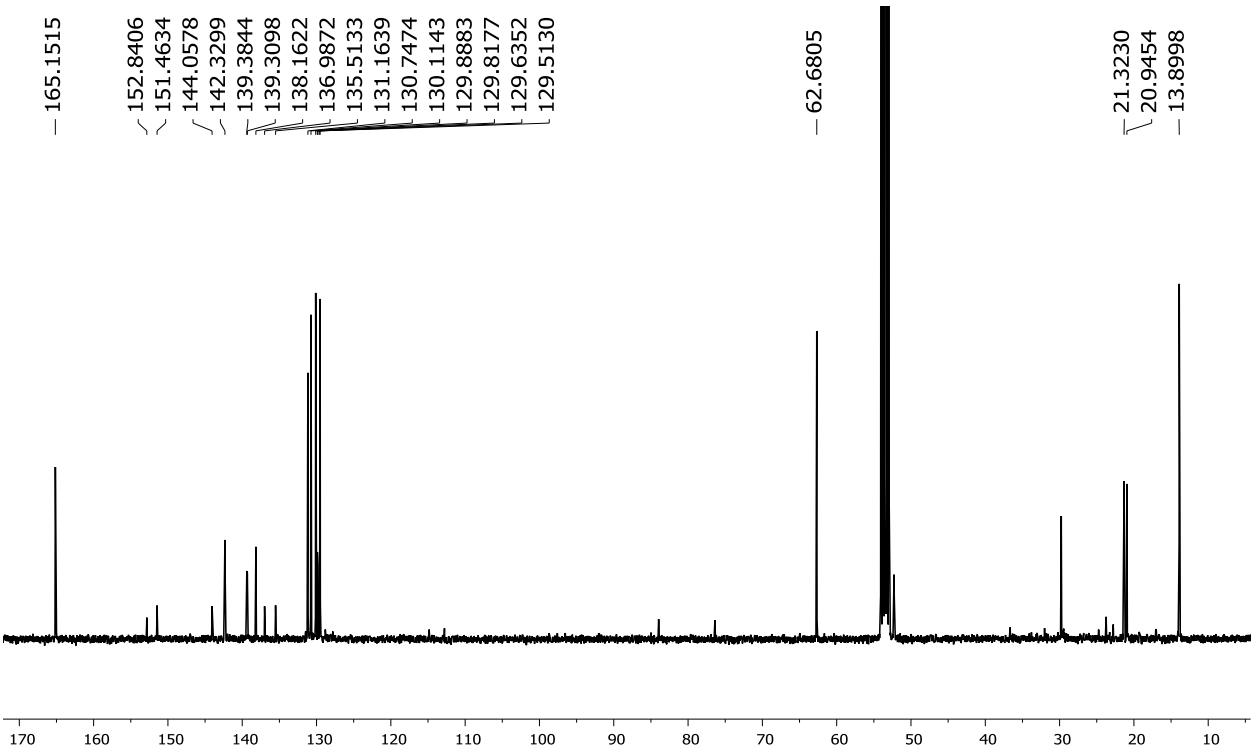

Figure B.50: ^{13}C NMR spectrum of **18** in CD_2Cl_2

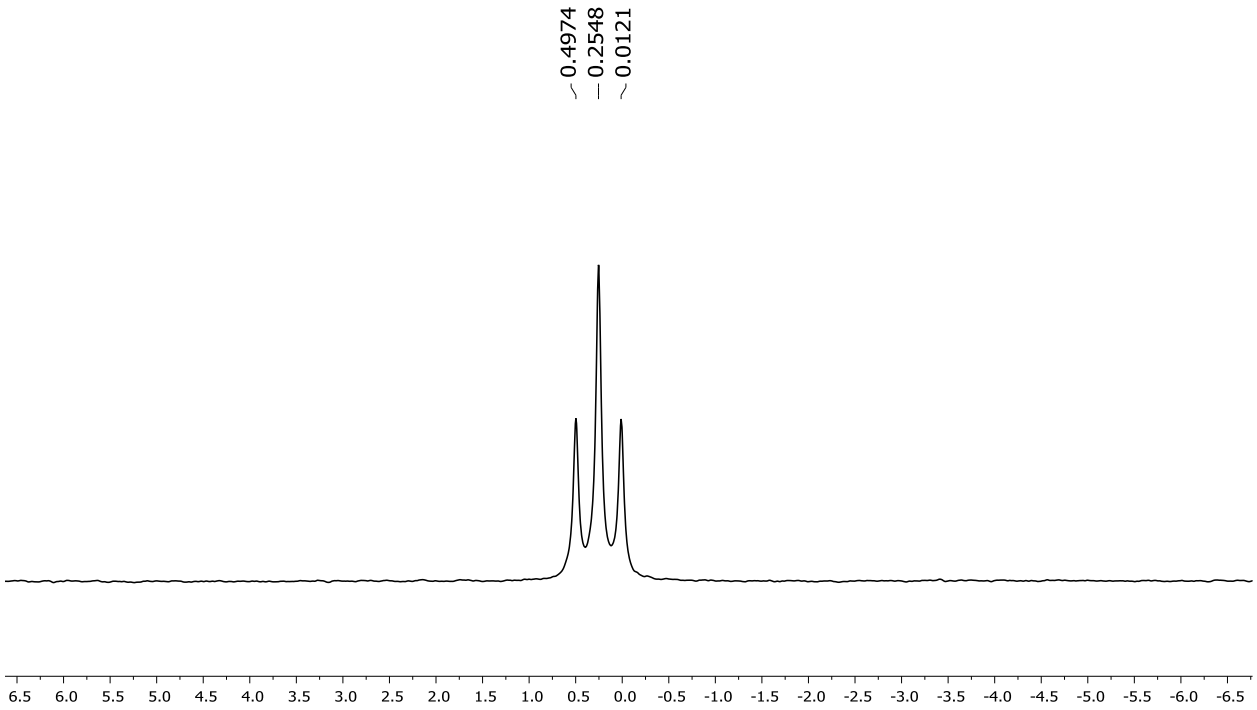

Figure B.51: ^{11}B NMR spectrum of **18** in CD_2Cl_2

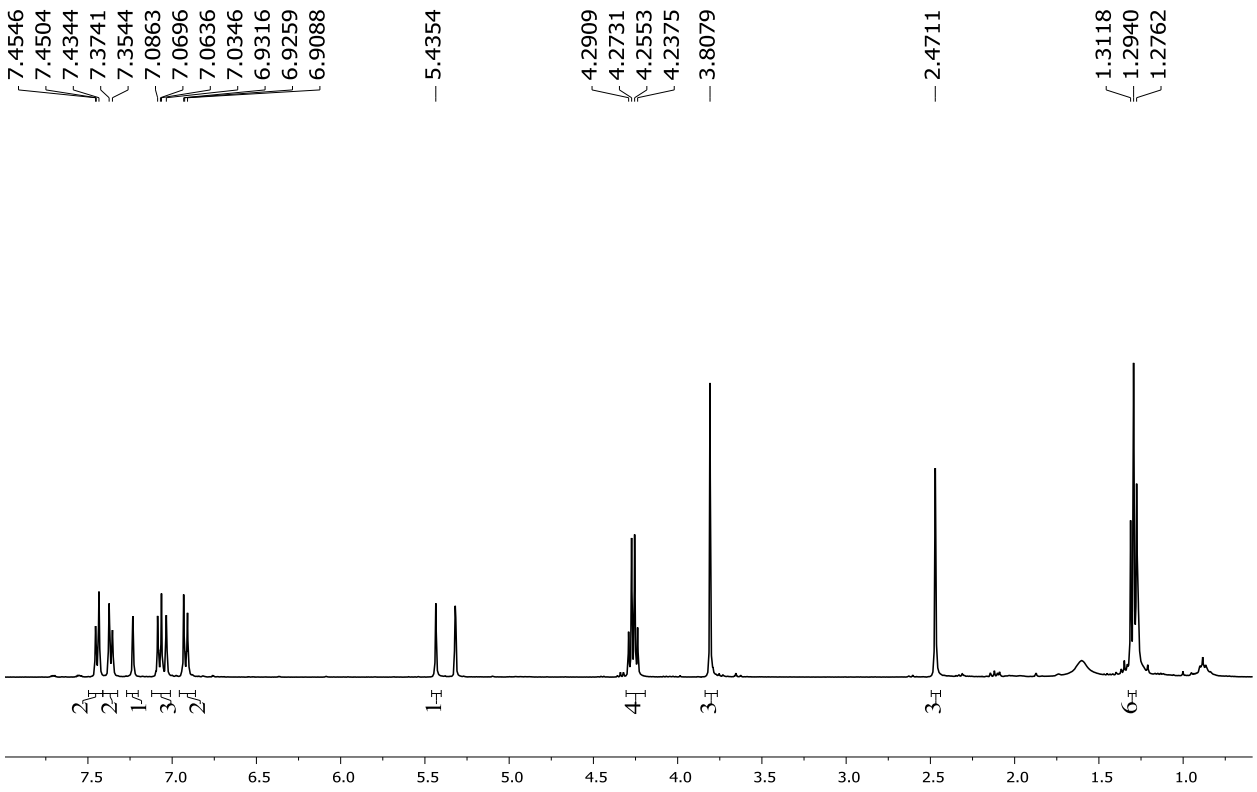

Figure B.52: ^{1}H NMR spectrum of **19** in $CDCl_3$

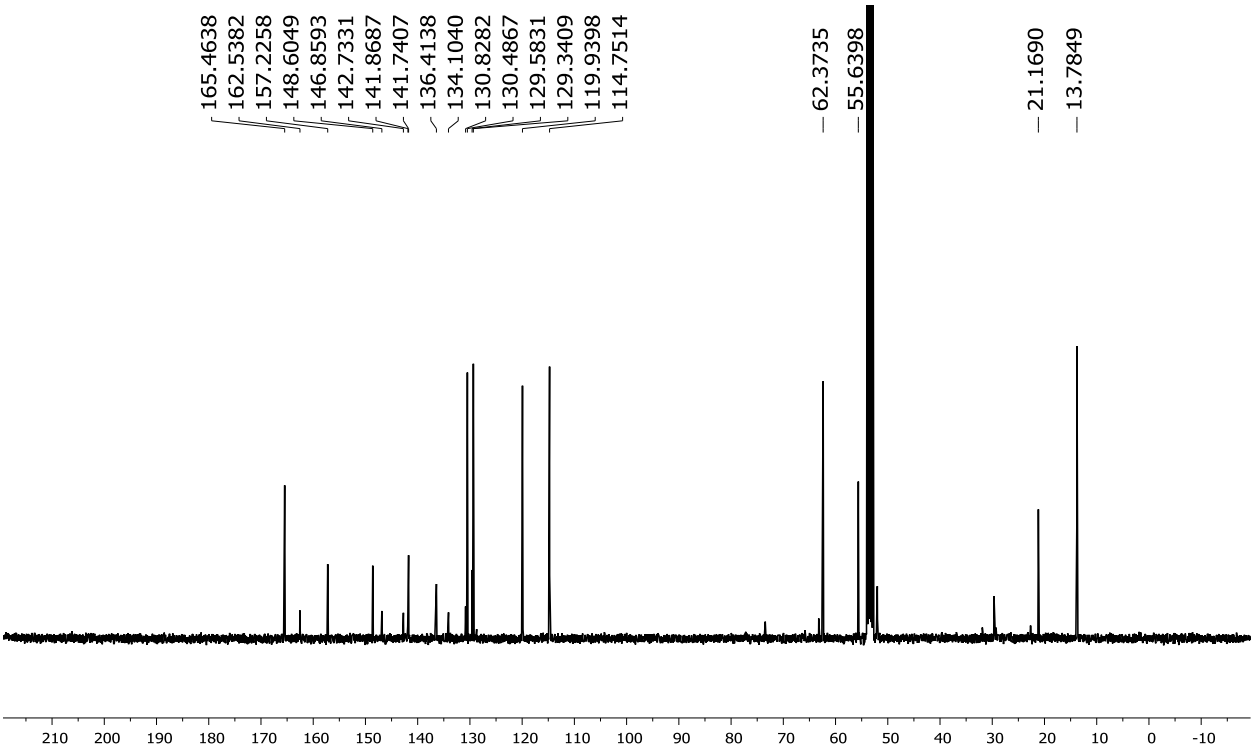

Figure B.53: ^{13}C NMR spectrum of **19** in $CDCl_3$

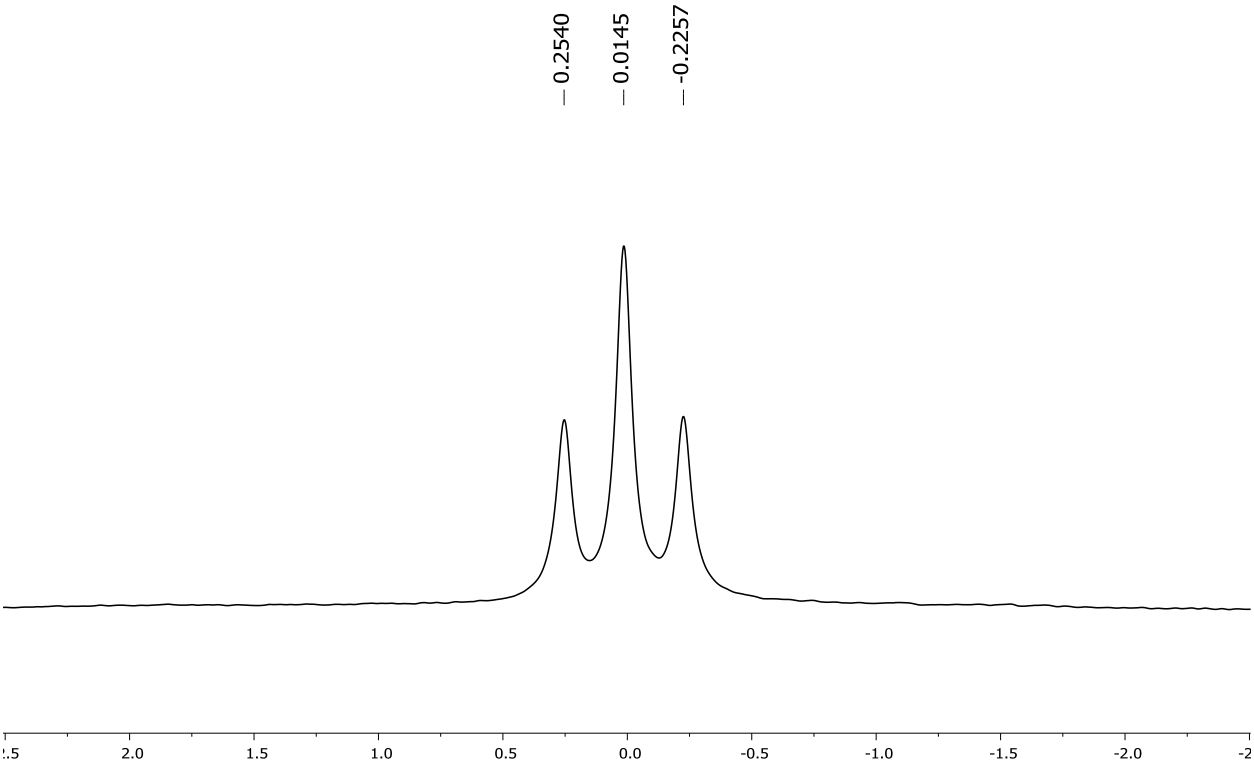

Figure B.54: ^{11}B NMR spectrum of **19** in $CDCl_3$

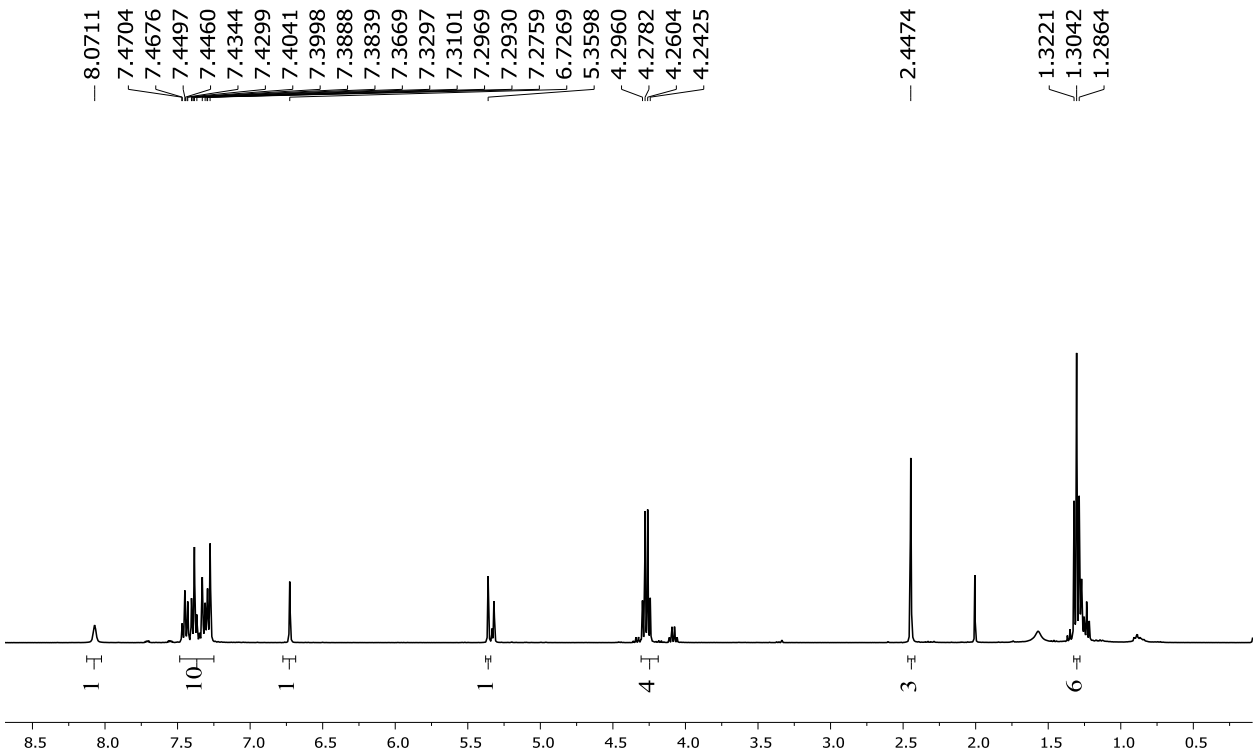

Figure B.55: ^{1}H NMR spectrum of **20** in CD_2Cl_2

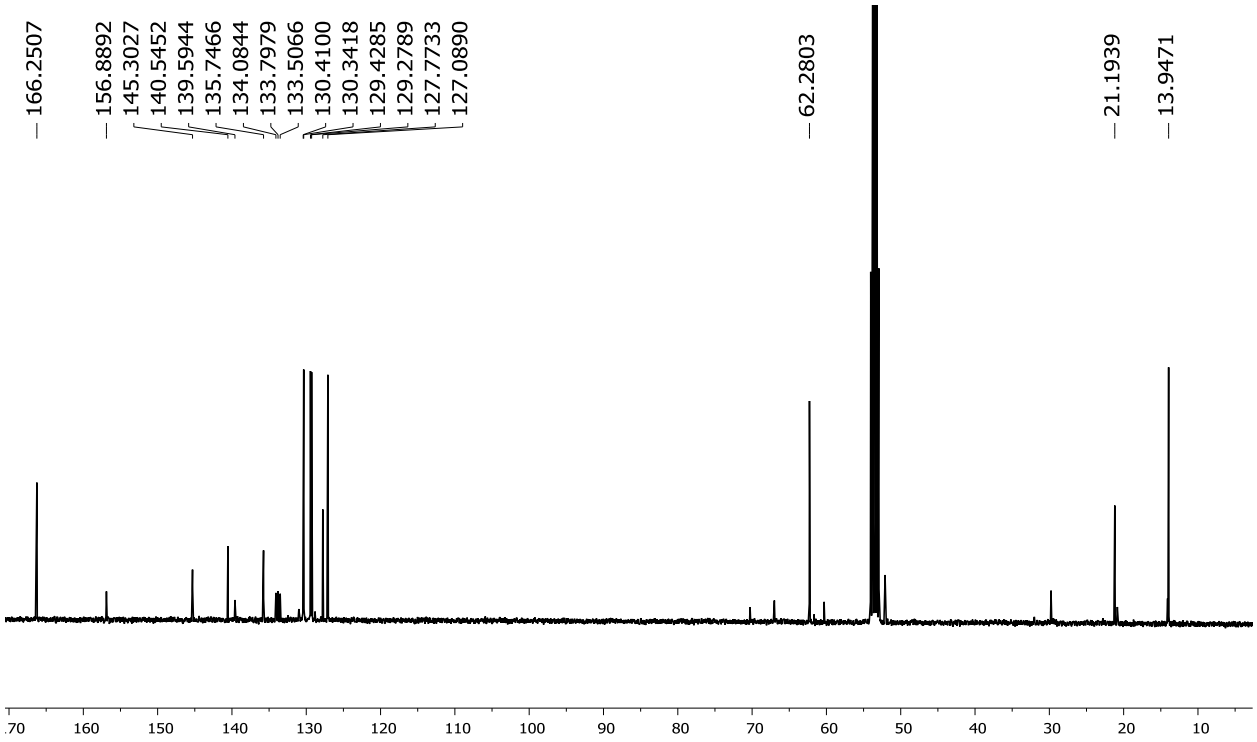

Figure B.56: ^{13}C NMR spectrum of **20** in CD_2Cl_2

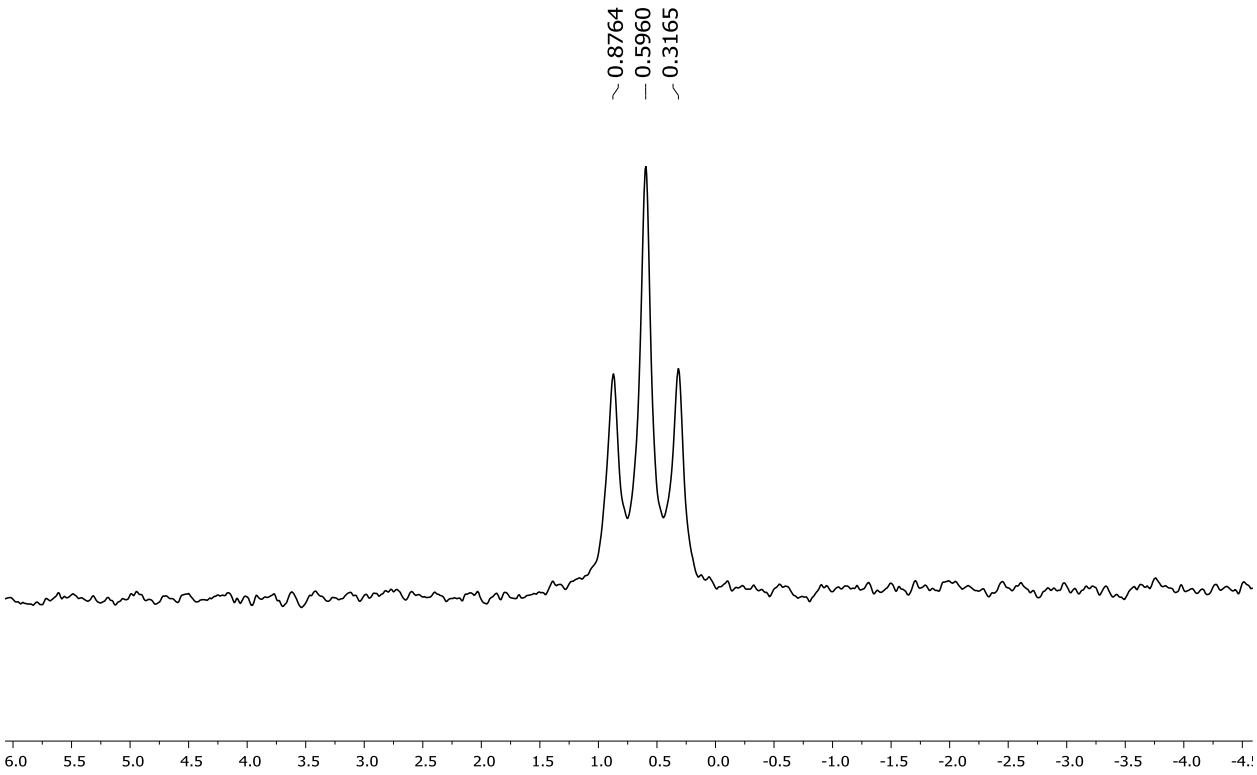

Figure B.57: ^{11}B NMR spectrum of **20** in CD_2Cl_2

APPENDIX C: NMR Characterization of Compounds Found in Chapter 4

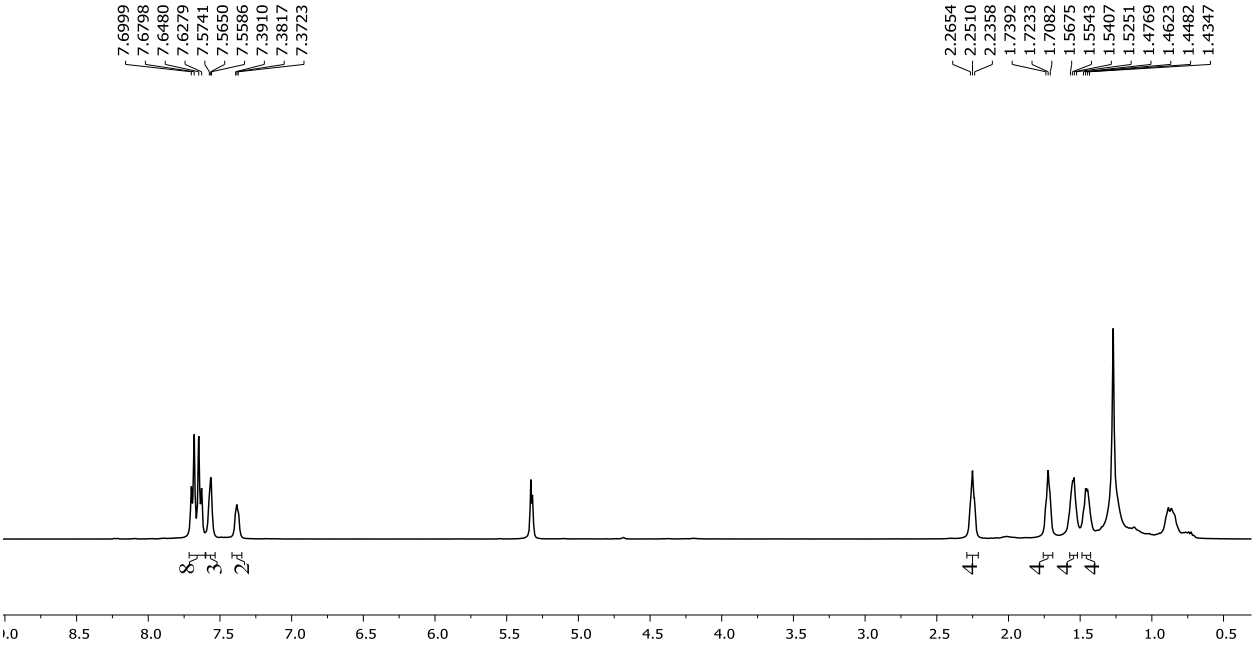

Figure C.1: ^{1}H NMR spectrum of BODIPY **2c** in CD_2Cl_2

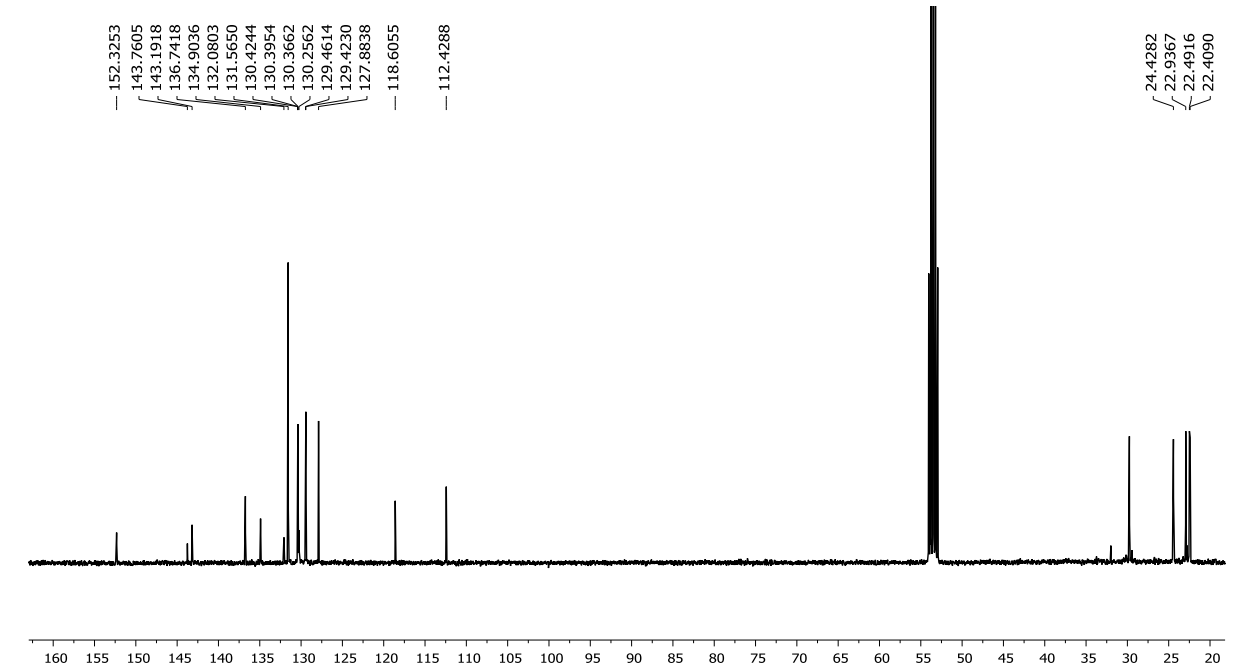

Figure C.2: ^{13}C NMR spectrum of BODIPY **2c** in CD_2Cl_2

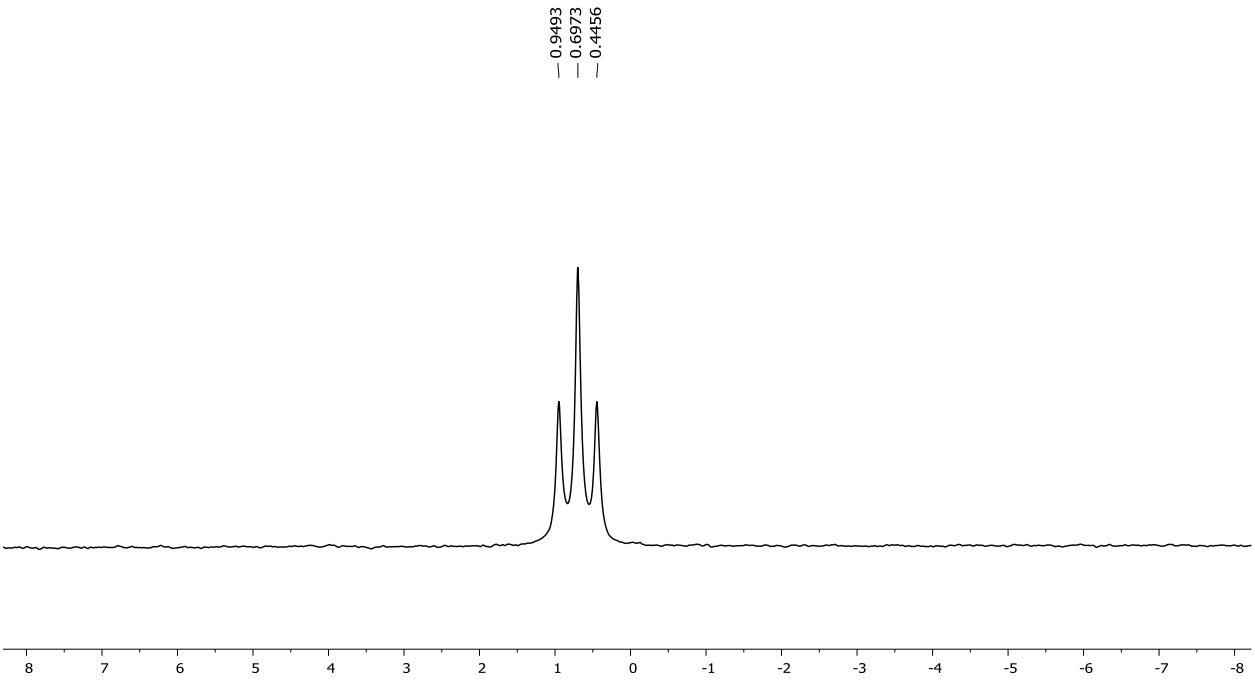

Figure C.3: ^{11}B NMR spectrum of BODIPY **2c** in CD_2Cl_2

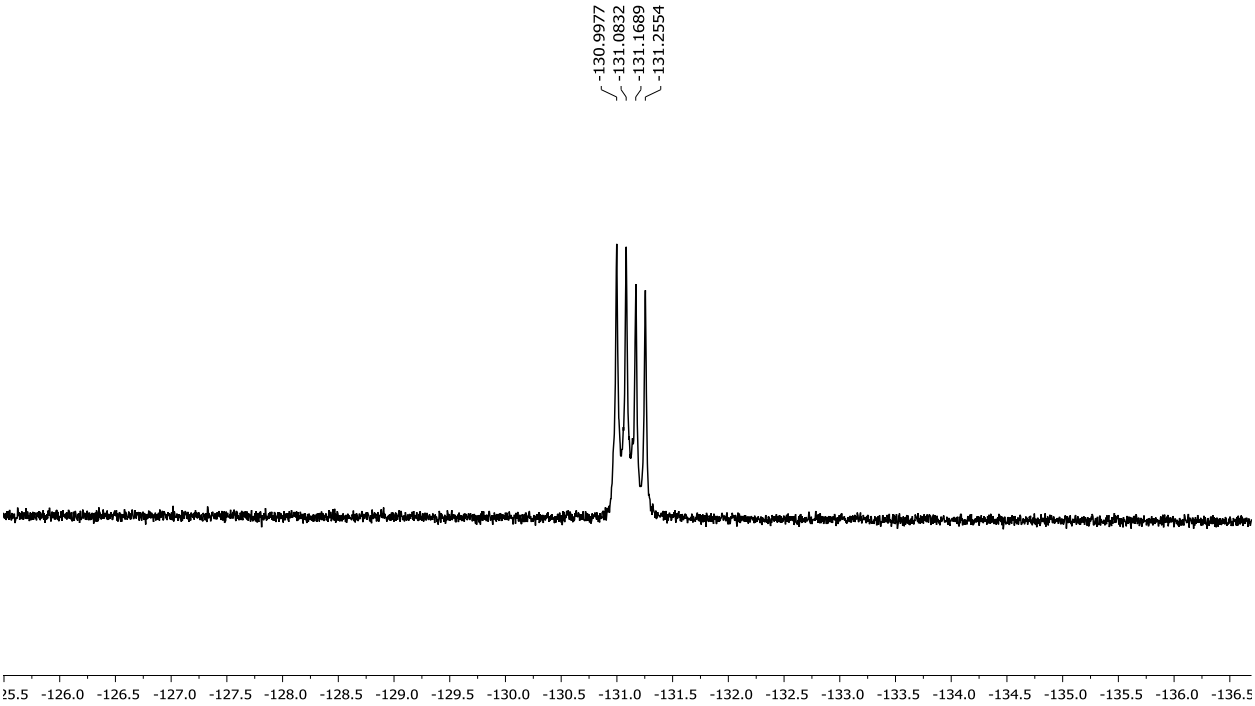

Figure C.4: ^{19}F NMR spectrum of BODIPY **2c** in CD_2Cl_2

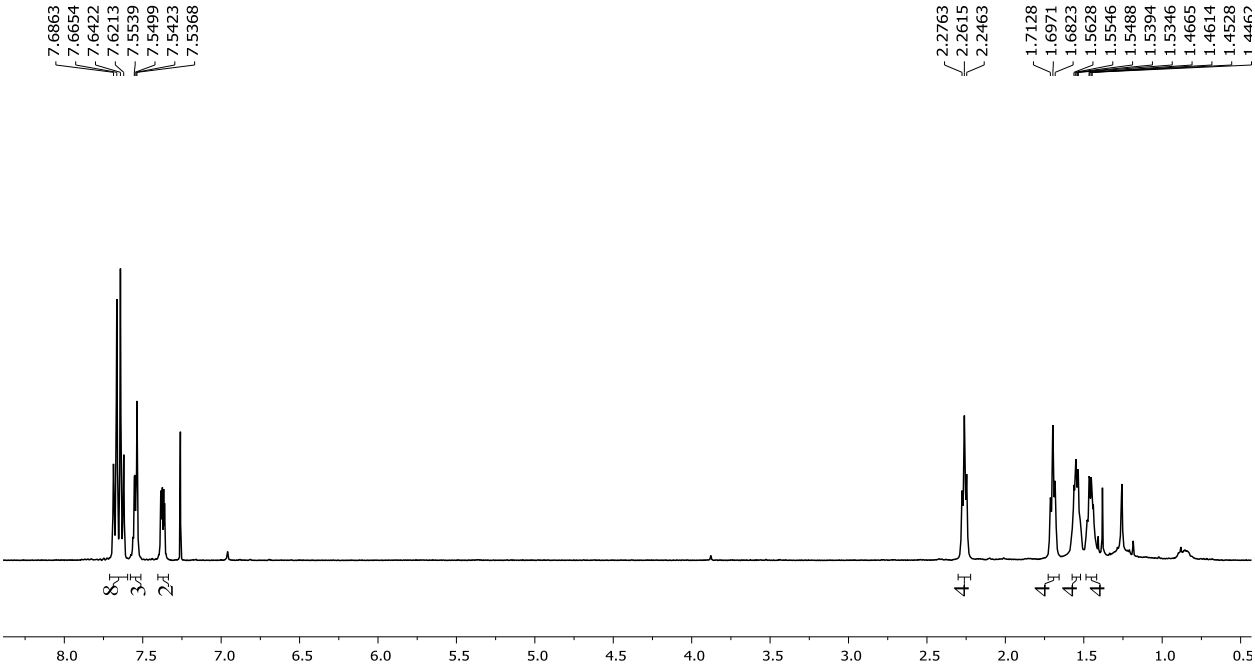

Figure C.5: ^{1}H NMR spectrum of BODIPY **2d** in $CDCl_3$

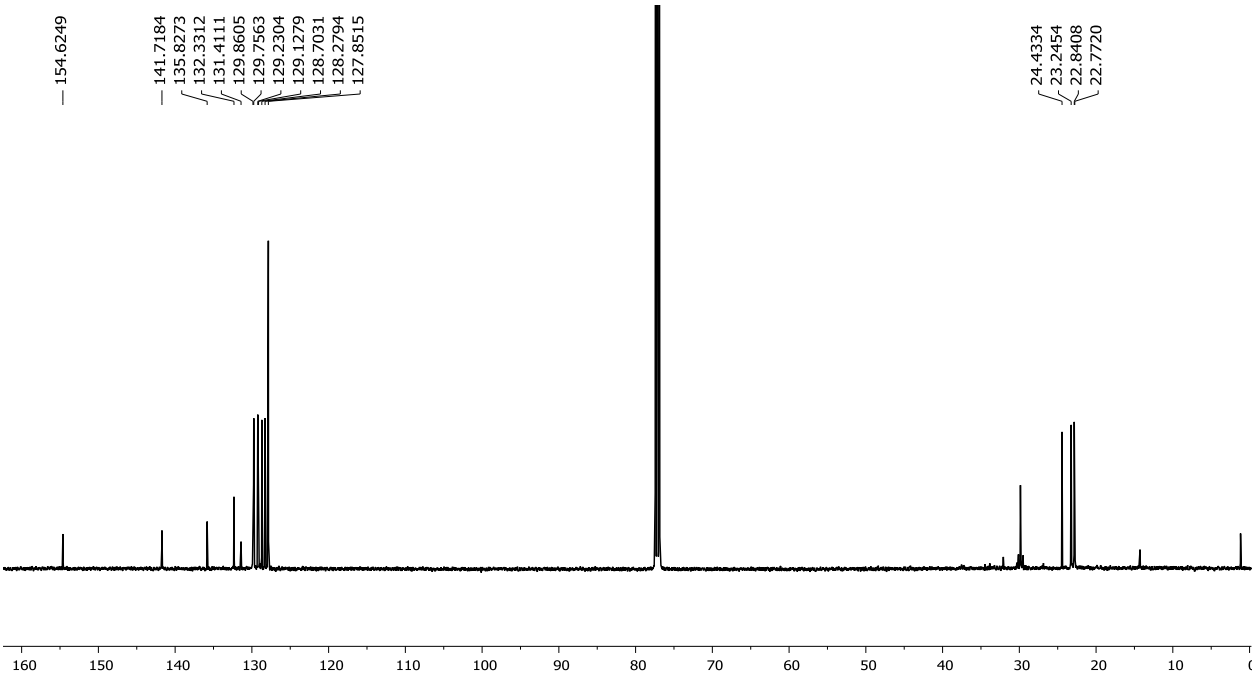

Figure C.6: ^{13}C NMR spectrum of BODIPY **2d** in $CDCl_3$

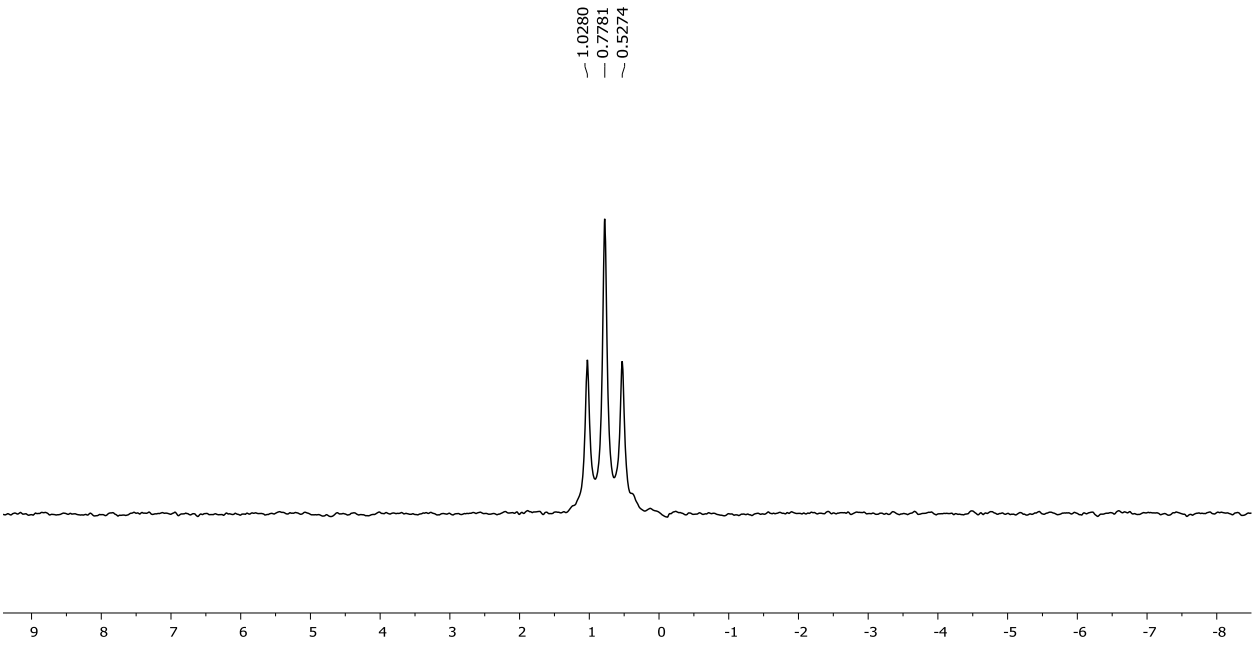

Figure C.7: ^{11}B NMR spectrum of BODIPY **2d** in $CDCl_3$

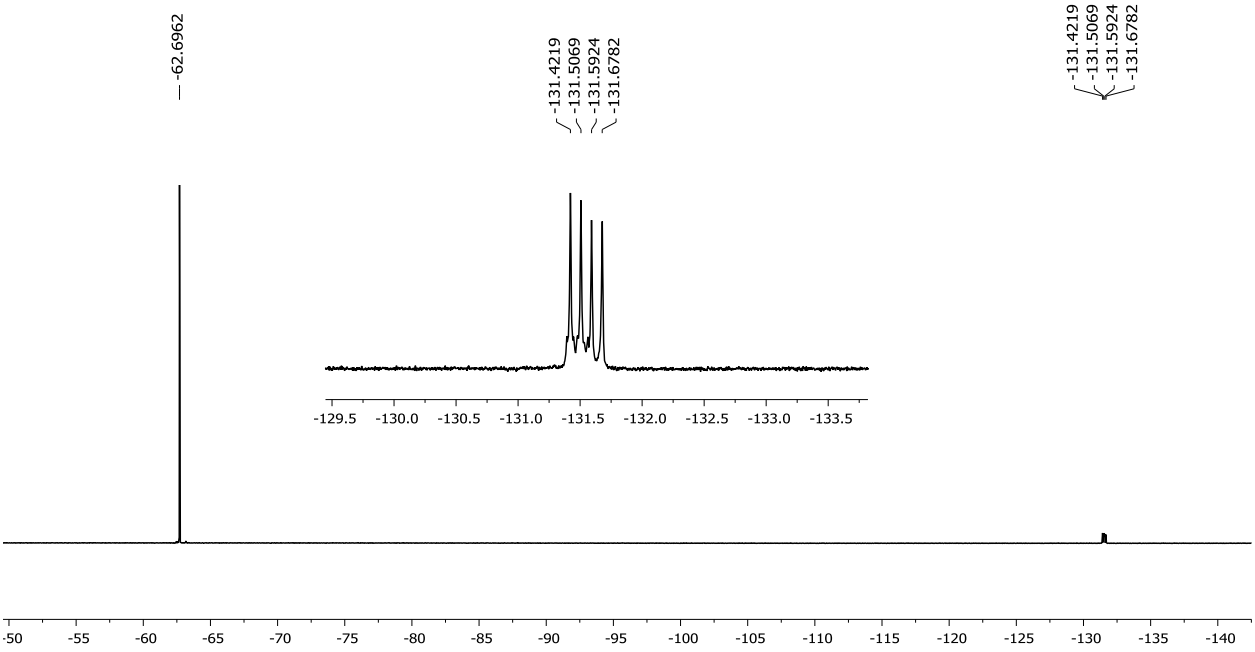

Figure C.8: ^{19}F NMR spectrum of BODIPY **2d** in $CDCl_3$

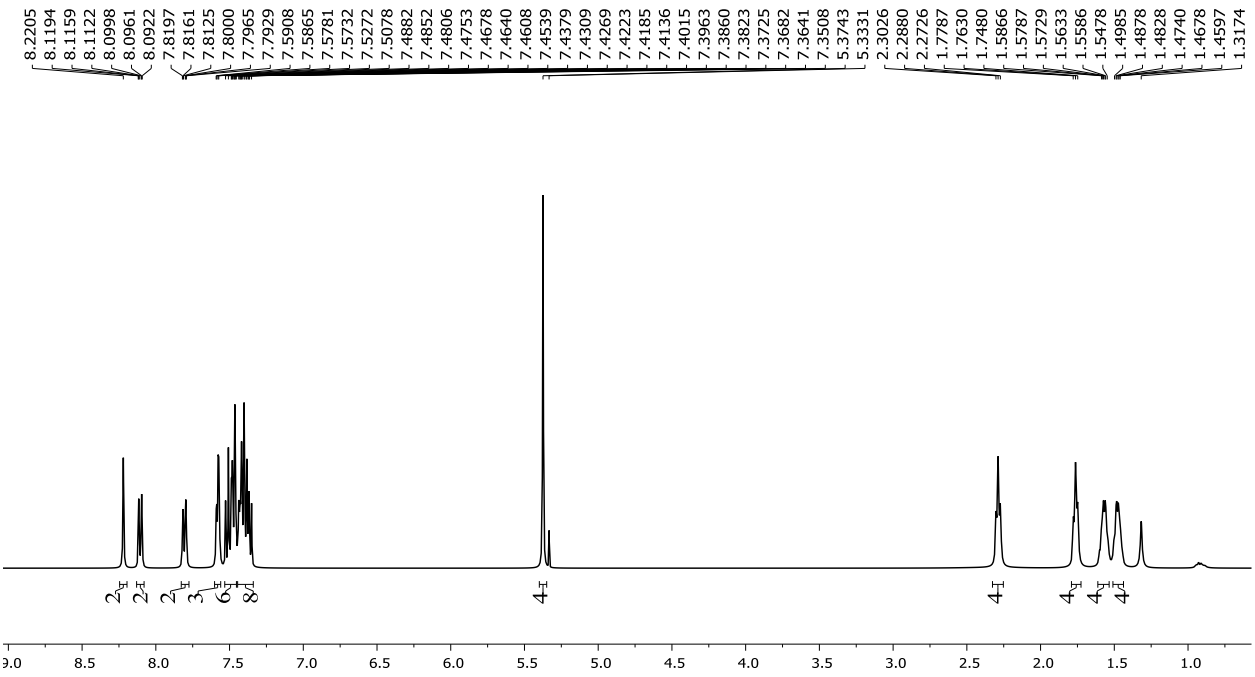

Figure C.9: ^{1}H NMR spectrum of BODIPY **2e** in CD_2Cl_2

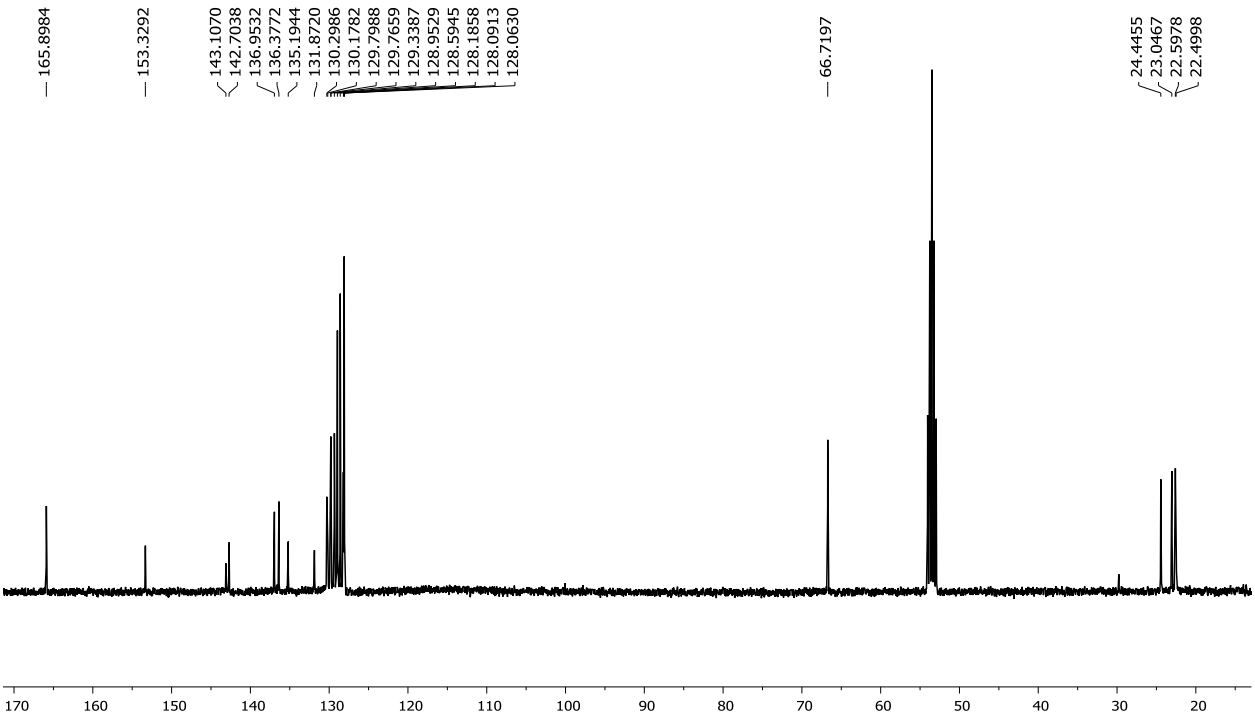

Figure C.10: ^{13}C NMR spectrum of BODIPY **2e** in CD_2Cl_2

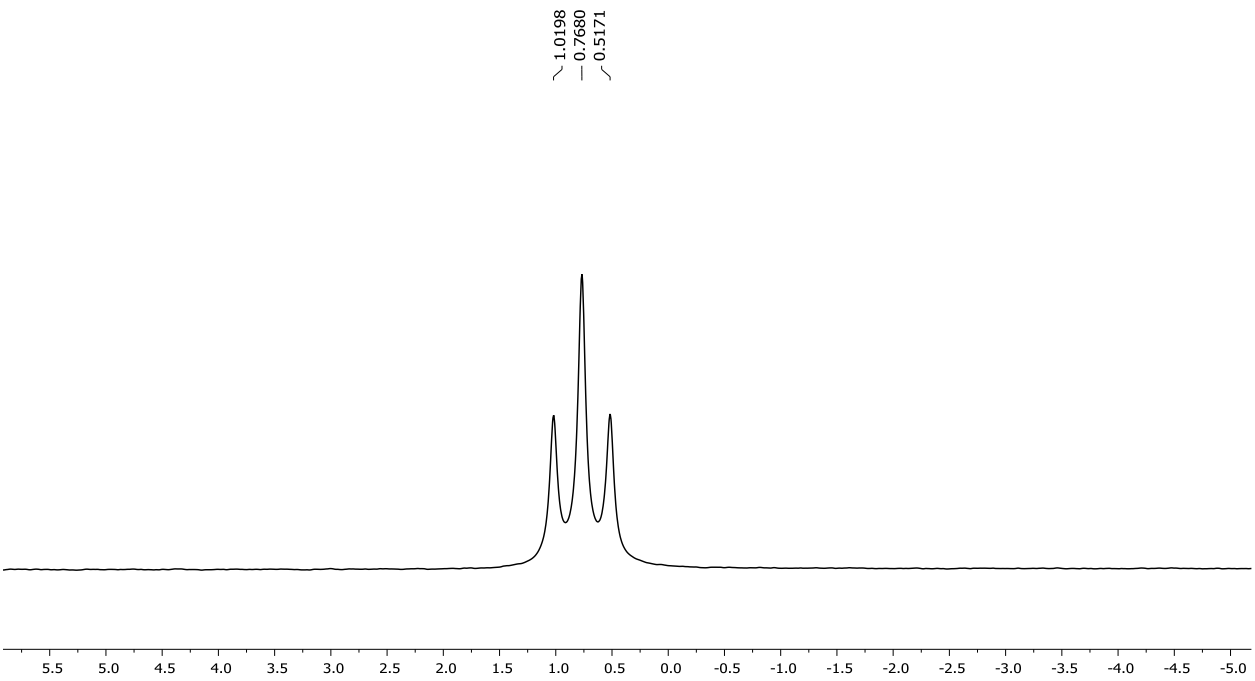

Figure C.11: ^{11}B NMR spectrum of BODIPY **2e** in CD_2Cl_2

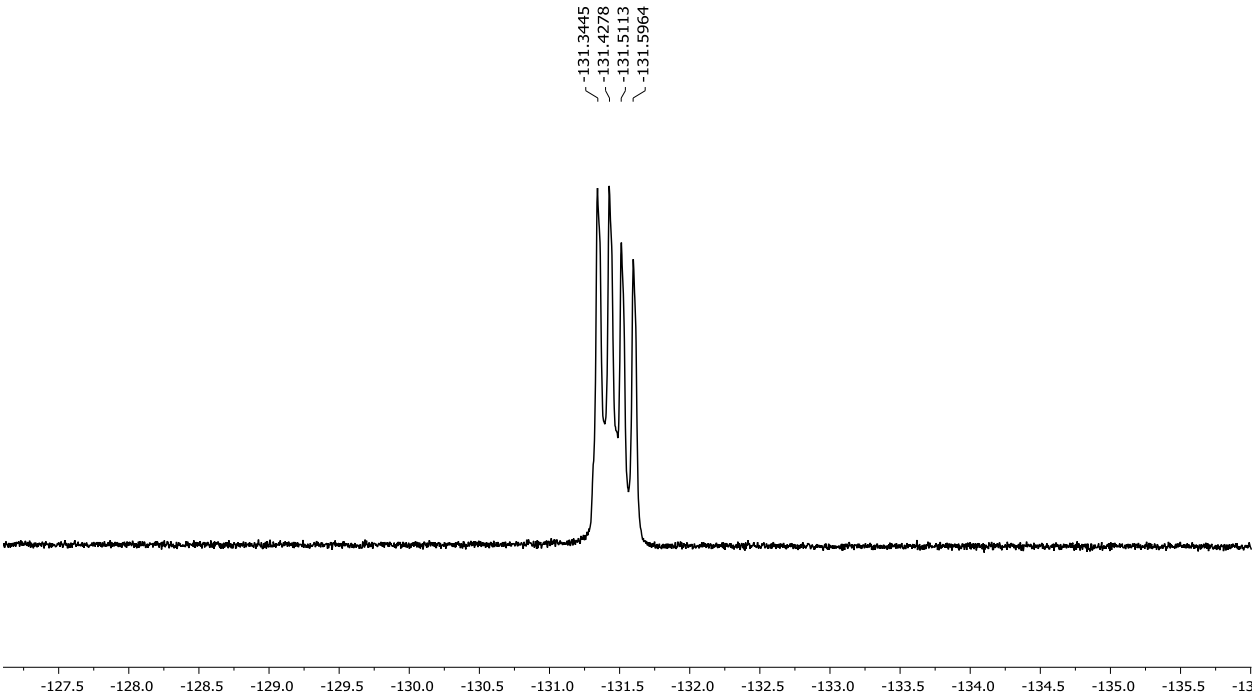

Figure C.12: ^{11}B NMR spectrum of BODIPY **2e** in CD_2Cl_2

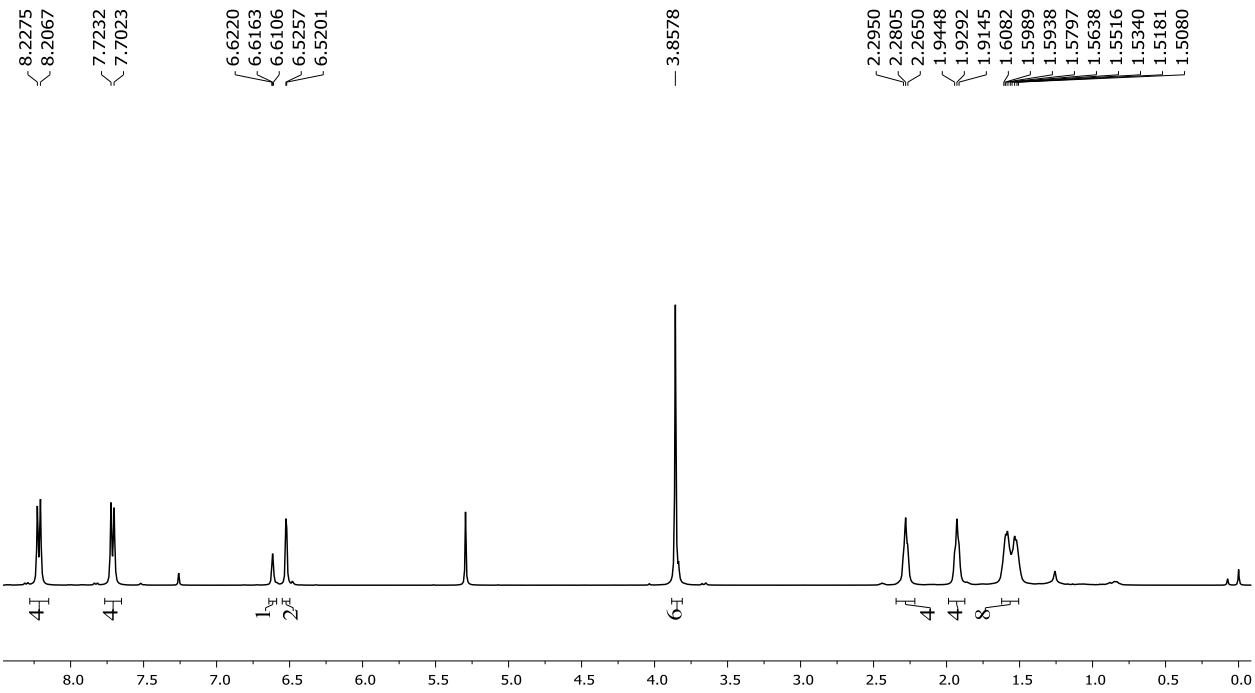

Figure C.13: ^{1}H NMR spectrum of BODIPY **2f** in $CDCl_3$

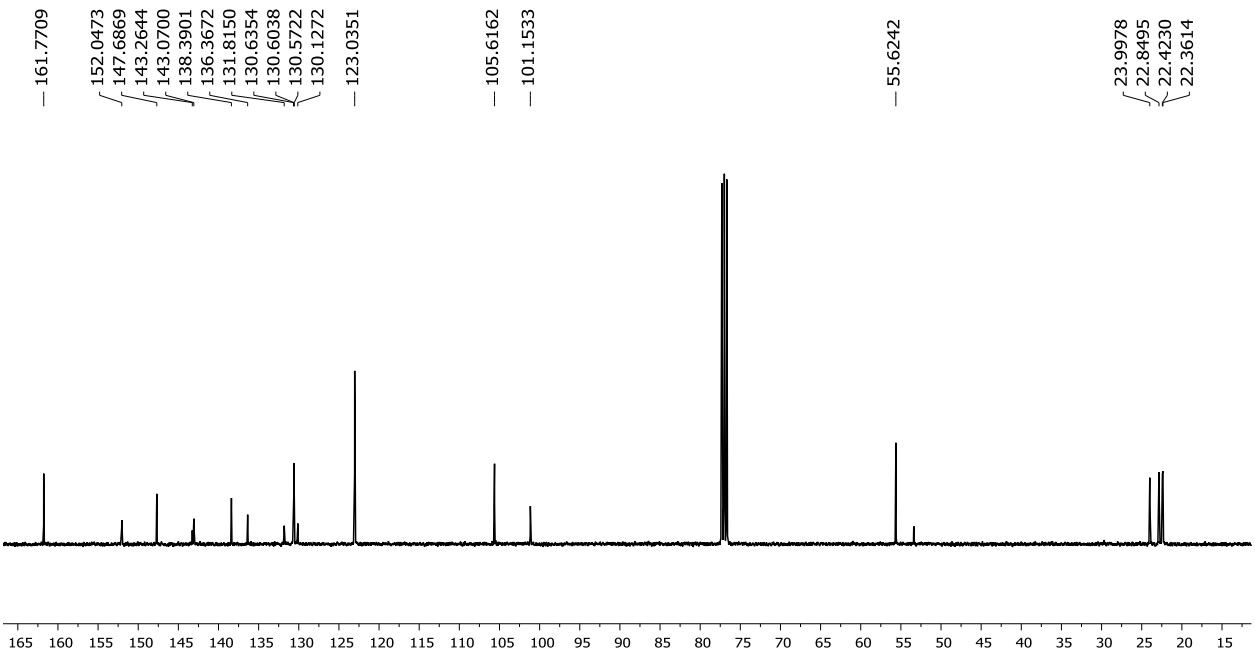

Figure C.14: ^{13}C NMR spectrum of BODIPY **2f** in $CDCl_3$

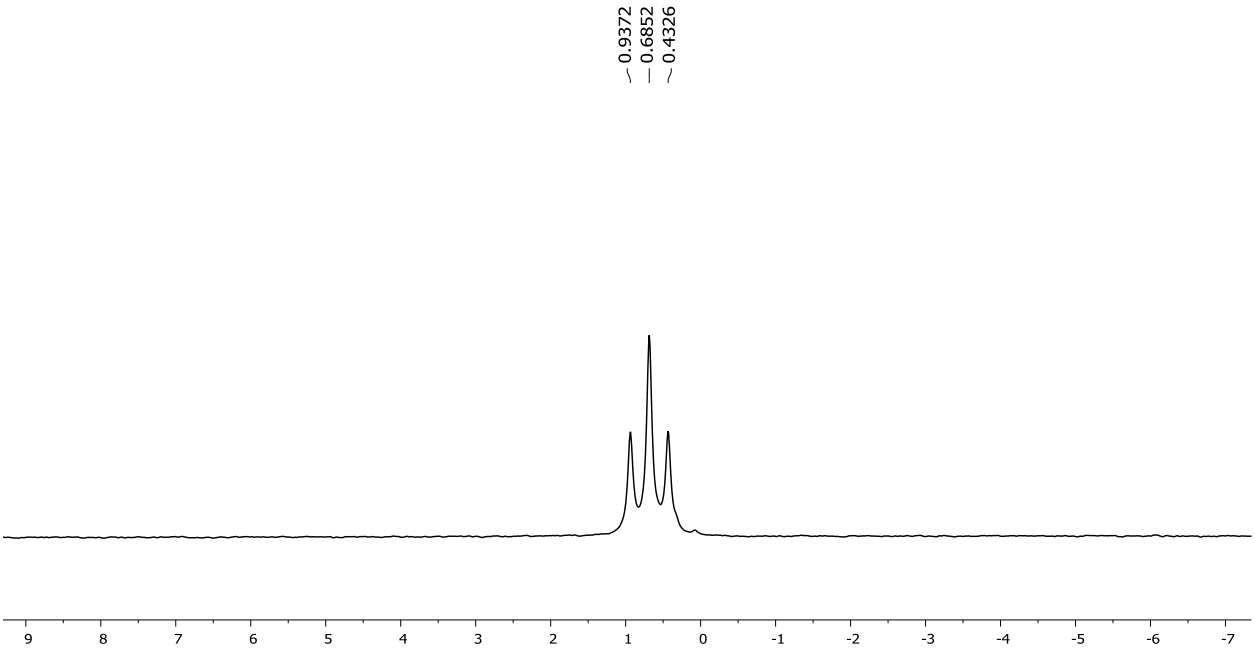

Figure C.15: ^{11}B NMR spectrum of BODIPY **2f** in $CDCl_3$

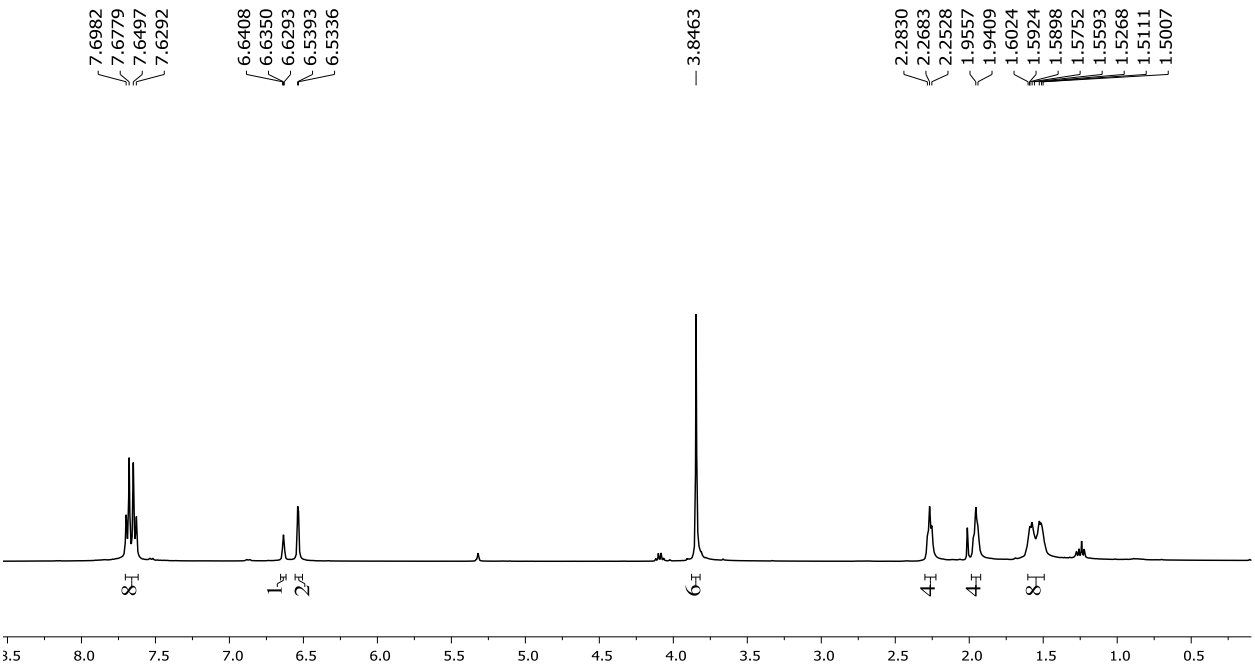

Figure C.16: ^{1}H NMR spectrum of BODIPY **2g** in CD_2Cl_2

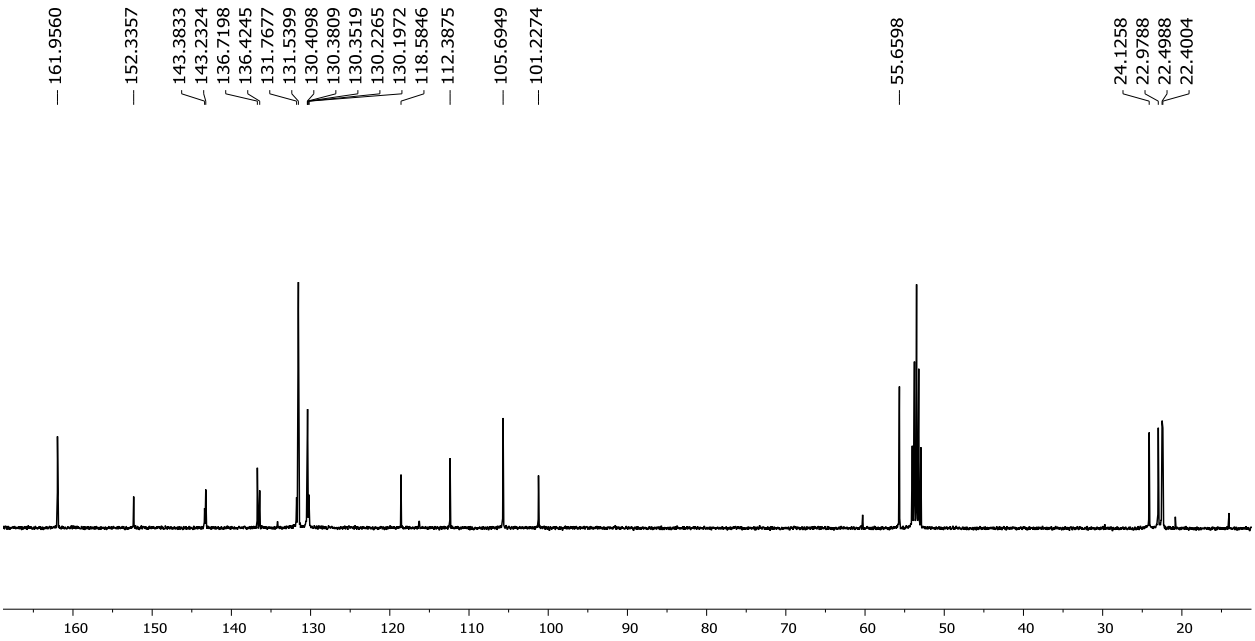

Figure C.17: ^{13}C NMR spectrum of BODIPY **2g** in CD_2Cl_2

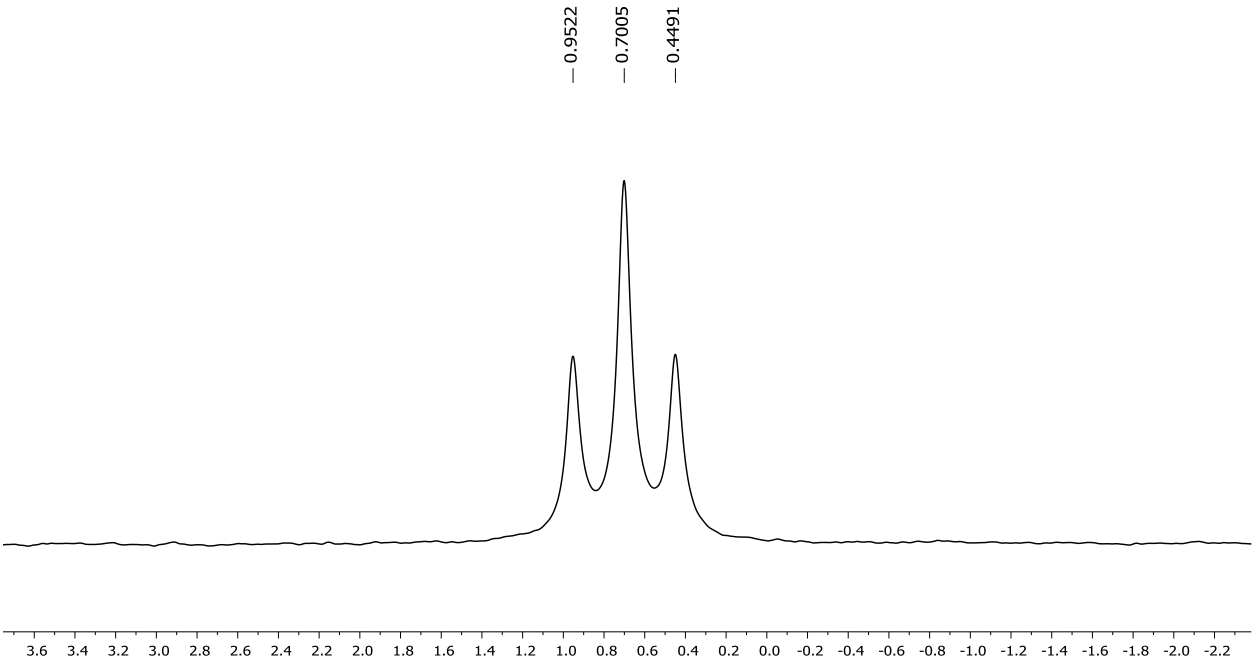

Figure C.18: ^{11}B NMR spectrum of BODIPY **2g** in CD_2Cl_2

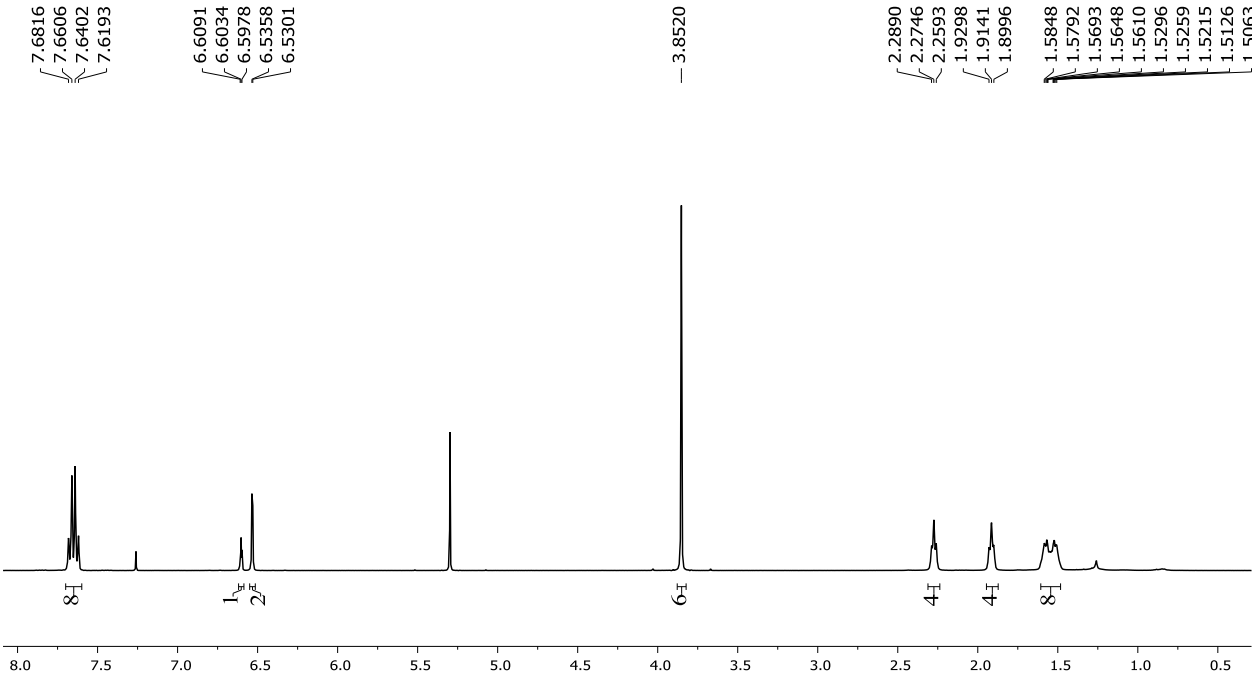

Figure C.19: ^{1}H NMR spectrum of BODIPY **2h** in $CDCl_3$

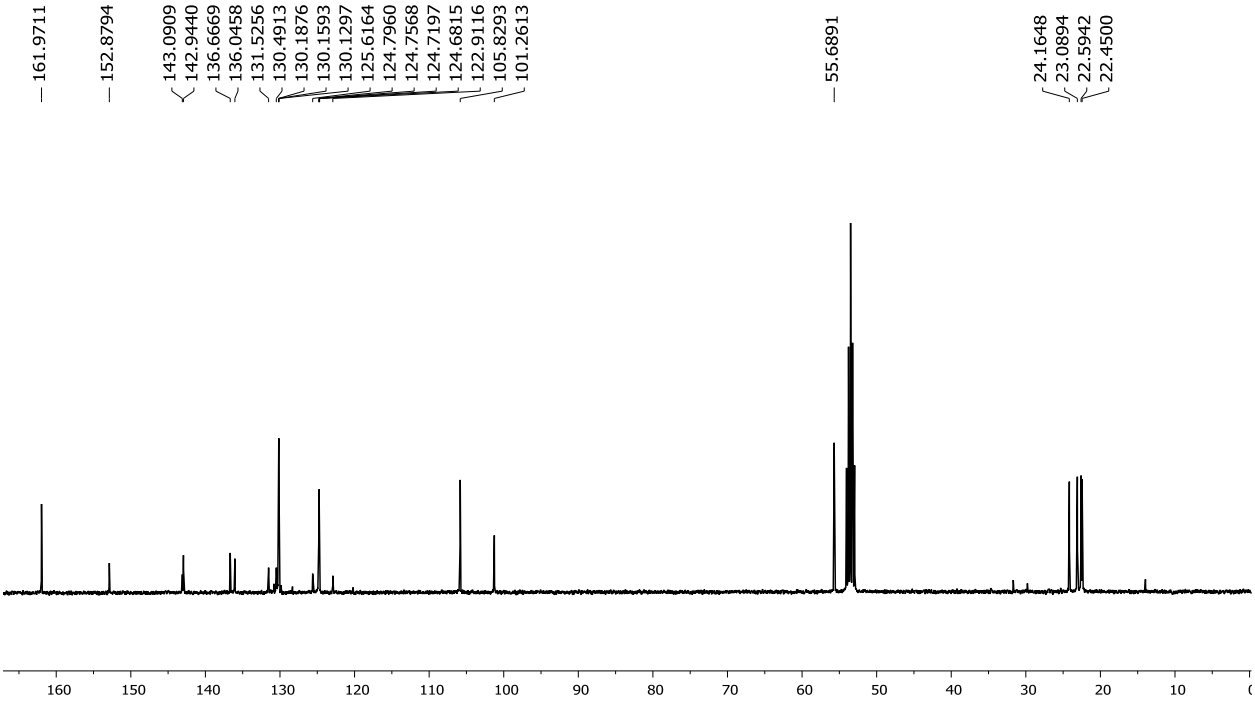

Figure C.20: ^{13}C NMR spectrum of BODIPY **2h** in CD_2Cl_2

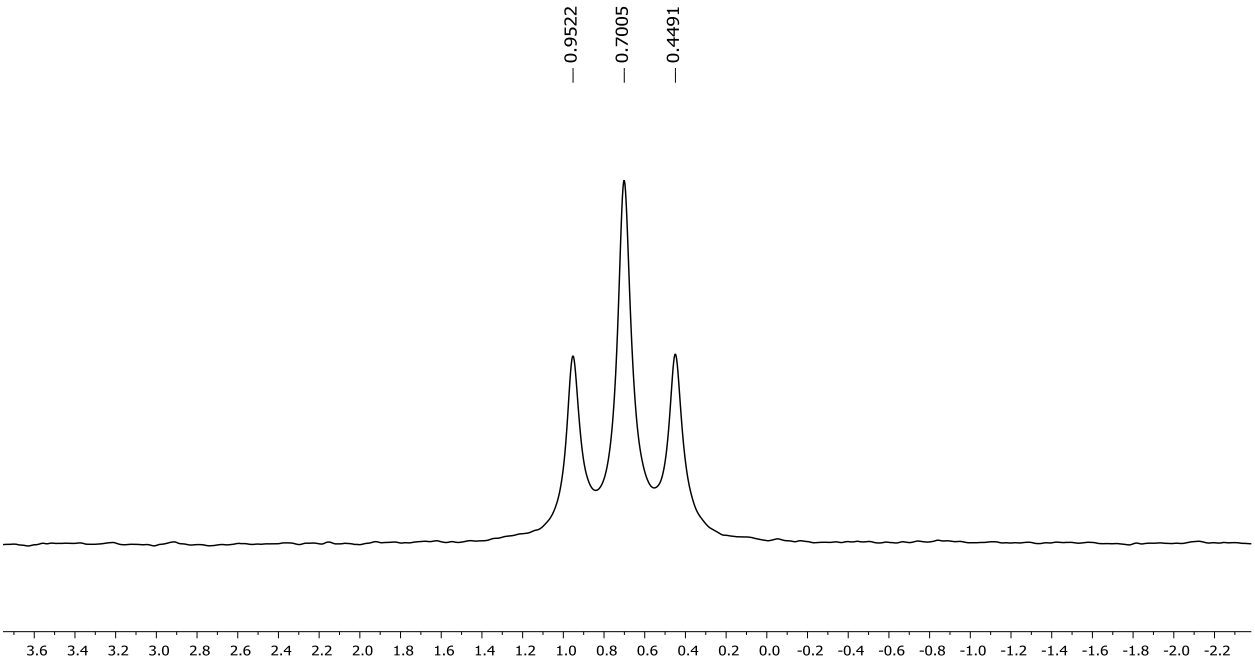

Figure C.21: ^{11}B NMR spectrum of BODIPY **2h** in CD_2Cl_2

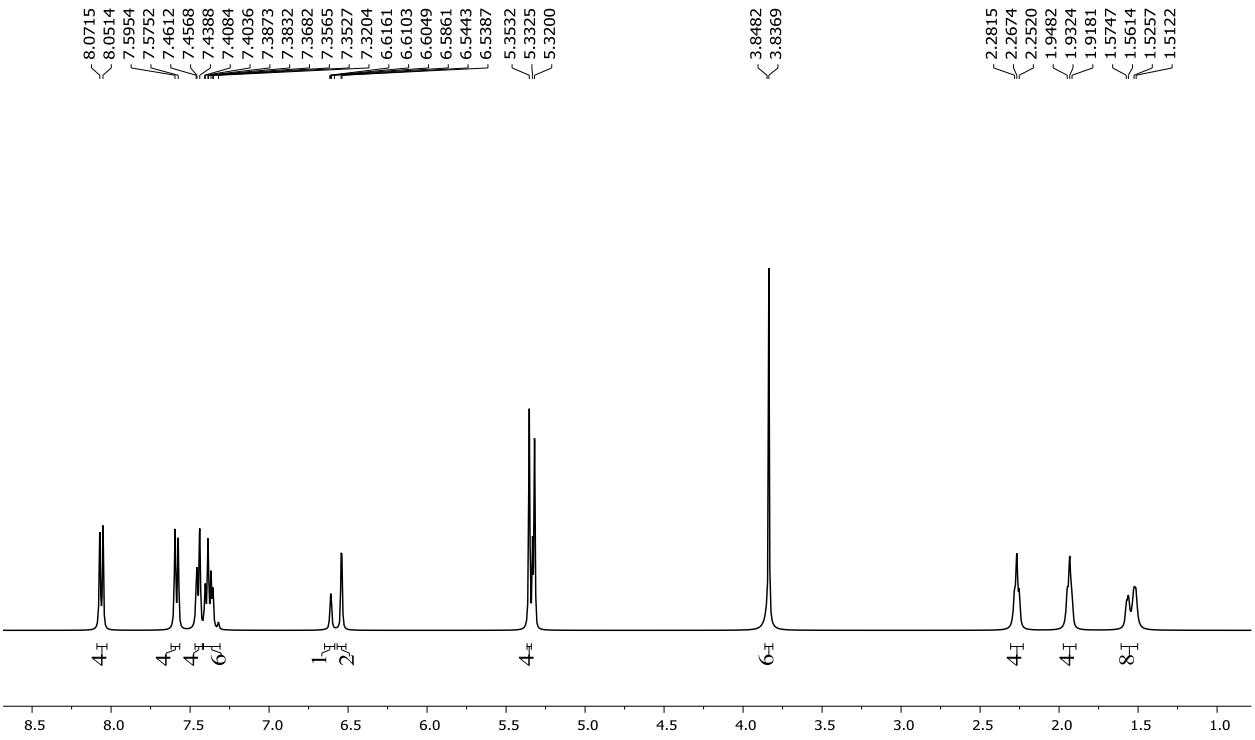

Figure C.22: ^{1}H NMR spectrum of BODIPY **2i** in CD_2Cl_2

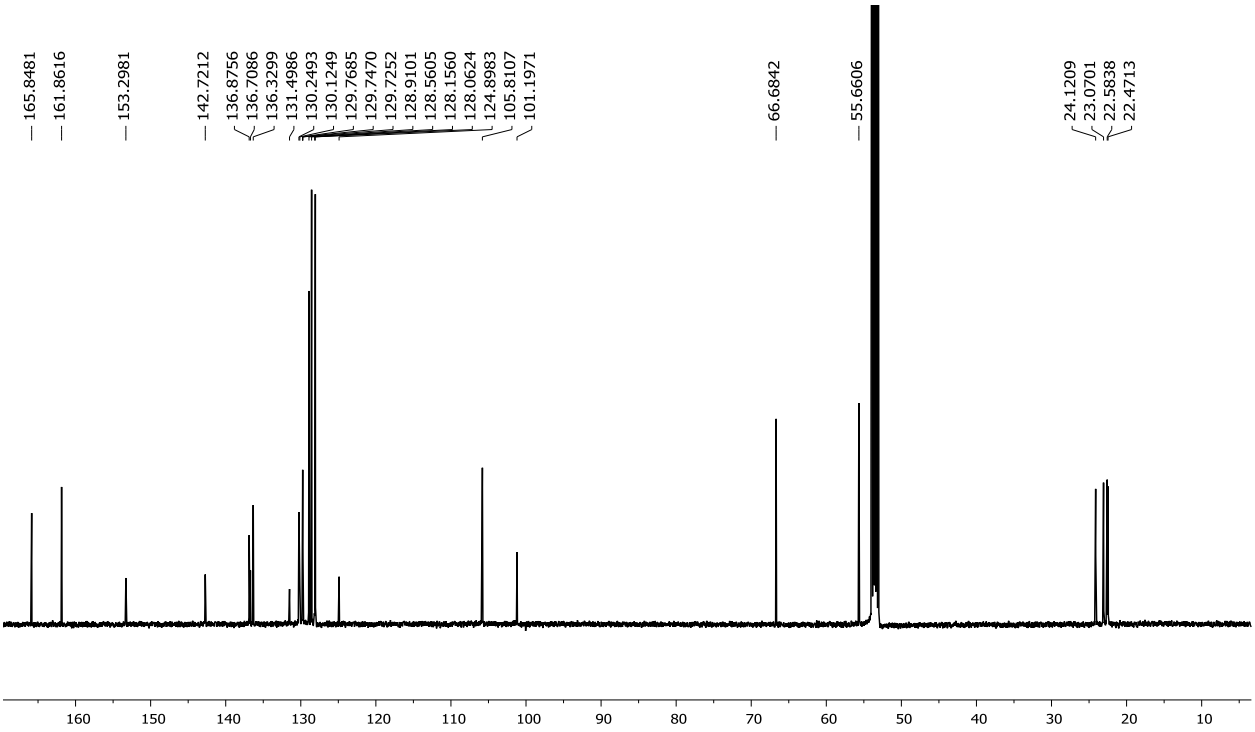

Figure C.23: ^{13}C NMR spectrum of BODIPY **2i** in CD_2Cl_2

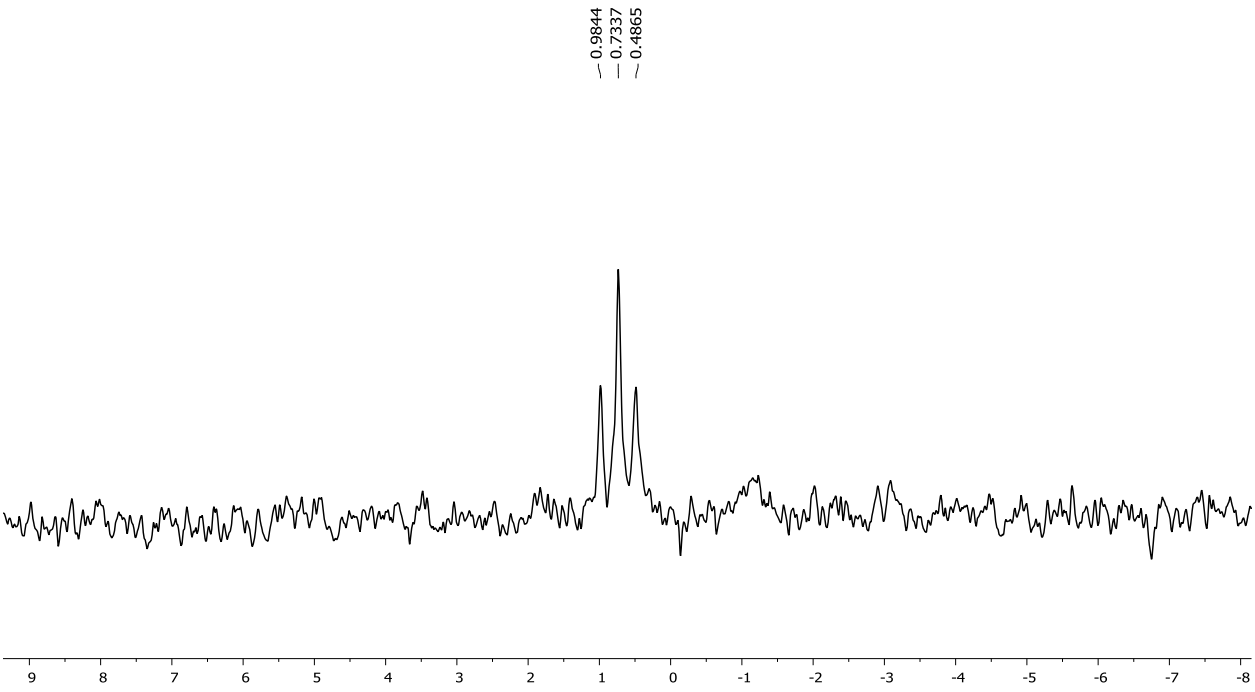

Figure C.24: ^{11}B NMR spectrum of BODIPY **2i** in CD_2Cl_2

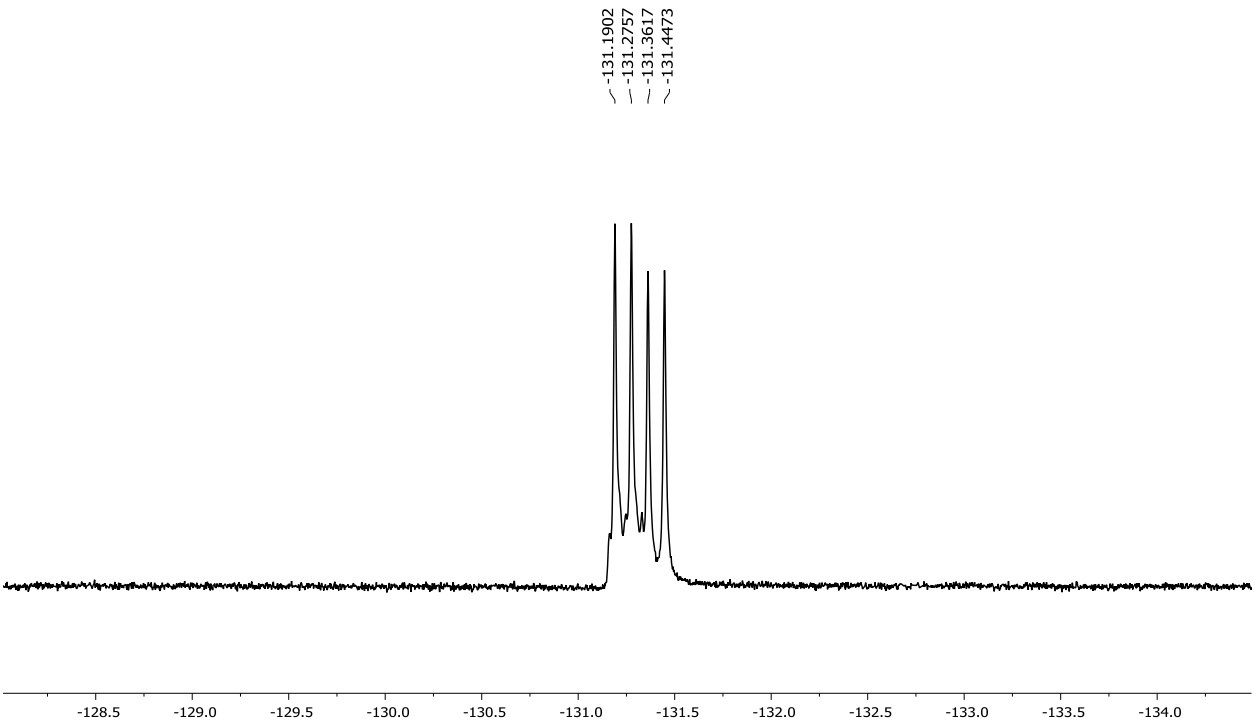

Figure C.25: ^{19}F NMR spectrum of BODIPY **2i** in CD_2Cl_2

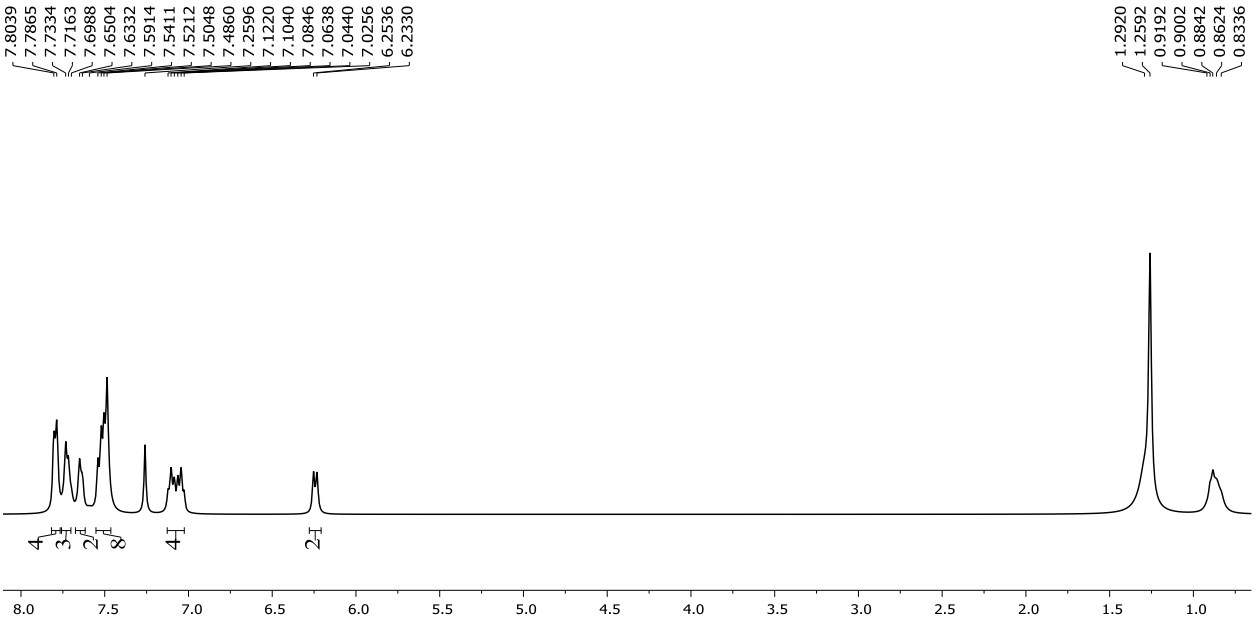

Figure C.26: ^{1}H NMR spectrum of BODIPY **4a** in $CDCl_3$

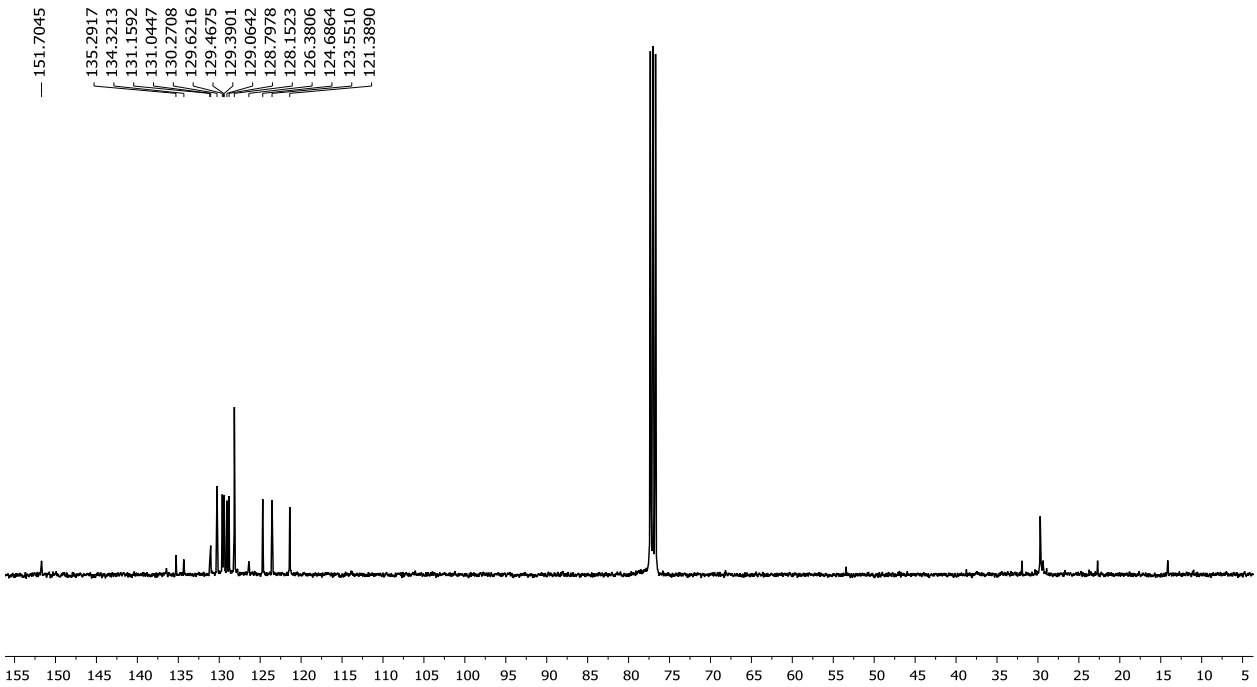

Figure C.27: ^{13}C NMR spectrum of BODIPY **4a** in $CDCl_3$

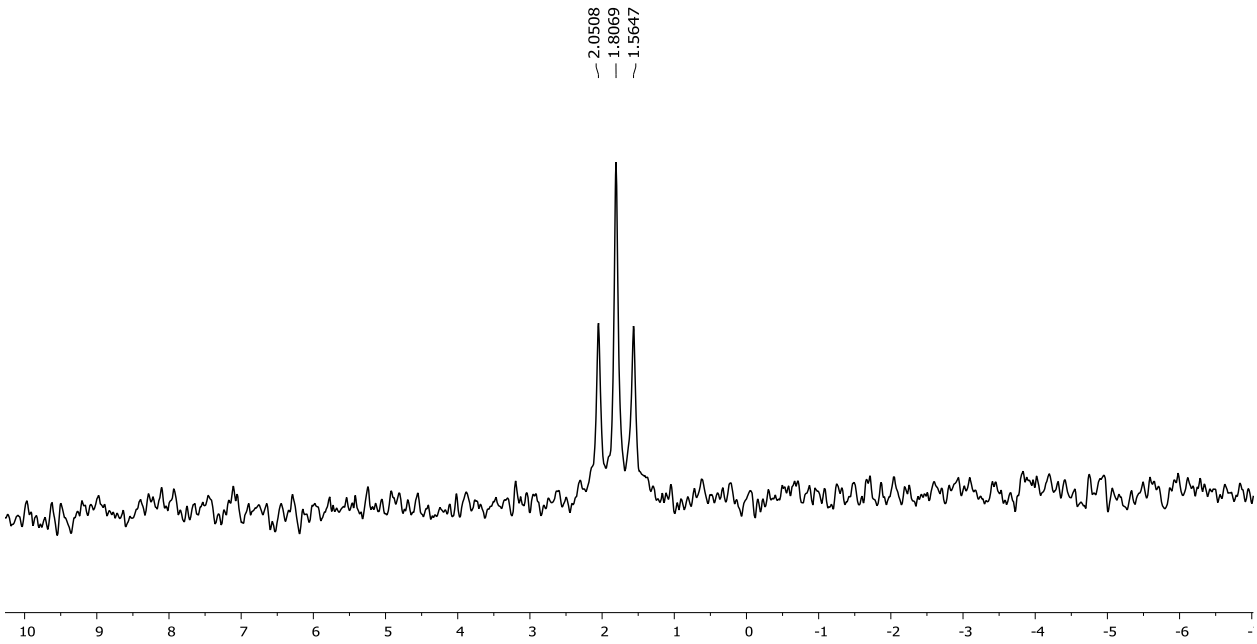

Figure C.28: ^{11}B NMR spectrum of BODIPY **4a** in $CDCl_3$

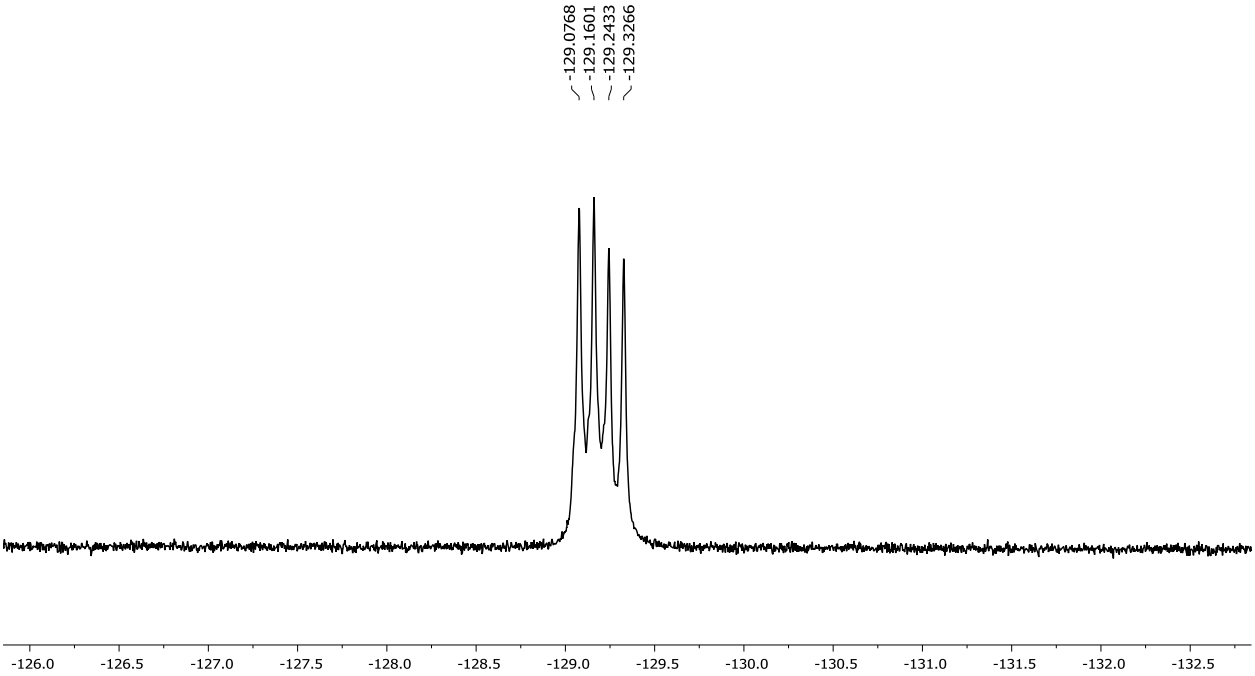

Figure C.29: ^{19}F NMR spectrum of BODIPY **4a** in $CDCl_3$

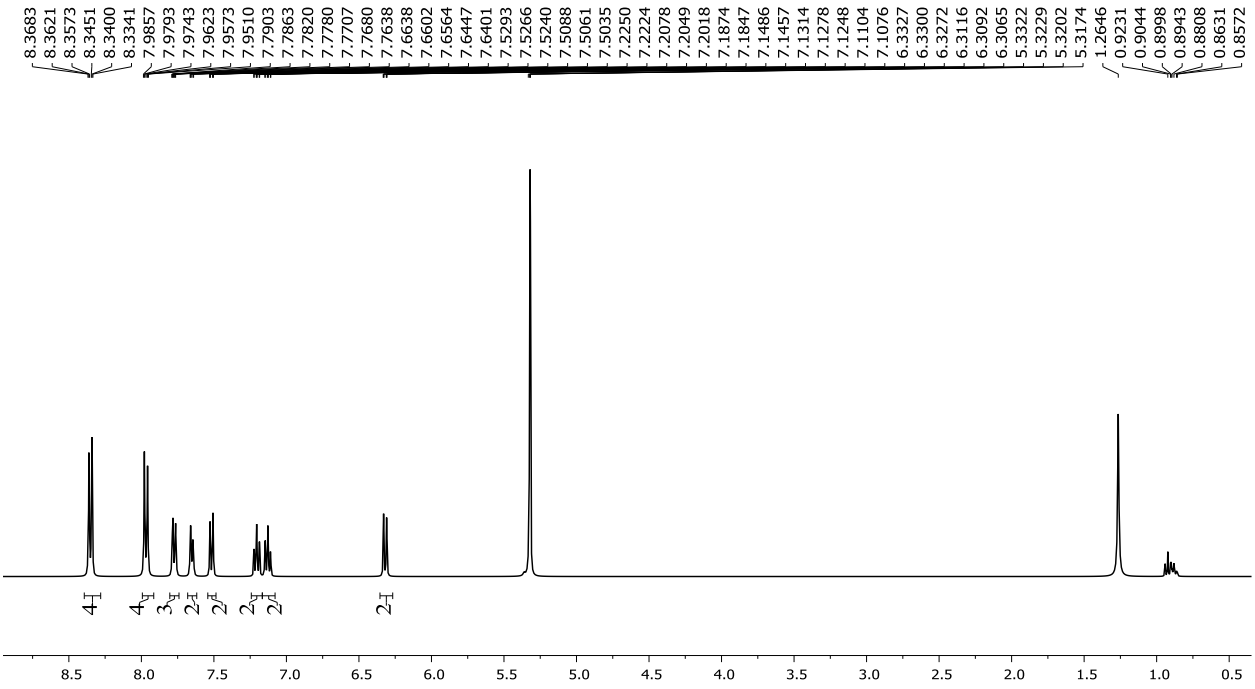

Figure C.30: ^{1}H NMR spectrum of BODIPY **4b** in CD_2Cl_2

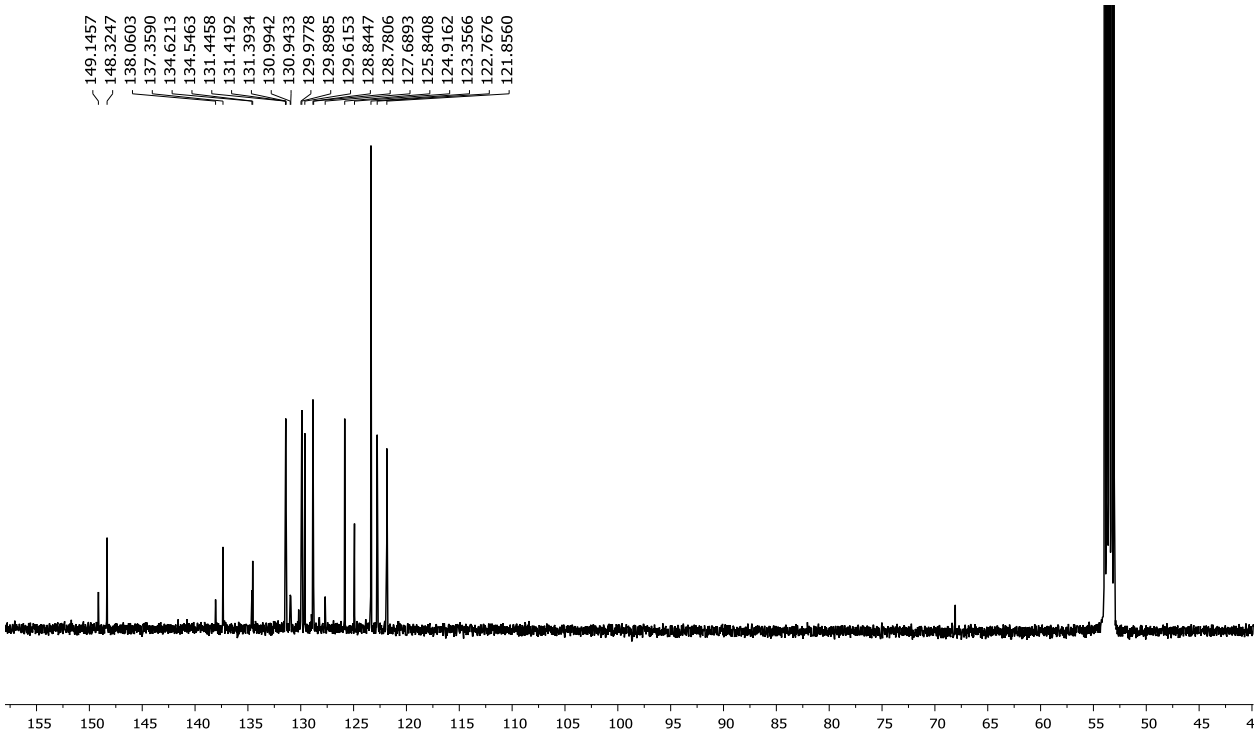

Figure C.31: ^{13}C NMR spectrum of BODIPY **4b** in CD_2Cl_2

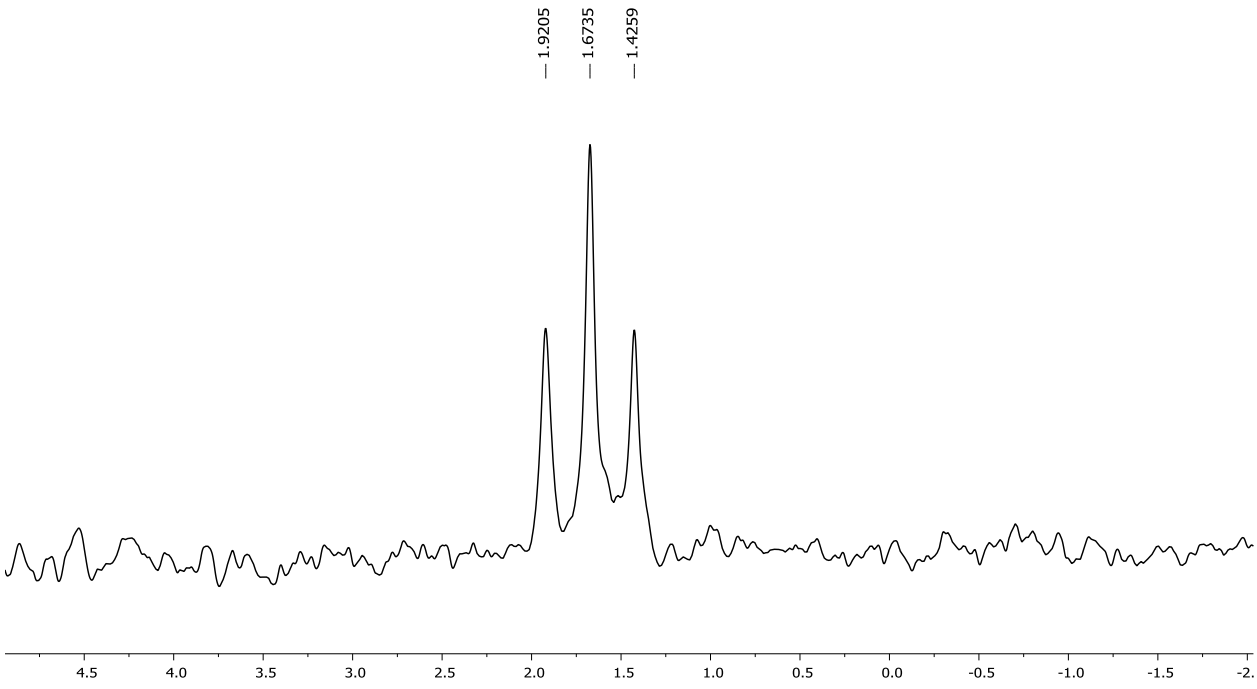

Figure C.32: ^{11}B NMR spectrum of BODIPY **4b** in CD_2Cl_2

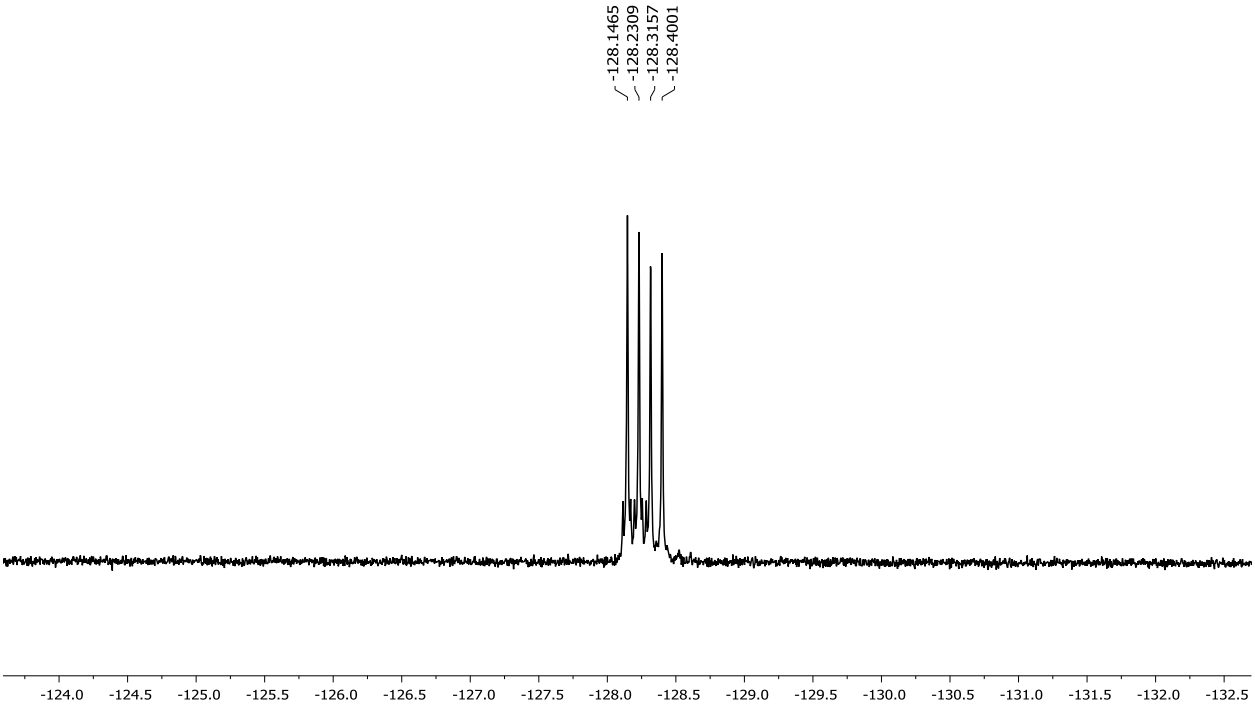

Figure C.33: ^{19}F NMR spectrum of BODIPY **4b** in CD_2Cl_2

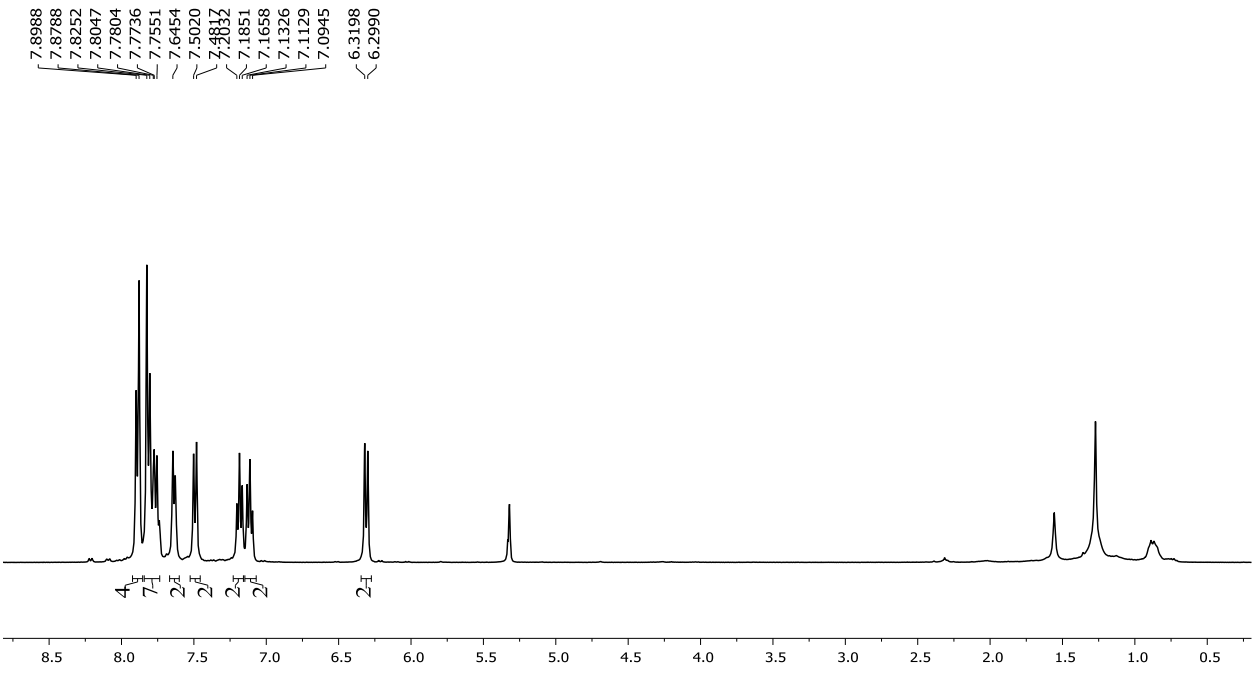

Figure C.34: ^{1}H NMR spectrum of BODIPY **4c** in CD_2Cl_2

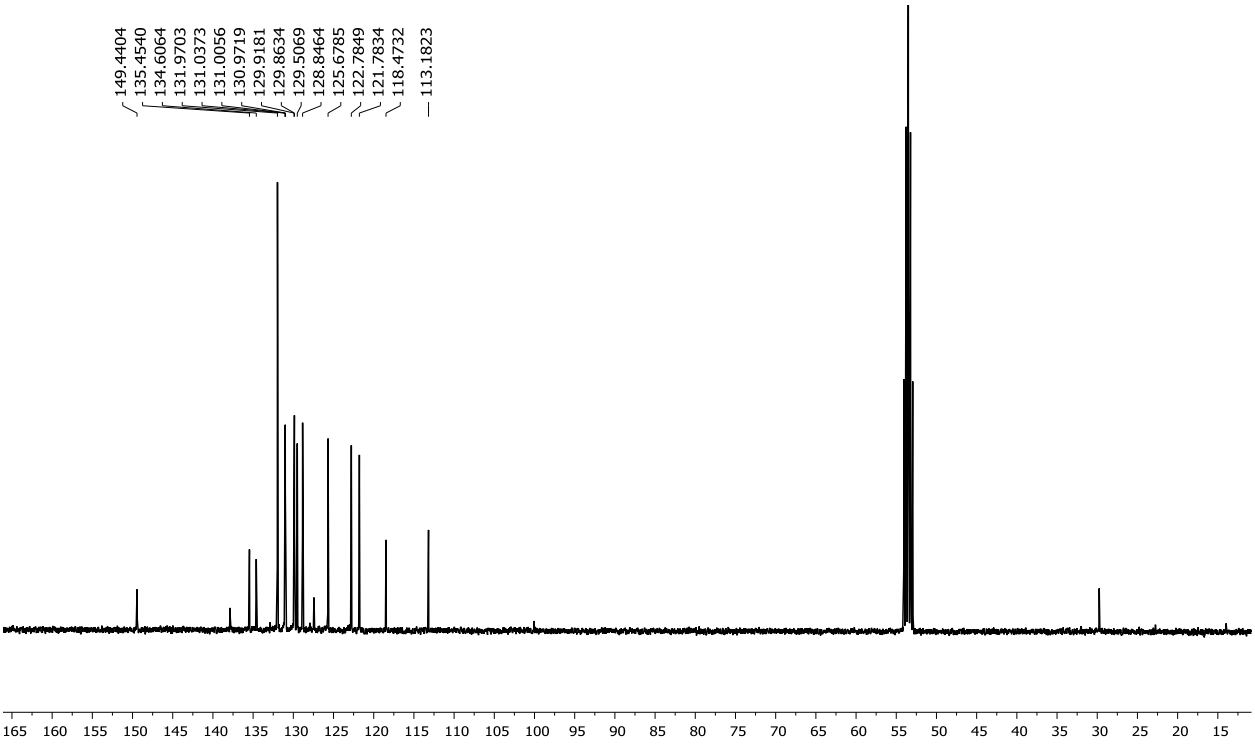

Figure C.35: ^{13}C NMR spectrum of BODIPY **2h** in CD_2Cl_2

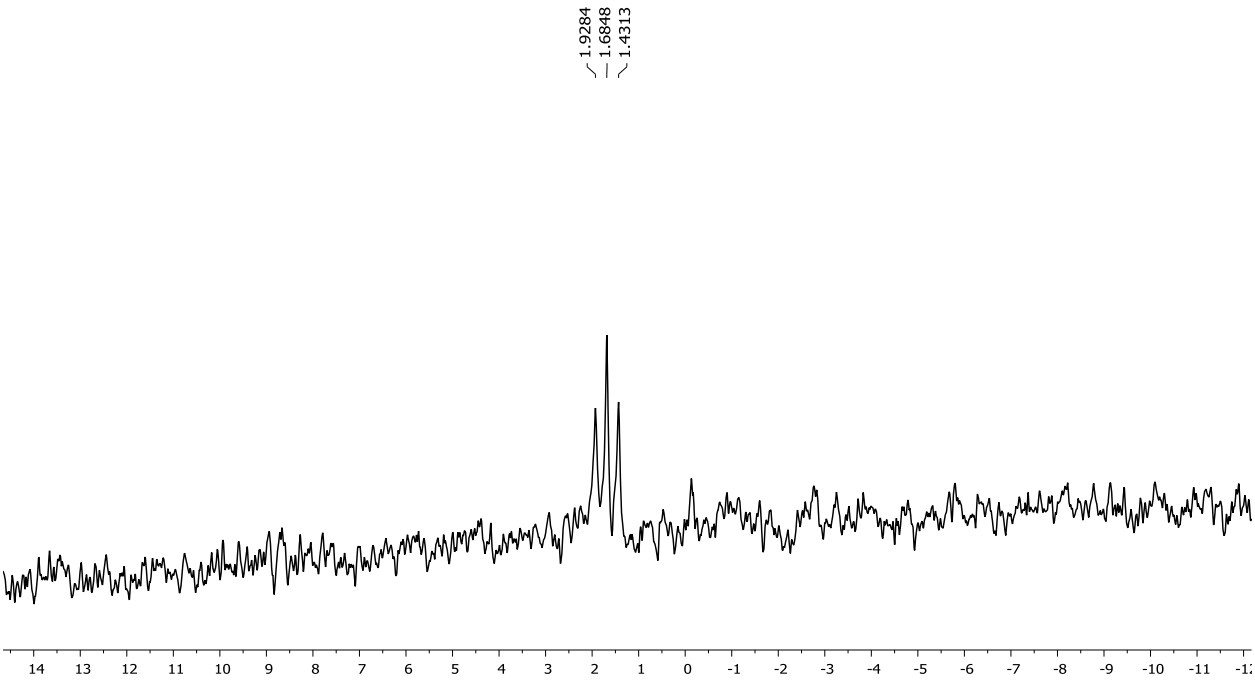

Figure C.36: ^{11}B NMR spectrum of BODIPY **4c** in CD_2Cl_2

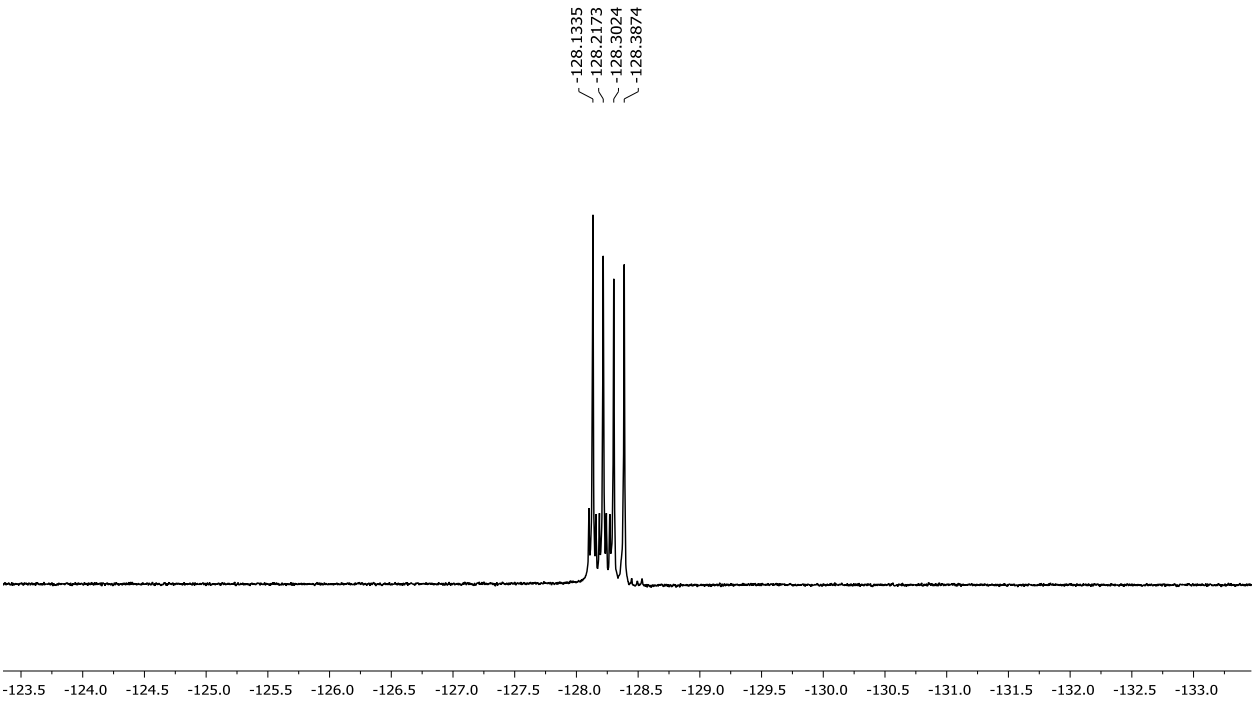

Figure C.37: ^{19}F NMR spectrum of BODIPY **4c** in CD_2Cl_2

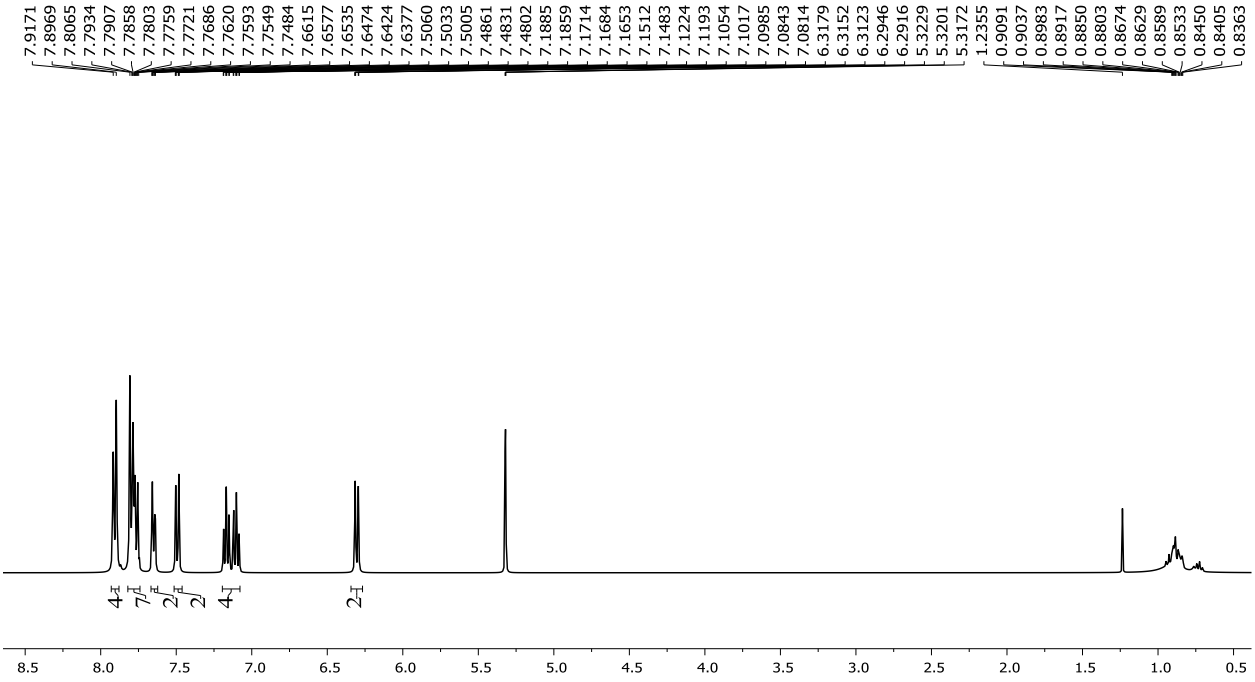

Figure C.38: ^{1}H NMR spectrum of BODIPY **4d** in CD_2Cl_2

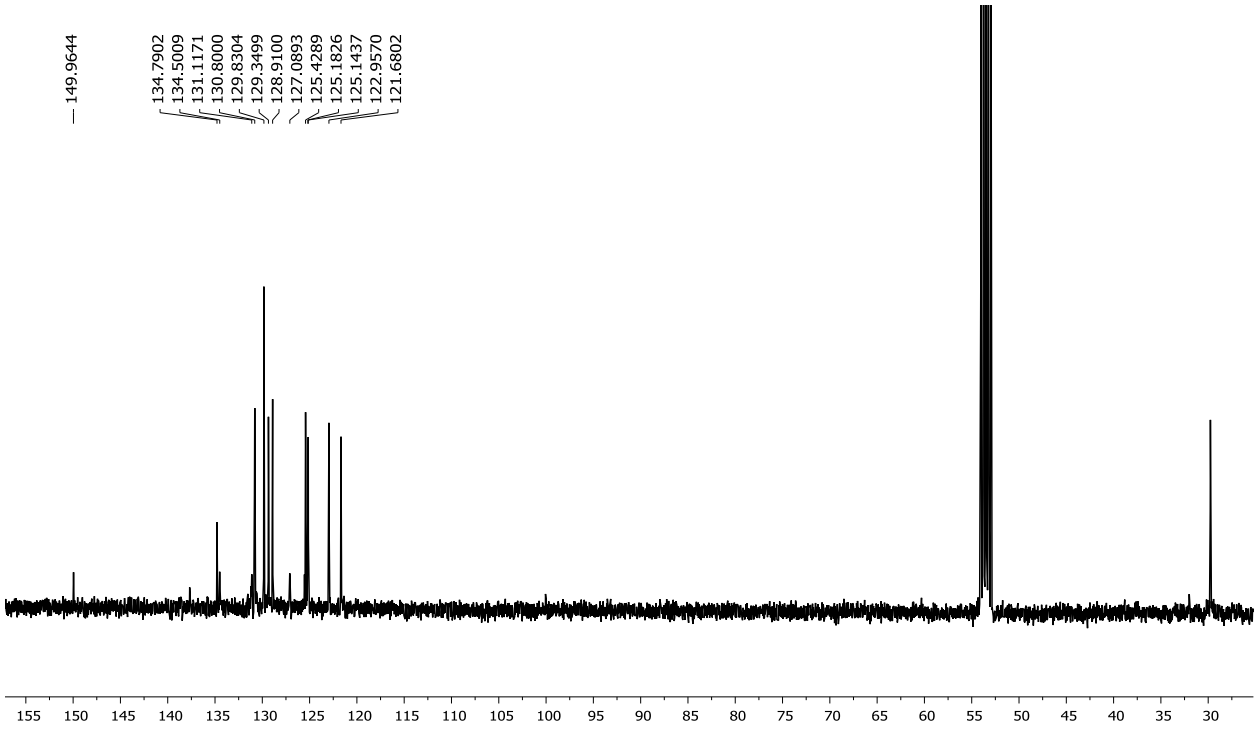

Figure C.39: ^{13}C NMR spectrum of BODIPY **4d** in CD_2Cl_2

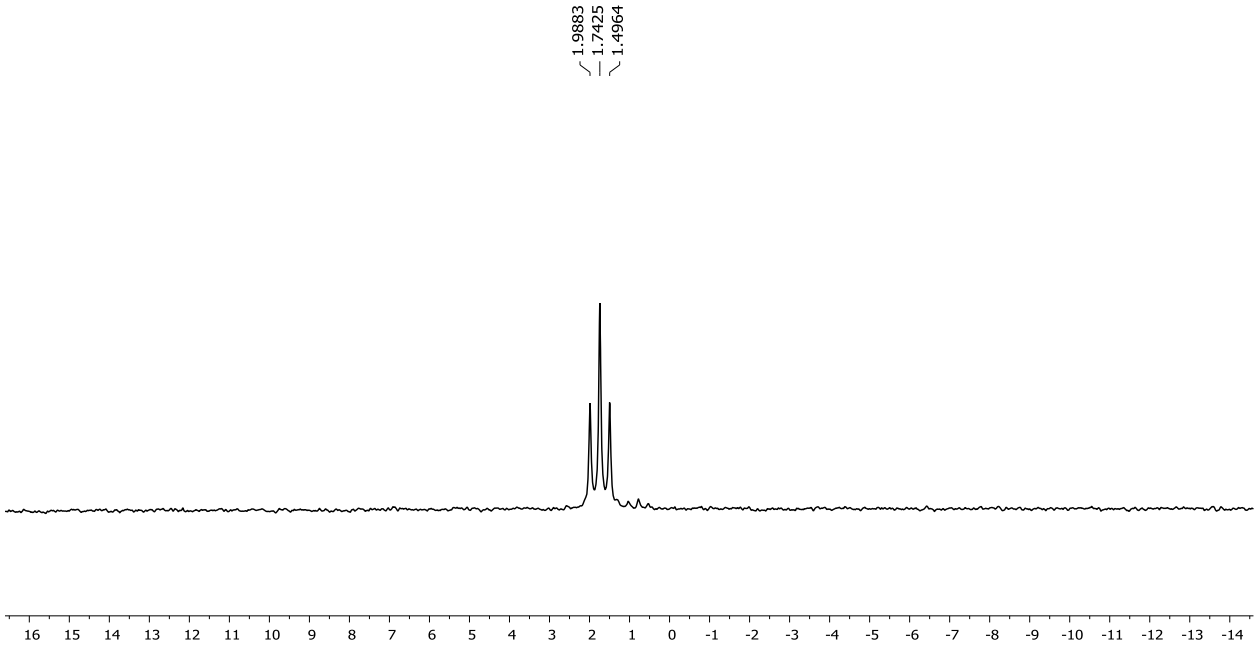

Figure C.40: ^{11}B NMR spectrum of BODIPY **4d** in CD_2Cl_2

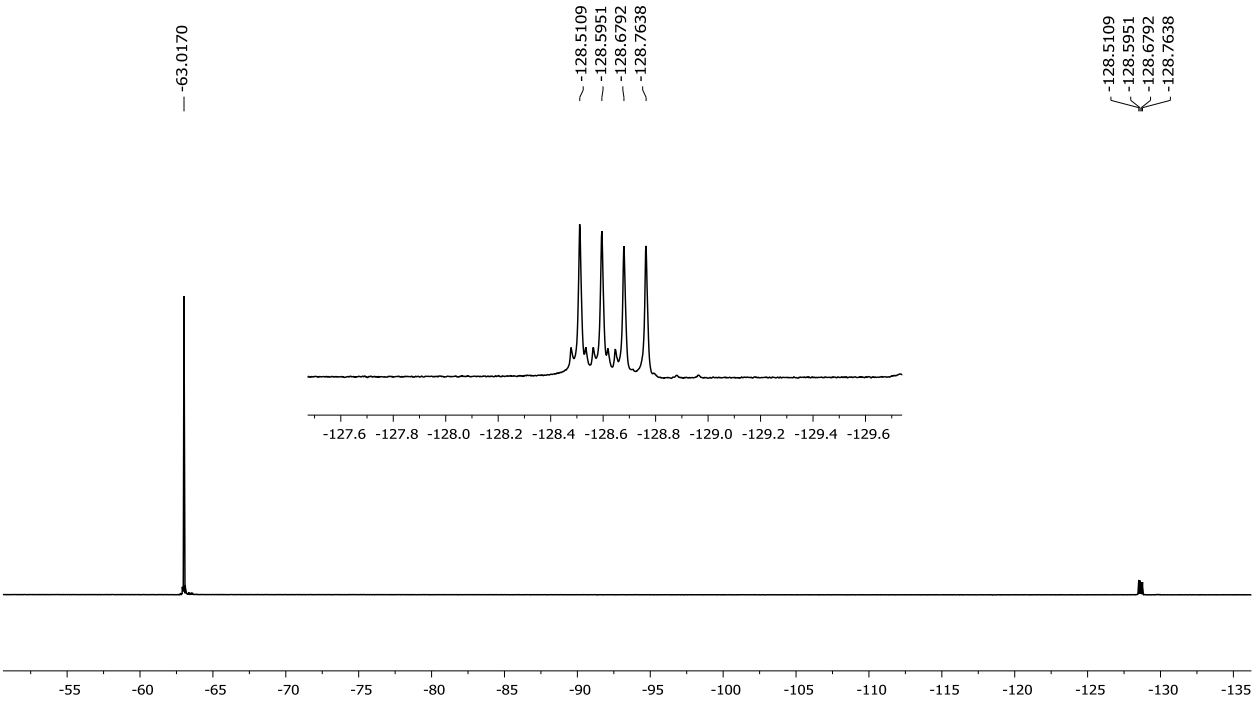

Figure C.41: ^{19}F NMR spectrum of BODIPY **4d** in CD_2Cl_2

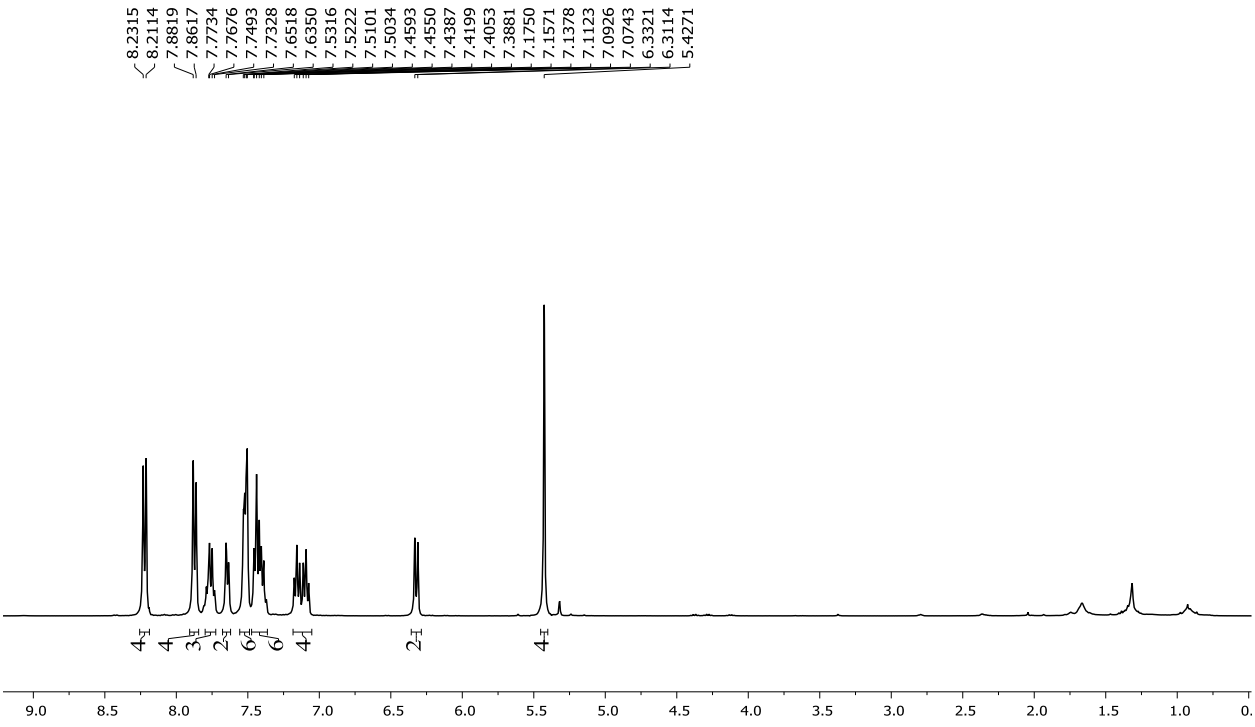

Figure C.42: ^{1}H NMR spectrum of BODIPY **4e** in CD_2Cl_2

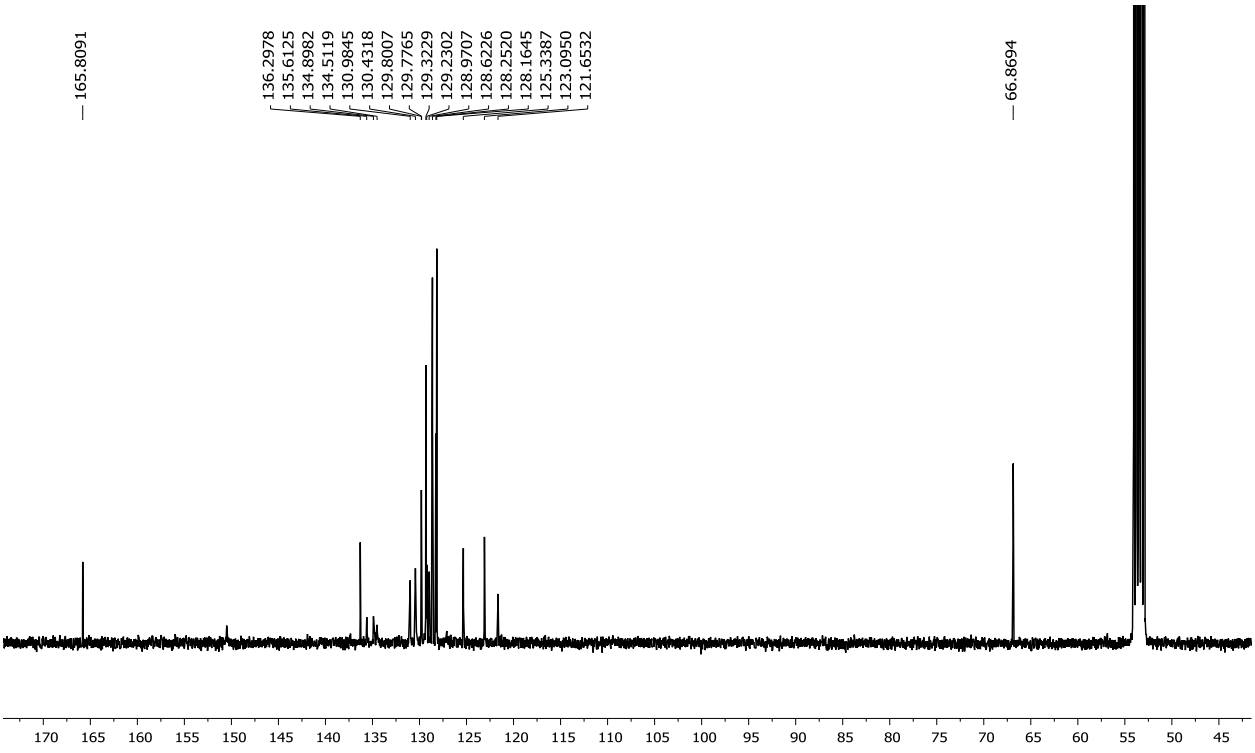

Figure C.43: ^{13}C NMR spectrum of BODIPY **4e** in CD_2Cl_2

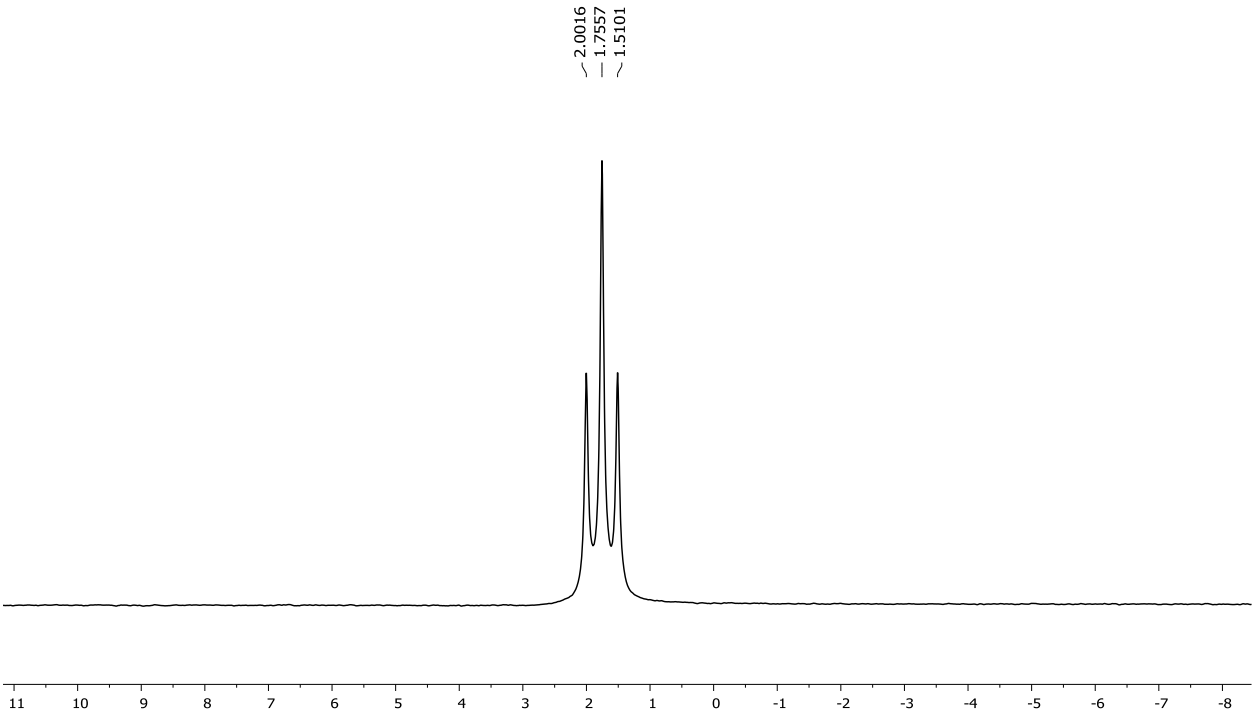

Figure C.44: ^{11}B NMR spectrum of BODIPY **4e** in CD_2Cl_2

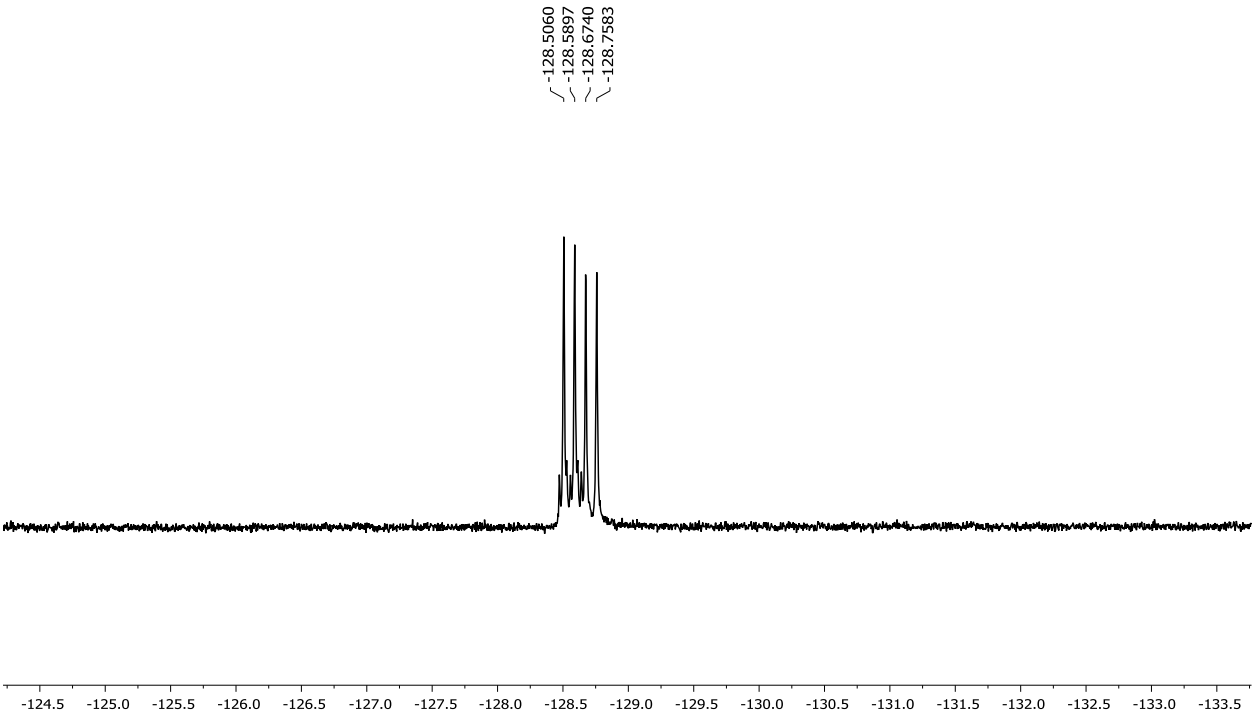

Figure C.45: ^{19}F NMR spectrum of BODIPY **4e** in CD_2Cl_2

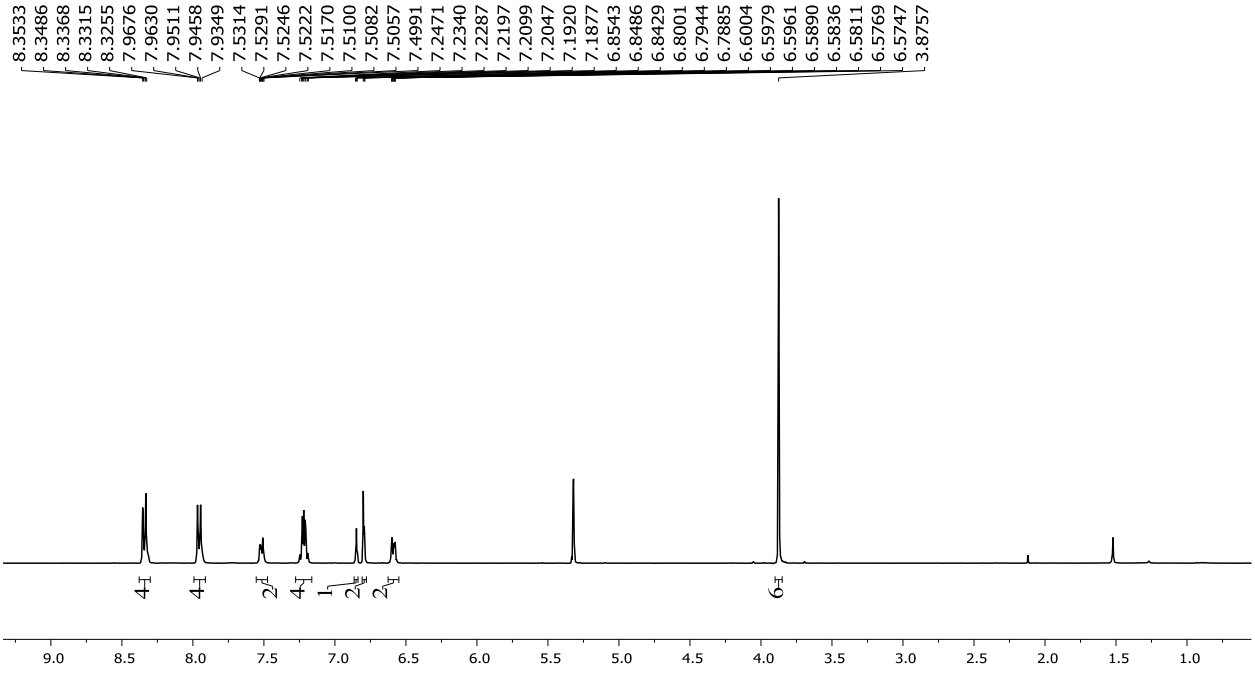

Figure C.46: ^{1}H NMR spectrum of BODIPY **4f** in CD_2Cl_2

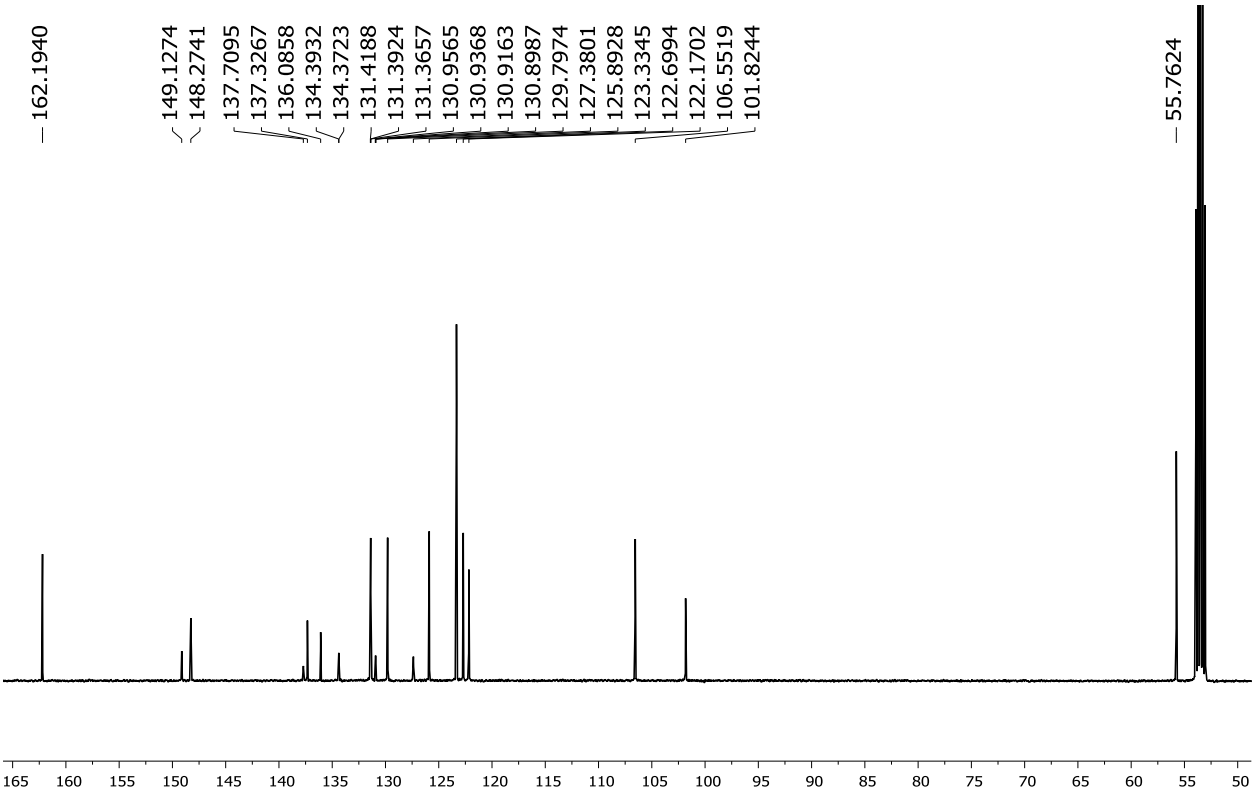

Figure C.47: ^{13}C NMR spectrum of BODIPY **4f** in CD_2Cl_2

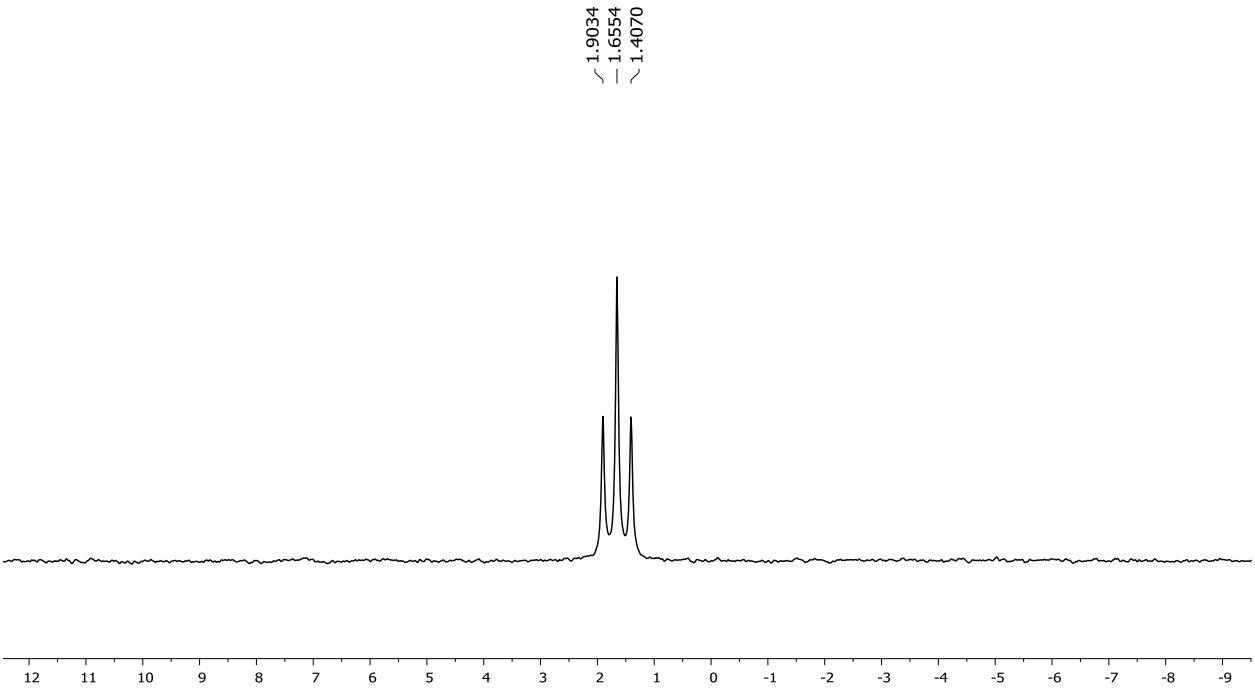

Figure C.48: ^{11}B NMR spectrum of BODIPY **4f** in CD_2Cl_2

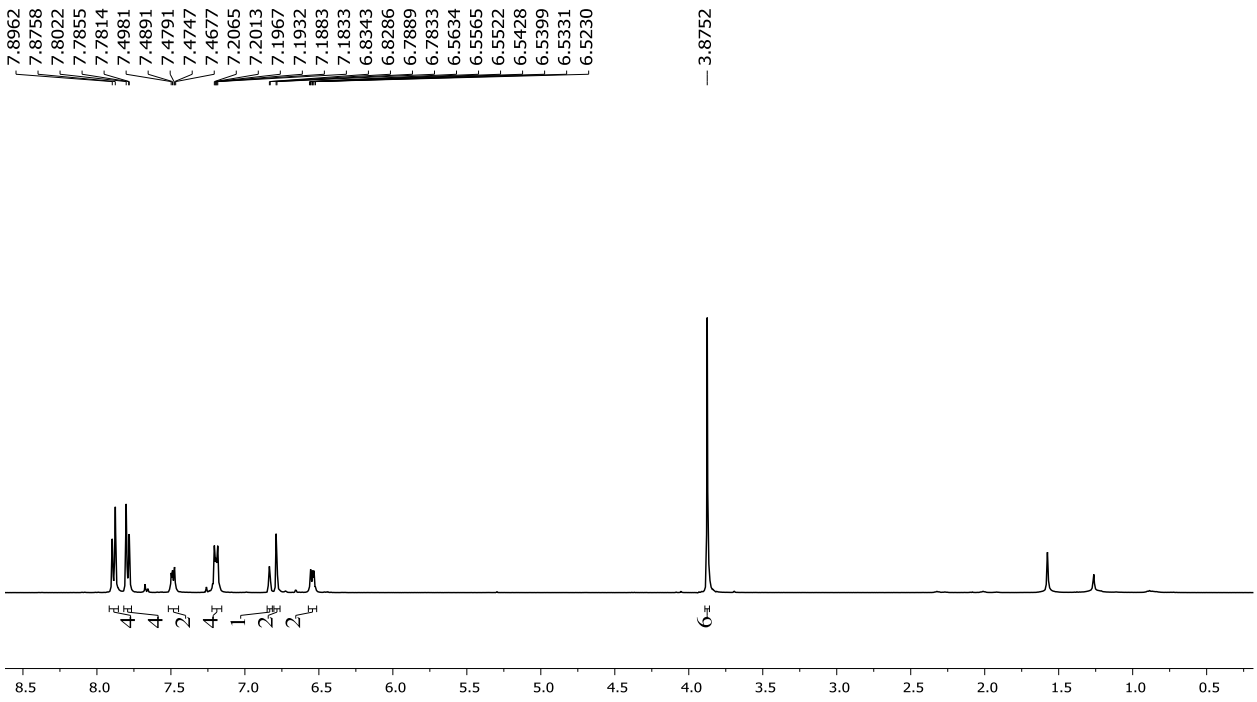

Figure C.49: ^{1}H NMR spectrum of BODIPY **4g** in $CDCl_3$

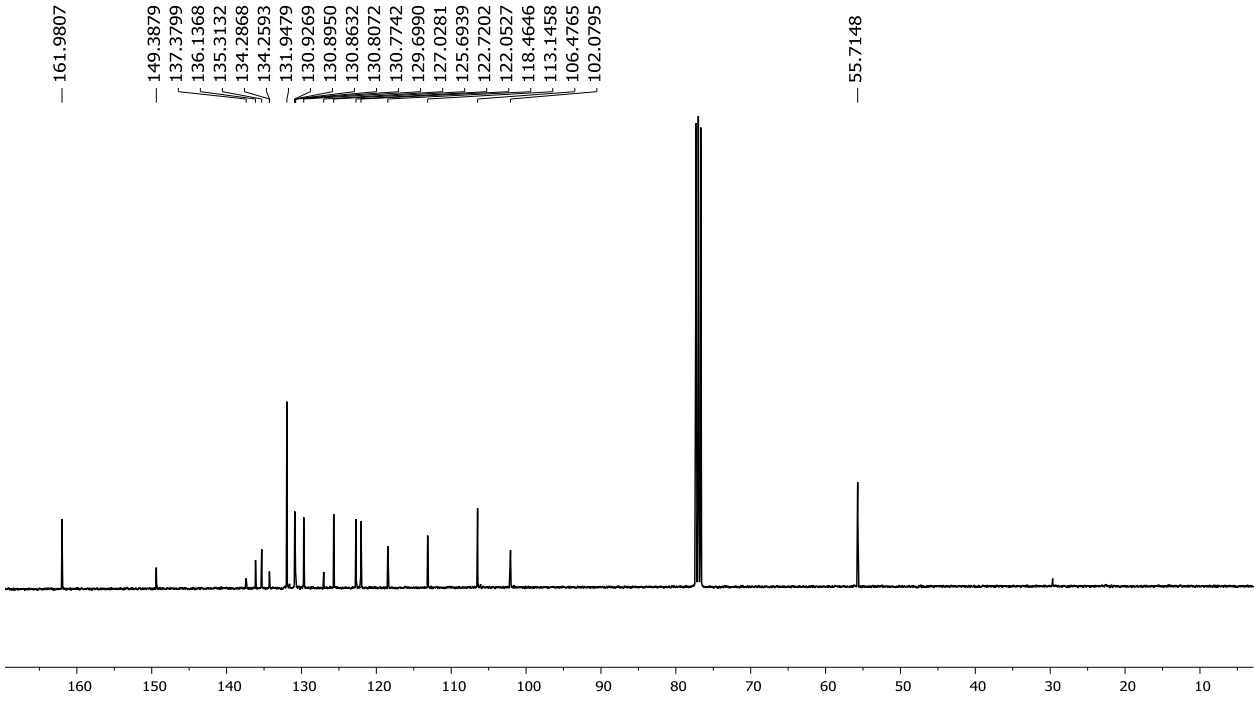

Figure C.50: ^{13}C NMR spectrum of BODIPY **4g** in CD_2Cl_2

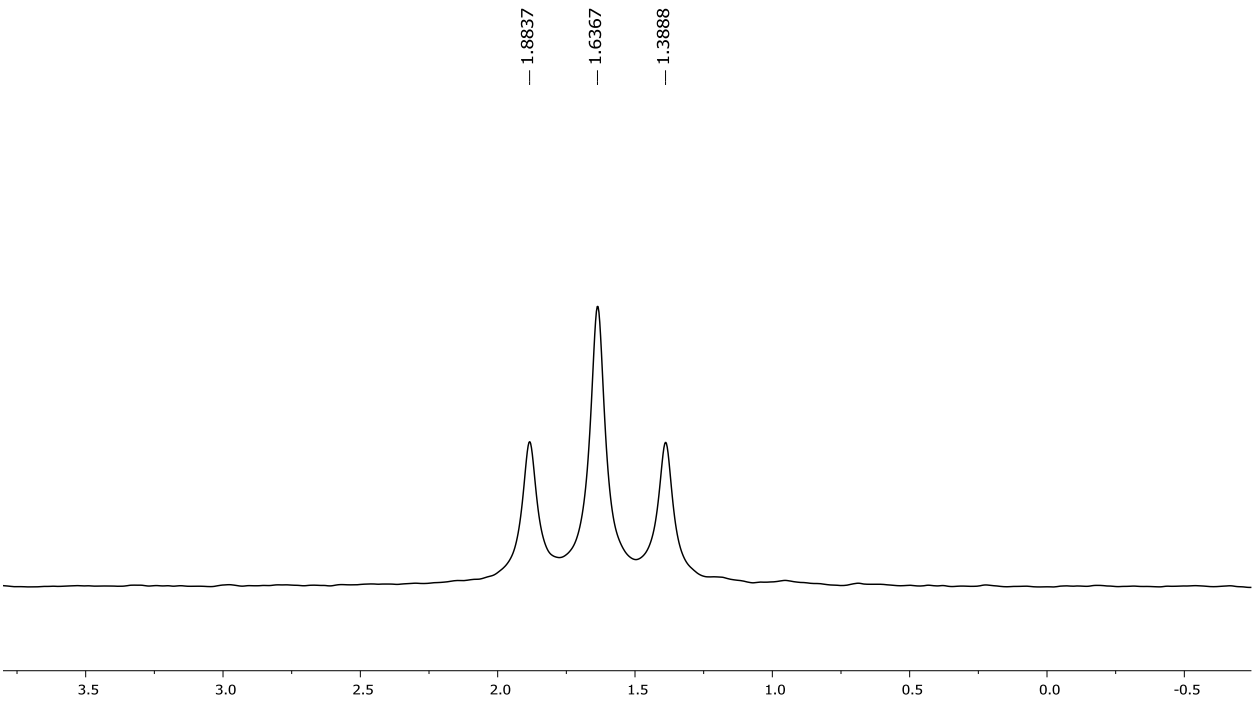

Figure C.51: ^{11}B NMR spectrum of BODIPY **4g** in CD_2Cl_2

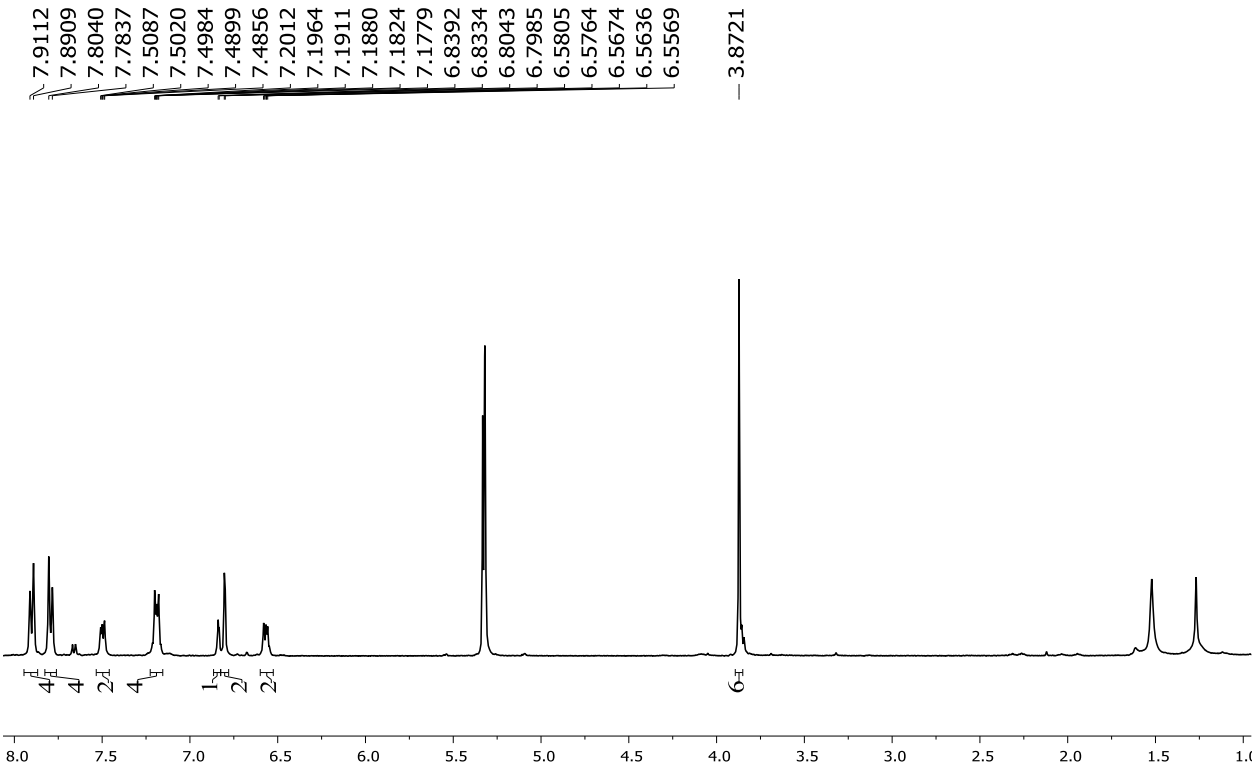

Figure C.52: ^{1}H NMR spectrum of BODIPY **4h** in CD_2Cl_2

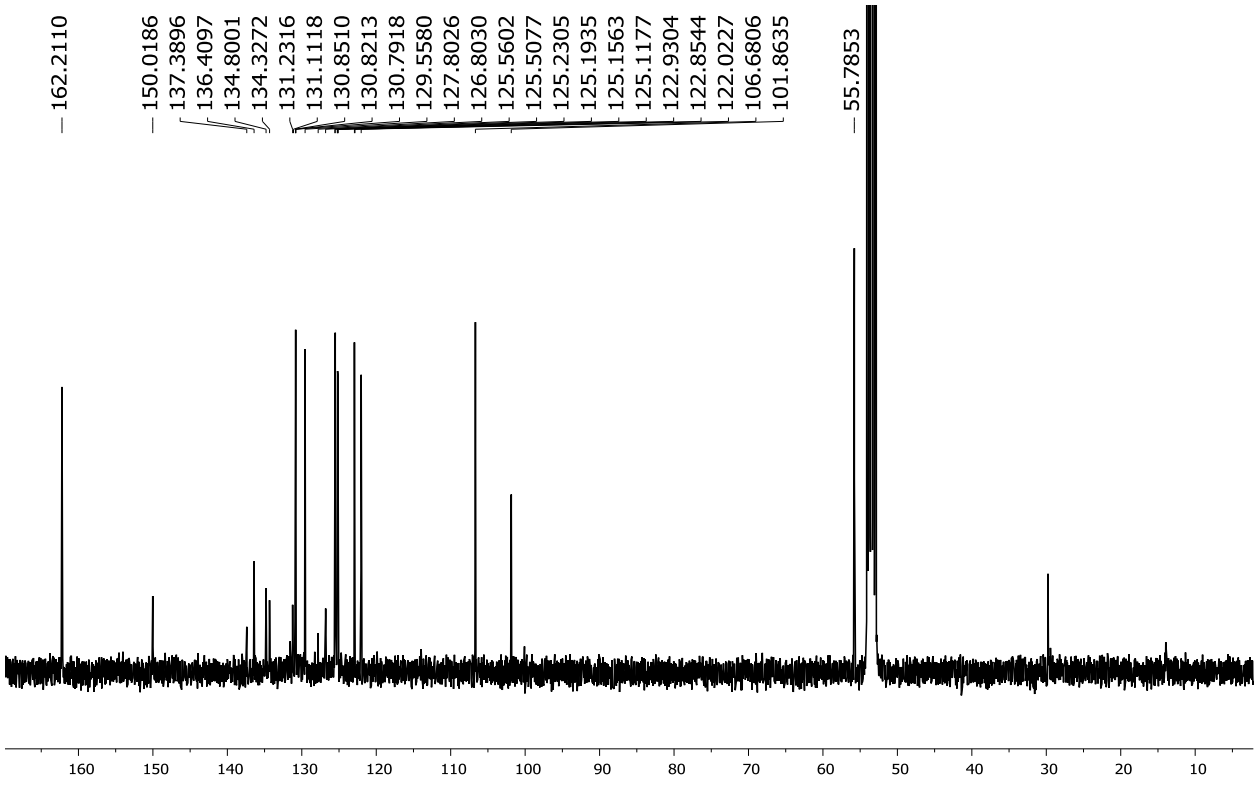

Figure C.53: ^{13}C NMR spectrum of BODIPY **4h** in CD_2Cl_2

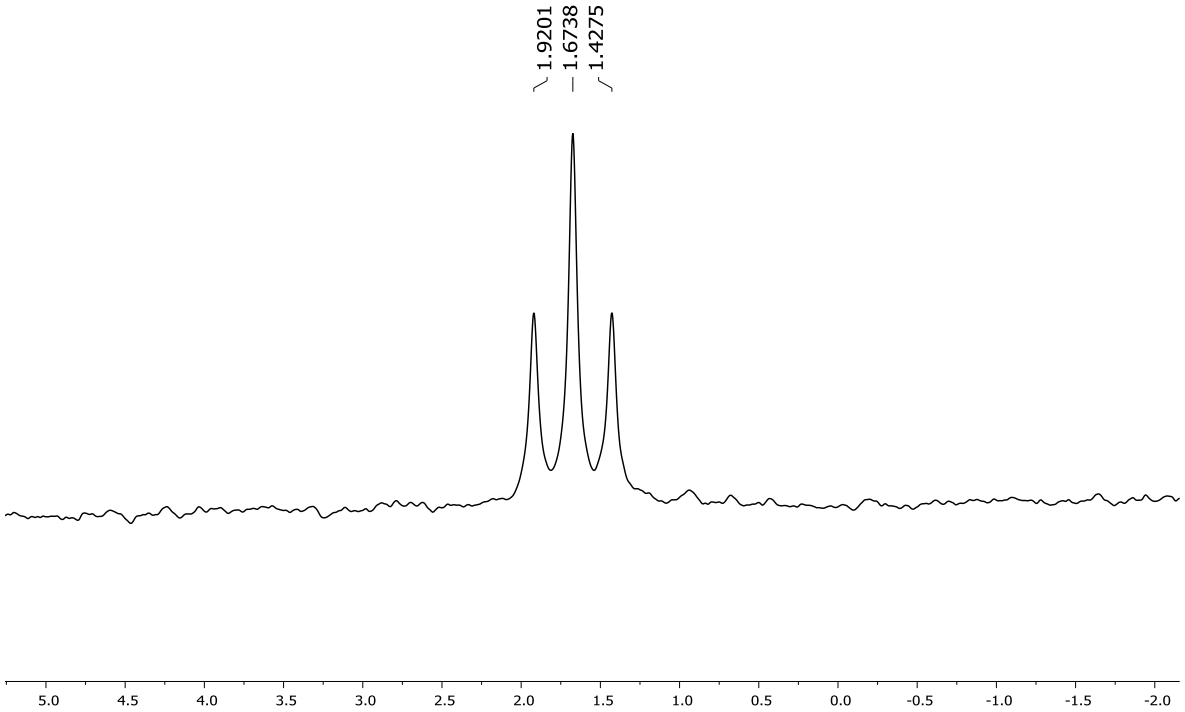

Figure C.54: ^{11}B NMR spectrum of BODIPY **4h** in CD_2Cl_2

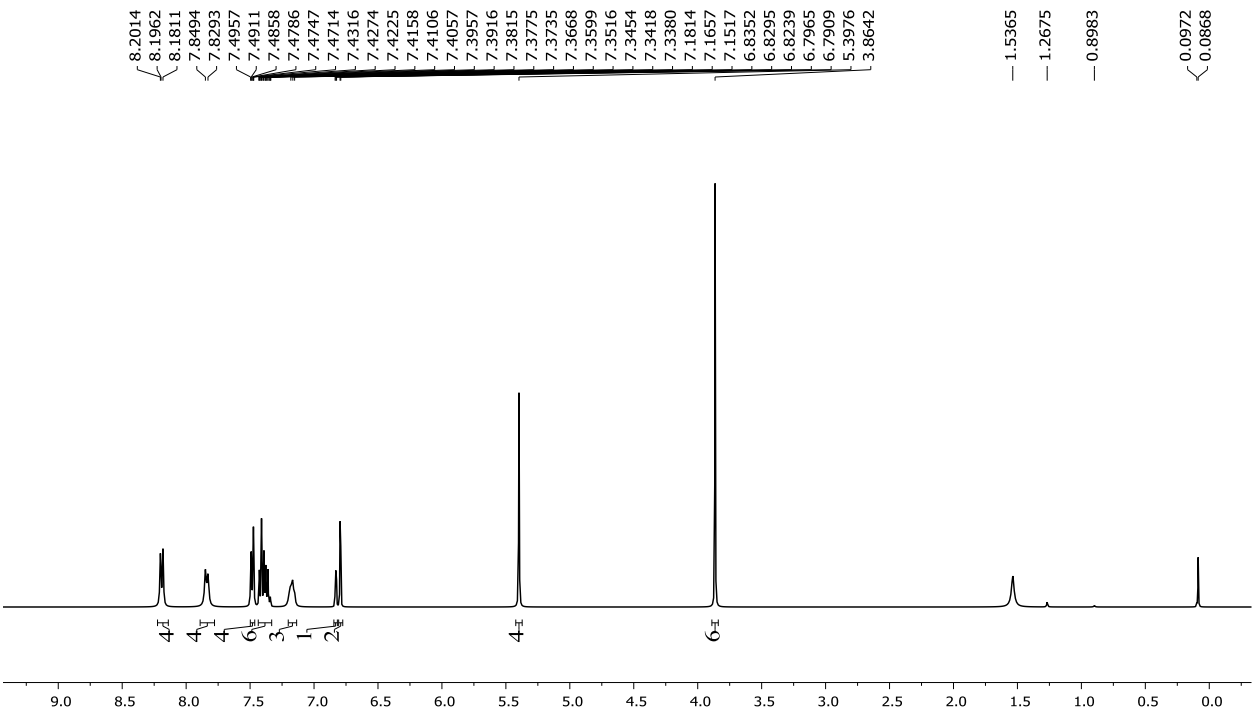

Figure C.55: ^{1}H NMR spectrum of BODIPY **4i** in CD_2Cl_2

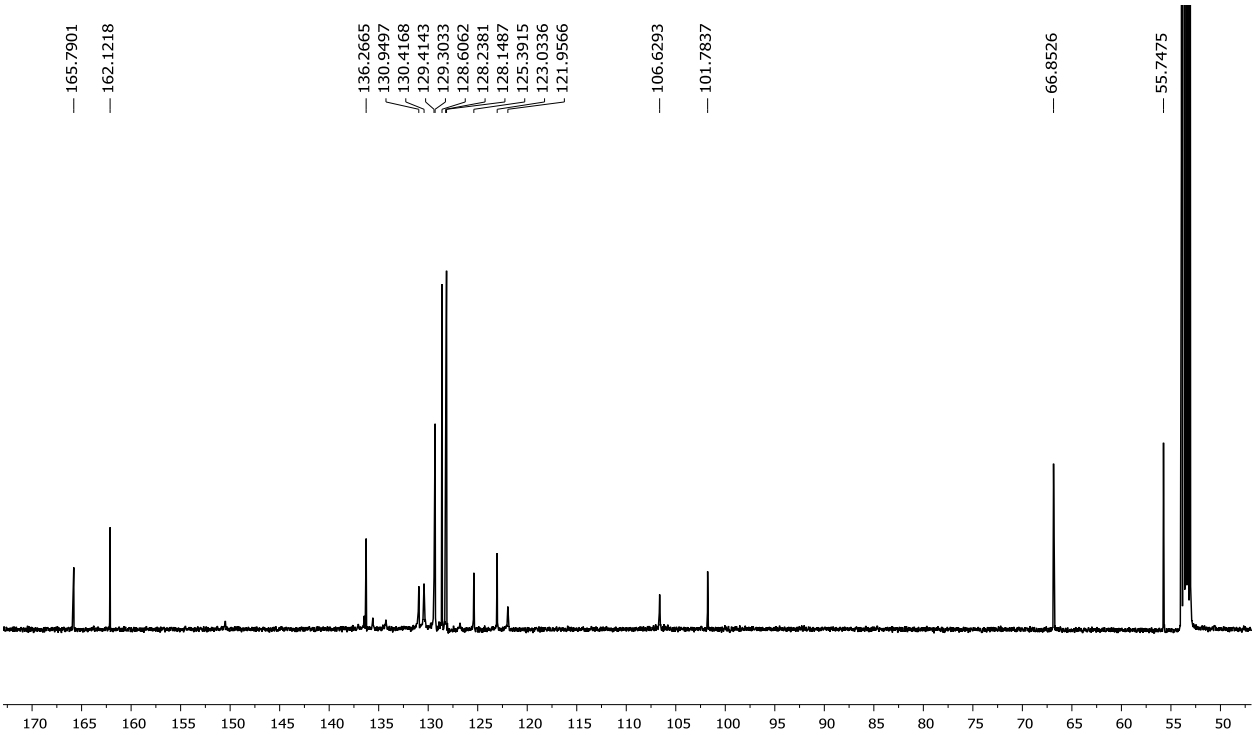

Figure C.56: ^{13}C NMR spectrum of BODIPY **4i** in CD_2Cl_2

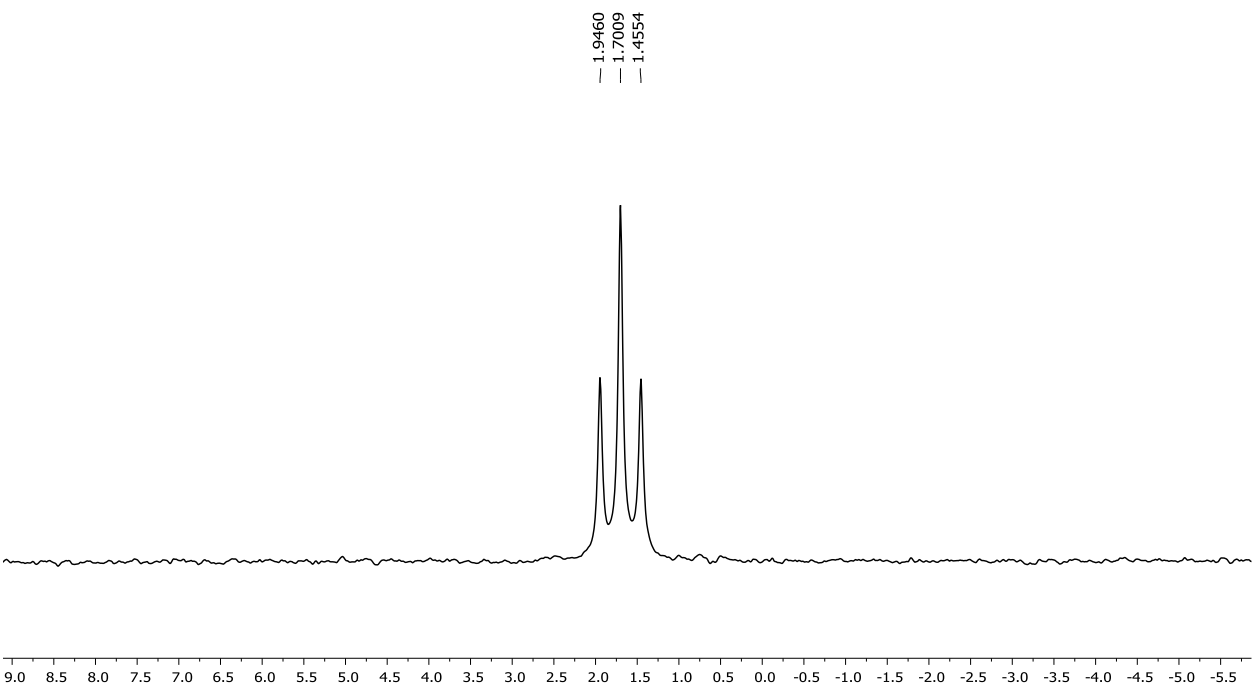

Figure C.57: ^{11}B NMR spectrum of BODIPY **4i** in CD_2Cl_2

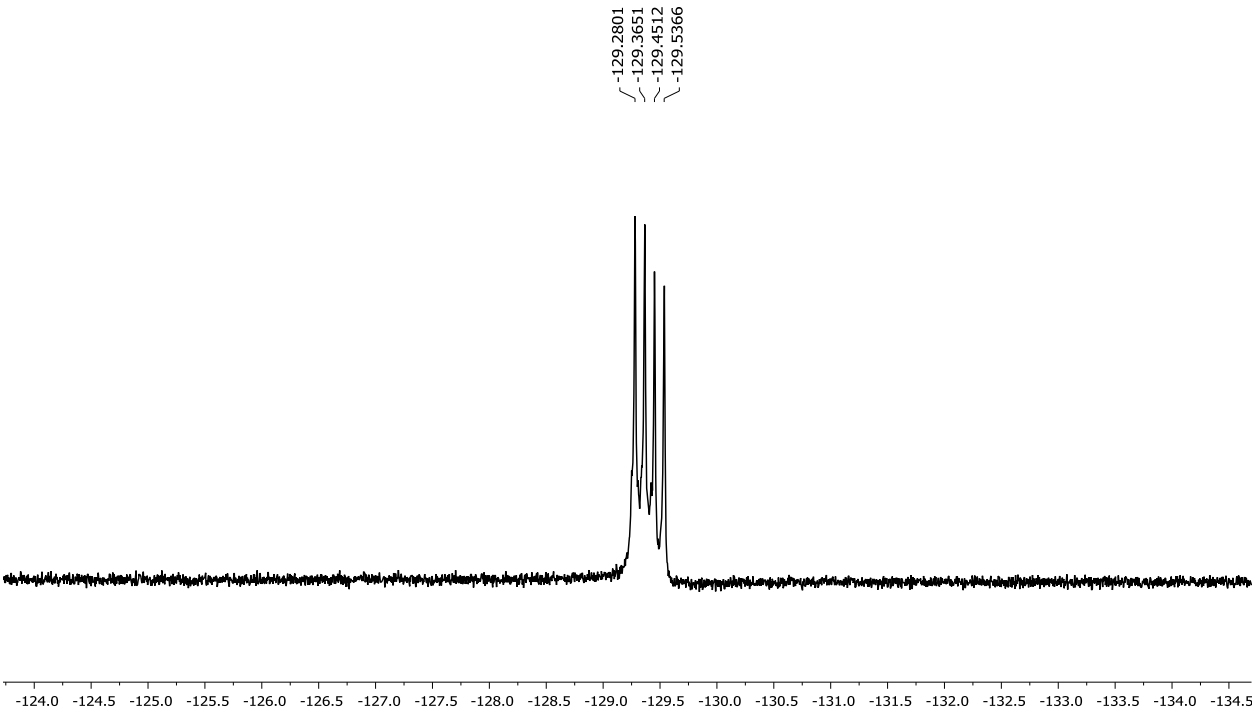

Figure C.58: ^{19}F NMR spectrum of BODIPY **4i** in CD_2Cl_2

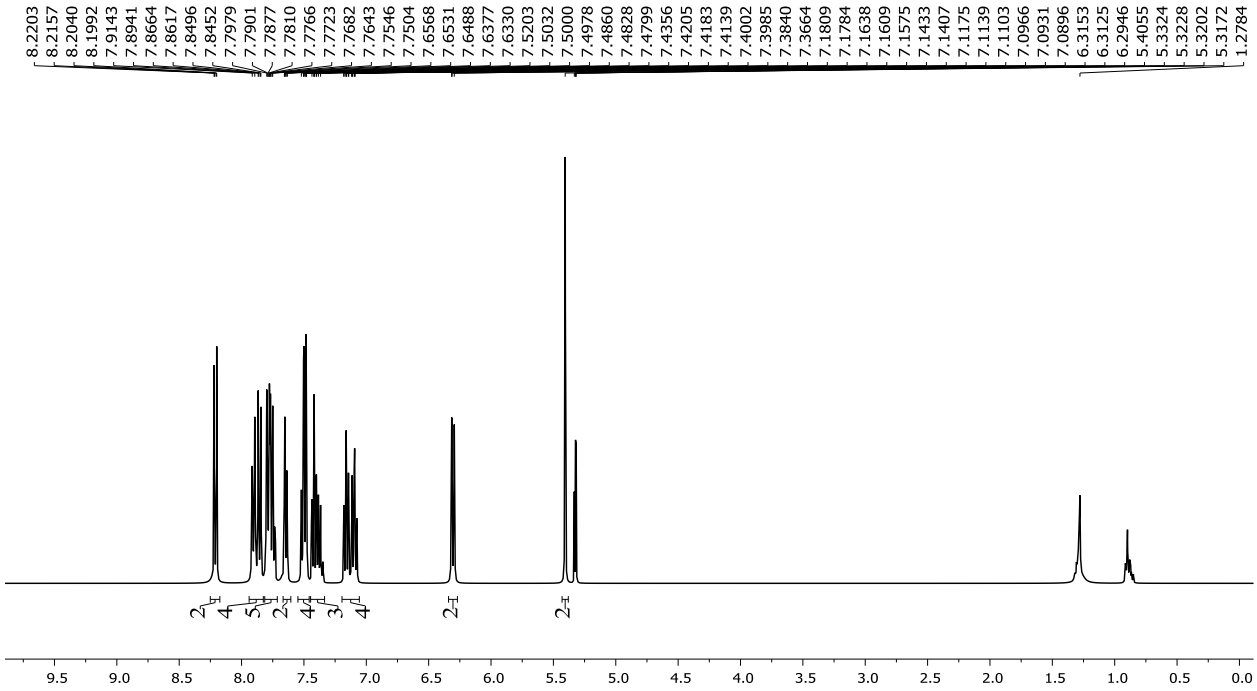

Figure C.59: ^{1}H NMR spectrum of BODIPY **4j** in CD_2Cl_2

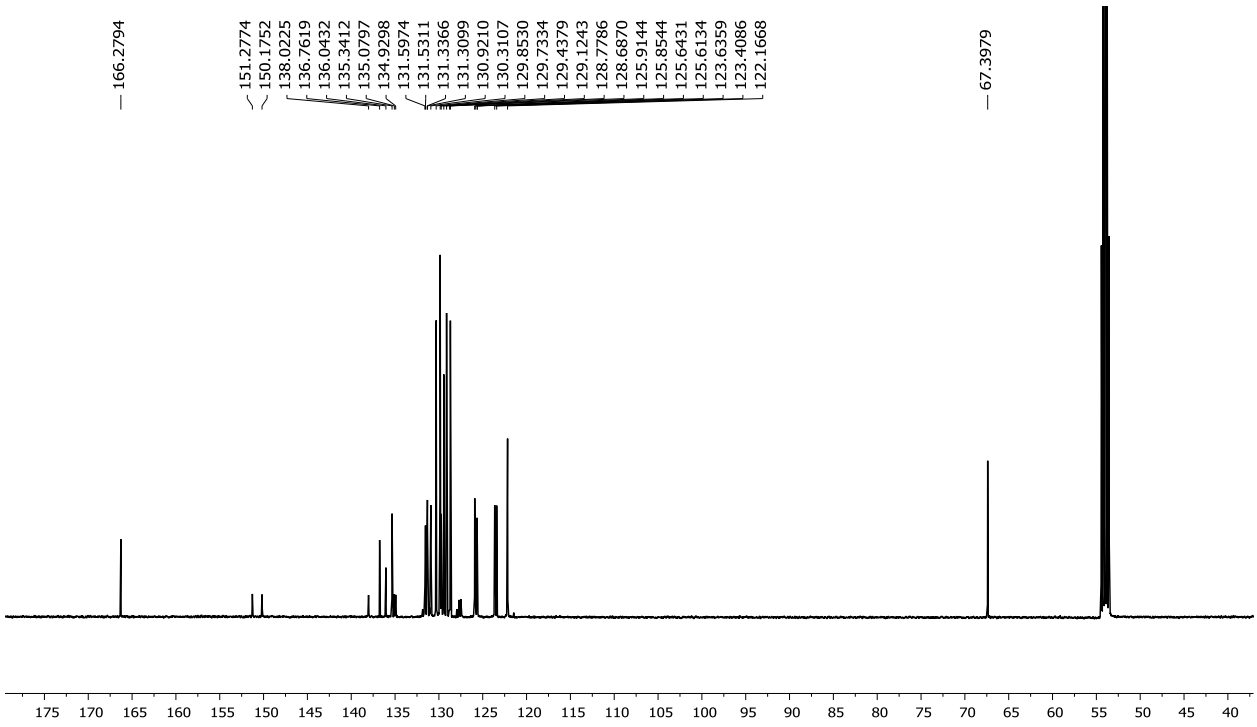

Figure C.60: ^{13}C NMR spectrum of BODIPY **4j** in CD_2Cl_2

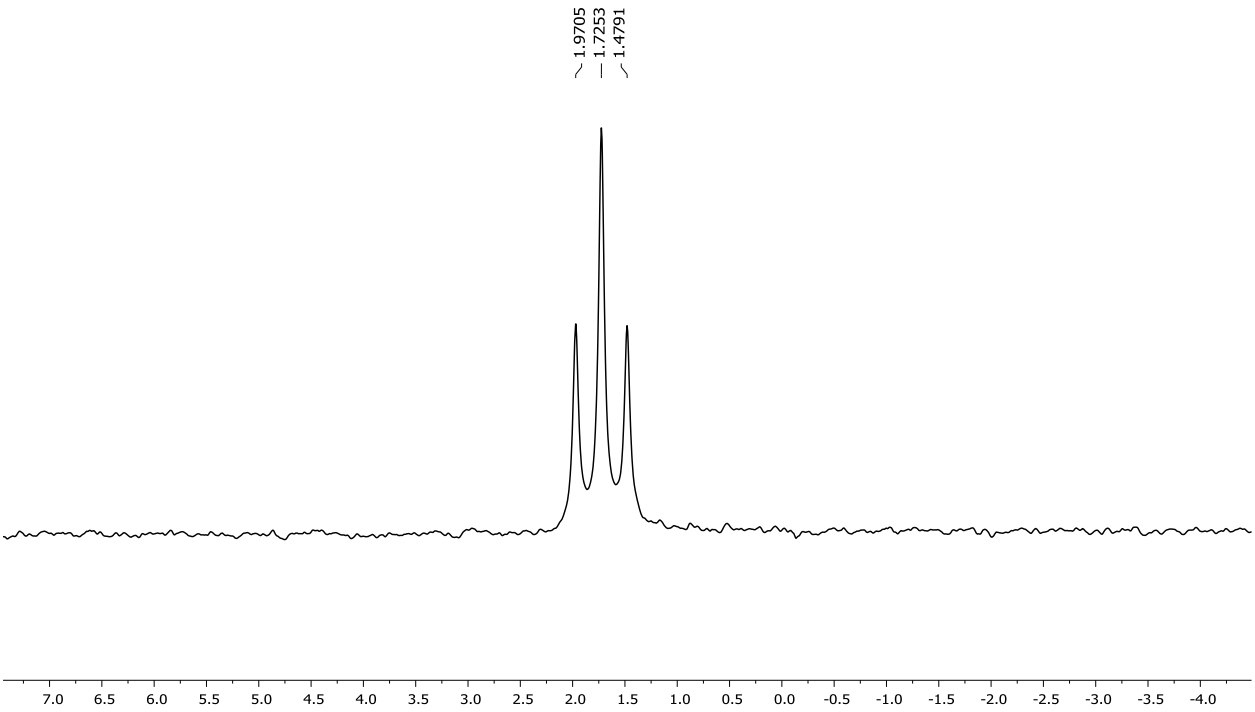

Figure C.61: ^{11}B NMR spectrum of BODIPY **4j** in CD_2Cl_2

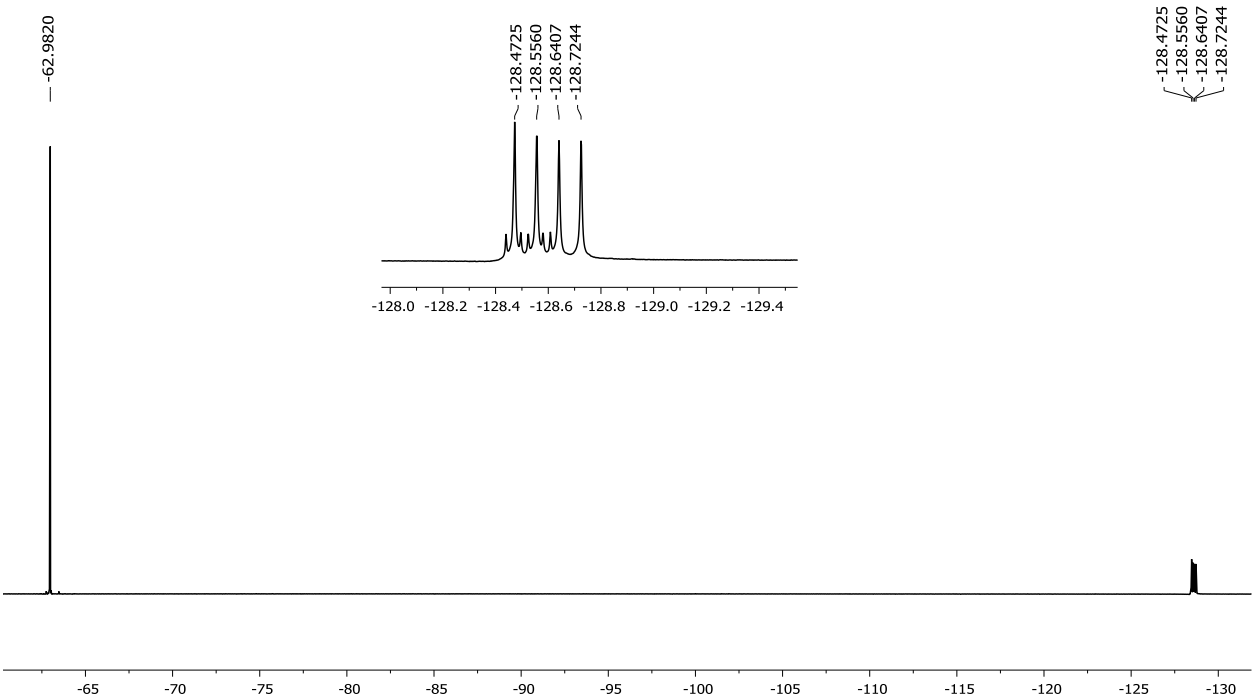

Figure C.62: ^{19}F NMR spectrum of BODIPY **4j** in CD_2Cl_2

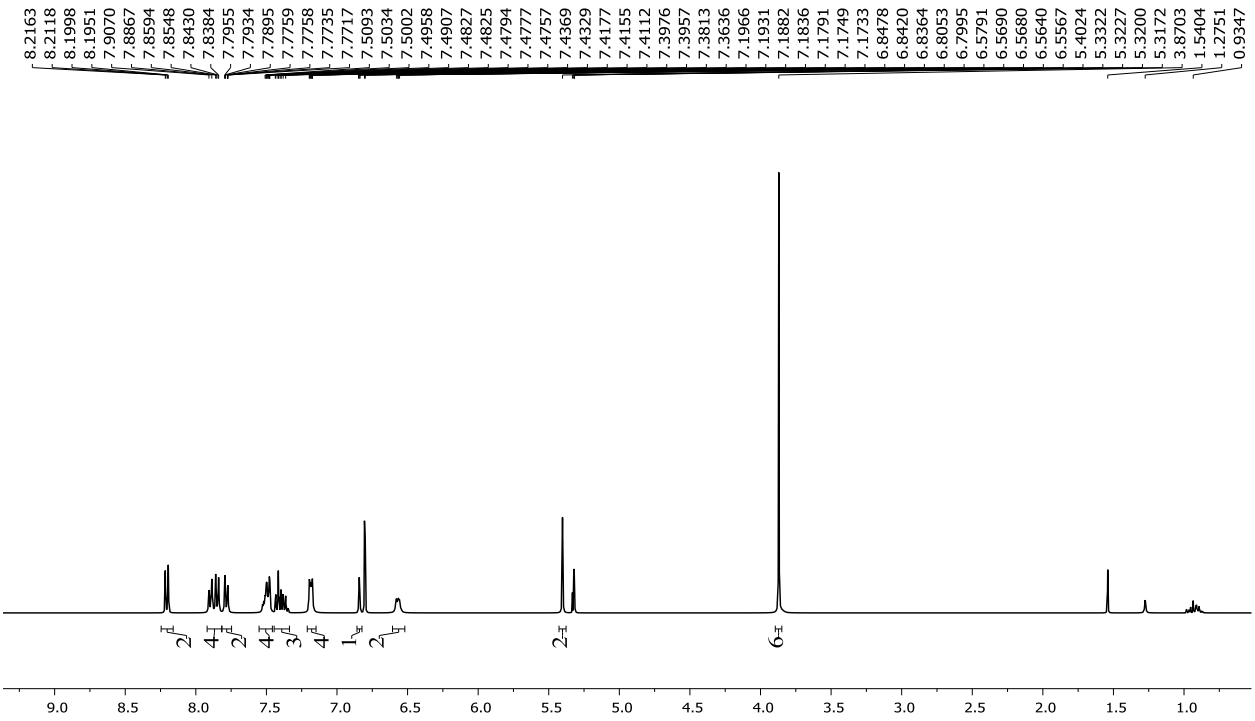

Figure C.63: ^{1}H NMR spectrum of BODIPY **4k** in CD_2Cl_2

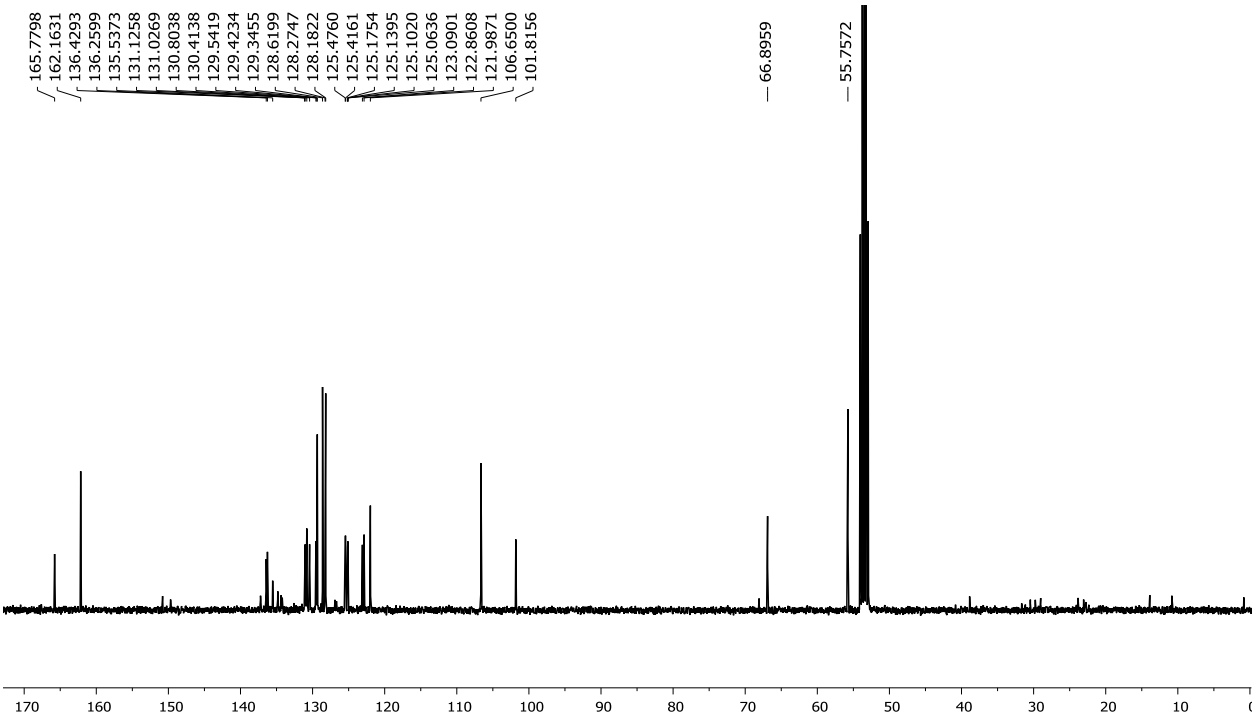

Figure C.64: ^{13}C NMR spectrum of BODIPY **4k** in CD_2Cl_2

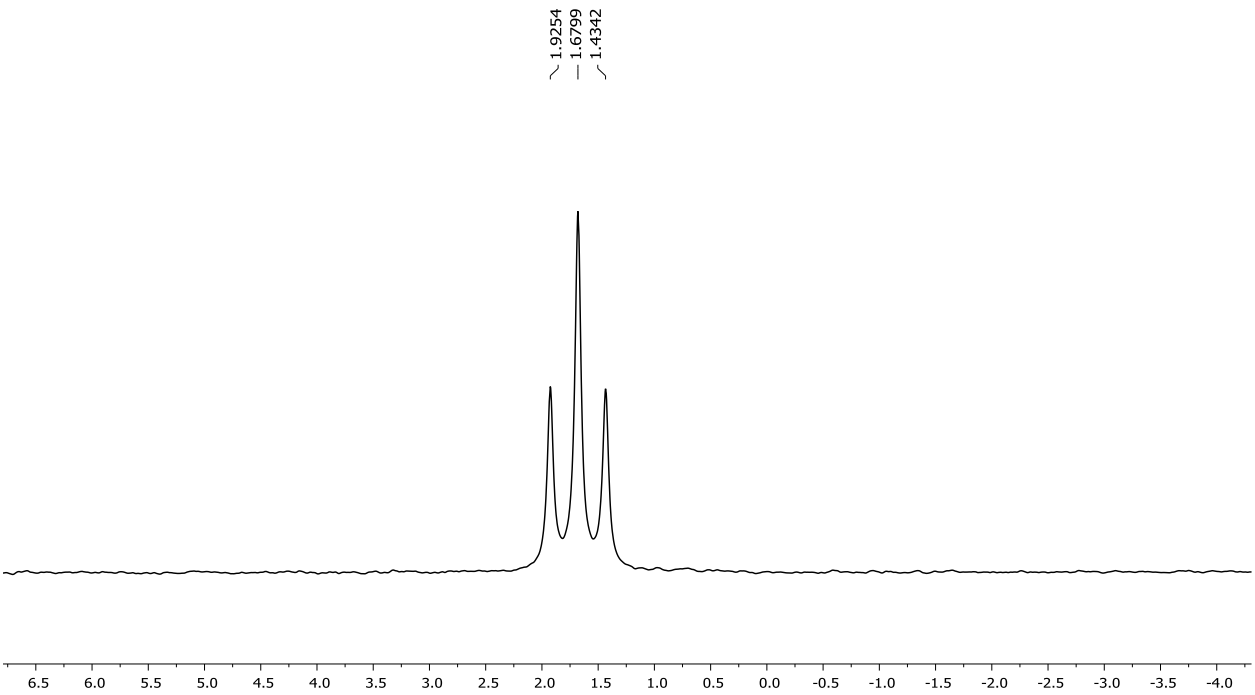

Figure C.65: ^{11}B NMR spectrum of BODIPY **4k** in CD_2Cl_2

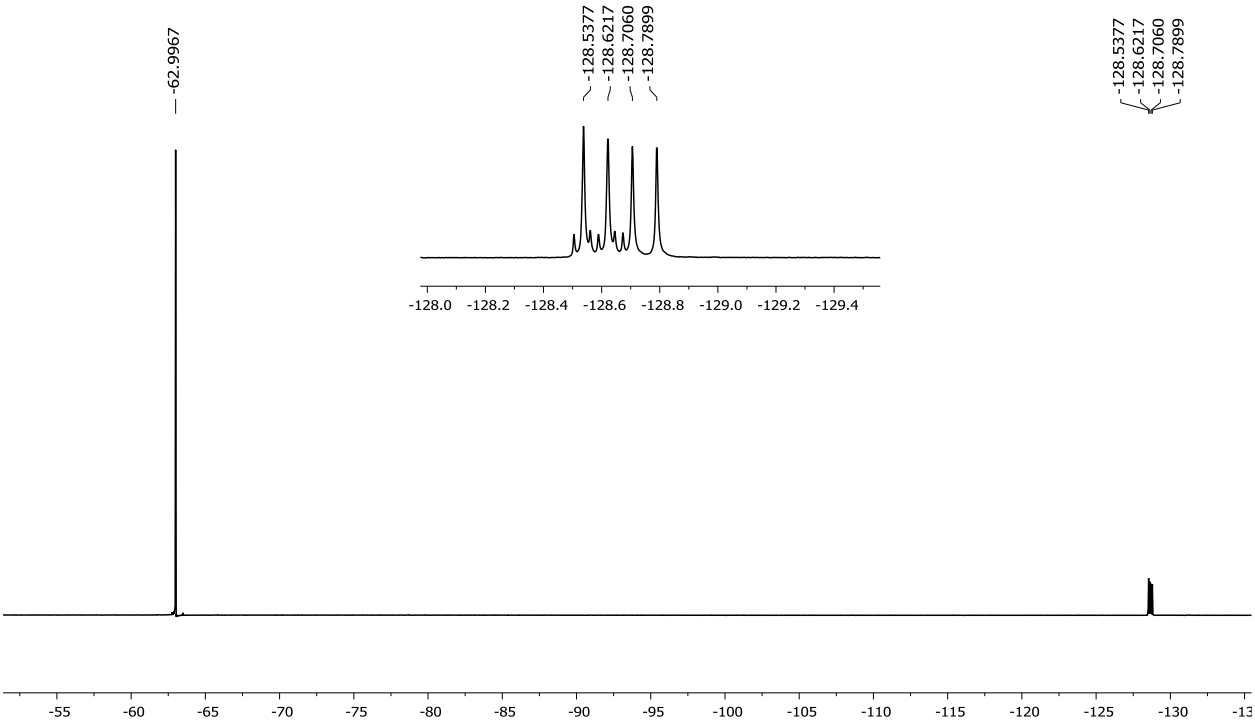

Figure C.66: ^{19}F NMR spectrum of BODIPY **4k** in CD_2Cl_2

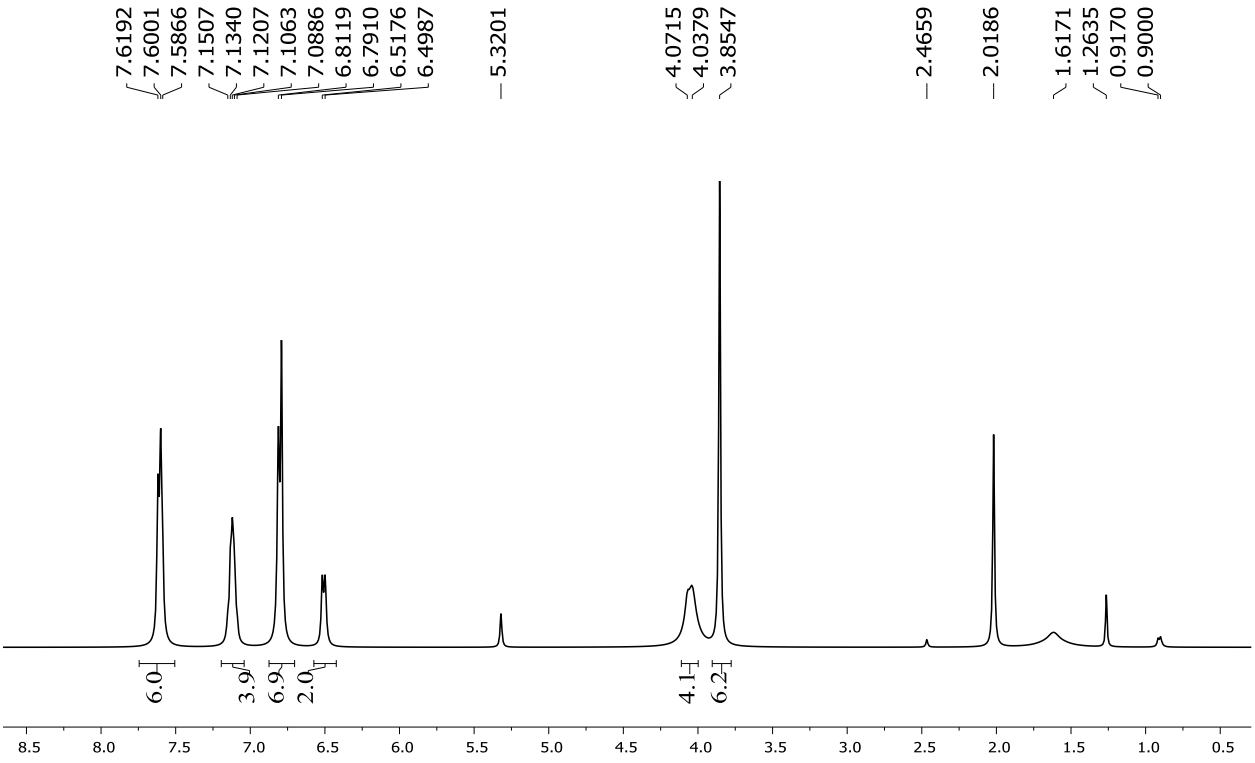

Figure C.67: ^{1}H NMR spectrum of BODIPY **5b** in CD_2Cl_2

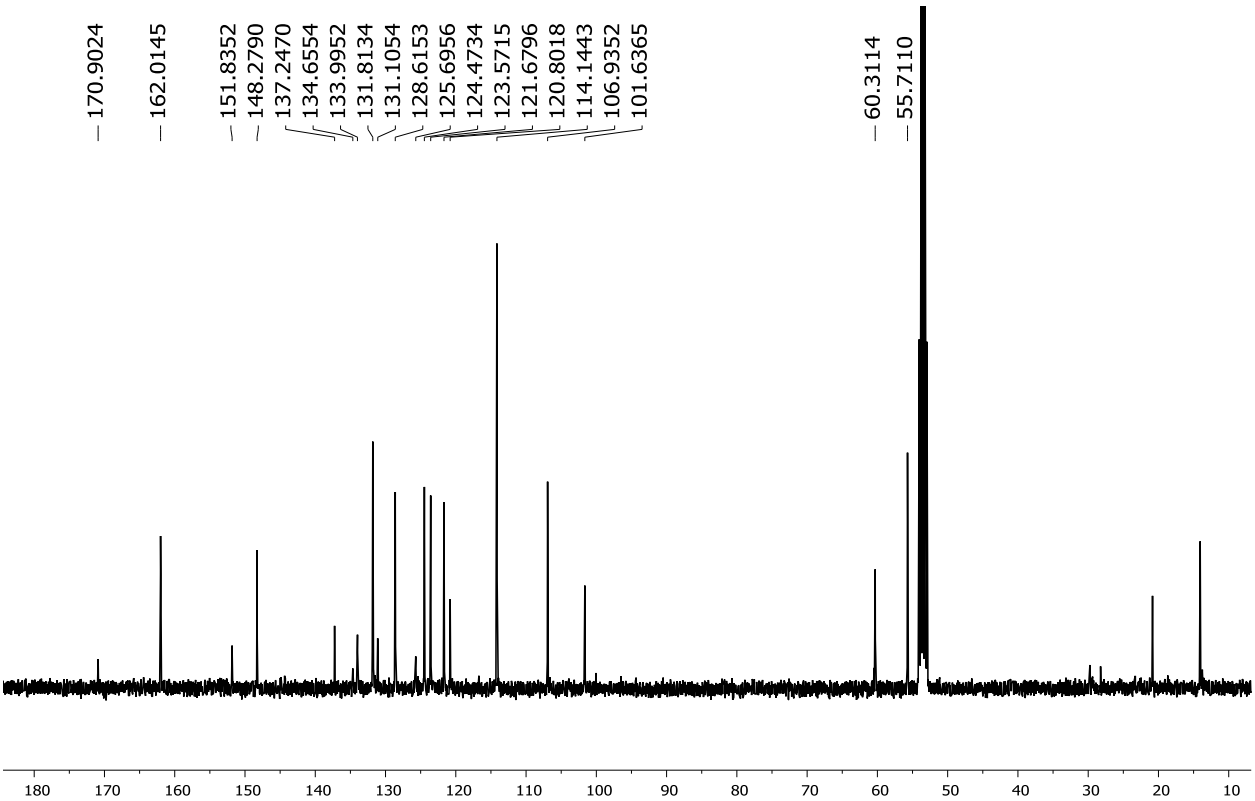

Figure C.68: ^{13}C NMR spectrum of BODIPY **5b** in CD_2Cl_2

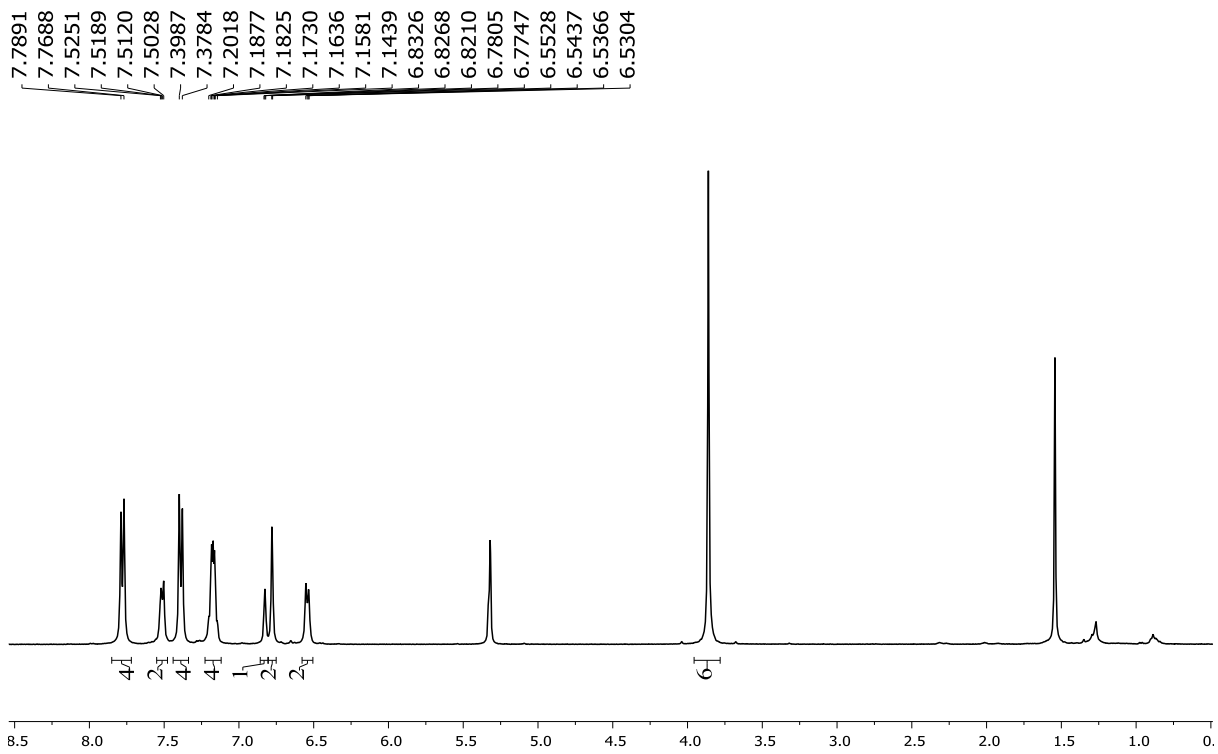

Figure C.69: ^{1}H NMR spectrum of BODIPY **6b** in CD_2Cl_2

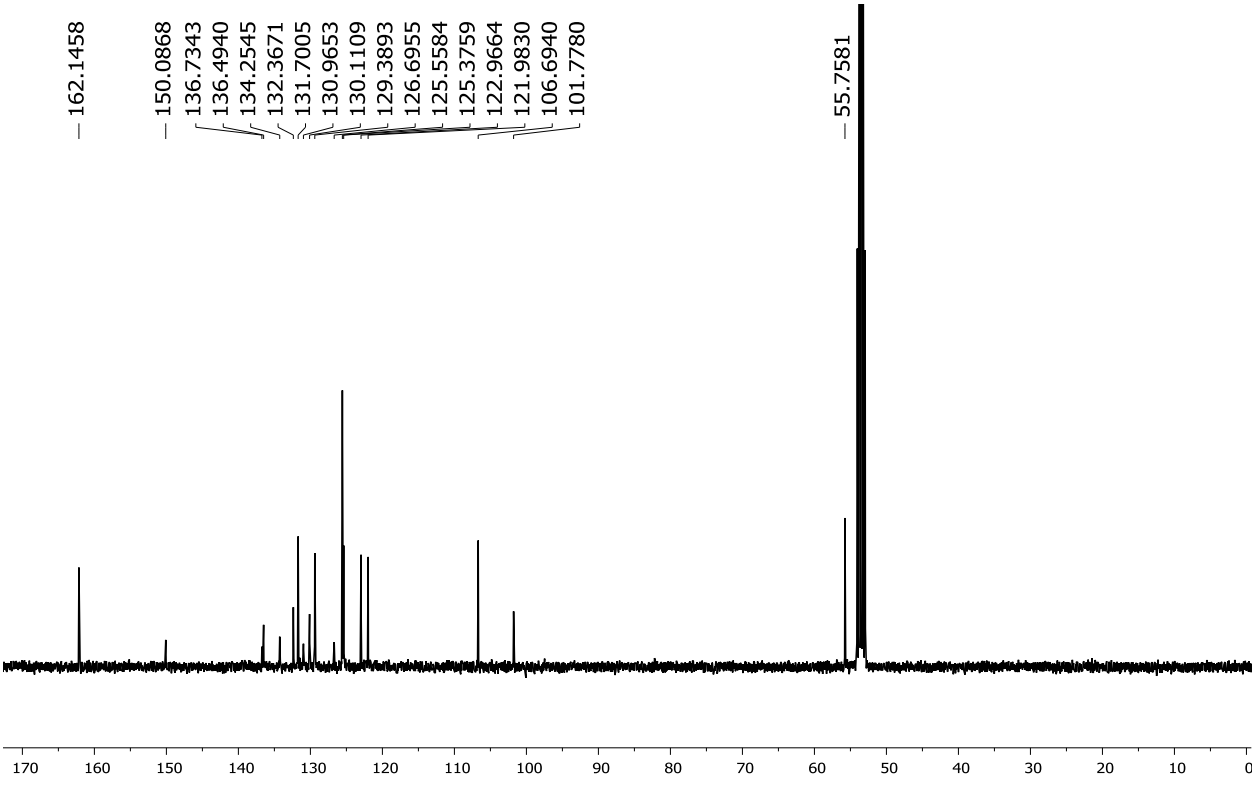

Figure C.70: ^{13}C NMR spectrum of BODIPY **6b** in CD_2Cl_2

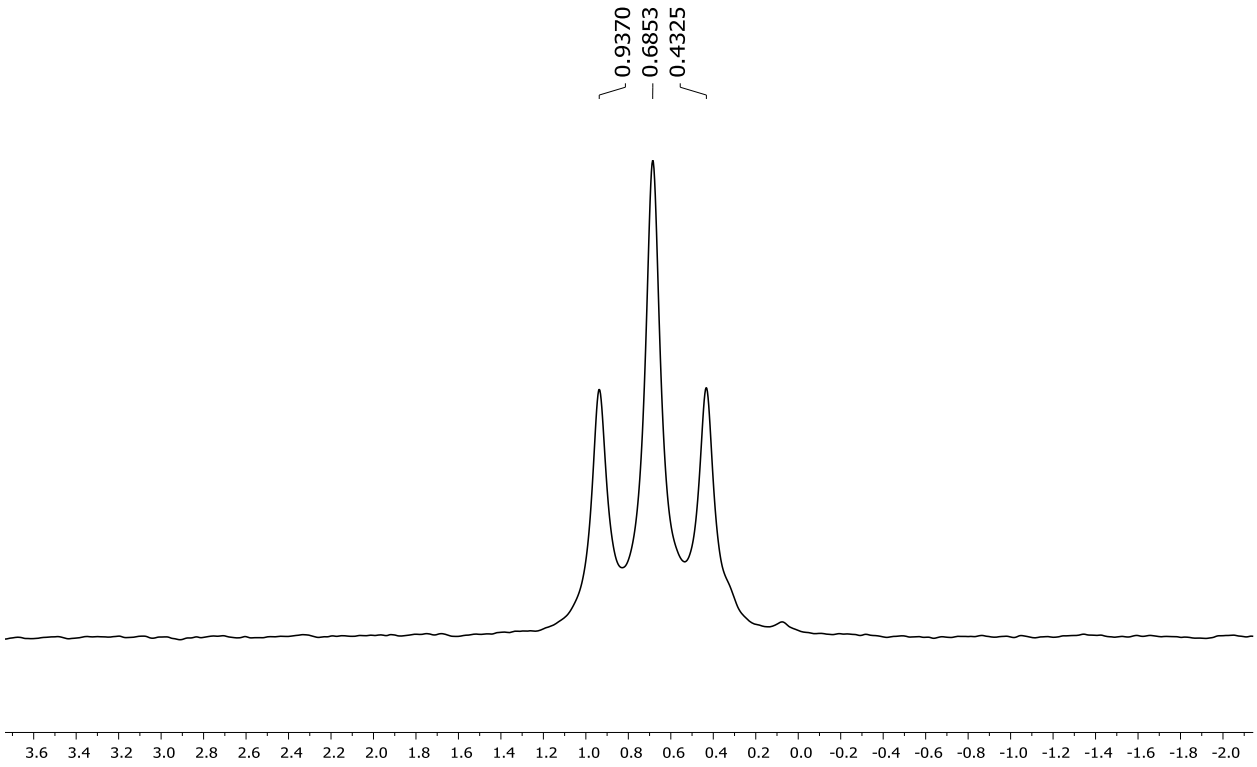

Figure C.71: ^{11}B NMR spectrum of BODIPY **6b** in CD_2Cl_2

APPENDIX D: NMR Characterization of Compounds Found in Chapter 5

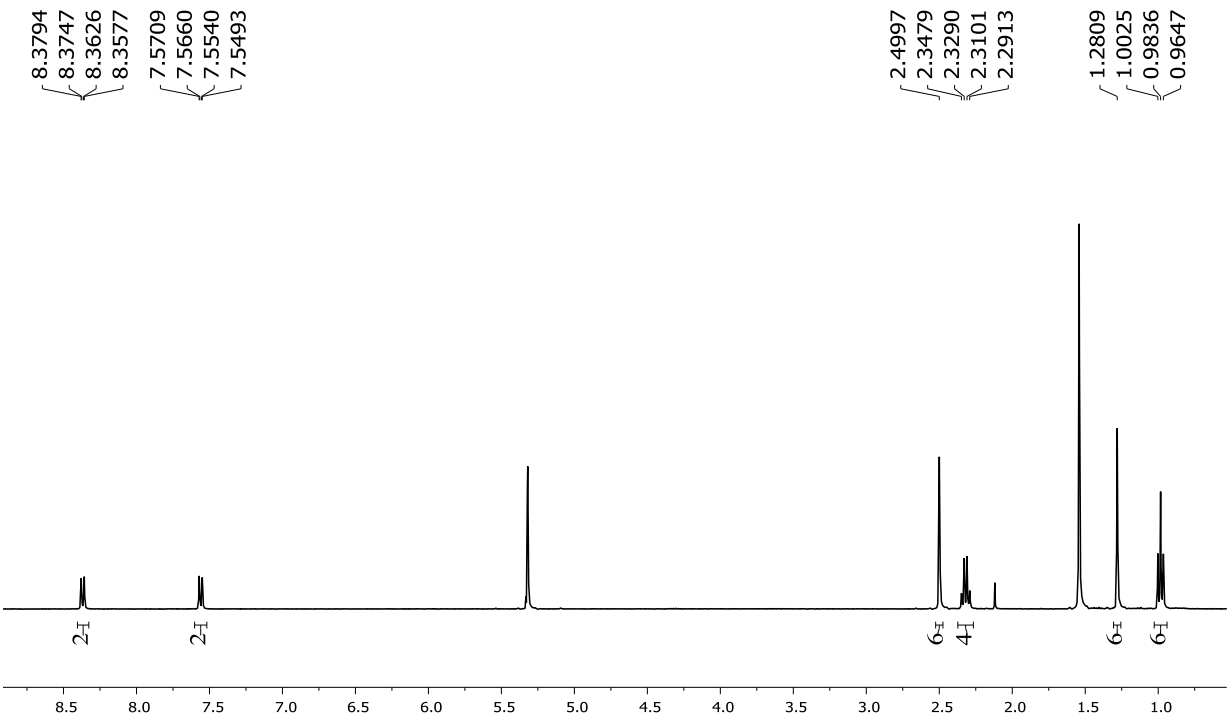

Figure D.1: ^{1}H NMR spectrum of **2** in CD_2Cl_2

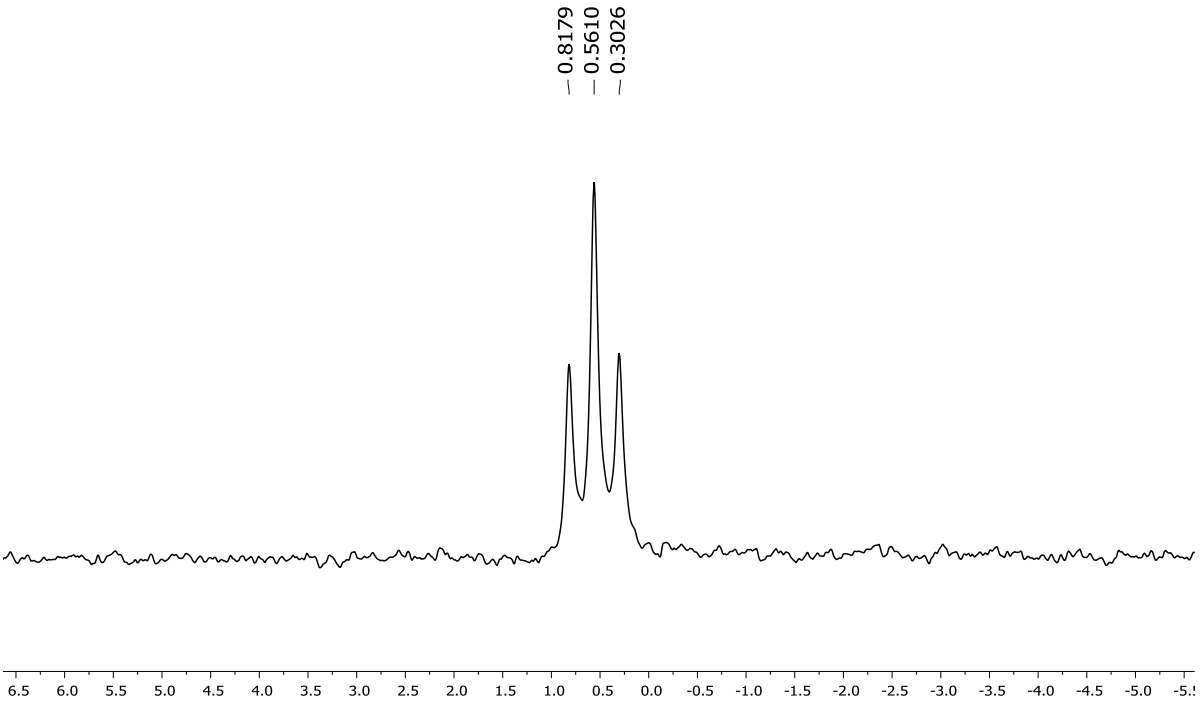

Figure D.2: ^{11}B NMR spectrum of **2** in CD_2Cl_2

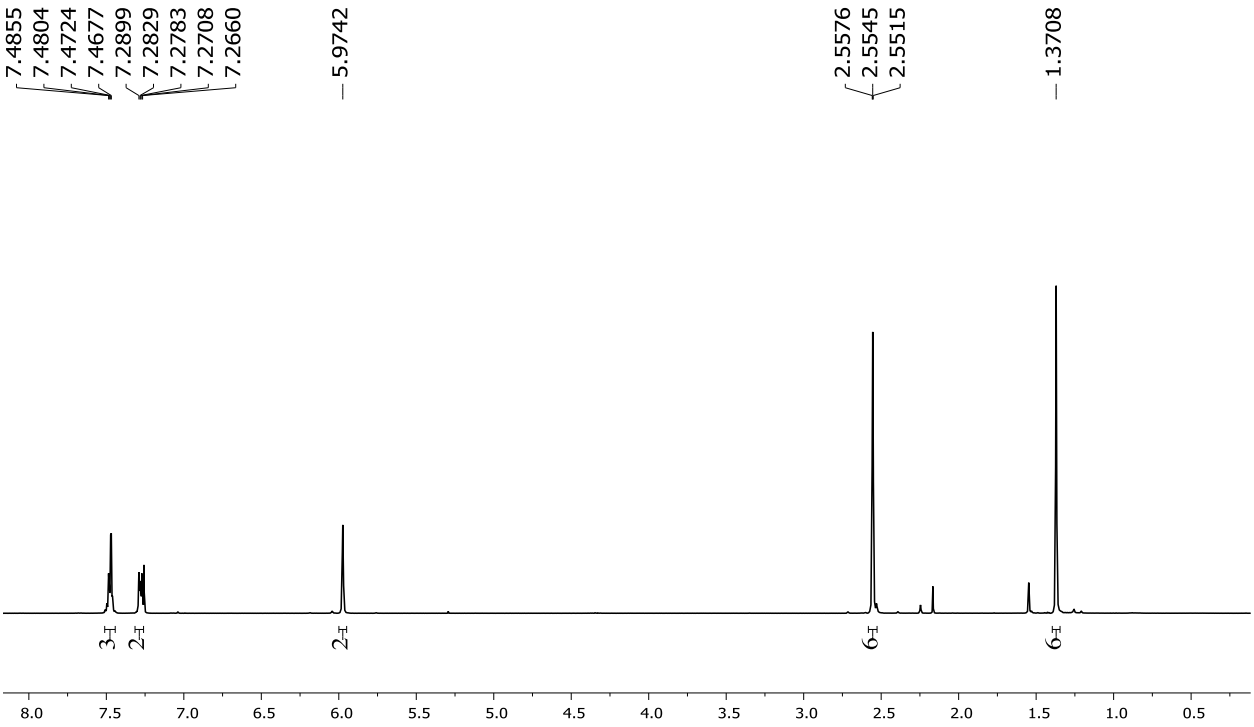

Figure D.3: ^{1}H NMR spectrum of **4** in $CDCl_3$

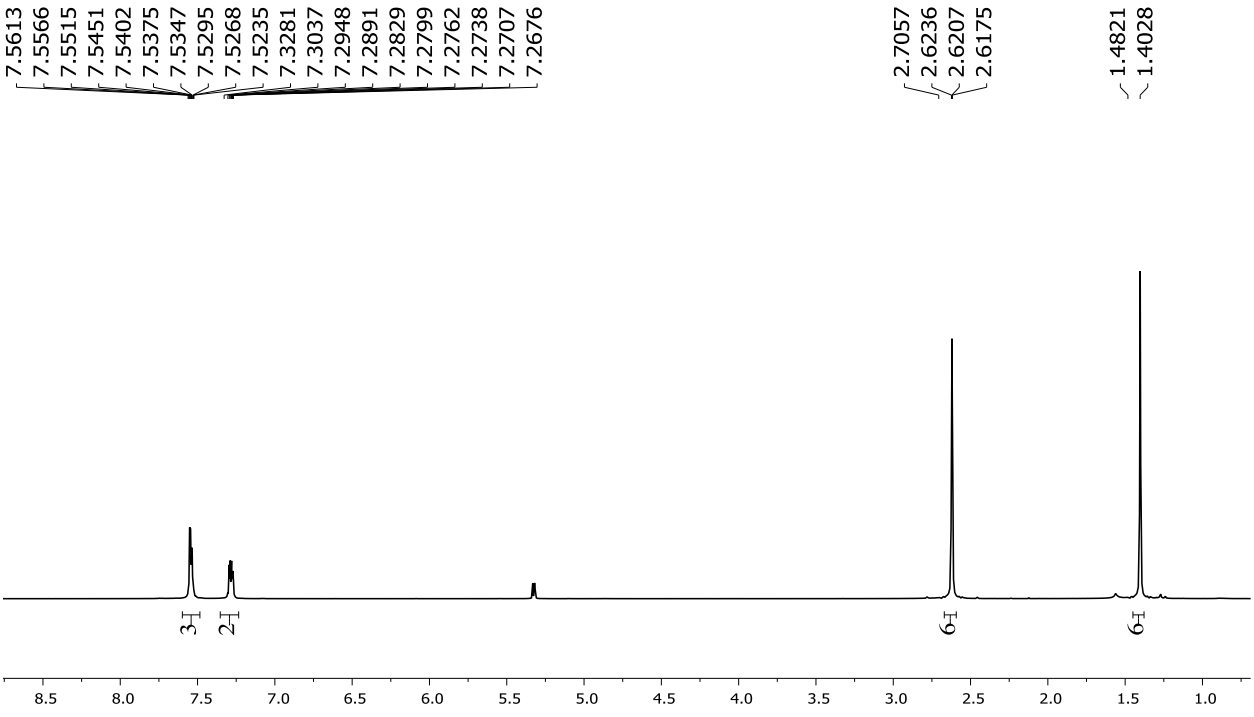

Figure D.4: ^{1}H NMR spectrum of **5** in CD_2Cl_2

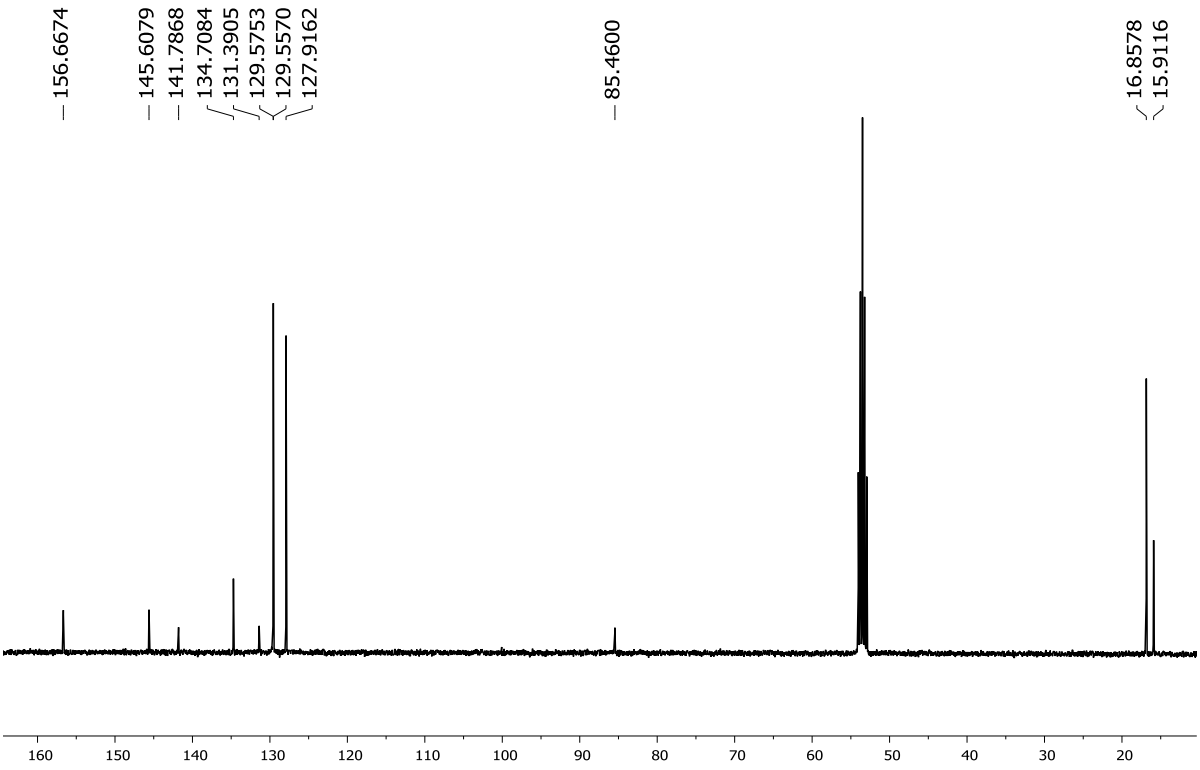

Figure D.5: ^{13}C NMR spectrum of **5** in CD_2Cl_2

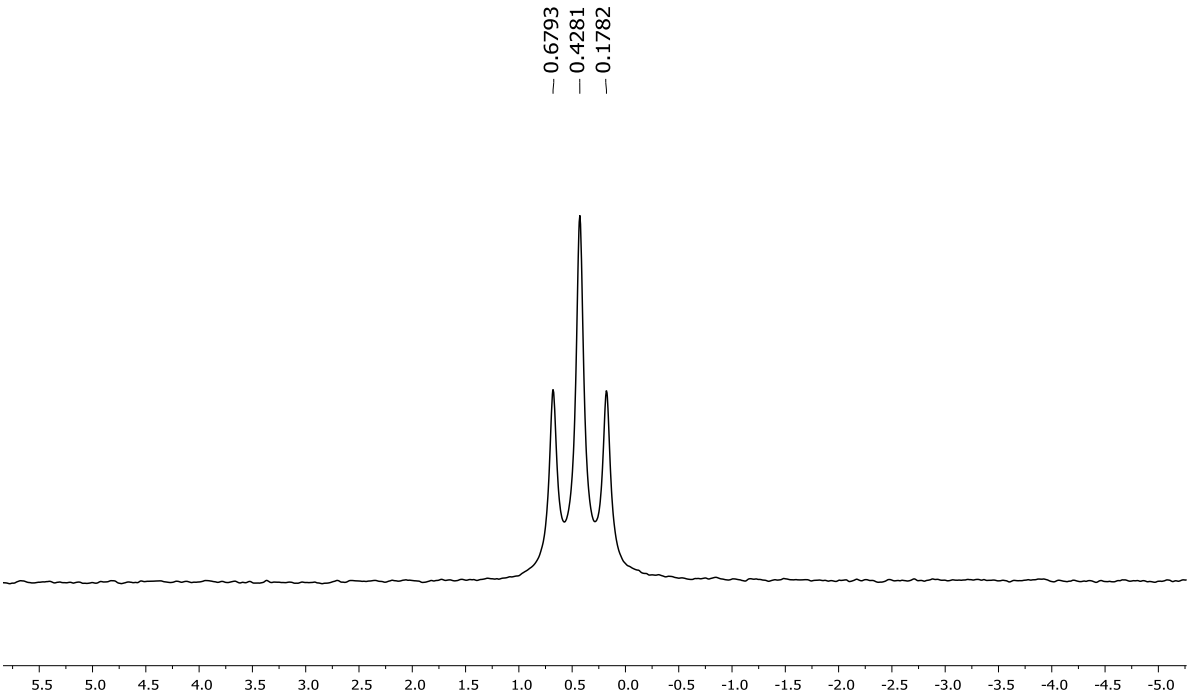

Figure D.6: ^{11}B NMR spectrum of **5** in CD_2Cl_2

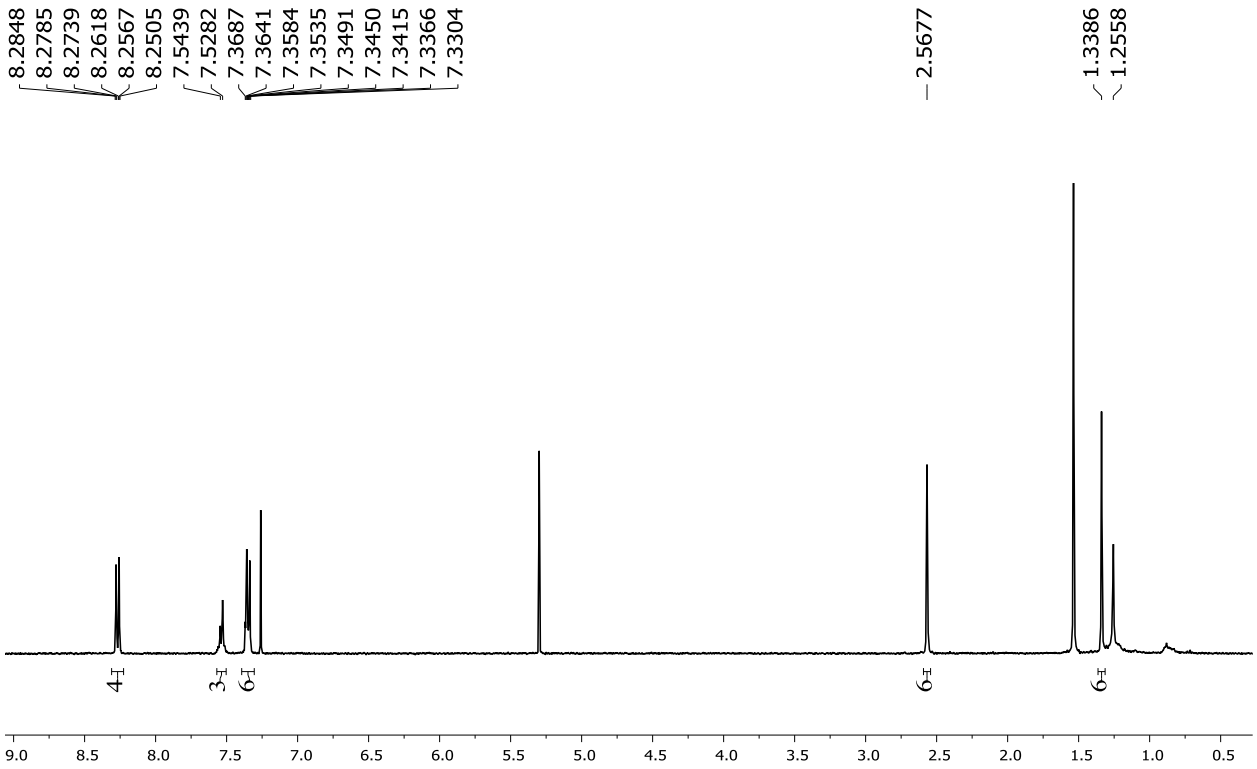

Figure D.7: ^{1}H NMR spectrum of **6** in CD_2Cl_2

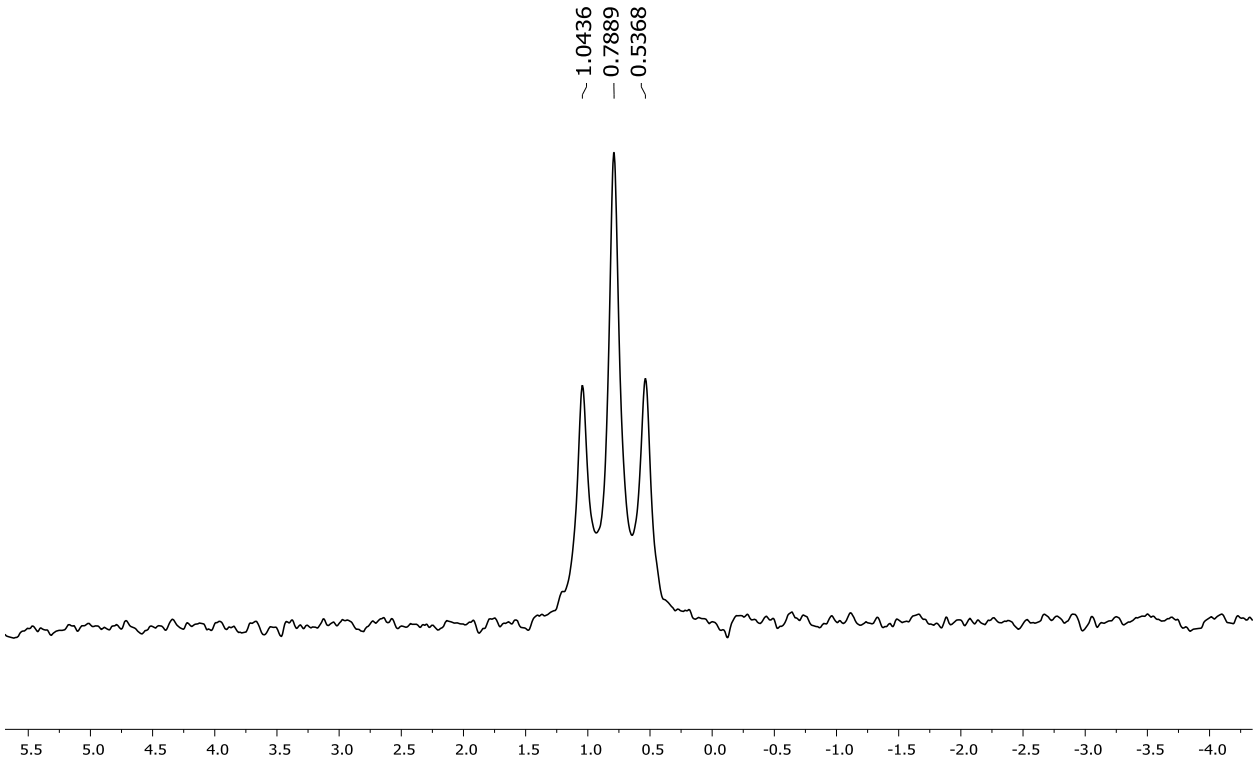

Figure D.8: ^{11}B NMR spectrum of **6** in CD_2Cl_2

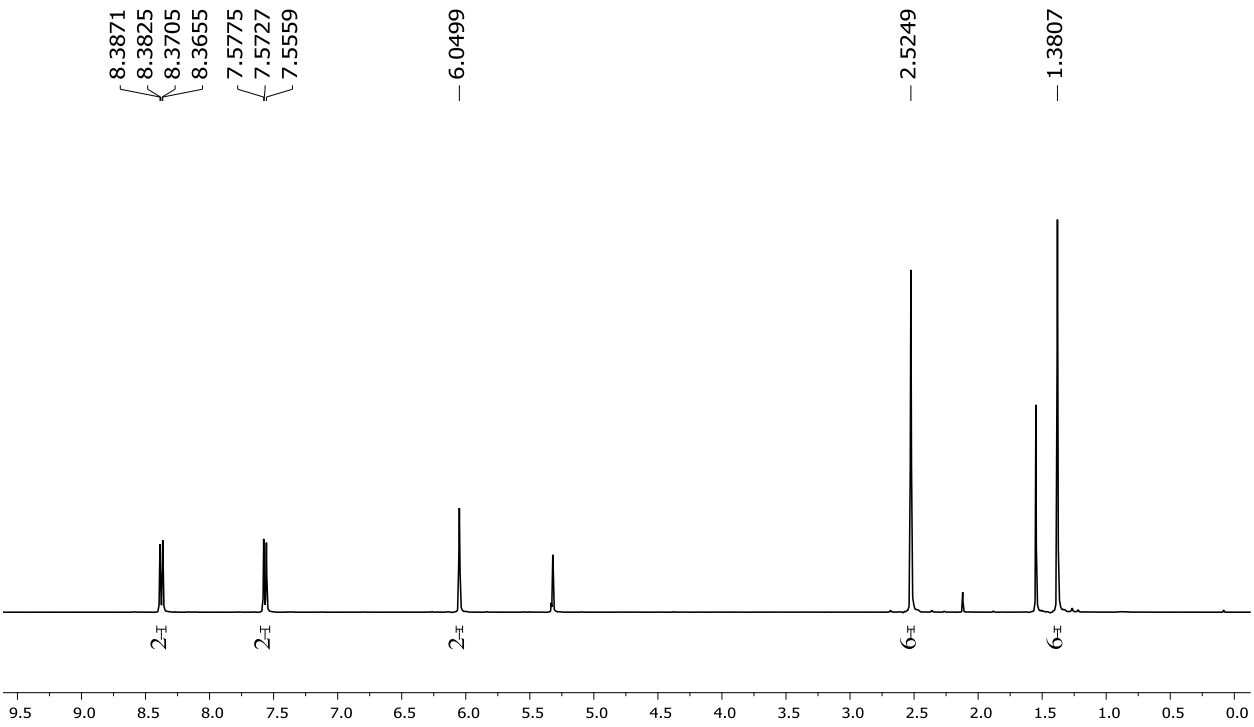

Figure D.9: ^{1}H NMR spectrum of **7** in CD_2Cl_2

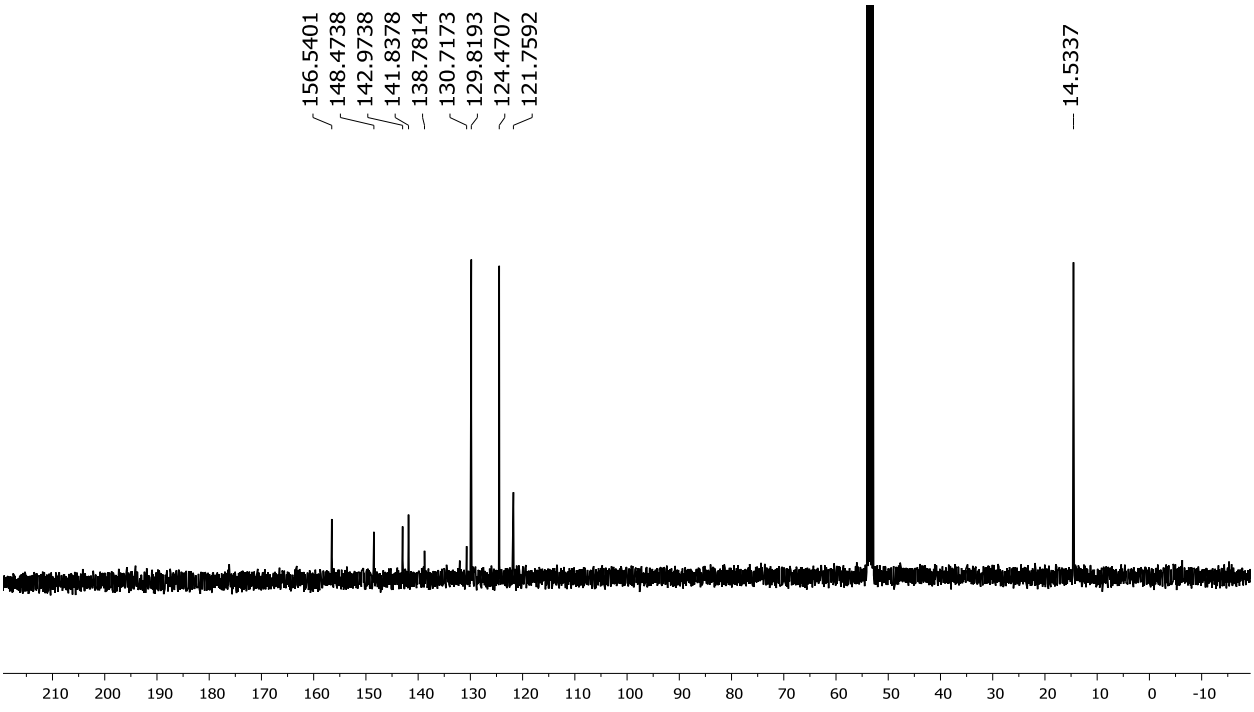

Figure D.10: ^{13}C NMR spectrum of **7** in CD_2Cl_2

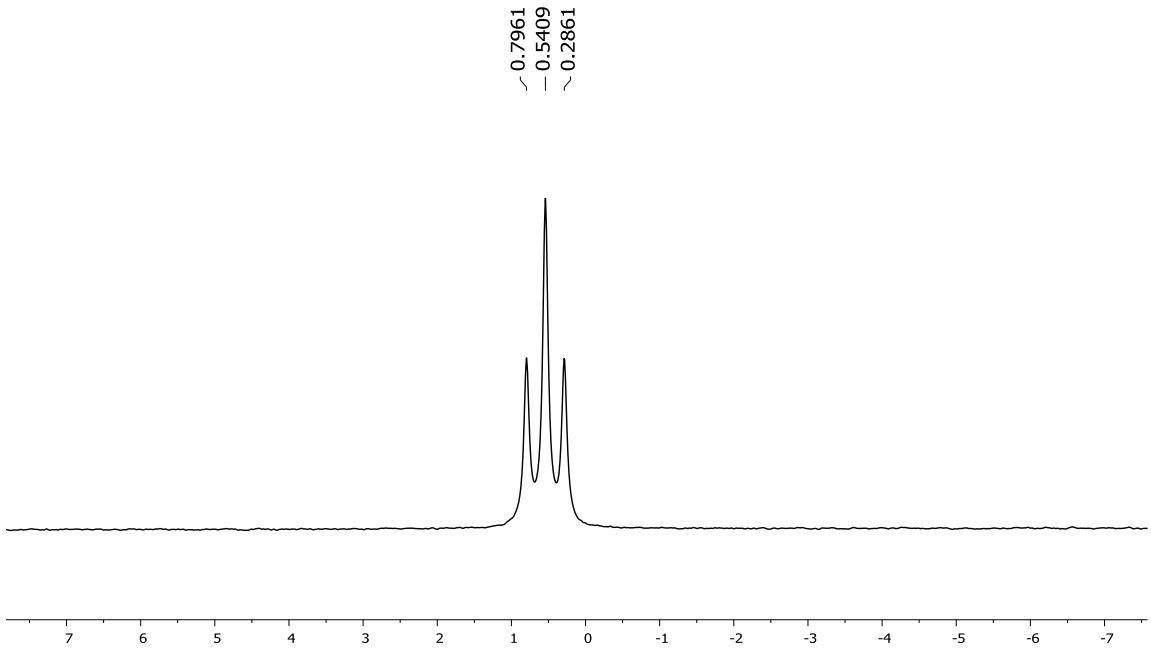

Figure D.11: ^{11}B NMR spectrum of **7** in CD_2Cl_2

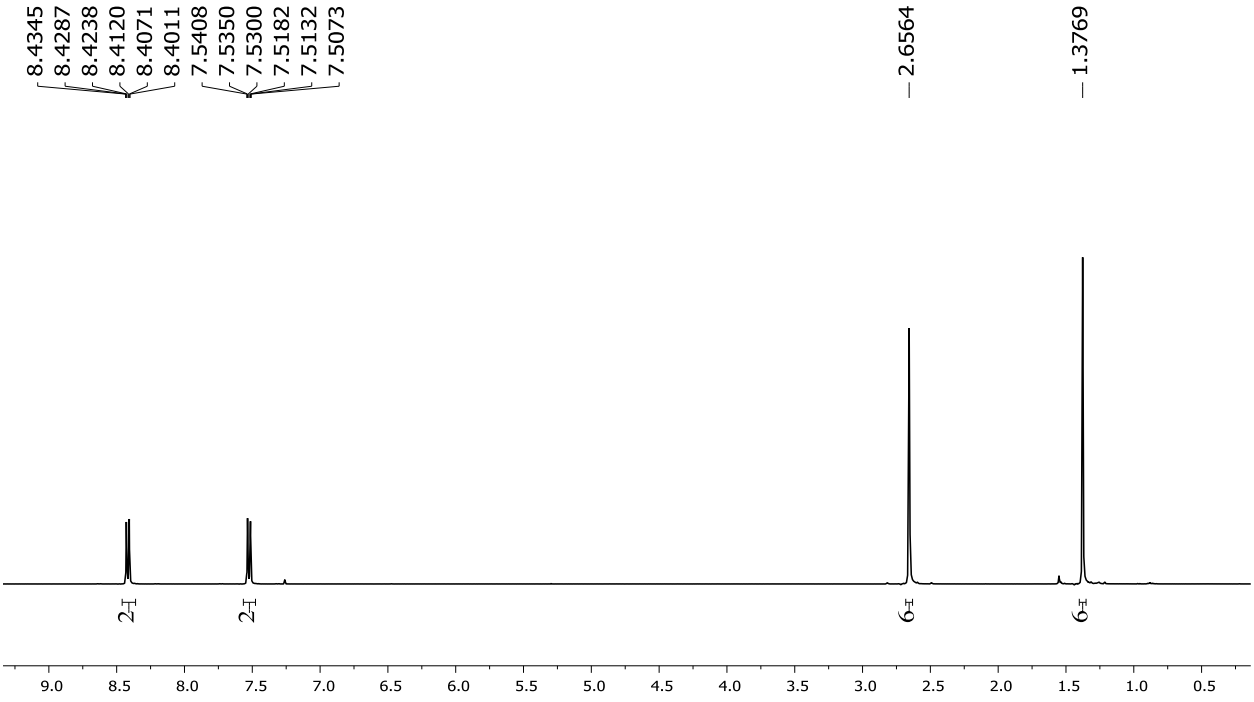

Figure D.12: ^{1}H NMR spectrum of **8** in $CDCl_3$

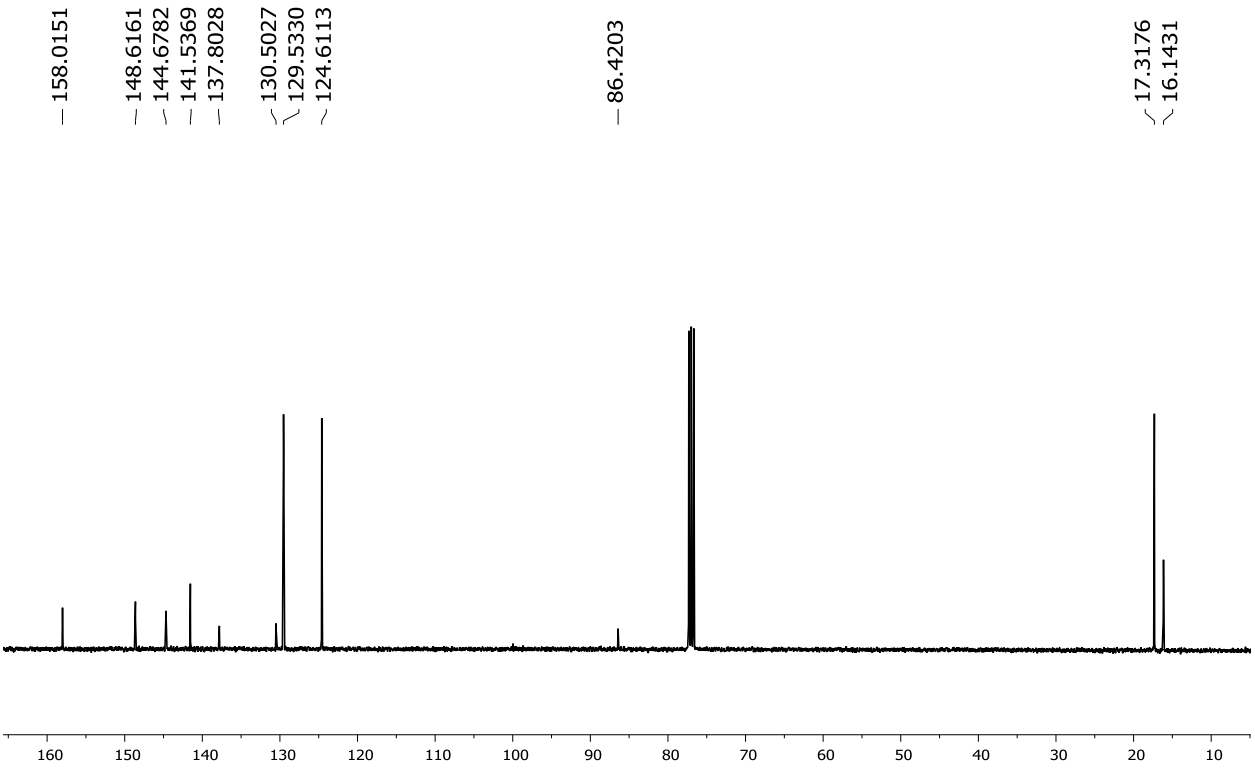

Figure D.13: ^{13}C NMR spectrum of **8** in $CDCl_3$

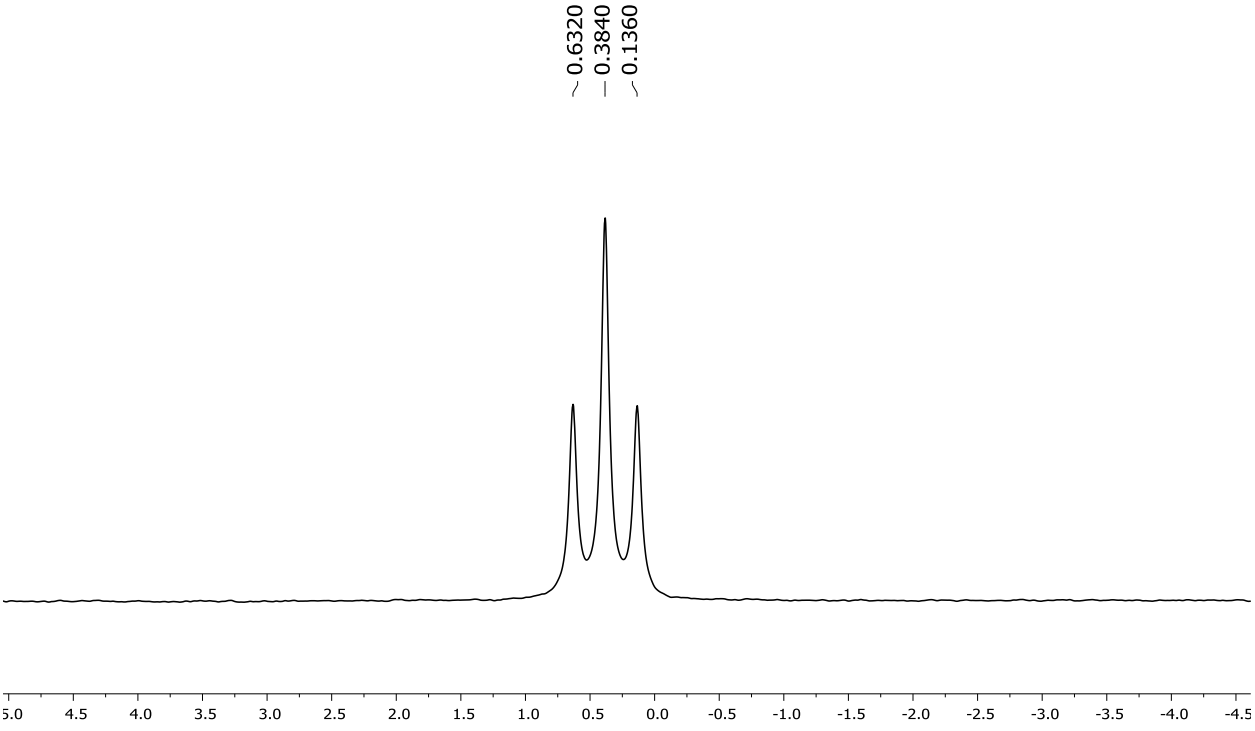

Figure D.14: ^{11}B NMR spectrum of **8** in $CDCl_3$

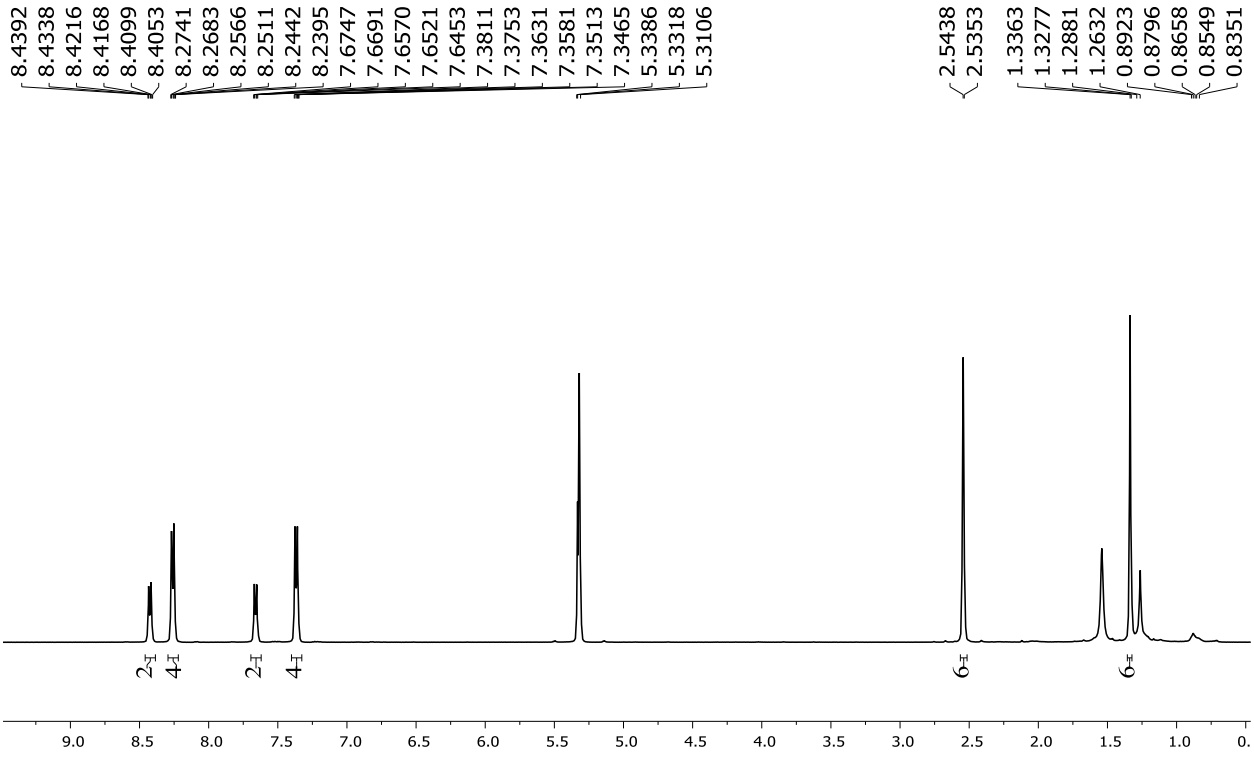

Figure D.15: ^{1}H NMR spectrum of **9** in CD_2Cl_2

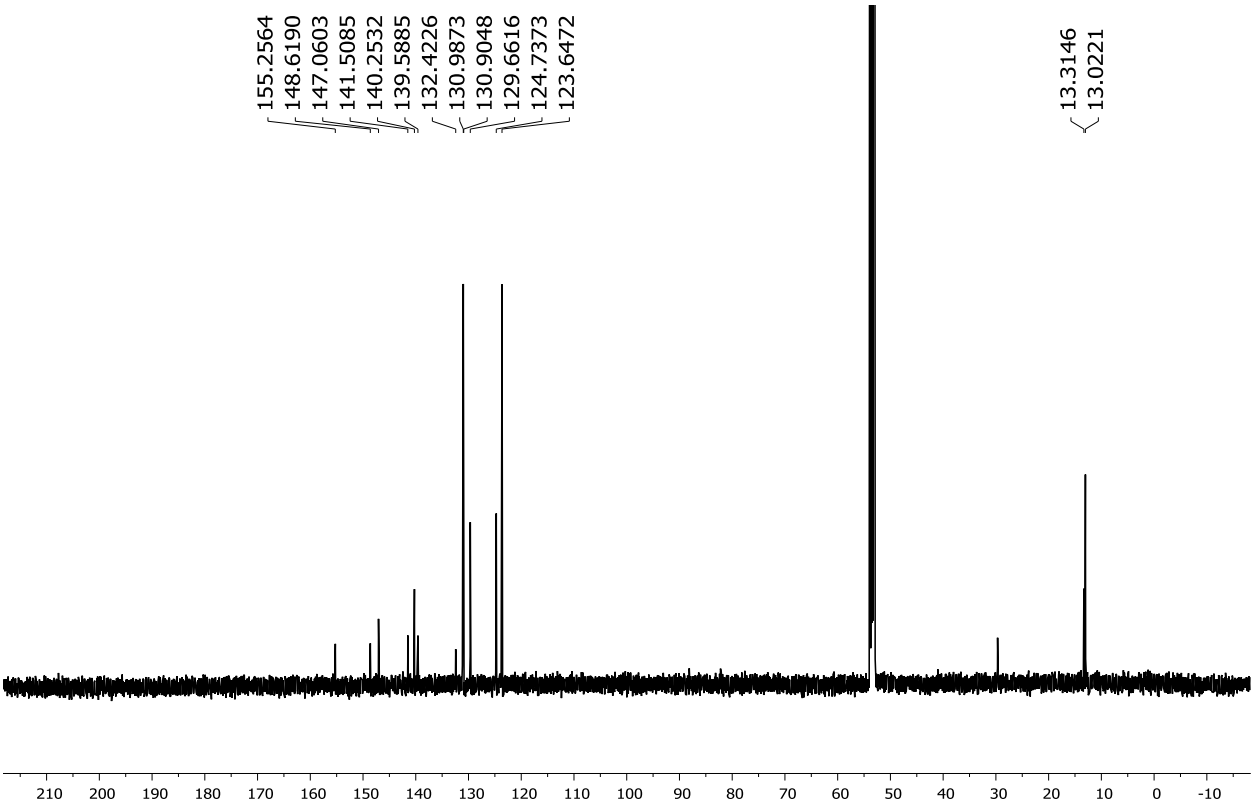

Figure D.16: ^{13}C NMR spectrum of **9** in CD_2Cl_2

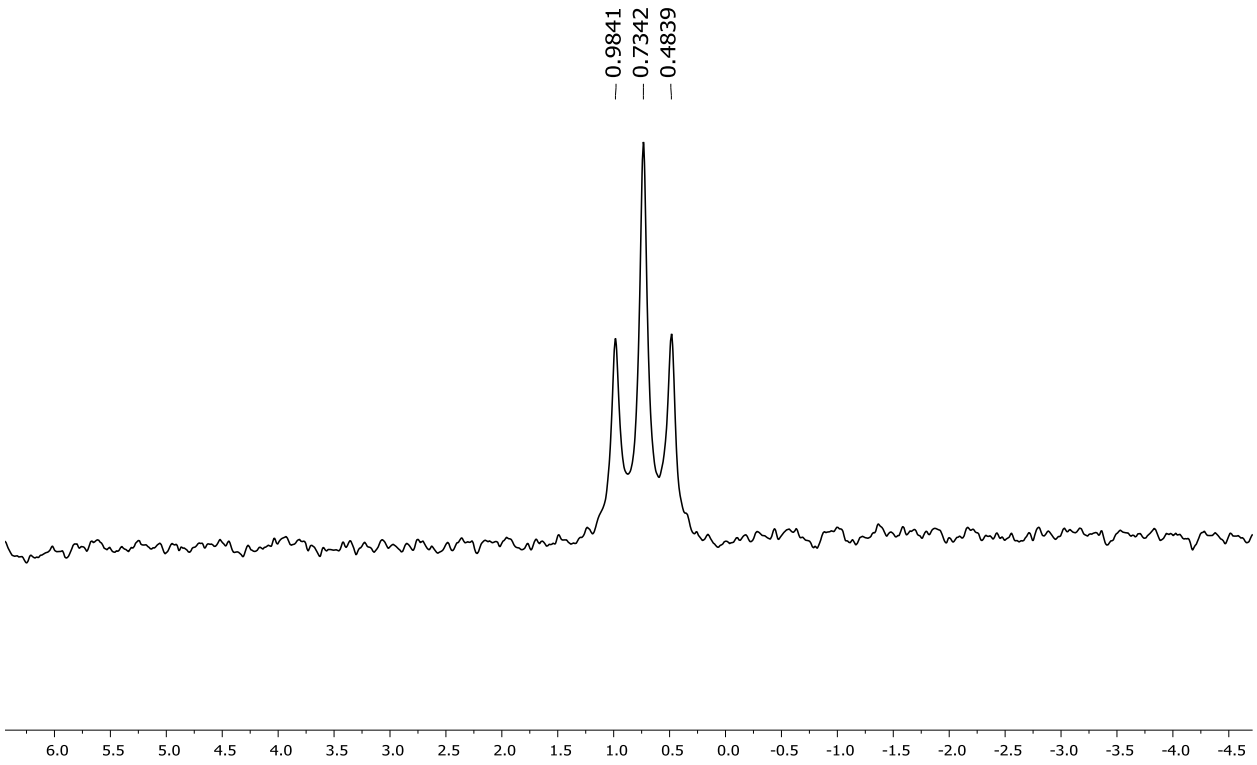

Figure D.17: ^{11}B NMR spectrum of **9** in CD_2Cl_2

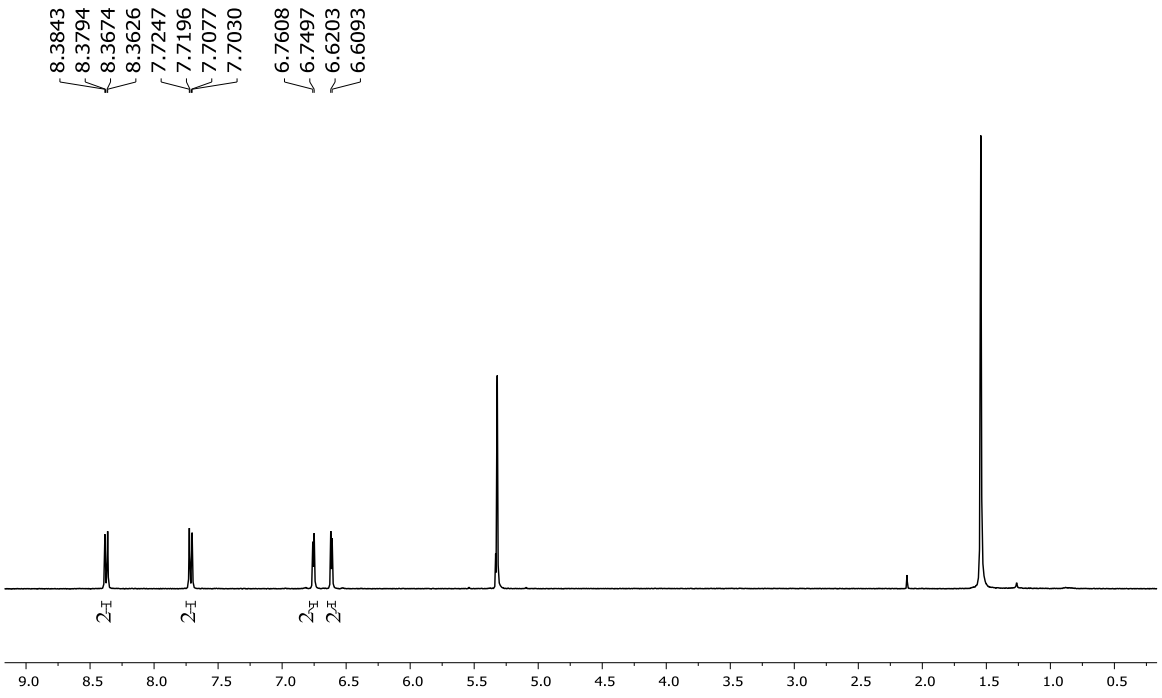

Figure D.18: ^{1}H NMR spectrum of **13** in CD_2Cl_2

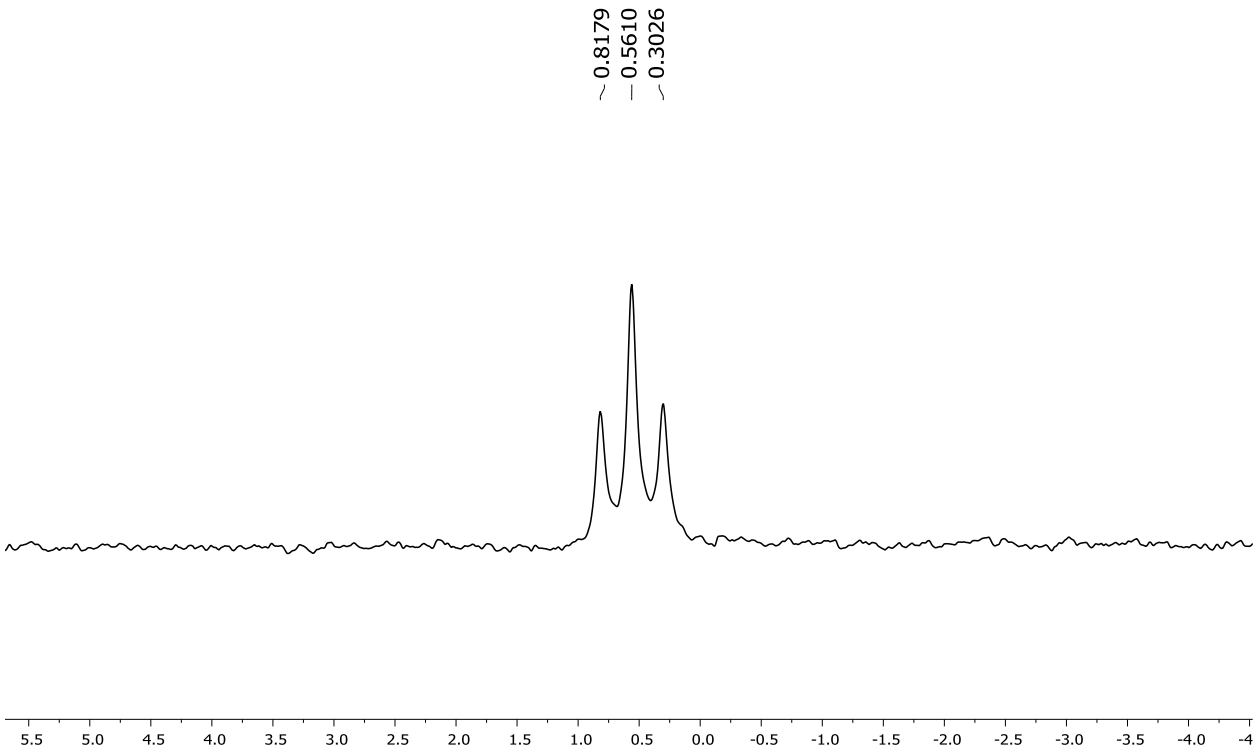

Figure D.19: ^{11}B NMR spectrum of **13** in CD_2Cl_2

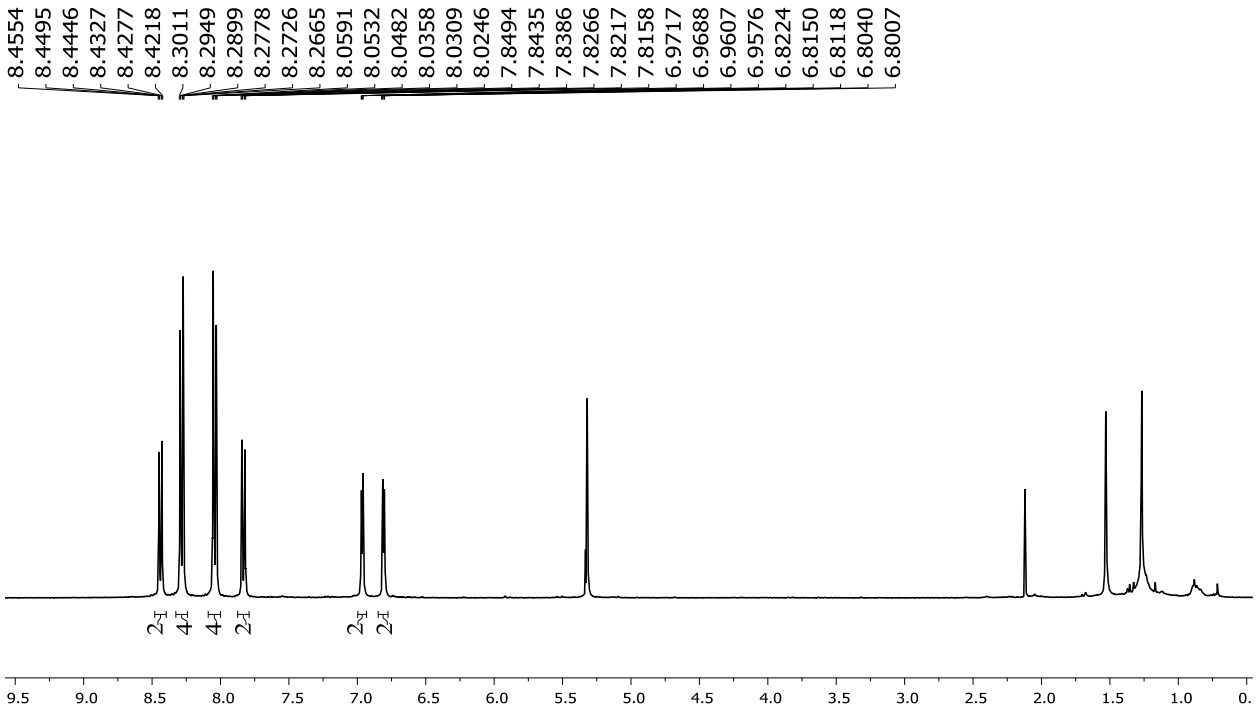

Figure D.20: ^{1}H NMR spectrum of **14** in CD_2Cl_2

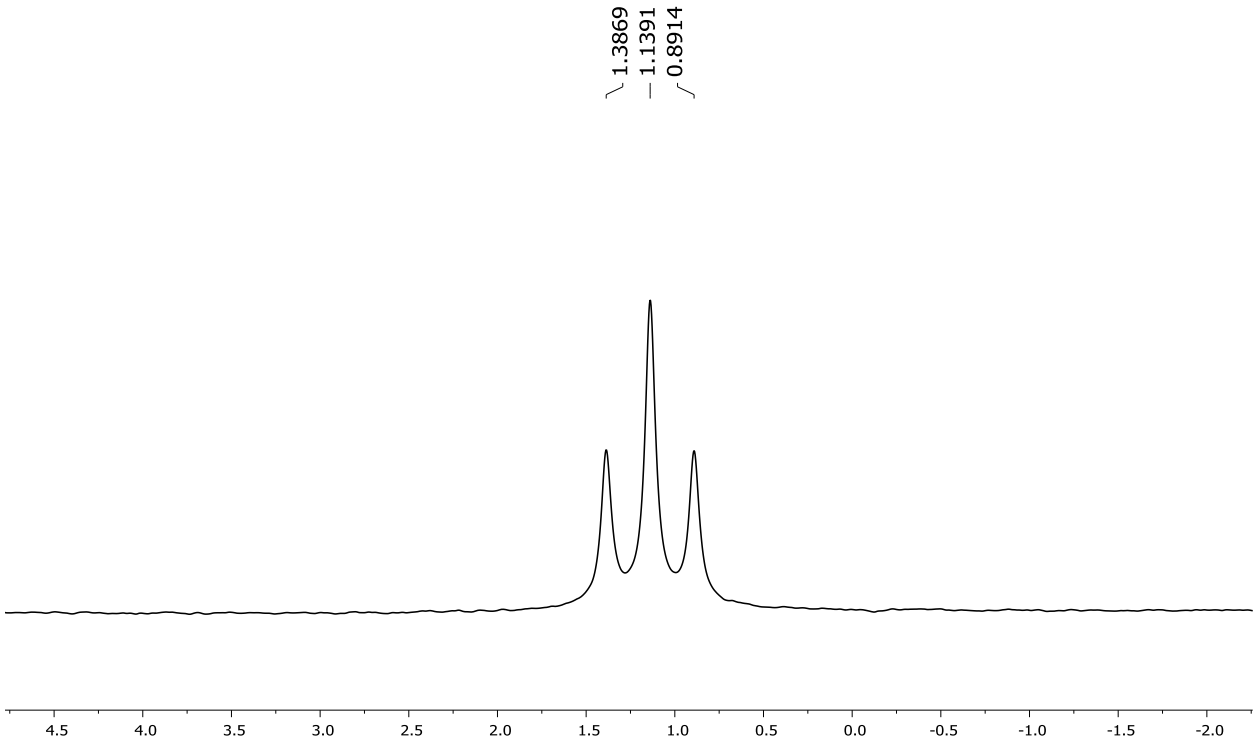

Figure D.21: ^{11}B NMR spectrum of **14** in CD_2Cl_2

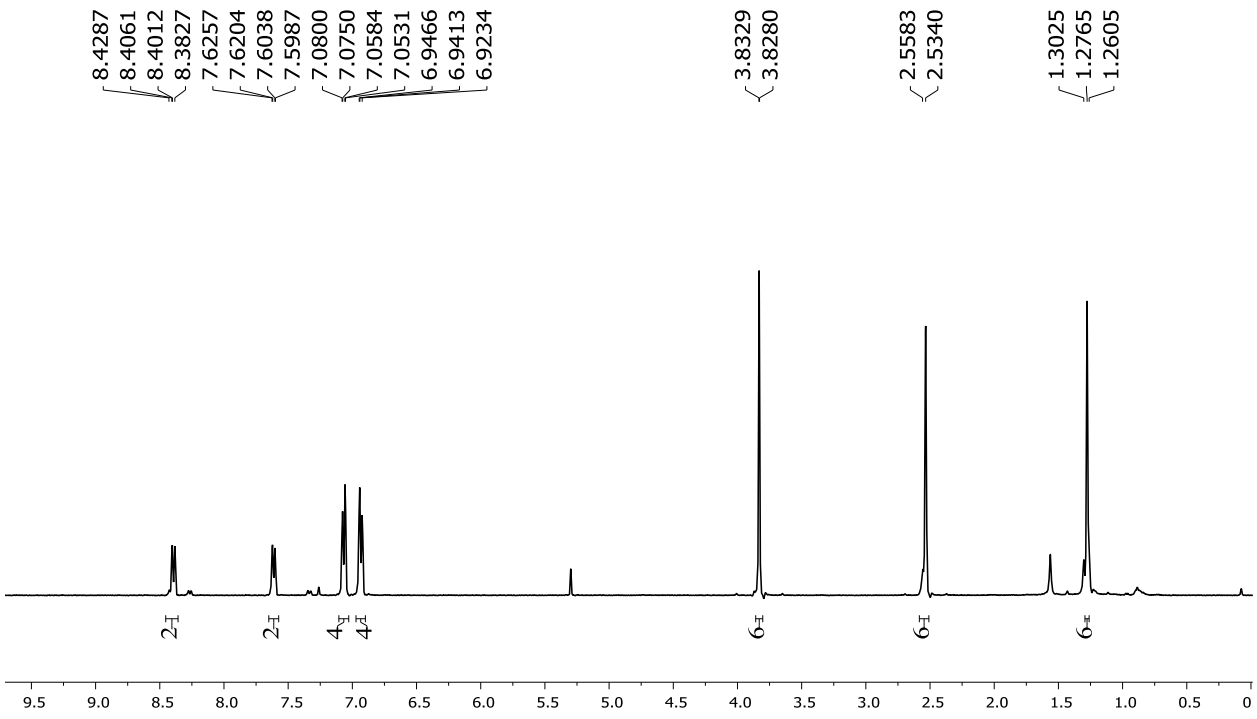

Figure D.22: ^{1}H NMR spectrum of **17** in $CDCl_3$

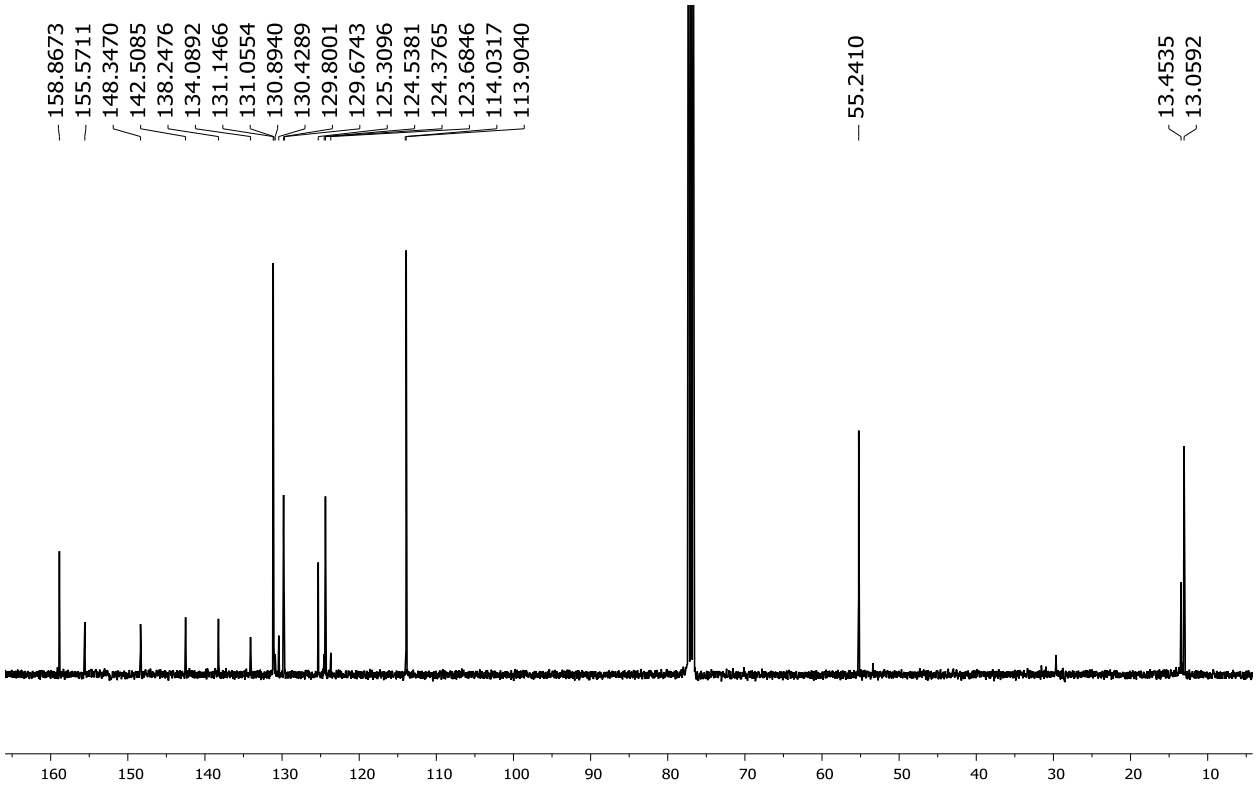

Figure D.23: ^{13}C NMR spectrum of **17** in $CDCl_3$

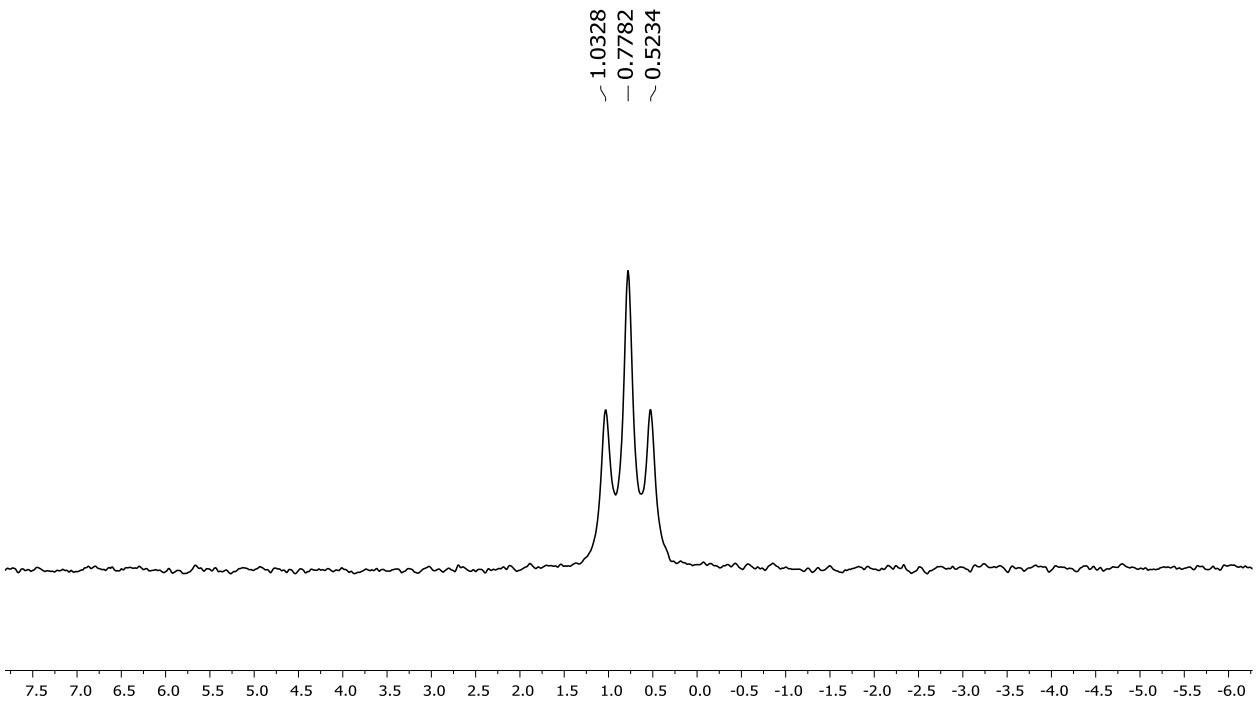

Figure D.24: ^{11}B NMR spectrum of **17** in $CDCl_3$

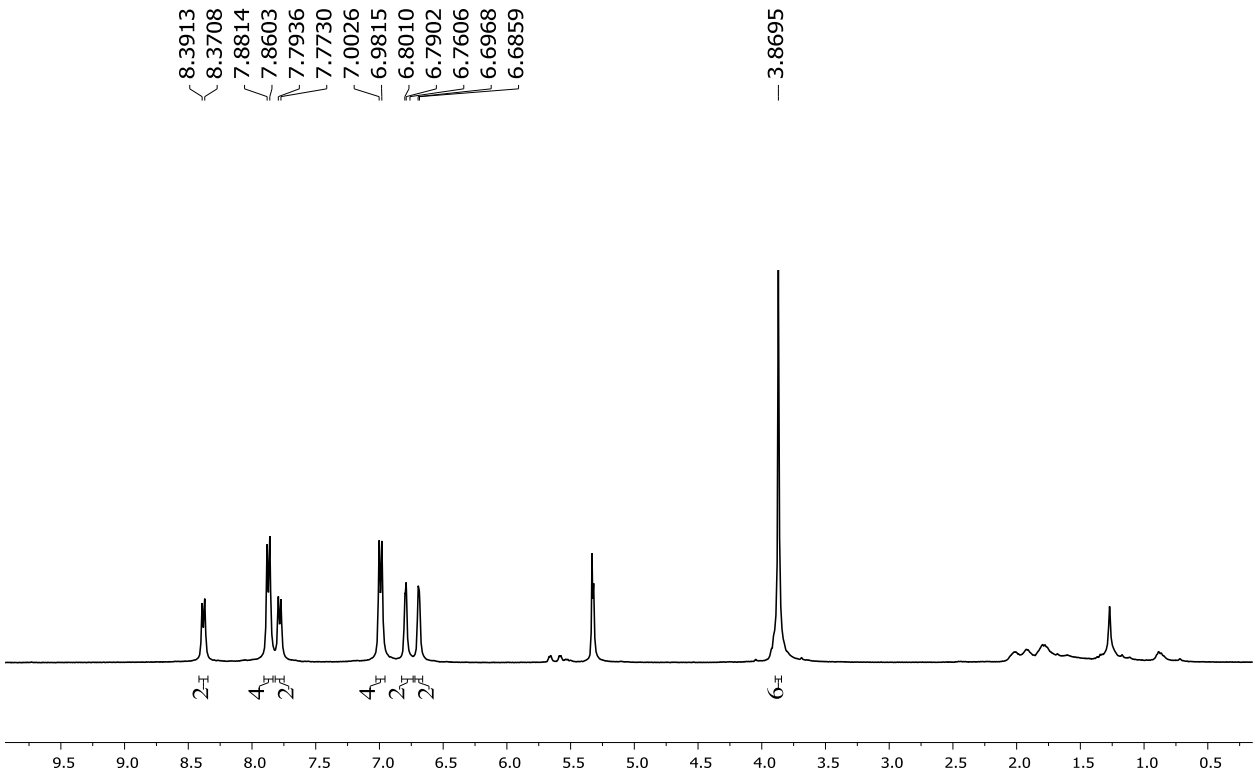

Figure D.25: ^{1}H NMR spectrum of **18** in CD_2Cl_2

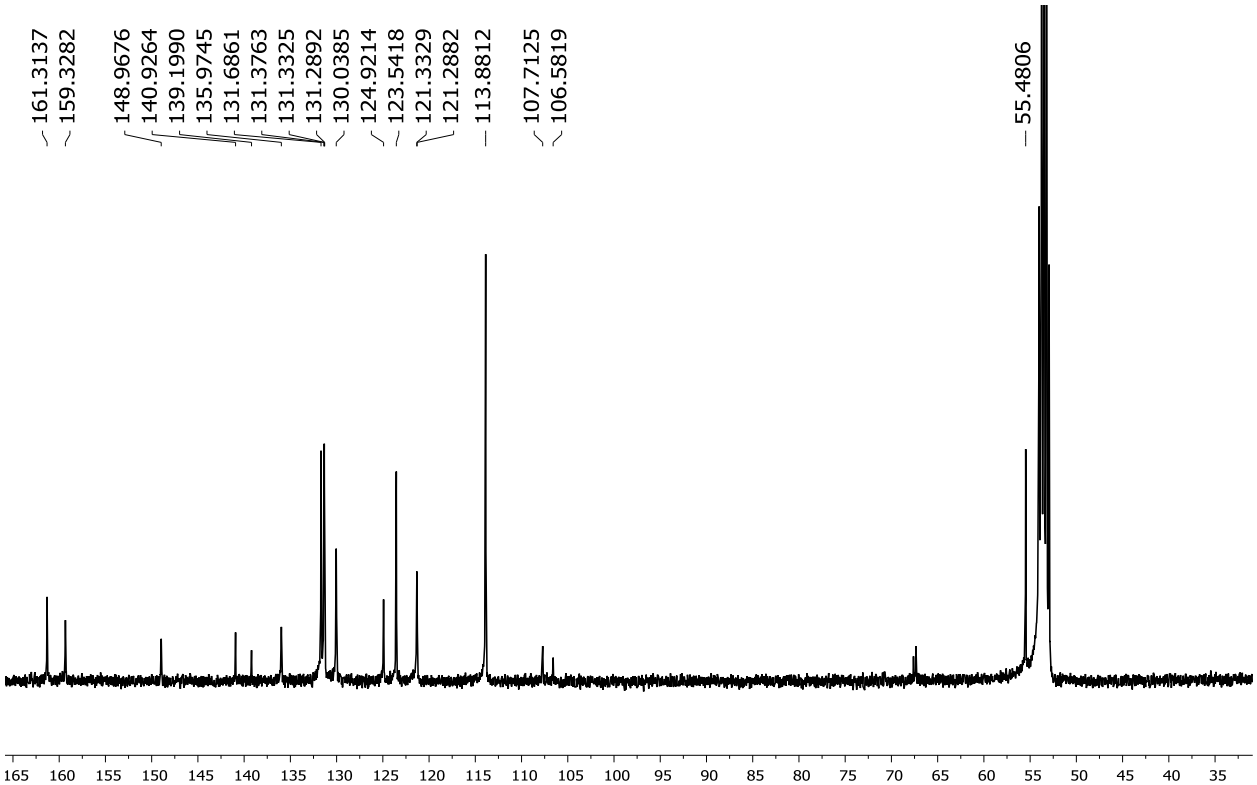

Figure D.26: ^{13}C NMR spectrum of **18** in CD_2Cl_2

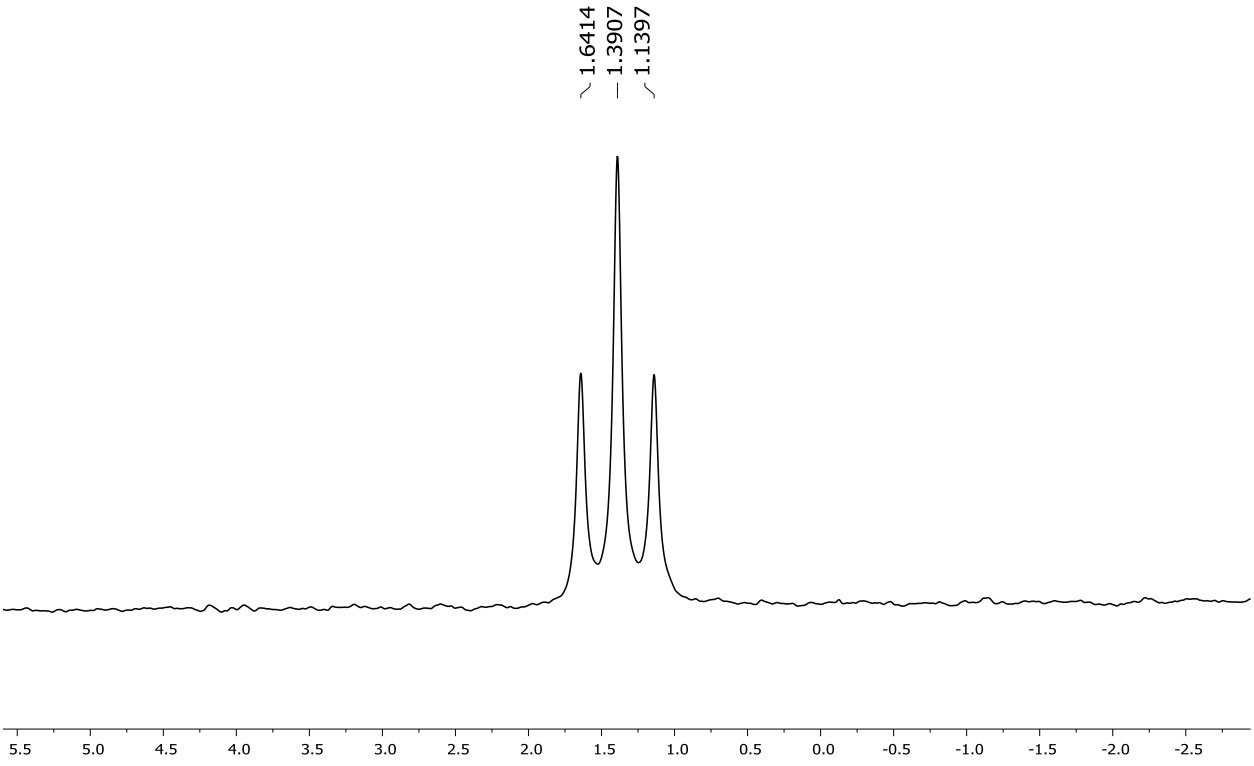

Figure D.27: ^{11}B NMR spectrum of **18** in CD_2Cl_2

Letters of Permission

Title: Bright Ideas for Chemical Biology
Author: Luke D. Lavis, Ronald T. Raines
Publication: ACS Chemical Biology
Publisher: American Chemical Society
Date: Mar 1, 2008

Logged in as:
Qianli Meng
LOGOUT

PERMISSION/LICENSE IS GRANTED FOR YOUR ORDER AT NO CHARGE

This type of permission/license, instead of the standard Terms & Conditions, is sent to you because no fee is being charged for your order. Please note the following:

- Permission is granted for your request in both print and electronic formats, and translations.
- If figures and/or tables were requested, they may be adapted or used in part.
- Please print this page for your records and send a copy of it to your publisher/graduate school.
- Appropriate credit for the requested material should be given as follows: "Reprinted (adapted) with permission from (COMPLETE REFERENCE CITATION). Copyright (YEAR) American Chemical Society." Insert appropriate information in place of the capitalized words.
- One-time permission is granted only for the use specified in your request. No additional uses are granted (such as derivative works or other editions). For any other uses, please submit a new request.

If credit is given to another source for the material you requested, permission must be obtained from that source.

BACK CLOSE WINDOW

ELSEVIER LICENSE
TERMS AND CONDITIONS

Mar 06, 2017

This Agreement between Qianli Meng ("You") and Elsevier ("Elsevier") consists of your license details and the terms and conditions provided by Elsevier and Copyright Clearance Center.

License Number	4063320713421
License date	
Licensed Content Publisher	Elsevier
Licensed Content Publication	Current Opinion in Chemical Biology
Licensed Content Title	In vivo near-infrared fluorescence imaging
Licensed Content Author	John V Frangioni
Licensed Content Date	October 2003
Licensed Content Volume	7
Licensed Content Issue	5
Licensed Content Pages	9
Start Page	626
End Page	634
Type of Use	reuse in a thesis/dissertation
Portion	figures/tables/illustrations
Number of figures/tables/illustrations	1
Format	both print and electronic
Are you the author of this Elsevier article?	No
Will you be translating?	No
Order reference number	
Original figure numbers	Figure 1
Title of your thesis/dissertation	Design, Synthesis, Characterization and Evaluation of Near Infrared BODIPY Dyes for Various Applications
Expected completion date	Apr 2017
Estimated size (number of pages)	250
Elsevier VAT number	GB 494 6272 12
Requestor Location	Qianli Meng 232 Choppin Hall Department of Chemistry BATON ROUGE, LA 70803 United States Attn: Qianli Meng
Publisher Tax ID	98-0397604
Total	0.00 USD

ELSEVIER LICENSE
TERMS AND CONDITIONS

Mar 06, 2017

This Agreement between Qianli Meng ("You") and Elsevier ("Elsevier") consists of your license details and the terms and conditions provided by Elsevier and Copyright Clearance Center.

License Number	4063321219938
License date	
Licensed Content Publisher	Elsevier
Licensed Content Publication	Tetrahedron Letters
Licensed Content Title	Synthesis of N,N-difluoroboryl complexes of 3,3′-diarylazadiisoindolylmethenes
Licensed Content Author	Valentina F. Donyagina,Soji Shimizu,Nagao Kobayashi,Evgeny A. Lukyanets
Licensed Content Date	13 October 2008
Licensed Content Volume	49
Licensed Content Issue	42
Licensed Content Pages	3
Start Page	6152
End Page	6154
Type of Use	reuse in a thesis/dissertation
Intended publisher of new work	other
Portion	figures/tables/illustrations
Number of figures/tables/illustrations	1
Format	both print and electronic
Are you the author of this Elsevier article?	No
Will you be translating?	No
Order reference number	
Original figure numbers	Figure 4
Title of your thesis/dissertation	Design, Synthesis, Characterization and Evaluation of Near Infrared BODIPY Dyes for Various Applications
Expected completion date	Apr 2017
Estimated size (number of pages)	250
Elsevier VAT number	GB 494 6272 12
Requestor Location	Qianli Meng 232 Choppin Hall Department of Chemistry BATON ROUGE, LA 70803

ELSEVIER LICENSE
TERMS AND CONDITIONS

Mar 07, 2017

This Agreement between Qianli Meng ("You") and Elsevier ("Elsevier") consists of your license details and the terms and conditions provided by Elsevier and Copyright Clearance Center.

License Number	4063890730281
License date	Mar 07, 2017
Licensed Content Publisher	Elsevier
Licensed Content Publication	Journal of Inorganic Biochemistry
Licensed Content Title	Cobalt triarylcorroles containing one, two or three nitro groups. Effect of NO2 substitution on electrochemical properties and catalytic activity for reduction of molecular oxygen in acid media
Licensed Content Author	Bihong Li,Zhongping Ou,Deying Meng,Jijun Tang,Yuanyuan Fang,Rui Liu,Karl M. Kadish
Licensed Content Date	July 2014
Licensed Content Volume	136
Licensed Content Issue	n/a
Licensed Content Pages	10
Start Page	130
End Page	139
Type of Use	reuse in a thesis/dissertation
Intended publisher of new work	other
Portion	figures/tables/illustrations
Number of figures/tables/illustrations	1
Format	both print and electronic
Are you the author of this Elsevier article?	No
Will you be translating?	No
Order reference number	
Original figure numbers	figure 1
Title of your thesis/dissertation	Design, Synthesis, Characterization and Evaluation of Near Infrared BODIPY Dyes for Various Applications
Expected completion date	Apr 2017
Estimated size (number of pages)	250
Elsevier VAT number	GB 494 6272 12
Requestor Location	Qianli Meng 232 Choppin Hall Department of Chemistry BATON ROUGE, LA 70803

VITA

Qianli Meng was born to Ming Meng and Min Li in Wuhu, Anhui, China. After completing his primary studies in 2007, he attended Anhui Normal University, Anhui, China where he earned Bachelor of Engineering in July of 2011. He then entered the Doctoral Program in the Department of Chemistry at Louisiana State University, Baton Rouge, Louisiana. He joined the research group of Prof. M. Graça H. Vicente from 2012. Qianli is currently a candidate for the Doctor of Philosophy degree in organic chemistry, which will be awarded at the May 2017 commencement.